Robustness Issues in Fault Diagnosis and Fault Tolerant Control

Stoustrup, Jakob; Zhou, Kemin

Published in:
Journal of Control Science and Engineering

DOI (link to publication from Publisher):
10.1155/2008/251973

Publication date:
2008

Document Version
Early version, also known as pre-print

Journal of Control Science and Engineering

Robustness Issues in Fault Diagnosis and Fault Tolerant Control

Guest Editors: Jakob Stoustrup and Kemin Zhou

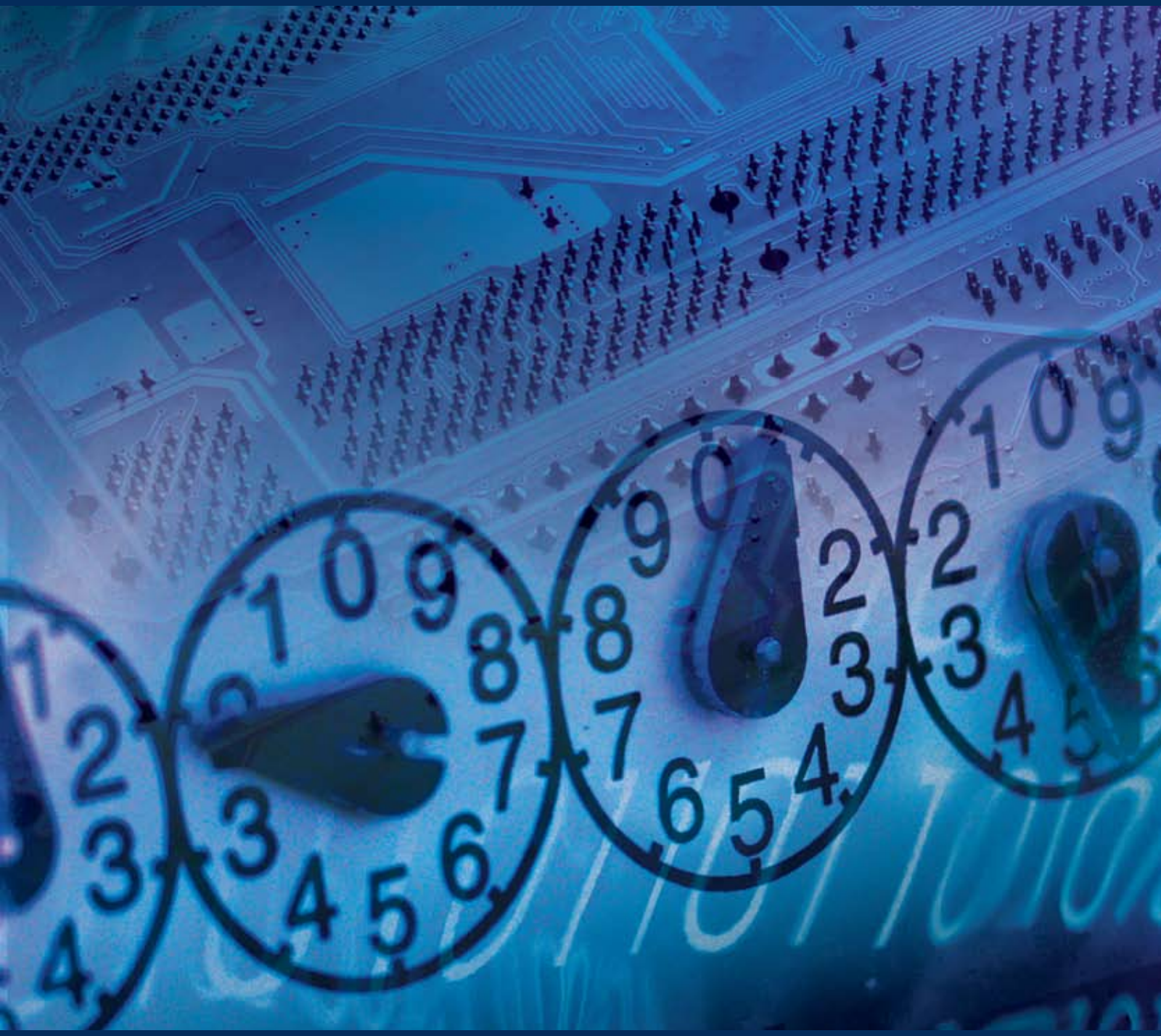

Robustness Issues in Fault Diagnosis and Fault Tolerant Control

Journal of Control Science and Engineering

Robustness Issues in Fault Diagnosis and Fault Tolerant Control

Guest Editors: Jakob Stoustrup and Kemin Zhou

Contents

Hindawi Publishing Corporation
Journal of Control Science and Engineering
Volume 2008, Article ID 251973, 2 pages
doi:10.1155/2008/251973

Editorial

Robustness Issues in Fault Diagnosis and Fault Tolerant Control

Jakob Stoustrup[1] and Kemin Zhou[2]

[1] *Section for Automation and Control, Department of Electronic Systems, Aalborg University, Fredrik Bajers Vej 7C, 9220 Aalborg, Denmark*
[2] *Department of Electrical and Computer Engineering, Louisiana State University, Baton Rouge, LA 70803, USA*

Correspondence should be addressed to Jakob Stoustrup, jakob@es.aau.dk

Received 24 January 2008; Accepted 24 January 2008

Fault diagnosis and fault tolerant control have become critically important in modern complex systems such as aircrafts and petrochemical plants. Since no system in the real world can work perfectly at all time under all conditions, it is crucial to be able to detect and identify the possible faults in the system as early as possible so that measures can be taken to prevent significant performance degradation or damages to the system. Fault diagnosis is not relevant only for safety critical systems, but also for a significant number of systems, where availability is a major issue.

In the past twenty some years, fault diagnosis of dynamic systems has received much attention and significant progress has been made in searching for model-based diagnosis techniques. Many techniques have been developed for fault detection and fault tolerant control. However, the issue of robustness of fault detection and fault tolerant control has not been sufficiently addressed. Since disturbances, noise, and model uncertainties are unavoidable for any practical system, it is essential in the design of any fault diagnosis/fault tolerant control system to take these effects into consideration, so that fault diagnosis/tolerant control can be done reliably and robustly. The objective of this special issue is to report some most recent developments and contributions in this direction.

The special issue is initiated by a paper by P. Zhang and S. Ding, which gives a review of standard fault detection formulations, focusing on robustness issues for model-based diagnosis systems.

N. Liu and K. Zhou then study a number of robust fault detection problems, such as $\mathcal{H}/\mathcal{H}$, $\mathcal{H}_2/\mathcal{H}$, and $\mathcal{H}/\mathcal{H}$ problems, and it is shown that these problems share the same optimal filters. The optimal filters are designed by solving an algebraic Riccati equation.

The robust fault detection and isolation problem is studied in the paper by E. Mazars et al., where an $\mathcal{H}$ criterion is used, giving rise to a quadratic matrix inequality problem. A jet engine example is provided.

D. Campos-Delgado et al. suggest an active fault-tolerant control, and a design strategy is provided, which takes model uncertainty into account. The methods are illustrated for a DC motor example.

Systems that can be described by linear parameter varying models are considered by S. Grenaille et al. where robustness constraints are included in the design of fault detection and isolation filters. An illustration of the methods is given in terms of an application to a nuclear power plant.

A method for design of a diagnosis and a fault tolerant control system using an integrated approach is presented in the paper by S. Yang and J. Chen. The design is illustrated for a double inverted pendulum system.

M. Benini et al. present both a linear and a nonlinear fault detection and isolation scheme. This paper focuses on robust fault diagnosis for an aircraft model, and has extensive simulations.

The fault tolerant scheme proposed by R. Dionisio and J. Lemos is capable of stabilizing systems with intermittent sensor faults. The approach is based on reconstructing the feedback signal, using a switching strategy where a model is used in the intermittent periods.

A design method for actuator fault diagnosis is proposed in the paper by Q. Zhang, where the focus is to obtain robustness with respect to nonlinear sensor distortion. A numerical example is given.

The problem of designing fault tolerant control systems for networked systems with actuator faults is treated in the

paper by Li et al. The proposed design method is demonstrated by a numerical example.

The notion of a reliability index is introduced by H. Li et al., for monitoring fault tolerant control systems. The reliability is evaluated based on semi-Markov models, and the approach is applied to an aircraft model.

The final paper of the special issue by N. Wu et al. addresses fault tolerant control of a distributed database system. The fault tolerant design relies on data redundancy in the partitioned system architecture. Robustness is represented by the introduction of additional states modeling delays and decision errors. The design is based on solving Markovian decision problems.

Jakob Stoustrup
Kemin Zhou

Hindawi Publishing Corporation
Journal of Control Science and Engineering
Volume 2008, Article ID 849546, 18 pages
doi:10.1155/2008/849546

Review Article

On Fault Detection in Linear Discrete-Time, Periodic, and Sampled-Data Systems

P. Zhang and S. X. Ding

Institute for Automatic Control and Complex Systems, Faculty of Engineering, University of Duisburg-Essen, Bismarckstrasse 81 BB, 47057 Duisburg, Germany

Correspondence should be addressed to S. X. Ding, steven.ding@uni-due.de

Received 30 April 2007; Accepted 4 October 2007

Recommended by Kemin Zhou

This paper gives a review of some standard fault-detection (FD) problem formulations in discrete linear time-invariant systems and the available solutions. Based on it, recent development of FD in periodic systems and sampled-data systems is reviewed and presented. The focus in this paper is on the robustness and sensitivity issues in designing model-based FD systems.

1. INTRODUCTION

With the increasing requirements of modern complex control systems on safety and reliability, model-based fault detection and isolation (FDI) technology has attracted remarkable attention during the last three decades [1–6]. In major industrial sectors, it has become an important supporting technology and is replacing the traditional hardware redundancy technique in part or totally. As a standard functional module, FDI systems are increasingly integrated in modern technical systems and provide valuable information for condition-based predictive maintenance, higher-level fault tolerant control, and plant-wide production optimization.

Though closely related to the development of control and filtering theory, there are several distinct features of the model-based FDI problems that justify the efforts made in this field. To evaluate the performance of an FDI system in practice, miss alarm rate, false alarm rate, and detection delay are the most important criteria that decide the acceptance of the methods. It is widely accepted that these functional requirements can be reformulated as a multi-objective problem. Enhancing the robustness of the FDI system to unknown disturbances and modeling errors is an essential objective. However, alone the robustness does not guarantee a good FDI performance. The sensitivity of the FDI system to faults should be simultaneously improved. To find the best compromise between the robustness and the sensitivity is thus the central problem in model-based FDI. This is the first difference of FDI problems from control and standard filtering problems, where the focus is put on disturbance attenuation. Bearing this in mind, full-decoupling problem and optimal design of FDI systems have been studied [3–6] and different types of indices have been introduced to describe the sensitivity to the faults. Secondly, for the purpose of FDI, a fault indicating signal, called residual, needs not only to be generated, but also to be evaluated and, based on it, a decision for the existence, location, and size of the faults needs to be made. Therefore, an FDI procedure includes residual generation and residual evaluation. An integrated design of these two parts is needed to guarantee the optimal FDI performance [7].

In this paper, we will first give a review of some standard fault detection (FD) problem formulations in discrete-time systems and the available solutions. There are two types of discrete-time model-based FD systems: the parity space and the observer-based ones. The former is, in its original form, specially dedicated to the discrete-time systems [8], while the latter is analogous to the continuous-time systems and its development shares the same essentials with the continuous-time systems. Perhaps for this reason, besides the early research activity on the parity space approaches, only few studies have been specifically devoted to the FD problems in discrete-time systems. Recently, the intensive research on networked control systems (NCS) and embedded systems

considerably stimulates the study on periodic, sampled-data systems [9]. The integration of data communication networks into control systems introduces natural periodic behavior in the system dynamics and the sampling effect is understood not only in view of the behavior of A/D and D/A converters but also in the context of data transmission among the subsystems. It can be observed that the recent studies on FD in periodic and sampled-data systems are mainly based on the discrete-time model-based FD methods. It is this fact that motivates us to give an overview of some standard FD methods for discrete-time systems and, based on it, to review and present some recent results on FD in periodic and sampled-data systems. Bearing in mind that fault isolation problems can be principally reformulated as a robust fault detection problem [4, 5], our focus in this paper is on the robustness issues in designing model-based FD systems.

The paper is organized as follows. In Section 2, we review FD methods for discrete-time systems and address some important relations between different methods. Section 3 is devoted to FD in discrete-time periodic systems. In Section 4, FD in sampled-data systems is addressed.

Throughout this paper, standard notations of robust control theory, for instance those used in [10], are adopted. We will use $\underline{\sigma}(X), \overline{\sigma}(X)$ to denote the minimum and maximum singular values of matrix X, respectively and $\sigma_i(X)$ to denote any singular value of X that satisfies $\underline{\sigma}(X) \le \sigma_i(X) \le \overline{\sigma}(X)$. $\|x\|_E$ denotes the Euclidean norm of vector x, $\|\xi\|_2$ the l_2-norm of discrete-time signal ξ or the $\mathcal{L}_2$-norm of continuous-time signal ξ, $\|\xi\|_{2,[a,b)}$ the 2 norm of ξ over the interval $[a, b)$, and $\|G\|_\infty$ the H_∞-norm of transfer function matrix G. The superscript T denotes the transpose of matrices and the superscript $*$ denotes the adjoint of operators. $\mathcal{RH}_\infty$ stands for the subspace that consists of all proper and real rational stable transfer function matrices. In this paper, we call a state-space model (A, B, C, D) regular, if it is detectable and has no invariant zeros on the unit circle and no unobservable modes at the origin.

2. FD OF DISCRETE LTI SYSTEMS

Linear time-invariant (LTI) systems are the simplest class of systems. Although the handling of FD problems in discrete LTI systems can often be done along the well-established framework of FD schemes for continuos LTI systems, study on FD in discrete LTI systems is of primary importance from the following three aspects:

(i) it gives insight and often motivates extensions to more complex systems like periodic and sampled-data systems addressed in the subsequent sections;
(ii) there are some methods that have been developed specially for discrete LTI systems;
(iii) due to its practical form for the direct online implementation, the discrete-time system form is often favored in the applications.

In this section, basic ideas and solution procedures of advanced FD methods for discrete LTI systems, divided into three groups, will be reviewed:

(i) parity space approaches, which are specific for discrete LTI systems and will be dealt to some details;
(ii) the parametrization of observer-based FD systems and postfilter design schemes;
(iii) fault detection filter schemes, which are mostly studied and closely related to robust control theory.

Thanks to the well-known relationships between the technical features of the discrete- and continuous-time systems, many well-established FD schemes for continuous LTI systems can be directly applied to the latter two FD schemes. For this reason, we will restrict ourselves to some representative methods and give a brief view of the analog application of the methods for continuous-time systems to the discrete FD systems. Another focus in this section is on the comparison and interpretation of the FD methods.

2.1. System models and problem formulation

Suppose that the discrete LTI systems are described by

$$\Sigma_{\text{LTI}}: \begin{cases} x(k+1) = Ax(k) + Bu(k) + E_d d(k) + E_f f(k), \\ y(k) = Cx(k) + Du(k) + F_d d(k) + F_f f(k), \end{cases} \tag{1}$$

where $x \in \mathcal{R}^n$ is the state vector, $u \in \mathcal{R}^p$ the vector of control inputs, $y \in \mathcal{R}^m$ the vector of process outputs, $d \in \mathcal{R}^{n_d}$ the vector of unknown disturbances, and $f \in \mathcal{R}^{n_f}$ the vector of faults to be detected, $A, B, E_d, E_f, C, D, F_d$, and F_f are known constant matrices of appropriate dimensions. In the frequency domain, system Σ_{LTI} can be equivalently described by

$$y(z) = G_u(z)u(z) + G_d(z)d(z) + G_f(z)f(z), \tag{2}$$

where $G_u(z), G_d(z)$, and $G_f(z)$ denote, respectively, the transfer function matrices from u, d, and f to y.

Although the design of a model-based FD systems mainly consists of three tasks: (a) residual generation, (b) residual evaluation, (c) threshold determination, major research attention has been focused on the residual generation with the following issues.

(i) *Full decoupling problem*, which deals with the design of a residual generator, so that the residual signal r satisfies

$$\forall u, d, \lim_{k\to\infty} r(k) = 0 \quad \text{if } f = 0, \qquad r(k) \neq 0 \quad \text{if } f_i(k) \neq 0,\ i = 1, \ldots, n_f. \tag{3}$$

If a full decoupling is realized, then the residual evaluation reduces to detect the nonzeroness of the residual signal.
(ii) *Optimal FD problem*, which is to design the residual generator so that the residual signal r is as small as possible if $f = 0$ and deviates from 0 as much as possible if $f_i(k) \neq 0$, $i = 1, \ldots, n_f$.

Considering that in the fault-free case the residual signal r would, due to the existence of d, differ from zero, evaluation

of the size of r is necessary in order to distinguish the influence of the faults from that of the disturbances. In this paper, the *norm-based evaluation* of the residual signal, denoted by $J = \|r\|$ and, based on it, *threshold determination* satisfying

$$J\text{th} = \sup_{f=0,d} \|r\| \tag{4}$$

will be briefly reviewed.

2.2. Parity space approach

The parity space approach is based on the so-called parity relation. Let s be an integer denoting the length of a moving time window. The output of system (1) over the moving window $[k-s, k]$ can be expressed by the initial state $x(k-s)$, the stacked control input vector $u_{k,s}$, the stacked disturbance vector $d_{k,s}$, and the stacked fault vector $f_{k,s}$ as

$$y_{k,s} = H_{o,s}x(k-s) + H_{u,s}u_{k,s} + H_{d,s}d_{k,s} + H_{f,s}f_{k,s}, \tag{5}$$

where

$$\xi_{k,s} = \begin{bmatrix} \xi(k-s) \\ \xi(k-s+1) \\ \vdots \\ \xi(k) \end{bmatrix} \quad \text{with } \xi \text{ standing for } y, u, d, f,$$

$$H_{o,s} = \begin{bmatrix} C \\ CA \\ \vdots \\ CA^s \end{bmatrix}, \qquad H_{u,s} = \begin{bmatrix} D & O & \cdots & O \\ CB & D & \ddots & \vdots \\ \vdots & \ddots & \ddots & O \\ CA^{s-1}B & \cdots & CB & D \end{bmatrix}, \tag{6}$$

$H_{d,s}$ and $H_{f,s}$ are constructed similarly as $H_{u,s}$ and can be achieved by replacing B, D, respectively, by E_d, F_d and E_f, F_f. To satisfy the requirement on the residual signal, a residual generator can be constructed as

$$r(k) = v_s(y_{k,s} - H_{u,s}u_{k,s}), \tag{7}$$

where a design parameter v_s called parity vector is introduced to modulate the residual dynamics and improve the sensitivity of the residual to the faults and the robustness to the disturbances and the initial state. Usually, $v_sH_{o,s} = 0$ is required to eliminate the influence of the initial state and the past input signals (before the time instant $k-s$).

If the existence condition

$$\text{rank}[H_{o,s} \;\; H_{d,s} \;\; H_{f,s}] > \text{rank}[H_{o,s} \;\; H_{d,s}] \tag{8}$$

is satisfied, then a full decoupling from both the initial state and the disturbances can be achieved by solving

$$v_s[H_{o,s} \;\; H_{d,s}] = 0, \qquad v_sH_{f,s} \neq 0, \tag{9}$$

for v_s, that is, v_s lies in the intersection between the left null space of $[H_{o,s} \;\; H_{d,s}]$ and the image space of $H_{f,s}$. If a full decoupling is not achievable or not desired, the FD problem is often formulated as to solve the optimization problem

$$\begin{aligned} \max_{v_s, v_sH_{o,s}=0} J_{\text{PS}}(v_s) &= \max_{v_s, v_sH_{o,s}=0} \frac{\sup_{d_{k,s}=0, f_{k,s}\neq 0}(r^T(k)r(k)/f_{k,s}^T f_{k,s})}{\sup_{f_{k,s}=0, d_{k,s}\neq 0}(r^T(k)r(k)/d_{k,s}^T d_{k,s})} \\ &= \max_{v_s, v_sH_{o,s}=0} \frac{v_sH_{f,s}H_{f,s}^T v_s^T}{v_sH_{d,s}H_{d,s}^T v_s^T} \end{aligned} \tag{10}$$

whose solution can be obtained by solving a generalized eigenvalue-eigenvector problem [11].

Solution to optimization problem (10)

Let N_{basis} denote the basis of the left null space of $H_{o,s}$. Assume that $\lambda_{\max}$ and $p_{s,\max}$ are the maximal generalized eigenvalue and the corresponding eigenvector to the generalized eigenvalue-eigenvector problem

$$p_{s,\max}\left(N_{\text{basis}}H_{f,s}H_{f,s}^T N_{\text{basis}}^T - \lambda_{\max} N_{\text{basis}}H_{d,s}H_{d,s}^T N_{\text{basis}}^T\right) = 0, \tag{11}$$

then optimization problem (10) is solved by

$$v_s = p_{s,\max} N_{\text{basis}}. \tag{12}$$

It is pointed out in [12] that the solutions of a full decoupling or (10) are achieved at the cost of (considerably) reduced fault detectability. This can be immediately seen with a look at the dynamics of the residual signal

$$r(k) = v_s(y_{k,s} - H_{u,s}u_{k,s}) = v_s(H_{f,s}f_{k,s} + H_{d,s}d_{k,s}) \tag{13}$$

which shows that the influence of the fault expressed by $v_sH_{f,s}$ is structurally reduced to a minimum, that is, rank $(v_sH_{f,s}) = 1$. Reference [12] proposed the use of a parity matrix V_s,

$$r(k) = V_s(y_{k,s} - H_{u,s}u_{k,s}) = V_s(H_{f,s}f_{k,s} + H_{d,s}d_{k,s}) \tag{14}$$

instead of a parity vector aiming at enhancing the influence of the faults on the residual signal. To this end, the following optimization problems are formulated as

$$\begin{aligned} &\max_{V_s, V_sH_{o,s}=0} J_{\text{PS},\infty/\infty}(V_s) \\ &\quad = \max_{V_s, V_sH_{o,s}=0} \frac{\sup_{d_{k,s}=0, f_{k,s}\neq 0}(r^T(k)r(k)/f_{k,s}^T f_{k,s})}{\sup_{f_{k,s}=0, d_{k,s}\neq 0}(r^T(k)r(k)/d_{k,s}^T d_{k,s})} \\ &\quad = \max_{V_s, V_sH_{o,s}=0} \frac{\overline{\sigma}^2(V_sH_{f,s})}{\overline{\sigma}^2(V_sH_{d,s})}, \end{aligned} \tag{15}$$

$$\begin{aligned} &\max_{V_s, V_sH_{o,s}=0} J_{\text{PS},-/\infty}(V_s) \\ &\quad = \max_{V_s, V_sH_{o,s}=0} \frac{\inf_{d_{k,s}=0, f_{k,s}\neq 0}(r^T(k)r(k)/f_{k,s}^T f_{k,s})}{\sup_{f_{k,s}=0, d_{k,s}\neq 0}(r^T(k)r(k)/d_{k,s}^T d_{k,s})} \\ &\quad = \max_{V_s, V_sH_{o,s}=0} \frac{\underline{\sigma}^2(V_sH_{f,s})}{\overline{\sigma}^2(V_sH_{d,s})}, \end{aligned} \tag{16}$$

$$\max_{V_s, V_sH_{o,s}=0} J_{\text{PS},i/\infty}(V_s) = \max_{V_s, V_sH_{o,s}=0} \frac{\sigma_i^2(V_sH_{f,s})}{\overline{\sigma}^2(V_sH_{d,s})}. \tag{17}$$

The difference in optimization problems (15)-(16) consists in that the former considers the maximal influence of the faults on the residual amplitude, while the latter considers the minimal influence. Optimization problem (17) is a generalization of (15)-(16) and takes into account the fault sensitivity in different directions. The achievable optimal performance index of optimization problem (15) is the same with that of (10). At the end of this subsection, we will show that the solution of (17) would lead to maximizing the fault detectability in the context of a tradeoff between false alarm rate and fault detectability.

Solution to optimization problems (15), (16), *and* (17)

A solution to optimization problem (17) that also solves (15)-(16) simultaneously is given in [12] as follows, which is derived based on the observation that for any matrices X_1 and X_2 of compatible dimensions,

$$\begin{aligned} \overline{\sigma}(X_1X_2) &\le \overline{\sigma}(X_1)\overline{\sigma}(X_2), \\ \underline{\sigma}(X_1X_2) &\le \overline{\sigma}(X_1)\underline{\sigma}(X_2), \\ \sigma_i(X_1X_2) &\le \overline{\sigma}(X_1)\sigma_i(X_2). \end{aligned} \tag{18}$$

Assume that there is the following singular value decomposition (SVD):

$$N_{\text{basis}}H_{d,s} = U[S \;\; O]V^T, \tag{19}$$

where U and V are unitary matrices, $S = \text{diag}\{\sigma_1, \ldots, \sigma_\gamma\}$, then optimization problems (15), (16), and (17) are solved by

$$V_s = \overline{P}_s S^{-1} U^T N_{\text{basis}}, \tag{20}$$

where $\overline{P}_s$ is any unitary matrix of compatible dimensions.

Note that the solutions to the above optimization problems are not unique. For instance, an alternative optimal solution for problem (16) is

$$V_s = \overline{P}_s P N_{\text{basis}}, \tag{21}$$

where P is the left inverse of $N_{\text{basis}}H_{f,s}$. On the other side, only solution (20) solves (15), (16), and (17) simultaneously. For this reason, (20) is called *unified parity space solution*.

To detect the faults successfully, the generated residual signal should be further evaluated. For a residual signal generated by means of the parity space approach, the Euclidean norm defined by

$$J = \|r(k)\|_E = \sqrt{r^T(k)r(k)} \tag{22}$$

is a reasonable evaluation function. It follows from (14) and (4) that the corresponding threshold is determined by

$$J\text{th} = \sup_{f=0,d} \|r(k)\|_E = \overline{\sigma}(V_sH_{d,s}) \max \|d_{k,s}\|_E. \tag{23}$$

Based on the decision logic

$$\|r(k)\|_E \le J\text{th} \Longrightarrow \text{fault-free, otherwise faulty}, \tag{24}$$

a decision for the occurrence of a fault can be finally made.

In practice, false alarm rate and miss detection rate are two important technical features for the performance evaluation of a fault detection system. Below, we will introduce these two concepts in the context of the norm-based residual evaluation (22) and briefly compare the above-presented parity space solutions.

*J*th *setting under a given false alarm rate*. Consider (23) and denote the upper bound of $\|d_{k,s}\|_E$ by δ_d. In the context of norm-based evaluation, the objective of J_{th} setting is to ensure that any disturbance whose size is not larger than the tolerant limit should not cause an alarm. To express the strongest disturbance that is allowed without causing a false alarm in relation to δ_d, we define false alarm rate (FAR) as

$$\text{FAR} = 1 - \frac{\alpha}{\delta_d}, \quad 0 \le \alpha \le \delta_d \Longrightarrow 0 \le 1 - \frac{\alpha}{\delta_d} \le 1, \tag{25}$$

that is, those disturbances whose size is not larger than $\alpha = (1 - \text{FAR})\delta_d$ should not cause an alarm. Suppose that the allowable FAR is now given. It is straightforward that the threshold should be set as

$$J\text{th} = \alpha\overline{\sigma}(V_sH_{d,s}) = (1 - \text{FAR})\delta_d\overline{\sigma}(V_sH_{d,s}). \tag{26}$$

Note that in the norm-based residual evaluation, Jth is often set as $\delta_d\overline{\sigma}(V_sH_{d,s})$ which leads to a zero FAR but may result in a very conservative Jth setting.

To express the miss detection rate (MDR), we introduce the set of detectable faults. Note that a fault can be detected if and only if

$$\|r\|_E > J\text{th} \Longleftrightarrow \|V_s(H_{d,s}d_{k,s} + H_{f,s}f_{k,s})\|_E > J\text{th}. \tag{27}$$

Hence, the *set of detectable faults* (SDF) $\Omega_{\text{DE}}(V_s, J\text{th}, d)$ is defined as follows: given V_s and Jth

$$\Omega_{\text{DE}}(V_s, J\text{th}, d) = \{f_{k,s} \mid (27) \text{ is satisfied}\}. \tag{28}$$

Given Jth, a parity space matrix $V_{s,\text{opt}}$ delivers a residual signal with the lowest MDR if

$$\forall V_s, \Omega_{\text{DE}}(V_s, J\text{th}, d) \subseteq \Omega_{\text{DE}}(V_{s,\text{opt}}, J\text{th}, d), \tag{29}$$

that is, $\Omega_{\text{DE}}(V_{s,\text{opt}}, J\text{th}, d)$ includes the largest number of detectable faults, which is equivalent with the lowest MDR.

The subsequent comparison study is done in the context of *maximizing SDF (i.e., minimizing MDR) under a given FAR*.

Note that (27) can be, according to (19), rewritten into

$$\begin{aligned} &\|V_s(H_{d,s}d_{k,s} + H_{f,s}f_{k,s})\|_E \\ &\quad > (1 - \text{FAR})\delta_d\overline{\sigma}(V_sH_{d,s}) \\ &\quad \Longleftrightarrow \left\|Q[I \;\; O]V^Td_{k,s} + QS^{-1}U^TN_{\text{basis}}H_{f,s}f_{k,s}\right\|_E \\ &\quad > (1 - \text{FAR})\delta_d\overline{\sigma}\left(Q[I \;\; O]V^T\right) \\ &\text{by setting } V_s = QS^{-1}U^TN_{\text{basis}}, \quad \text{for some } Q. \end{aligned} \tag{30}$$

It turns out that $\forall Q \neq 0$, (30) holds only if

$$\left\|[I \;\; O]V^Td_{k,s} + S^{-1}U^TN_{\text{basis}}H_{f,s}f_{k,s}\right\|_E > (1 - \text{FAR})\delta_d. \tag{31}$$

It means that a parity matrix that ensures (31) would provide a maximal SDF. Note that the unified parity space solution (20) delivers exactly (31). Thus, *the unified parity space solution maximizes SDF (i.e., minimizes MDR) under a given FAR*.

For comparison, denote the SVD of $N_{\text{basis}}H_{f,s}$ by

$$N_{\text{basis}}H_{f,s} = U_f[S_f \quad O]V_f^T. \tag{32}$$

Then the vector-valued solution (12) to optimization problem (10) and the matrix-valued solution (21) to optimization problem (16) can be, respectively, rewritten into

$$\begin{aligned} v_s &= p_s S^{-1}U^T N_{\text{basis}}, \\ p_s(S^{-1}U^T U_f S_f^2 U_f^T U S^{-1} - \lambda_{\max} I) &= 0, \\ V_s &= (\overline{P}_s S_f^{-1} U_f^T U S) S^{-1} U^T N_{\text{basis}}. \end{aligned} \tag{33}$$

Since, generally, $p_s, \overline{P}_s S_f^{-1} U_f^T U S$ are not unitary matrices, we have finally

$$\begin{aligned} \Omega_{\text{DE}}(V_s, J\text{th}, d) \subset \Omega_{\text{DE}}(V_{s,\text{opt}}, J\text{th}, d), \quad V_s &= p_{s,\max} N_{\text{basis}}, \\ V_{s,\text{opt}} &= \overline{P}_s S^{-1} U^T N_{\text{basis}}, \\ \Omega_{\text{DE}}(V_s, J\text{th}, d) \subset \Omega_{\text{DE}}(V_{s,\text{opt}}, J\text{th}, d), \quad V_s &= \overline{P}_s P N_{\text{basis}}, \\ V_{s,\text{opt}} &= \overline{P}_s S^{-1} U^T N_{\text{basis}}. \end{aligned} \tag{34}$$

With the following remarks we would like to conclude this subsection.

(i) Parity-space-based FD system design is characterized by the simple mathematical handling. It only deals with matrix- and vector-valued operations. This fact attracts attention from the industry for the application of parity-space-based methods.

(ii) There is a one-to-one relationship between the parity-space approach and the observer-based approach that allows the design of an observer-based residual generator based on a given parity vector [13, 14]. Based on this result, a strategy called *parity-space design, observer-based implementation* has been developed, which makes use of the computational advantage of parity-space approaches for the FD system design (selection of a parity vector or matrix) and then realizes the solution in the observer form to ensure a numerically stable and less consuming online computation. This strategy has been successfully used in the sensor-fault detection in vehicles [15].

(iii) In the parity-space approaches, a high order s will improve the optimal performance index J_{PS} but, on the other side, increase the online computational effort [16]. By introducing a low-order IIR (infinite impulse response) filter, the performance of the parity-relation-based residual generator can be much improved without significant increase of the order of the parity relation [17]. Similar effect can be achieved by the closed-loop-observer-based implementation, as pointed out by [18].

(iv) The algebraic form of the parity-space-based FD system allows a statistic test and norm-based residual evaluation and threshold determination [19]. It may well bridge the statistical methods [1] and the observer-based methods.

(v) In the framework of parity-space-based FD system design, system dynamic features like transmission zeros, zeros in the right half plane (RHP), and so forth are not taken into account. This may cause trouble at the online implementation. Also for this reason, we are of the opinion that the strategy of *parity space design, observer-based implementation* would be helpful to solve this problem.

2.3. Parametrization of FD systems and postfilter design

Observer-based FD system design for continuous LTI systems has been widely studied in the literature [3–6]. In this and the next subsections, the analog form of those known results will be briefly reviewed. Attention will be paid to the comparison study when it is special for discrete LTI systems.

Let $(\widehat{M}_u(z), \widehat{N}_u(z))$ be a left coprime factorization pair of $G_u(z)$, that is, $G_u(z) = \widehat{M}_u^{-1}(z)\widehat{N}_u(z), \widehat{M}_u(z), \widehat{N}_u(z) \in \mathcal{RH}_\infty$ [10]. In [20], a parametrization of all LTI residual generators for system (1) described by

$$r(z) = R(z)(\widehat{M}_u(z)y(z) - \widehat{N}_u(z)u(z)) \tag{35}$$

is presented, where $R(z) \in \mathcal{RH}_\infty$ is the so-called postfilter that is arbitrarily selectable. Suppose that $G_u(z) = (A, B, C, D)$ is a detectable state space realization of $G_u(z)$. Then $\widehat{M}_u(z), \widehat{N}_u(z)$ can be computed as follows [10]:

$$\begin{aligned} \widehat{M}_u(z) &= I - C(zI - A + LC)^{-1}L, \\ \widehat{N}_u(z) &= D + C(zI - A + LC)^{-1}(B - LD). \end{aligned} \tag{36}$$

It is now a well-known result that

(i) $\widehat{M}_u(z)y(z) - \widehat{N}_u(z)u(z) = y(z) - \hat{y}(z)$, where $\hat{y}(z)$ is the output estimation delivered by a full-order observer;

(ii) given L_1 and L_2, there exists an $\mathcal{RH}_\infty$-invertible postfilter $Q(z) = I + C(zI - A + L_1C)^{-1}(L_2 - L_1)$ so that

$$\begin{aligned} &\widehat{M}_{u,L_1}(z)y(z) - \widehat{N}_{u,L_1}(z)u(z) \\ &\quad = Q(z)(\widehat{M}_{u,L_2}(z)y(z) - \widehat{N}_{u,L_2}(z)u(z)), \end{aligned} \tag{37}$$

where $(\widehat{M}_{u,L_1}(z), \widehat{N}_{u,L_1}(z))$ and $(\widehat{M}_{u,L_2}(z), \widehat{N}_{u,L_2}(z))$ are the left coprime factorization pair of $G_u(z)$, which are computed according to (36) with $L = L_1$ and $L = L_2$, respectively.

(iii) all LTI residual generators can be expressed by a series connection of a full-order observer and a postfilter, and are therefore called observer-based residual generators. Moreover, the selection of the postfilter can be done independent of the observer design.

Due to the latter fact, we concentrate in this subsection on the selection of $R(z)$. The dynamics of a residual generator (35) is governed by

$$r(z) = R(z)\widehat{M}_u(z)(G_d(z)d(z) + G_f(z)f(z)). \tag{38}$$

The full decoupling problem is to find the postfilter $R(z)$ so that

$$R(z)\widehat{M}_u(z)G_d(z) = 0, \qquad R(z)\widehat{M}_u(z)G_f(z)\neq 0. \tag{39}$$

If the l_2-norm of the residual signal is used as evaluation function, then the optimal FD problem is formulated as optimization problems

$$\sup_{R(z)\in\mathcal{RH}_\infty} J_{\mathrm{FRE},\infty/\infty}(R) = \sup_{R(z)\in\mathcal{RH}_\infty} \frac{\left\|R(z)\widehat{M}_u(z)G_f(z)\right\|_\infty}{\left\|R(z)\widehat{M}_u(z)G_d(z)\right\|_\infty}, \tag{40}$$

$$\sup_{R(z)\in\mathcal{RH}_\infty} J_{\mathrm{FRE},-/\infty}(R) = \sup_{R(z)\in\mathcal{RH}_\infty} \frac{\left\|R(z)\widehat{M}_u(z)G_f(z)\right\|_-}{\left\|R(z)\widehat{M}_u(z)G_d(z)\right\|_\infty}, \tag{41}$$

$$\sup_{R(z)\in\mathcal{RH}_\infty} J_{\mathrm{FRE},i/\infty}(R) = \sup_{R(z)\in\mathcal{RH}_\infty} \frac{\sigma_i(R(e^{j\omega})\widehat{M}_u(e^{j\omega})G_f(e^{j\omega}))}{\left\|R(z)\widehat{M}_u(z)G_d(z)\right\|_\infty} \tag{42}$$

$$\begin{aligned}\sup_{R(z)\in\mathcal{RH}_\infty^{1\times m}} J_{\mathrm{FRE},2/2}(R) = \sup_{R(z)\in\mathcal{RH}_\infty^{1\times m}} \Bigg(&\int_0^{2\pi} R(e^{j\omega})\widehat{M}_u(e^{j\omega})G_f(e^{j\omega})G_f^*(e^{j\omega}) \\ &\times \widehat{M}_u^*(e^{j\omega})R^*(e^{j\omega})d\omega \Big/ \int_0^{2\pi} R(e^{j\omega}) \\ &\times \widehat{M}_u(e^{j\omega})G_d(e^{j\omega})G_d^*(e^{j\omega})\widehat{M}_u^*(e^{j\omega}) \\ &\times R^*(e^{j\omega})d\omega\Bigg),\end{aligned} \tag{43}$$

where $\sigma_i(R(e^{j\omega})\widehat{M}_u(e^{j\omega})G_f(e^{j\omega}))$ represents the fault sensitivity at different levels at the frequency ω,

$$\begin{aligned}\left\|R(z)\widehat{M}_u(z)G_f(z)\right\|_- &= \inf_\omega\left(\underline{\sigma}(R(e^{j\omega})\widehat{M}_u(e^{j\omega})G_f(e^{j\omega}))\right) \\ &= \inf_{\omega,i}\left(\sigma_i(R(e^{j\omega})\widehat{M}_u(e^{j\omega})G_f(e^{j\omega}))\right)\end{aligned} \tag{44}$$

though not a norm, it is interpreted as the worst-case fault sensitivity. Optimization problems (40), (41), and (43) are often called the H_∞/H_∞, H_-/H_∞, and H_2/H_2 optimization, respectively.

The ratio-type performance index given in (40) and (43) is the first one that was introduced for the FD purpose [11, 21]. Currently, the index of the form

$$\left\|R(z)\widehat{M}_u(z)G_d(z)\right\| < \gamma, \qquad \left\|R(z)\widehat{M}_u(z)G_f(z)\right\| > \beta \tag{45}$$

becomes more popular, where γ, β are some constants. The FD system design is often formulated as maximizing β under a given γ. The third index type is often met in the robust control theory and formulated as

$$J_{f-d} = \alpha_f\left\|R(z)\widehat{M}_u(z)G_f(z)\right\| - \alpha_d\left\|R(z)\widehat{M}_u(z)G_d(z)\right\|, \tag{46}$$

where $\alpha_f, \alpha_d > 0$ are some given constants. The FD system design is then achieved by maximizing J_{f-d}. In [22], it has been demonstrated that the above three types indices are equivalent in a certain sense. With this fact in mind, in this paper we only consider optimizations under ratio-type indices (40)–(43).

Solution to optimization problems (40)–(42)

Let $\widehat{M}_u(z)G_d(z) = G_{do}(z)G_{di}(z)$ be a co-inner-outer factorization of $\widehat{M}_u(z)G_d(z)$ [10], where $G_{do}(z)$ is the $\mathcal{RH}_\infty$-left-invertible co-outer, $G_{di}(z)$ is the co-inner containing all the right half complex plane zeros of $\widehat{M}_u(z)G_d(z)$ and satisfying $G_{di}(z)G_{di}^*(z) = I$. Based on the relations

$$\begin{aligned}\left\|G_1(z)G_2(z)\right\|_\infty &\le \left\|G_1(z)\right\|_\infty\left\|G_2(z)\right\|_\infty, \\ \left\|G_1(z)G_2(z)\right\|_- &\le \left\|G_1(z)\right\|_\infty\left\|G_2(z)\right\|_- \\ \sigma_i(G_1(e^{j\omega})G_2(e^{j\omega})) &\le \left\|G_1(z)\right\|_\infty\sigma_i(G_2(e^{j\omega})), \quad \forall i,\end{aligned} \tag{47}$$

it has been proven in [23, 24], similar to the results for continuous LTI systems given in [22] and recently in [25], that optimization problems (40)–(42) are solved simultaneously by

$$R(z) = G_{do}^{-1}(z). \tag{48}$$

For this reason, (48) is called unified solution.

Another solution to optimization problem (41), if $G_f(z)$ is $\mathcal{RL}_\infty$-left-invertible, is

$$R(z) = G_{fo}^{-1}(z), \tag{49}$$

where $G_{fo}(z)$ is the co-outer of $\widehat{M}_u(z)G_f(z)$.

The main purpose of the co-inner-outer factorization is to separate the nonminimum phase zeros so that the rest part of $\widehat{M}_u(z)G_d(z)$ or $\widehat{M}_u(z)G_f(z)$ is $\mathcal{RH}_\infty$-left invertible. Note that the co-inner-outer factorization is not unique. Therefore, the optimal postfilter $R(z)$ is also not unique [26].

Solution to optimization problem (43)

The optimal solution to optimization problem (43) is a frequency selector as follows [27]:

$$R(z) = f_{\omega_0}(z)p(z), \qquad J_{\mathrm{FRE},2/2,\mathrm{opt}} = \sup_\omega \lambda_{\max}(\omega), \tag{50}$$

where $f_{\omega_0}(z)$ is an ideal frequency-selective filter with the selective frequency at ω_0, which satisfies

$$\begin{aligned}&f_{\omega_0}(e^{j\omega})q(e^{j\omega}) = 0, \quad \omega\neq\omega_0 \\ &\int_0^{2\pi} f_{\omega_0}(e^{j\omega})q(e^{j\omega})q^*(e^{j\omega})f_{\omega_0}^*(e^{j\omega})d\omega \\ &\qquad = q(e^{j\omega_0})q^*(e^{j\omega_0}), \quad \forall q^T(z)\in\mathcal{RH}_2,\end{aligned} \tag{51}$$

$\lambda_{\max}(\omega), p(e^{j\omega})$ are, respectively, the maximal generalized eigenvalue and corresponding eigenvector of the following generalized eigenvalue-eigenvector problem:

$$p(e^{j\omega})\left(\lambda_{\max}(\omega)\widehat{M}_u(e^{j\omega})G_d(e^{j\omega})G_d^*(e^{j\omega})\widehat{M}_u^*(e^{j\omega}) - \widehat{M}_u(e^{j\omega})G_f(e^{j\omega})G_f^*(e^{j\omega})\widehat{M}_u^*(e^{j\omega})\right) = 0 \tag{52}$$

and ω_0 is the frequency at which $\lambda_{\max}(\omega)$ achieves its maximum, that is,

$$\lambda_{\max}(\omega_0) = \sup_{\omega} \lambda_{\max}(\omega). \tag{53}$$

In practice, usually a narrow bandpass filter is implemented as frequency selector. From the viewpoint of FAR and MDR, the frequency selector may cause loss of fault sensitivity and restrict the application of the H_2/H_2 optimal residual generator.

Recently, [27] reported a very interesting result on the relationship between the parity-space vector and the solution to optimization problem (43). It has been shown that

$$\lim_{s\to\infty} \min_{v_s} \frac{v_s H_{f,s} H_{f,s}^T v_s^T}{v_s H_{d,s} H_{d,s}^T v_s^T} = \lambda_{\max}(\omega_{\text{opt}}) \tag{54}$$

and $\lim_{s\to\infty} v_s$ correspond to a bandpass filter. This result not only reveals the physical interpretation of the standard optimal selection of parity vectors but also provides us with an efficient tool to approximate the optimal solution to optimization problem (43). Moreover, based on it, advanced parity-space approaches using wavelet transform have been proposed [28, 29].

As to the residual evaluation and threshold determination, the l_2-norm is the mostly used evaluation function, which leads to

$$\begin{aligned} J &= \|r\|_2, \\ J\text{th} &= \sup_{f=0,d} \|r\|_2 = \left\|R(z)\widehat{M}_u(z)G_d(z)\right\|_\infty \max \|d\|_2. \end{aligned} \tag{55}$$

In case of applying the unified solution (48), we have

$$J\text{th} = \sup_{f=0,d} \|r\|_2 = \max \|d\|_2. \tag{56}$$

Analog with the results in [30] and the discussion in the last subsection, it can be proven that the unified solution (48) minimizes MDR under a given FAR, where MDR and FAR are defined in the context of the norm-based residual evaluation.

2.4. fault detection filter design

fault detection filter (FDF) is a special kind of observer-based FD systems (35) with a constant postfilter and constructed as

$$\begin{aligned} \hat{x}(k+1) &= A\hat{x}(k) + Bu(k) + L\big(y(k) - \hat{y}(k)\big), \\ r(k) &= W\big(y(k) - \hat{y}(k)\big), \\ \hat{y}(k) &= C\hat{x}(k) + Du(k), \end{aligned} \tag{57}$$

where the observer gain matrix L and the weighting matrix W are design parameters. Due to its state space expression and close relation to the observer design, FDF study receives most research attention. The dynamics of residual generator (57) is governed by

$$\begin{aligned} r(z) &= G_{rd}(z)d(z) + G_{rf}(z)f(z), \\ G_{rd}(z) &= W\left(F_d + C(zI - A + LC)^{-1}(E_d - LF_d)\right), \\ G_{rf}(z) &= W\left(F_f + C(zI - A + LC)^{-1}(E_f - LF_f)\right). \end{aligned} \tag{58}$$

In the FDF design, the full-decoupling problem is to design L and W such that

$$G_{rd}(z) = 0, \qquad G_{rf}(z) \neq 0 \tag{59}$$

while the optimal FD problems are formulated so as to choose matrices L, W that solve the optimization problem [5, 7, 31]

$$\sup_{L,W} J_{\text{OBS},\infty/\infty}(L, W) = \sup_{L,W} \frac{\left\|G_{rf}(z)\right\|_\infty}{\left\|G_{rd}(z)\right\|_\infty}, \tag{60}$$

$$\sup_{L,W} J_{\text{OBS},-/\infty}(L, W) = \sup_{L,W} \frac{\left\|G_{rf}(z)\right\|_-}{\left\|G_{rd}(z)\right\|_\infty}, \tag{61}$$

$$\sup_{L,W} J_{\text{OBS},i/\infty}(L, W) = \sup_{L,W} \frac{\sigma_i\left(G_{rf}(e^{j\omega})\right)}{\left\|G_{rd}(z)\right\|_\infty}. \tag{62}$$

Solution to optimization problems (60)–(62)

Because the FDF (57) is a special case of (35), the optimal solutions to optimization problems (60)–(62) can be derived based on the state space realization of the optimal postfilter $R(z)$ given by (48), as shown in [24]. A unified optimal solution to optimization problems (60)–(62) is associated to a discrete-time algebraic Riccati system (DTARS) [24, 32]. Assume that (A, E_d, C, F_d) is regular, then

$$L = -L_d^T, \qquad W = W_d \tag{63}$$

solve optimization problems (60)–(62) simultaneously, where W_d is the left inverse of a full column rank matrix H_d satisfying $H_d H_d^T = CX_dC^T + F_dF_d^T$ and (X_d, L_d) is the stabilizing solution to the DTARS

$$\begin{bmatrix} AX_dA^T - X_d + E_dE_d^T & AX_dC^T + E_dF_d^T \\ CX_dA^T + F_dE_d^T & CX_dC^T + F_dF_d^T \end{bmatrix} \begin{bmatrix} I \\ L_d \end{bmatrix} = 0. \tag{64}$$

An alternative solution to optimization problem (61), if (A, E_f, C, F_f) is regular, is given by

$$L = -L_f^T, \qquad W = W_f, \tag{65}$$

where W_f is the left inverse of a full column rank matrix H_f satisfying $H_f H_f^T = CX_fC^T + F_fF_f^T$ and (X_f, L_f) is the stabilizing solution to the DTARS

$$\begin{bmatrix} AX_fA^T - X_f + E_fE_f^T & AX_fC^T + E_fF_f^T \\ CX_fA^T + F_fE_f^T & CX_fC^T + F_fF_f^T \end{bmatrix} \begin{bmatrix} I \\ L_f \end{bmatrix} = 0. \tag{66}$$

Recently, application of LMI-technique (linear matrix inequality) to solve (60) and (61) for continuous LTI systems has been reported [33–36]. The core of those approaches consists in formulating (60) or (61) as a multiobjective optimization problem and solving them based on an iterative computation of two LMIs. It can be proven that these solutions can, in the ideal case, converge to the optimal solution (63). The extension of these results to the discrete FDF is straightforward and will not be discussed in this paper.

At the end of this subsection, we would like to introduce a very interesting result achieved by the comparison study between the well-known Kalman-filter-based residual generation [37] and the unified solution (63). Given system

$$\begin{aligned} x(k+1) &= Ax(k) + Bu(k) + E_d\zeta(k), \\ y(k) &= Cx(k) + Du(k) + F_d\eta(k), \end{aligned} \tag{67}$$

where $\zeta(k), \eta(k)$ are independent zero-mean Gaussian white noise processes with $\operatorname{cov}(\zeta(k)\zeta^T(k)) = I$, $\operatorname{cov}(\eta(k)\eta^T(k)) = I$, then a Kalman filter with

$$\hat{x}(k+1 \mid k) = A\hat{x}(k \mid k-1) + Bu(k) + L\big(y(k) - \hat{y}(k \mid k-1)\big), \tag{68}$$

$$\hat{y}(k \mid k-1) = C\hat{x}(k \mid k-1) + Du(k), \tag{69}$$

$$L = APC^T\big(CPC^T + R\big)^{-1}, \quad R = F_dF_d^T (> 0), \tag{70}$$

$$APA^T - P - APC^T\big(CPC^T + R\big)^{-1}CPA^T + E_dE_d^T = 0, \quad P > 0, \tag{71}$$

delivers an innovation as residual signal, where $\hat{x}(k \mid k-1)$ is a prediction of $x(k)$ based on the data up to $k-1$. Comparing the above Kalman filter algorithm with the unified solution (63) makes it clear that both solutions are quite similar. Indeed, (67) can be brought into the general form of (1) by letting $d = [\,\zeta^T \ \eta^T\,]^T$ and, as a result, (71) can be regarded as a special case of (64). Remember that the Kalman filter delivers, in the context of statistic tests, a minimum MDR under a given FAR. In comparison, in the context of norm-based definition of MDR and FAR, the unified solution (63) provides us with the same result.

3. FD OF DISCRETE-TIME LINEAR PERIODIC SYSTEMS

In this section, we review some recent results on FD in discrete linear time periodic (LTP) systems. LTP is a special kind of linear time-varying systems described by

$$\Sigma_{\text{LTP}}: \begin{cases} x(k+1) \\ \quad = A(k)x(k) + B(k)u(k) + E_d(k)d(k) + E_f(k)f(k), \\ y(k) \\ \quad = C(k)x(k) + D(k)u(k) + F_d(k)d(k) + F_f(k)f(k), \end{cases} \tag{72}$$

where $A(k), B(k), C(k), D(k), E_d(k), E_f(k), F_d(k)$, and $F_f(k)$ are known bounded and real periodic matrices of period θ, that is, $\forall k$, $A(k+\theta) = A(k)$, and so forth. There is not only continuous interest and development of periodic control and filtering theory [38–42], but also increasing applications of periodic control in practice like helicopter vibration control, satellite attitude control as well as wind turbine. The FD problem of periodic systems has been considered in [24, 32, 43–45]. Basically, there are two ways to handle the FD problem of LTP systems, as shown below.

3.1. FD schemes based on lifted LTI reformulation

It is well known that there is a strong correspondence between discrete LTP systems and discrete LTI systems [42]. Therefore, FD system design for the LTP system (72) can be carried out as follows:

(i) lift the LTP system (72) into a discrete LTI system,
(ii) design residual generator(s) based on the lifted LTI reformulation,
(iii) using either parallel residual generators or select the parameters of the residual generator to satisfy the causality condition.

Let $\Psi_{A(k)}(k_1, k_0)$ ($k_1 \geq k_0$) denote the state transition matrix of LTP system (72)

$$\Psi_{A(k)}(k_1, k_0) = \begin{cases} I & \text{if } k_1 = k_0, \\ A(k_1-1)A(k_1-2)\cdots A(k_0) & \text{if } k_1 > k_0. \end{cases} \tag{73}$$

Periodic system (72) can be lifted into a discrete LTI system described by [42]

$$\begin{aligned} \widetilde{x}_\tau((k+1)\theta + \tau) &= \widetilde{A}_\tau\widetilde{x}_\tau(k\theta+\tau) + \widetilde{B}_\tau\widetilde{u}_\tau(k\theta+\tau) \\ &\quad + \widetilde{E}_{d,\tau}\widetilde{d}_\tau(k\theta+\tau) + \widetilde{E}_{f,\tau}\widetilde{f}_\tau(k\theta+\tau), \\ \widetilde{y}_\tau(k\theta+\tau) &= \widetilde{C}_\tau\widetilde{x}_\tau(k\theta+\tau) + \widetilde{D}_\tau\widetilde{u}_\tau(k\theta+\tau) \\ &\quad + \widetilde{F}_{d,\tau}\widetilde{d}_\tau(k\theta+\tau) + \widetilde{F}_{f,\tau}\widetilde{f}_\tau(k\theta+\tau), \end{aligned} \tag{74}$$

where τ is an integer between 0 and $\theta - 1$ denoting the initial time, the state vector of the lifted system is $\widetilde{x}_\tau(k\theta+\tau) = x(k\theta+\tau)$, $\widetilde{\eta}_\tau$ with η standing for u, y, d, f is the augmented signal defined by

$$\widetilde{\eta}_\tau(k\theta+\tau) = \begin{bmatrix} \eta(k\theta+\tau) \\ \eta(k\theta+\tau+1) \\ \vdots \\ \eta(k\theta+\tau+\theta-1) \end{bmatrix},$$

$$\widetilde{A}_\tau = \Psi_{A(k)}(\tau+\theta, \tau),$$

$$\widetilde{B}_\tau = \begin{bmatrix} X' & Y' & \cdots & Z' \end{bmatrix},$$

$$\widetilde{C}_\tau = \begin{bmatrix} C(\tau) \\ C(\tau+1)\Psi_{A(k)}(\tau+1, \tau) \\ \vdots \\ C(\tau+\theta-1)\Psi_{A(k)}(\tau+\theta-1, \tau) \end{bmatrix},$$

$$\widetilde{D}_\tau = \begin{bmatrix} \widetilde{D}_{\tau,1,1} & O & \cdots & O \\ \widetilde{D}_{\tau,2,1} & \widetilde{D}_{\tau,2,2} & \ddots & \vdots \\ \vdots & \ddots & \ddots & O \\ \widetilde{D}_{\tau,\theta,1} & \cdots & \widetilde{D}_{\tau,\theta,\theta-1} & \widetilde{D}_{\tau,\theta,\theta} \end{bmatrix},$$

$$\widetilde{D}_{\tau,i,j} = \begin{cases} D(\tau+i-1) & \text{for } i = j, \\ C(\tau+i-1)\Psi_{A(k)}(\tau+i-1, \tau+j) & \\ \quad B(\tau+j-1) & \text{for } i > j, \end{cases} \tag{75}$$

where $\widetilde{B}_{\tau,1} = \Psi_{A(k)}(\tau+\theta,\tau+1)B(\tau)$, $\widetilde{B}_{\tau,2} = \Psi_{A(k)}(\tau+\theta,\tau+2)B(\tau+1)$, $\widetilde{B}_{\tau,\theta} = B(\tau+\theta-1)$, and $\widetilde{E}_{d,\tau}, \widetilde{F}_{d,\tau}$ and $\widetilde{E}_{f,\tau}, \widetilde{F}_{f,\tau}$ are defined in a way similar to $\widetilde{C}_\tau, \widetilde{D}_\tau$.

3.1.1. Observer-based FD system design and implementation

Assume that $(A(k), C(k))$ is detectable. Then $(\widetilde{A}_\tau, \widetilde{C}_\tau)$ is detectable and an observer-based LTI residual generator can be designed based on lifted reformulation (74) as

$$\begin{aligned}\hat{\widetilde{x}}_\tau((k+1)\theta+\tau) &= \widetilde{A}_\tau\hat{\widetilde{x}}_\tau(k\theta+\tau) + \widetilde{B}_\tau\widetilde{u}_\tau(k\theta+\tau) \\ &\quad + L_\tau(\widetilde{y}_\tau(k\theta+\tau) - \hat{\widetilde{y}}_\tau(k\theta+\tau)), \\ r_\tau(k\theta+\tau) &= W_\tau(\widetilde{y}_\tau(k\theta+\tau) - \hat{\widetilde{y}}_\tau(k\theta+\tau)), \\ \hat{\widetilde{y}}_\tau(k) &= \widetilde{C}_\tau\hat{\widetilde{x}}_\tau(k\theta+\tau) + \widetilde{D}_\tau\widetilde{u}_\tau(k\theta+\tau),\end{aligned} \tag{76}$$

where L_τ and W_τ are constant matrices and can be designed with FD approaches for the discrete LTI systems introduced in the last section to realize full decoupling or optimal FD. Observer (76) reconstructs the outputs over one period $y(k\theta+\tau),\ldots,y(k\theta+\tau+\theta-1)$ based on the estimation of state vector $x(k\theta+\tau)$. Both the state vector of observer (76) and the residual signal are updated every θ time instants.

In fault detection, the detection delay should be as small as possible. Therefore, it is advantageous if a residual signal can be obtained at each time instant. To this aim,

(i) a bank of LTI residual generators (76) can be used, each of which is designed for $\tau = 0, 1, \ldots, \theta-1$, respectively [43]. This scheme is characterized by a simple design but needs much online computational efforts.

(ii) If the weighting matrix W_τ is designed to satisfy the causality constraint, that is, W_τ is a lower block triangular matrix in the form of

$$W_\tau = \begin{bmatrix} W_{\tau,1,1} & O & \cdots & O \\ W_{\tau,2,1} & W_{\tau,2,2} & \ddots & \vdots \\ \vdots & \ddots & \ddots & O \\ W_{\tau,\theta,1} & \cdots & W_{\tau,\theta,\theta-1} & W_{\tau,\theta,\theta} \end{bmatrix}, \tag{77}$$

then, for a given integer τ, the residual generator (76) can be implemented as

$$\begin{aligned}&\hat{\widetilde{x}}_\tau((k+1)\theta+\tau) \\ &\quad= \widetilde{A}_\tau\hat{\widetilde{x}}_\tau(k\theta+\tau) + \widetilde{B}_\tau\widetilde{u}_\tau(k\theta+\tau) \\ &\qquad + L_\tau\left(\begin{bmatrix} y(k\theta+\tau) \\ \vdots \\ y(k\theta+\tau+\theta-1) \end{bmatrix} - \begin{bmatrix} \hat{y}(k\theta+\tau) \\ \vdots \\ \hat{y}(k\theta+\tau+\theta-1) \end{bmatrix}\right), \\ &r(k\theta+\tau+j) \\ &\quad= \begin{bmatrix} W_{\tau,j+1,1} & \cdots & W_{\tau,j+1,j+1} \end{bmatrix} \\ &\qquad \times \left(\begin{bmatrix} y(k\theta+\tau) \\ \vdots \\ y(k\theta+\tau+j) \end{bmatrix} - \begin{bmatrix} \hat{y}(k\theta+\tau) \\ \vdots \\ \hat{y}(k\theta+\tau+j) \end{bmatrix}\right), \\ &\hat{y}(k\theta+\tau+j) \\ &\quad= C(\tau+j)\Psi_{A(k)}(\tau+j,\tau)\hat{\widetilde{x}}_\tau(k\theta+\tau) \\ &\qquad + \begin{bmatrix} \widetilde{D}_{\tau,j+1,1} & \cdots & \widetilde{D}_{\tau,j+1,j+1} \end{bmatrix} \begin{bmatrix} u(k\theta+\tau) \\ \vdots \\ u(k\theta+\tau+j) \end{bmatrix}, \\ &\qquad j = 0, 1, \ldots, \theta-1.\end{aligned} \tag{78}$$

In this case, the state estimation is still updated at every θ time instants, but at each time instant $k\theta+\tau+j$, $j = 0, 1, \ldots, \theta-1$, a residual signal $r(k\theta+\tau+j)$ is calculated from control input and measured outputs available up to the time instant $k\theta+\tau+j$.

3.1.2. Parity-relation-based FD system design and implementation

Similarly, a parity-relation-based LTI residual generator can be built as follows:

$$\begin{aligned} r_\tau(k\theta+\tau) &= V_{\tau,s}(\widetilde{y}_{\tau,k,s} - \widetilde{H}_{u,s}\widetilde{u}_{\tau,k,s}), \\ \widetilde{y}_{\tau,k,s} &= \begin{bmatrix} \widetilde{y}_\tau((k-s)\theta+\tau) \\ \widetilde{y}_\tau((k-s+1)\theta+\tau) \\ \vdots \\ \widetilde{y}_\tau(k\theta+\tau) \end{bmatrix}, \\ \widetilde{u}_{\tau,k,s} &= \begin{bmatrix} \widetilde{u}_\tau((k-s)\theta+\tau) \\ \widetilde{u}_\tau((k-s+1)\theta+\tau) \\ \vdots \\ \widetilde{u}_\tau(k\theta+\tau) \end{bmatrix}, \\ \widetilde{H}_{u,s} &= \begin{bmatrix} \widetilde{D}_\tau & O & \cdots & O \\ \widetilde{C}_\tau\widetilde{B}_\tau & \widetilde{D}_\tau & \ddots & \vdots \\ \vdots & \ddots & \ddots & O \\ \widetilde{C}_\tau\widetilde{A}_\tau^{s-1}\widetilde{B}_\tau & \cdots & \widetilde{C}_\tau\widetilde{B}_\tau & \widetilde{D}_\tau \end{bmatrix}, \end{aligned} \tag{79}$$

where $V_{\tau,s}$ is a constant parity matrix,

$$V_{\tau,s}\begin{bmatrix} \widetilde{C}_\tau \\ \widetilde{C}_\tau\widetilde{A}_\tau \\ \vdots \\ \widetilde{C}_\tau\widetilde{A}_\tau^s \end{bmatrix} = 0. \tag{80}$$

To get a residual signal at each time instant, we can use a bank of parity-relation-based residual generators, each one

for $\tau = 0, 1, \ldots, \theta - 1$, respectively. Alternatively, we can also impose a structural constant on parity matrix $V_{\tau,s}$ as

$$V_{\tau,s} = \begin{bmatrix} V_{\tau,s,0} & V_{\tau,s,1} & \cdots & V_{\tau,s,s-1} & V_{\tau,s,s} \end{bmatrix},$$
$$V_{\tau,s,s} = \begin{bmatrix} (V_{\tau,s,s})_{1,1} & O & \cdots & O \\ (V_{\tau,s,s})_{2,1} & (V_{\tau,s,s})_{2,2} & \ddots & \vdots \\ \vdots & \ddots & \ddots & O \\ (V_{\tau,s,s})_{\theta,1} & \cdots & (V_{\tau,s,s})_{\theta,\theta-1} & (V_{\tau,s,s})_{\theta,\theta} \end{bmatrix}, \tag{81}$$

that is, the last block in $V_{\tau,s}$ is a lower triangular matrix, then for a fixed τ, residual generator (79) can be implemented in such a way that only control inputs and measured outputs available up to the time instant $k\theta + \tau + j$ are needed for the calculation of $r(k\theta + \tau + j)$, $j = 0, 1, \ldots, \theta - 1$.

3.2. FD schemes based on periodic model

In this subsection, we will show that the parity-space approach and the observer-based FD approach can be directly extended to periodic systems, which do not need the temporary step of lifted LTI reformulation and lead to a simplified design and implementation.

3.2.1. Periodic parity-space approach

The extension of the parity-space approach to periodic systems is straightforward, because the parity-space approach can handle each time instant independently [45]. The input-output relation of periodic system (72) during the moving window $[k - s, k]$ can be expressed by

$$y_{k,s} = H_{o,s,k}x(k - s) + H_{u,s,k}u_{k,s} + H_{d,s,k}d_{k,s} + H_{f,s,k}f_{k,s}. \tag{82}$$

While the vectors $y_{k,s}, u_{k,s}, d_{k,s}$, and $f_{k,s}$ in (82) are built in exactly the same way as in the LTI case according to (6), the matrices $H_{o,s,k}, H_{u,s,k}, H_{d,s,k}$, and $H_{f,s,k}$ in (82) are not constant matrices but the following periodic matrices:

$$H_{o,s,k} = \begin{bmatrix} C(k-s) \\ C(k-s+1)A(k-s) \\ \vdots \\ C(k)A(k-1)\cdots A(k-s+1)A(k-s) \end{bmatrix},$$
$$H_{u,s,k} = \begin{bmatrix} D(k-s) & O & \cdots & O \\ C(k-s+1)B(k-s) & D(k-s+1) & \ddots & \vdots \\ \vdots & \ddots & \ddots & O \\ C(k)A(k-1)\cdots & \cdots & & D(k) \\ A(k-s+1)B(k-s) & & & \end{bmatrix}, \tag{83}$$

$H_{d,s,k}$, and $H_{f,s,k}$ are similar as $H_{u,s,k}$ with $B(j), D(j)$ replaced, respectively, by $E_d(j), F_d(j)$, and $E_f(j), F_f(j)$, $j = k-s, \ldots, k$.

A periodic residual generator can be built as

$$r(k) = V_k(y_{k,s} - H_{u,s,k}u_{k,s}), \tag{84}$$
$$\overset{(a)}{=} V_k(H_{d,s,k}d_{k,s} + H_{f,s,k}f_{k,s}), \tag{85}$$

where V_k is a θ-periodic parity matrix (or vector) that satisfies $V_kH_{o,s,k} = 0$, equation (85) represents the residual dynamics.

If the rank condition

$$\text{rank}\,[H_{o,s,k} \;\; H_{d,s,k} \;\; H_{f,s,k}] > \text{rank}\,[H_{o,s,k} \;\; H_{d,s,k}] \tag{86}$$

holds for any k, then a full decoupling can be achieved by solving

$$V_k[H_{o,s,k} \;\; H_{d,s,k}] = 0, \qquad V_kH_{f,s,k} \neq 0 \tag{87}$$

for V_k over one period at $k, k + 1, \ldots, k + \theta - 1$. The residual evaluation consists in detecting the deviation of residual $r(k)$ from 0. Especially, if

$$\text{rank}[H_{o,s,0}\cdots H_{o,s,\theta-1} \;\; H_{d,s,0}\cdots H_{d,s,\theta-1} \;\; H_{f,s,0}\cdots H_{f,s,\theta-1}] > \text{rank}[H_{o,s,0} \;\; \cdots \;\; H_{o,s,\theta-1} \;\; H_{d,s,0} \;\; \cdots \;\; H_{d,s,\theta-1}], \tag{88}$$

then the full decoupling can be achieved by a constant parity matrix (or vector) V_k. However, condition (88) is rather restrictive in practice.

In case that a full decoupling is not achievable, optimization problems similar to (15)–(17) are formulated as

$$\max_{V_k, V_kH_{o,s,k}=0} J_{\text{LTP,PS},\infty/\infty}(V_k) = \max_{V_k, V_kH_{o,s,k}=0} \frac{\overline{\sigma}^2(V_kH_{f,s,k})}{\overline{\sigma}^2(V_kH_{d,s,k})}, \tag{89}$$

$$\max_{V_k, V_kH_{o,s,k}=0} J_{\text{LTP,PS},-/\infty}(V_k) = \max_{V_k, V_kH_{o,s,k}=0} \frac{\underline{\sigma}^2(V_kH_{f,s,k})}{\overline{\sigma}^2(V_kH_{d,s,k})}, \tag{90}$$

$$\max_{V_k, V_kH_{o,s,k}=0} J_{\text{LTP,PS},i/\infty}(V_k) = \max_{V_k, V_kH_{o,s,k}=0} \frac{\sigma_i^2(V_kH_{f,s,k})}{\overline{\sigma}^2(V_kH_{d,s,k})}, \tag{91}$$

which are solved over one period to get the optimal periodic parity matrix V_k. Because the parity-space approach handles each time instant independently and there is no stability problem, the solutions of problems (87)–(91) at each time instant are independent of each other and can be obtained following the procedures introduced in Section 2.2. The threshold Jth can be calculated by (23) or (26) according to the requirement on FAR, while the residual evaluation function is selected as the amplitude (22) of the residual signal.

If the order s of the parity relation (82) is an integer multiple of the period θ, then the periodic parity-space approach is equivalent with a bank of residual generators (79). In comparison, the periodic parity space approach provides more flexibility. The order of the parity relation s needs not to be related to the period θ. Moreover, s may take different values at different time instants. In this case, the threshold for the residual evaluation may need to be chosen differently at different time.

3.2.2. Periodic observer-based approach

Assume that $(A(k), C(k))$ is detectable. A periodic observer-based residual generator can be constructed as

$$\begin{aligned}\hat{x}(k+1) &= A(k)\hat{x}(k) + B(k)u(k) + L(k)\big(y(k) - \hat{y}(k)\big),\\ r(k) &= W(k)\big(y(k) - \hat{y}(k)\big),\\ \hat{y}(k) &= C(k)\hat{x}(k) + D(k)u(k),\end{aligned} \tag{92}$$

where $L(k)$ and $W(k)$ are θ-periodic observer gain matrix and weighting matrix, respectively. The residual dynamics is governed by

$$\begin{aligned}e(k+1) &= \big(A(k) - L(k)C(k)\big)e(k) + \big(E_d(k) - L(k)F_d(k)\big)d(k)\\ &\quad + \big(E_f(k) - L(k)F_f(k)\big)f(k),\\ r(k) &= W(k)\big(C(k)e(k) + F_d(k)d(k) + F_f(k)f(k)\big),\end{aligned} \tag{93}$$

where $e(k) = x(k) - \hat{x}(k)$.

To enhance the robustness of the FD system to the unknown disturbances without loss of the sensitivity to the faults, the optimal design problem is formulated as

$$\begin{aligned}&\sup_{L(k),W(k)} J_{\mathrm{LTP,OBS},\infty/\infty}\big(L(k), W(k)\big)\\ &\quad = \sup_{L(k),W(k)} \frac{\sup_{d=0, f\in l_2-\{0\}}\big(\|r\|_2/\|f\|_2\big)}{\sup_{f=0, d\in l_2-\{0\}}\big(\|r\|_2/\|d\|_2\big)},\end{aligned} \tag{94}$$

$$\begin{aligned}&\sup_{L(k),W(k)} J_{\mathrm{LTP,OBS},-/\infty}\big(L(k), W(k)\big)\\ &\quad = \sup_{L(k),W(k)} \frac{\inf_{d=0, f\in l_2-\{0\}}\big(\|r\|_2/\|f\|_2\big)}{\sup_{f=0, d\in l_2-\{0\}}\big(\|r\|_2/\|d\|_2\big)}.\end{aligned} \tag{95}$$

The solutions of optimization problems (94)-(95) are derived by solving an equivalent optimization problem for the cyclically lifted LTI systems first and then recover the periodic matrices $L(k)$ and $W(k)$ [24].

Solution to optimization problems (94)-(95)

Assume that $(A(k), E_d(k), C(k), F_d(k))$ is regular. Then

$$L(k) = -L_d^T(k), \qquad W(k) = W_d(k) \tag{96}$$

solve optimization problems (94)-(95) simultaneously, where $W_d(k)$ is the left inverse of a full column rank matrix $H_d(k)$ satisfying $H_d(k)H_d^T(k) = C(k)X_d(k)C^T(k) + F_d(k)F_d^T(k)$, and $(X_d(k), L_d(k))$ is the stabilizing solution to the difference periodic Riccati system (DPRS)

$$\begin{bmatrix}\Omega_{d,11} & \Omega_{d,12}\\ \Omega_{d,12}^T & \Omega_{d,22}\end{bmatrix} \times \begin{bmatrix}I\\ L_d(k)\end{bmatrix} = 0\,, \tag{97}$$

where $\Omega_{d,11} = A(k)X_d(k)A^T(k) - X_d(k+1) + E_d(k)E_d^T(k)$, $\Omega_{d,12} = A(k)X_d(k)C^T(k) + E_d(k)F_d^T(k)$, and $\Omega_{d,22} = C(k)X_d(k)C^T(k) + F_d(k)F_d^T(k)$. An alternative solution to problem (95), if $(A(k), E_f(k),\ C(k), F_f(k))$ is regular, is given by

$$L(k) = -L_f^T(k), \qquad W(k) = W_f(k), \tag{98}$$

where $W_f(k)$ is the left inverse of a full column rank matrix $H_f(k)$ satisfying $H_f(k)H_f^T(k) = C(k)X_f(k)C^T(k) + F_f(k)F_f^T(k)$, and $(X_f(k), L_f(k))$ is the stabilizing solution to the DPRS

$$\begin{bmatrix}\Omega_{f,11} & \Omega_{f,12}\\ \Omega_{f,12}^T & \Omega_{f,22}\end{bmatrix} \times \begin{bmatrix}I\\ L_f(k)\end{bmatrix} = 0, \tag{99}$$

where $\Omega_{f,11} = A(k)X_f(k)A^T(k) - X_f(k+1) + E_f(k)E_f^T(k)$, $\Omega_{f,12} = A(k)X_f(k)C^T(k) + E_f(k)F_f^T(k)$, and $\Omega_{f,22} = C(k)X_f(k)C^T(k) + F_f(k)F_f^T(k)$. It is interesting to note the following connections between different approaches.

(i) Periodic observer-based residual generator (92) can be rewritten into the form of lifted reformulation-based LTI observer (76) with

$$\begin{aligned}L_\tau &= \begin{bmatrix}L_{\tau,1} & L_{\tau,2} & \cdots & L_{\tau,\theta}\end{bmatrix},\\ L_{\tau,i} &= \Psi_{A(k)-L(k)C(k)}(\tau+\theta, \tau+i)L(\tau+i-1),\\ W_\tau &= \begin{bmatrix}W_{\tau,1,1} & O & \cdots & O\\ W_{\tau,2,1} & W_{\tau,2,2} & \ddots & \vdots\\ \vdots & \ddots & \ddots & O\\ W_{\tau,\theta,1} & \cdots & W_{\tau,\theta,\theta-1} & W_{\tau,\theta,\theta}\end{bmatrix},\\ W_{\tau,i,j} &= W(\tau+i-1), \quad \text{if } i = j,\\ W_{\tau,i,j} &= -W(\tau+i-1)C(\tau+i-1)\\ &\quad \times \Psi_{A(k)-L(k)C(k)}(\tau+i-1, \tau+j)L(\tau+j-1)\\ &\quad \text{if } i > j,\ i = 1, 2, \ldots, \theta,\ \ j = 1, 2, \ldots, \theta.\end{aligned} \tag{100}$$

Recalling the discussion in Section 3.1.1, the physical meaning is that the periodic observer-based residual generator naturally satisfies the causality condition. It is further proven that, if the parameters $(L(k), W(k))$ of the periodic observer-based residual generator (92) solve optimization problems (94) or (95), then the parameters (L_τ, W_τ) of the LTI observer (76) got by (100) will solve optimization problems in the form of (60)-(61).

(ii) Similar as in LTI systems, the periodic parity-space approach and periodic observer-based approach are closely related. Assume that the periodic vector

$$v_k = \begin{bmatrix}v_{k,0} & v_{k,1} & \cdots & v_{k,s}\end{bmatrix} \tag{101}$$

satisfies $v_k H_{o,s,k} = 0$. Then a periodic functional observer-based residual generator in the form of

$$\begin{aligned}z(k+1) &= G(k)z(k) + H(k)u(k) + L(k)y(k),\\ r(k) &= w(k)z(k) + q(k)u(k) + p(k)y(k)\end{aligned} \tag{102}$$

with $z \in \mathcal{R}^s$, $r \in \mathcal{R}$, can be readily obtained as [45]

$$G(k) = \begin{bmatrix} 0 & 0 & \cdots & 0 & g_{k,1} \\ 1 & 0 & \ddots & \vdots & g_{k,2} \\ \vdots & \ddots & \ddots & 0 & \vdots \\ 0 & \cdots & 1 & 0 & g_{k,s-1} \\ 0 & \cdots & 0 & 1 & g_{k,s} \end{bmatrix},$$

$$L(k) = -\begin{bmatrix} v_{k+s,0} \\ v_{k+s-1,1} \\ \vdots \\ v_{k+1,s-1} \end{bmatrix} - \begin{bmatrix} g_{k,1} \\ g_{k,2} \\ \vdots \\ g_{k,s} \end{bmatrix} v_{k,s}, \tag{103}$$

$$w(k) = [0 \;\; 0 \;\; \cdots \;\; 0 \;\; -1],$$

$$p(k) = v_{k,s},$$

$$H(k) = T(k+1)B(k) - L(k)D(k),$$

$$q(k) = -p(k)D(k),$$

where periodic scalars $g_{k,1}, \ldots, g_{k,s}$ appearing in matrices $G(k), L(k)$ are free parameters and should be selected to guarantee the stability of $G(k)$. Moreover, if v_k realizes a full decoupling from the unknown disturbances, that is, $v_k[H_{o,s,k} \;\; H_{d,s,k}] = 0$, then the functional observer-based residual generator (102) also achieves a full decoupling, that is, $r(k) = 0$, $\forall u(k), d(k)$. This provides an approach to design full decoupling observer-based residual generator.

(iii) We would like to point out that, for the LTI system (1), a residual generator with periodic gain matrix $L(k)$ and periodic weighting matrix $W(k)$ will not improve the FD performance under performance index (94).

4. FD OF SAMPLED-DATA SYSTEMS

The study on FD problems of sampled-data (SD) systems has been motivated by the digital implementation of controllers and monitoring systems. Figure 1 sketches a typical application of an FD system in a process control system. The process under consideration is a continuous-time process. Both the controller and the FD system are discrete-time systems which are implemented on a computer system or on an embedded microprocessor. The sensor output signals are discretized by the A/D converters and then fed to the controller as well as to the FD system. The D/A converters convert the discrete-time control input signals into continuous-time signals. Since both continuous-time and discrete-time signals exist in the system, the system design should be indeed considered from the viewpoint of an SD system [46, 47]. The intersample behavior is the main factor that should be considered in developing FD algorithms for the SD systems. In practice, it happens often that the A/D and D/A converters are working at different sampling rates [48–53]. In this section, we will review the FD methods for the SD systems with various sampling mechanisms.

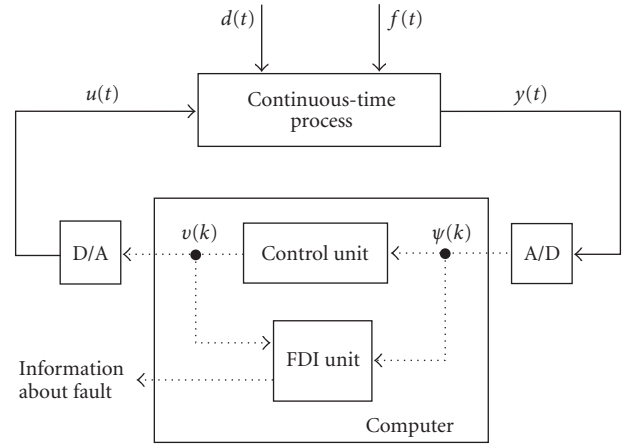

Figure 1: Schematic description of the application of an FDI system in a process control system.

4.1. System description

Assume that, in the SD systems, the process is a continuous LTI process represented by

$$\begin{aligned} \dot{x}(t) &= A_c x(t) + B_c u(t) + E_{dc} d(t) + E_{fc} f(t), \\ y(t) &= Cx(t), \end{aligned} \tag{104}$$

where A_c, B_c, E_{dc}, E_{fc}, and C are known constant matrices of appropriate dimensions. In *single-rate sampled-data (SSD)* systems, the A/D converter and the D/A converter are, respectively, described by

$$\psi(k) = y(kh), \tag{105}$$

$$u(t) = v(k), \quad kh \leqslant t < (k+1)h, \tag{106}$$

where h is the sampling period, $\psi \in \mathcal{R}^m$ is the sampled process output signal, $v \in \mathcal{R}^p$ is the discrete-time control input sequence delivered by the controller program. In *multirate sampled-data (MSD)* systems, the A/D converters and the D/A converters may work with different sampling rates and thus modeled, respectively, by

$$\psi_l(k^l) = y_l(k^l T_{y,l}), \quad l = 1, 2, \ldots, m;\ k^l = 0, 1, 2, \ldots, \tag{107}$$

$$\begin{aligned} u_j(t) &= v_j(k^j), \quad k^j T_{u,j} \leq t < (k^j + 1) T_{u,j}, \\ & j = 1, 2, \ldots, p;\ k^j = 0, 1, 2, \ldots, \end{aligned} \tag{108}$$

where $T_{y,l}$ and $T_{u,j}$ denote, respectively, the sampling periods of the A/D converter in the lth output channel and the D/A converter in the jth input channel. A more general class of systems are *nonuniformly sampled-data (NSD)* systems, where the sampling instants may be multirate, asynchronous, and nonequidistantly distributed, that is,

$$\begin{aligned} \psi_l(k^l) &= y_l(t_{y,k^l}), \quad l = 1, 2, \ldots, m;\ k^l = 0, 1, 2, \ldots, \\ u_j(t) &= v_j(k^j), \quad t_{u,k^j} \leq t < t_{u,k^j+1}, \\ & j = 1, 2, \ldots, p;\ k^j = 0, 1, 2, \ldots, \end{aligned} \tag{109}$$

where t_{y,k^l} represent the sampling instants in the lth output channel and t_{u,k^j} the time instants at which the jth control input is updated. It is worth mentioning that a special kind of NSD systems, where the sampling instants are nonequidistant spaced but periodic, has been studied in the literature rather intensively [54–57].

4.2. FD of SSD systems

Conventionally, an FD system can be designed for the SSD system by indirect approaches, that is,

(i) *analog design and SD implementation*, or
(ii) *discrete-time design based on the discretization of the process model*.

Motivated by the development of sampled-data control [46, 47], in the last years the FD problem of the SSD systems have been studied from the viewpoint of *direct design* to take into account the intersample behavior and eliminate the approximation made during the design [26, 58–60].

The dynamics of the SSD system at the sampling instants can be described by

$$\begin{aligned} x(k+1) &= Ax(k) + Bv(k) + \overline{d}(k) + \overline{f}(k), \\ \psi(k) &= Cx(k), \end{aligned} \tag{110}$$

where

$$\begin{aligned} A &= e^{A_c h}, \qquad B = \int_0^h e^{A_c t} B_c dt, \\ \overline{d}(k) &= \int_0^h e^{A_c(h-\tau)} E_{dc} d(kh+\tau) d\tau, \\ \overline{f}(k) &= \int_0^h e^{A_c(h-\tau)} E_{fc} f(kh+\tau) d\tau. \end{aligned} \tag{111}$$

It is worth noticing that in SD systems there is a significant difference between $u(t)$ and $d(t), f(t)$. Due to the D/A converter (106), $u(t)$ is a piecewise constant signal. The influence of $u(t)$ on $y(t)$ is exactly known from the information of $v(k)$ and can thus be completely compensated in residual generation. In comparison, $d(t)$ and $f(t)$ are unknown signals. Hence, the key is to study the influence of continuous-time signals $d(t)$ and $f(t)$ on the discrete-time sampled output signals $\psi(k)$ and residual signals $r(k)$.

4.2.1. Parity-relation-based FD scheme for SSD systems

A parity-relation-based residual generator

$$r(k) = V_s(\psi_{k,s} - H_{u,s} v_{k,s}) \tag{112}$$

can be used for residual generation, where $V_s H_{o,s} = 0$, $\psi_{k,s}, v_{k,s}, H_{o,s}$, and $H_{u,s}$ are constructed according to (6). To describe the intersample behavior, for a continuous-time signal $\delta(t)$ with δ standing for d and f, an operator is defined as follows:

$$\begin{aligned} \Psi^\delta \delta_{k,s}(t) &= \begin{bmatrix} \overline{\delta}(k-s) \\ \overline{\delta}(k-s+1) \\ \vdots \\ \overline{\delta}(k) \end{bmatrix} \\ &= \begin{bmatrix} \int_0^h e^{A_c(h-\tau)} E_{\delta c} \delta((k-s)h+\tau) d\tau \\ \int_0^h e^{A_c(h-\tau)} E_{\delta c} \delta((k-s+1)h+\tau) d\tau \\ \vdots \\ \int_0^h e^{A_c(h-\tau)} E_{\delta c} \delta(kh+\tau) d\tau \end{bmatrix}. \end{aligned} \tag{113}$$

The residual dynamics can be expressed with the help of operators as

$$\begin{aligned} r(k) &= V_s H(\Psi^d d_{k,s}(t) + \Psi^f f_{k,s}(t)), \\ H &= \begin{bmatrix} O & O & \cdots & O \\ C & O & \ddots & \vdots \\ \vdots & \ddots & \ddots & O \\ CA^{s-1} & \cdots & C & O \end{bmatrix}. \end{aligned} \tag{114}$$

The influence of the continuous-time signal $\delta(t)$ over the time interval $[(k-s)h, (k+1)h)$ on the discrete-time signal $\Psi^\delta \delta_{k,s}(t)$ is measured by

$$\begin{aligned} \overline{\sigma}(V_s H \Psi^\delta (\Psi^\delta)^* H^T V_s^T) &= \sup_{\delta \in \mathcal{L}_{2,[(k-s)h,(k+1)h)}} \frac{r^T(k) r(k)}{\|\delta\|^2_{2,[(k-s)h,(k+1)h)}}, \\ \underline{\sigma}(V_s H \Psi^\delta (\Psi^\delta)^* H^T V_s^T) &= \inf_{\delta \in \mathcal{L}_{2,[(k-s)h,(k+1)h)}} \frac{r^T(k) r(k)}{\|\delta\|^2_{2,[(k-s)h,(k+1)h)}}, \end{aligned} \tag{115}$$

where $(\Psi^\delta)^*$ denotes the adjoint of the operator Ψ^δ which uniquely satisfies

$$\langle \Psi^\delta \delta_{k,s}(t), \beta_s(k) \rangle = \langle \delta_{k,s}(t), (\Psi^\delta)^* \beta_s(k) \rangle \tag{116}$$

for any vector $\beta_s(k)$ of compatible dimensions. The optimization problems are thus formulated as

$$\begin{aligned} \max_{V_s, V_s H_{o,s}=0} J_{\mathrm{SSD,PS},\infty/\infty}(V_s) &= \max_{V_s, V_s H_{o,s}=0} \frac{\overline{\sigma}(V_s H \Psi^f (\Psi^f)^* H^T V_s^T)}{\overline{\sigma}(V_s H \Psi^d (\Psi^d)^* H^T V_s^T)}, \\ \max_{V_s, V_s H_{o,s}=0} J_{\mathrm{SSD,PS},-/\infty}(V_s) &= \max_{V_s, V_s H_{o,s}=0} \frac{\underline{\sigma}(V_s H \Psi^f (\Psi^f)^* H^T V_s^T)}{\overline{\sigma}(V_s H \Psi^d (\Psi^d)^* H^T V_s^T)}, \\ \max_{V_s, V_s H_{o,s}=0} J_{\mathrm{SSD,PS,i}/\infty}(V_s) &= \max_{V_s, V_s H_{o,s}=0} \frac{\sigma_i(V_s H \Psi^f (\Psi^f)^* H^T V_s^T)}{\overline{\sigma}(V_s H \Psi^d (\Psi^d)^* H^T V_s^T)}. \end{aligned} \tag{117}$$

An analytical expression can be obtained for $\Psi^\delta (\Psi^\delta)^*$ as

$$\begin{aligned} \Psi^\delta (\Psi^\delta)^* &= \mathrm{diag}\{\overline{E}_\delta \overline{E}_\delta^T, \overline{E}_\delta \overline{E}_\delta^T, \ldots, \overline{E}_\delta \overline{E}_\delta^T\}, \\ \overline{E}_\delta \overline{E}_\delta^T &= \int_0^h e^{A_c \tau} E_{\delta c} E_{\delta c}^T e^{A_c^T \tau} d\tau. \end{aligned} \tag{118}$$

As a result, optimization problems (117) are transformed into some equivalent optimization problems:

$$\begin{aligned}
\max_{V_s,V_sH_{o,s}=0} J_{\mathrm{SSD,PS},\infty/\infty}(V_s) &= \max_{V_s,V_sH_{o,s}=0} \frac{\overline{\sigma}^2(V_s\overline{H}_{f,s})}{\overline{\sigma}^2(V_s\overline{H}_{d,s})},\\
\max_{V_s,V_sH_{o,s}=0} J_{\mathrm{SSD,PS},-/\infty}(V_s) &= \max_{V_s,V_sH_{o,s}=0} \frac{\underline{\sigma}^2(V_s\overline{H}_{f,s})}{\overline{\sigma}^2(V_s\overline{H}_{d,s})},\\
\max_{V_s,V_sH_{o,s}=0} J_{\mathrm{SSD,PS},i/\infty}(V_s) &= \max_{V_s,V_sH_{o,s}=0} \frac{\sigma_i^2(V_s\overline{H}_{f,s})}{\overline{\sigma}^2(V_s\overline{H}_{d,s})},
\end{aligned} \tag{119}$$

where $\overline{H}_{f,s}$ and $\overline{H}_{d,s}$ are built based on $(A,\overline{E}_f,C,O)$ and $(A,\overline{E}_d,C,O)$ in a way similar to $H_{u,s}$ in (6). The equivalent optimization problems (119) are of the standard form and can be solved as introduced in Section 2.2.

4.2.2. Observer-based FD scheme for SSD systems

An observer-based residual generator is constructed as

$$\begin{aligned}
\hat{x}(k+1) &= A\hat{x}(k)+B\upsilon(k)+L(\psi(k)-\hat{\psi}(k)),\\
r(k) &= W(\psi(k)-\hat{\psi}(k)) \quad \hat{\psi}(k)=C\hat{x}(k).
\end{aligned} \tag{120}$$

To describe the influence of continuous-time signals $d(t)$ and $f(t)$ on the discrete-time residual signal $r(k)$ in the frequency domain, operator Γ_δ (δ standing for d or f) is introduced as

$$\begin{aligned}
\Gamma_\delta\delta(j\omega) &= \frac{1}{h}\sum_{k=-\infty}^{\infty} G_\delta(j\omega+jk\omega_s)\delta(j\omega+jk\omega_s),\\
G_\delta(s) &= C(sI-A_c)^{-1}E_{\delta c}, \qquad \omega_s=\frac{2\pi}{h}.
\end{aligned} \tag{121}$$

Based on it, the residual dynamics can be expressed as

$$\begin{aligned}
r(e^{j\omega h}) &= W\widehat{M}_u(e^{j\omega h})(\Gamma_d d(j\omega)+\Gamma_f f(j\omega)),\\
\widehat{M}_u(e^{j\omega h}) &= I-C(e^{jwh}I-A+LC)^{-1}L.
\end{aligned} \tag{122}$$

Let $\overline{E}_\delta$ be given by (118). Then

$$\Gamma_\delta\Gamma_\delta^* = C(e^{j\omega h}I-A)^{-1}\overline{E}_\delta\overline{E}_\delta^T(e^{-j\omega h}I-A^T)^{-1}C^T. \tag{123}$$

Based on it, the H_2/H_2 optimal design problem is solved [59]. Further, it was shown that the H_∞/H_∞, H_-/H_∞ and H_i/H_∞ design problems of the SSD system are equivalent to that of a discrete LTI system and can be obtained by solving equivalent optimization problems [26, 60]:

$$\begin{aligned}
\sup_{L,W} J_{\mathrm{SSD,OBS},\infty/\infty}(L,W) &= \sup_{L,W}\frac{\sup_{d=0,f\in\mathcal{L}_2-\{0\}}(\|r\|_2/\|f\|_2)}{\sup_{f=0,d\in\mathcal{L}_2-\{0\}}(\|r\|_2/\|d\|_2)}\\
&= \sup_{L,W}\frac{\|\overline{G}_{rf}(z)\|_\infty}{\|\overline{G}_{rd}(z)\|_\infty},\\
\sup_{L,W} J_{\mathrm{SSD,OBS},-/\infty}(L,W) &= \sup_{L,W}\frac{\inf_{d=0,f\in\mathcal{L}_2-\{0\}}(\|r\|_2/\|f\|_2)}{\sup_{f=0,d\in\mathcal{L}_2-\{0\}}(\|r\|_2/\|d\|_2)}\\
&= \sup_{L,W}\frac{\|\overline{G}_{rf}(z)\|_-}{\|\overline{G}_{rd}(z)\|_\infty},\\
\sup_{L,W} J_{\mathrm{SSD,OBS},i/\infty}(L,W) &= \sup_{L,W}\frac{\sigma_i(\overline{G}_{rf}(e^{j\omega h}))}{\|\overline{G}_{rd}(z)\|_\infty}\\
\overline{G}_{r\delta}(z) &= WC(zI-A+LC)^{-1}\overline{E}_\delta, \quad \delta=d,f.
\end{aligned} \tag{124}$$

4.2.3. Influence of sampling on full decoupling

No matter which residual generation approach is adopted, due to the sampling effect, the full decoupling becomes more difficult in SD systems than in the original continuous-time systems, because after sampling the dimension of the influence space of the unknown disturbances becomes

$$\begin{aligned}
\operatorname{rank}\overline{E}_d &= \operatorname{rank}\overline{E}_d\overline{E}_d^T = \operatorname{rank}\int_0^h e^{A_c\tau}E_{dc}E_{dc}^Te^{A_c^T\tau}d\tau\\
&\geq \operatorname{rank}E_{dc},
\end{aligned} \tag{125}$$

that is, the equivalent number of the unknown disturbances may increase [58].

4.3. FD of MSD systems

Under some assumptions, the FD problem of MSD systems has been considered in [61–64]. The MSD system is in nature a periodic system. The system period, denoted by T, is the least common multiple of the sampling periods [52]. The maximal common multiplier of the sampling periods is often called base period. From the FD viewpoint, in MSD systems only those time instants with sampled outputs are of interest. In [65], the basic idea of the proposed FD approach is to get the input-output relations of the MSD at the base periods at first and then downsample them according to different sampling periods to get the parity relation of the MSD system. In [66], a so-called fast rate residual generator is proposed, which generates a residual signal as soon as a new measurement is available. The basic idea is to reformulate the MSD system as a system with periodic output equations. The problem of fast rate residual generation is further pursued by [67, 68], where the basic ideas are, respectively, to compute the parity matrix V_s and the postfilter $R(z)$ for lifted system model. To satisfy the causality constraint, the freedoms in matrix $\overline{P}_s$ and $R(z)$ are used. Most recently, a unified and simplified approach to the FD of the MSD systems is proposed by [69], which considers the special problem formulation of fault detection and shows clearly the difference between control problem and FD problem. The basic idea of [69] is to remodel the MSD system as a nonuniformly sampled-data system and then use periodic or time varying system theory to design the FD system.

Denote with $\{t_k\}$ the sequence of time instants at which one or more sampled outputs are available, $t_0<t_1<\cdots<t_k<t_{k+1}<\cdots$. Let $\overline{\psi}(k)$ represent the vector of sampled output signals at time instant t_k. The dimension of $\overline{\psi}(k)$ is time-varying and upper bounded by m. Let $x(k)=x(t_k)$. For the purpose of FD, the MSD system described by (104), (107), and (108) can be equivalently remodeled as

$$\begin{aligned}
x(k+1) &= A(k)x(k)+\overline{u}(k)+\overline{d}(k)+\overline{f}(k),\\
\overline{\psi}(k) &= C(k)x(k),
\end{aligned} \tag{126}$$

where

$$\begin{aligned} A(k) &= e^{A_c(t_{k+1}-t_k)}, \\ \overline{u}(k) &= \int_{t_k}^{t_{k+1}} e^{A_c(t_{k+1}-t)} B_c u(t)dt, \\ \overline{d}(k) &= \int_{t_k}^{t_{k+1}} e^{A_c(t_{k+1}-t)} E_{dc} d(t)dt, \\ \overline{f}(k) &= \int_{t_k}^{t_{k+1}} e^{A_c(t_{k+1}-t)} E_{fc} f(t)dt. \end{aligned} \tag{127}$$

The new description is different from other descriptions available in the literature [66–68] and considers the transition of system dynamics only at the time instants with sampled outputs. The terms $\overline{d}(k)$ and $\overline{f}(k)$ characterize, respectively, the influence of the disturbances and the faults on the sampled outputs. As $v_1, \ldots, v_p$ are available and the models of the D/A converters (108) are known, $\overline{u}(k)$ and thus the influence of the control input vector on the sampled outputs can be completely reconstructed and easily compensated. The matrices $A(k)$ and $C(k)$ are time varying matrices, as $t_{k+1} - t_k$ is time-varying with respect to time k. In the MSD system, due to the periodicity of the sampling time sequence, $A(k), C(k)$ are periodic matrices. FD systems can be designed for the MSD system based on the time-varying model (126).

4.3.1. Parity-relation-based FD scheme for MSD systems

The input-output relationship of (126) over the moving horizon $[t_{k-s}, t_k]$, where s denotes the length of the moving horizon, is

$$\widetilde{\psi}(k) = H_{o,s,k} x(k-s) + H_{s,k}\big(\widetilde{u}(k) + \widetilde{d}(k) + \widetilde{f}(k)\big), \tag{128}$$

where $\widetilde{\psi}(k), \widetilde{u}(k), \widetilde{d}(k)$, and $\widetilde{f}(k)$ are stacked vectors based on $\overline{\psi}(j), \overline{u}(j), \overline{d}(j)$, and $\overline{f}(j)$, $j = k-s, \ldots, k$, respectively, $H_{o,s,k}$ is constructed according to (83),

$$H_{s,k} = \begin{bmatrix} O & O & \cdots \\ C(k-s+1) & \ddots & \ddots \\ \vdots & \ddots & O \\ C(k)A(k-1)\cdots A(k-s+1) & \cdots & C(k) \end{bmatrix}. \tag{129}$$

Build a parity-relation-based residual generator with

$$r(k) = V_k\big(\widetilde{\psi}(k) - H_{s,k}\widetilde{u}(k)\big), \qquad V_k H_{o,s,k} = 0, \tag{130}$$

where V_k is a periodically time-varying parity matrix (or vector). To describe the influence of continuous-time signals $d(t), f(t)$ on the multirate-sampled outputs, linear time-varying operators Ψ_k^δ (δ standing for d or f),

$$\widetilde{\delta}(k) = \Psi_k^\delta \delta_k(t) = \begin{bmatrix} \int_{t_{k-s}}^{t_{k-s+1}} e^{A_c(t_{k-s+1}-t)} E_{\delta c}\delta(t)dt \\ \int_{t_{k-s+1}}^{t_{k-s+2}} e^{A_c(t_{k-s+2}-t)} E_{\delta c}\delta(t)dt \\ \vdots \\ \int_{t_{k-1}}^{t_k} e^{A_c(t_k-t)} E_{\delta c}\delta(t)dt \end{bmatrix}, \tag{131}$$

are introduced and the residual dynamics is described by

$$r(k) = V_k H_{s,k}\big(\widetilde{d}(k) + \widetilde{f}(k)\big) = V_k H_{s,k}\big(\Psi_k^d d_k(t) + \Psi_k^f f_k(t)\big). \tag{132}$$

The optimal selection of V_k can be formulated similar to (117) with $\Psi^d(\Psi^d)^*$ and $\Psi^f(\Psi^f)^*$ substituted by $\Psi_k^d(\Psi_k^d)^*$ and $\Psi_k^f(\Psi_k^f)^*$, respectively. Using the same technique, $\Psi_k^\delta(\Psi_k^\delta)^*$ are derived to be

$$\begin{aligned} \Psi_k^\delta(\Psi_k^\delta)^* &= \operatorname{diag}\{\Psi_{k,s}^\delta, \ldots, \Psi_{k,1}^\delta\}, \\ \Psi_{k,j}^\delta &= \int_0^{t_{k-j+1}-t_{k-j}} e^{A_c t} E_{\delta c} E_{\delta c}^T e^{A_c^T t} dt, \quad j = s, \ldots, 1. \end{aligned} \tag{133}$$

Due to the periodicity of $\Psi_k^\delta(\Psi_k^\delta)^*$, the optimization problem needs to be solved over one period.

4.3.2. Observer-based FD scheme for MSD systems

For the aim of fault detection, a fast rate time-varying observer-based residual generator can be constructed as

$$\begin{aligned} \hat{x}(k+1) &= A(k)\hat{x}(k) + \overline{u}(k) + L(k)\big(\overline{\psi}(k) - \hat{\psi}(k)\big), \\ r(k) &= W(k)\big(\overline{\psi}(k) - \hat{\psi}(k)\big), \qquad \hat{\psi}(k) = C(k)\hat{x}(k), \end{aligned} \tag{134}$$

where the gain matrix $L(k)$ and the weighting matrix $W(k)$ are time-varying matrices to be determined. The dimensions of $L(k)$ and $W(k)$ may change with the number of available sampled output signals. Considering the periodicity of the matrices $A(k), C(k)$, (134) can be designed as a periodic observer. Define the state estimation error as $e(k) = x(k) - \hat{x}(k)$. The dynamics of residual generator (134) is governed by

$$\begin{aligned} e(k+1) &= \big(A(k) - L(k)C(k)\big)e(k) + \overline{d}(k) + \overline{f}(k), \\ r(k) &= W(k)C(k)e(k). \end{aligned} \tag{135}$$

Introduce linear time-varying operators Γ_k^δ (δ standing for d or f),

$$\Gamma_k^\delta \delta_k(t) = \int_{t_k}^{t_{k+1}} e^{A_c(t_{k+1}-t)} E_{\delta c}\delta(t)dt, \tag{136}$$

to rewrite the residual dynamics as

$$\begin{aligned} e(k+1) &= \big(A(k) - L(k)C(k)\big)e(k) + \Gamma_k^d d_k(t) + \Gamma_k^f f_k(t), \\ r(k) &= W(k)C(k)e(k). \end{aligned} \tag{137}$$

To enhance the robustness of the FD system to the unknown disturbances without loss of the sensitivity to the faults, the design problem is formulated as

$$\begin{aligned}&\sup_{L(k),W(k)} J_{\mathrm{MSD,OBS},\infty/\infty}(L(k),W(k))\\&\quad=\sup_{L(k),W(k)}\frac{\sup_{d=0,f\in\mathcal{L}_2-\{0\}}(\|r\|_2/\|f\|_2)}{\sup_{f=0,d\in\mathcal{L}_2-\{0\}}(\|r\|_2/\|d\|_2)},\\&\sup_{L(k),W(k)} J_{\mathrm{MSD,OBS},-/\infty}(L(k),W(k))\\&\quad=\sup_{L(k),W(k)}\frac{\inf_{d=0,f\in\mathcal{L}_2-\{0\}}(\|r\|_2/\|f\|_2)}{\sup_{f=0,d\in\mathcal{L}_2-\{0\}}(\|r\|_2/\|d\|_2)}.\end{aligned}\tag{138}$$

By analyzing $\Gamma_k^\delta(\Gamma_k^\delta)^*$, optimization problems (138) are transformed into equivalent optimization problems of discrete LTP system

$$\begin{aligned}e(k+1)&=(A(k)-L(k)C(k))e(k)+\overline{E}_d(k)d_{\mathrm{eq}}(k)+\overline{E}_f(k)f_{\mathrm{eq}}(k),\\r(k)&=W(k)C(k)e(k),\end{aligned}\tag{139}$$

where the l_2-norms of $d_{\mathrm{eq}}(k)$ and $f_{\mathrm{eq}}(k)$ in (139) have the same upper bounds, respectively, with the $\mathcal{L}_2$-norms of $d(t)$ and $f(t)$ in (104), the matrices $\overline{E}_d(k)$ and $\overline{E}_f(k)$ are time-varying matrices reflecting the sampling effect and satisfy

$$\overline{E}_\delta(k)\overline{E}_\delta^T(k)=\int_0^{t_{k+1}-t_k}e^{A_c t}E_{\delta c}E_{\delta c}^T e^{A_c^T t}dt.\tag{140}$$

Then, optimization problems (138) can be solved with the approaches introduced in Section 3.2.2.

4.4. FD of NSD systems

The same design procedures introduced in the last subsection can be applied to the FD of NSD systems by reordering the sampling instants. The main difference lies in that in general NSD systems, $A(k), C(k), \overline{E}_d(k), \overline{E}_f(k)$ are time-varying matrices but not periodic matrices. In consequence, for the NSD systems

(i) if the parity space approach is used, then the time-varying parity matrix $V(k)$ needs to be calculated at each time instant,

(ii) if the observer-based approach is adopted, then the observer gain matrix $L(k)$ needs to guarantee the stability of the resulting linear time-varying system.

4.5. Influence of sampling period on optimal FD performance

Sampling period is an important parameter in SD systems. Recently, the influence of the sampling period on the optimal FD performance has been investigated in [70, 71]. Suppose that for a given continuous-time process (104) three different sampling schemes are considered: single-rate sampling with sampling period h, single-rate sampling with sampling period ρh, multirate sampling with base period h and system period ρh, where $\rho \geq 1$ is an integer. It is proven that the optimal performance indeces are related by

$$\begin{aligned}J_{\mathrm{SSD,OBS},\infty/\infty,h}&\geq J_{\mathrm{MSD,OBS},\infty/\infty}\geq J_{\mathrm{SSD,OBS},\infty/\infty,\rho h},\\J_{\mathrm{SSD,PS},\infty/\infty,h}&\geq J_{\mathrm{MSD,PS},\infty/\infty}\geq J_{\mathrm{SSD,PS},\infty/\infty,\rho h}.\end{aligned}\tag{141}$$

That means that, with the increase of the sampling period, the FD performance will become worse. It can be intuitively interpreted as the consequence of information reduction caused by the increase of the sampling period. However, we would like to emphasize that such a conclusion does not hold for all performance indices, for instance, the H_-/H_∞ index.

5. CONCLUDING REMARKS

In this paper, standard methods for FD in discrete LTI systems have been reviewed and recent development in FD for discrete LTP and SD systems has been summarized. In case of discrete LTI systems, the basic idea, full decoupling and optimization problems, and the corresponding solutions are introduced. It can be seen that different FD approaches are closely related to each other. The FD problem of discrete LTP systems can be handled either indirectly by lifting or directly by considering the periodicity of the system matrices. In SD systems the main problem is to take into account the intersample behavior and to develop direct FD approaches. With the aid of operators, the FD problem of SSD, MSD, and NSD systems can be transformed, respectively, into the FD problem of discrete LTI, LTP, and linear time-varying systems. The methods introduced in this paper have found several interesting applications in the emerging research area of embedded networked control systems (emNCS) [72, 73]. Because of the limited data rate, the sampling mechanisms become an important design parameter in emNCS and have decisive influence on the real-time network and computing performance and FD performance.

REFERENCES

[1] M. Basseville and I. Nikiforov, *Detection of Abrupt Changes — Theory and Application*, Prentice-Hall, Englewood Cliffs, NJ, USA, 1993.

[2] J. Gertler, *Fault Detection and Diagnosis in Engineering Systems*, Marcel Dekker, New York, NY, USA, 1998.

[3] R. Mangoubi, *Robust Estimation and Failure Detection*, Springer, New York, NY, USA, 1998.

[4] J. Chen and R. J. Patton, *Robust Model-Based Fault Diagnosis for Dynamic Systems*, Kluwer Academic Publishers, Boston, Mass, USA, 1999.

[5] R. J. Patton, P. M. Frank, and R. N. Clark, *Issues of Fault Diagnosis for Dynamic Systems*, Springer, London, UK, 2000.

[6] M. Blanke, M. Kinnaert, J. Lunze, and M. Staroswiecki, *Diagnosis and Fault-Tolerant Control*, Springer, New York, NY, USA, 2003.

[7] P. M. Frank, S. X. Ding, and T. Marcu, "Model-based fault diagnosis in technical processes," *Transactions of the Institute of Measurement and Control*, vol. 22, no. 1, pp. 57–101, 2000.

[8] E. Y. Chow and A. S. Willsky, "Analytical redundancy and the design of robust failure detection systems," *IEEE Transactions on Automatic Control*, vol. 29, pp. 603–614, 1984.

[9] H. Ishii and B. Francis, *Limited Data Rate in Control Systems with Networks*, Springer, Berlin, Germany, 2002.

[10] K. Zhou, *Essential of Robust Control*, Prentice-Hall, Englewood Cliffs, NJ, USA, 1998.

[11] J. Wuennenberg, *Observer-Based Fault Detection in Dynamic Systems*, Ph.D. thesis, University of Duisburg, Duisburg, Germany, 1990.

[12] S. X. Ding, E. L. Ding, T. Jeinsch, and P. Zhang, "An approach to a unified design of FDI systems," in *Proceedings of the 3rd Asian Control Conference*, pp. 2812–2817, Shanghai, China, July 2000.

[13] S. X. Ding, E. L. Ding, and T. Jeinsch, "A numerical approach to optimization of FDI systems," in *Proceedings of the 37th IEEE Conference on Decision and Control (CDC '98)*, pp. 1137–1142, Tampa, Fla, USA, December 1998.

[14] S. X. Ding, E. L. Ding, and T. Jeinsch, "An approach to analysis and design of observer and parity relation based FDI systems," in *Proceedings of the 14th Triennial World Congress of the International Federation of Automatic Control*, pp. 37–42, Beijing, China, July 1999.

[15] S. Schneider, N. Weinhold, S. X. Ding, and A. Rehm, "Parity space based FDI-scheme for vehicle lateral dynamics," in *Proceedings of the IEEE International Conference on Control Applications (CCA '05)*, pp. 1409–1414, Toronto, Canada, August 2005.

[16] X. Ding, L. Guo, and T. Jeinsch, "A characterization of parity space and its application to robust fault detection," *IEEE Transactions on Automatic Control*, vol. 44, no. 2, pp. 337–343, 1999.

[17] H. Ye, G. Z. Wang, S. X. Ding, and H. Y. Su, "An IIR filter based parity space approach for fault detection," in *Proceedings of the 15th Triennial World Congress of the International Federation of Automatic Control*, Barcelona, Spain, July 2002.

[18] P. Zhang and S. X. Ding, "Multi-objective design of robust fault detection systems," in *Proceedings of the 6th IFAC Symposium on Fault Detection, Supervision and Safety of Technical Processes (SAFEPROCESS '06)*, pp. 1453–1458, Beijing, China, August-September 2006.

[19] S. X. Ding, P. Zhang, B. Huang, E. L. Ding, and P. M. Frank, "An approach to norm and statistical methods based residual evaluation," in *Proceedings of the 10th IEEE International Conference on Methods and Models in Automation and Robotics (MMAR '04)*, pp. 777–780, Miedzyzdroje, Poland, August-September 2004.

[20] X. Ding and P. M. Frank, "Fault detection via factorization approach," *Systems and Control Letters*, vol. 14, no. 5, pp. 431–436, 1990.

[21] X. Ding and P. M. Frank, "Fault detection via optimally robust detection filters," in *Proceedings of the 28th Conference on Decision and Control (CDC '89)*, vol. 2, pp. 1767–1772, Tampa, Fla, USA, December 1989.

[22] S. X. Ding, T. Jeinsch, P. M. Frank, and E. L. Ding, "A unified approach to the optimization of fault detection systems," *International Journal of Adaptive Control and Signal Processing*, vol. 14, no. 7, pp. 725–745, 2000.

[23] P. Zhang, S. X. Ding, G. Z. Wang, and D. H. Zhou, "An approach to fault detection of sampled-data systems," Tech. Rep., submitted to *IEEE Transactions on Automatic Control*.

[24] P. Zhang, S. X. Ding, G. Z. Wang, and D. H. Zhou, "Fault detection of linear discrete-time periodic systems," *IEEE Transactions on Automatic Control*, vol. 50, no. 2, pp. 239–244, 2005.

[25] N. Liu and K. Zhou, "Optimal and analytic solutions to robust fault detection problems," submitted to *IEEE Transactions on Automatic Control*.

[26] P. Zhang, S. X. Ding, G. Z. Wang, D. H. Zhou, and E. L. Ding, "An H_∞ approach to fault detection for sampled-data systems," in *Proceedings of the American Control Conference (ACC '02)*, vol. 3, pp. 2196–2201, Anchorage, Alaska, USA, May 2002.

[27] P. Zhang, H. Ye, S. X. Ding, G. Z. Wang, and D. H. Zhou, "On the relationship between parity space and H_2 approaches to fault detection," *Systems and Control Letters*, vol. 55, no. 2, pp. 94–100, 2006.

[28] H. Ye, S. X. Ding, and G. Z. Wang, "Integrated design of fault detection systems in time-frequency domain," *IEEE Transactions on Automatic Control*, vol. 47, no. 2, pp. 384–390, 2002.

[29] H. Ye, G. Z. Wang, and S. X. Ding, "A new parity space approach for fault detection based on stationary wavelet transform," *IEEE Transactions on Automatic Control*, vol. 49, no. 2, pp. 281–287, 2004.

[30] S. X. Ding, P. M. Frank, E. L. Ding, and T. Jeinsch, "Fault detection system design based on a new trade-off strategy," in *Proceedings of the 39th IEEE Conference on Decision and Control (CDC '00)*, vol. 4, pp. 4144–4149, Sydney, Australia, December 2000.

[31] P. M. Frank and X. Ding, "Frequency domain approach to optimally robust residual generation and evaluation for model-based fault diagnosis," *Automatica*, vol. 30, no. 5, pp. 789–904, 1994.

[32] P. Zhang, S. X. Ding, G. Z. Wang, and D. H. Zhou, "Fault detection for linear discrete-time periodic systems," in *Proceedings of the 5th IFAC Symposium on Fault Detection, Supervision and Safety of Technical Processes (SAFEPROCESS '03)*, pp. 247–252, Washington, DC, USA, 2003.

[33] M. Hou and R. J. Patton, "An LMI approach to H_-/H_∞ fault detection observers," in *Proceedings of the UKACC International Conference on Control*, vol. 1, pp. 305–310, Exeter, UK, September 1996.

[34] F. Rambeaux, F. Hamelin, and D. Sauter, "Robust residual generation via LMI," in *Proceedings of the 14th Triennial World Congress of the International Federation of Automatic Control*, pp. 240–246, Beijing, China, July 1999.

[35] D. Henry and A. Zolghadri, "Design and analysis of robust residual generators for systems under feedback control," *Automatica*, vol. 41, no. 2, pp. 251–264, 2005.

[36] J. Liu, J. L. Wang, and G.-H. Yang, "An LMI approach to minimum sensitivity analysis with application to fault detection," *Automatica*, vol. 41, no. 11, pp. 1995–2004, 2005.

[37] R. H. Chen, D. L. Mingori, and J. L. Speyer, "Optimal stochastic fault detection filter," *Automatica*, vol. 39, no. 3, pp. 377–390, 2003.

[38] S. Bittanti and P. Colaneri, "Analysis of discrete-time linear periodic systems," *Control and Dynamics Systems*, vol. 78, pp. 313–339, 1996.

[39] P. Colaneri and V. Kucera, "The model matching problem for periodic discrete-time systems," *IEEE Transactions on Automatic Control*, vol. 42, no. 10, pp. 1472–1476, 1997.

[40] B. P. Lampe, M. A. Obraztsov, and E. N. Rosenwasser, "Statistical analysis of stable FDLCP systems by parametric transfer matrices," *International Journal of Control*, vol. 78, no. 10, pp. 747–761, 2005.

[41] S. Bittanti and P. Colaneri, "Periodic Control," in *John Wiley Encyclopaedia on Electrical and Electronic Engineering*, J. Webster, Ed., vol. 16, pp. 240–253, John Wiley & Sons, New York, NY, USA, 1999.

[42] S. Bittanti and P. Colaneri, "Invariant representations of discrete-time periodic systems," *Automatica*, vol. 36, no. 12, pp. 1777–1793, 2000.

[43] M. S. Fadali and S. Gummuluri, "Robust observer-based fault detection for periodic systems," in *Proceedings of the American Control Conference (ACC '01)*, vol. 1, pp. 464–469, Arlington,Va, USA, June 2001.

[44] A. Varga, "Design of fault detection filters for periodic systems," in *Proceedings of the 43rd IEEE Conference on Decision and Control (CDC '04)*, pp. 4800–4805, Atlantis, Bahamas, December 2004.

[45] P. Zhang, S. X. Ding, and T. Jeinsch, "Study on full decoupling problem of linear periodic systems," in *Proceedings of the 16th Triennial World Congress of the International Federation of Automatic Control*, Prague, Czech Republic, July 2005.

[46] T. W. Chen and B. Francis, *Optimal Sampled-Data Control Systems*, Springer, London, UK, 1995.

[47] E. Rosenwasser and B. P. Lampe, *Computer Controlled Systems–Analysis and Design with Process-Orientated Models*, Springer, London, UK, 2000.

[48] G. M. Kranc, "Input-output analysis of multirate feedback systems," *IRE Transactions on Automatic Control*, vol. 3, no. 1, pp. 21–28, 1957.

[49] R. E. Kalman and J. E. Bertram, "A unified approach to the theory of sampling systems," *Journal of the Franklin Institute*, vol. 267, no. 5, pp. 405–436, 1959.

[50] R. A. Meyer and C. S. Burrus, "A unified analysis of multirate and periodically time-varying digital filters," *IEEE Transactions on Circuits and Systems*, vol. 22, no. 3, pp. 162–168, 1975.

[51] M. Araki and T. Hagiwara, "Pole assignment by multirate sampled-data output feedback," *International Journal of Control*, vol. 44, no. 6, pp. 1661–1673, 1986.

[52] L. Qiu and T. W. Chen, "Multirate sampled-data systems: all H_∞ suboptimal controllers and the minimum entropy controller," *IEEE Transactions on Automatic Control*, vol. 44, no. 3, pp. 537–550, 1999.

[53] S. Lall and G. Dullerud, "An LMI solution to the robust synthesis problem for multi-rate sampled-data systems," *Automatica*, vol. 37, no. 12, pp. 1909–1922, 2001.

[54] J. Sheng, T. W. Chen, and S. L. Shah, "Generalized predictive control for non-uniformly sampled systems," *Journal of Process Control*, vol. 12, no. 8, pp. 875–885, 2002.

[55] G. Kreisselmeier, "On sampling without loss of observability/controllability," *IEEE Transactions on Automatic Control*, vol. 44, no. 5, pp. 1021–1025, 1999.

[56] W. Li, S. L. Shah, and D. Y. Xiao, "Kalman filters for non-uniformly sampled multirate systems," in *Proceedings of the 16th Triennial World Congress of the International Federation of Automatic Control*, Prague, Czech Republic, July 2005.

[57] W. Li, Z. Han, and S. L. Shah, "Subspace identification for FDI in systems with non-uniformly sampled multirate data," *Automatica*, vol. 42, no. 4, pp. 619–627, 2006.

[58] P. Zhang, S. X. Ding, G. Z. Wang, and D. H. Zhou, "An FDI approach for sampled-data systems," in *Proceedings of the American Control Conference (ACC '01)*, vol. 4, pp. 2702–2707, Arlington, Va, USA, June 2001.

[59] P. Zhang, S. X. Ding, G. Z. Wang, and D. H. Zhou, "A frequency domain approach to fault detection in sampled-data systems," *Automatica*, vol. 39, no. 7, pp. 1303–1307, 2003.

[60] P. Zhang, S. X. Ding, G. Z. Wang, and D. H. Zhou, "An approach to fault detection of sampled-data systems," Tech. Rep., Institute of Automatic Control and Complex Systems(AKS), University of Duisburg, Duisburg, Germany, 2003.

[61] N. Viswanadham and K. D. Minto, "Fault diagnosis in multirate sampled data systems," in *Proceedings of the 29th IEEE Conference on Decision and Control (CDC '90)*, vol. 6, pp. 3666–3671, Honolulu, Hawaii, USA, December 1990.

[62] M. S. Fadali and W. Liu, "Fault detection for systems with multirate sampling," in *Proceedings of the American Control Conference (ACC '98)*, pp. 3302–3306, Philadelphia, Pa, USA, June 1998.

[63] M. S. Fadali and W. Liu, "Observer-based robust fault detection for a class of multirate sampled-data linear systems," in *Proceedings of the American Control Conference (ACC '99)*, vol. 1, pp. 97–98, San Diego, Calif, USA, June 1999.

[64] M. S. Fadali and H. E. Emara-Shabaik, "Robust fault detection for a class of multirate linear systems," in *Proceedings of the American Control Conference (ACC '00)*, vol. 2, pp. 1210–1214, Chicago, Ill, USA, June 2000.

[65] P. Zhang, S. X. Ding, G. Z. Wang, and D. H. Zhou, "Fault detection for multirate sampled-data systems with time delays," *International Journal of Control*, vol. 75, no. 18, pp. 1457–1471, 2002.

[66] P. Zhang, S. X. Ding, G. Z. Wang, and D. H. Zhou, "Observer-based approaches to fault detection in multirate sampled-data systems," in *Proceedings of the 4th Asian Control Conference*, pp. 1367–1372, Singapore, September 2002.

[67] I. Izadi, Q. Zhao, and T. W. Chen, "An optimal scheme for fast rate fault detection based on multirate sampled data," *Journal of Process Control*, vol. 15, no. 3, pp. 307–319, 2005.

[68] I. Izadi, Q. Zhao, and T. W. Chen, "An H_∞ approach to fast rate fault detection for multirate sampled-data systems," *Journal of Process Control*, vol. 16, no. 6, pp. 651–658, 2006.

[69] P. Zhang and S. X. Ding, "Fault detection of multirate sampled-data systems based on periodic system theory," in *Proceedings of the European Control Conference*, Kos, Greece, July 2007.

[70] P. Zhang, S. X. Ding, R. J. Patton, and C. Kambhampati, "Adaptive and cooperative sampling in networked control systems," in *Proceedings of the IEEE International Conference on Networking, Sensing and Control (ICNSC '07)*, pp. 398–403, London, UK, April 2007.

[71] P. Zhang and S. X. Ding, "On monotonicity of a class of optimal fault detection performance vs. sampling period," in *Proceedings of the 46th IEEE Conference on Decision and Control (CDC '07)*, New Orleans, La, USA, December 2007.

[72] S. X. Ding, P. Zhang, and E. L. Ding, "Observer-based monitoring of distributed net-worked control systems," in *Proceedings of the 6th IFAC Symposium on Fault Detection, Supervision and Safety of Technical Processes (SAFEPROCESS '06)*, pp. 337–342, Beijing, China, August-September 2006.

[73] P. Zhang and S. X. Ding, "Fault detection of networked control systems with limited communication," in *Proceedings of the 6th IFAC Symposium on Fault Detection, Supervision and Safety of Technical Processes (SAFEPROCESS '06)*, pp. 1135–1140, Beijing, China, August-September 2006.

Hindawi Publishing Corporation
Journal of Control Science and Engineering
Volume 2008, Article ID 829459, 16 pages
doi:10.1155/2008/829459

Research Article

Optimal Robust Fault Detection for Linear Discrete Time Systems

Nike Liu and Kemin Zhou

Department of Electrical and Computer Engineering, Louisiana State University, Baton Roug, LA 70803, USA

Correspondence should be addressed to Kemin Zhou, kemin@ece.lsu.edu

Received 30 December 2006; Accepted 7 October 2007

Recommended by Jakob Stoustrup

This paper considers robust fault-detection problems for linear discrete time systems. It is shown that the optimal robust detection filters for several well-recognized robust fault-detection problems, such as $\mathcal{H}_-/\mathcal{H}_\infty$, $\mathcal{H}_2/\mathcal{H}_\infty$, and $\mathcal{H}_\infty/\mathcal{H}_\infty$ problems, are the same and can be obtained by solving a standard algebraic Riccati equation. Optimal filters are also derived for many other optimization criteria and it is shown that some well-studied and seeming-sensible optimization criteria for fault-detection filter design could lead to (optimal) but useless fault-detection filters.

1. INTRODUCTION

It is well recognized that many practical dynamical systems are subject to various environmental changes, unknown disturbances, and changing operating conditions, thus sensors/actuators/components failure and faults in those systems are inevitable. Since any faults/failures in a dynamical system may lead to significant performance degradation, serious system damages, and even loss of human life, it is essential to be able to detect and identify faults and failures in a timely manner so that necessary protective measures can be taken in advance. To that end, fault diagnosis of dynamic systems has received much attention and significant progress has been made in recent years in searching for both data-driven and model-based diagnosis techniques: see [1–5] and the references therein.

Much attention has been devoted to the development of robust fault-detection methods under external disturbances for continuous time systems. Since most (continuous) dynamical systems are nowadays controlled using digital devices, it is also important to understand those theoretical development in the digital (sampled-data) setting. Furthermore, it has been shown in [6] that sample-data fault-detection problem can be converted to equivalent discrete time-detection problem using certain discretization method and thus discrete time fault-detection is of great importance and most nature for modern digital implementation.

One of the particular interesting techniques among all the model-based techniques is observer-based fault-detection filter design [1]. It has been shown in many theoretical studies and applications that suitably designed observer-based fault-detection filters are easy to implement in discrete systems and can be very effective in detecting sensors, actuators, and system components faults. There are significant amount of works addressing this problem using Kalman filter related techniques [7–9]. Nevertheless, finding systemic design methods for systems subject to unknown disturbances and model uncertainties have been proven to be difficult. Since known/unknown disturbances, noise, and model uncertainties are unavoidable for any practical systems, it is essential in the design of any fault-detection filter to take these effects into consideration so that fault detection can be done reliably and robustly. To that effect, many robust filter design techniques, such as $\mathcal{H}_\infty$ optimization, LMI, parity space, and eigen-structure assignment techniques, have been applied to fault detection filter design with limited success [10–15]. The reason is that a fault detection filter design is really a multiple objective design task. It needs not only rejecting disturbance, noise and being insensitive to model uncertainties, it also needs to be as sensitive as possible to possible faults so that early detection of faults is possible. Unfortunately, these two design objectives are almost always conflicting with each other. Hence a design tradeoff between these two objectives is unavoidable and needs to be addressed

explicitly in the design process. To do that, some suitable design criteria for both objectives have to be defined. It has been widely accepted in the field that $\mathcal{H}_2$ norm and $\mathcal{H}_\infty$ of the transfer matrix from disturbances to fault detection residuals are good candidates for measuring up the disturbance rejection capability of a fault detection system. In some cases, $\mathcal{H}_2$ norm of the transfer function matrix from faults to fault detection residual signals is also suitable for evaluating the fault detection system's sensitivity to faults. It has also been recognized that the $\mathcal{H}_-$ index, first introduced by Hou and Patton [16] and further extended by Liu et al. [17], seems to be a very appropriate measure of the fault-detection sensitivity [1–3]. Although this concept was originally proposed for continuous time system, it is quite straightforward to extend this concept to discrete time systems. With such defined performance objectives, several discrete time fault detection design problems can be formulated as multiple objective optimization problems by minimizing the effects of disturbances and maximizing the fault sensitivity, for example, $\mathcal{H}_-/\mathcal{H}_\infty$ problem, $\mathcal{H}_\infty/\mathcal{H}_\infty$ problem, $\mathcal{H}_2/\mathcal{H}_\infty$ problem, $\mathcal{H}_-/\mathcal{H}_2$ problem, and $\mathcal{H}_2/\mathcal{H}_2$ problem. These problems have attracted a great deal of attention recently, [6, 18–25]. However, most of the results obtained in the existing literature are either conservative or complicate to apply. Furthermore, they are usually not guaranteed to be optimal. A notable exception is the work by Ding et al. in [26], where optimal solutions to some formulations of continuous $\mathcal{H}_-/\mathcal{H}_\infty$ and $H_\infty/\mathcal{H}_\infty$ problems are given. Zhang et al. in [27] also give an optimal solution to $\mathcal{H}_\infty/\mathcal{H}_\infty$ problem for linear discrete time periodic systems.

We have developed a new technique to solve the above problems for continuous time systems in [28]. In this paper, we will carry out the parallel development for discrete time problems. Although there are considerable similarities between the continuous and the discrete time solutions, there are also significant differences in some cases where we can give more explicit solutions in discrete time cases that cannot be done in continuous time cases. In addition, explicit discrete time solutions have their own merits in applications. It turns out that our solutions are surprising simple once the problems are suitably formulated.

The rest of this paper is organized as follows: Section 2 introduces the notations and summarizes some key facts that will be used in the later sections. Section 3 gives the mathematical formulations of various fault-detection problems to be solved in this paper. The analytic and optimal solutions for $\mathcal{H}_-/\mathcal{H}_\infty$ problem and $\mathcal{H}_\infty/\mathcal{H}_\infty$ problem are given in Section 4. The solution for $\mathcal{H}_2/\mathcal{H}_\infty$ problem is given in Section 5. The solutions for various $\mathcal{H}_-/\mathcal{H}_2$ problems are discussed in Sections 6–8. Some numerical examples of our fault detection designs are shown in Section 9. Some conclusions are given in Section 10.

2. NOTATIONS AND PRELIMINARY RESULTS

The notations used in this paper are quite standard. The set of m by n real (complex) matrices is denoted as $\mathcal{R}^{m\times n}$ ($\mathcal{C}^{m\times n}$). For a matrix $A \in \mathcal{C}^{m\times n}$ we use A^T to denote its transpose and A' for its complex conjugate transpose. For a Hermitian matrix $A = A' \in \mathcal{C}^{m\times n}$, $\overline{\lambda}(A)$ represents the largest eigenvalue of A and $\underline{\lambda}(A)$ represents the smallest eigenvalue value of A. For $A \in \mathcal{C}^{m\times n}$, $\overline{\sigma}(A) = \sqrt{\overline{\lambda}(AA')} = \sqrt{\overline{\lambda}(A'A)}$ denotes the largest singular value of A and $\underline{\sigma}(A) = \sqrt{\underline{\lambda}(AA')}$ ($\sqrt{\underline{\lambda}(A'A)}$) denotes the smallest singular value of A if $m \le n$ ($m \ge n$). The $n \times n$ identity matrix is denoted as I_n and the $m \times n$ zero matrix is denoted as $0_{m,n}$, with the subscripts dropped if they can be inferred from context.

Discrete transfer matrices and $\mathcal{Z}$-transforms of signals are represented using bold characters and sometimes in dependence of the variable z. A state-space realization of a transfer matrix $\mathbf{G}(z)$ is denoted as

$$\mathbf{G}(z) = \left[\begin{array}{c|c} A & B \\ \hline C & D \end{array}\right] \tag{1}$$

such that $\mathbf{G}(z) = D + C(zI - A)^{-1}B$. We define $\mathbf{G}^{\sim}(z) := \mathbf{G}^T(z^{-1})$ and denote $\mathbf{G}^{-1}(z)$ as the inverse of $\mathbf{G}(z)$ if $\mathbf{G}(z)$ is square and invertible. Now suppose

$$\mathbf{G}(z) = \left[\begin{array}{c|c} A & B \\ \hline C & C \end{array}\right] \tag{2}$$

is square and D is nonsingular, then we have from [29]

$$\mathbf{G}^{-1} = \left[\begin{array}{c|c} A - BD^{-1}C & -BD^{-1} \\ \hline D^{-1}C & D^{-1} \end{array}\right]. \tag{3}$$

We use $\mathcal{RL}_2^{m\times n}$ to denote the set of $m \times n$ real rational transfer matrices with no poles on the unit circle. The superscripts for dimensions will usually be dropped when they are either not important or clear from context. $\mathcal{RH}_2$ ($= \mathcal{RH}_\infty$) is the set of all stable proper transfer matrices.

For $\mathbf{G}(z) \in \mathcal{RH}_2$ we define the $\mathcal{H}_2$ norm of $\mathbf{G}$ as

$$\|\mathbf{G}\|_2 = \sqrt{\frac{1}{2\pi}\int_0^{2\pi} \mathrm{Trace}[\mathbf{G}^{\sim}(e^{j\theta})\mathbf{G}(e^{j\theta})]\,d\theta}. \tag{4}$$

For $\mathbf{G} \in \mathcal{RH}_\infty$ we define the $\mathcal{H}_\infty$ norm of $\mathbf{G}$ as

$$\|\mathbf{G}\|_\infty = \sup_{\theta\in[0,2\pi]} \overline{\sigma}[\mathbf{G}(e^{j\theta})]. \tag{5}$$

Similar to the $\mathcal{H}_-$ definitions of continuous system in [16, 17], we define the $\mathcal{H}_-$ index of a discrete transfer matrix $\mathbf{G}$ on the whole unit circle as

$$\|\mathbf{G}\|_-^{[0,2\pi]} = \inf_{\theta\in[0,2\pi]} \underline{\sigma}(\mathbf{G}(e^{j\theta})). \tag{6}$$

The $\mathcal{H}_-$ index of $\mathbf{G}$ over a finite frequency range $[\theta_1, \theta_2]$ is defined as

$$\|\mathbf{G}\|_-^{[\theta_1,\theta_2]} = \inf_{\theta\in[\theta_1,\theta_2]} \underline{\sigma}(\mathbf{G}(e^{j\theta})). \tag{7}$$

In particular the $\mathcal{H}_-$ index defined at $\theta = 0$ is

$$\|\mathbf{G}\|_-^{[0]} = \underline{\sigma}(\mathbf{G}(1)). \tag{8}$$

If no superscript is added to the $\mathcal{H}_-$ symbol, such as $\|\mathbf{G}\|_-$, then it represents all possible $\mathcal{H}_-$ definitions. In many literatures $\mathcal{H}_-$ index is also called $\mathcal{H}_-$ norm, although it is actually not a norm.

It is easy to show from the definition of singular value of a matrix that we have the following result [30].

Lemma 1. *Let $A \in \mathcal{C}^{m\times n}$ and $B \in \mathcal{C}^{n\times p}$ be two matrices with appropriate dimensions, then $\underline{\sigma}(AB) \le \overline{\sigma}(A)\underline{\sigma}(B)$.*

The following transfer matrix factorizations will be frequently used in this paper and can be found from [29].

Lemma 2 (left coprime factorization). *Let $\mathbf{G}(z)$ be a proper real rational transfer matrix. A left coprime factorization (LCF) of $\mathbf{G}$ is a factorization*

$$\mathbf{G} = \mathbf{M}^{-1}\mathbf{N}, \tag{9}$$

where $\mathbf{N}$ and $\mathbf{M}$ are left-coprime over $\mathcal{RH}_\infty$. Let

$$\mathbf{G} = \left[\begin{array}{c|c} A & B \\ \hline C & D \end{array}\right] \tag{10}$$

be a detectable state-space realization of $\mathbf{G}$ and let L be a matrix with appropriate dimensions such that $A + LC$ is stable, then a left coprime factorization of $\mathbf{G}$ is given by

$$[\mathbf{M}\ \ \mathbf{N}] = \left[\begin{array}{c|cc} A+LC & L & B+LD \\ \hline C & I & D \end{array}\right]. \tag{11}$$

Lemma 3 (Spectral factorization). *Let $\mathbf{G}(z)$ be a proper real rational transfer matrix and let*

$$\mathbf{G} = \left[\begin{array}{c|c} A & B \\ \hline C & D \end{array}\right] \tag{12}$$

be a detectable realization of $\mathbf{G}$. Suppose D has full row rank and $\left[\begin{smallmatrix} A-e^{j\theta}I & B \\ C & D \end{smallmatrix}\right]$ has full row rank for all $\theta \in [0, 2\pi]$. Let $P \ge 0$ be the stabilizing solution to the following algebraic Riccati equation:

$$\begin{aligned} APA' - P - (APC' + BD')(DD' + CPC')^{-1} \\ \times (DB' + CPA') + BB' = 0 \end{aligned} \tag{13}$$

such that $A - (APC' + BD')(DD' + CPC')^{-1}C$ is stable and let $R := DD' + CPC'$. Then the following spectral factorization holds

$$\mathbf{W}\mathbf{W}^{\sim} = \mathbf{G}\mathbf{G}^{\sim}, \tag{14}$$

where $\mathbf{W}^{-1} \in \mathcal{RH}_\infty$ and

$$\mathbf{W} = \left[\begin{array}{c|c} A & (APC' + BD')R^{-1/2} \\ \hline C & R^{1/2} \end{array}\right]. \tag{15}$$

3. PROBLEM FORMULATION

Consider a discrete time invariant system with disturbance and possible faults as:

$$\begin{aligned} x(k+1) &= Ax(k) + Bu(k) + B_d d(k) + B_f f(k), \\ y(k) &= Cx(k) + Du(k) + D_d d(k) + D_f f(k), \end{aligned} \tag{16}$$

where $x(k) \in \mathcal{R}^n$ is the state vector, $y(k) \in \mathcal{R}^{n_y}$ is the output measurement, $d(k) \in \mathcal{R}^{n_d}$ represents the unknown/uncertain disturbance and measurement noise, and $f(k) \in \mathcal{R}^{n_f}$ denotes the process, sensor or actuator fault vector. $f(k)$ and $d(k)$ can be modeled as different types of signals, depending on specific situations under consideration. See Chapters 4 and 8 of [29] and [1] for some detailed discussions. Two frequently used assumptions on $d(k)$ and $f(k)$ are:

(i) unknown signal with bounded energy or bounded power;
(ii) white noise.

Different assumptions on $d(k)$ and $f(k)$ will lead to different fault detection problem formulations and the solutions for all these problems will be discussed in this paper.

All coefficient matrices in (16) are assumed to be known constant matrices. Furthermore, the following assumptions are made.

Assumption 1. (A, C) is detectable.

This is a standard assumption for all fault-detection problems.

Assumption 2. D_d has full row rank.

This means that $n_y \le n_d$ and every measurement of the output signals is either affected by some disturbance or corrupted with some measurement noise. We argue that this assumption can be made without loss of any generality since it is impossible to take perfect measurement in any practical system and furthermore it is reasonable to assume that the measurement noise is independent of each other. So it is reasonable to assume that D_d has full row rank. In the case of some simplified model where D_d does not have full row rank, we can simply add some columns to make it full row rank. For example, suppose that D_d does not have full row rank, then let

$$\widetilde{d} = \begin{bmatrix} d \\ d_\epsilon \end{bmatrix}, \qquad \widetilde{B}_d = [B_d \ \ 0_{n\times n_y}], \qquad \widetilde{D}_d = [D_d \ \ \epsilon I_{n_y}] \tag{17}$$

for a small $\epsilon > 0$. Then $\widetilde{D}_d$ has full row rank.

Assumption 3. $\left[\begin{smallmatrix} A-e^{j\theta}I & B_d \\ C & D_d \end{smallmatrix}\right]$ has full row rank for all $\theta \in [0, 2\pi]$ or, equivalently, the transfer function matrix

$$\mathbf{G}_d := \left[\begin{array}{c|c} A & B_d \\ \hline C & D_d \end{array}\right] \tag{18}$$

has no transmission zero on the unit circle.

This assumption can be relaxed in the same way as in the continuous time case [28].

Remark 1. We want to point out that in several recent work on continuous time fault detection problems [17, 19, 21, 22], it is assumed that D_f has full column rank. We believe that this assumption is extremely restrictive. The assumption implies that measurement y contains directly the independent information on every faulty component of f. In particular,

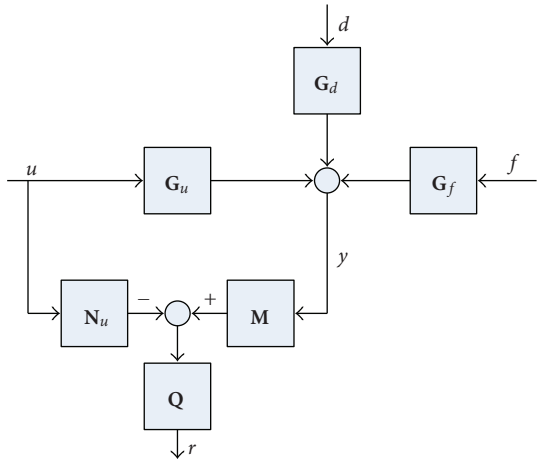

Figure 1: General fault-detection filter structure.

this implies that D_f cannot be zero which is usually not the case when there is only actuator/system component fault and no sensor fault. Furthermore, we believe that the fault detection for sensor fault is relatively easier than that for actuator/system fault.

By taking $\mathcal{Z}$-transform of (16) we have the system input/output equation

$$\mathbf{y} = \mathbf{G}_u\mathbf{u} + \mathbf{G}_d\mathbf{d} + \mathbf{G}_f\mathbf{f}, \tag{19}$$

where $\mathbf{G}_u$, $\mathbf{G}_d$, and $\mathbf{G}_f$ are $n_y \times n_u$, $n_y \times n_d$ and $n_y \times n_f$ transfer matrices, respectively and their state-space realizations are

$$\left[\mathbf{G}_u \;\; \mathbf{G}_d \;\; \mathbf{G}_f\right] = \left[\begin{array}{c|ccc} A & B & B_d & B_f \\ \hline C & D & D_d & D_f \end{array}\right]. \tag{20}$$

Since the state-space realization of $\mathbf{G}_u$, $\mathbf{G}_d$, and $\mathbf{G}_f$ share the same A and C matrices, applying Lemma 2 we can find an LCF for the system (20)

$$\left[\mathbf{G}_u \;\; \mathbf{G}_d \;\; \mathbf{G}_f\right] = \mathbf{M}^{-1}\left[\mathbf{N}_u \;\; \mathbf{N}_d \;\; \mathbf{N}_f\right], \tag{21}$$

where

$$\left[\mathbf{M} \;\; \mathbf{N}_u \;\; \mathbf{N}_d \;\; \mathbf{N}_f\right] = \left[\begin{array}{c|cccc} A+LC & L & B+LD & B_d+LD_d & B_f+LD_f \\ \hline C & I & D & D_d & D_f \end{array}\right] \tag{22}$$

and L is a matrix such that $A + LC$ is stable.

It has been shown in [2] that, without loss of generality, the fault detection filter can take the following general form:

$$\mathbf{r} = \mathbf{Q}(\mathbf{M}\mathbf{y} - \mathbf{N}_u\mathbf{u}) = \mathbf{Q}\left[\mathbf{M} - \mathbf{N}_u\right]\begin{bmatrix}\mathbf{y}\\ \mathbf{u}\end{bmatrix}, \tag{23}$$

where $\mathbf{r}$ is the residual vector for detection, $\mathbf{Q} \in \mathcal{RH}_\infty^{n_y \times n_y}$ is a free stable transfer matrix to be designed. The filter structure is shown in Figure 1. Replacing $\mathbf{y}$ in (23) by the right-hand side of (19) and (21) we have

$$\mathbf{r} = \mathbf{Q}\left[\mathbf{N}_d \;\; \mathbf{N}_f\right]\begin{bmatrix}\mathbf{d}\\ \mathbf{f}\end{bmatrix} = \mathbf{Q}\mathbf{N}_d\mathbf{d} + \mathbf{Q}\mathbf{N}_f\mathbf{f}. \tag{24}$$

Denote the transfer matrices from $\mathbf{d}$ and $\mathbf{f}$ to $\mathbf{r}$ by $\mathbf{G}_{\mathrm{rd}}$ and $\mathbf{G}_{\mathrm{rf}}$, respectively, then

$$\mathbf{G}_{\mathrm{rd}} = \mathbf{Q}\mathbf{N}_d, \qquad \mathbf{G}_{\mathrm{rf}} = \mathbf{Q}\mathbf{N}_f. \tag{25}$$

In general a good fault-detection filter must make a tradeoff between two conflicting performance objectives: robustness to disturbance rejection and sensitivity to faults. To achieve good robustness to disturbance, the influence of disturbance must be minimized at the output of the residual signals. On the other hand, the residual signal should be as sensitive as possible to the faults. Therefore, we need to choose certain performance criteria for measuring these two aspects so that the fault-detection filter design has satisfactory fault detection sensitivity and guaranteed disturbance rejection effect.

Since an $\mathcal{H}_-$ index is a good measurement for a transfer function's smallest gain, $\|\mathbf{G}_{\mathrm{rf}}\|_-$ is a reasonable performance criterion for measuring fault detection sensitivity if $f(k)$ is modeled as unknown energy or power bounded signals. If $d(k)$ is modeled as unknown energy or power bounded signals, then $\mathcal{H}_\infty$ norm is a widely accepted worst case measure and $\|\mathbf{G}_{\mathrm{rd}}\|_\infty$ is a good indicator of disturbance rejection performance. On the other hand, if $d(k)$ and/or $f(k)$ are white noise, the $\mathcal{H}_2$ norms of $\mathbf{G}_{\mathrm{rd}}$ and/or $\mathbf{G}_{\mathrm{rf}}$ seem to be more suitable criteria. See [29] for more detailed discussions and motivations on various performance measures.

We will now formulate several fault-detection filter design problems.

Problem 1 ($\mathcal{H}_-/\mathcal{H}_\infty$ problem). Let an uncertain system be described by (16)–(20) and let $\gamma > 0$ be a given disturbance rejection level. Find a stable transfer matrix $\mathbf{Q} \in \mathcal{RH}_\infty^{n_y \times n_y}$ in (23)–(25) such that $\|\mathbf{G}_{\mathrm{rd}}\|_\infty \le \gamma$ and $\|\mathbf{G}_{\mathrm{rf}}\|_-$ is maximized, that is,

$$\max_{\mathbf{Q}\in\mathcal{RH}_\infty^{n_y\times n_y}} \{\|\mathbf{Q}\mathbf{N}_f\|_- : \|\mathbf{Q}\mathbf{N}_d\|_\infty \le \gamma\}. \tag{26}$$

Problem 2 ($\mathcal{H}_2/\mathcal{H}_\infty$ problem). Let an uncertain system be described by (16)–(20) and let $\gamma > 0$ be a given disturbance rejection level. Find a stable transfer matrix $\mathbf{Q} \in \mathcal{RH}_\infty^{n_y \times n_y}$ in (23)–(25) such that $\|\mathbf{G}_{\mathrm{rd}}\|_\infty \le \gamma$ and $\|\mathbf{G}_{\mathrm{rf}}\|_2$ is maximized, that is,

$$\max_{\mathbf{Q}\in\mathcal{RH}_\infty^{n_y\times n_y}} \{\|\mathbf{Q}\mathbf{N}_f\|_2 : \|\mathbf{Q}\mathbf{N}_d\|_\infty \le \gamma\}. \tag{27}$$

Problem 3 ($\mathcal{H}_-/\mathcal{H}_2$ problem). Let an uncertain system be described by (16)–(20) and let $\gamma > 0$ be a given disturbance rejection level. Find a stable transfer matrix $\mathbf{Q} \in \mathcal{RH}_\infty^{n_y \times n_y}$ in (23)–(25) such that $\|\mathbf{G}_{\mathrm{rd}}\|_2 \le \gamma$ and $\|\mathbf{G}_{\mathrm{rf}}\|_-$ is maximized, that is,

$$\max_{\mathbf{Q}\in\mathcal{RH}_\infty^{n_y\times n_y}} \{\|\mathbf{Q}\mathbf{N}_f\|_- : \|\mathbf{Q}\mathbf{N}_d\|_2 \le \gamma\}. \tag{28}$$

Remark 2. A more conventional formulation of the above problems is to optimize the following:

$$\max_{\mathbf{Q}\in\mathcal{RH}_\infty^{n_y\times n_y}} \frac{\|\mathbf{Q}\mathbf{N}_f\|_X}{\|\mathbf{Q}\mathbf{N}_d\|_Y}, \tag{29}$$

where X and Y can be 2, ∞, or $-$. The problem that $X = Y = 2$ is classical and optimal solution is available [2]. The case for $X = -, \infty$ and $Y = \infty$ has been solved recently in [26] for continuous-time systems. A discrete solution has also been obtained recently in [27] for the cases of $X = \infty$ and $Y = \infty$.

Before we proceed to the solutions of the above problems, we will first establish some preliminary results.

Lemma 4. *Suppose Assumption 3 is satisfied and let $\mathbf{G}_d = \mathbf{M}^{-1}\mathbf{N}_d$ be any left coprime factorization over $\mathcal{RH}_\infty$. Then $\mathbf{N}_d$ has no transmission zero on the unit circle or, equivalently, for any appropriately dimensioned matrix L,*

$$\begin{bmatrix} A + LC - e^{j\theta}I & B_d + LD_d \\ C & D_d \end{bmatrix} \tag{30}$$

has full row rank for all $\theta \in [0, 2\pi]$.

Proof. The result follows by noting that

$$\begin{bmatrix} A + LC - e^{j\theta}I & B_d + LD_d \\ C & D_d \end{bmatrix} = \begin{bmatrix} I & L \\ 0 & I \end{bmatrix} \begin{bmatrix} A - e^{j\theta}I & B_d \\ C & D_d \end{bmatrix} \tag{31}$$

and the fact that all coprime factors have the same unstable transmission zeros [29]. □

An immediate consequence of the above result is the following spectral factorization formula.

Lemma 5. *Suppose Assumptions 1–3 are satisfied and let $\mathbf{G}_d = \mathbf{M}^{-1}\mathbf{N}_d$ be any left coprime factorization over $\mathcal{RH}_\infty$. Then there is a square transfer matrix $\mathbf{V} \in \mathcal{RH}_\infty^{n_y \times n_y}$ such that $\mathbf{V}^{-1} \in \mathcal{RH}_\infty^{n_y \times n_y}$ and*

$$\mathbf{V}\mathbf{V}^{\sim} = \mathbf{N}_d\mathbf{N}_d^{\sim}. \tag{32}$$

In particular, if a state-space representation of $\mathbf{N}_d$ is given as in (22), then a state space representation of $\mathbf{V}$ is given by

$$\mathbf{V} = \left[\begin{array}{c|c} A + LC & [(A + LC)PC' + (B_d + LD_d)D_d']R_d^{-1/2} \\ \hline C0 & R_d^{1/2} \end{array}\right] \tag{33}$$

with

$$\mathbf{V}^{-1} = \left[\begin{array}{c|c} A - (APC' + B_dD_d')R_d^{-1}C & -(APC' + B_dD_d')R_d^{-1} - L \\ \hline R_d^{-1/2}C & R_d^{-1/2} \end{array}\right], \tag{34}$$

where $P \geq 0$ is the stabilizing solution to the Riccati equation

$$\begin{aligned} APA' - P - (APC' + B_dD_d')(D_dD_d' + CPC')^{-1} \\ \times (D_dB_d' + CPA') + B_dB_d' = 0 \end{aligned} \tag{35}$$

such that $A - (APC' + B_dD_d')(D_dD_d' + CPC')^{-1}C$ is stable and $R_d := D_dD_d' + CPC'$.

Proof. Since Assumptions 1–3 are satisfied, Lemmas 3 and 4 can be applied to $\mathbf{N}_d$ to get $\mathbf{V}\mathbf{V}^{\sim} = \mathbf{N}_d\mathbf{N}_d^{\sim}$, where $P \geq 0$ satisfies the following Riccati equation

$$\begin{aligned} A_{LC}PA_{LC}' - P - (A_{LC}PC' + B_{LD}D_d')R_d^{-1} \\ \times (D_dB_{LD}' + CPA_{LC}') + B_{LD}B_{LD}' = 0, \\ A_{LC} := A + LC, \qquad B_{LD} := B + LD. \end{aligned} \tag{36}$$

It is easy to show that the above algebraic Riccati equation can be simplified to (35). The rest of the proof follows from some simple algebraic manipulations. □

The following lemma is the key to the solutions of all the above problems.

Lemma 6. *Suppose Assumptions 1–3 are satisfied. Let $\mathbf{V}, \mathbf{V}^{-1} \in \mathcal{RH}_\infty$ be defined as in (32). Let*

$$\mathbf{Q} = \Psi\mathbf{V}^{-1} \tag{37}$$

for $\Psi \in \mathcal{RH}_\infty$ and denote $\widetilde{\mathbf{N}}_f = \mathbf{V}^{-1}\mathbf{N}_f \in \mathcal{RH}_\infty$. Then the fault-detection Problems 1–3 are equivalent to Problems 4–6 below, respectively.

Problem 4.

$$\max_{\Psi \in \mathcal{RH}_\infty^{n_y \times n_y}} \{\|\Psi\widetilde{\mathbf{N}}_f\|_- : \|\Psi\|_\infty \leq \gamma\}. \tag{38}$$

Problem 5.

$$\max_{\Psi \in \mathcal{RH}_\infty^{n_y \times n_y}} \{\|\Psi\widetilde{\mathbf{N}}_f\|_2 : \|\Psi\|_\infty \leq \gamma\}. \tag{39}$$

Problem 6.

$$\max_{\Psi \in \mathcal{RH}_2^{n_y \times n_y}} \{\|\Psi\widetilde{\mathbf{N}}_f\|_- : \|\Psi\|_2 \leq \gamma\}. \tag{40}$$

Proof. We will first show that Problems 1 and 2 are equivalent to Problems 4 and 5, respectively.

Note that by Lemma 6 there exists $\mathbf{V} \in \mathcal{RH}_\infty$ such that $\mathbf{V}\mathbf{V}^{\sim} = \mathbf{N}_d\mathbf{N}_d^{\sim}$ and $\mathbf{V}^{-1} \in \mathcal{RH}_\infty$. Therefore,

$$\begin{aligned} \|\mathbf{Q}\mathbf{N}_d\|_\infty^2 &= \sup_{\theta \in [0,2\pi]} \overline{\sigma}(\mathbf{Q}(e^{j\theta})\mathbf{N}_d(e^{j\theta})\mathbf{N}_d^{\sim}(e^{j\theta})\mathbf{Q}^{\sim}(e^{j\theta})) \\ &= \sup_{\theta \in [0,2\pi]} \overline{\sigma}(\mathbf{Q}(e^{j\theta})\mathbf{V}(e^{j\theta})\mathbf{V}^{\sim}(e^{j\theta})\mathbf{Q}^{\sim}(e^{j\theta})) \\ &= \|\mathbf{Q}\mathbf{V}\|_\infty^2, \end{aligned} \tag{41}$$

that is, $\|\mathbf{Q}\mathbf{N}_d\|_\infty = \|\mathbf{Q}\mathbf{V}\|_\infty$. We can, therefore without loss of generality, take $\mathbf{Q}$ in the form of $\mathbf{Q} = \Psi\mathbf{V}^{-1}$ for some $\Psi \in \mathcal{RH}_\infty$. Hence $\|\mathbf{Q}\mathbf{N}_d\|_\infty = \|\mathbf{Q}\mathbf{V}\|_\infty = \|\Psi\|_\infty$, so that $\|\mathbf{Q}\mathbf{N}_d\|_\infty \leq \gamma$ is equivalent to $\|\Psi\|_\infty \leq \gamma$. Moreover, $\mathbf{Q}\mathbf{N}_f = \Psi\mathbf{V}^{-1}\mathbf{N}_f = \Psi\widetilde{\mathbf{N}}_f$, hence Problem 1 is equivalent to Problem 4 and Problem 2 is equivalent to Problem 5.

Next we show that Problem 3 is equivalent to Problem 6. Note that in Problem 3, we have $\mathbf{Q}\mathbf{N}_d \in \mathcal{RH}_2$. Hence,

$$\begin{aligned} \|\mathbf{Q}\mathbf{N}_d\|_2^2 &= \frac{1}{2\pi}\int_0^{2\pi} \mathrm{Trace}\{\mathbf{Q}(e^{j\theta})\mathbf{N}_d(e^{j\theta})\mathbf{N}_d^{\sim}(e^{j\theta})\mathbf{Q}^{\sim}(e^{j\theta})\}\,d\theta \\ &= \frac{1}{2\pi}\int_0^{2\pi} \mathrm{Trace}\{\mathbf{Q}(e^{j\theta})\mathbf{V}(e^{j\theta})\mathbf{V}^{\sim}(e^{j\theta})\mathbf{Q}^{\sim}(e^{j\theta})\}\,d\theta \\ &= \|\mathbf{Q}\mathbf{V}\|_2^2 \end{aligned} \tag{42}$$

such that $\|\mathbf{QN}_d\|_2 = \|\mathbf{QV}\|_2$. Since $\mathbf{QV} \in \mathcal{RH}_2$ and $\mathbf{V}, \mathbf{V}^{-1} \in \mathcal{RH}_\infty$, we can let $\mathbf{Q} = \Psi\mathbf{V}^{-1}$ for some $\Psi \in \mathcal{RH}_2$. Therefore, $\|\mathbf{QN}_d\|_2 = \|\mathbf{QV}\|_2 = \|\Psi\|_2$ so that $\|\mathbf{QN}_d\|_2 \le \gamma$ is equivalent to $\|\Psi\|_2 \le \gamma$. Moreover, $\mathbf{QN}_f = \Psi\mathbf{V}^{-1}\mathbf{N}_f = \Psi\widetilde{\mathbf{N}}_f$, hence Problem 3 is equivalent to Problem 6. □

We will provide optimal solutions for each of the above problems in the following sections.

4. $\mathcal{H}_-/\mathcal{H}_\infty$ FAULT-DETECTION FILTER DESIGN

In this section, we give a complete solution for the $\mathcal{H}_-/\mathcal{H}_\infty$ fault-detection filter design problem, that is, Problem 1 or Problem 4.

Theorem 1. *Suppose Assumptions 1–3 are satisfied. Let*

$$\begin{bmatrix}\mathbf{G}_u & \mathbf{G}_d & \mathbf{G}_f\end{bmatrix} = \mathbf{M}^{-1}\begin{bmatrix}\mathbf{N}_u & \mathbf{N}_d & \mathbf{N}_f\end{bmatrix} \tag{43}$$

be any left coprime factorization over $\mathcal{RH}_\infty$ and let $\mathbf{V} \in \mathcal{RH}_\infty$ be a square transfer matrix such that $\mathbf{V}^{-1} \in \mathcal{RH}_\infty$ and $\mathbf{VV}^{\sim} = \mathbf{N}_d\mathbf{N}_d^{\sim}$. Then

$$\max_{\mathbf{Q}\in\mathcal{RH}_\infty^{n_y\times n_y}} \{||\mathbf{QN}_f||_- : ||\mathbf{QN}_d||_\infty \le \gamma\} = \gamma||\mathbf{V}^{-1}\mathbf{N}_f||_- \tag{44}$$

and an optimal fault-detection filter for Problem 1 is given by

$$\mathbf{r} = \mathbf{Q}_{\text{opt}}[\mathbf{M} - \mathbf{N}_u]\begin{bmatrix}\mathbf{y}\\ \mathbf{u}\end{bmatrix}, \tag{45}$$

where

$$\mathbf{Q}_{\text{opt}} = \gamma\mathbf{V}^{-1}. \tag{46}$$

Proof. Note that by Lemma 6, we only need to solve Problem 4:

$$\max_{\Psi\in\mathcal{RH}_\infty^{n_y\times n_y}} \{||\Psi\widetilde{\mathbf{N}}_f||_- : \|\Psi\|_\infty \le \gamma\}. \tag{47}$$

From Lemma 1 we know that for every frequency $\theta \in [0, 2\pi]$,

$$\underline{\sigma}(\Psi(e^{j\theta})\widetilde{\mathbf{N}}_f(e^{j\theta})) \le \overline{\sigma}(\Psi(e^{j\theta}))\underline{\sigma}(\widetilde{\mathbf{N}}_f(e^{j\theta})) \tag{48}$$

so that

$$||\Psi\widetilde{\mathbf{N}}_f||_- \le \|\Psi\|_\infty||\widetilde{\mathbf{N}}_f||_- \le \gamma||\widetilde{\mathbf{N}}_f||_-. \tag{49}$$

By letting $\Psi = \gamma I$, we have $\|\Psi\|_\infty = \gamma$ and $\|\Psi\widetilde{\mathbf{N}}_f\|_- = \gamma\|\widetilde{\mathbf{N}}_f\|_-$, which means that $\Psi = \gamma I$ is an optimal solution achieving the maximum. □

Remark 3. The optimal fault-detection filter given in Theorem 1 does not depend on B_f and D_f matrices.

Remark 4. Note that the solution given in the above theorem does not depend on the specific definitions of $\mathcal{H}_-$ index. Hence, the solution provided here is an optimal solution for all $\mathcal{H}_-$ indices. However, it should be pointed out that this optimal filter is not the only optimal solution for some $\mathcal{H}_-$ index criterion. For example, let $\mathbf{Q} = \gamma\mathbf{L}(z)\mathbf{V}^{-1}$ where $L \in \mathcal{RH}_\infty$ is a low-pass filter with a very small bandwidth so that $\|\mathbf{L}(z)\|_\infty = 1$ and $\mathbf{L}(1) = I$. Then this $\mathbf{Q}$ is also an optimal solution for

$$\max_{\mathbf{Q}\in\mathcal{RH}_\infty^{n_y\times n_y}} \left\{||\mathbf{QN}_f||_-^{[0]} : ||\mathbf{QN}_d||_\infty \le \gamma\right\}, \tag{50}$$

even though this is obviously a bad fault-detection filter because the low-pass filter $L(z)$ would make the filter much less sensitive to faults.

Note also that the solution given in the above theorem is completely general and it does not depend on specific state space representation of those coprime factorization and spectral factorization, which may be necessary in some fault tolerant control applications [5, 31]. On the other hand, if those specific state-space coprime and spectral factorizations in the previous sections are used, the optimal filter can be written in a very simple form.

Theorem 2. *Suppose Assumptions 1–3 are satisfied. Let $P \ge 0$ be the stabilizing solution to the Riccati equation*

$$\begin{aligned}APA' - P - (APC' + B_dD_d')(D_dD_d' + CPC')^{-1}\\ \times(D_dB_d' + CPA') + B_dB_d' = 0\end{aligned} \tag{51}$$

such that $A - (APC' + B_dD_d')(D_dD_d' + CPC')^{-1}C$ is stable and let $R_d = D_dD_d' + CPC'$. Define

$$L_0 = -(APC' + B_dD_d')R_d^{-1}. \tag{52}$$

Then

$$\max_{\mathbf{Q}\in\mathcal{RH}_\infty^{n_y\times n_y}} \{||\mathbf{QN}_f||_- : ||\mathbf{QN}_d||_\infty \le \gamma\} = \gamma||\mathbf{V}^{-1}\mathbf{N}_f||_- \tag{53}$$

and an optimal $\mathcal{H}_-/\mathcal{H}_\infty$ fault-detection filter has the following state space representation

$$\mathbf{r} = \mathbf{Q}_{\text{opt}}[\mathbf{M} - \mathbf{N}_u]\begin{bmatrix}\mathbf{y}\\ \mathbf{u}\end{bmatrix}, \tag{54}$$

where

$$\begin{aligned}\mathbf{Q}_{\text{opt}}[\mathbf{M} - \mathbf{N}_u] &= \gamma\left[\begin{array}{c|cc} A + L_0C & -L_0 & B + L_0D\\ \hline -R_d^{-1/2}Ct & R_d^{-1/2} & -R_d^{-1/2}D\end{array}\right],\\ \mathbf{V}^{-1}\mathbf{N}_f &= \left[\begin{array}{c|c} A + L_0C & B_f + L_0D_f\\ \hline R_d^{-1/2}C & R_d^{-1/2}D_f\end{array}\right].\end{aligned} \tag{55}$$

In other words, the optimal $\mathcal{H}_-/\mathcal{H}_\infty$ fault-detection filter is the following observer:

$$\begin{aligned}\hat{x}(k+1) &= (A + L_0C)\hat{x}(k) - L_0y(t) + (B + L_0D)u(k)\\ r(k) &= \gamma R_d^{-1/2}(y(k) - C\hat{x}(k) - Du(k)).\end{aligned} \tag{56}$$

Proof. Note that

$$\begin{bmatrix}\mathbf{M} & \mathbf{N}_u\end{bmatrix} = \left[\begin{array}{c|cc} A + LC & L & B + LD\\ \hline C & I & D\end{array}\right], \tag{57}$$

where L is a matrix with appropriate dimensions such that $A + LC$ is stable. Note from Theorem 1 and Lemma 5 that

$$\mathbf{Q}_{\text{opt}} = \gamma \mathbf{V}^{-1} = \gamma \left[\begin{array}{c|c} A + L_0 C & L_0 - L \\ \hline R_d^{-1/2} C & R_d^{-1/2} \end{array}\right]. \tag{58}$$

Then

$$\begin{aligned}
&\mathbf{Q}_{\text{opt}}[\mathbf{M} - \mathbf{N}_u] \\
&= \gamma \left[\begin{array}{c|c} A + L_0 C & L_0 - L \\ \hline R_d^{-1/2} C & R_d^{-1/2} \end{array}\right] \left[\begin{array}{c|cc} A + LC & L & -(B + LD) \\ \hline C & I & -D \end{array}\right] \\
&= \gamma \left[\begin{array}{cc|cc} A + L_0 C & L_0 C - LC & L_0 - L & -(L_0 - L)D \\ 0 & A + LC & L & -(B + LD) \\ \hline R_d^{-1/2} C & R_d^{-1/2} C & R_d^{-1/2} & -R_d^{-1/2} D \end{array}\right] \\
&= \gamma \left[\begin{array}{cc|cc} A + L_0 C & 0 & L_0 & -(B + L_0 D) \\ 0 & A + LC & L & -(B + LD) \\ \hline R^{-1/2} C & 0 & R_d^{-1/2} & -R_d^{-1/2} D \end{array}\right] \\
&= \gamma \left[\begin{array}{c|cc} A + L_0 C & L_0 & -(B + L_0 D) \\ \hline R_d^{-1/2} C & R_d^{-1/2} & -R_d^{-1/2} D \end{array}\right] \\
&= \gamma \left[\begin{array}{c|cc} A + L_0 C & -L_0 & B + L_0 D \\ \hline -R_d^{-1/2} C & R_d^{-1/2} & -R_d^{-1/2} D \end{array}\right].
\end{aligned} \tag{59}$$

Similarly, we have

$$\begin{aligned}
&\mathbf{V}^{-1}\mathbf{N}_f \\
&= \left[\begin{array}{c|c} A + L_0 C & L_0 - L \\ \hline R_d^{-1/2} C & R_d^{-1/2} \end{array}\right] \left[\begin{array}{c|c} A + LC & B_f + LD_f \\ \hline C & D_f \end{array}\right] \\
&= \left[\begin{array}{cc|c} A + L_0 C & (L_0 - L)C & (L_0 - L)D_f \\ 0 & A + LC & B_f + LD_f \\ \hline R_d^{-1/2} C & R_d^{-1/2} C & R_d^{-1/2} D_f \end{array}\right] \\
&= \left[\begin{array}{cc|c} A + L_0 C & 0 & B_f + L_0 D_f \\ 0 & A + LC & B_f + LD_f \\ \hline R_d^{-1/2} C & 0 & R_d^{-1/2} D_f \end{array}\right] \\
&= \left[\begin{array}{c|c} A + L_0 C & B_f + L_0 D_f \\ \hline R_d^{-1/2} C & R_d^{-1/2} D_f \end{array}\right].
\end{aligned} \tag{60}$$

□

Remark 5. Note that the optimal fault-detection filter $\mathbf{Q}_{\text{opt}}[\mathbf{M} - \mathbf{N}_u]$ is independent of the choice of L matrix.

Remark 6. It is easy to see that our optimal filter given in Theorems 1 and 2 is also optimal for the so-called $\mathcal{H}_\infty/\mathcal{H}_\infty$ problem

$$\max_{\mathbf{Q} \in \mathcal{RH}_\infty^{n_y \times n_y}} \{ ||\mathbf{Q}\mathbf{N}_f||_\infty : ||\mathbf{Q}\mathbf{N}_d||_\infty \le \gamma \} \tag{61}$$

and it turns out this filter is the same as the one given by Zhang et al. in [27] under the following equivalent optimization criterion:

$$\max_{\mathbf{Q}} \frac{||\mathbf{Q}\mathbf{N}_f||_\infty}{||\mathbf{Q}\mathbf{N}_d||_\infty}. \tag{62}$$

5. $\mathcal{H}_2/\mathcal{H}_\infty$ FAULT-DETECTION FILTER DESIGN

In this section, we give an optimal solution for the $\mathcal{H}_2/\mathcal{H}_\infty$ problem stated in Section 3 as Problem 2. Similar to the solution for $\mathcal{H}_-/\mathcal{H}_\infty$ problem given in Theorems 1 and 2, we have the following parallel results for the $\mathcal{H}_2/\mathcal{H}_\infty$ problem.

Theorem 3. *Suppose Assumptions 1–3 are satisfied. Let*

$$[\mathbf{G}_u \;\; \mathbf{G}_d \;\; \mathbf{G}_f] = \mathbf{M}^{-1}[\mathbf{N}_u \;\; \mathbf{N}_d \;\; \mathbf{N}_f] \tag{63}$$

be any left coprime factorization over $\mathcal{RH}_\infty$ and let $\mathbf{V} \in \mathcal{RH}_\infty$ be a square transfer matrix such that $\mathbf{V}^{-1} \in \mathcal{RH}_\infty$ and $\mathbf{V}\mathbf{V}^{\sim} = \mathbf{N}_d\mathbf{N}_d^{\sim}$. Then

$$\max_{\mathbf{Q} \in \mathcal{RH}_\infty^{n_y \times n_y}} \{ ||\mathbf{Q}\mathbf{N}_f||_2 : ||\mathbf{Q}\mathbf{N}_d||_\infty \le \gamma \} = \gamma ||\mathbf{V}^{-1}\mathbf{N}_f||_2 \tag{64}$$

and the optimal fault-detection filter for Problem 1 given in Theorems 1 and 2 is also the optimal filter for this problem.

Proof. Note that by Lemma 6, we only need to solve Problem 5:

$$\max_{\Psi \in \mathcal{RH}_\infty^{n_y \times n_y}} \{ ||\Psi\tilde{\mathbf{N}}_f||_2 : \|\Psi\|_\infty \le \gamma \}. \tag{65}$$

Note that

$$||\Psi\tilde{\mathbf{N}}_f||_2 \le \|\Psi\|_\infty ||\tilde{\mathbf{N}}_f||_2 \le \gamma ||\tilde{\mathbf{N}}_f||_2. \tag{66}$$

By letting $\Psi = \gamma I$, we have $\|\Psi\|_\infty = \gamma$ and $\|\Psi\tilde{\mathbf{N}}_f\|_2 = \gamma\|\tilde{\mathbf{N}}_f\|_2$, which means that $\Psi = \gamma I$ is an optimal solution achieving the maximum. □

6. $\mathcal{H}_-/\mathcal{H}_2$ FAULT-DETECTION FILTER DESIGN: CASE 1

From Lemma 6 we know that the $\mathcal{H}_-/\mathcal{H}_2$ problem is equivalent to Problem 6, that is,

$$\max_{\Psi \in \mathcal{RH}_2^{n_y \times n_y}} \{ ||\Psi\tilde{\mathbf{N}}_f||_- : \|\Psi\|_2 \le \gamma \}. \tag{67}$$

Unlike the $\mathcal{H}_-/\mathcal{H}_\infty$ problem studied in Section 4, we have different solutions for the $\mathcal{H}_-/\mathcal{H}_2$ problem if different $\mathcal{H}_-$ definitions are considered. In this section and the next two sections we will illustrate this point and give solutions for all cases.

Theorem 4. *Suppose Assumptions 1–3 are satisfied. Then*

$$\sup_{\mathbf{Q} \in \mathcal{RH}_\infty^{n_y \times n_y}} \left\{ ||\mathbf{Q}\mathbf{N}_f||_-^{[0]} : ||\mathbf{Q}\mathbf{N}_d||_2 \le \gamma \right\} = \infty. \tag{68}$$

Furthermore, for any given $\alpha > 0$, let $2 > \epsilon > 0$ and

$$\mathbf{Q}_{\text{sub}} = \frac{\gamma\sqrt{\epsilon(2 - \epsilon)}}{z - 1 + \epsilon}\mathbf{V}^{-1}. \tag{69}$$

Then

$$\left\{ ||\mathbf{Q}_{\text{sub}}\mathbf{N}_f||_-^{[0]} > \alpha,\ ||\mathbf{Q}_{\text{sub}}\mathbf{N}_d||_2 \le \gamma \right\} \tag{70}$$

is satisfied for a sufficiently small $\epsilon > 0$.

Proof. Again note that the equivalent Problem 6 in this case is

$$\sup_{\Psi\in\mathcal{RH}_2^{n_y\times n_y}}\left\{\left|\left|\Psi\tilde{\mathbf{N}}_f\right|\right|_-^{[0]}:\|\Psi\|_2\le\gamma\right\}. \tag{71}$$

Take $\Psi(z)=\left(\gamma\sqrt{\epsilon(2-\epsilon)}\right)/(z-1+\epsilon)I$ such that $2>\epsilon>0$. Then $\Psi(1)=\gamma\sqrt{2-\epsilon/\epsilon}I$ and $\|\Psi\|_2=\gamma$. Let $\epsilon\to 0$, then $\Psi(1)\to\infty$, so that

$$\left|\left|\Psi\tilde{\mathbf{N}}_f\right|\right|_-^{[0]}=\underline{\sigma}(\Psi(1)\tilde{\mathbf{N}}_f(1))=\gamma\sqrt{\frac{2-\epsilon}{\epsilon}}\underline{\sigma}(\tilde{\mathbf{N}}_f(1))\longrightarrow\infty. \tag{72}$$

□

Remark 7. We should point out that an optimal filter designed using Theorem 4 is not necessarily good for fault detection since this optimal filter can be extremely narrowbanded near 0 frequency so that any higher frequency component of fault may not be detected.

7. $\mathcal{H}_-/\mathcal{H}_2$ FAULT-DETECTION FILTER DESIGN: CASE 2

In this section, we will consider another special case where the $\mathcal{H}_-$ index is defined for all frequencies but with D_f full column rank. As we have mentioned before, this is a very restrictive case. We are interested in this case because an analytic solution is possible.

Lemma 7. *Suppose D_f has full column rank. Then an optimal solution Ψ_{opt} to Problem 6*

$$\max_{\Psi\in\mathcal{RH}_2^{n_y\times n_y}}\left\{\left|\left|\Psi\tilde{\mathbf{N}}_f\right|\right|_-^{[0,2\pi]}:\|\Psi\|_2\le\gamma\right\} \tag{73}$$

has the form $\Psi_{\text{opt}}=U\Psi_o$ and

$$\Psi_o\tilde{\mathbf{N}}_f=\begin{bmatrix}\alpha I_{n_f}\\ 0_{(n_y-n_f)\times n_f}\end{bmatrix}, \tag{74}$$

where α is a positive scalar and U is an $n_y\times n_y$ all-pass stable transfer matrix.

Proof. We will first show

$$\underline{\sigma}\left(\Psi_{\text{opt}}(e^{j\theta})\tilde{\mathbf{N}}_f(e^{j\theta})\right)=C\quad\text{for every }\theta\in[0,2\pi], \tag{75}$$

where C is a nonnegative scalar.

Suppose there exists a Ψ_{opt} such that $\underline{\sigma}(\Psi_{\text{opt}}(e^{j\theta})\tilde{\mathbf{N}}_f(e^{j\theta}))=C$ does not hold. Let Θ_1 denote the set of all θ values such that $\underline{\sigma}(\Psi_{\text{opt}}(e^{j\theta})\tilde{\mathbf{N}}_f(e^{j\theta}))=\|\Psi_{\text{opt}}\tilde{\mathbf{N}}_f\|_-^{[0,2\pi]}$ is achieved. Let $\Theta_2:=[0,2\pi]-\Theta_1$ such that

$$\underline{\sigma}(\Psi_{\text{opt}}(e^{j\theta})\tilde{\mathbf{N}}_f(e^{j\theta}))_{\theta\in\Theta_1}<\underline{\sigma}(\Psi_{\text{opt}}(e^{j\theta})\tilde{\mathbf{N}}_f(e^{j\theta}))_{\theta\in\Theta_2}. \tag{76}$$

Then there exists a weighting function $\mathbf{W}\in\mathcal{RH}_\infty^{n_y\times n_y}$ such that $\|\mathbf{W}\Psi_{\text{opt}}\|_2=\|\Psi_{\text{opt}}\|_2$ and

$$\begin{aligned}&\underline{\sigma}(\Psi_{\text{opt}}(e^{j\theta})\mathbf{N}_f(e^{j\theta}))_{\theta\in\Theta_1}\\&<\underline{\sigma}(\mathbf{W}(e^{j\theta})\Psi_{\text{opt}}(e^{j\theta})\tilde{\mathbf{N}}_f(e^{j\theta}))_{\theta\in\Theta_1}\\&\le\underline{\sigma}(\mathbf{W}(e^{j\theta})\Psi_{\text{opt}}(e^{j\theta})\mathbf{N}_f(e^{j\theta}))_{\theta\in\Theta_2}.\end{aligned} \tag{77}$$

Therefore, $\|\mathbf{W}\Psi_{\text{opt}}\tilde{\mathbf{N}}_f\|_-^{[0,2\pi]}>\|\Psi_{\text{opt}}\tilde{\mathbf{N}}_f\|_-^{[0,2\pi]}$ and Ψ_{opt} is not an optimal solution. Hence, it must be true that $\underline{\sigma}(\Psi_{\text{opt}}(e^{j\theta})\tilde{\mathbf{N}}_f(e^{j\theta}))=C$ for every $\theta\in[0,2\pi]$.

Next we show that

$$\begin{aligned}&\overline{\sigma}(\Psi_{\text{opt}}(e^{j\theta})\tilde{\mathbf{N}}_f(e^{j\theta}))\\&\quad=\underline{\sigma}(\Psi_{\text{opt}}(e^{j\theta})\tilde{\mathbf{N}}_f(e^{j\theta}))\quad\text{for every }\theta\in[0,2\pi].\end{aligned} \tag{78}$$

Suppose there exists a Ψ_{opt} such that $\overline{\sigma}(\Psi_{\text{opt}}(e^{j\theta_1})\tilde{\mathbf{N}}_f(e^{j\theta_1}))\neq\underline{\sigma}(\Psi_{\text{opt}}(e^{j\theta_1})\tilde{\mathbf{N}}_f(e^{j\theta_1}))$ for some θ_1, that is,

$$\begin{aligned}\overline{\sigma}(\Psi_{\text{opt}}(e^{j\theta_1})\tilde{\mathbf{N}}_f(e^{j\theta_1}))&>\underline{\sigma}(\Psi_{\text{opt}}(e^{j\theta_1})\tilde{\mathbf{N}}_f(e^{j\theta_1}))\\&=\left|\left|\Psi_{\text{opt}}\tilde{\mathbf{N}}_f\right|\right|_-^{[0,2\pi]}.\end{aligned} \tag{79}$$

Then a Ψ_1 can be selected such that

$$\begin{aligned}&\underline{\sigma}(\Psi_1(e^{j\theta})\tilde{\mathbf{N}}_f(e^{j\theta}))=\underline{\sigma}(\Psi_{\text{opt}}(e^{j\theta})\tilde{\mathbf{N}}_f(e^{j\theta})),\quad\forall\,\theta\in[0,2\pi],\\&\overline{\sigma}(\Psi_1(e^{j\theta_1})\tilde{\mathbf{N}}_f(e^{j\theta_1}))<\overline{\sigma}(\Psi_{\text{opt}}(e^{j\theta_1})\tilde{\mathbf{N}}_f(e^{j\theta_1})),\\&\left|\left|\Psi_1\right|\right|_2<\left|\left|\Psi_{\text{opt}}\right|\right|_2.\end{aligned} \tag{80}$$

Since $\underline{\sigma}(\Psi_{\text{opt}}(e^{j\theta})\tilde{\mathbf{N}}_f(e^{j\theta}))=C$ for every $\theta\in[0,2\pi]$, $\|\Psi_1\tilde{\mathbf{N}}_f\|_-^{[0,2\pi]}=\|\Psi_{\text{opt}}\tilde{\mathbf{N}}_f\|_-^{[0,2\pi]}$. Let $\Psi_2=\|\Psi_{\text{opt}}\|_2/\|\Psi_1\|_2\Psi_1$, then $\|\Psi_2\|_2=\|\Psi_{\text{opt}}\|_2$ and

$$\begin{aligned}\left|\left|\Psi_2\tilde{\mathbf{N}}_f\right|\right|_-^{[0,2\pi]}&=\frac{\left|\left|\Psi_{\text{opt}}\right|\right|_2}{\left|\left|\Psi_1\right|\right|_2}\left|\left|\Psi_1\tilde{\mathbf{N}}_f\right|\right|_-^{[0,2\pi]}\\&=\frac{\left|\left|\Psi_{\text{opt}}\right|\right|_2}{\left|\left|\Psi_1\right|\right|_2}\left|\left|\Psi_{\text{opt}}\,\tilde{\mathbf{N}}_f\,\right|\right|_-^{[0,2\pi]}>\left|\left|\Psi_{\text{opt}}\tilde{\mathbf{N}}_f\right|\right|_-^{[0,2\pi]}.\end{aligned} \tag{81}$$

Therefore, Ψ_{opt} is not optimal and by contradiction the assumption is false. So $\overline{\sigma}(\Psi_{\text{opt}}(e^{j\theta})\tilde{\mathbf{N}}_f(e^{j\theta}))=\underline{\sigma}(\Psi_{\text{opt}}(e^{j\theta})\tilde{\mathbf{N}}_f(e^{j\theta}))$ holds for every $\theta\in[0,2\pi]$.

Since $\overline{\sigma}(\Psi_{\text{opt}}(e^{j\theta})\tilde{\mathbf{N}}_f(e^{j\theta}))=\underline{\sigma}(\Psi_{\text{opt}}(e^{j\theta})\tilde{\mathbf{N}}_f(e^{j\theta}))=C$ for every $\theta\in[0,2\pi]$, and that D_f has full column rank implies $n_y\ge n_f$, $\Psi_{\text{opt}}\tilde{\mathbf{N}}_f$ has the form

$$\mathbf{\Psi}_{\text{opt}}\tilde{\mathbf{N}}_f=U\begin{bmatrix}\alpha I_{n_f}\\ 0_{(n_y-n_f)\times n_f}\end{bmatrix}, \tag{82}$$

where U is an all-pass stable transfer matrix and α is a positive scalar. Let $\Psi_{\text{opt}}=U\Psi_o$, then

$$\Psi_o\tilde{\mathbf{N}}_f=\begin{bmatrix}\alpha I_{n_f}\\ 0_{(n_y-n_f)\times n_f}\end{bmatrix}. \tag{83}$$

□

Lemma 8. *Suppose D_f has full column rank. Then Problem 6*

$$\max_{\Psi\in\mathcal{RH}_2^{n_y\times n_y}}\left\{\left|\left|\Psi\tilde{\mathbf{N}}_f\right|\right|_-^{[0,2\pi]}:\|\Psi\|_2\le\gamma\right\} \tag{84}$$

is equivalent to the following problem.

Problem 7.

$$\min_{\widetilde{\mathbf{N}}_f^+ \in \mathcal{RH}_2^{n_f \times n_y}} \{ \| \widetilde{\mathbf{N}}_f^+ \|_2 : \widetilde{\mathbf{N}}_f^+ \widetilde{\mathbf{N}}_f = I \}. \tag{85}$$

Proof. From Lemma 7 we know that the optimal solution to Problem 6 has the form $\Psi_{\text{opt}} = U\Psi_o$ and

$$\Psi_o \widetilde{\mathbf{N}}_f = \begin{bmatrix} \alpha I_{n_f} \\ 0_{(n_y - n_f)\times n_f} \end{bmatrix}. \tag{86}$$

Let $\Psi_o = \left[\begin{smallmatrix} \Psi_1 \\ \Psi_2 \end{smallmatrix}\right]$, where Ψ_1 is $n_f \times n_y$ and Ψ_2 is $(n_y - n_f) \times n_y$. Then $\left[\begin{smallmatrix} \Psi_1 \widetilde{\mathbf{N}}_f \\ \Psi_2 \widetilde{\mathbf{N}}_f \end{smallmatrix}\right] = \left[\begin{smallmatrix} \alpha I \\ 0 \end{smallmatrix}\right]$ so $\Psi_2 = 0$ and $\|\Psi_o\|_2 = \|\Psi_1\|_2$. Since Problem 6 needs to maximize $\|\Psi \widetilde{\mathbf{N}}_f\|_-$ with the constraint $\|\Psi\|_2 \le \gamma$, it is equivalent to find a Ψ_1 with the smallest $\mathcal{H}_2$ norm such that $\Psi_1 \widetilde{\mathbf{N}}_f = I$. Denote $\Psi_1 = \widetilde{\mathbf{N}}_f^+$, then Problem 6 is equivalent to Problem 7. □

In [32] the solution to a dual problem of Problem 7 is given. Similarly, we have the solution to Problem 7 given by the following lemma.

Lemma 9. *Assume*

$$\mathbf{H}(z) = \left[\begin{array}{c|c} A & B \\ \hline C & D \end{array}\right] \tag{87}$$

is strictly minimum phase and D has full column rank. Let $D^+ = D(D'D)^{-1}, D_\perp$ is chosen such that $D_\perp' D_\perp = I - D(D'D)^{-1}D'$ and $A_0 = A - B(D^+)'C$, then the optimal solution to problem

$$\min_{\mathbf{H}^+(z) \in \mathcal{RH}_2^{n_f \times n_y}} \{ \| \mathbf{H}^+(z) \|_2 : H^+(z)\mathbf{H}(z) = I \} \tag{88}$$

is given by

$$\mathbf{H}^+(z)_{\text{opt}} = \left[\begin{array}{c|c} A + KC & K \\ \hline RC & R \end{array}\right], \tag{89}$$

where $Q \ge 0$ is the solution to the algebraic Ricatti equation

$$\begin{aligned} Q &= A_0' Q A_0 - A_0' Q C' D_\perp' \left(I + D_\perp C Q C' D_\perp'\right)^{-1} D_\perp C Q A_0 \\ &\quad + B(D'D)^{-1}B', \\ K &= -B(D^+)' - A_0 Q C' D_\perp' \left(I + D_\perp C Q C' D_\perp'\right)^{-1} D_\perp, \\ R &= (D^+)' \left(I + C Q C' D_\perp' D_\perp\right)^{-1}. \end{aligned} \tag{90}$$

Proof. The equation $\mathbf{H}^+(z)\mathbf{H}(z) = I$ is equivalent to $\mathbf{H}^T(z)(\mathbf{H}^+(z))^T = I$, so Problem 7 is equivalent to finding an $\mathbf{H}^{(\text{rinv})}(z)$ with the smallest $\mathcal{H}_2$ norm such that $\mathbf{H}^T(z)\mathbf{H}^{(\text{rinv})}(z) = I$. Hence the conclusion in [32] can be applied to $\mathbf{H}^T(z)$ to get the optimal $\mathbf{H}^{(\text{rinv})}(z)_{\text{opt}}$. $\mathbf{H}^+(z)_{\text{opt}}$ is then obtained by taking transpose of $\mathbf{H}^{(\text{rinv})}(z)_{\text{opt}}$. □

Theorem 5. *Suppose Assumptions 1–3 are satisfied. Let G_f has all zeros inside the unit circle and D_f has full column rank. Let*

$$[\mathbf{G}_u \;\; \mathbf{G}_d \;\; \mathbf{G}_f] = \mathbf{M}^{-1}[\mathbf{N}_u \;\; \mathbf{N}_d \;\; \mathbf{N}_f] \tag{91}$$

be any left coprime factorization over $\mathcal{RH}_\infty$ and let $\mathbf{V} \in \mathcal{RH}_\infty$ be a square transfer matrix such that $\mathbf{V}^{-1} \in \mathcal{RH}_\infty$ and $\mathbf{V}\mathbf{V}^\sim = \mathbf{N}_d \mathbf{N}_d^\sim$. Let $(\widetilde{\mathbf{N}}_f^+)_{\text{opt}} = (\mathbf{V}^{-1}\mathbf{N}_f)^+_{\text{opt}}$ be the optimal solution to Problem 7. Then

$$\max_{\mathbf{Q} \in \mathcal{RH}_2^{n_y \times n_y}} \left\{ \| \mathbf{Q}\mathbf{N}_f \|_-^{[0,2\pi]} : \| \mathbf{Q}\mathbf{N}_d \|_\infty \le \gamma \right\} = \frac{\gamma}{\| (\mathbf{V}^{-1}\mathbf{N}_f)^+_{\text{opt}} \|_2} \tag{92}$$

and an optimal fault detection filter is given by

$$\mathbf{r} = \mathbf{Q}_{\text{opt}} [\mathbf{M} - \mathbf{N}_u] \begin{bmatrix} \mathbf{y} \\ \mathbf{u} \end{bmatrix}, \tag{93}$$

where

$$\mathbf{Q}_{\text{opt}} = \frac{\gamma}{\| (\mathbf{V}^{-1}\mathbf{N}_f)^+_{\text{opt}} \|_2} \begin{bmatrix} (\mathbf{V}^{-1}\mathbf{N}_f)^+_{\text{opt}} \mathbf{V}^{-1} \\ 0 \end{bmatrix}. \tag{94}$$

Proof. Note that by Lemma 6, we only need to solve Problem 6

$$\max_{\Psi \in \mathcal{RH}_2^{n_y \times n_y}} \left\{ \| \Psi \widetilde{\mathbf{N}}_f \|_-^{[0,2\pi]} : \| \Psi \|_2 \le \gamma \right\}. \tag{95}$$

Since G_f has all zeros inside the unit circle and $\mathbf{V}^{-1} \in \mathcal{RH}_\infty$, $\widetilde{\mathbf{N}}_f$ is strictly minimum phase. From Lemmas 7–9 we know that the optimal solutionto Problem 6 is given by

$$\Psi_{\text{opt}} = U \frac{\gamma}{\| (\widetilde{\mathbf{N}}_f^+)_{\text{opt}} \|_2} \begin{bmatrix} (\widetilde{\mathbf{N}}_f^+)_{\text{opt}} \\ 0 \end{bmatrix}, \tag{96}$$

where $(\widetilde{\mathbf{N}}_f^+)_{\text{opt}} = (\mathbf{V}^{-1}\mathbf{N}_f)^+_{\text{opt}}$ is the optimal solution to Problem 7 and U is a unitary matrix. Take $U = I$, then an optimal solution is given by

$$\begin{aligned} \mathbf{Q}_{\text{opt}} &= \frac{\gamma}{\| (\widetilde{\mathbf{N}}_f^+)_{\text{opt}} \|_2} \begin{bmatrix} (\widetilde{\mathbf{N}}_f^+)_{\text{opt}} \mathbf{V}^{-1} \\ 0 \end{bmatrix} \\ &= \frac{\gamma}{\| (\mathbf{V}^{-1}\mathbf{N}_f)^+_{\text{opt}} \|_2} \begin{bmatrix} (\mathbf{V}^{-1}\mathbf{N}_f)^+_{\text{opt}} \mathbf{V}^{-1} \\ 0 \end{bmatrix}. \end{aligned} \tag{97}$$

□

Again the solution given in the above theorem is general and it does not depend on specific state-space representation of those coprime factorization and spectral factorization. If specific state-space coprime and spectral factorization in the previous section are used, the optimal filter can be written in an explicit form.

Theorem 6. *Suppose Assumptions 1–3 are satisfied. Let G_f has all zeros inside the unit circle and D_f has full column rank. Let $P \ge 0$ be the stabilizing solution to the Riccati equation*

$$\begin{aligned} APA' - P - \left(APC' + B_d D_d'\right)\left(D_d D_d' + CPC'\right)^{-1} \\ \times \left(D_d B_d' + CPA'\right) + B_d B_d' = 0 \end{aligned} \tag{98}$$

such that $A-(APC'+B_dD_d')(D_dD_d'+CPC')^{-1}C$ *is stable. Let* $R_d=D_dD_d'+CPC'$ *and define*

$$L_0=-(APC'+B_dD_d')R_d^{-1}. \tag{99}$$

Let $D^+=R_d^{-1/2}D_f(D_f'R_d^{-1}D_f)^{-1}$, $D_\perp$ *is chosen such that* $D_\perp'D_\perp=I-R_d^{-1/2}D_f(D_f'R_d^{-1}D_f)^{-1}D_f'R_d^{-1/2}$ *and* $A_0=A+L_0C-(B_f+L_0D_f)(D^+)'R_d^{-1/2}C$. *Let* $Q\geq 0$ *is the solution to the algebraic Ricatti equation*

$$\begin{aligned}Q=&A_0'QA_0'-A_0'QC'D_\perp'(I+D_\perp CQC'D_\perp')^{-1}D_\perp CQA_0\\&+(B_f+L_0D_f)(D_f'R_d^{-1}D_f)^{-1}(B_f+L_0D_f)'\end{aligned} \tag{100}$$

and define

$$\begin{aligned}K_0=&-(B_f+L_0D_f)(D^+)'\\&-A_0QC'R_d^{-1/2}D_\perp'(I+D_\perp R_d^{-1/2}CQC'R_d^{-1/2}D_\perp')^{-1}D_\perp,\\R_0=&(D^+)'(I+R_d^{-1/2}CQC'R_d^{-1/2}D_\perp'D_\perp)^{-1}.\end{aligned} \tag{101}$$

Then

$$\max_{\mathbf{Q}\in\mathcal{RH}_2^{n_y\times n_y}}\left\{\|\mathbf{QN}_f\|_-^{[0,2\pi]}:\|\mathbf{QN}_d\|_\infty\leq\gamma\right\}=\frac{\gamma}{\left\|(\mathbf{V}^{-1}\mathbf{N}_f)_{\text{opt}}^+\right\|_2}, \tag{102}$$

where

$$(\mathbf{V}^{-1}\mathbf{N}_f)_{\text{opt}}^+=\left[\begin{array}{c|c}A+K_0C&K_0-L_0\\\hline R_0C&R_0\end{array}\right] \tag{103}$$

and an optimal $\mathcal{H}_-/\mathcal{H}_2$ *fault-detection filter has the following state-space representation:*

$$\mathbf{r}=\mathbf{Q}_{\text{opt}}[\mathbf{M}-\mathbf{N}_u]\begin{bmatrix}\mathbf{y}\\\mathbf{u}\end{bmatrix}, \tag{104}$$

where

$$\begin{aligned}\mathbf{Q}_{\text{opt}}=&\frac{\gamma}{\left\|(\mathbf{V}^{-1}\mathbf{N}_f)_{\text{opt}}^+\right\|_2}\begin{bmatrix}(\mathbf{V}^{-1}\mathbf{N}_f)_{\text{opt}}^+\mathbf{V}^{-1}\\0\end{bmatrix},\\\mathbf{Q}_{\text{opt}}[\mathbf{M}-\mathbf{N}_u]=&\frac{\gamma}{\left\|(\mathbf{V}^{-1}\mathbf{N}_f)_{\text{opt}}^+\right\|_2}\\&\times\left[\begin{array}{c|c}\begin{bmatrix}A+L_0C&0\\KL5&A+K_0C\end{bmatrix}&\begin{bmatrix}-L_0&B+L_0D\\KL7&KL8\end{bmatrix}\\\hline\begin{bmatrix}-R_0R_d^{-1/2}C&R_0C\\0&\end{bmatrix}&\begin{bmatrix}R_0R_d^{-1/2}&-R_0R_d^{-1/2}D\end{bmatrix}\end{array}\right],\end{aligned} \tag{105}$$

where $KL5=-(K_0-L_0)R_d^{-1/2}C$, $KL7=(K_0-L_0)R_d^{-1/2}$, *and* $KL8=-(K_0-L_0)R_d^{-1/2}D$.

Proof. Note that

$$\begin{bmatrix}\mathbf{M}&\mathbf{N}_u\end{bmatrix}=\left[\begin{array}{c|cc}A+LC&L&B+LD\\\hline C&I&D\end{array}\right], \tag{106}$$

where L is a matrix with appropriate dimensions such that $A+LC$ is stable. From Theorem 1

$$\mathbf{V}^{-1}=\left[\begin{array}{c|c}A+L_0C&L_0-L\\\hline R_d^{-1/2}C&R_d^{-1/2}\end{array}\right]. \tag{107}$$

From Theorem 2

$$\begin{aligned}\mathbf{V}^{-1}\mathbf{N}_f=&\left[\begin{array}{c|c}A+L_0C&B_f+L_0D_f\\\hline R_d^{-1/2}C&R_d^{-1/2}\end{array}\right],\\\mathbf{V}^{-1}[\mathbf{M}-\mathbf{N}_u]=&\left[\begin{array}{c|cc}A+L_0C&-L_0&B+L_0D\\\hline -R_d^{-1/2}C&R_d^{-1/2}&-R_d^{-1/2}D\end{array}\right].\end{aligned} \tag{108}$$

From Lemma 9

$$(\mathbf{V}^{-1}\mathbf{N}_f)_{\text{opt}}^+=\left[\begin{array}{c|c}A+K_0C&K_0-L_0\\\hline R_0C&R_0\end{array}\right]. \tag{109}$$

Therefore,

$$\begin{aligned}&\mathbf{Q}_{\text{opt}}[\mathbf{M}-\mathbf{N}_u]\\&=\frac{\gamma}{\left\|(\mathbf{V}^{-1}\mathbf{N}_f)_{\text{opt}}^+\right\|_2}\begin{bmatrix}(\mathbf{V}^{-1}\mathbf{N}_f)_{\text{opt}}^+\\0\end{bmatrix}\mathbf{V}^{-1}[\mathbf{M}-\mathbf{N}_u]\\&=\frac{\gamma}{\left\|(\mathbf{V}^{-1}\mathbf{N}_f)_{\text{opt}}^+\right\|_2}\left[\begin{array}{c}\left[\begin{array}{c|c}A+K_0C&K_0-L_0\\\hline R_0C&R_0\end{array}\right]\\0\end{array}\right]\\&\quad\times\left[\begin{array}{c|cc}A+L_0C&-L_0&B+L_0D\\\hline -R_d^{-1/2}C&R_d^{-1/2}&-R_d^{-1/2}D\end{array}\right]\\&=\frac{\gamma}{\left\|(\mathbf{V}^{-1}\mathbf{N}_f)_{\text{opt}}^+\right\|_2}\\&\quad\times\left[\begin{array}{c}\left[\begin{array}{cc|cc}A+L_0C&0&-L_0&B+L_0D\\MN5&A+K_0C&MN7&MN8\\\hline -R_0R_d^{-1/2}C&R_0C&R_0R_d^{-1/2}&-R_0R_d^{-1/2}D\end{array}\right]\\0\end{array}\right].\end{aligned} \tag{110}$$

where $MN5=-(K_0-L_0)R_d^{-1/2}C$, $MN7=c(K_0-L_0)R_d^{-1/2}$, and $MN8=-(K_0-L_0)R_d^{-1/2}D$. □

Remark 8. Note that the optimal fault-detection filter $\mathbf{Q}_{\text{opt}}[\mathbf{M}-\mathbf{N}_u]$ is independent of the choice of Lmatrix.

Remark 9. Note that the strictly minimum phase assumption for $\widetilde{N}_f$ is not needed. In general, if $\widetilde{N}_f$ does not have any zeros on the unit circle, one can always factorize $\widetilde{N}_f=\widetilde{N}_f^{\min}\widetilde{N}_f^a$ so that $\widetilde{N}_f^{\min}$ is strictly minimum phase and $\widetilde{N}_f^a$ is a stable all-pass matrix. Then the solution can be computed by using $\widetilde{N}_f^{\min}$ in place of $\widetilde{N}_f$. In the case when $\widetilde{N}_f$ has zeros on the unit circle, approximation factorization can also be carried out to obtain an approximation solution.

8. $\mathcal{H}_-/\mathcal{H}_2$ FAULT-DETECTION FILTER DESIGN: CASE 3

When Problem 3 is considered with the $\mathcal{H}_-$ index defined over a finite frequency range $[\theta_1,\theta_2]$, the solution becomes much more complicated. We will now state this as a separate problem as below.

Problem 8 (interval $\mathcal{H}_-/\mathcal{H}_2$ problem). Let an uncertain system be described by (16)–(20) and let $\gamma > 0$ be a given disturbance rejection level. Find a stable transfer matrix $\mathbf{Q} \in \mathcal{RH}_\infty^{n_y \times n_y}$ in (23)–(25) such that $\|\mathbf{G}_{\mathrm{rd}}\|_2 \le \gamma$ and $\|\mathbf{G}_{\mathrm{rf}}\|_-^{[\theta_1,\theta_2]}$ is maximized, that is,

$$\max_{\mathbf{Q}\in\mathcal{RH}_\infty^{n_y\times n_y}} \left\{ \left\|\left|\mathbf{QN}_f\right\|\right|_-^{[\theta_1,\theta_2]} : \left\|\mathbf{QN}_d\right\|_2 \le \gamma \right\} \tag{111}$$

or, equivalently, let $\mathbf{Q} = \Psi\mathbf{V}^{-1}$ and solve

$$\max_{\Psi\in\mathcal{RH}_2^{n_y\times n_y}} \left\{ \left\|\left|\Psi\widetilde{\mathbf{N}}_f\right\|\right|_-^{[\theta_1,\theta_2]} : \|\Psi\|_2 \le \gamma \right\}. \tag{112}$$

Remark 10. It is not hard to see that there is no rational function solution to the above problem. This is because an optimal Ψ must satisfy $\Psi(e^{j\theta}) = 0$ almost every where for any $\theta \notin [\theta_1, \theta_2]$. Hence, an analytic optimal solution seems to be impossible. Nevertheless, it is intuitively feasible to find some rational approximations so that a rational Ψ has the form of a bandpass filter with the pass-band close to $[\theta_1, \theta_2]$ and $\|\Psi\|_2 = \gamma$.

Remark 11. When the condition that D_f has full column rank is not satisfied, the rational optimal solution to the problem

$$\max_{\mathbf{Q}\in\mathcal{RH}_\infty^{n_y\times n_y}} \left\{ \left\|\left|\mathbf{QN}_f\right\|\right|_-^{[0,2\pi]} : \left\|\mathbf{QN}_d\right\|_2 \le \gamma \right\} \tag{113}$$

may not exist. In this case, we also need to find some rational approximate solutions. Moreover, this problem is a special case of Problem 8 by letting $\theta_1 = 0$ and $\theta_2 = 2\pi$, we will only consider the solution to Problem 8.

In the following, we will describe an optimization approach to find a good rational approximation for the two cases above. To do that, we will need a state-space parametrization of a stable rational function with a given $\mathcal{H}_2$ norm [33].

Lemma 10. *Let*

$$\Psi = \left[\begin{array}{c|c} A_\psi & B_\psi \\ \hline C_\psi & D_\psi \end{array}\right] \in \mathcal{RH}_2^{n_y\times n_y} \tag{114}$$

be an n_ψth order proper stable transfer matrix. Then the state space parameters of Ψ can be expressed as $A_\psi = (I + A_{\psi k})(I - A_{\psi k})^{-1}(I - C_\psi' C_\psi)^{1/2}$ for some $A_{\psi k} = -A_{\psi k}'$ and some C_ψ satisfies $\|C_\psi\| \le 1$. Furthermore, $\|\Psi\|_2^2 = \mathrm{Trace}(D_\psi' D_\psi + B_\psi' B_\psi)$.

Proof. Assume that

$$\Psi = \left[\begin{array}{c|c} \hat{A}_\psi & \hat{B}_\psi \\ \hline \hat{C}_\psi & \hat{D}_\psi \end{array}\right] \in \mathcal{RH}_2 \tag{115}$$

is an n_ψth order observable realization, then the Observability Gramian L_o satisfies

$$\hat{A}_\psi' L_o \hat{A}_\psi - L_o + \hat{C}_\psi' \hat{C}_\psi = 0. \tag{116}$$

Since $L_o > 0$, there exists a Cholesky factorization of $L_o = T'T$ where T is invertible. Perform a similarity transformation on Ψ such that

$$\Psi = \left[\begin{array}{c|c} T\hat{A}_\psi T^{-1} & T\hat{B}_\psi \\ \hline \hat{C}_\psi T^{-1} & \hat{D}_\psi \end{array}\right] = \left[\begin{array}{c|c} A_\psi & B_\psi \\ \hline C_\psi & D_\psi \end{array}\right]. \tag{117}$$

Thus, $A_\psi' A_\psi - I + C_\psi' C_\psi = 0$, so that $A_\psi = O(I - C_\psi' C_\psi)^{1/2}$ where O is an orthogonal matrix and $I - C_\psi' C_\psi$ is a nonnegative definite. Since an orthogonal matrix O with no eigenvalue equals -1 can be represented as $A = (I + A_{\psi k})(I - A_{\psi k})^{-1}$, where $A_{\psi k} = -A_{\psi k}'$ is a skew-symmetric matrix, we have

$$A_\psi = (I + A_{\psi k})(I - A_{\psi k})^{-1}(I - C_\psi' C_\psi)^{1/2} \tag{118}$$

and $\|C_\psi\| \le 1$. Consequently, $\|\Psi\|_2^2 = \mathrm{Trace}(D_\psi' D_\psi + B_\psi' B_\psi)$. □

If we use directly the elements of A_ψ, B_ψ, C_ψ, and D_ψ as optimization variables the total number of variables is $n_\psi^2 + 2n_y n_\psi + n_y^2$. However, from Lemma 10 A_ψ can be computed from C_ψ and $A_{\psi k}$ so the elements $A_{\psi k}$, B_ψ, C_ψ, and D_ψ are all (necessary) optimization variables. Using this technique, the total number of optimization variables is $n_\psi(n_\psi - 1)/2 + 2n_y n_\psi + n_y^2$ and the reduction is $n_\psi(n_\psi + 1)/2$.

In order to carry out the subsequent optimization effectively, we need an effective method of computing $\mathcal{H}_-$ index fast and exactly. Enlightened by the bisection method of computing $\mathcal{H}_\infty$ norm of a transfer matrix [34], we now present a bisection algorithm to compute the $\mathcal{H}_-$ index defined over $[\theta_1, \theta_2]$.

The following result shows the main idea used in our algorithm.

Lemma 11. *Suppose*

$$\mathbf{G}(z) = \left[\begin{array}{c|c} A & B \\ \hline C & D \end{array}\right] \in \mathcal{RH}_\infty \tag{119}$$

and $\theta \in [\theta_1, \theta_2]$, then

$$\min_\theta \underline{\sigma}[\mathbf{G}(e^{j\theta})] > \beta \tag{120}$$

if and only if $\underline{\sigma}[D + C(I - A)^{-1}] > \beta$, and

$$S = \begin{bmatrix} HK1 & HK2 \\ -(A' + C'DR^{-1}B')^{-1}C'\beta^2R^{-1}C & (A' + C'DR^{-1}B')^{-1} \end{bmatrix}, \tag{121}$$

where $HK1 = A + BR^{-1}D'C - BR^{-1}B'(A' + C'DR^{-1}B')^{-1}C'\beta^2R^{-1}C$ and $HK2 = BR^{-1}B'(A' + C'DR^{-1}B')^{-1}$ has no eigenvalues on the segment of unit circle between $\theta = \theta_1$ and $\theta = \theta_2$, where $R = \beta^2 I - D'D$.

The detailed procedure of our algorithm for computing $\mathcal{H}_-$ index is summarized below.

(1) Give an initial guess on lower bound and upper bound such that

$$0 \le \beta_1 \le \min_{\theta\in[\theta_1,\theta_2]} \underline{\sigma}(\mathbf{G}(e^{j\theta})) \le \beta_2 \tag{122}$$

and give a tolerance $\epsilon > 0$.

(2) Let $\beta = (1/2)(\beta_1 + \beta_2)$. Compute the eigenvalues of

$$S = \begin{bmatrix} MP1 & MP2 \\ -(A' + C'DR^{-1}B')^{-1}C'\beta^2R^{-1}C & (A' + C'DR^{-1}B')^{-1} \end{bmatrix} \tag{123}$$

where $MP1 = A + BR^{-1}D'CBR^{-1}B'(A' + C'DR^{-1}B')^{-1}C'\beta^2R^{-1}C$ and $MP2 = R^{-1}B'(A' + C'DR^{-1}B')^{-1}$.

(3) If S has no eigenvalue on the segment of unit circle between $\theta = \theta_1$ and $\theta = \theta_2$, which means that

$$\min_{\theta\in[\theta_1,\theta_2]} \underline{\sigma}(\mathbf{G}(e^{j\theta})) > \beta \tag{124}$$

is true, then let $\beta_1 = \beta$; else let $\beta_2 = \beta$.

(4) Repeat steps (2) and (3) until $\beta_2 - \beta_1 < \epsilon$ is satisfied. And the approximate value of

$$\min_{\theta\in[\theta_1,\theta_2]} \underline{\sigma}(\mathbf{G}(e^{j\theta})) \tag{125}$$

is given by $(1/2)(\beta_1 + \beta_2)$ with tolerance ϵ.

With the state-space parametrization of Ψ on $\mathcal{RH}_2$ space and our bisection algorithm for computing $\mathcal{H}_-$ index, the optimization process for solving Problem 8,

$$\max_{\|\Psi\|_2\le\gamma} \|\Psi\widetilde{\mathbf{N}}_f\|_-^{[\theta_1,\theta_2]}, \tag{126}$$

can be performed as

$$\max_{A_{\psi k},B_\psi,C_\psi,D_\psi,\|C_\psi\|\le 1,\mathrm{Trace}(D_\psi'D_\psi+B_\psi'B_\psi)\le\gamma^2} \left\| \left[\begin{array}{c|c} (I + A_{\psi k})(I - A_{\psi k})^{-1}(I - C_\psi'C_\psi)^{1/2} & B_\psi \\ \hline C_\psi & D_\psi \end{array}\right] \widetilde{\mathbf{N}}_f \right\|_-^{[\theta_1,\theta_2]}. \tag{127}$$

Furthermore, we introduce a penalty function $\Theta(B_\psi, C_\psi, D_\psi)$ to ensure the conditions $\mathrm{Trace}(D_\psi'D_\psi + B_\psi'B_\psi) \le \gamma^2$ and $\|C_\psi\| \le 1$. Θ is defined as

$$\Theta(B_\psi, C_\psi, D_\psi) = \begin{cases} C, & \text{if } \mathrm{Trace}(B_\psi'B_\psi + D_\psi'D_\psi) > \gamma^2 \\ & \text{or } \|C_\psi\| > 1; \\ 0 & \text{else,} \end{cases} \tag{128}$$

where C is a large positive number. Therefore, the new optimization scheme is

$$\max_{A_{\psi k},B_\psi,C_\psi,D_\psi} \left\| \left[\begin{array}{c|c} (I+A_{\psi k})(I - A_{\psi k})^{-1}(I-C_\psi'C_\psi)^{1/2} & B_\psi \\ \hline C_\psi & D_\psi \end{array}\right] \widetilde{\mathbf{N}}_f \right\|_-^{[\theta_1,\theta_2]} - \Theta(B_\psi, C_\psi, D_\psi). \tag{129}$$

For this optimization scheme we have developed a two-stage optimization algorithm which is a combination of genetic algorithm [35, 36] and Nelder-Mead simplex method [10, 26]. Genetic algorithm is good at searching for the right direction for global optimum but has slow convergence, while Nelder-Mead simplex method is good at searching for small neighborhood. So the result obtained by genetic algorithm is used as the starting point for the second-step optimization by Nelder-Mead simplex method, the latter gives the final results of the optimization process.

Theoretically, Ψ can be a transfer matrix of any order. However, in practice we try to find a Ψ with low degree. Thus, we run the optimization process as follows: first set Ψ with a given starting order, searching for the optimal value; then increase the order of Ψ, run the searching algorithm again and compare the results with the former one; if higher degree Ψ gives a better performance and the Ψ's degree does not exceed the predefined limit, then keep increasing the degree of Ψ and redo the searching process; else the optimization process ends. Example 4 will demonstrate the effectiveness of this optimization method.

9. NUMERICAL EXAMPLES

In this section, we give some numerical examples to show the effectiveness of our approaches for solving the fault-detection problems.

Example 1. We consider Problem 1 for a third-order system:

$$\begin{aligned} A &= \begin{bmatrix} -0.1964 & -0.3962 & -0.5884 \\ 1 & 2 & 3 \\ -0.5428 & -1.0879 & -1.6291 \end{bmatrix}, \\ B_d &= \begin{bmatrix} 0.01 & 0 \\ 0 & 0.01 \\ 0 & 0 \end{bmatrix}, \qquad B_f = \begin{bmatrix} 1 & -3 \\ -0.5 & 1 \\ 0.5 & 0 \end{bmatrix}, \\ C &= \begin{bmatrix} -0.1964 & -0.3962 & -0.5884 \\ -0.3650 & -2.1320 & -3.0951 \end{bmatrix}, \\ D_d &= \begin{bmatrix} 0.02 & 0 \\ 0 & 0.02 \end{bmatrix}, \qquad D_f = \begin{bmatrix} 0 & 0.7 \\ 0 & 1 \end{bmatrix}. \end{aligned} \tag{130}$$

Let the pair (γ, β) represents the performance of an $\mathcal{H}_-/\mathcal{H}_\infty$ fault-detection filter such that $\|\mathbf{G}_{\mathrm{rd}}\|_\infty \le \gamma$ and $\|\mathbf{G}_{\mathrm{rf}}\|_-^{[0,2\pi]} \ge \beta$. Using our approach an optimal fault-detection filter has the form in Theorem 2 with

$$L_0 = \begin{bmatrix} -0.05 & 0 \\ 0 & -0.05 \\ 0 & 0 \end{bmatrix}. \tag{131}$$

Let $\gamma = 1$, we have the optimal $\beta = \gamma\|\widetilde{\mathbf{N}}_f\|_-^{[0,2\pi]} = 0.7632$. The singular value plots of $\mathbf{G}_{\mathrm{rd}}$ and $\mathbf{G}_{\mathrm{rf}}$ are shown in Figures 2 and 3, respectively.

Example 2. We consider Problem 2 for the same system in Example 1. Let the pair (γ, β) represents the performance of an $\mathcal{H}_2/\mathcal{H}_\infty$ fault-detection filter such that $\|\mathbf{G}_{\mathrm{rd}}\|_\infty \le \gamma$ and

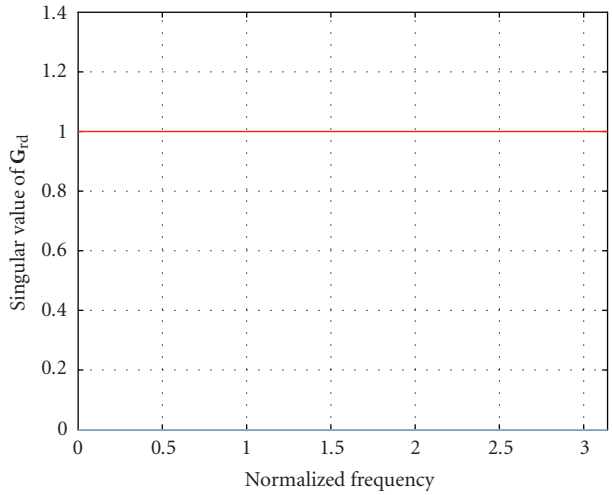

FIGURE 2: The singular value plot of $\mathbf{G}_{rd}$, $\|\mathbf{G}_{rd}\|_\infty = 1$, for Example 1.

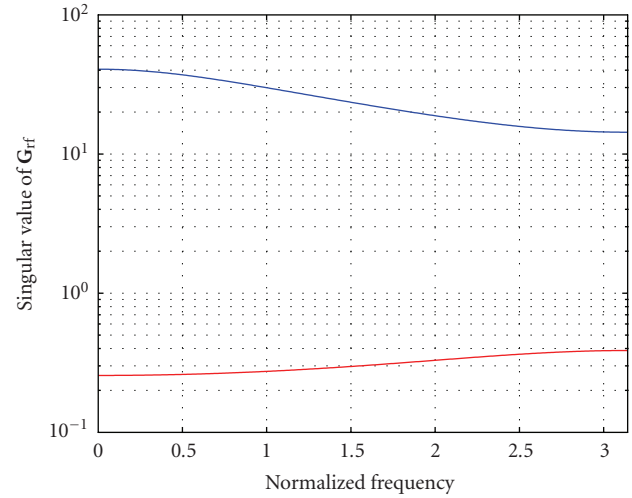

FIGURE 3: The singular value plot of $\mathbf{G}_{rf}$, $\|\mathbf{G}_{rf}\|_-^{[0,2\pi]} = 0.75$, for Example 1.

$\|\mathbf{G}_{rf}\|_2^{[0,2\pi]} \geq \beta$. From Theorem 3 the optimal fault-detection filter in Example 1 is also optimal for this example. Let $\gamma = 1$, the optimal $\beta = \gamma\|\tilde{\mathbf{N}}_f\|_2 = 9.7591$.

Note that if the so-called $\mathcal{H}_\infty/\mathcal{H}_\infty$ problem is considered for this system, the above fault-detection filter is also the optimal $\mathcal{H}_\infty/\mathcal{H}_\infty$ filter. Let $\|\mathbf{G}_{rd}\|_\infty \leq 1$, then the optimal $\|\mathbf{G}_{rf}\|_\infty$ is 11.4598.

Example 3. We consider Problem 3 for the system

$$
\begin{aligned}
A &= \begin{bmatrix} -0.1964 & -0.3962 & -0.5884 \\ 1 & 2 & 3 \\ -0.5428 & -1.0879 & -1.6291 \end{bmatrix}, \\
B_d &= \begin{bmatrix} 0.01 & 0 \\ 0 & 0.01 \\ 0 & 0 \end{bmatrix}, \qquad B_f = \begin{bmatrix} 1 & 0 \\ 1 & 1 \\ 0.5 & 0 \end{bmatrix}, \\
C &= \begin{bmatrix} -0.1964 & -0.3962 & -0.5884 \\ -0.3650 & -2.1320 & -3.0951 \end{bmatrix}, \\
D_d &= \begin{bmatrix} 0.02 & 0 \\ 0 & 0.02 \end{bmatrix}, \qquad D_f = \begin{bmatrix} 1 & 0.7 \\ 0 & 1 \end{bmatrix}.
\end{aligned} \tag{132}
$$

We let the pair (γ, β) represents the performance of an $\mathcal{H}_-/\mathcal{H}_2$ fault-detection filter such that $\|\mathbf{G}_{rd}\|_2 \leq \gamma$ and $\|\mathbf{G}_{rf}\|_-^{[0,2\pi]} \geq \beta$. Since this $\mathbf{G}_f$ has all zeros inside the unit circle and D_f has full column rank, we get from Theorem 6

$$
\begin{aligned}
&(\mathbf{V}^{-1}\mathbf{N}_f)_{\text{opt}}^{+} \\
&= \left[\begin{array}{ccc|cc} -0.2555 & -1.4924 & -2.1666 & 0.1900 & -0.1400 \\ 1.3059 & 3.0358 & 4.5169 & 0.2000 & 0.0500 \\ -0.5723 & -1.6360 & -2.4182 & 0.1000 & -0.0700 \\ \hline -0.0591 & -1.0962 & -1.5782 & 0.2000 & -0.1400 \\ 0.3650 & 2.1320 & 3.0951 & 0 & 0.2000 \end{array}\right]
\end{aligned} \tag{133}
$$

and the optimal filter

$$
\begin{aligned}
&\mathbf{Q}_{\text{opt}} \\
&= \frac{\gamma}{\left\|(\mathbf{V}^{-1}\mathbf{N}_f)_{\text{opt}}^{+}\right\|_2}(\mathbf{V}^{-1}\mathbf{N}_f)_{\text{opt}}^{+}\mathbf{V}^{-1} \\
&= \left[\begin{array}{ccc|cc} -0.0740 & 0.3126 & -0.8467 & -1.2003 & 0.3892 \\ -2.8761 & 1.3720 & -5.9237 & 5.7439 & -0.2946 \\ -0.4110 & 0.2304 & -0.9359 & 0.8321 & -0.0352 \\ \hline 0.7188 & -0.7509 & 2.5122 & 0.7430 & -0.5201 \\ -1.7340 & 1.3456 & -4.8682 & 0 & 0.7430 \end{array}\right].
\end{aligned} \tag{134}
$$

Let $\gamma = 1$ the optimal

$$
\beta = \frac{\gamma}{\left\|(\mathbf{V}^{-1}\mathbf{N}_f)_{\text{opt}}^{+}\right\|_2} = 0.7430. \tag{135}
$$

The singular value plots of $\mathbf{G}_{rd}$ and $\mathbf{G}_{rf}$ are shown in Figures 4 and 5, respectively.

Example 4. We consider Problem 8 for a system

$$
\begin{aligned}
A &= \begin{bmatrix} -0.1964 & -0.3962 & -0.5884 \\ 1.0000 & 2.0000 & 3.0000 \\ -0.5428 & -1.0879 & -1.6291 \end{bmatrix}, \\
B_d &= \begin{bmatrix} 0.01 \\ 0.01 \\ 0 \end{bmatrix}, \qquad B_f = \begin{bmatrix} 1.0 \\ -0.5 \\ 0.5 \end{bmatrix} \\
C &= \begin{bmatrix} -0.1964 & -0.3962 & -0.5884 \end{bmatrix}, \\
D_d &= 0.02, \qquad D_f = 0,
\end{aligned} \tag{136}
$$

where $\theta_1 = 0$ and $\theta_2 = \pi/2$.

As discussed in Section 8 we use optimization method to search for a good solution. Let us denote the maximum of

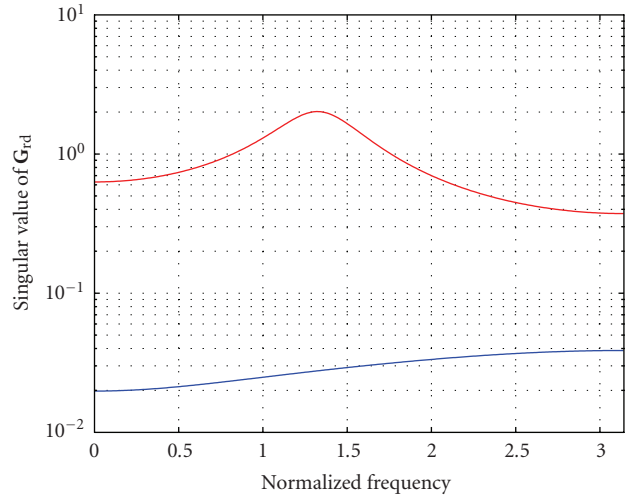

FIGURE 4: Singular value plot of $\mathbf{G}_{rd}$, $\|\mathbf{G}_{rd}\|_2 = 1$, for Example 3.

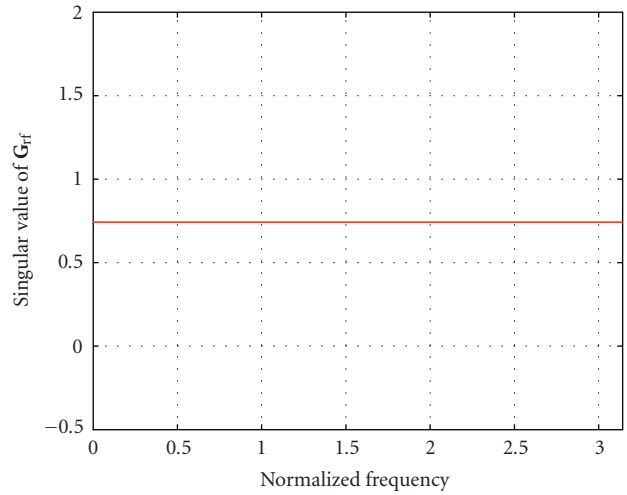

FIGURE 5: Singular value plot of $\mathbf{G}_{rf}$, $\|\mathbf{G}_{rf}\|_- = 0.7430$, for Example 3.

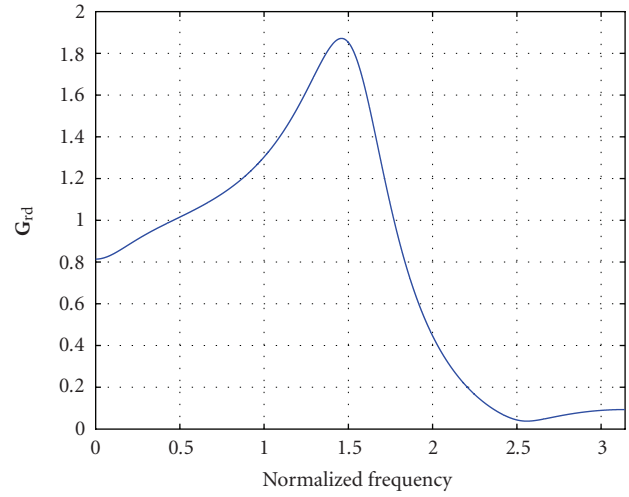

FIGURE 6: Singular value plot of $\mathbf{G}_{rd}$ with a third order Ψ, $\|\mathbf{G}_{rd}\|_2 = 1$, for Example 4.

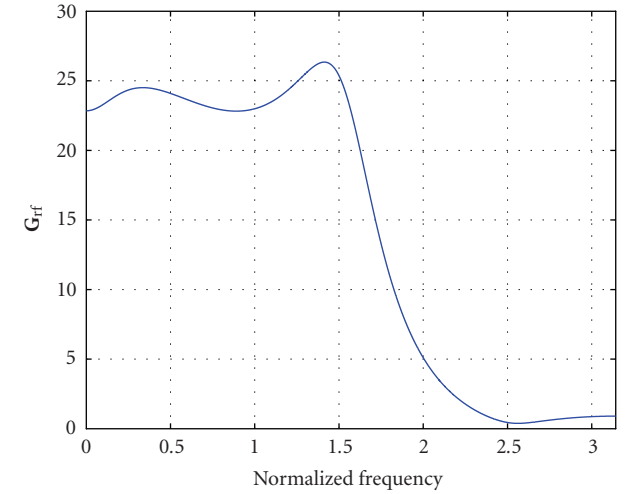

FIGURE 7: Singular value plot of $\mathbf{G}_{rf}$ with a third order Ψ, $\|\mathbf{G}_{rf}\|_-^{[0,\pi/2]} = 22.8182$, for Example 4.

TABLE 1: Results for different Ψ's order.

Ψ's order	First	Second	Third
β	14.2661	22.5345	22.8182

$\|\mathbf{G}_{rf}\|_-^{[\theta_1,\theta_2]}$ as β when $\|\mathbf{G}_{rd}\|_2 \le 1$. In Table 1 the results obtained using our optimization algorithm with different predefined Ψ orders are given. It is clear that the results improve with the increasing order of Ψ. In particular, a third-order Ψ design achieving $\beta = 22.8182$ is given by

$$\Psi = \left[\begin{array}{cccc|c} 0.1187 & -0.0019 & 0.4270 & -0.1424 \\ -0.8445 & 0.4220 & 0.3270 & 0.2363 \\ -0.3536 & -0.9012 & 0.2408 & 0.8865 \\ \hline 0.3844 & 0.0988 & 0.8079 & 0.3714 \end{array}\right]. \quad (137)$$

The singular value plots of $\mathbf{G}_{rd}$ and $\mathbf{G}_{rf}$ are shown in Figures 6 and 7 for this third-order Ψ. Figure 8 demonstrates how the smallest singular value of $\mathbf{G}_{rf}$ changes in the frequency range of $[0, \pi/2]$ with the order of Ψ. It is seen that the improvement on the performance with any Ψ of higher order than 3 is insignificant.

It is interesting to note that the Ψ is trying to invert $\widetilde{\mathbf{N}}_f$ in the frequency interval $[0, \pi/2]$.

10. CONCLUSION

In this paper, we have presented optimal solutions to various robust fault-detection problems for linear discrete time systems in parallel with our continuous time results in [28]. We have shown that an optimal filter for both $\mathcal{H}_-/\mathcal{H}_\infty$ and $\mathcal{H}_2/\mathcal{H}_\infty$ can be obtained by solving one Riccati equation. It is also interesting to note that we are able to give analytic

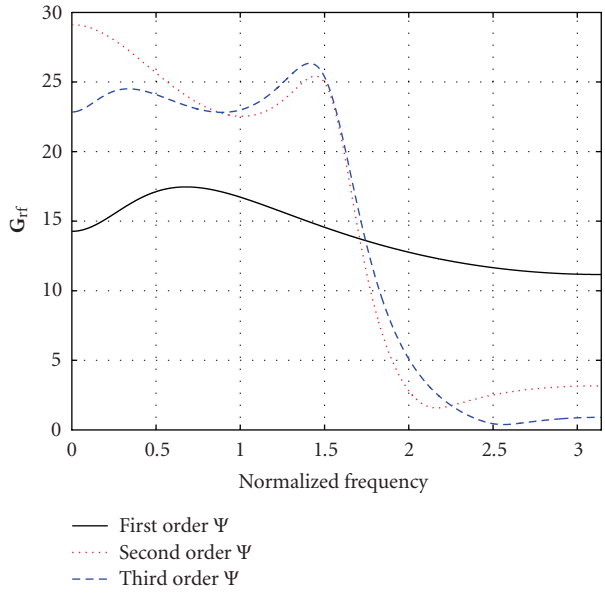

FIGURE 8: Singular value plot of $\mathbf{G}_{rf}$ for different order of Ψ: first order (solid line), second order (dotted line), and third order (dashed line), for Example 4.

solution to an $\mathcal{H}_-/\mathcal{H}_2$ problem defined on the entire frequency range $[0, 2\pi]$ when D_f has full column rank. In contrast, the corresponding continuous time problem does not make any sense [28]. The critical reason for this difference is because the entire frequency range in discrete time is finite ($\leq 2\pi$) while the entire frequency range in continuous time is infinite. We have also shown that many design criteria considered in the literature do not give desirable fault-detection designs.

ACKNOWLEDGMENTS

This work was supported in part by grants from NASA (NCC5-573), LEQSF (NASA/LEQSF(2001-04)-01), and the NNSFC Young Investigator Award for Overseas Collaborative Research (60328304).

REFERENCES

[1] J. Chen and R. J. Patton, *Robust Model-Based Fault Diagnosis for Dynamic Systems*, Kluwer Academic Publishers, Norwell, Mass, USA, 1999.

[2] P. M. Frank and X. Ding, "Survey of robust residual generation and evaluation methods in observer-based fault detection systems," *Journal of Process Control*, vol. 7, no. 6, pp. 403–424, 1997.

[3] R. J. Patton, "Robustness in model-based fault diagnosis:the 1995 situation," *Annual Reviews in Control*, vol. 21, pp. 103–123, 1997.

[4] Y. M. Zhang and J. Jiang, "Bibliographical review on reconfigurable fault-tolerant control systems," in *Proceedings of the 5th IFAC Symposium on Fault Detection, Supervision and Safety of Technical Processes (SAFEPROCESS '03)*, pp. 265–276, Washington, DC, USA, June 2003.

[5] K. Zhou and Z. Ren, "A new controller architecture for high performance, robust, and fault-tolerant control," *IEEE Transactions on Automatic Control*, vol. 46, no. 10, pp. 1613–1618, 2001.

[6] I. Izadi, T. Chen, and Q. Zhao, "Norm invariant discretization for sampled-data fault detection," *Automatica*, vol. 41, no. 9, pp. 1633–1637, 2005.

[7] F. Caliskan and C. M. Hajiyev, "EKF based surface fault detection and reconfiguration in aircraft control systems," in *Proceedings of the American Control Conference (ACC '00)*, vol. 2, pp. 1220–1224, Chicago, Ill, USA, 2000.

[8] B. Jiang and F. N. Chowdhury, "Fault estimation and accommodation for linear MIMO discrete-time systems," *IEEE Transactions on Control Systems Technology*, vol. 13, no. 3, pp. 493–499, 2005.

[9] Y. Zhang and J. Jiang, "Design of integrated fault detection, diagnosis and reconfigurable control systems," in *Proceedings of the 38th IEEE Conference on Decision and Control (CDC '99)*, vol. 4, pp. 3587–3592, Phoenix, Ariz, USA, December 1999.

[10] G. P. Liu, J. B. Yang, and J. F. Whidborne, *Multiobjective Optimization and Control*, Research Studies Press, Baldock, UK, 2001.

[11] M. A. Sadrnia, J. Chen, and R. J. Patton, "Robust fault diagnosis observer design using $\mathcal{H}_\infty$ optimisation and μ synthesis," in *IEE Colloquium on Modeling and Signal Processing for Fault Diagnosis*, p. 9, Leicester, UK, September 1996.

[12] R. J. Patton, J. Chen, and J. H. P. Miller, "A robust disturbance decoupling approach to fault detection in process systems," in *Proceedings of the 30th IEEE Conference on Decision and Control (CDC '91)*, vol. 2, pp. 1543–1548, Brighton, UK, December 1991.

[13] P. Zhang, H. Ye, S. X. Ding, G. Z. Wang, and D. H. Zhou, "On the relationship between parity space and H_2 approaches to fault detection," *Systems and Control Letters*, vol. 55, no. 2, pp. 94–100, 2006.

[14] M. Zhong, S. X. Ding, B. Tang, P. Zhang, and T. Jeinsch, "A LMI approach to robust fault detection filter design for discrete-time systems with model uncertainty," in *Proceedings of the 40th Conference on Desision and Control (CDC '01)*, vol. 4, pp. 3613–3618, Orlando, Fla, USA, December 2001.

[15] M. Zhong, S. X. Ding, J. Lam, and H. Wang, "An LMI approach to design robust fault detection filter for uncertain LTI systems," *Automatica*, vol. 39, no. 3, pp. 543–550, 2003.

[16] M. Hou and R. J. Patton, "LMI approach to $\mathcal{H}_-/\mathcal{H}_\infty$ fault detection observers," in *Proceedings of the UKACC International Conference on Control*, vol. 1, pp. 305–310, Exeter, UK, September 1996.

[17] J. Liu, J. L. Wang, and G.-H. Yang, "An LMI approach to minimum sensitivity analysis with application to fault detection," *Automatica*, vol. 41, no. 11, pp. 1995–2004, 2005.

[18] I. Izadi, Q. Zhao, and T. Chen, "An $\mathcal{H}_\infty$ approach to fast rate fault detection for multirate sampled-data systems," *Journal of Process Control*, vol. 16, no. 6, pp. 651–658, 2006.

[19] I. M. Jaimoukha, Z. Li, and V. Papakos, "A matrix factorization solution to the $\mathcal{H}_-$ / $\mathcal{H}_\infty$ fault detection problem," *Automatica*, vol. 42, no. 11, pp. 1907–1912, 2006.

[20] B. Jiang, M. Staroswiecki, and V. Cocquempot, "$\mathcal{H}_\infty$ fault detection filter design for linear discrete-time systems with multiple time delays," *International Journal of Systems Science*, vol. 34, no. 5, pp. 365–373, 2003.

[21] F. Tao and Q. Zhao, "Fault detection observer design with unknown inputs," in *Proceedings of the IEEE Conference on Control Applications (CCA '05)*, pp. 1275–1280, Toronto, Canada, August 2005.

[22] H. B. Wang, L. Lam, S. X. Ding, and M. Y. Zhong, "Iterative linear matrix inequality algorithms for fault detection with unknown inputs," *Journal of Systems and Control Engineering*, vol. 219, no. 2, pp. 161–172, 2005.

[23] H. Ye, S. X. Ding, and G. Wang, "Integrated design of fault detection systems in time-frequency domain," *IEEE Transactions on Automatic Control*, vol. 47, no. 2, pp. 384–390, 2002.

[24] P. Zhang, S. X. Ding, G. Z. Wang, and D. H. Zhou, "Fault detection for uncertain sampled-data systems," in *Proceedings of the World Congress on Intelligent Control and Automation (WCICA '02)*, vol. 4, pp. 2728–2732, Shanghai, China, June 2002.

[25] P. Zhang, S. X. Ding, G. Z. Wang, D. H. Zhou, and E. L. Ding, "An $\mathcal{H}_\infty$ approach to fault detection for sampled-data systems," in *Proceedings of the American Control Conference (ACC '02)*, vol. 3, pp. 2196–2201, Anchorage, Alaska, USA, May 2002.

[26] S. X. Ding, T. Jeinsch, P. M. Frank, and E. L. Ding, "A unified approach to the optimization of fault detection systems," *International Journal of Adaptive Control and Signal Processing*, vol. 14, no. 7, pp. 725–745, 2000.

[27] P. Zhang, S. X. Ding, G. Z. Wang, and D. H. Zhou, "Fault detection of linear discrete-time periodic systems," *IEEE Transactions on Automatic Control*, vol. 50, no. 2, pp. 239–244, 2005.

[28] N. Liu and K. Zhou, "Optimal solutions to multi-objective robust fault detection problems," in *Proceedings of the 46th IEEE Conference on Decision and Control (CDC '07)*, New Orleans, La, USA, December 2007.

[29] K. Zhou, J. C. Doyle, and K. Clover, *Robust and Optimal Control*, Prentice-Hall, Upper Saddle River, NJ, USA, 1996.

[30] R. C. Horn and C. R. Johnson, *Topics in Matrix Analysis*, Cambridge University Press, Cambridge, UK, 1991.

[31] H. Niemann and J. Stoustrup, "An architecture for fault tolerant controllers," *International Journal of Control*, vol. 78, no. 14, pp. 1091–1110, 2005.

[32] L. Li and G. Gu, "Design of optimal zero-forcing precoders for MIMO channels via optimal full information control," *IEEE Transactions on Signal Processing*, vol. 53, no. 8, pp. 3238–3246, 2005.

[33] D. U. Campos-Delgado and K. Zhou, "A parametric optimization approach to $\mathcal{H}_\infty$ and $\mathcal{H}_2$ strong stabilization," *Automatica*, vol. 39, no. 7, pp. 1205–1211, 2003.

[34] S. Boyd, V. Balakrishnan, and P. Kabamba, "A bisection method for computing the$\mathcal{H}_\infty$ norm of a transfer matrix and related problems," *Mathematics of Control, Signals, and Systems*, vol. 2, no. 3, pp. 207–219, 1989.

[35] M. Gen and R. W. Chenge, *Genetic Algorithms and Engineering Optimization*, John Wiley & Sons, New York, NY, USA, 2000.

[36] R. J. Patton, J. Chen, and G. P. Liu, "Robust fault detection of dynamic systems via genetic algorithms," in *Proceedings of the 1st International Conference on Genetic Algorithms in Engineering Systems: Innovations and Applications (GALESIA '95)*, no. 414, pp. 511–516, Sheffield, UK, September 1995.

Hindawi Publishing Corporation
Journal of Control Science and Engineering
Volume 2008, Article ID 790893, 12 pages
doi:10.1155/2008/790893

Research Article

Computation of a Reference Model for Robust Fault Detection and Isolation Residual Generation

Emmanuel Mazars, Imad M. Jaimoukha, and Zhenhai Li

Control and Power Group, Department of Electrical and Electronic Engineering, Imperial College, London SW7 2AZ, UK

Correspondence should be addressed to Imad M. Jaimoukha, i.jaimouka@imperial.ac.uk

Received 30 March 2007; Revised 31 August 2007; Accepted 3 November 2007

Recommended by Kemin Zhou

This paper considers matrix inequality procedures to address the robust fault detection and isolation (FDI) problem for linear time-invariant systems subject to disturbances, faults, and polytopic or norm-bounded uncertainties. We propose a design procedure for an FDI filter that aims to minimize a weighted combination of the sensitivity of the residual signal to disturbances and modeling errors, and the deviation of the faults to residual dynamics from a fault to residual reference model, using the $\mathcal{H}_\infty$-norm as a measure. A key step in our procedure is the design of an optimal fault reference model. We show that the optimal design requires the solution of a quadratic matrix inequality (QMI) optimization problem. Since the solution of the optimal problem is intractable, we propose a linearization technique to derive a numerically tractable suboptimal design procedure that requires the solution of a linear matrix inequality (LMI) optimization. A jet engine example is employed to demonstrate the effectiveness of the proposed approach.

1. INTRODUCTION

In the past decade, great attention has been devoted to the design of model-based fault detection systems and their robustness [1, 2]. With the rapid development of robust control theory and $\mathcal{H}_\infty$ optimization control techniques, more and more methods have been presented to solve the robust FDI problem. The $\mathcal{H}_\infty$-filter is designed such that the $\mathcal{H}_\infty$-norm of the estimation error is minimized (see [3–5] and the references therein). Some of the approaches used for this problem include frequency domain approaches [6], left and right eigenvector assignment [7], structure parity equation [8], and an unknown input observer with disturbances decoupled in the state estimation error [9]. Recently developed LMI approaches offer numerically attractive techniques [10–12].

A reference residual model is an ideal solution for robust FDI under the assumption that there are no disturbances or model uncertainty. The idea is to design a filter for the uncertain system that approximates the solution given by the reference model [13]. In [14], a new performance index is proposed using such a reference residual model. Frisk and Nielsen [15] give an algorithm to design a reference model and a robust FDI filter that fits into the framework of standard robust $\mathcal{H}_\infty$-filtering relying on established and efficient methods. However, their framework consists in solving two optimization problems successively, which results in a suboptimal solution.

In this paper, we propose a performance index that captures the requirements of fault isolation and disturbance rejection as well as the design of the optimal reference model. The fault isolation performance is measured by the size of the deviation of the fault to residual dynamics from the reference dynamics model, while the disturbance rejection performance is measured by the size of the input to residual and disturbance to residual dynamics. In all cases, the $\mathcal{H}_\infty$ norm is used as a measure. The design of the optimal reference model is incorporated in the robust FDI framework. We consider systems subject to norm-bounded or polytopic uncertainties. For systems described by polytopic and unstructured norm-bounded uncertainties, we derive an optimal FDI filter obtained as the solution of a QMI optimization. For systems described by structured uncertainties, we derive a suboptimal QMI-based solution. Since the solution

of a QMI optimization is, in general, intractable, we propose a linearization technique to derive a suboptimal design procedure that requires the solution of a numerically tractable LMI optimization. This note extends our work in [16] by proposing algorithms for the design of suboptimal reference dynamics.

The structure of the work is as follows. After defining the notation, we review filter-based FDI techniques for residual signal generation and give the problem formulation in Section 2. Section 3 presents a matrix inequality formulation for the FDI problem, and gives the solution and the design of the optimal reference model for both norm-bounded and polytopic uncertainties in a form of QMI's. Section 4 gives a suboptimal solution in both cases through the use of an algorithm that necessitates solving LMI's. Finally, a numerical example is presented in Section 5, and Section 6 summarizes our results.

The notation we use is fairly standard. The set of real $n \times m$ matrices is denoted by $\mathcal{R}^{n\times m}$. For $A \in \mathcal{R}^{n\times m}$, we use the notation A^T to denote transpose. For $A = A^T \in \mathcal{R}^{n\times n}$, $A \succ 0$ ($A \prec 0$) denotes that A is positive (negative) definite, that is, all the eigenvalues of A are greater (less) than zero. The $n \times n$ identity matrix is denoted as I_n and the $n \times m$ null matrix is denoted as $0_{n,m}$ with the subscripts occasionally dropped if they can be inferred from context.

Let $\mathcal{L}_2$ be the set of square integrable functions. The $\mathcal{L}_2$-norm of $u \in \mathcal{L}_2$ is defined as $\|u\|_2 = \sqrt{\int_0^\infty u(t)^T u(t)dt}$. A transfer matrix $G(s) = D + C(sI - A)^{-1}B$ will be denoted as $G(s) \stackrel{s}{=} (A, B, C, D)$ or

$$G(s) \stackrel{s}{=} \left[\begin{array}{c|c} A & B \\ \hline C & D \end{array}\right], \tag{1}$$

and dependence on the variable s will be suppressed. For a stable transfer matrix G, we define

$$\begin{aligned} \|G\|_\infty &= \sup\{\|Gu\|_2/\|u\|_2 : 0 \neq u \in \mathcal{L}_2\}, \\ \|G\|_- &= \inf\{\|Gu\|_2/\|u\|_2 : 0 \neq u \in \mathcal{L}_2\}. \end{aligned} \tag{2}$$

In section 3, we use the following result.

Lemma 1 (see [17]). *Let $\phi(s) = R + B^T(-sI - A^T)^{-1}C + C^T(sI - A)^{-1}B + B^T(-sI - A^T)^{-1}Q(sI - A)^{-1}B$ with (A, B) sign controllable, $R^T = R$, and $Q^T = Q$. Then $\phi(s)$ has a spectral factor $G(s) \in \mathcal{RL}_\infty^{m\times p}$ (i.e., $\phi(s) = G^T(-s)G(s)$) if and only if there exists symmetric P that satisfies the following linear matrix inequality:*

$$\begin{bmatrix} PA + A^TP + Q & PB + C \\ (PB + C)^T & R \end{bmatrix} \succeq 0. \tag{3}$$

2. PROBLEM FORMULATION

Consider a linear time-invariant dynamic system subject to disturbances, modeling errors and process, sensor and actuator faults modeled as

$$\begin{bmatrix} \dot{x}(t) \\ y(t) \end{bmatrix} = \overbrace{\begin{bmatrix} A & B & B_d & B_f \\ C & D & D_d & D_f \end{bmatrix}}^{\mathcal{M}} \begin{bmatrix} x(t) \\ u(t) \\ d(t) \\ f(t) \end{bmatrix}, \tag{4}$$

where $x(t) \in \mathcal{R}^n$, $u(t) \in \mathcal{R}^{n_u}$, and $y(t) \in \mathcal{R}^{n_y}$ are the process state and input and output vectors, respectively, and where $d(t) \in \mathcal{R}^{n_d}$ and $f(t) \in \mathcal{R}^{n_f}$ are the disturbance and fault vectors, respectively. Here, $B_f \in \mathcal{R}^{n\times n_f}$ and $D_f \in \mathcal{R}^{n_y\times n_f}$ are the component and instrument fault distribution matrices, respectively, while $B_d \in \mathcal{R}^{n\times n_d}$ and $D_d \in \mathcal{R}^{n_y\times n_d}$ are the corresponding disturbance distribution matrices [18].

We consider two types of uncertainties: norm-bounded and polytopic uncertainties. In the case of norm-bounded uncertainties,

$$\begin{aligned} \mathcal{M} \in \Bigg\{ &\overbrace{\begin{bmatrix} A^o & B^o & B_d^o & B_f^o \\ C^o & D^o & D_d^o & D_f^o \end{bmatrix}}^{\mathcal{M}^o} \\ &+ \begin{bmatrix} F_A \\ F_C \end{bmatrix} \Delta_H \begin{bmatrix} E_A & E_B & E_d & E_f \end{bmatrix} : \Delta \in \mathbf{\Delta} \Bigg\} =: \boldsymbol{\mathcal{M}}_{\mathbf{\Delta}}, \end{aligned} \tag{5}$$

where $\mathcal{M}^o$ represents the nominal model, $\Delta_H = \Delta(I - H\Delta)^{-1}$, where

$$\begin{aligned} \mathbf{\Delta} := \{&\Delta = \operatorname{diag}(\delta_1 I_{q1}, \ldots, \delta_l I_{ql}, \Delta_{l+1}, \ldots, \Delta_{l+f}) : \|\Delta\| \leq 1, \\ &\delta_i \in \mathcal{R}, \Delta_i \in \mathcal{R}^{q_i\times q_i}\} \subset \mathcal{R}^{n_\Delta \times n_\Delta}, \end{aligned} \tag{6}$$

and where F_A, F_C, E_A, E_B, E_d, E_f, and H are known and constant matrices with appropriate dimensions. This linear fractional representation of uncertainty, which is assumed to be well-posed over $\mathbf{\Delta}$ (i.e., $\det(I - H\Delta) \neq 0$ for all $\Delta \in \mathbf{\Delta}$), has great generality and is widely used in control theories.

In the case of polytopic uncertainties,

$$\mathcal{M} \in \left\{ \sum_{i=1}^p \xi_i \overbrace{\begin{bmatrix} A^i & B^i & B_d^i & B_f^i \\ C^i & D^i & D_d^i & D_f^i \end{bmatrix}}^{\mathcal{M}^i} : \sum_{i=1}^p \xi_i = 1,\ \xi_i \geq 0 \right\} =: \boldsymbol{\mathcal{M}}_{\boldsymbol{\xi}}, \tag{7}$$

where $\mathcal{M}^i$, $i = 1, \ldots, p$, are known constant matrices with appropriate dimensions.

A residual signal in an FDI system should represent the inconsistency between the system variables and the mathematical model. The objective is to design an FDI filter of the form

$$\begin{bmatrix} \dot{\hat{x}}(t) \\ r(t) \end{bmatrix} = \begin{bmatrix} A_k & B_{ku} & B_{ky} \\ C_k & D_{ku} & D_{ky} \end{bmatrix} \begin{bmatrix} \hat{x}(t) \\ u(t) \\ y(t) \end{bmatrix}, \tag{8}$$

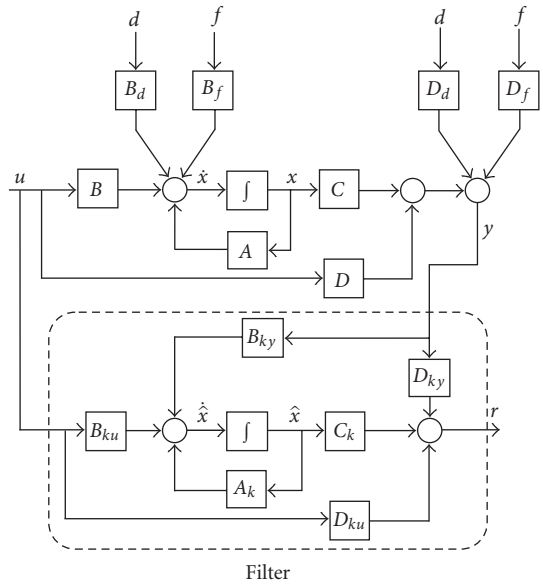

FIGURE 1: Filter-based robust FDI scheme.

where $\hat{x}(t) \in \mathcal{R}^{n_k}$ is the filter state and $r(t) \in \mathcal{R}^{n_f}$ is the residual signal. Figure 1 illustrates this filter in the robust residual generation scheme.

By defining an augmented state $z(t) = [\, x(t)^T \ \hat{x}(t)^T \,]^T$ the residual dynamics are given by

$$\begin{bmatrix} \dot{z}(t) \\ r(t) \end{bmatrix} = \begin{bmatrix} \widetilde{A} & \widetilde{B}_f & \widetilde{B}_d & \widetilde{B}_u \\ \widetilde{C} & \widetilde{D}_f & \widetilde{D}_d & \widetilde{D}_u \end{bmatrix} \begin{bmatrix} z(t) \\ f(t) \\ d(t) \\ u(t) \end{bmatrix} \tag{9}$$

or

$$\begin{aligned} &\begin{bmatrix} T_{rf}^{\mathcal{M}} & T_{rd}^{\mathcal{M}} & T_{ru}^{\mathcal{M}} \end{bmatrix} \\ &\quad \stackrel{s}{=} \left[\begin{array}{c|ccc} \widetilde{A} & \widetilde{B}_f & \widetilde{B}_d & \widetilde{B}_u \\ \hline \widetilde{C} & \widetilde{D}_f & \widetilde{D}_d & \widetilde{D}_u \end{array}\right] \\ &\quad = \left[\begin{array}{cc|ccc} A & 0 & B_f & B_d & B \\ B_{ky}C & A_k & B_{ky}D_f & B_{ky}D_d & B_{ku} + B_{ky}D \\ \hline D_{ky}C & C_k & D_{ky}D_f & D_{ky}D_d & D_{ku} + D_{ky}D \end{array}\right], \end{aligned} \tag{10}$$

where $T_{rf}^{\mathcal{M}}$, $T_{rd}^{\mathcal{M}}$, and $T_{ru}^{\mathcal{M}}$ denote the dynamics from faults, disturbances, and inputs to the residual, respectively. Note that dependence on the uncertain data is indicated by a superscript $\mathcal{M}$.

Ideally, the residual signal is required to be sensitive only to faults. This corresponds to $T_{rd}^{\mathcal{M}} = 0$, $T_{ru}^{\mathcal{M}} = 0$, and $T_{rf}^{\mathcal{M}} \neq 0$. For fault isolation, it is further required that the fault signature can be deduced from the residual. This corresponds to $T_{rf}^{\mathcal{M}} \in \mathcal{S}$, where $\mathcal{S}$ is a set of transfer matrices with a special structure that depends on the nature of the faults, for example, if the faults can occur simultaneously, $\mathcal{S}$ is the set of stable diagonal transfer matrices with nonzero diagonal entries. Unfortunately, characterizing a general structured set $\mathcal{S}$ is intractable, and we will assume that we can define a subset

$$\begin{aligned} \mathcal{S} = \Big\{ T_{\text{ref}} \stackrel{s}{=} (A_{\text{ref}}, B_{\text{ref}}, C_{\text{ref}}, D_{\text{ref}}) :\ & A_{\text{ref}} \in \mathcal{S}_A \subseteq \mathcal{R}^{n_{\text{ref}} \times n_{\text{ref}}}, \\ & B_{\text{ref}} \in \mathcal{S}_B \subseteq \mathcal{R}^{n_{\text{ref}} \times n_f},\ C_{\text{ref}} \in \mathcal{S}_C \subseteq \mathcal{R}^{n_f \times n_{\text{ref}}}, \\ & D_{\text{ref}} \in \mathcal{S}_D \subseteq \mathcal{R}^{n_f \times n_f} \Big\} \subseteq \mathcal{S} \end{aligned} \tag{11}$$

such that subsequent optimizations over the structured state-space data sets $\mathcal{S}_A$, $\mathcal{S}_B$, $\mathcal{S}_C$, and $\mathcal{S}_D$ are tractable. For example, if $\mathcal{S}$ denotes the set of all stable $n_f \times n_f$ diagonal transfer matrices with nonzero diagonal entries, we may define $\mathcal{S}_A$ as the set of all $n_f \times n_f$ diagonal matrices with negative entries, and $\mathcal{S}_B$, $\mathcal{S}_C$, and $\mathcal{S}_D$ as the sets of all $n_f \times n_f$ diagonal matrices. An example of this simplification procedure is given in Section 5 below. We also replace the requirement of nonzero diagonal entries for $\mathcal{S}$ by a condition of the form $\|T_{\text{ref}}\|_- \geq \beta > 0$ for all $T_{\text{ref}} \in \mathcal{S}$.

Due to the presence of disturbances and modelling uncertainties, exact FDI is not possible. For robust FDI, we propose the following, more realistic, problem formulation.

Problem 1. Assume that the system dynamics in (4) are quadratically stable. For any $\gamma > 0$, find a stable fault reference dynamics $T_{\text{ref}} \stackrel{s}{=} (A_{\text{ref}}, B_{\text{ref}}, C_{\text{ref}}, D_{\text{ref}}) \in \mathcal{S}$ such that $\|T_{\text{ref}}\|_- \geq 1$ (to ensure the requirement of nonzero diagonal entries for $\mathcal{S}$), and find a stable filter of the form given in (8), if it exists, such that the residual dynamics in (10) are quadratically stable and

$$\sup_{\mathcal{M} \in \boldsymbol{\mathcal{M}}} \left\| \begin{bmatrix} T_{rf}^{\mathcal{M}} - T_{\text{ref}} & T_{rd}^{\mathcal{M}} & T_{ru}^{\mathcal{M}} \end{bmatrix} \right\|_\infty < \gamma, \tag{12}$$

where $\boldsymbol{\mathcal{M}} = \boldsymbol{\mathcal{M}}_{\boldsymbol{\Delta}}$ for norm-bounded uncertainties and $\boldsymbol{\mathcal{M}} = \boldsymbol{\mathcal{M}}_{\boldsymbol{\xi}}$ for polytopic uncertainties.

Recall that quadratic stability for the dynamics in (4) is equivalent to the existence of $P = P^T \succ 0$ such that $A^T P + PA \prec 0$ for all A (see [19] for more details).

A modified version of Problem 1 uses a weighted cost function, say, of the form

$$\left\| \begin{bmatrix} (T_{rf}^{\mathcal{M}} - T_{\text{ref}}) W_f & T_{rd}^{\mathcal{M}} W_d & T_{ru}^{\mathcal{M}} W_u \end{bmatrix} \right\|_\infty, \tag{13}$$

where W_f, W_d, and W_u are constant or frequency-dependent weighting functions that can vary the emphasis between fault detection (small $\|T_{rd}^{\mathcal{M}}\|_\infty$ and $\|T_{ru}^{\mathcal{M}}\|_\infty$) and fault isolation (small $\|T_{rf}^{\mathcal{M}} - T_{\text{ref}}\|_\infty$). In the sequel, we assume that any such weighting functions are absorbed in the system data.

Remark 1. The objective is to find the smallest γ for which (12) is satisfied. Indeed, by minimizing γ, we will ensure $\|T_{rd}^{\mathcal{M}}\|_\infty$ (which measures the disturbance rejection level), $\|T_{ru}^{\mathcal{M}}\|_\infty$ (which measures the effect of uncertainty), and $\|T_{rf}^{\mathcal{M}} - T_{\text{ref}}\|_\infty$ (which measures the deviation of the fault to residual dynamics from the reference dynamics, and hence is a measure of fault isolation capability) to be small.

A poorly chosen reference model can result in a residual generator with poor robustness. Here, we incorporate its design into our scheme so as to improve the robustness of the FDI filter.

In some approaches, a common assumption is that $D_f = 0$ and/or CB_f has full rank [20, 21]; in others, the assumption D_f has full rank and is widely used [22, 23]. Here, we do not impose any of these assumptions. Note, however, that if D_f does not have full column rank, for example, if $D_f = 0$, then this will have an adverse effect on the minimum values of γ since $\gamma \geq \|[\ T_{rf}^{\mathcal{M}} - T_{\text{ref}}\ \ T_{rd}^{\mathcal{M}}\ \ T_{ru}^{\mathcal{M}}\ ]\|_\infty \geq \|T_{rf}^{\mathcal{M}}(\infty) - T_{\text{ref}}(\infty)\| = \|D_{ky}D_f - D_{\text{ref}}\| = \|D_{\text{ref}}\| \geq 1$. This would therefore limit the overall performance of the filter, which is measured by the value of γ.

3. MATRIX INEQUALITY FORMULATION

In this section, we derive a matrix inequality formulation of Problem 1. The main idea is to express (12) in terms of QMIs using the bounded real lemma and change of variables techniques, and then to derive necessary and sufficient conditions for solvability.

The dynamics in (12) can be written as

$$\left[\begin{array}{c|cc} T_{rf}^{\mathcal{M}} - T_{\text{ref}} & T_{rd}^{\mathcal{M}} & T_{ru}^{\mathcal{M}} \end{array}\right] \overset{s}{=} \left[\begin{array}{c|c} A_c^{\mathcal{M}} & B_c^{\mathcal{M}} \\ \hline C_c^{\mathcal{M}} & D_c^{\mathcal{M}} \end{array}\right] := \left[\begin{array}{cc|ccc} A_{\text{ref}} & 0 & B_{\text{ref}} & 0 & 0 \\ 0 & \widetilde{A} & \widetilde{B}_f & \widetilde{B}_d & \widetilde{B}_u \\ \hline -C_{\text{ref}} & \widetilde{C} & \widetilde{D}_f - D_{\text{ref}} & \widetilde{D}_d & \widetilde{D}_u \end{array}\right]. \tag{14}$$

It follows from the bounded real lemma that there exists a stable filter of the form given in (8) such that (12) is satisfied if and only if there exists $P_c = P_c^T$ such that $P_c \succ 0$ and

$$\begin{bmatrix} (A_c^{\mathcal{M}})^T P_c + P_c A_c^{\mathcal{M}} & P_c B_c^{\mathcal{M}} & (C_c^{\mathcal{M}})^T \\ (B_c^{\mathcal{M}})^T P_c & -\gamma I & (D_c^{\mathcal{M}})^T \\ C_c^{\mathcal{M}} & D_c^{\mathcal{M}} & -\gamma I \end{bmatrix} \prec 0 \tag{15}$$

for all $\mathcal{M}$ (see [24, Theorem 3]). We deal separately with norm-bounded and polytopic uncertainties.

3.1. Solution with norm-bounded uncertainties

For norm-bounded uncertainties, we separate the terms involving modeling uncertainties from the other terms as

$$(A_c^{\mathcal{M}}, B_c^{\mathcal{M}}, C_c^{\mathcal{M}}, D_c^{\mathcal{M}}) = (A_c^o + A_c^\Delta, B_c^o + B_c^\Delta, C_c^o + C_c^\Delta, D_c^o + D_c^\Delta), \tag{16}$$

where

$$\left[\begin{array}{c|c} A_c^o & B_c^o \\ \hline C_c^o & D_c^o \end{array}\right] = \left[\begin{array}{ccc|ccc} A_{\text{ref}} & 0 & 0 & B_{\text{ref}} & 0 & 0 \\ 0 & A^o & 0 & B_f^o & B_d^o & B^o \\ 0 & B_{ky}C^o & A_k & B_{ky}D_f^o & B_{ky}D_d^o & B_{ku}+B_{ky}D^o \\ \hline -C_{\text{ref}} & D_{ky}C^o & C_k & D_{ky}D_f^o - D_{\text{ref}} & D_{ky}D_d^o & D_{ku}+D_{ky}D^o \end{array}\right], \tag{17}$$

$$\left[\begin{array}{c|c} A_c^\Delta & B_c^\Delta \\ \hline C_c^\Delta & D_c^\Delta \end{array}\right] = \begin{bmatrix} F_{r1} \\ F_{r2} \end{bmatrix} \Delta_H \begin{bmatrix} E_{r1} & E_{r2} \end{bmatrix} := \left[\begin{array}{c} 0 \\ F_A \\ B_{ky}F_C \\ \hline D_{ky}F_C \end{array}\right] \Delta_H \left[\begin{array}{ccc|ccc} 0 & E_A & 0 & E_f & E_d & E_B \end{array}\right]. \tag{18}$$

Using this separation, the inequality (15) can be rewritten as

$$\overbrace{\begin{bmatrix} (A_c^o)^T P_c + P_c A_c^o & P_c B_c^o & (C_c^o)^T \\ (B_c^o)^T P_c & -\gamma I & (D_c^o)^T \\ C_c^o & D_c^o & -\gamma I \end{bmatrix}}^{T_c^o} + \overbrace{\begin{bmatrix} (A_c^\Delta)^T P_c + P_c A_c^\Delta & P_c B_c^\Delta & (C_c^\Delta)^T \\ (B_c^\Delta)^T P_c & 0 & (D_c^\Delta)^T \\ C_c^\Delta & D_c^\Delta & 0 \end{bmatrix}}^{T_c^\Delta} \prec 0. \tag{19}$$

A calculation shows that $T_c^\Delta = \widetilde{F}\Delta_H\widetilde{E} + \widetilde{E}^T\Delta_H\widetilde{F}^T$, where

$$\widetilde{F} = \begin{bmatrix} (P_c F_{r1})^T & 0 & F_{r2}^T \end{bmatrix}^T, \qquad \widetilde{E} = \begin{bmatrix} E_{r1} & E_{r2} & 0 \end{bmatrix}. \tag{20}$$

The next result uses the fact that $\Delta \in \mathbf{\Delta}$ to remove explicit dependence on Δ.

Lemma 2 (see [25]). *Let $\mathbf{\Delta}$ be as described in (6) and define the subspaces*

$$\begin{aligned} \mathbf{\Sigma} &= \{\text{diag}\,(S_1, \ldots, S_l, \lambda_1 I_{ql+1}, \ldots, \lambda_s I_{ql+f}) : \\ &\qquad S_i = S_i^T \in \mathcal{R}^{q_i \times q_i}, \lambda_j \in \mathcal{R}\}, \\ \mathbf{\Gamma} &= \{\text{diag}\,(G_1, \ldots, G_l, 0_{ql+1}, \ldots, 0_{ql+f}) : \\ &\qquad G_i = -G_i^T \in \mathcal{R}^{q_i \times q_i}\}. \end{aligned} \tag{21}$$

Let $R = R^T$, F, E, and H be matrices with appropriate dimensions. We have $\det(I - H\Delta) \neq 0$ and $R + F\Delta(I - H\Delta)^{-1}E + E^T(I - \Delta^T H^T)^{-1}\Delta^T F^T \prec 0$ for every $\Delta \in \mathbf{\Delta}$ if there exist $S \in \mathbf{\Sigma}$ and $G \in \mathbf{\Gamma}$ such that $S \succ 0$ and

$$\begin{bmatrix} R + E^T S E & F + E^T S H + E^T G \\ F^T + H^T S E + G E & H^T S H + H^T G + G H - S \end{bmatrix} \prec 0. \tag{22}$$

If $\mathbf{\Delta}$ *is unstructured* (*i.e., if* $\mathbf{\Delta} = \{\Delta \in \mathcal{R}^{n_\Delta \times n_\Delta} : \|\Delta\| \le 1\}$), *then* (22) *becomes*

$$\begin{bmatrix} R + \lambda E^T E & F + \lambda E^T H \\ F^T + \lambda H^T E & \lambda(H^T H - I) \end{bmatrix} \prec 0 \tag{23}$$

for some scalar $\lambda \ge 0$. *In this case, condition* (23) *is both necessary and sufficient.*

When the uncertainty set is unstructured, then Lemma 2 implies that

$$\begin{aligned} (19) &\iff T_c^o + \widetilde{F}\Delta_H \widetilde{E} + \widetilde{E}^T \Delta_H{}^T \widetilde{F}^T \prec 0 \\ &\iff \begin{bmatrix} T_c^o + \lambda \widetilde{E}^T \widetilde{E} & \widetilde{F} + \lambda \widetilde{E}^T H \\ \widetilde{F}^T + \lambda H^T \widetilde{E} & \lambda(H^T H - I) \end{bmatrix} \prec 0 \end{aligned} \tag{24}$$

for some $\lambda \ge 0$. Using a Schur complement argument shows that (19) is equivalent to

$$\overline{T}_c := \begin{bmatrix} (A_c^o)^T P_c + \star & P_c B_c^o & (C_c^o)^T & P_c F_{r1} & \lambda E_{r1}^T \\ \star & -\gamma I & (D_c^o)^T & 0 & \lambda E_{r2}^T \\ \star & \star & -\gamma I & F_{r2} & 0 \\ \star & \star & \star & -\lambda I & \lambda H^T \\ \star & \star & \star & \star & -\lambda I \end{bmatrix} \prec 0, \tag{25}$$

where $\star$ denotes terms readily inferred from symmetry. Next, we introduce a change of variables to linearize the above matrix inequality [26]. Assume that $n_k = n_{\text{ref}} + n$, that is, the filter order is equal to the order of the system plus the order of the reference model. Let

$$\begin{aligned} P_c &= \begin{bmatrix} Y & N \\ N^T & \hat{Y} \end{bmatrix}, \qquad P_c^{-1} = \begin{bmatrix} X & M \\ M^T & \hat{X} \end{bmatrix}, \\ \Pi_1 &= \begin{bmatrix} I & I \\ M^T Z & 0 \end{bmatrix}, \end{aligned} \tag{26}$$

where $X, Y, \hat{X}, \hat{Y} \in \mathcal{R}^{n_k \times n_k}$ are symmetric matrices, and $Z = X^{-1}$. Define $T = \operatorname{diag}(\Pi_1, I)$. Then $\overline{T}_c \prec 0$ if and only if $T^T \overline{T}_c T \prec 0$. From $P_c P_c^{-1} = I$, we have the following calculations, where boldface letters are used to indicate optimization variables:

$$\begin{aligned} \mathcal{L}_{11} &:= \Pi_1^T P_c A_c^o \Pi_1 \\ &= \begin{bmatrix} \mathbf{Z}\overline{A} + \mathbf{Z}E_1 \mathbf{A}_{\text{ref}} E_1^T & \mathbf{Z}\overline{A} + \mathbf{Z}E_1 \mathbf{A}_{\text{ref}} E_1^T \\ \mathbf{Y}\overline{A} + \mathbf{Y}E_1 \mathbf{A}_{\text{ref}} E_1^T + \hat{\mathbf{A}} + \hat{\mathbf{B}}_y \overline{C} & \mathbf{Y}\overline{A} + \mathbf{Y}E_1 \mathbf{A}_{\text{ref}} E_1^T + \hat{\mathbf{B}}_y \overline{C} \end{bmatrix}, \end{aligned} \tag{27}$$

$$\begin{aligned} \mathcal{L}_{12} &:= \Pi_1^T P_c B_c^o \\ &= \begin{bmatrix} \mathbf{Z}\overline{B}_f + \mathbf{Z}E_1 \mathbf{B}_{\text{ref}} & \mathbf{Z}\overline{B}_d & \mathbf{Z}\overline{B} \\ \mathbf{Y}\overline{B}_f + \mathbf{Y}E_1 \mathbf{B}_{\text{ref}} + \hat{\mathbf{B}}_y D_f^o & \mathbf{Y}\overline{B}_d + \hat{\mathbf{B}}_y D_d^o & \mathbf{Y}\overline{B} + \hat{\mathbf{B}}_y D^o + \hat{\mathbf{B}}_u \end{bmatrix}, \end{aligned} \tag{28}$$

$$\mathcal{L}_{13} := (C_c^o \Pi_1)^T = \begin{bmatrix} (\hat{\mathbf{D}}_y \overline{C} - \mathbf{C}_{\text{ref}} E_2 + \hat{\mathbf{C}})^T \\ (\hat{\mathbf{D}}_y \overline{C} - \mathbf{C}_{\text{ref}} E_2)^T \end{bmatrix}, \tag{29}$$

$$\mathcal{L}_{14} := \Pi_1^T P_c F_{r1} = \begin{bmatrix} \mathbf{Z}\overline{F}_A \\ \mathbf{Y}\overline{F}_A + \hat{\mathbf{B}}_y F_C \end{bmatrix}, \tag{30}$$

$$\mathcal{L}_{15} := \Pi_1^T E_{r1}^T = \begin{bmatrix} \overline{E}_A^T \\ \overline{E}_A^T \end{bmatrix}, \tag{31}$$

$$\mathcal{L}_{23}^T = \begin{bmatrix} \hat{\mathbf{D}}_y D_f^o - \mathbf{D}_{\text{ref}} & \hat{\mathbf{D}}_y D_d^o & \hat{\mathbf{D}}_y D^o + \hat{\mathbf{D}}_u \end{bmatrix}, \tag{32}$$

$$\mathcal{L}_{25}^T = \begin{bmatrix} E_f & E_d & E_B \end{bmatrix}, \tag{33}$$

where we have defined

$$\left[\begin{array}{cccccc} \overline{A} & E_1 & \overline{B}_f & \overline{B}_d & \overline{B} & \overline{F}_A \end{array}\right] := \left[\begin{array}{cc|cccccc} 0 & 0 & I_{n_{\text{ref}}} & 0 & 0 & 0 & 0 \\ 0 & A^o & 0 & B_f^o & B_d^o & B^o & F_A \end{array}\right], \tag{34}$$

$$\begin{bmatrix} \overline{C} \\ E_2 \\ \overline{E}_A \end{bmatrix} := \begin{bmatrix} 0 & C^o \\ I_{n_{\text{ref}}} & 0 \\ 0 & E_A \end{bmatrix}, \tag{35}$$

$$\begin{bmatrix} \hat{\mathbf{A}} & \hat{\mathbf{B}}_y & \hat{\mathbf{B}}_u \\ \hat{\mathbf{C}} & \hat{\mathbf{D}}_y & \hat{\mathbf{D}}_u \end{bmatrix} = \begin{bmatrix} N A_k M^T Z & N B_{ky} & N B_{ku} \\ C_k M^T Z & D_{ky} & D_{ku} \end{bmatrix}. \tag{36}$$

If M and N are invertible, the variables A_k, C_k, B_{ky}, B_{ku}, D_{ky}, D_{ku} can be replaced by the new variables $\hat{\mathbf{A}}$, $\hat{\mathbf{B}}_y$, $\hat{\mathbf{B}}_u$, $\hat{\mathbf{C}}$, $\hat{\mathbf{D}}_y$, $\hat{\mathbf{D}}_u$ without loss of generality. We can now rewrite (19) as

$$\begin{bmatrix} \mathcal{L}_{11} + \mathcal{L}_{11}^T & \mathcal{L}_{12} & \mathcal{L}_{13} & \mathcal{L}_{14} & \boldsymbol{\lambda}\mathcal{L}_{15} \\ \star & -\gamma I & \mathcal{L}_{23} & 0 & \boldsymbol{\lambda}\mathcal{L}_{25} \\ \star & \star & -\gamma I & \hat{\mathbf{D}}_y F_C & 0 \\ \star & \star & \star & -\boldsymbol{\lambda} I & \boldsymbol{\lambda} H^T \\ \star & \star & \star & \star & -\boldsymbol{\lambda} I \end{bmatrix} \prec 0, \tag{37}$$

which is nonlinear in the variables. Note that the nonlinearities involve the terms $\mathbf{A}_{\text{ref}}$ and $\mathbf{B}_{\text{ref}}$ only. The constraint $P_c \succ 0$ can be expressed as an LMI as follows:

$$P_c \succ 0 \iff \Pi_1^T P_c \Pi_1 \succ 0 \iff \begin{bmatrix} \mathbf{Z} & \mathbf{Z} \\ \mathbf{Z} & \mathbf{Y} \end{bmatrix} \succ 0. \tag{38}$$

The constraint $\|T_{\text{ref}}\|_- \ge 1$ can be expressed as a quadratic matrix inequality using the next lemma.

Lemma 3. *Let* T_{ref} *be as defined above. Then* $\|T_{\text{ref}}\|_- \ge 1$ *if and only if there exists* $\mathbf{P}_{\text{ref}} = \mathbf{P}_{\text{ref}}{}^T \in \mathcal{R}^{n_{\text{ref}} \times n_{\text{ref}}}$ *such that*

$$\begin{aligned} &T_{\text{ro}} \\ &:= \begin{bmatrix} \mathbf{P}_{\text{ref}} \mathbf{A}_{\text{ref}} + \mathbf{A}_{\text{ref}}{}^T \mathbf{P}_{\text{ref}} + \mathbf{C}_{\text{ref}}{}^T \mathbf{C}_{\text{ref}} & \mathbf{P}_{\text{ref}} \mathbf{B}_{\text{ref}} + \mathbf{C}_{\text{ref}}{}^T \mathbf{D}_{\text{ref}} \\ \mathbf{B}_{\text{ref}}{}^T \mathbf{P}_{\text{ref}} + \mathbf{D}_{\text{ref}}{}^T \mathbf{C}_{\text{ref}} & \mathbf{D}_{\text{ref}}{}^T \mathbf{D}_{\text{ref}} - I_{n_f} \end{bmatrix} \\ &\ge 0. \end{aligned} \tag{39}$$

Proof. Let $\phi(s) = T_{\text{ref}}^{\sim}(s)T_{\text{ref}}(s) - I_{n_f}$. Then $\phi(s) \succeq 0$ if and only if $\|T_{\text{ref}}\|_- \geq 1$. It is easy to show that $\phi(s)$ can be written as follows:

$$\begin{aligned}\phi(s) = {} & \mathbf{D}_{\text{ref}}{}^T\mathbf{D}_{\text{ref}} - I_{nf} + \mathbf{B}_{\text{ref}}{}^T\left(-sI_{nf} - \mathbf{A}_{\text{ref}}{}^T\right)^{-1}\mathbf{C}_{\text{ref}}{}^T\mathbf{D}_{\text{ref}} \\ & + \left(\mathbf{C}_{\text{ref}}{}^T\mathbf{D}_{\text{ref}}\right)^T\left(sI_{nf} - \mathbf{A}_{\text{ref}}\right)^{-1}\mathbf{B}_{\text{ref}} \\ & + \mathbf{B}_{\text{ref}}{}^T\left(-sI_{nf} - \mathbf{A}_{\text{ref}}{}^T\right)^{-1}\mathbf{C}_{\text{ref}}{}^T\mathbf{C}_{\text{ref}}\left(sI_{nf} - \mathbf{A}_{\text{ref}}\right)^{-1}\mathbf{B}_{\text{ref}}.\end{aligned} \tag{40}$$

The result then follows from Lemma 1. □

The next lemma summarizes our result so far by giving necessary and sufficient conditions for the solution of Problem 1, in the case that the uncertainty set is unstructured, in the form of a QMI feasibility problem.

Lemma 4. *Assume that $\mathbf{\Delta}$ is unstructured. Then there exist a stable filter of the form given in* (8) *and a stable fault reference dynamics model $T_{\text{ref}} \stackrel{s}{=} (\mathbf{A}_{\text{ref}}, \mathbf{B}_{\text{ref}}, \mathbf{C}_{\text{ref}}, \mathbf{D}_{\text{ref}}) \in \mathcal{S}$, where $\mathcal{S}$ is defined in* (11)*, such that $\|T_{\text{ref}}\|_- \geq 1$, residual dynamics in* (10) *are quadratically stable, and* (12) *is satisfied for $\mathcal{M} = \mathcal{M}_\Delta$ if and only if there exist $\mathbf{A}_{\text{ref}} \in \mathcal{S}_A$, $\mathbf{B}_{\text{ref}} \in \mathcal{S}_B$, $\mathbf{C}_{\text{ref}} \in \mathcal{S}_C$, $\mathbf{D}_{\text{ref}} \in \mathcal{S}_D$, $\hat{\mathbf{A}}$, $\hat{\mathbf{B}}_y$, $\hat{\mathbf{B}}_u$, $\hat{\mathbf{C}}$, $\hat{\mathbf{D}}_y$, $\hat{\mathbf{D}}_u, \boldsymbol{\lambda}$, and symmetric matrices $\mathbf{P}_{\text{ref}}$, $\mathbf{Y}$, and $\mathbf{Z}$ such that* (37), (38), *and* (39) *are satisfied. If such variables exist, the filter dynamics are obtained by solving* (36) *where M and N are chosen such that $NM^T = I - \mathbf{Y}\mathbf{Z}^{-1}$.*

Approximate solutions to these QMIs can be obtained by using algorithms with guaranteed global convergence [27, 28], as well as local numerical search algorithms that converge (without a guarantee) much faster [29, 30]. A related discussion of the solution algorithms for QMIs can also be found in [31]. In Section 4 below, we develop an alternative procedure for the approximate solution of these QMIs.

Remark 2. In the case that T_{ref} is preassigned to a known value, (37) becomes linear and (39) becomes irrelevant, therefore, the optimal solution is given in a form of an LMI optimization. This case has been considered in [16].

When $\mathbf{\Delta}$ is structured, we proceed as follows. By using (22) from Lemma 2, we get

$$\begin{aligned}(19) &\Longleftrightarrow T_c^o + \widetilde{F}\Delta_H\widetilde{E} + \widetilde{E}^T\Delta_H{}^T\widetilde{F}^T \prec 0 \\ &\Longleftarrow \exists \mathbf{S} \in \mathbf{\Sigma}\ \&\ \mathbf{G} \in \mathbf{\Gamma} \quad \text{s.t. } \mathbf{S} \succ 0\ \&\ T_{SG} \prec 0,\end{aligned} \tag{41}$$

where

$$T_{SG} = \begin{bmatrix} T_c^o & \widetilde{F} + \widetilde{E}^T\mathbf{G} \\ \widetilde{F}^T + \mathbf{G}^T\widetilde{E} & H^T\mathbf{G} + \mathbf{G}^TH - \mathbf{S} \end{bmatrix} + \begin{bmatrix} \widetilde{E}^T \\ H^T \end{bmatrix} \mathbf{S} \begin{bmatrix} \widetilde{E} & H \end{bmatrix}. \tag{42}$$

Using a Schur complement argument and the expression of $\widetilde{E}$ and $\widetilde{F}$ in (20), we get

$$\begin{aligned}T_{SG} \prec 0 &\Longleftrightarrow \overline{T}_{SG} \\ &:= \begin{bmatrix} \left(A_c^o\right)^TP_c + \star & P_cB_c^o & \left(C_c^o\right)^T & P_cF_{r1} + E_{r1}^T\mathbf{G} & E_{r1}^T\mathbf{S} \\ \star & -\gamma I & \left(D_c^o\right)^T & E_{r2}^T\mathbf{G} & E_{r2}^T\mathbf{S} \\ \star & \star & -\gamma I & F_{r2} & 0 \\ \star & \star & \star & H^T\mathbf{G} + \mathbf{G}^TH - \mathbf{S} & H^T\mathbf{S} \\ \star & \star & \star & \star & -\mathbf{S} \end{bmatrix} \\ &\prec 0.\end{aligned} \tag{43}$$

As we did for unstructured uncertainties, we use the same matrix $T = \operatorname{diag}(\Pi_1, I)$ to allow to change variables, it follows that $\overline{T}_{SG} \prec 0$ if and only if $\widetilde{T}_{SG} := T\overline{T}_{SG}T^T \prec 0$. We multiply $\widetilde{T}_{SG}$ by $K = \operatorname{diag}(I, \mathbf{S})$ and K^T from left and right, respectively, to get $T_{SG} \prec 0$ if and only if

$$\begin{bmatrix} \mathcal{L}_{11} + \mathcal{L}_{11}^T & \mathcal{L}_{12} & \mathcal{L}_{13} & \mathcal{L}_{14} + \mathcal{L}_{15}\mathbf{G} & \mathcal{L}_{15}\mathbf{S} \\ \star & -\gamma I & \mathcal{L}_{23} & 0 & \mathcal{L}_{25}\mathbf{S} \\ \star & \star & -\gamma I & \hat{\mathbf{D}}_yF_C & 0 \\ \star & \star & \star & H^T\mathbf{G} + \mathbf{G}^TH - \mathbf{S} & H^T\mathbf{S} \\ \star & \star & \star & \star & -\mathbf{S} \end{bmatrix} \prec 0. \tag{44}$$

Therefore, when $\mathbf{\Delta}$ is structured, we have the following sufficient condition for solvability.

Lemma 5. *Suppose that $\mathbf{\Delta}$ has the structure defined in* (6)*. Then there exist a stable filter of the form given in* (8) *and a stable fault reference dynamics model $T_{\text{ref}} \stackrel{s}{=} (\mathbf{A}_{\text{ref}}, \mathbf{B}_{\text{ref}}, \mathbf{C}_{\text{ref}}, \mathbf{D}_{\text{ref}}) \in \mathcal{S}$, where $\mathcal{S}$ is defined in* (11)*, such that $\|T_{\text{ref}}\|_- \geq 1$, the residual dynamics in* (10) *are quadratically stable, and* (12) *is satisfied for $\mathcal{M} = \mathcal{M}_\Delta$ if there exist $\mathbf{A}_{\text{ref}} \in \mathcal{S}_A$, $\mathbf{B}_{\text{ref}} \in \mathcal{S}_B$, $\mathbf{C}_{\text{ref}} \in \mathcal{S}_C$, $\mathbf{D}_{\text{ref}} \in \mathcal{S}_D$, $\hat{\mathbf{A}}$, $\hat{\mathbf{B}}_y$, $\hat{\mathbf{B}}_u$, $\hat{\mathbf{C}}$, $\hat{\mathbf{D}}_y$, $\hat{\mathbf{D}}_u$, $\mathbf{S} \in \mathbf{\Sigma}$, $\mathbf{G} \in \mathbf{\Gamma}$, and symmetric matrices $\mathbf{P}_{\text{ref}}$, $\mathbf{Y}$, and $\mathbf{Z}$ such that* (38), (39), *and* (44) *are satisfied.*

3.2. Solution with polytopic uncertainties

In this section, we derive necessary and sufficient conditions for solvability of the robust FDI problem for a system subject to polytopic uncertainties, in the form of LMIs. Now,

$$\left[\begin{array}{c|c} A_c^{\mathcal{M}} & B_c^{\mathcal{M}} \\ \hline C_c^{\mathcal{M}} & D_c^{\mathcal{M}} \end{array}\right] \in \left\{ \sum_{i=1}^{p} \xi_i \left[\begin{array}{c|c} A_c^i & B_c^i \\ \hline C_c^i & D_c^i \end{array}\right], \sum_{i=1}^{p} \xi_i = 1, \xi_i \geq 0 \right\}, \tag{45}$$

where $(A_c^i, B_c^i, C_c^i, D_c^i)$ are as defined in (17), but with superscript (o) replaced by (i). We assume that the polytopic system is quadratically stable. Recall that (12) is satisfied if and only if (15) is satisfied for all $\mathcal{M}$. Now,

$$(15) \Longleftrightarrow \sum_{i=1}^{p} \xi_i \overbrace{\begin{bmatrix} (A_c^i)^T P_c + P_c A_c^i & P_c B_c^i & (C_c^i)^T \\ (B_c^i)^T P_c & -\gamma I & (D_c^i)^T \\ C_c^i & D_c^i & -\gamma I \end{bmatrix}}^{T_{\text{pol}}^i} \prec 0,$$

$$\forall \xi_i \text{ s.t. } \sum_{i=1}^{p} \xi_i = 1, \quad \xi_i \succeq 0,$$

$$\Longleftrightarrow T_{\text{pol}}^i \prec 0, \quad i = 1, \ldots, p. \tag{46}$$

Noting that the change of variable defined in (36) is independent of $\mathcal{M}^i$, we can therefore use it in this scheme as well. Letting $T = \operatorname{diag}(\Pi_1, I)$, it follows that

$$T_{\text{pol}}^i \prec 0 \Longleftrightarrow \overline{T}_{\text{pol}}^i := T T_{\text{pol}}^i T^T = \begin{bmatrix} \mathcal{L}_{11}^i + (\mathcal{L}_{11}^i)^T & \mathcal{L}_{12}^i & \mathcal{L}_{13}^i \\ \star & -\gamma I & \mathcal{L}_{23}^i \\ \star & \star & -\gamma I \end{bmatrix} \prec 0, \tag{47}$$

where the $(\mathcal{L}_{jk}^i)^T s$ are as defined in (27)–(33) and (34)-(35), but with the nominal model data $\mathcal{M}^o$ replaced by $\mathcal{M}^i$. Therefore, for polytopic uncertainties, we can derive necessary and sufficient conditions for solvability of Problem 1 in the form of a QMI feasibility problem as follows.

Lemma 6. *Let $\boldsymbol{\mathcal{M}} = \boldsymbol{\mathcal{M}}_\xi$. Then there exist a stable filter of the form given in* (8) *and a stable fault reference dynamics model $T_{\text{ref}} \stackrel{s}{=} (\mathbf{A}_{\text{ref}}, \mathbf{B}_{\text{ref}}, \mathbf{C}_{\text{ref}}, \mathbf{D}_{\text{ref}}) \in \mathcal{S}$, where $\mathcal{S}$ is defined in* (11), *such that $\|T_{\text{ref}}\|_- \geq 1$, the residual dynamics in* (10) *are quadratically stable, and* (12) *is satisfied for $\boldsymbol{\mathcal{M}} = \boldsymbol{\mathcal{M}}_\Delta$ if and only there exist $\mathbf{A}_{\text{ref}} \in \mathcal{S}_A$, $\mathbf{B}_{\text{ref}} \in \mathcal{S}_B$, $\mathbf{C}_{\text{ref}} \in \mathcal{S}_C$, $\mathbf{D}_{\text{ref}} \in \mathcal{S}_D$, $\hat{\mathbf{A}}$, $\hat{\mathbf{B}}_y$, $\hat{\mathbf{B}}_u$, $\hat{\mathbf{C}}$, $\hat{\mathbf{D}}_y$, $\hat{\mathbf{D}}_u$, $\mathbf{S} \in \boldsymbol{\Sigma}$, $\mathbf{G} \in \boldsymbol{\Gamma}$, and symmetric matrices $\mathbf{P}_{\text{ref}}$, $\mathbf{Y}$, and $\mathbf{Z}$ such that* (38), (39), *and $\overline{T}_{\text{pol}}^i \prec 0$ are satisfied for $i = 1, \ldots, p$.*

4. ROBUST FDI FILTER DESIGN USING LMIS

In this section, we give a suboptimal solution to Problem 1. An optimal solution would necessitate the solution of a quadratic matrix inequality and is in general intractable. Here, we propose a linearization procedure to derive an upper bound on the optimal solution that requires solving an LMI optimization problem.

The following general result demonstrates that if we have one feasible solution to a QMI optimization, then we can construct an LMI optimization problem whose solution gives an upper bound on the QMI problem.

Lemma 7. *Let $Q_o, R_o \in \mathcal{R}^{m\times n}$ and $S = S^T \in \mathcal{R}^{m\times m}$ be given and let $E_o = Q_o - R_o$ and $F_o = Q_o + R_o$. For $Q, R \in \mathcal{R}^{m\times n}$, define*

$$\mathcal{M}(Q,R) = S + QR^T + RQ^T,$$

$$\mathcal{N}(Q,R) = \begin{bmatrix} S + E_o E_o^T - (Q-R)E_o^T - E_o(Q-R)^T & R & Q \\ R^T & -I & 0 \\ Q^T & 0 & -I \end{bmatrix},$$

$$\mathcal{O}(Q,R) = \begin{bmatrix} S - F_o F_o^T + (Q+R)F_o^T + F_o(Q+R)^T & R & Q \\ R^T & I & 0 \\ Q^T & 0 & I \end{bmatrix}. \tag{48}$$

Then

$$\mathcal{N}(Q,R) \prec 0 \Longrightarrow \mathcal{M}(Q,R) \prec 0, \tag{49}$$

$$\mathcal{M}(Q_o,R_o) \prec 0 \Longrightarrow \mathcal{N}(Q_o,R_o) \prec 0, \tag{50}$$

$$\mathcal{O}(Q,R) \succ 0 \Longrightarrow \mathcal{M}(Q,R) \succ 0, \tag{51}$$

$$\mathcal{M}(Q_o,R_o) \succ 0 \Longrightarrow \mathcal{O}(Q_o,R_o) \succ 0. \tag{52}$$

Proof. Let $\mathcal{J}(Q,R) = S + QQ^T + RR^T + E_o E_o^T - (Q-R)E_o^T - E_o(Q-R)^T$. Then by using a Schur complement argument, we get

$$\mathcal{N}(Q,R) \prec 0 \Longleftrightarrow \mathcal{J}(Q,R) \prec 0. \tag{53}$$

Let $\xi(Q,R) = (Q-R-E_o)(Q-R-E_o)^T$. Now,

$$S + \xi(Q,R) = S + (Q-R)(Q-R)^T - (Q-R)E_o^T - E_o(Q-R)^T + E_o E_o^T, \tag{54}$$

and it follows that

$$S + QR^T + RQ^T = S + QQ^T + RR^T + E_o E_o^T - (Q-R)E_o^T - E_o(Q-R)^T - \xi(Q,R). \tag{55}$$

That is,

$$\mathcal{M}(Q,R) = \mathcal{J}(Q,R) - \xi(Q,R). \tag{56}$$

Using (53) and noting that $\xi(Q,R) \succeq 0$ and $\xi(Q_o,R_o) = 0$, we have

$$\mathcal{N}(Q,R) \prec 0 \Longrightarrow \mathcal{J}(Q,R) \prec 0 \Longrightarrow \mathcal{M}(Q,R) \prec 0,$$
$$\mathcal{M}(Q_o,R_o) \prec 0 \Longrightarrow \mathcal{J}(Q_o,R_o) \prec 0 \Longrightarrow \mathcal{N}(Q_o,R_o) \prec 0. \tag{57}$$

A similar proof can be used to derive (51) and (52). □

In order to simplify the subsequent analysis, we adopt the convention that variables appended with a subscript "x" denote feasible values of the variables for the QMIs (37) and (39).

In (37), the only nonlinear terms are $\mathbf{Z}E_1\mathbf{A}_{\text{ref}}E_1^T$, $\mathbf{Y}IE_1\mathbf{A}_{\text{ref}}E_1^T$, $\mathbf{Z}E_1\mathbf{B}_{\text{ref}}$, and $\mathbf{Y}E_1\mathbf{B}_{\text{ref}}$. We denote the matrix in (37) by T_{rfw}, and set S_{rfw} to be the matrix T_{rfw}, with the nonlinear terms removed.

Let $Z_x = Z_x^T \in \mathcal{R}^{n_k\times n_k}$, $Y_x = Y_x^T \in \mathcal{R}^{n_k\times n_k}$, $A_{\text{ref}_x} \in \mathcal{R}^{n_{\text{ref}}\times n_{\text{ref}}}$, and $B_{\text{ref}_x} \in \mathcal{R}^{n_{\text{ref}}\times n_f}$ be given. We use Lemma 7 to derive an LMI formulation. We can write T_{rfw} as

$$T_{rfw} = S_{rfw} + Q_c R_c^T + R_c Q_c^T, \tag{58}$$

where

$$Q_c = \begin{bmatrix} \mathbf{Z}E_1 & 0 \\ 0 & \mathbf{Y}E_1 \\ 0 & 0 \\ 0 & 0 \\ 0 & 0 \\ 0 & 0 \\ 0 & 0 \\ 0 & 0 \end{bmatrix}, \qquad R_c = \begin{bmatrix} E_1\mathbf{A}_{\text{ref}}{}^T & 0 \\ E_1\mathbf{A}_{\text{ref}}{}^T & E_1\mathbf{A}_{\text{ref}}{}^T \\ \mathbf{B}_{\text{ref}}{}^T & \mathbf{B}_{\text{ref}}{}^T \\ 0 & 0 \\ 0 & 0 \\ 0 & 0 \\ 0 & 0 \\ 0 & 0 \end{bmatrix}. \tag{59}$$

Let Q_{c_x} denote the value of Q_c when $\mathbf{Z}$ and $\mathbf{Y}$ are replaced by Z_x and Y_x, respectively, let R_{c_x} denote the value of R_c when $\mathbf{A}_{\text{ref}}$ and $\mathbf{B}_{\text{ref}}$ are replaced by A_{ref_x} and B_{ref_x}, respectively, and define $E_x = Q_{c_x} - R_{c_x}$. Using (49) from Lemma 7, we get

$$T_{rfw}^{\text{lin}} \prec 0 \Longrightarrow T_{rfw} \prec 0, \tag{60}$$

where

$$T_{rfw}^{\text{lin}} = \begin{bmatrix} S_{rfw} + E_x E_x^T - (Q_c - R_c)E_x^T - E_x(Q_c - R_c)^T & R_c & Q_c \\ R_c^T & -I & 0 \\ Q_c^T & 0 & -I \end{bmatrix}. \tag{61}$$

To linearize the matrix inequality in (39), we need Lemma 7 and the following lemma, whose proof is similar to that of Lemma 7 and is therefore dropped.

Lemma 8. *Let $U_o \in \mathcal{R}^{m\times n}$ and $S = S^T \in \mathcal{R}^{m\times m}$. For $U \in \mathcal{R}^{m\times n}$, define*

$$\begin{aligned} \mathcal{M}(U) &= S + UU^T = \mathcal{M}(U)^T, \\ \mathcal{N}(U) &= S + UU_o^T + U_oU^T - U_oU_o^T = \mathcal{N}(U)^T. \end{aligned} \tag{62}$$

Then

$$\begin{aligned} \mathcal{N}(U) \succ 0 &\Longrightarrow \mathcal{M}(U) \succ 0, \\ \mathcal{M}(U_o) \succ 0 &\Longrightarrow \mathcal{N}(U_o) \succ 0. \end{aligned} \tag{63}$$

Let $P_{\text{ref}_x} = P_{\text{ref}_x}^T \in \mathcal{R}^{n_{\text{ref}}\times n_{\text{ref}}}$, $C_{\text{ref}_x} \in \mathcal{R}^{n_f\times n_{\text{ref}}}$, and $D_{\text{ref}_x} \in \mathcal{R}^{n_f\times n_f}$ be given. Using (51) from Lemmas 7 and 8, it is easy to get

$$T_{\text{ro}}^{\text{lin}} \succeq 0 \Longrightarrow T_{\text{ro}} \succeq 0, \tag{64}$$

where

$$T_{\text{ro}}^{\text{lin}} = \begin{bmatrix} V & \star & \star & \star \\ V' & V'' & \star & \star \\ \mathbf{P}_{\text{ref}} & 0 & I & \star \\ \mathbf{A}_{\text{ref}} & \mathbf{B}_{\text{ref}} & 0 & I \end{bmatrix}, \tag{65}$$

where $V = \{(\mathbf{P}_{\text{ref}} + \mathbf{A}_{\text{ref}}{}^T)(P_{\text{ref}_x} + A_{\text{ref}_x}) + \star - C_{\text{ref}_x}^T C_{\text{ref}_x} + \mathbf{C}_{\text{ref}}{}^T C_{\text{ref}_x} + \star - (P_{\text{ref}_x} + A_{\text{ref}_x}^T)(P_{\text{ref}_x} + A_{\text{ref}_x})\}$, $V' = \{\mathbf{D}_{\text{ref}}^T C_{\text{ref}_x} + D_{\text{ref}_x}^T \mathbf{C}_{\text{ref}} - B_{\text{ref}_x}^T(P_{\text{ref}_x} + A_{\text{ref}_x}) - D_{\text{ref}_x}^T C_{\text{ref}_x} + \mathbf{B}_{\text{ref}}^T(P_{\text{ref}_x} + A_{\text{ref}_x}) + B_{\text{ref}_x}^T(\mathbf{P}_{\text{ref}} + \mathbf{A}_{\text{ref}})\}$, $V'' = \{\mathbf{D}_{\text{ref}}{}^T D_{\text{ref}_x} + D_{\text{ref}_x}^T \mathbf{D}_{\text{ref}} - B_{\text{ref}_x}^T B_{\text{ref}_x} - D_{\text{ref}_x}^T D_{\text{ref}_x} - I + \mathbf{B}_{\text{ref}}^T B_{\text{ref}_x} + \star\}$. The next lemma summarizes the results of this section by giving a linearized formulation of the optimization problem defined in Lemma 4 using (60) and (64).

Lemma 9. *Assume that $\mathbf{\Delta}$ is unstructured. Let $Z_x = Z_x^T \in \mathcal{R}^{n_k\times n_k}$, $Y_x = Y_x^T \in \mathcal{R}^{n_k\times n_k}$, $P_{\text{ref}_x} = P_{\text{ref}_x}^T \in \mathcal{R}^{n_{\text{ref}}\times n_{\text{ref}}}$, $A_{\text{ref}_x} \in \mathcal{A}$, $B_{\text{ref}_x} \in \mathcal{B}$, $C_{\text{ref}_x} \in \mathcal{C}$, and $D_{\text{ref}_x} \in \mathcal{D}$ be given. Then there exist a stable filter of the form given in* (8) *and a stable fault reference dynamics model $T_{\text{ref}} \stackrel{s}{=} (\mathbf{A}_{\text{ref}}, \mathbf{B}_{\text{ref}}, \mathbf{C}_{\text{ref}}, \mathbf{D}_{\text{ref}}) \in \mathcal{S}$, where $\mathcal{S}$ is defined in* (11), *such that $\|T_{\text{ref}}\|_- \geq 1$, residual dynamics in* (10) *are quadratically stable, and* (12) *is satisfied for $\mathcal{M} = \mathcal{M}_{\mathbf{\Delta}}$ if there exist $\mathbf{A}_{\text{ref}} \in \mathcal{A}$, $\mathbf{B}_{\text{ref}} \in \mathcal{B}$, $\mathbf{C}_{\text{ref}} \in \mathcal{C}$, $\mathbf{D}_{\text{ref}} \in \mathcal{D}$, $\hat{\mathbf{A}}$, $\hat{\mathbf{B}}_y$, $\hat{\mathbf{B}}_u$, $\hat{\mathbf{C}}$, $\hat{\mathbf{D}}_y$, $\hat{\mathbf{D}}_u$, $\boldsymbol{\lambda}$, and symmetric matrices $\mathbf{P}_{\text{ref}}$, $\mathbf{Y}$, and $\mathbf{Z}$ such that*

$$T_{rfw}^{\text{lin}} \prec 0, \tag{66}$$

$$T_{\text{ro}}^{\text{lin}} \succeq 0, \tag{67}$$

$$\begin{bmatrix} \mathbf{Z} & \mathbf{Z} \\ \mathbf{Z} & \mathbf{Y} \end{bmatrix} \succ 0. \tag{68}$$

Remark 3. This scheme can also be applied to Lemmas 5 and 6 to obtain a suboptimal solution involving linear matrix inequalities.

Next, we need to choose the initial parameters (Z_x, Y_x, P_{ref_x}, A_{ref_x}, B_{ref_x}, C_{ref_x}, and D_{ref_x}) to reduce γ. The idea is to derive an algorithm where at each iteration, we solve the optimization problem given in Lemma 9, using the solution of this problem at the previous iteration, for initial parameters. The algorithm will use initial values Z_x^{init}, Y_x^{init}, $P_{\text{ref}_x}^{\text{init}}$, $A_{\text{ref}_x}^{\text{init}}$, $B_{\text{ref}_x}^{\text{init}}$, $C_{\text{ref}_x}^{\text{init}}$, and $D_{\text{ref}_x}^{\text{init}}$, which must guarantee that the LMI constraints (66) and (67) will be feasible.

From the above discussion, an algorithm for choosing the initial parameters can be listed as follows.

Algorithm 1. (1) Set initial values $A_{\text{ref}_x}^{\text{init}}$, $B_{\text{ref}_x}^{\text{init}}$, $C_{\text{ref}_x}^{\text{init}}$, and $D_{\text{ref}_x}^{\text{init}}$ such that $T_{\text{ref}}^{\text{init}} \stackrel{s}{=} (A_{\text{ref}_x}^{\text{init}}, B_{\text{ref}_x}^{\text{init}}, C_{\text{ref}_x}^{\text{init}}, D_{\text{ref}_x}^{\text{init}})$ satisfies $\|T_{\text{ref}}^{\text{init}}\|_- \geq 1$ and $T_{\text{ref}}^{\text{init}} \in \mathcal{S}$.

(2) Find the solutions $\mathbf{Z}$, $\mathbf{Y}$, and $\mathbf{P}_{\text{ref}}$ of the optimization derived from Lemmas 3 and 4, which is linear since the matrix inequalities (37), (38), and (39) become linear when $T_{\text{ref}} := T_{\text{ref}}^{\text{init}}$ is fixed. (The matrices $\mathbf{Z}$, $\mathbf{Y}$, and $\mathbf{P}_{\text{ref}}$ always exist since the cost function in (12) is bounded because $\mathbf{\Delta}$ is bounded).

(3) Set $Z_x^{\text{init}} := \mathbf{Z}$, $Y_x^{\text{init}} := \mathbf{Y}$, and $P_{\text{ref}_x}^{\text{init}} := \mathbf{P}_{\text{ref}}$.

(4) Start loop.

(5) Since the initial values are feasible for (37), (38), and (39), the LMIs (66) to (68) have feasible solutions from (50) and (63) in Lemmas 7 and 8. Compute solutions ($\mathbf{Z}$, $\mathbf{Y}$, etc.) of (66) to (68) to minimize γ.

(6) Rename $Z_x^{\text{init}} = \mathbf{Z}$, $Y_x^{\text{init}} = \mathbf{Y}$, $P_{\text{ref}_x}^{\text{init}} = \mathbf{P}_{\text{ref}}$, $A_{\text{ref}_x}^{\text{init}} = \mathbf{A}_{\text{ref}}$, $B_{\text{ref}_x}^{\text{init}} = \mathbf{B}_{\text{ref}}$, $C_{\text{ref}_x}^{\text{init}} = \mathbf{C}_{\text{ref}}$, and $D_{\text{ref}_x}^{\text{init}} = \mathbf{D}_{\text{ref}}$, and go to Step 5.

(7) End loop.

Algorithm 1 is convergent, possibly to a local minimum, in the sense that the quantity γ is nonincreasing after each iteration. This can be easily shown using (50) and (52) from Lemma 7, and (63) from Lemma 8.

Remark 4. Lemmas 7, 8, and Algorithm 1 can also be applied to other problems involving QMIs and bilinear matrix inequalities (BMIs). The procedure potentially gives an improvement and seems to work well in practice.

Remark 5. In the case that we choose a diagonal structure for T_{ref}, we may use

$$\begin{aligned} A_{\text{ref}}^{\text{init}} &= -I_{n_{\text{ref}}}, \qquad B_{\text{ref}}^{\text{init}} = 0_{n_{\text{ref}}\times n_f}, \\ C_{\text{ref}}^{\text{init}} &= 0_{n_f\times n_{\text{ref}}}, \qquad D_{\text{ref}}^{\text{init}} = I_{n_f}, \end{aligned} \tag{69}$$

as initial values. This will ensure that T_{ref} is stable and $\|T_{\text{ref}}\|_- = 1$. We can solve the LMI optimization problem given in Lemma 4. This will give Z_x^{init}, Y_x^{init}, $P_{\text{ref}_x}^{\text{init}}$, and so forth. These initial values are not unique and can be chosen using other criteria.

Remark 6. A more systematic technique for generating valid initial values is as follows: first, generate any $B_{\text{ref}}^{\text{init}}$, $C_{\text{ref}}^{\text{init}}$, $D_{\text{ref}}^{\text{init}}$, and a stable $A_{\text{ref}}^{\text{init}}$ with the structure chosen, then, compute $\alpha = \|T_{\text{ref}}^{\text{init}}\|_-$. If $\alpha > 0$, redefine the matrices as $A_{\text{ref}}^{\text{init}} = A_{\text{ref}}^{\text{init}}/\alpha$, $B_{\text{ref}}^{\text{init}} = B_{\text{ref}}^{\text{init}}/\alpha$, $C_{\text{ref}}^{\text{init}} = C_{\text{ref}}^{\text{init}}/\alpha$, and $D_{\text{ref}}^{\text{init}} = D_{\text{ref}}^{\text{init}}/\alpha$, which fulfill that the conditions $T_{\text{ref}}^{\text{init}}$ are stable and $\|T_{\text{ref}}^{\text{init}}\|_- = 1$.

Remark 7. The requirement for T_{ref} to be diagonal is to ensure fault isolability in the case that all faults may occur simultaneously. If we ignore disturbances and uncertainty, and assuming perfect fault isolation, then $r = T_{\text{ref}} f$ so that fault f_i only affects residual r_i. If none of the faults can occur simultaneously, then we need only to impose the constraint that T_{ref} is upper (or lower) triangular. While it is not difficult to modify our analysis under these conditions, we only consider the case when T_{ref} is diagonal so that all faults may occur simultaneously since our contribution is focussed on reducing the effect of disturbances and uncertainties under the most stringent fault scenarios.

5. NUMERICAL EXAMPLE

In order to illustrate the efficiency of Algorithm 1 and the importance of the choice of T_{ref}, we consider a jet engine state-space model [32] supplied by NASA Glenn Research Center given as

$$\begin{aligned} \dot{x}(t) &= (A^o + F_A\Delta_H E_A)x(t) + (B^o + F_A\Delta_H E_B)u(t) \\ &\quad + B_d d(t) + B_f f(t), \\ y(t) &= (C^o + F_C\Delta_H E_A)x(t) + (D^o + F_C\Delta_H E_B)u(t) \\ &\quad + D_d d(t) + D_f f(t), \end{aligned} \tag{70}$$

where

$$\begin{aligned} A^o &= \begin{bmatrix} -0.9835 & -0.0110 & -0.0039 \\ -0.0004 & -0.9858 & -0.0026 \\ 0 & 0.0002 & -0.9891 \end{bmatrix}, \\ B^o &= \begin{bmatrix} 0.0080 & 0.2397 & -0.0383 \\ 0.0068 & 0.1565 & 0.0248 \\ 0.0003 & -0.0003 & 0.0003 \end{bmatrix}, \\ C^o &= \begin{bmatrix} 0.2383 & 0.4871 & 0.1390 \\ 0 & -.0008 & 0.0004 \\ 0.00002 & -0.00004 & 0 \end{bmatrix}, \\ D^o &= \begin{bmatrix} 0.4171 & -4.4920 & 0.4875 \\ 0.0008 & -0.0050 & 0.0003 \\ 0 & 0.0005 & -0.0021 \end{bmatrix}. \end{aligned} \tag{71}$$

The system is subject to three disturbances and three potential faults. Here, the setup is given by

$$\begin{aligned} B_d &= \begin{bmatrix} 0.1 & 0 & 0 \\ 0 & 0.1 & 0 \\ 0 & 0 & 0.01 \end{bmatrix}, \\ B_f &= \begin{bmatrix} 0.0080 & 0.2397 & -0.0383 \\ 0.0068 & 0.1565 & 0.0248 \\ 0.0003 & -0.0003 & 0.0003 \end{bmatrix}, \\ D_d &= 0.1 \times I_3, \\ D_f &= \begin{bmatrix} -0.0205 & 0.6217 & 0.8115 \\ 0.2789 & -1.7506 & 0.6363 \\ 1.0583 & 0.6973 & 1.3101 \end{bmatrix}. \end{aligned} \tag{72}$$

Since no uncertainty parameters were given in this example, we assume an unstructured norm-bounded uncertainty, with matrices F_A, F_C, E_A, E_B, and H randomly generated as

$$\begin{aligned} H &= \begin{bmatrix} -0.319 & -0.080 & 0.142 \\ -0.288 & 0.138 & 0.258 \\ 0.114 & 0.163 & 0.133 \end{bmatrix}, \\ E_A &= \begin{bmatrix} -0.060 & -0.008 & -0.135 \\ -0.015 & 0.154 & 0.047 \\ -0.044 & -0.061 & -0.090 \end{bmatrix}, \\ E_B &= \begin{bmatrix} 0.134 & 0.630 & 0.451 \\ 0.207 & 0.371 & 0.044 \\ 0.607 & 0.575 & 0.027 \end{bmatrix}, \\ F_C &= \begin{bmatrix} -0.055 & 0.066 & -0.012 \\ -0.085 & -0.085 & -0.007 \\ -0.025 & -0.120 & 0.049 \end{bmatrix}, \\ F_A &= \begin{bmatrix} 0.148 & -0.129 & -0.084 \\ 0.114 & -0.007 & 0.050 \\ -0.068 & -0.033 & 0.149 \end{bmatrix}. \end{aligned} \tag{73}$$

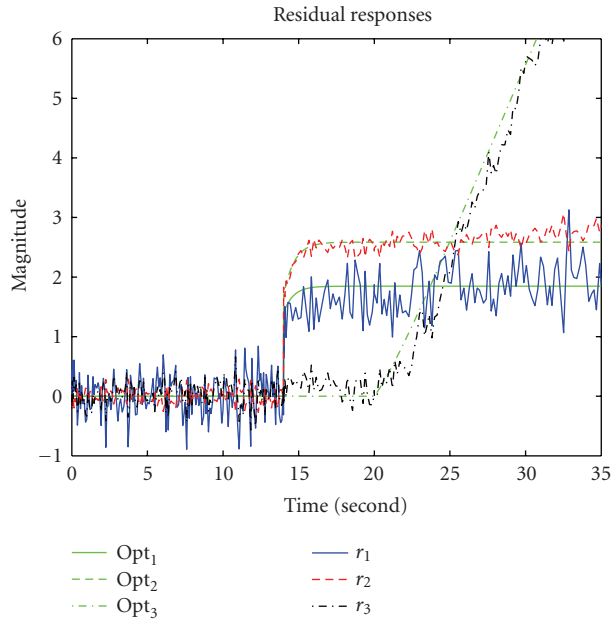

FIGURE 2: Time response of the residual before the optimization.

A square and diagonal structure for T_{ref} is necessary to get fault isolation in the case that the faults occur at the same time.

Remark 8. If A_{ref}, B_{ref}, and C_{ref} are chosen diagonal, then

$$\begin{aligned} T_{\text{ref}}(s) &= C_{\text{ref}}(sI - A_{\text{ref}})^{-1}B_{\text{ref}} + D_{\text{ref}} \\ &= C_{\text{ref}}B_{\text{ref}}(sI - A_{\text{ref}})^{-1} + D_{\text{ref}}. \end{aligned} \tag{74}$$

The terms in B_{ref} can be incorporated in C_{ref}. It follows that we can set $B_{\text{ref}} = I$. Therefore, the nonlinearity in (37) comes only from bilinear terms $\mathbf{Z}E_1\mathbf{A}_{\text{ref}}E_1^T$ and $\mathbf{Y}E_1\mathbf{A}_{\text{ref}}E_1^T$.

To initialize Algorithm 1, $T_{\text{ref}}^{\text{init}}$ is generated following Remark 6 as

$$\begin{aligned} A_{\text{ref}}^{\text{init}} &= \begin{bmatrix} -1.60 & 0 & 0 \\ 0 & -1.44 & 0 \\ 0 & 0 & -0.57 \end{bmatrix}, \\ B_{\text{ref}}^{\text{init}} &= I_3, \\ C_{\text{ref}}^{\text{init}} &= \begin{bmatrix} 0.71 & 0 & 0 \\ 0 & 1.29 & 0 \\ 0 & 0 & 0.67 \end{bmatrix}, \\ D_{\text{ref}}^{\text{init}} &= \begin{bmatrix} 1.40 & 0 & 0 \\ 0 & 1.69 & 0 \\ 0 & 0 & 1.81 \end{bmatrix}. \end{aligned} \tag{75}$$

Then, by following the first two steps of Algorithm 1, we get the optimal γ as

$$\gamma = 0.6273 \tag{76}$$

and the values given below for Z, Y, and P_{ref_x}, which will be used to initialize the main loop of the algorithm as follows.

$$\begin{aligned} Z_{\text{ref}} &= \begin{bmatrix} 0.5010 & -0.4385 & 0.0309 & 0.6192 & -0.4313 & 0.4861 \\ -0.4385 & 0.8184 & 0.0844 & -0.3629 & -0.6083 & -0.8105 \\ 0.0309 & 0.0844 & 0.0651 & 0.0986 & -0.3323 & -0.1397 \\ 0.6192 & -0.3629 & 0.0986 & 1.4722 & -1.2716 & 0.9082 \\ -0.4313 & -0.6083 & -0.3323 & -1.2716 & 5.7926 & -1.5337 \\ 0.4861 & -0.8105 & -0.1397 & 0.9082 & -1.5337 & 2.5593 \end{bmatrix}, \\ Y_{\text{ref}} &= \begin{bmatrix} 5.0059 & 19.1311 & 2.7518 & 0.1860 & 3.0607 & 0.7016 \\ 19.1311 & 165.3233 & 12.5435 & -13.2886 & 32.4525 & -15.3595 \\ 2.7518 & 12.5435 & 7.7249 & -4.8209 & 0.6873 & -3.4439 \\ 0.1860 & -13.2886 & -4.8209 & 7.4800 & -5.3595 & 4.9329 \\ 3.0607 & 32.4525 & 0.6873 & -5.3595 & 22.7920 & -4.1575 \\ 0.7016 & -15.3595 & -3.4439 & 4.9329 & -4.1575 & 8.6769 \end{bmatrix}, \\ P_{\text{ref}_x} &= \begin{bmatrix} -0.0492 & 1.4322 & -0.1444 \\ 1.4322 & -63.1246 & 8.1628 \\ -0.1444 & 8.1628 & -1.2084 \end{bmatrix}. \end{aligned} \tag{77}$$

Taking into account Remark 8, we implemented Algorithm 1 in Matlab to minimize γ. Table 1 shows the evolution of the optimization following Algorithm 1.

Algorithm 1 can clearly improve the result in a few iterations; γ is reduced by 33% compared to the one obtained with a fixed T_{ref}. This shows that the choice of T_{ref} is essential in our FDI scheme. We get

$$\begin{aligned} A_{\text{ref}} &= \begin{bmatrix} -18.1665 & 0 & 0 \\ 0 & -9.2781 & 0 \\ 0 & 0 & -6.0914 \end{bmatrix}, \\ B_{\text{ref}} &= I_3, \\ C_{\text{ref}} &= \begin{bmatrix} 0.0007 & 0 & 0 \\ 0 & -0.3959 & 0 \\ 0 & 0 & 0.0572 \end{bmatrix}, \\ D_{\text{ref}} &= \begin{bmatrix} 1.2438 & 0 & 0 \\ 0 & 4.3768 & 0 \\ 0 & 0 & 1.8216 \end{bmatrix}. \end{aligned} \tag{78}$$

Remark 9. In our numerical experimentation, other choices for $T_{\text{ref}}^{\text{init}}$ have been used; however, all converged to the same solution but with different numbers of iterations.

In order to show that our filter is robust against disturbances and model uncertainties, we introduce a randomly generated Δ given by

$$\Delta = \begin{bmatrix} 0.4058 & -0.0534 & -0.3600 \\ -0.4097 & -0.5466 & 0.4822 \\ -0.0067 & 0.0877 & -0.2743 \end{bmatrix}, \tag{79}$$

Table 1

Iterations	0	1	2	5	10	20	50	100
γ	0.6273	0.6248	0.5791	0.5476	0.5253	0.4739	0.4641	0.4641

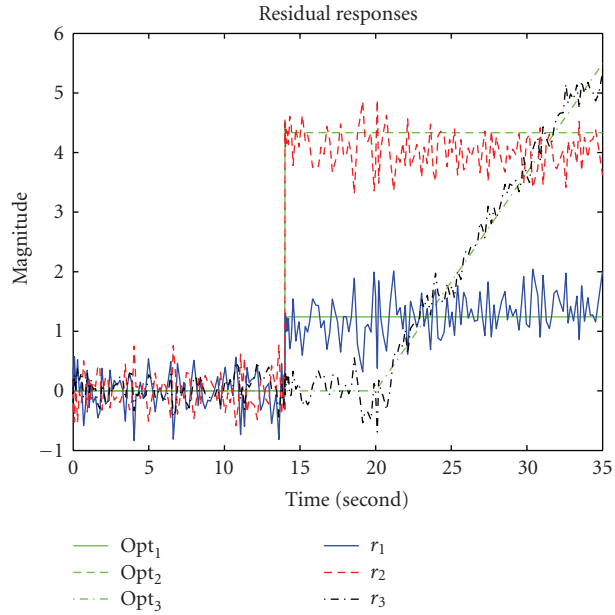

Figure 3: Time response of the residual after the optimization.

as well as three disturbances. Simulated through MATLAB and SIMULINK, these disturbances are three-band-limited white noises with mean 0 and standard deviation 2. Faults f_1 and f_2 are both simulated by a unit positive jump connected from the 14th second. Fault f_3, simulated by a soft bias (slope = 0.2), is connected from the 20th second. Figure 2 gives the residual responses before the algorithm, where each residual is dedicated to a particular fault, while Figure 3 gives the optimized residual response using our algorithm.

The lines opt_1, opt_2, and opt_3 represent the optimal trajectories that each residual must follow

$$\begin{bmatrix} \text{opt}_1(s) \\ \text{opt}_2(s) \\ \text{opt}_3(s) \end{bmatrix} = T_{\text{ref}} \begin{bmatrix} f_1(s) \\ f_2(s) \\ f_3(s) \end{bmatrix}. \tag{80}$$

In both figures, each fault can be distinguished from the others and the disturbances; however, in Figure 3, the faults can be more easily distinguished and each residual follows its optimal trajectory (green line) with more accuracy. Furthermore, the disturbances are more attenuated compared to Figure 2, and the jumps that indicate faults are clearer in Figure 3 since their amplitudes are bigger and therefore allow a better fault detection using thresholds [33, 34]. The isolation performance is clearly effective as each fault produces a deviation of its residual only, without modifying the trajectory of the others. This example illustrates that the designed filter satisfies the performance requirement of FDI which is sufficiently robust against disturbances and modeling errors.

Figure 3 also justifies the efficiency of Algorithm 1 to improve the design of the reference model and therefore the overall performance of our filter.

6. CONCLUSION

This paper has addressed the problem of fault detection and isolation for linear time-invariant systems subject to faults, disturbances, and model uncertainties. We proposed a performance index that captures the FDI requirements. Through QMI formulations, we gave the design of an optimal filter for polytopic or unstructured norm-bounded uncertainties, and a suboptimal filter for structured norm-bounded uncertainties. Suboptimality in the latter case is inherited from the bounded real lemma, which gives only sufficient LMI conditions for structured uncertainties (see Lemma 2). By allowing the reference model T_{ref} to be variable in our formulation, we get its optimal design, which can be used in other schemes dedicated to fault isolation. The optimal design of this reference model is initially given in a form of a QMI optimization, then a suboptimal solution is obtained by using a linearization procedure which derives an upper bound on the optimal solution of the QMI formulation that requires the solution of an LMI optimization. Note, however, that we have no indication concerning the deviation of our design from the optimal filter. We have also illustrated the effectiveness of our algorithm using a jet-engine example.

ACKNOWLEDGMENT

This work was partially supported by the Ministry of Defence through the Data and Information Fusion Defence Technology Centre.

REFERENCES

[1] Z. Gao and H. Wang, "Descriptor observer approaches for multivariable systems with measurement noises and application in fault detection and diagnosis," *Systems and Control Letters*, vol. 55, no. 4, pp. 304–313, 2006.

[2] C. Jiang and D. H. Zhou, "Fault detection and identification for uncertain linear time-delay systems," *Computers and Chemical Engineering*, vol. 30, no. 2, pp. 228–242, 2005.

[3] M. Fu, C. E. De Souza, and Z.-Q. Luo, "Finite-horizon robust kalman filter design," *IEEE Transactions on Signal Processing*, vol. 49, no. 9, pp. 2103–2112, 2001.

[4] K. M. Nagpal and P. P. Khargonekar, "Filtering and smoothing in an $\mathcal{H}_\infty$ setting," *IEEE Transactions on Automatic Control*, vol. 36, no. 2, pp. 152–166, 1991.

[5] A. H. Sayed, "A framework for state-space estimation with uncertain models," *IEEE Transactions on Automatic Control*, vol. 46, no. 7, pp. 998–1013, 2001.

[6] S. H. Zad and M.-A. Massoumnia, "Generic solvability of the failure detection and identification problem," *Automatica*, vol. 35, no. 5, pp. 887–893, 1999.

[7] R. J. Patton and J. Chen, "On eigenstructure assignment for robust fault diagnosis," *International Journal of Robust and Nonlinear Control*, vol. 10, no. 14, pp. 1193–1208, 2000.

[8] P. Zhang, H. Ye, S. X. Ding, G. Z. Wang, and D. H. Zhou, "On the relationship between parity space and $\mathcal{H}_2$ approaches to fault detection," *Systems and Control Letters*, vol. 55, no. 2, pp. 94–100, 2006.

[9] J. Chen, R. J. Patton, and H.-Y. Zhang, "Design of unknown input observers and robust fault detection filters," *International Journal of Control*, vol. 63, no. 1, pp. 85–105, 1996.

[10] I. M. Jaimoukha, Z. Li, and E. F.M. Mazars, "Linear matrix inequality solution to the $\mathcal{H}_-/\mathcal{H}_\infty$, fault detection problem," in *Proceedings of the 7th International Conference on Control and Applications, the International Association of Science and Technology for Development (IASTED '05)*, pp. 183–188, Cancun, Mexico, May 2005.

[11] I. M. Jaimoukha, Z. Li, and E. Mazars, "Fault isolation filter with linear matrix inequality solution to optimal decoupling," in *Proceedings of the American Control Conference (ACC '06)*, vol. 2006, pp. 2339–2344, Minneapolis, Minn, USA, 2006.

[12] Z. Li, E. Mazars, and I. M. Jaimoukha, "State space solution to the $\mathcal{H}_-/\mathcal{H}_\infty$ fault detection problem.," in *Proceedings of the IEEE 45th Conference on Decision and Control (CDC '06)*, pp. 2177–2182, San Diego, Calif, USA, December 2006.

[13] E. Frisk and L. Nielsen, "Robust residual generation for diagnosis including a reference model for residual behavior," in *Proceedings of the 14th World Congress International Federation of Automatic Control (IFAC '99)*, pp. 55–60, Beijing, China, July 1999.

[14] M. Zhong, S. X. Ding, J. Lam, and H. Wang, "An LMI approach to design robust fault detection filter for uncertain LTI systems," *Automatica*, vol. 39, no. 3, pp. 543–550, 2003.

[15] E. Frisk and L. Nielsen, "Robust residual generation for diagnosis including a reference model for residual behavior," *Automatica*, vol. 42, no. 3, pp. 437–445, 2006.

[16] E. Mazars, I. M. Jaimoukha, and Z. Li, "Linear matrix solutions to a robust fault detection and isolation problem," under review in *European Journal of Control*.

[17] D. J. Clements, B. D.O. Anderson, A. J. Laub, and J. B. Matson, "Spectral factorization with imaginary-axis zeros," *Linear Algebra and Its Applications*, vol. 250, pp. 225–252, 1997.

[18] P. M. Frank and X. Ding, "Survey of robust residual generation and evaluation methods in observer-based fault detection systems," *Journal of Process Control*, vol. 7, no. 6, pp. 403–424, 1997.

[19] S. P. Boyd, L. El Ghaoui, E. Feron, and V. Balakrishnan, *Linear Matrix Inequalities in Systems and Control Theory*, SIAM, Philadelphia, Pa, USA, 1994.

[20] W. H. Chung and J. L. Speyer, "A game theoretic fault detection filter," *IEEE Transactions on Automatic Control*, vol. 43, no. 2, pp. 143–161, 1998.

[21] R. K. Douglas and J. L. Speyer, "Robust fault detection filter design," in *Proceedings of the American Control Conference (ACC '95)*, vol. 1, pp. 91–96, Seattle, Wash, USA, June 1995.

[22] I. M. Jaimoukha, Z. Li, and V. Papakos, "A matrix factorization solution to the $\mathcal{H}_-/\mathcal{H}_\infty$ fault detection problem," *Automatica*, vol. 42, no. 11, pp. 1907–1912, 2006.

[23] H. B. Wang, L. Lam, S. X. Ding, and M. Y. Zhong, "Iterative linear matrix inequality algorithms for fault detection with unknown inputs," *Journal of Systems and Control Engineering*, vol. 219, no. 2, pp. 161–172, 2005.

[24] H. D. Tuan, P. Apkarian, and T. Q. Nguyen, "Robust filtering for uncertain nonlinearly parameterized plants," *IEEE Transactions on Signal Processing*, vol. 51, no. 7, pp. 1806–1815, 2003.

[25] L. El Ghaoui and J. P. Folcher, "Multiobjective robust control of LTI systems subject to unstructured perturbations," *Systems and Control Letters*, vol. 28, no. 1, pp. 23–30, 1996.

[26] C. Scherer, P. Gahinet, and M. Chilali, "Multi-objective output-feedback control via LMI optimization," *IEEE Transactions on Automatic Control*, vol. 42, no. 7, pp. 896–911, 1997.

[27] K.-C. Goh, M. G. Safonov, and G. P. Papavassilopoulos, "Global optimization approach for the BMI problem," in *Proceedings of the IEEE Conference on Decision and Control (CDC '94)*, vol. 3, pp. 2009–2014, Lake Buena Vista, Fla, USA, 1994.

[28] Yamada, Hara, and Fujioka, "Global optimization for constantly scaled $\mathcal{H}_\infty$ control problem," in *Proceedings of the American Control Conference (ACC '95)*, vol. 1, pp. 427–430, Seattle, Wash, USA, June 1995.

[29] J. C. Geromel, P. L. D. Peres, and S. R. De Souza, "Output feedback stabilization of uncertain systems through a min/max problem," in *Proceedings of the 12th World Congress International Federation of Automatic Control (IFAC '93)*, vol. 6, pp. 35–38, The Institute of Engineers, Sydney, Australia, July 1993, in preprints of papers.

[30] E. Beran and K. Grigoriadis, "A combined alternating projections and semidefinite programming algorithm for low-order control design," in *Proceedings of the 13th World Congress, International Federation of Automatic Control (IFAC '96)*, pp. 85–90, San Francisco, Calif, USA, July 1996.

[31] A. Saberi, P. Sannuti, and B. M. Chen, *H_2 optimal control system and control engineering*, Prentice Hall, London, UK, 1995.

[32] T. D. Curry and E. G. Collins Jr., "Robust fault detection and isolation using robust ℓ 1 estimation," *Journal of Guidance, Control, and Dynamics*, vol. 28, no. 6, pp. 1131–1139, 2005.

[33] X. C. Ding and P. M. Frank, "Frequency domain approach and threshold selector for robust model-based fault detection and isolation," in *IFAC/IMACS Symposium on Fault Detection, Supervision and Safety for Technical Processes—SAFEPROCESS '91 (IFAC '92)*, vol. 6, pp. 271–276, Baden-Baden, Germany, 1992.

[34] F. Rambeaux, F. Hamelin, and D. Sauter, "Optimal thresholding for robust fault detection of uncertain systems," *International Journal of Robust and Nonlinear Control*, vol. 10, no. 14, pp. 1155–1173, 2000.

Hindawi Publishing Corporation
Journal of Control Science and Engineering
Volume 2008, Article ID 853275, 15 pages
doi:10.1155/2008/853275

Research Article

Fault Detection, Isolation, and Accommodation for LTI Systems Based on GIMC Structure

D. U. Campos-Delgado,[1] E. Palacios,[1] and D. R. Espinoza-Trejo[2]

[1] *Facultad de Ciencias, Zona Universitaria, Universidad Autonoma de San Luis Potosí, 78290 San Luis Potosí, SLP, Mexico*
[2] *Facultad de Ingeniería, Universidad Autonoma de San Luis Potosí, Av. Dr. Manuel Nava 8, Zona Universitaria, 78290 C.P., SLP, Mexico*

Correspondence should be addressed to D. U. Campos-Delgado, ducd@fciencias.uaslp.mx

Received 31 December 2006; Revised 28 July 2007; Accepted 13 November 2007

Recommended by Kemin Zhou

In this contribution, an active fault-tolerant scheme that achieves fault detection, isolation, and accommodation is developed for LTI systems. Faults and perturbations are considered as additive signals that modify the state or output equations. The accommodation scheme is based on the generalized internal model control architecture recently proposed for fault-tolerant control. In order to improve the performance after a fault, the compensation is considered in two steps according with a fault detection and isolation algorithm. After a fault scenario is detected, a general fault compensator is activated. Finally, once the fault is isolated, a specific compensator is introduced. In this setup, multiple faults could be treated simultaneously since their effect is additive. Design strategies for a nominal condition and under model uncertainty are presented in the paper. In addition, performance indices are also introduced to evaluate the resulting fault-tolerant scheme for detection, isolation, and accommodation. Hard thresholds are suggested for detection and isolation purposes, meanwhile, adaptive ones are considered under model uncertainty to reduce the conservativeness. A complete simulation evaluation is carried out for a DC motor setup.

1. INTRODUCTION

In the early stages of control applications, closed-loop performance was the main objective for the control engineer. To achieve this goal, the implementations of these feedback configurations involved sensors, actuators, electronic instrumentation, and signal processors. However, during a normal operation, these parts could fail in some degree, and the resulting performance of the closed-loop will be largely deteriorated, or even instability can be observed. In fact, for some processes besides performance, safety is also a necessary and important objective. Therefore, it is desirable to detect these malfunctions to take proper action in order to avoid a dangerous situation. Nowadays, the advance in electronics has made possible to have digital signal processors as microcontrollers, DSP's and FPGA boards that can perform, in real time, very complex algorithms. Hence this extra processing capacity could be applied to perform in parallel fault diagnosis strategies to the nominal control schemes. The problem of fault diagnosis is indeed a challenging one, and its importance in applications has attracted the attention of the research community in control theory and signal processing [1–4].

In any process, the faults can be classified in two sets: *unrecoverable* and *recoverable*. The unrecoverable ones represent all faults that cannot be compensated or accommodated while the system is running. On the other hand, the recoverable faults comprise any fault whose outcome can still be safely compensated by the control algorithm with a possible deterioration of performance, but still allowing the necessary conditions to maintain closed-loop stability. Obviously, this classification depends on the problem at hand, and requires knowledge about the operation of the system. From a control point of view, the focus is on the *recoverable faults*, where a degree of robustness or reconfigurability in the control scheme is desirable to accommodate these faults and still preserve closed-loop performance. These ideas have triggered a research line called fault-tolerant control (FTC) [5–9].

FTC can be approached from two perspectives: passive and active. In the passive approach, the faults are treated as disturbances into the closed-loop system. As a result, a single

controller is designed to achieve stability and performance against all studied faults. The main drawback of this scheme is the conservativeness that can be incorporated, however, no extra complexity in the control implementation is carried out. For LTI systems, the passive approach can be treated as a simultaneous stabilization or robust $\mathcal{H}_\infty$ design [9]. Meanwhile, for nonlinear systems, a variable structure control (sliding mode) methodology can be applied [10]. On the other hand, the active approach relies on a fault diagnosis stage, followed by a controller reconfiguration or accommodation [6]. Compared to the passive approach, the active one requires more computational power during implementations, but it can provide less conservative results and better closed-loop performance after faults. Applications of the active approach have been suggested for LTI [7, 8, 11, 12], LPV [13, 14], and nonlinear systems [15, 16]. Three major trends are devised in active FTC according to the required information of the FDI stage as follows.

(A) Estimate the faults profiles and update the nominal control law to cancel completely their effect (*fault decoupling*). Therefore, this idea requires a reliable fault isolation and identification scheme.
(B) Design a compensation signal for the nominal control law that depends on the fault affecting the system. Hence according to the transfer function from a specific fault to the output measurements or input control signal (*fault signature transfer matrices*), an accommodation control law is designed to reduce its effect into the closed-loop system. Alternatively, the nominal control law can be reconfigurated according to the isolated fault, for example, using reconfigurable control gains under a state-feedback control law. As a result, these approaches rely on the information from the fault isolation stage to properly operate.
(C) Switch to a robust control law that maintains closed-loop stability for a studied set of faults. In consequence, this scheme depends just on the information of a fault detection block. However, the post-fault performance can be pretty conservative.

This work looks to extend the ideas initially presented in [12, 17, 18]. Hence fault detection, isolation, and accommodation are discussed in a more general framework under the GIMC control structure for additive faults. The contribution of this paper lies in the following lines.

(i) A two-step active FTC scheme is proposed for LTI systems under an additive fault scenario.
(ii) Design strategies are proposed for diagnosis and accommodation based on general optimization criteria.
(iii) Performance indices are suggested in order to evaluate the active FTC from a worst-case perspective.
(iv) A complete analysis is introduced for the synthesis algorithms under model uncertainty. Hard and adaptive thresholds are provided for detection and isolation purposes.

Consequently, the FTC philosophies (B) and (C) are adopted in this work, looking to reduce the conservativeness in the post-fault performance, but avoiding the necessity of fault identification. The paper is structured as follows. Section 2 describes the problem formulation. The FTC scheme is presented in Section 3. First, the general methodology is introduced, and the design criteria for diagnostic, isolation, and accommodation are detailed next. Section 4 analyzes the effect of model uncertainty in the FTC scheme. Finally, Section 5 presents an illustrative example, and Section 6 gives some concluding remarks.

2. PROBLEM FORMULATION

The problem addressed in this paper is fault detection, isolation, and accommodation for LTI systems under additive faults and perturbations. In this way, consider a system $P(s)$ affected by disturbances $d \in \mathbb{R}^r$ and possible faults $f \in \mathbb{R}^l$, as shown in Figure 1, described by

$$P(s)\begin{cases}\dot{x} = Ax + Bu + F_1 f + E_1 d,\\ y = Cx + Du + F_2 f + E_2 d,\end{cases} \tag{1}$$

where $x \in \mathbb{R}^n$ represents the vector of states, $u \in \mathbb{R}^m$ the vector of inputs, and $y \in \mathbb{R}^p$ the vector of outputs. Thus matrix $F_1 \in \mathbb{R}^{n\times l}$ stands for the distribution matrix of the actuator or system faults, and $F_2 \in \mathbb{R}^{p\times l}$ for sensor faults. Denote as $F_1^i \in \mathbb{R}^n$ and $F_2^i \in \mathbb{R}^p$ with $i = 1, \ldots, l$ the columns of the fault signature matrices F_1 and F_2, respectively, that is,

$$F_1 = \begin{bmatrix} F_1^1 & \cdots & F_1^l \end{bmatrix}, \qquad F_2 = \begin{bmatrix} F_2^1 & \cdots & F_2^l \end{bmatrix}. \tag{2}$$

Thus matrices (F_1^i, F_2^i) will represent the signature of the ith component f_i in the fault vector f. The nominal system (A, B, C, D) is considered controllable and observable. On the other hand, the system response y can be analyzed in a transfer matrix form (frequency domain) as follows:

$$y(s) = P_{uy}u(s) + P_{fy}f(s) + P_{dy}d(s), \tag{3}$$

where

$$\begin{aligned} P_{uy} &= C(sI - A)^{-1}B + D,\\ P_{dy} &= C(sI - A)^{-1}E_1 + E_2,\\ P_{fy} &= C(sI - A)^{-1}F_1 + F_2. \end{aligned} \tag{4}$$

A left coprime factorization for each transfer matrix can be derived by obtaining matrix $L \in \mathbb{R}^{n\times p}$ such that $\Re\{\lambda_i(A + LC)\} < 0$ [19, 20], as it is shown next:

$$\begin{bmatrix} \widetilde{N} & \widetilde{M} & \widetilde{N}_d & \widetilde{N}_f \end{bmatrix} = \left[\begin{array}{c|cccc} A + LC & B + LD & L & E_1 + LE_2 & F_1 + LF_2 \\ \hline C & D & I & E_2 & F_2 \end{array}\right]. \tag{5}$$

Consequently, the LTI systems in (4) can be written as

$$P_{uy} = \widetilde{M}^{-1}\widetilde{N}, \qquad P_{dy} = \widetilde{M}^{-1}\widetilde{N}_d, \qquad P_{fy} = \widetilde{M}^{-1}\widetilde{N}_f, \tag{6}$$

where $\widetilde{M}, \widetilde{N}, \widetilde{N}_d, \widetilde{N}_f \in \mathcal{RH}_\infty$. An initial question about the fault diagnosis and isolation process relies on the necessary conditions to achieve this objective, hence the condition originally presented in [1, 4] are assumed as follows:

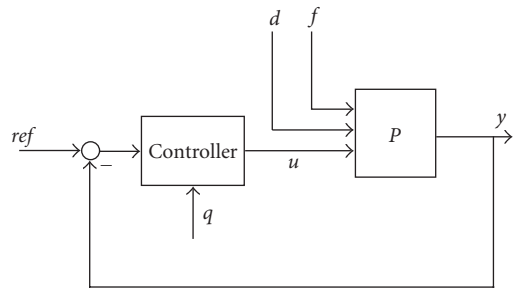

Figure 1: Problem formulation for control.

(1) for isolation of the fault vector f,

$$\text{rank}\left(\begin{bmatrix} F_1 \\ F_2 \end{bmatrix}\right) = l; \tag{7}$$

(2) for the simultaneous isolation of faults under unknown perturbations,

$$\text{normrank}\left(\begin{bmatrix} \widetilde{N}_d & \widetilde{N}_f \end{bmatrix}\right) \geq \text{normrank}\,(\widetilde{N}_d) + l, \tag{8}$$

where normrank stands for the normal rank of the corresponding transfer matrix [20].

Now, it is assumed that a nominal controller K stabilizes the nominal plant P_{uy}, and it provides a desired closed-loop performance in terms of robustness, transient, and steady-state responses. The controller K is considered observable, and consequently, it can also be expressed by a left coprime factorization, that is, $K = \widetilde{V}^{-1}\widetilde{U}$ where $\widetilde{U}, \widetilde{V} \in \mathcal{RH}_\infty$,

$$K = \left[\begin{array}{c|c} A_k & B_k \\ \hline C_k & D_k \end{array}\right] \Longrightarrow \begin{bmatrix} \widetilde{U} & \widetilde{V} \end{bmatrix} = \left[\begin{array}{c|cc} A_k + L_k C_k & B_k + L_k D_k & L_k \\ \hline C_k & D_k & I \end{array}\right]. \tag{9}$$

The nominal controller can be synthesized following classical techniques or optimal control: lead/lag compensator, PI, PID, LQG/$\mathcal{H}_2$, $\mathcal{H}_\infty$ loop shaping design, and so on. Consequently, the *control objective* is presented as follows. *Design an active fault-tolerant scheme such that it detects and isolates the occurrence of a fault in the closed-loop system, and provides an appropriate compensation signal q to the controller in order to maintain closed-loop performance* (see Figure 1).

Remark 1. The problem formulation in (1) assumes no previous knowledge of the time profiles of the fault components $f_i\, i = 1, \ldots, l$. Thus the fault vector f is modeled as an unknown exogenous input for the system $P(s)$. However, if explicit knowledge about the faults time profiles is available, then this information can be incorporated at the FDI stage to improve the residual design and evaluation. Nonetheless, the fault-accommodation scheme presented in the next section is consistent with this assumption, and it does not require an explicit identification of the faults affecting the system. Furthermore, the additive faults representation in (1) might be able to describe some common faults that cause changes on system parameters or loss of effectiveness in actuators, but in those cases, the faults time profiles will be related to states or control inputs (as it will be shown in Section 5).

The definition of the following system performance indexes will be very important for the synthesis and analysis of the fault detection, isolation, and accommodation algorithms [19–21]:

$$\begin{aligned}
\|G\|_1 &= \max_{1\leq i\leq n} \sum_{j=1}^{m} \int_0^\infty |g_{ij}(t)|\, dt, \\
\|G\|_2 &= \sqrt{\frac{1}{2\pi}\int_{-\infty}^{\infty} \text{Trace}\{G^*(j\omega)G(j\omega)\}\, d\omega}, && G \in \mathcal{RH}_2, \\
\|G\|_\infty &= \sup_{\omega\in\mathbb{R}} \overline{\sigma}(G(j\omega)), && G \in \mathcal{RH}_\infty, \\
\|G\|_- &= \inf_{\omega\in\mathbb{R}} \underline{\sigma}(G(j\omega)), \\
\|G\|_-^{[\omega_1,\omega_2]} &= \inf_{\omega\in[\omega_1,\omega_2]} \underline{\sigma}(G(j\omega)), && 0 \leq \omega_1 < \omega_2 < \infty,
\end{aligned} \tag{10}$$

where G is a $n \times m$ Hurwitz matrix transfer function, and $g_{ij}(t) = \mathcal{L}^{-1}\{G_{ij}(s)\}$ $(1 \leq i \leq n,\ 1 \leq j \leq m)$ are the impulse responses corresponding to every component in the transfer matrix G. The next inequalities will be useful to derive thresholds for residual evaluation:

$$\begin{aligned}
\|y\|_\infty &\leq \|G\|_1 \|u\|_\infty, \\
\|y\|_2 &\leq \|G\|_\infty \|u\|_2,
\end{aligned} \tag{11}$$

where $y = Gu$, the signal norms are defined as

$$\begin{aligned}
\|y\|_\infty &= \sup_{t\in[0,\infty)} \|y(t)\|, \\
\|y\|_2 &= \sqrt{\int_0^\infty \|y(t)\|^2 dt},
\end{aligned} \tag{12}$$

and $\|\cdot\|$ denotes the Euclidean norm.

3. FAULT-TOLERANT CONTROL SCHEME

The proposed FTC scheme relies on a fault diagnosis and isolation (FDI) algorithm, followed by a fault accommodation into the nominal controller. For LTI systems and additive faults, several FTC control structures have been suggested [12, 22–24] departing from the Youla parametrization of all stabilizing controllers [20]. In this configuration, a free parameter $Q \in \mathcal{RH}_\infty$ is selected to achieve the fault compensation, with the assurance that closed-loop stability is achieved after the fault accommodation. In this fashion, the accommodation scheme adopted in this work is motivated by a new implementation of the Youla parametrization called *generalized internal model control (GIMC)* [7, 12]. In this configuration, the nominal controller K is represented by its left coprime factorization, that is, $K = \widetilde{V}^{-1}\widetilde{U}$. In addition, the GIMC configuration allows to perform the FDI process and accommodation in the same structure, where these two processes are carried out by selecting two design parameters $Q, H \in \mathcal{RH}_\infty$ (see Figure 2). Consequently, the residual r is generated by selecting the detection/isolation filter

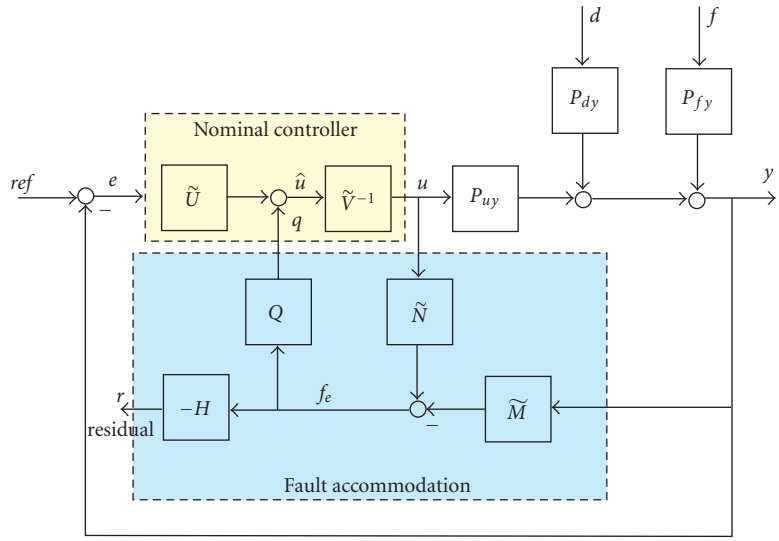

Figure 2: GIMC with additive perturbations and faults.

H, and the accommodation signal q by the compensator Q, using the filtered signal f_e with the following criteria.

(1) $H(s)$: the fault detection/isolation filter must diminish the effect of the disturbances or uncertainty into the residual signal, and maximize the effect of the faults.
(2) $Q(s)$: the robustification controller must provide robustness into the closed-loop system in order to maintain acceptable performance against faults.

3.1. Fault detection and isolation

From Figure 2, it can be observed that $f_e \in R^p$ contains information of perturbations d and faults f as follows:

$$f_e(s) = -\widetilde{N}_d d(s) - \widetilde{N}_f f(s). \tag{13}$$

Hence a residual r is naturally constructed by using the information of the coprime factorization of the nominal plant through f_e [1];

$$r(s) = -H f_e(s) = H[\widetilde{N}_d d(s) + \widetilde{N}_f f(s)]. \tag{14}$$

In order to improve the accuracy of the FDI stage, it is proposed to carry out this task in two consecutive steps: (a) first, fault detection, and next, (b) fault isolation. This idea is also appealing for fault accommodation, and its benefits will be explained in the next section. As a result, the FDI algorithm is designed in two parts as follows.

(1) A detection filter H_D is first synthesized to determine a general fault scenario.
(2) Next, an isolation filter H_I is computed to identify the faults affecting the system.

First, the detection filter H_D is constructed to obtain a scalar residual, that is, H_D is a $1 \times p$ transfer matrix such that it attenuates the contribution from the perturbations d while maximizing the faults f effect. Hence the following design criteria are suggested:

$$\begin{aligned} &\sup_{H_D \in \mathcal{RH}_\infty} \frac{||H_D \widetilde{N}_f||_k}{||H_D \widetilde{N}_d||_j} \quad \text{or} \\ &\sup_{H_D \in \mathcal{RH}_\infty} ||H_D \widetilde{N}_f||_k \quad \text{s.t.} \, ||H_D \widetilde{N}_d||_j \le \gamma, \end{aligned} \tag{15}$$

where $\gamma > 0$ denotes a desired attenuation factor for the unknown perturbations contribution, and k, j represent the performance indexes in (10). In [21, 25], the previous multiobjective optimizations have been studied where optimal and approximation solutions are provided. Alternatively, the ∞/∞ and 2/2 optimizations can be solved using well-known algorithms through a characterization by a linear fractional transformation (LFT) [20];

$$\begin{aligned} &\min_{H_D \in \mathcal{RH}_\infty} \left|\left| \begin{bmatrix} 0 & h \end{bmatrix} - H_D \begin{bmatrix} \widetilde{N}_d & \widetilde{N}_f \end{bmatrix} \right|\right|_j \\ &\quad = \min_{H_D \in \mathcal{RH}_\infty} ||F_l(G_{H_D}, H_D)||_j, \quad j = 2, \infty, \end{aligned} \tag{16}$$

where $h \in \mathcal{RH}_\infty$ is a $1 \times l$ transfer matrix that describes the faults frequency bandwidth, $F_l(\cdot, \cdot)$ represents a lower LFT [20], and G_{H_D} the generalized plant (see Figure 3) given by

$$G_{H_D} = \begin{bmatrix} 0 & h & -1 \\ \widetilde{N}_d & \widetilde{N}_f & 0 \end{bmatrix}. \tag{17}$$

One advantage of the LFT characterization is that it can be augmented to include model uncertainty in the problem formulation. Meanwhile, the isolation filter H_I ($l \times p$ transfer matrix) is designed to isolate the fault vector f and decouple the perturbations d, that is,

(i) $H_I \widetilde{N}_d(s) \approx 0$,
(ii) $H_I \widetilde{N}_f(s) \approx T$,

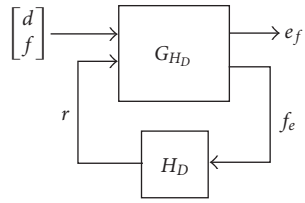

Figure 3: LFT formulation for detection filter H_D.

where $T \in \mathcal{RH}_\infty$ is a diagonal transfer matrix. Transfer matrix T is a design parameter, and it should be chosen according to the frequency response of $\widetilde{N}_f$, in order to achieve the isolation and decoupling objectives. Nevertheless, nonminimum phase zeros of $\widetilde{N}_f$ could limit the resulting performance [26]. Once more, the design criterion can be proposed by combining both objectives measured by a system norm $j = 2, \infty$ as follows:

$$\min_{H_I \in \mathcal{RH}_\infty} \left\| \begin{bmatrix} 0 & T \end{bmatrix} - H_I \begin{bmatrix} \widetilde{N}_d & \widetilde{N}_f \end{bmatrix} \right\|_j = \min_{H_I \in \mathcal{RH}_\infty} \left\| F_l(G_{H_I}, H_I) \right\|_j, \tag{18}$$

where G_{H_I} stands for the generalized plant associated to the LFT formulation given by

$$G_{H_I} = \begin{bmatrix} 0 & T & -I \\ \widetilde{N}_d & \widetilde{N}_f & 0 \end{bmatrix}. \tag{19}$$

Hence once a fault is detected, in the isolation stage, the filter H_I has to provide a good estimate of the fault affecting the system. Therefore, it is fundamental that H_I could render diagonally the product $H_I\widetilde{N}_f$, or at least diagonally dominant. In fact, this issue has to be verified after H_I is designed for a correct fault identification.

Remark 2. Assumptions (7) and (8) about the rank properties of the perturbations and faults transfer matrices provide necessary conditions to achieve the decoupling objective. Therefore, it is expected that the optimal filters obtained through (16) and (18) will guarantee good fault detection and isolation properties of the residuals.

Now, perfect disturbance decoupling is hard to achieve in a general scenario. As a result, the residuals will not be zero in a fault-free condition. Two possible techniques can be followed in order to detect a fault: hard or adaptive thresholds [3, 27, 28]. Since the perturbations are considered unknown and no uncertainty is assumed at this stage, hard thresholds are adopted. Departing from the signal norms in (12), a windowed residual evaluation criteria can be chosen as follows:

$$\|r\| = \|r\|_{2,t,T_o} = \sqrt{\int_{t-T_o}^{t} \|r(\tau)\| d\tau}, \tag{20}$$

$$\|r\| = \|r\|_{\infty,t,T_o} = \sup_{t-T_o \le \tau \le t} \|r\|, \tag{21}$$

where T_o is the window length or evaluation horizon. Hence to avoid a false alarm in the evaluation due to perturbations [27], a threshold value is selected such that

$$J_{\text{th}} = \sup_{f=0, \forall d} \|r\| \tag{22}$$

in the case of the windowed 2 norm, and considering bounded energy perturbations, that is, $\|d\|_{2,t,T_o} < \gamma_2^d$, then an initial detection threshold can be calculated by applying (11) as

$$J_{\text{th}}^D = \gamma_2^d \|H_D \widetilde{N}_d\|_\infty. \tag{23}$$

On the other hand, if the perturbations are now assumed bounded for all time, that is, $\|d\|_\infty < \gamma_\infty^d$, then a new detection threshold can be employed as follows:

$$J_{\text{th}}^D = \gamma_\infty^d \|H_D \widetilde{N}_d\|_1. \tag{24}$$

The hard thresholds in (23) and (24) are conservative starting values since they are derived from the norms inequalities in (11). Nevertheless, they have to be adjusted online for proper fault detection. Now, with respect to the isolation stage, a hard threshold has to be obtained for each output of the filter H_I that represents the estimated fault. However, if the product $H_I\widetilde{N}_f$ is not diagonal, then each output is affected at some degree by all faults and perturbations. Assuming that the ith output is evaluated, then the following thresholds are proposed:

$$J_{\text{th}}^{Ii} = \sum_{\substack{j=1 \\ j \neq i}}^{l} \|[H_I \widetilde{N}_f]_{ij}\|_\infty \gamma_2^i + \sum_{k=1}^{r} \|[H_I \widetilde{N}_d]_{ik}\|_\infty \gamma_2^d, \tag{25}$$

or

$$J_{\text{th}}^{Ii} = \sum_{\substack{j=1 \\ j \neq i}}^{l} \|[H_I \widetilde{N}_f]_{ij}\|_1 \gamma_\infty^i + \sum_{k=1}^{r} \|[H_I \widetilde{N}_d]_{ik}\|_1 \gamma_\infty^d, \tag{26}$$

where $i = 1, \ldots, l$, $[\cdot]_{ij}$ denotes the ij term in the transfer matrix, $\|f_i\|_{2,t,T_o} < \gamma_2^i$, and $\|f_i\|_\infty < \gamma_\infty^i$. Consequently, some information about the energy or time upper-bound on each fault is necessary to compute (25) and (26). Once more, it is important to point out that (25) and (26) are just starting values for the threshold selection during the residual evaluation, since they rely on inequalities that involve some inherit conservativeness.

3.2. Fault accommodation

In order to derive the fault accommodation scheme, the effect of the compensation signal q in the GIMC structure of Figure 2 is analyzed. Define the following nominal closed-loop transfer matrices:

(i) input sensitivity: $S_i \triangleq (I + KP_{uy})^{-1}$,
(ii) output sensitivity: $S_o \triangleq (I + P_{uy}K)^{-1}$,
(iii) complementary output sensitivity: $T_o \triangleq I - S_o = (I + P_{uy}K)^{-1}P_{uy}K$.

The next lemma originally presented in [17] characterizes the dynamic behavior of the compensated control input u and output y of the closed-loop system.

Lemma 1. *In the GIMC configuration of Figure 2 considering additive faults, the resulting closed-loop characteristics for the control signal u and output y are given by*

$$u(s) = S_i K\, ref(s) - S_i \widetilde{V}^{-1}(\widetilde{U}\widetilde{M}^{-1} + Q)(\widetilde{N}_d d(s) + \widetilde{N}_f f(s)),$$
$$y(s) = T_o\, ref(s) + S_o \widetilde{M}^{-1}(I - \widetilde{N}\widetilde{V}^{-1}Q)(\widetilde{N}_d d(s) + \widetilde{N}_f f(s)). \tag{27}$$

The resulting closed-loop system is stable, provided that $Q \in \mathcal{RH}_\infty$, since the nominal controller K internally stabilizes the nominal plant P_{uy} (proof in Appendix B).

By a simple inspection of (27), two results can be concluded by considering the complete decoupling of perturbations d and faults f from the control input u and output y of the system.

Corollary 1 (see [17]). *If the nominal plant $P_{uy} \in \mathcal{RH}_\infty$, then $\widetilde{M}^{-1} \in \mathcal{RH}_\infty$, and the complete disturbance and fault decoupling can be achieved at the control signal u by letting $Q = -\widetilde{U}\widetilde{M}^{-1} \in \mathcal{RH}_\infty$. As a result, it is obtained that*

$$u(s) = S_i K\, ref(s), \tag{28}$$
$$y(s) = T_o\, ref(s) + \widetilde{M}^{-1}(\widetilde{N}_d d(s) + \widetilde{N}_f f(s)). \tag{29}$$

Therefore, if the nominal plant P_{uy} is stable by properly choosing the compensator Q, the control signal is not affected by faults and perturbations. The compensation suggested in Corollary 1 is particularly useful under a sensor fault scenario [24] since it is not desirable to adjust the control signal dynamics against erroneous information given by a sensor. Note that from (29), perturbations and faults are decoupled from the closed-loop feedback dynamics since they appear in an open-loop fashion at the output. However, the perturbations are affecting the outputs with a feedforward structure, which is an undesirable effect of this compensation. Consequently, as it was suggested in [18], if some estimation of the perturbations $\hat{d}$ could be deduced by steady-state relations of the system or by an observer using state-augmentation, the compensation q could incorporate this new information to improve the closed-loop performance. In general, if the FDI stage could provide a reliable identification of the fault vector $\hat{f}$, then this estimation can be also applied under the compensation suggested in Corollary 1 to decouple the faults from the closed-loop system. The compensation including perturbations and faults estimations will be given by

$$q(s) = -\widetilde{U}\widetilde{M}^{-1}[\widetilde{N}u(s) + \widetilde{N}_d\hat{d}(s) + \widetilde{N}_f\hat{f}(s) - \widetilde{M}y(s)], \tag{30}$$

and the resulting output dynamics are given now by

$$y(s) = T_o\, ref(s) + \widetilde{M}^{-1}[\widetilde{N}_d\{d(s) - \hat{d}(s)\} + \widetilde{N}_f\{f(s) - \hat{f}(s)\}]. \tag{31}$$

Therefore, the accuracy in the perturbations and faults estimations ($d(s) - \hat{d}(s)$ and $f(s) - \hat{f}(s)$) will dictate the resulting performance deterioration. However, in a practical scenario, it is difficult to have these estimations available or to have a stable plant. Hence it is important that the compensator Q could simultaneously attenuate perturbations and faults into the closed-loop system. On the other hand, if P_{uy} has also a stable inverse, a complete output decoupling for perturbations and faults can be achieved.

Corollary 2 (see [17]). *If the nominal plant satisfies P_{uy}, $P_{uy}^{-1} \in \mathcal{RH}_\infty$, then $\widetilde{N}^{-1} \in \mathcal{RH}_\infty$ and with $Q = \widetilde{V}\widetilde{N}^{-1} \in \mathcal{RH}_\infty$, the resulting output is decoupled perfectly from the perturbations and faults, that is,*

$$u(s) = S_i K\, ref(s) - \widetilde{N}^{-1}(\widetilde{N}_d d(s) + \widetilde{N}_f f(s)),$$
$$y(s) = T_o\, ref(s). \tag{32}$$

Note that the compensation proposed in Corollary 2 is particularly useful for an actuator or system fault, since the output is perfectly decoupled from faults and perturbations. However, it should be avoided in a sensor fault scenario. In fact, the decoupling conditions of Corollaries 1 and 2 could be very restrictive. For this reason, by analyzing (27), if it is desired to minimize the faults effect at the control signal, while reducing the perturbations contribution at the output, the compensator Q should be designed by following the optimization strategy

$$\min_{Q\in\mathcal{RH}_\infty} \left\|\left[Z_1 Z_2\right]\right\|_j = \min_{Q\in\mathcal{RH}_\infty} \left\|\left[Z_3 Z_4\right]\right\|_j, \tag{33}$$

where

$$Z_1 = \alpha_d S_o \widetilde{M}^{-1}(I - \widetilde{N}\widetilde{V}^{-1}Q)\widetilde{N}_d,$$
$$Z_2 = -\alpha_f S_i \widetilde{V}^{-1}(\widetilde{U}\widetilde{M}^{-1} + Q)\widetilde{N}_f,$$
$$Z_3 = \alpha_d S_o (P_{dy} - P_{uy}\widetilde{V}^{-1}Q\widetilde{N}_d),$$
$$Z_4 = -\alpha_f S_i (KP_{fy} + \widetilde{V}^{-1}Q\widetilde{N}_f), \tag{34}$$

j represents the $\mathcal{H}_2$ or $\mathcal{H}_\infty$ norms in (10), $\alpha_d, \alpha_f \in [0, 1]$ are two weighting factors to balance the tradeoff between perturbations and faults reduction, and the normalized coprime factors relations in (6) are applied. However, the optimization problem in (33) cannot be solved using standard robust control algorithms [19, 20]. Therefore, it is proposed to extend the cost function to have a feasible problem as follows:

$$\min_{Q\in\mathcal{RH}_\infty} \left\| \begin{bmatrix} \alpha_d S_o P_{dy} & 0 \\ 0 & -\alpha_f S_i K P_{fy} \end{bmatrix} + \begin{bmatrix} -\alpha_d S_o P_{uy}\widetilde{V}^{-1} \\ -\alpha_f S_i \widetilde{V}^{-1} \end{bmatrix} Q \begin{bmatrix} \widetilde{N}_d & \widetilde{N}_f \end{bmatrix} \right\|_j = \min_{Q\in\mathcal{RH}_\infty} \left\| F_l(G_{Q_u}, Q) \right\|_j, \tag{35}$$

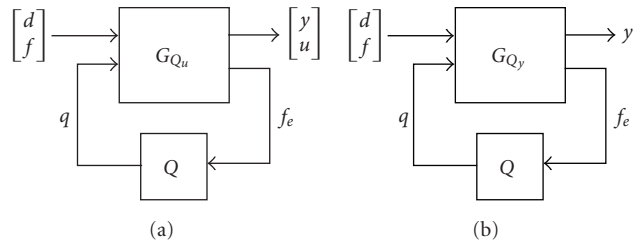

Figure 4: LFT formulations for compensator Q: (a) Control signal and output attenuation, and (b) output signal attenuation.

where G_{Q_u} represents the generalized plant (see Figure 4) given by

$$G_{Q_u} = \begin{bmatrix} \alpha_d S_o P_{dy} & 0 & -\alpha_d S_o P_{uy} \widetilde{V}^{-1} \\ 0 & -\alpha_f S_i K P_{fy} & -\alpha_f S_i \widetilde{V}^{-1} \\ \widetilde{N}_d & \widetilde{N}_f & 0 \end{bmatrix}. \tag{36}$$

Meanwhile, if it is desired to attenuate both faults and perturbations at the output y, then the next optimization scheme is suggested:

$$\begin{aligned} &\min_{Q\in\mathcal{RH}_\infty} \left\| S_o \widetilde{M}^{-1} (I - \widetilde{N}\widetilde{V}^{-1} Q) \begin{bmatrix} \alpha_d \widetilde{N}_d & \alpha_f \widetilde{N}_f \end{bmatrix} \right\|_j \\ &\quad = \min_{Q\in\mathcal{RH}_\infty} \left\| F_l \left(G_{Q_y}, Q \right) \right\|_j, \end{aligned} \tag{37}$$

where G_{Q_y} is given by

$$G_{Q_y} = \begin{bmatrix} \alpha_d S_o P_{dy} & \alpha_f S_o P_{fy} & -S_o P_{uy} \widetilde{V}^{-1} \\ \alpha_d \widetilde{N}_d & \alpha_f \widetilde{N}_f & 0 \end{bmatrix}. \tag{38}$$

Remark 3. The optimization criteria for Q in (35) and (37) can be interpreted as approximation or normalization problems with certain postweighting and preweighting given by the frequency content of the perturbations $\widetilde{N}_d$ or faults $\widetilde{N}_f$. In fact, (35) introduces a combined optimization: (i) a normalization process of $\widetilde{N}\widetilde{V}^{-1}$ by Q with a frequency postweighting given by the nominal output sensitivity S_o and $\widetilde{M}^{-1}$, and (ii) an approximation problem to $-\widetilde{U}\widetilde{M}^{-1}$ with a frequency postweighting given by the nominal input sensitivity S_i and $\widetilde{V}^{-1}$.

Remark 4. Note that the compensators Q designed by the criteria in (35) and (37) can be conservative since it is required to attenuate the effect of all types of faults analyzed in (1), and it is also assumed that all of them have the same structure.

To improve the post-fault performance, it is then proposed to design specific compensators $Q_i \in \mathcal{RH}_\infty$ for $i = 1,\ldots,l$ for every studied fault, depending if their effect is on the state (*actuator or system faults*) or the output (*sensor faults*) equations in (1), using the previous optimization algorithms as follows:

(i) *actuator or system faults*:

$$\min_{Q_i\in\mathcal{RH}_\infty} \left\| S_o \widetilde{M}^{-1} (I - \widetilde{N}\widetilde{V}^{-1} Q_i) \begin{bmatrix} \alpha_d \widetilde{N}_d & \alpha_f \widetilde{N}_f^i \end{bmatrix} \right\|_j; \tag{39}$$

(ii) *sensor faults*:

$$\begin{aligned} \min_{Q_i\in\mathcal{RH}_\infty} \Bigg\| &\begin{bmatrix} \alpha_d S_o P_{dy} & 0 \\ 0 & -\alpha_f S_i K P_{fy}^i \end{bmatrix} \\ &+ \begin{bmatrix} -\alpha_d S_o P_{uy} \widetilde{V}^{-1} \\ -\alpha_f S_i \widetilde{V}^{-1} \end{bmatrix} Q_i \begin{bmatrix} \widetilde{N}_d & \widetilde{N}_f^i \end{bmatrix} \Bigg\|_j, \end{aligned} \tag{40}$$

where

$$\widetilde{N}_f^i = \left[\begin{array}{c|c} A + LC & F_1^i + LF_2^i \\ \hline C & F_2^i \end{array}\right] \tag{41}$$

and $P_{fy}^i = \widetilde{M}^{-1}\widetilde{N}_f^i$. In this way, the fault accommodation scheme of Figure 5 is proposed, and the overall active FTC algorithm consists of three stages according to the information of the FDI block as follows:

(1) in the fault-free case, just the nominal control loop is active;
(2) after a fault scenario is detected into the system, a general compensator Q designed by (35) is activated;
(3) finally, after the fault is classified and isolated, an specific compensator Q_i designed by (39) or (40) is selected.

In a general fault condition, it is then decided to decouple (if possible) or attenuate the effect of faults at the control signal u, until the fault is well-characterized during the isolation stage. As a result, after the fault is isolated, the specific compensation is injected into the closed-loop configuration to improve the postfault performance.

Remark 5. Since the fault accommodation is based on the Youla parametrization, and since the faults are additive, the closed-loop stability after each reconfiguration is guaranteed, provided that $Q, Q_i \in \mathcal{RH}_\infty$, and any nonlinear behavior is avoided into the closed-loop system, like saturations, rate limiters, and so on. However, if the fault profile depends on the states or outputs then closed-loop stability could not be assured after all.

Remark 6. In the proposed configuration, multiple and intermittent faults could be handled. Once they are identified by the FDI scheme, the corresponding compensator should be activated to perform its accommodation. However, if FDI algorithm detects that the fault is no longer present, the compensation is removed.

3.3. Performance evaluation

One important question, after the design stage is completed, is the resulting performance of the fault detection, isolation and accommodation algorithms. To address this problem, different quantification indices will be proposed using the

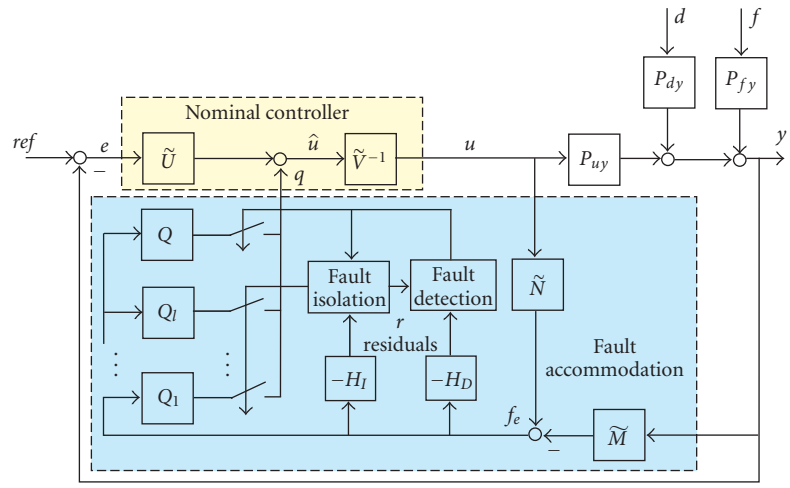

Figure 5: GIMC accommodation setup.

system performance indexes in (10) of the resulting transfer functions. The selection of the applied performance index in (10) will depend on the a priori faults information, for example, the faults frequency content, or the desired interpretation of the quantification index, for example, the worst case condition in the evaluation. The next indices are motivated from the optimization algorithms used for synthesis in the previous sections.

(1) *Fault evaluation.* The capability of the detection filter H_D of reducing the perturbations frequency content compared to increasing the faults sensitivity is evaluated by

$$I_{\mathrm{FD}} \triangleq \frac{\|H_D\widetilde{N}_f\|_k}{\|H_D\widetilde{N}_d\|_j}. \tag{42}$$

Hence a large value of I_{FD} will indicate good evaluation characteristics.

(2) *Fault isolation.* This index is constructed by analyzing the property of H_I of diagonalizing $\widetilde{N}_f$ while attenuating the disturbances frequency content:

$$I_{\mathrm{FI}} \triangleq \frac{\left\|[H_I\widetilde{N}_f]_{\mathrm{diag}}\right\|_k}{\left\|[H_I\widetilde{N}_f]_{\mathrm{nondiag}}\right\|_k + \left\|H_I\widetilde{N}_d\right\|_j}, \tag{43}$$

where $[\cdot]_{\mathrm{diag}}$ denotes the diagonal part of the transfer matrix, and $[\cdot]_{\mathrm{nondiag}}$ the off diagonal structure. In fact, I_{FI} is usually denoted as signal-to-noise and interference ratio (SNIR) in the signal processing community. Thus if I_{FI} is large, then fault isolation can be achieved.

(3) *Fault accommodation.* The fault accommodation is quantified in terms of the property of reducing the effect of faults and perturbations simultaneously into the closed-loop system. The accommodation performance criteria is defined for the ith fault f_i as

$$I^i_{\mathrm{FA}} \triangleq \alpha_f\|W^i_A\widetilde{N}^i_f\|_k + \alpha_d\|S_o\widetilde{M}^{-1}(I-\widetilde{N}\widetilde{V}^{-1}Q_i)\widetilde{N}_d\|_j, \tag{44}$$

where the weighting W^i_A is selected according to the fault effect:

$$W^i_A \triangleq \begin{cases} S_o\widetilde{M}^{-1}(I-\widetilde{N}\widetilde{V}^{-1}Q_i) & \text{actuator/system fault,} \\ S_i\widetilde{V}^{-1}(\widetilde{U}\widetilde{M}^{-1}+Q_i) & \text{sensor fault,} \end{cases} \tag{45}$$

where (α_d, α_f) are the positive weighting factors to judge the importance of perturbations or faults attenuation. Now, a small value of I^i_{FA} will indicate good fault accommodation. Note that this value is related to a worst-case performance degradation level expected in the FTC scheme [29].

The overall synthesis algorithms for fault detection, isolation, and accommodation including performance evaluation are described in Appendix A. The synthesis procedure includes samples of MATLAB commands that could be used for numerical calculations.

4. FAULT TOLERANT APPROACH UNDER MODEL UNCERTAINTY

During the implementation of any control strategy, there is always some model uncertainty in the mathematical description used for design. If the characterization of this uncertainty could be obtained during the problem formulation, this information could be used at the design stage to improve the closed-loop performance, and understand also the practical limitations. In this work, additive model uncertainty is considered [19, 20] as shown in Figure 6, that is, the actual nominal plant $\hat{P}_{uy}$ is given by

$$\hat{P}_{uy} = P_{uy} + \Delta_{uy}, \quad \Delta_{uy} \triangleq W_2\Delta W_1, \tag{46}$$

where $W_1, W_2 \in \mathcal{RH}_\infty$ represent pre- and post-uncertainty weighting functions, and $\Delta \in \mathcal{RH}_\infty$ a normalized uncertain transfer matrix $\|\Delta\|_\infty < 1$. As presented in [18], other uncertainty representations (parametric, multiplicative, etc.) could be also fitted under an additive uncertainty structure, but at the price of introducing some conservativeness in the design.

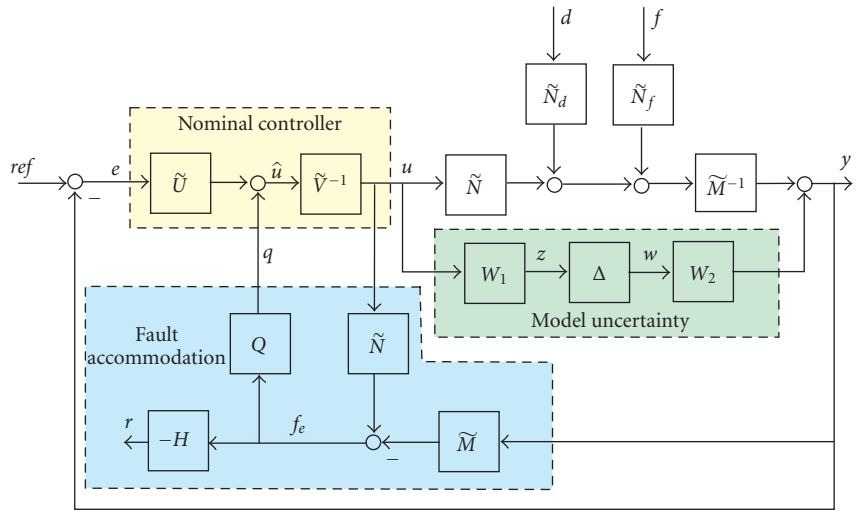

Figure 6: GIMC with additive perturbations, faults, and model uncertainty.

First of all, note that under model uncertainty, the signal f_e in the GIMC configuration is no longer decoupled from the control signal u (see Figure 6). The results are summarized as follows [17].

Lemma 2. *Considering additive model uncertainty in the GIMC configuration of Figure 2, the resulting closed-loop characteristics are given by*

$$f_e(s) = -\widetilde{M}\Delta_{uy}u(s) - \widetilde{N}_d d(s) - \widetilde{N}_f f(s), \tag{47}$$

$$u(s) = W_u^{-1}\left[K\,ref(s) - \widetilde{V}^{-1}\left(\widetilde{U}\widetilde{M}^{-1}+Q\right)\left(\widetilde{N}_d d(s)+\widetilde{N}_f f(s)\right)\right], \tag{48}$$

$$\begin{aligned} y(s) = {} & \left(P_{uy}+\Delta_{uy}\right)W_u^{-1}K\,ref(s) \\ & - \left[\left(P_{uy}+\Delta_{uy}\right)W_u^{-1}\widetilde{V}^{-1}\left(\widetilde{U}\widetilde{M}^{-1}+Q\right) - \widetilde{M}^{-1}\right] \\ & \times \left(\widetilde{N}_d d(s)+\widetilde{N}_f f(s)\right), \end{aligned} \tag{49}$$

where

$$\begin{aligned} W_u &\triangleq I + K\left(P_{uy}+\Delta_{uy}\right) + \widetilde{V}^{-1}Q\widetilde{M}\Delta_{uy} \\ &= I + KP_{uy} + \widetilde{V}^{-1}\left(\widetilde{U}+Q\widetilde{M}\right)\Delta_{uy}. \end{aligned} \tag{50}$$

(Proof is in Appendix C)

4.1. Robust fault isolation

Note that by including additive uncertainty, an extra requirement is evident, the detection/isolation filter H should cancel or diminish the uncertainty contribution at the residual output r for a robust detection and isolation, that is, $H\widetilde{M}\Delta_{uy} \approx 0$. As described in Section 2, there are necessary conditions related to the rank of the involved transfer matrices to guarantee proper fault isolation. Consequently, this condition can be extended for robust fault isolation, considering the worst-case uncertainty as

$$\begin{aligned} &\text{normrank}\left(\left[\widetilde{M}W_2W_1 \;\; \widetilde{N}_d \;\; \widetilde{N}_f\right]\right) \\ &\quad \geq \text{normrank}\left(\left[\widetilde{M}W_2W_1 \;\; \widetilde{N}_d\right]\right) + l. \end{aligned} \tag{51}$$

Since the description of the uncertainty is posed in terms of the ∞ norm, the optimization problems for the detection H_D and isolation H_I filters are also proposed in terms of this norm. As a result, the following robust performance criteria are adopted for both synthesis procedures:

(i) *fault detection:*

$$\begin{aligned} &\min_{\substack{H_D\in\mathcal{RH}_\infty \\ \|\Delta\|_\infty<1}} \left\| \left[0 \;\; 0 \;\; h\right] - H_D\left[\widetilde{M}W_2 \;\; \Delta W_1 \;\; \widetilde{N}_d \;\; \widetilde{N}_f\right] \right\|_\infty \\ &\qquad = \min_{\substack{H_D\in\mathcal{RH}_\infty \\ \|\Delta\|_\infty<1}} \left\| F_l\left(F_u\left(G^{\Delta}_{H_D},\Delta\right),H_D\right)\right\|_\infty, \end{aligned} \tag{52}$$

(ii) *fault isolation:*

$$\begin{aligned} &\min_{\substack{H_D\in\mathcal{RH}_\infty \\ \|\Delta\|_\infty<1}} \left\| \left[0 \;\; 0 \;\; T\right] - H_I\left[\widetilde{M}W_2 \;\; \Delta W_1 \;\; \widetilde{N}_d \;\; \widetilde{N}_f\right] \right\|_\infty \\ &\qquad = \min_{\substack{H_D\in\mathcal{RH}_\infty \\ \|\Delta\|_\infty<1}} \left\| F_l\left(F_u\left(G^{\Delta}_{H_I},\Delta\right),H_I\right)\right\|_\infty, \end{aligned} \tag{53}$$

where $F_u(\cdot,\cdot)$ stands for an upper LFT [20], and the respective generalized plants $G^{\Delta}_{H_D}$ and $G^{\Delta}_{H_I}$ are given by

$$\begin{aligned} G^{\Delta}_{H_D} &= \begin{bmatrix} 0 & W_1 & 0 & 0 & 0 \\ 0 & 0 & 0 & h & -1 \\ \widetilde{M}W_2 & 0 & \widetilde{N}_d & \widetilde{N}_f & 0 \end{bmatrix}, \\ G^{\Delta}_{H_I} &= \begin{bmatrix} 0 & W_1 & 0 & 0 & 0 \\ 0 & 0 & 0 & T & -I \\ \widetilde{M}W_2 & 0 & \widetilde{N}_d & \widetilde{N}_f & 0 \end{bmatrix}. \end{aligned} \tag{54}$$

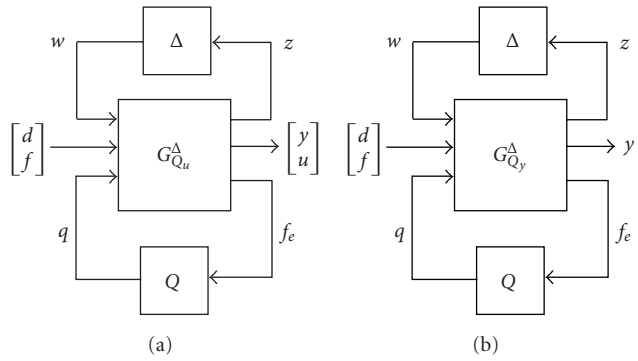

FIGURE 7: LFT formulations for compensator Q under model uncertainty: (a) control signal and output attenuation, and (b) output signal attenuation.

The optimization problems in (52) and (53) can be solved by using μ-synthesis design or LMI's [19, 20]. On the other hand, at the residual evaluation, it is observed that the uncertainty Δ_{uy} is affected by the control signal u at (47). Thus the residual is directly dependent on the control signal u, and its profile will appear in the resulting dynamic behavior, but since this signal is known, an adaptive threshold [3, 28] can be used in order to reduce the conservativeness in the fault detection process introduced by the uncertain term as

$$J^{D}_{\text{th}}(t) = ||H_D \widetilde{M} W_1 W_2||_\infty ||u||_{2,t,T_o} + \gamma_2^d ||H_D \widetilde{N}_d||_\infty, \tag{55}$$

where γ_2^d is the bound on the windowed energy of the perturbations, and the inequalities in (11) are applied. This characterization is appropriate since the uncertainty Δ is quantified in terms of the $\|\cdot\|_\infty$ norm. Similarly, an adaptive threshold can be formulated for fault isolation as

$$\begin{aligned} J^{Ii}_{\text{th}}(t) = {} & \sum_{\substack{j=1 \\ j\neq i}}^{l} ||[H_I \widetilde{N}_f]_{ij}||_\infty \gamma_2^i \\ & + \sum_{k=1}^{m} ||[H_I \widetilde{M} W_1 W_2]_{ik}||_\infty ||u_k||_{2,t,T_o} \\ & + \sum_{k=1}^{r} ||[H_I \widetilde{N}_d]_{ir}||_\infty \gamma_2^d, \end{aligned} \tag{56}$$

where $i = 1, \ldots, l$. As mentioned in the previous section, the thresholds in (55) and (56) are derived from norms inequalities, so their values could be conservative and they have to be tuned online to optimize the fault detection capabilities.

Remark 7. It is clear that hard thresholds could lead to a conservative fault diagnosis stage, or fault misdetection due to a change in the operating conditions or model uncertainty. However, adaptive thresholds require a prior knowledge of the possible uncertainty or maximum variability of the residuals in nominal conditions for a correct implementation.

4.2. Robust fault accommodation

In general, no guarantee of closed-loop stability is granted although $Q \in \mathcal{RH}_\infty$ as in the uncertainty free case. From the results in Lemma 2, it can be seen that for a special case (stable nominal plant), the uncertainty can be decoupled from the control signal as in Corollary 1, and closed-loop stability can be deduced if the nominal controller internally stabilizes the nominal plant.

Corollary 3. *If the nominal plant satisfies $P_{uy} \in \mathcal{RH}_\infty$, then complete disturbance, fault, and uncertainty decoupling can be achieved at the control signal u by letting $Q = -\widetilde{U}\widetilde{M}^{-1}$, and consequently*

$$\begin{aligned} u(s) &= S_i K\, ref(s), \\ y(s) &= (P_{uy} + \Delta_{uy}) S_i K\, ref(s) + \widetilde{M}^{-1}(\widetilde{N}_d d(s) + \widetilde{N}_f f(s)). \end{aligned} \tag{57}$$

Moreover, the closed-loop is stable if K internally stabilizes P_{uy}.

Similarly to the result in Corollary 1, with the compensation suggested in Corollary 3, the perturbations d and faults f affect the output in an open-loop fashion. Therefore, if an estimation of the perturbations $\hat{d}$ and faults $\hat{f}$ are available, then the feedforward structure in (30) could be followed to attenuate their effect at the output. On the other hand, for a general design case by looking at (48) and (49), a robust criteria (performance and stability) should be targeted to reduce the faults effects at the control signal u and the perturbations contribution at the output y by

$$\begin{aligned} \min_{\substack{Q\in\mathcal{RH}_\infty \\ \|\Delta\|_\infty<1}} \Bigg\| & \begin{bmatrix} -\alpha_d(\hat{P}_{uy} W_u^{-1} K - I) P_{dy} & 0 \\ 0 & -\alpha_f W_u^{-1} K P_{fy} \end{bmatrix} \\ & + \begin{bmatrix} -\alpha_d \hat{P}_{uy} W_u^{-1} \widetilde{V}^{-1} \\ -\alpha_f W_u^{-1} \widetilde{V}^{-1} \end{bmatrix} Q \begin{bmatrix} \widetilde{N}_d & \widetilde{N}_f \end{bmatrix} \Bigg\|_\infty \\ = \min_{\substack{Q\in\mathcal{RH}_\infty \\ \|\Delta\|_\infty<1}} & ||F_l(F_u(G^{\Delta}_{Q_u}, \Delta), Q)||_\infty, \end{aligned} \tag{58}$$

where W_u is defined in (50), and the generalized plant $G^{\Delta}_{Q_u}$ (see Figure 7) including uncertainty information is given by

$$G^{\Delta}_{Q_u} = \begin{bmatrix} -W_1 S_i K W_2 & -W_1 S_i K P_{dy} & -W_1 S_i K P_{fy} & W_1 S_i \widetilde{V}^{-1} \\ \alpha_d S_o W_2 & \alpha_d S_o P_{dy} & 0 & \alpha_d S_o P_{uy} \widetilde{V}^{-1} \\ -\alpha_f S_i K W_2 & 0 & -\alpha_f S_i K P_{fy} & \alpha_f S_i \widetilde{V}^{-1} \\ -\widetilde{M} W_2 & -\widetilde{N}_d & -\widetilde{N}_f & 0 \end{bmatrix}. \tag{59}$$

Meanwhile, if robust attenuation is now looked at the output y, the following robust performance problem is formulated:

$$\begin{aligned} \min_{\substack{Q\in\mathcal{RH}_\infty \\ \|\Delta\|_\infty<1}} \Big\| & - (\hat{P}_{uy} W_u^{-1} \widetilde{V}^{-1} (\widetilde{U}\widetilde{M}^{-1} + Q) - \widetilde{M}^{-1}) \\ & \times \begin{bmatrix} \alpha_d \widetilde{N}_d & \alpha_f \widetilde{N}_f \end{bmatrix} \Big\|_\infty \\ = \min_{\substack{Q\in\mathcal{RH}_\infty \\ \|\Delta\|_\infty<1}} & ||F_l(F_u(G^{\Delta}_{Q_y}, \Delta), Q)||_\infty, \end{aligned} \tag{60}$$

where the corresponding generalized plant $G^{\Delta}_{Q_y}$ is given by

$$G^{\Delta}_{Q_y} = \begin{bmatrix} -W_1 S_i K W_2 & -\alpha_d W_1 S_i K P_{dy} & -\alpha_f W_1 S_i K P_{fy} & W_1 S_i \widetilde{V}^{-1} \\ S_o W_2 & \alpha_d S_o P_{dy} & \alpha_f S_o P_{fy} & S_o P_{uy} \widetilde{V}^{-1} \\ -\widetilde{M} W_2 & -\alpha_d \widetilde{N}_d & -\alpha_f \widetilde{N}_f & 0 \end{bmatrix}. \tag{61}$$

As in the nominal case, in order to improve the closed-loop performance after the fault has been isolated, a specific compensator $Q_i \in \mathcal{RH}_\infty$ can be designed using the optimization criteria in (58) and (60), depending if the fault is affecting the state or output equations on the state-space representation (1). For these cases, in the generalized plants $(G^{\Delta}_{Q_u}, G^{\Delta}_{Q_y})$ presented in (59) and (61), $\widetilde{N}_f$ is replaced by the information of the analyzed fault $\widetilde{N}^i_f$ for $i = 1, \ldots, l$.

The robust stability condition is very important since it is needed that the fault accommodation scheme will preserve closed-loop stability after the compensation despite model uncertainty. However, the size of the uncertainty and its frequency content will dictate the degree of conservativeness introduced. Assume that the ith fault f_i is analyzed, then define the transfer matrix $M_i(s)$ by closing the lower feedback path with its specific compensator Q_i in the LFT configuration, that is,

$$M_i(s) = F_l(P_i, Q_i) = \begin{bmatrix} M_i^{11} & M_i^{12} \\ M_i^{21} & M_i^{22} \end{bmatrix}, \tag{62}$$

where P_i represents the generalized plant in (59) (*sensor faults*) or (61) (*actuator or system fault*) by replacing $\widetilde{N}_f$ with $\widetilde{N}^i_f$. Then robust stability with respect to the ith compensator Q_i is tested by the condition [20] as follows:

$$\|M_i^{11}\| \leq 1. \tag{63}$$

4.3. Robust performance evaluation

Finally, some indices are suggested to evaluate the robust performance of the resulting FTC structure.

(1) *Fault evaluation*. The size of the worst-case uncertainty is applied to obtain an estimate of the evaluation performance as

$$I_{\text{RFD}} \triangleq \frac{\left\|H_D \widetilde{N}_f\right\|_k}{\left\|H_D \widetilde{N}_d\right\|_j + \left\|H_D \widetilde{M} W_2 W_1\right\|_\infty}. \tag{64}$$

Consequently, if I_{RFD} is large, then good evaluation characteristics are devised.

(2) *Fault isolation*. The structure of the index (43) is maintained, but the worst-case uncertainty information is appended as

$$I_{\text{RFI}} \triangleq \frac{\left\|\left[H_I \widetilde{N}_f\right]_{\text{diag}}\right\|_k}{\left\|\left[H_I \widetilde{N}_f\right]_{\text{nondiag}}\right\|_k + \left\|H_I \widetilde{N}_d\right\|_j + \left\|H_I \widetilde{M} W_2 W_1\right\|_\infty}. \tag{65}$$

(3) *Fault accommodation*. The fault accommodation performance is evaluated in terms of the faults and perturbations attenuation subject to model uncertainty. For this purpose, a robust performance analysis is carried out by using the structured singular value μ_Δ [19, 20]. Then the fault accommodation performance with respect to the ith fault is defined by

$$I^i_{\text{RFA}} = \sup_{\omega \in \mathbb{R}} \mu_{\Delta_p}[M_i(j\omega)], \tag{66}$$

where $\Delta_p = \text{diag}(\Delta, \Delta_f)$ is an augmented uncertainty block to address the performance specifications. Thus internal stability is guaranteed for $\|\Delta\|_\infty < 1/I^i_{\text{RFA}}$, and the worst-case performance is bounded $F_u(M_i, \Delta) \leq I^i_{\text{RFA}}$. As a result, if the index I^i_{RFA} is lower than one, then robust stability is granted.

5. ILLUSTRATIVE EXAMPLE

In order to illustrate the ideas presented in the paper, the design of an active FTC scheme for a separately excited DC motor is considered. The dynamics of a second-order actuator are appended to the motor description. To have a more realistic simulation, the actuator gain is limited by a saturation function. Hence the control signal u is limited to the interval $[0, 10]$ V. Thus a system with one input and three outputs (armature voltage V_a and current i_a, and angular velocity ω) is studied [30]. The load torque is modeled as an unknown constant or slowly time-varying external disturbance d into the system. The control objective is defined as the regulation of the angular velocity to a prescribed reference. Note that since there are three measurements and one unknown perturbation, then only the effect of two different faults could be analyzed simultaneously [4]. The studied faults are actuator f_1 (gain of the dc drive) and sensor f_2 (angular velocity measurement). The parameters of the dc motor are shown in Table 1. The mathematical model of the studied system is presented next:

$$\begin{aligned} \begin{bmatrix} \dot{x}_1 \\ \dot{x}_2 \\ \dot{x}_3 \\ \dot{x}_4 \end{bmatrix} &= \begin{bmatrix} -\frac{R_a}{L_a} & -\frac{K_b}{L_a} & 0 & \frac{1}{L_a} \\ \frac{K_b}{J} & -\frac{B}{J} & 0 & 0 \\ 0 & 0 & 0 & -1 \\ 0 & 0 & \omega_a^2 & -2\zeta_a\omega_a \end{bmatrix} \begin{bmatrix} x_1 \\ x_2 \\ x_3 \\ x_4 \end{bmatrix} \\ &\quad + \begin{bmatrix} 0 \\ 0 \\ K_a \\ 0 \end{bmatrix} u + \begin{bmatrix} 0 \\ -\frac{1}{J} \\ 0 \\ 0 \end{bmatrix} d + \begin{bmatrix} 0 & 0 \\ 0 & 0 \\ K_a & 0 \\ 0 & 0 \end{bmatrix} \begin{bmatrix} f_1 \\ f_2 \end{bmatrix}, \\ \begin{bmatrix} i_a \\ \omega \\ V_a \end{bmatrix} &= \begin{bmatrix} 1 & 0 & 0 & 0 \\ 0 & 1 & 0 & 0 \\ 0 & 0 & 0 & 1 \end{bmatrix} \begin{bmatrix} x_1 \\ x_2 \\ x_3 \\ x_4 \end{bmatrix} + \begin{bmatrix} 0 & 0 \\ 0 & 1 \\ 0 & 0 \end{bmatrix} \begin{bmatrix} f_1 \\ f_2 \end{bmatrix}. \end{aligned} \tag{67}$$

In fact, the model described in (67), with the parameters in Table 1, is stable and satisfies the isolation conditions presented in (7) and (8). The nominal controller is designed following a PI structure with respect to the velocity reference

error $\omega_{ref} - \omega$, plus a constant feedback from i_a and V_a, that is,

$$\begin{aligned} \dot{x}_k &= \omega_{ref} - \omega, \\ u &= K_i x_k + K_p^{\omega}(\omega_{ref} - \omega) + K_p^i i_a + K_p^V V_a, \end{aligned} \tag{68}$$

where $K_i = 0.5$, $K_p^{\omega} = 0.1$, $K_p^i = 0.2$, and $K_p^V = -0.01$. This control law satisfies the performance specifications by achieving internal stability and asymptotic tracking. Now, the detection and isolation filters (H_D, H_I) were designed following the optimization indices (16) and (18) with $j = \infty$, and selecting

$$\begin{aligned} h(s) &= \begin{bmatrix} 1 & 1 \end{bmatrix} \times \frac{1}{s/100 + 1}, \\ T(s) &= \frac{1}{s/10^4 + 1} \begin{bmatrix} 1 & 0 \\ 0 & 1 \end{bmatrix}. \end{aligned} \tag{69}$$

All the numerical calculations were carried out in MATLAB by using two toolboxes: (i) control system, and (ii) LMI control (see Appendix A). The transfer matrix $T(s)$ was chosen as a diagonal low-pass filter since the frequency content of $\widetilde{N}_f$ allows perfect decoupling in the low frequency. The residual evaluation was computed by the windowed 2 norm in (20). Consequently, assuming a time window T_o and $\|d\|_{\infty} \leq d_{\max}$, then a hard threshold for fault evaluation is calculated by

$$J_{\text{th}}^D = \|H_D \widetilde{N}_d\|_{\infty} \sqrt{T_o} d_{\max}, \tag{70}$$

since $\|d\|_{2,t,T_o} \leq d_{\max}\sqrt{T_o}$. Meanwhile, for isolation purposes, two new thresholds are also computed as follows:

$$\begin{aligned} J_{\text{th}}^{I1} &= \|[H_I \widetilde{N}_d]_1\|_{\infty} \sqrt{T_o} d_{\max} + \|[H_I \widetilde{N}_f]_{12}\|_{\infty} \sqrt{T_o} f_{2\max}, \\ J_{\text{th}}^{I2} &= \|[H_I \widetilde{N}_d]_2\|_{\infty} \sqrt{T_o} d_{\max} + \|[H_I \widetilde{N}_f]_{21}\|_{\infty} \sqrt{T_o} f_{1\max}, \end{aligned} \tag{71}$$

where $\|f_1\|_{\infty} \leq f_{1\max}$, and $\|f_2\|_{\infty} \leq f_{2\max}$. Next, the fault accommodation compensators Q, Q_1, and Q_2 were synthesized by (35), (39), and (40) with $\alpha_f = 1.0$ and $\alpha_d = 0.0$. The performance indices in (42), (43), and (44) were computed taking the ∞ norm ($k = j = \infty$), and they are listed in Table 2. The weight α_d is chosen null since the perturbation is assumed constant or slowly time varying, so the integral part of the nominal controller can compensate effectively its effect. Hence the results in Table 2 reflect that the active FTC will provide good performance in the detection, isolation, and accommodation stages. Furthermore, no degradation should be expected in a steady state since $I_{\text{FA}} = I_{\text{FA}}^1 = I_{\text{FA}}^2 = 0$. However, some transient changes have to be anticipated due to control switching (see Figure 5). The velocity reference ω_{ref} is defined as a square wave that oscillates between 75 and 125 rad/s at a frequency of 4 Hz. The load torque d is initialized to 1 Nm. The following scenario is tested under numerical simulation:

Table 1: DC motor parameters.

Parameter	Description
$R_a = 0.699\,\Omega$	Armature resistance
$L_a = 0.297\,\text{H}$	Armature inductance
$B = 4.544 \times 10^{-3}\,\text{Nm/rad/s}$	Friction coefficient
$J = 2.79 \times 10^{-3}\,\text{kg m}$	Inertia
$K_b = 0.746\,\text{V/rad/s}$	Electromagnetic constant
$K_a = 40$	Actuator gain
$\omega_a = 2\pi \times 360\,\text{rad/s}$	Actuator natural frequency
$\zeta_a = 0.7$	Actuator damping factor

Table 2: FTC performance indices.

Index	Value
I_{FD}	6.17×10^3
I_{FI}	106.5
I_{FA}	0
I_{FA}^1	0
I_{FA}^2	0
I_{RFD}	1.63
I_{RFI}	1.05

(i) at 2.5 s, there is a perturbation step change from 1 Nm to 2 Nm;
(ii) from 4 to 8 s, fault f_2 is active as a complete sensor outage, that is, $f_2 = -\omega$;
(iii) from 10 to 14 s, fault f_1 is triggered as a 50% reduction in the actuator gain, that is, $f_1 = -0.5\,u$;
(iv) finally, from 16 to 20 s, fault f_2 is once more active.

The results are presented in Figures 8 and 9. For comparison, the nominal controller (without compensation) and the active FTC are plotted simultaneously in Figure 8. From the simulation results, the nominal controller saturates the control signal u when f_2 is triggered, and the actuator delivers its maximum output voltage to the motor. As a result, the angular velocity is dangerously raised to ≈ 500 rad/s. This behavior could induce severe mechanical stresses in the motor, and practically, an instability scenario is faced, but limited by the actuator saturation. Meanwhile, the active FTC scheme can accommodate effectively this fault, with some transient oscillation due to the control switching. However, for fault f_1, the nominal controller and the FTC scheme can compensate its appearance by the integral action in the nominal controller, but although the nominal control law can inherently accommodate this fault, there is no record of this faulty condition in the closed-loop system. Now, the results of the fault detection and isolation stages are illustrated in Figure 9. Faults f_1 and f_2 are correctly isolated, and the disturbance step change is not mistaken by a fault in the FDI stage. In fact, f_1 and f_2 are almost instantaneously isolated. Note that the active FTC scheme is able to maintain good performance after both faults, and also when the faults are removed from the system, the nominal performance is recovered.

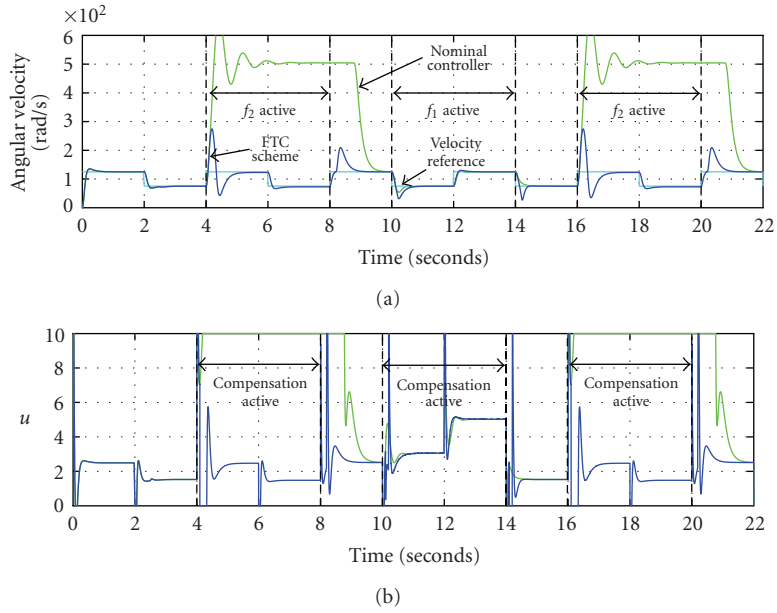

FIGURE 8: Simulation evaluation of FTC scheme: (a) angular velocity, and (b) control signal.

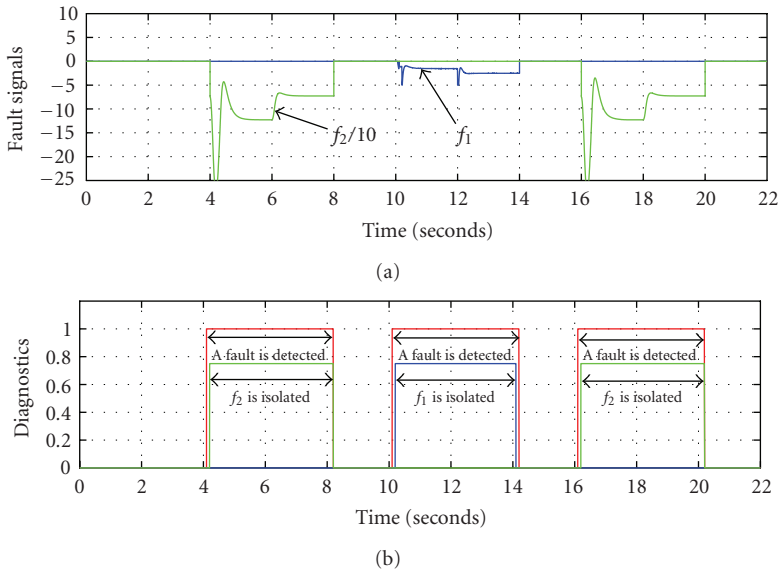

FIGURE 9: Simulation evaluation of FTC scheme: (a) fault signals, (b) detection and isolation results.

Now, in order to evaluate the fault diagnosis and isolation under model uncertainty, the performance of the previously designed filters H_D and H_I under uncertainty in the measurements i_a and ω is analyzed. So, consider the following output uncertainty weight W_2 as follows:

$$W_2(s) = \begin{bmatrix} \dfrac{0.2}{s/10+1} \\ \dfrac{0.15}{s/1000+1} \\ 0 \end{bmatrix}. \tag{72}$$

The interpretation of W_2 is the following: (a) there is a maximum error of 20% at the low frequency of the armature current measurement, and there is a 15% error in the measurement of the angular velocity sensor over the whole frequency bandwidth. The robust performance indices in (64) and (65) were calculated ($k = j = \infty$), and the results are presented in Table 2. The results show that there is a severe deterioration in the diagnosis and isolation capabilities under that uncertainty profile, but there are still some degree of separability to achieve the diagnosis and isolation stage.

6. CONCLUSIONS

In this paper, a control methodology for fault detection, isolation, and accommodation to address LTI systems has been

detailed. The FTC scheme is based on the GIMC configuration [12] which extends the use of the Youla parametrization to FTC. Design strategies were presented for the FDI process and accommodation. Multiple and intermittent faults can be treated in this FTC scheme. Closed-loop stability is always guaranteed after each configuration but only if the additive faults profiles do not depend on the states or outputs. Moreover, the analysis of the design schemes under model uncertainty was carried out. For detection and isolation purposes, a hard threshold is suggested for the nominal case, and an adaptive one is considered when model uncertainty affects the output measurements. Performance indices are also suggested to evaluate the detection, isolation, and accommodation schemes. The FTC structure was tested in numerical simulation over a DC motor setup, and the advantages over a nominal control law were clearly presented.

APPENDICES

A. FAULT TOLERANT SYNTHESIS ALGORITHMS

The synthesis algorithm for fault diagnosis, isolation, and accommodation in the nominal case is presented in this section. The algorithm follows the ideas exposed in Section 3. The synthesis procedure is based on MATLAB, and it could be implemented using the next toolboxes: (i) control system, (ii) LMI control, (iii) μ analysis and synthesis, and (iv) robust control. After each step in the algorithm, the MATLAB commands used for numerical synthesis are introduced inside parentheses as follows.

(1) Define the state-space description of the plant and nominal controller in (1) and (9) (*ss, ltisys, pack* and *mksys*).
(2) Construct the left coprime factorizations of plant (5) and controller (9) (*lqr, place* and *acker*), in order to avoid numerical problems, use a balance realization for all the coprime factors (*balreal, sbalanc, sysbal* and *obalreal*).
(3) Check conditions (7) and (8) to verify the solvability of the synthesis schemes.
(4) Define the filters $h, T \in \mathcal{RH}_\infty$, and obtain H_D, H_I by solving the optimization problems (16) and (18) (*hinflmi, hinfric, hinfsyn, h2syn, hinfopt*, and *h2lqg*).
(5) Evaluate the fault diagnosis performance through (42), and isolation property by extracting the diagonal and nondiagonal parts of the product $H_I\widetilde{N}_f$ using the state-space realization and computing (43) (*norm, norminf, norm2, h2norm, hinfnorm, normh2, normhinf, ssdata, ltiss, unpck*, and *branch*).
(6) Obtain the general accommodation compensator Q using (35), and the specific compensators Q_i by (39) or (40) (*hinflmi, hinfric, hinfsyn, h2syn, hinfopt*, and *h2lqg*).
(7) Evaluate the fault accommodation performance by (44) (*norm, norminf, norm2, h2norm, hinfnorm, normh2*, and *normhinf*).

Alternatively, the synthesis procedure can be computed using open source numerical programs as Scilab [31] and Octave [32]. In fact, freely in the web, there are toolboxes for these two programs that implement the same synthesis algorithms as in MATLAB.

B. PROOF OF LEMMA 1

From the block diagram in Figure 2, it is observed that the internal signal f_e is given by (13), and as a result, the internal control signal $\hat{u}$ is constructed as

$$\begin{aligned}\hat{u}(s) &= q(s) + \widetilde{U}e(s) = Qf_e(s) + \widetilde{U}(ref(s) - y(s)) \\ &= -Q[\widetilde{N}_d d(s) + \widetilde{N}_f f(s)] + \widetilde{U}[ref(s) - y(s)].\end{aligned} \tag{B.1}$$

Thus the control signal u contains information from the faults, perturbations, references, and outputs:

$$\begin{aligned}u(s) = \widetilde{V}^{-1}\hat{u}(s) &= K[ref(s) - y(s)] \\ &- \widetilde{V}^{-1}Q[\widetilde{N}_d d(s) + \widetilde{N}_f f(s)].\end{aligned} \tag{B.2}$$

Finally, by a direct substitution of (3) into (B.2), the results in (27) are deduced.

C. PROOF OF LEMMA 2

From the block diagram of Figure 6 under additive uncertainty, (47) is obtained directly to describe f_e by recalling (13). Next, the control signal u is derived as

$$u(s) = \widetilde{V}^{-1}[Qf_e(s) + \widetilde{U}(ref(s) - y(s))], \tag{C.1}$$

and by a substitution of (3) and (46) into the previous equation, the effects of the reference, perturbations, and faults can be isolated from the control signal u :

$$\begin{aligned}&[I + \widetilde{V}^{-1}QM\Delta_{uy} + K(P_{uy} + \Delta_{uy})]u(s) \\ &\quad = K\,ref(s) + \widetilde{V}^{-1}(\widetilde{U}\widetilde{M}^{-1} + Q)(\widetilde{N}_d d(s) + \widetilde{N}_f f(s)).\end{aligned} \tag{C.2}$$

Hence by defining the term W_u in (50), the result in (48) is obtained. Finally, substituting (48) and (46) into the output equation (3), the contributions of the references, perturbations, and faults into the output are described by (49).

ACKNOWLEDGMENTS

This research is supported in part by grants from FAI (Grant no. C06-FAI-11-34.71) and CONACYT (Grant no. C07-ACIPC-08.4.4, no.52314). D. R. Espinoza-Trejo acknowledges the support provided by CONACYT through a doctoral scholarship (no. 166718).

REFERENCES

[1] J. Chen and R. J. Patton, *Robust Model-Based Fault Diagnosis for Dynamic Systems*, Kluwer Academic, Dordrecht, The Netherlands, 1999.
[2] R. Isermann and P. Ballé, "Trends in the application of model-based fault detection and diagnosis of technical processes," *Control Engineering Practice*, vol. 5, no. 5, pp. 709–719, 1997.

[3] R. Isermann, *Fault-Diagnosis Systems: An Introduction from Fault Detection to Fault Tolerance*, Springer, New York, NY, USA, 2006.
[4] A. Saberi, A. A. Stoorvogel, P. Sannuti, and H. Niemann, "Fundamental problems in fault detection and identification," *International Journal of Robust and Nonlinear Control*, vol. 10, no. 14, pp. 1209–1236, 2000.
[5] M. Blanke, R. Izadi-Zamanabadi, S. A. Bøgh, and C. P. Lunau, "Fault-tolerant control systems—a holistic view," *Control Engineering Practice*, vol. 5, no. 5, pp. 693–702, 1997.
[6] M. Blanke, M. Kinnaert, J. Lunze, and M. Staroswiecki, *Diagnosis and Fault-Tolerant Control*, Springer, New York, NY, USA, 2003.
[7] D. U. Campos-Delgado and K. Zhou, "Reconfigurable fault-tolerant control using GIMC structure," *IEEE Transactions on Automatic Control*, vol. 48, no. 5, pp. 832–838, 2003.
[8] H. Noura, D. Sauter, F. Hamelin, and D. Theilliol, "Fault-tolerant control in dynamic systems: application to a winding machine," *IEEE Control Systems Magazine*, vol. 20, no. 1, pp. 33–49, 2000.
[9] J. Stoustrup and V. D. Blondel, "Fault tolerant control: a simultaneous stabilization result," *IEEE Transactions on Automatic Control*, vol. 49, no. 2, pp. 305–310, 2004.
[10] D. Kim and Y. Kim, "Robust variable structure controller design for fault tolerant flight control," *Journal of Guidance, Control, and Dynamics*, vol. 23, no. 3, pp. 430–437, 2000.
[11] P. Zhang, S. X. Ding, G. Z. Wang, T. Jeinsch, and D. H. Zhou, "Application of robust observer-based FDI systems to fault tolerant control," in *Proceedings of the 15th Triennial IFAC World Congress*, Barcelona, Spain, 2002.
[12] K. Zhou and Z. Ren, "A new controller architecture for high performance, robust, and fault-tolerant control," *IEEE Transactions on Automatic Control*, vol. 46, no. 10, pp. 1613–1618, 2001.
[13] J.-Y. Shin, N. E. Wu, and C. Belcastro, "Adaptive linear parameter varying control synthesis for actuator failure," *Journal of Guidance, Control, and Dynamics*, vol. 27, no. 5, pp. 787–794, 2004.
[14] J.-Y. Shin and C. M. Belcastro, "Performance analysis on fault tolerant control system," *IEEE Transactions on Control Systems Technology*, vol. 14, no. 5, pp. 920–925, 2006.
[15] M. Ji, Z. Zhang, G. Biswas, and N. Sarkar, "Hybrid fault adaptive control of a wheeled mobile robot," *IEEE/ASME Transactions on Mechatronics*, vol. 8, no. 2, pp. 226–233, 2003.
[16] X. Zhang, T. Parisini, and M. M. Polycarpou, "Adaptive fault-tolerant control of nonlinear uncertain systems: an information-based diagnostic approach," *IEEE Transactions on Automatic Control*, vol. 49, no. 8, pp. 1259–1274, 2004.
[17] D. U. Campos-Delgado, E. R. Palacios, and D. R. Espinoza-Trejo, "Fault accommodation strategy for LTI systems based on GIMC structure: additive faults," in *Proceedings of the 44th IEEE Conference on Decision and Control, and the European Control Conference (CDC-ECC '05)*, vol. 2005, pp. 6292–6297, Seville, Spain, December 2005.
[18] D. U. Campos-Delgado, S. Martínez-Martínez, and K. Zhou, "Integrated fault-tolerant scheme for a DC speed drive," *IEEE/ASME Transactions on Mechatronics*, vol. 10, no. 4, pp. 419–427, 2005.
[19] G. E. Dullerud and F. Paganini, *A Course in Robust Control Theory*, Springer, New York, NY, USA, 2000.
[20] K. Zhou, J. C. Doyle, and K. Glover, *Robust and Optimal Control*, Prentice Hall, Upper Saddle River, NJ, USA, 1996.
[21] S. X. Ding, T. Jeinsch, P. M. Frank, and E. L. Ding, "A unified approach to the optimization of fault detection systems," *International Journal of Adaptive Control and Signal Processing*, vol. 14, no. 7, pp. 725–745, 2000.
[22] B. Marx, D. Koenig, and D. Georges, "Robust fault-tolerant control for descriptor systems," *IEEE Transactions on Automatic Control*, vol. 49, no. 10, pp. 1869–1875, 2004.
[23] H. Niemann and J. Stoustrup, "Fault tolerant controllers for sampled-data systems," in *Proceedings of the American Control Conference*, vol. 4, pp. 3490–3495, 2004.
[24] S. S. Yang and J. Chen, "Sensor faults compensation for MIMO fault-tolerant control systems," *Transactions of the Institute of Measurement and Control*, vol. 28, no. 2, pp. 187–205, 2006.
[25] N. Liu and K. Zhou, "Optimal solutions to multi-objective robust fault detection problems," in *Proccedings of the 2007 IEEE Conference on Decision and Control*, New Orleans, LA, USA, December 2007.
[26] H. Niemann and J. Stoustrup, "Fault diagnosis for nonmininum phase systems using H_∞ optimization," in *Proceedings of the American Control Conference*, vol. 6, pp. 4432–4436, 2001.
[27] A. Emami-Naeini, M. M. Akhter, and S. M. Rock, "Effect of model uncertainty on failure detection: the threshold selector," *IEEE Transactions on Automatic Control*, vol. 33, no. 12, pp. 1106–1116, 1988.
[28] M. G. Perhinschi, M. R. Napolitano, G. Campa, B. Seanor, J. Burken, and R. Larson, "An adaptive threshold approach for the design of an actuator failure detection and identification scheme," *IEEE Transactions on Control Systems Technology*, vol. 14, no. 3, pp. 519–525, 2006.
[29] J. Jiang and Y. Zhang, "Accepting performance degradation in fault-tolerant control system design," *IEEE Transactions on Control Systems Technology*, vol. 14, no. 2, pp. 284–292, 2006.
[30] R. Krishnan, *Electric Motor Drives: Modeling, Analysis, and Control*, Prentice Hall, Upper Saddle River, NJ, USA, 2001.
[31] http://www.scilab.org/.
[32] http://www.octave.org/.

Hindawi Publishing Corporation
Journal of Control Science and Engineering
Volume 2008, Article ID 231697, 11 pages
doi:10.1155/2008/231697

Research Article

A Method for Designing Fault Diagnosis Filters for LPV Polytopic Systems

Sylvain Grenaille, David Henry, and Ali Zolghadri

Université Bordeaux 1, Approche Robuste et Intégrée de l'Automatique, Laboratory IMS, 351 Cours de la Libération, 33405 Talence Cedex, France

Correspondence should be addressed to David Henry, david.henry@laps.ims-bordeaux.fr

Received 30 March 2007; Accepted 25 September 2007

Recommended by Kemin Zhou

The work presented in this paper focuses on the design of robust Fault Detection and Isolation (FDI) filters for dynamic systems characterized by LPV (Linear Parameter Varying) polytopic models. A sufficient condition is established to guarantee sensitivity performance of the residual signal vector to faults. Robustness constraints against model perturbations and disturbances are also taken into account in the design method. A key feature of the proposed method is that the residual structuring matrices are optimized as an integral part of the design, together with the dynamic part (i.e. the filter). The design problem is formulated as a convex optimization problem and solved using LMI (Linear Matrix Inequalities) techniques. The proposed method is illustrated on the secondary circuit of a Nuclear Power Plant.

1. INTRODUCTION AND MOTIVATIONS

The issue of Fault Detection and Isolation (FDI) in dynamic systems has been an active research area in the last two decades. Model-based FDI techniques use mathematical models of the monitored process and extract features from measured signals, to generate fault indicating signals, that is, the residuals. LTI models have been widely used to solve the problem of FDI. Tools are now available to enhance robustness against small parameter variations and other disturbances (see, [1–3] for surveys). The resulting robust FDI problem is generally formulated as a min-max optimization setting to maximize fault sensitivity performance and at the same time, to minimize the influence of unknowns inputs.

More recently, some research works have appeared that consider Linear Parameter Varying (LPV) modeling of the monitored system to take into account wider and more rapid parameters variations. Such models can be used efficiently to represent some nonlinear systems (see, e.g., [4, 5]). This motivates some researchers from the FDI community to develop model-based methods using LPV models (see [6–8] among others). The two commonly used approaches are fault estimation methods where the fault indicating signal is an estimate of the fault signal, and residual generation methods where the residuals are synthesized to be robust against modeling errors and unknown inputs, while being sensitive to the faults. In this context, a geometric approach is proposed in [6] to design a LPV observer in a Luenberger form. A procedure is derived to obtain the observer parameters via the construction of a suitable family of invariant subspaces (parameter varying (C, A)-invariant and un-observability subspaces). In [7], a multi-model approach is used to solve the FDI problem for nonlinear systems. The nonlinear system is modeled using polytopic models and a robust polytopic unknown input observer is then synthesized by means of pole assignment. The method uses LMI optimization techniques to synthesize the observer gain. The major limitation of this approach is that sensitivity of the residual signal against faults can only be checked a posteriori. More precisely, if the distribution matrices of the fault model and the effects that faults could have on the decoupled state is not of full column rank, then faults could go undetectable. To overcome this problem, a solution is provided in [8] where the main idea is to build a fault estimate using a LPV filter such that the worst-case gain (i.e., the H_∞ performances measure for LPV systems) from disturbances and faults to the estimation error, is minimized.

In this paper a different approach based on residual generation is considered for LPV systems that can be modeled within a LPV polytopic setting. Robustness against exogenous disturbances and sensitivity against faults are considered in a framework similar to the well-known H_∞/H_- setting for LTI systems. The robustness objectives are expressed in terms of a minimization problem using the H_∞ norm for LPV systems, and the sensitivity requirement is formulated in terms of a maximization constraint using also the H-index for LPV systems. The main difference between this problem and the standard H_∞ problem for LPV systems is that it involves the residual structuring matrices that are unknown.

The paper is organized as follows: In Section 2, the general FDI filter design problem and the corresponding solution are presented. In Section 3, the proposed method is applied to real data set coming from the secondary circuit of a nuclear power plant in France. Finally, some concluding remarks are made in a final section.

Preliminaries

The Euclidean norm is always used for vectors and is written without a subscript; for example $\|x\|$. Similarly in the matrix case, the induced vector norm is used: $\|A\| = \overline{\sigma}(A)$ where $\overline{\sigma}(A)$ denotes the maximum singular value of A. Signals, for example $w(t)$ or w, are assumed to be of bounded energy, and their norm is denoted by $\|w\|_2$, that is, $\|w\|_2 = (\int_{-\infty}^{+\infty}\|w(t)\|^2 dt)^{1/2} < \infty$. LTI models, for example, $P(s)$ or simply P, are assumed to be in RH_∞, real rational functions with $\|P\|_\infty = \sup_\omega \overline{\sigma}(P(j\omega)) < \infty$. $\|P\|_\infty$, that is, the largest gain of P, is accompanied by the smallest gain of P, $\inf_\omega \underline{\sigma}(P(j\omega))$, which may be equal to zero for some P (e.g., strictly proper systems), if the frequency range of interest is infinite. This motivated [1, 9–12] to define the nonzero smallest gain of P, that is, the H-index, as the restriction of $\inf_\omega \underline{\sigma}(P(j\omega))$ to a finite frequency domain Ω, that is, $\|P\|_- = \inf_{\omega\in\Omega}\underline{\sigma}(P(j\omega))$.

In [1, 9], an evaluation function $\|\bullet\|_e$ which is a restriction of the H_2 signal norm to Ω, is defined by the authors as $\|w\|_e = \|w\|_{2,\Omega} = (\int_{\omega_1}^{\omega_2}\|w(j\omega)\|_2^2 d\omega)^{1/2}$. Then, given P so that $y = Pu$, it follows that

$$\begin{aligned}\|y\|_e^2 &= \frac{1}{2\pi}\int_{\omega_1}^{\omega_2}\|P(j\omega)u(j\omega)\|_2^2 d\omega \\ &= \frac{1}{2\pi}\int_{\omega_1}^{\omega_2}\left\|P(j\omega)\frac{u(j\omega)}{\|u\|_2}\right\|_2^2 \|u\|_2^2 d\omega \geq \|P\|_-^2\|u\|_e^2\end{aligned} \tag{1}$$

and thus that $\|P\|_- \leq \|y\|_e/\|u\|_e$. This motivates the introduction of an evaluation function, denoted $\|\bullet\|_{\text{sens}}$, which is defined according to:

$$\|P\|_{\text{sens}} = \inf_{\|u\|_e\neq 0}\frac{\|y\|_e}{\|u\|_e} \geq \|P\|_-. \tag{2}$$

From (2), it follows that $\|P\|_{\text{sens}}$ takes the sense of the smallest value of a singular value of $P(j\omega)$ evaluated on Ω. Then it follows that $\|P\|_- \leq \|P\|_{\text{sens}} \leq \|P\|_\infty$.

The underlying LPV system is modeled by the following state space representation

$$\begin{aligned}\dot{x} &= A(\theta(t))x + B(\theta(t))u \\ y &= C(\theta(t))x + D(\theta(t))u\end{aligned} \tag{3}$$

which is denoted in a compact form as

$$M(\theta) = \begin{pmatrix} A(\theta) & B(\theta) \\ C(\theta) & D(\theta)\end{pmatrix}. \tag{4}$$

x is the state vector, u is the input vector, y is the output vector and $\theta(t)$ is a varying parameter vector. It is assumed that all parameters $\theta_i(t)$, $i = 1,\ldots,r$ are bounded, measurable (or estimated) in real time and take their values in the domain Θ, so that Θ is a convex polytope.

The LPV system (3) admits a (non-conservatism) polytopic model if it is possible to determine a set of matrices M_i, $i = 1,\ldots,N$, constituting the vertices of a polytope defined by

$$\text{Co}\{\beta_1,\ldots,\beta_N\} = \left\{\sum_{i=1}^N \beta_i M(\Pi_i),\ \beta_i \geq 0,\ \sum_{i=1}^N \beta_i = 1\right\} \tag{5}$$

and such that it corresponds to the image by M of the domain Θ:

$$\{M(\theta), \theta\in\Theta\} \equiv \text{Co}\{M(\Pi_1),\ldots,M(\Pi_N)\}. \tag{6}$$

Then, β_i, $i = 1,\ldots,N$ define barycentric coordinates of Θ and the following convex decomposition yields:

$$\theta(t) = \beta_1\Pi_1 + \cdots + \beta_N\Pi_N, \quad \beta_i \geq 0, \quad \sum_{i=1}^N \beta_i = 1. \tag{7}$$

Referring to the LPV system (3), the worst-case RMS gain from u to y which is known as the H_∞-norm for LPV systems is defined by:

$$\|M(\theta)\|_\infty = \sup_{\substack{\forall\theta\in\Theta \\ \|u\|_2\neq 0}} = \frac{\|y\|_2}{\|u\|_2}. \tag{8}$$

Following the definition of the index $\|\bullet\|_{\text{sens}}$ of a LTI transfer given by (2), we will introduce the following evaluation function, that will be useful in the following to formulate fault sensitivity requirements for LPV fault detection schemes:

$$\|M(\theta)\|_{\text{sens}} = \inf_{\substack{\forall\theta\in\Theta \\ \|u\|_e\neq 0}} = \frac{\|y\|_e}{\|u\|_e} \tag{9}$$

$\|M(\theta)\|_{\text{sens}}$ is also a generalization of (2) to LPV case.

2. FDI FILTERS FOR LPV SYSTEMS

2.1. Problem setting

Consider the general FDI design problem for LPV systems represented on Figure 1. $G(\theta)$ is a polytopic LPV model.

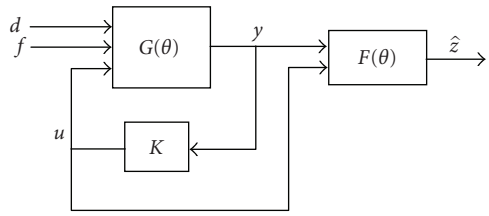

Figure 1: The general FDI filter design problem.

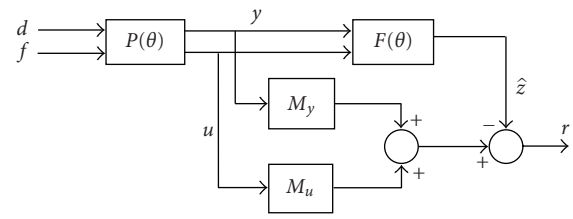

Figure 2: General setup for FDI/LPV filter design problem.

K is a known controller. $d \in R^{q_d}$ represents exogenous disturbances and $f \in R^{q_f}$ represents the faults to be detected. $F(\theta)$ is the FDI LPV filter to be designed. $\hat{z} \in R^{q_r}$ is an estimation of $z = M_y y + M_u u$, a subset of the measurements $y \in R^m$ and the controlled inputs $u \in R^p$. $M_y \in R^{q_r \times m}$ and $M_u \in R^{q_r \times p}$ are the two residual structuring matrices to be designed.

It is assumed that the problem depicted on Figure 1 is well posed and thus the lower fractional transformation $F_1(G(\theta), K)$ always exists.

The FDI design problem we are interested in can then be formulated as follows.

Problem 1. Assume that the faults f are detectable (the interested reader can refer to [13] for a discussion on fault detectability).

The goal is to find the state space matrices $A_F(\theta) \in R^{n_F \times n_F}$, $B_F(\theta) \in R^{n_F \times (m+p)}$, $C_F(\theta) \in R^{q_r \times n_F}$ and $D_F(\theta) \in R^{q_r \times (m+p)}$ of the (stable) polytopic LPV filter $F(\theta)$ and the residual structuring matrices $M_y \in R^{q_r \times m}$ and $M_u \in R^{q_r \times p}$ defining the residual vector

$$r = z - \hat{z} = M_y y + M_u u - F(\theta) \begin{pmatrix} y \\ u \end{pmatrix}, \quad r \in R^{q_r} \tag{10}$$

such that the residual vector meets the following requirements:

$$\|T_{rd}(\theta)\|_\infty < \gamma_1 \tag{11}$$

$$\|T_{rf}(\theta)\|_{\text{sens}} > \gamma_2 \tag{12}$$

where T_{rd} and T_{rf} denote the looped transfers between d and r and f and r, respectively. This problem can be represented by the block diagram illustrated on Figure 2, where $P(\theta)$ is derived from $F_1(G(\theta), K)$ so that $\left(\begin{smallmatrix} y \\ u \end{smallmatrix}\right) = P(\theta)\left(\begin{smallmatrix} d \\ f \end{smallmatrix}\right)$. In this formulation, γ_1 and γ_2 are two positive constants referring respectively to the robustness and sensitivity performances levels.

Equation (11) represents the worst-case robustness of the residual to disturbances d for all $\theta \in \Theta$, in the H_∞-norm sense. Under plant perturbation, the effect that the exogenous disturbances have on the residuals, can greatly increase and the fault detection performance may then be considerably degraded. A robust fault sensitivity specification is then needed to maintain a detection performance level of the FDI unit. Here the sensitivity measure (9) for LPV fault detection scheme is used to guarantee the worst-case sensitivity of the residual to faults.

Of course, the smaller γ_1 and the bigger γ_2 are the better the fault detection performance will be.

Remark 1. In Problem 1 formulation, it is assumed that the structuring matrices M_y and M_u do not depend on θ. If this assumption vanishes, it can be verified that the following theoretical developments still yields. The only difference in such a case is that, if we consider $M_y(\theta)$ and $M_u(\theta)$ in Problem 1, a set of structuring matrices $M_y(\Pi_i)$ and $M_u(\Pi_i)$ for each vertex of the polytope Θ would be obtained rather than constant matrices.

2.2. Design of the FDI filter

In this section, a solution is provided to compute simultaneously M_y, M_u and $F(\theta)$ so that the requirements (11) and (12) are satisfied. It is straightforward to verify that the major difficulty in this problem is related to the fault sensitivity requirement (12) since (11) can be solved using the techniques developed in the robust control community (see, e.g., [14] or [15]). To overcome this problem, a sufficient condition is established in terms of a fictitious H_∞ problem. It is then shown in the following that a solution to this fictitious problem is a solution of the original one.

2.2.1. Standard setup for the filter design problem

To proceed, let

$$P(\theta) = \begin{pmatrix} A(\theta) & B_d(\theta) & B_f(\theta) \\ C(\theta) & D_d(\theta) & D_f(\theta) \end{pmatrix}. \tag{13}$$

Using some algebra manipulations, the filter design problem illustrated on Figure 2, can be re-casted into the setup depicted in Figure 3, where $\overline{P}(\theta, M_y, M_u)$ is deduced from $P(\theta), M_y$ and M_u, according to:

$$\overline{P}(\theta, M_y, M_u) =$$

$$\begin{pmatrix} A(\theta) & B_d(\theta) & B_f(\theta) & 0_{n \times q_r} \\ (M_y \;\; M_u)C(\theta) & (M_y \;\; M_u)D_d(\theta) & (M_y \;\; M_u)D_f(\theta) & -I_{q_r} \\ C(\theta) & D_d(\theta) & D_f(\theta) & 0_{(m+p) \times q_r} \end{pmatrix} \tag{14}$$

where I_{q_r} and $0_{i \times j}$ denote respectively the identity matrix of dimension q_r and the null matrix of dimension $i \times j$. n is also the order of $\overline{P}(\theta, M_y, M_u)$, that is, $A(\theta) \in R^{n \times n}$.

Following the method proposed in [10, 11], the requirements (11) and (12) are now expressed in terms of loop

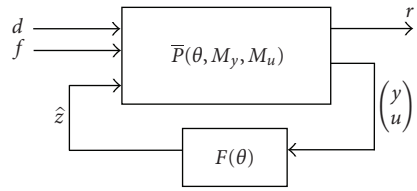

Figure 3: FDI/LPV filter design problem.

shapes, that is, of desired gain responses for the appropriate closed-loop transfers. These shaping objectives are then turned into uniform bounds by means of the shaping filters. Let W_d and W_f denote the (dynamical) shaping filters associated with (11) and (12) respectively, so that:

$$||W_d||_\infty \leq \gamma_1 \tag{15}$$

$$||W_f||_- \geq \gamma_2 \tag{16}$$

$\|W_d\|_\infty$ and $\|W_f\|_-$ denote respectively the H_∞ and H_- norm of the LTI transfer W_d and W_f (see preliminaries).

Assume that W_d is invertible (this can be done without loss of generality because it is always possible to add zeros in W_d to make it invertible). W_d and W_f are also defined in order to tune the gain responses for, respectively, $T_{rd}(\theta)$ and $T_{rf}(\theta)$. Then it is straightforward to verify that the specification (11) yields if the following constraint is satisfied:

$$||T_{r\tilde{d}}(\theta)||_\infty < 1. \tag{17}$$

In this formulation, $\tilde{d} \in R^{q_{\tilde{d}}}$ is a fictitious signal generating d through W_d (see Figure 4(a) for easy reference) and $T_{r\tilde{d}}$ denotes the looped transfer between r and $\tilde{d}$.

The following lemma allows the sensitivity constraint (12) to be transformed into a fictitious H_∞ one.

Lemma 1. *Consider an invertible transfer matrix W_F such that $\|W_f\|_- = (\gamma_2/\lambda)\|W_F\|_-$ and $\|W_F\|_- > \lambda$ where $\lambda = 1 + \gamma_2$. Define the (fictitious) signal $\tilde{r} \in R^{q_r}$ such that $\tilde{r} = r - W_F f$ (see Figure 4(a)). Then a sufficient condition for the specification* (12) *to hold, is:*

$$||T_{\tilde{r}f}(\theta)||_\infty < 1, \tag{18}$$

where $T_{\tilde{r}f}$ denote the looped transfer between $\tilde{r}$ and f.

Proof of Lemma 1. Consider the signal $\tilde{r}$ introduced in Figure 4, that is,

$$\tilde{r} = r - W_F f, \tag{19}$$

where W_F is define as in Lemma 1. Then it can be verified that the following relation yields:

$$||T_{rf}(\theta)||_{\text{sens}} \geq ||W_F||_- - ||T_{rf}(\theta) - W_F||_\infty \tag{20}$$

that can be re-written due to the definition of $\tilde{r}$ given by (19):

$$||T_{rf}(\theta)||_{\text{sens}} \geq ||W_F||_- - ||T_{\tilde{r}f}(\theta)||_\infty. \tag{21}$$

Now consider the weighting function W_F defined in Lemma 1. Since, W_F is supposed to be invertible, we get

$$\frac{1}{||W_F||_-} = ||W_F^+||_{\infty,\Omega}, \tag{22}$$

where $\|W_F^+\|_{\infty,\Omega} = \sup_{\omega\in\Omega}\overline{\sigma}(W_F^+(j\omega))\cdot W_F^+$ denotes the inverse of W_F which always exists by assumption (see Lemma 1). Then, factorizing the right term of (21) by $\|W_F\|_-$ gives

$$||T_{rf}(\theta)||_{\text{sens}} \geq \left(1 - \frac{||T_{\tilde{r}f}(\theta)||_\infty}{||W_F||_-}\right)||W_F||_- \tag{23}$$

that can be done since, by definition, $\|W_F\|_- \neq 0$. With (22), it then follows that:

$$||T_{rf}(\theta)||_{\text{sens}} \geq \left(1 - ||T_{\tilde{r}f}(\theta)||_\infty ||W_F^+||_{\infty,\Omega}\right)||W_F||_-. \tag{24}$$

Now, since by construction $\|W_F\|_- > \lambda$, it is straightforward to verify that the following relation yields:

$$||W_F^+||_{\infty,\Omega} < \frac{1}{\lambda}. \tag{25}$$

Suppose now that inequality (18) yields, that is, $\|T_{\tilde{r}f}(\theta)\|_\infty < 1$. From (25), it follows that

$$||T_{\tilde{r}f}(\theta)||_\infty ||W_F^+||_{\infty,\Omega} < \frac{1}{\lambda} \tag{26}$$

and with (24), we get

$$||T_{rf}(\theta)||_{\text{sens}} > \frac{\lambda - 1}{\lambda}||W_F||_-. \tag{27}$$

Thus, if $\|W_f\|_- = (\gamma_2/\gamma)\|W_F\|_-$ *with* $\lambda = 1 + \gamma_2$, then (27) implies that

$$||T_{rf}(\theta)||_{\text{sens}} > ||W_f||_- \tag{28}$$

which terminates the proof. □

Following (17) and (18), the design problem can be re-casted in a fictitious LPV H_∞-framework as depicted in Figure 4(a), where $\tilde{d}$ and $\tilde{r}$ are two fictitious signals, so that $\tilde{d} = W_d d$ and $\tilde{r} = r - W_F f$. Then, including γ_1, λ, W_F and W_d^{-1} into the model $\overline{P}(\theta, M_y, M_u)$ leads to the equivalent block diagram of Figure 4(b), where $\widetilde{P}(\theta, M_y, M_u)$ is defined according to:

$$\begin{pmatrix} r \\ \tilde{r} \end{pmatrix} = F_1\left(\widetilde{P}(\theta, M_y, M_u), F(\theta)\right)\begin{pmatrix} \tilde{d} \\ f \end{pmatrix}. \tag{29}$$

The residual generation problem can now be formulated in a framework which looks like a standard H_∞ problem for LPV systems, by combining both requirements (17) and (18) into a single H_∞ constraint. Using Lemma 1, it can be verified that a sufficient condition for (17) and (18) to hold, is

$$||F_1\left(\widetilde{P}(\theta, M_y, M_u), F(\theta)\right)||_\infty < 1. \tag{30}$$

As mentioned above, this equation seems to be similar to a standard H_∞ LPV problem. In fact, this is not the case since the transfer $\widetilde{P}(\theta, M_y, M_u)$ depends on M_y and M_u that are unknown. In the following section, a procedure is given to overcome this problem.

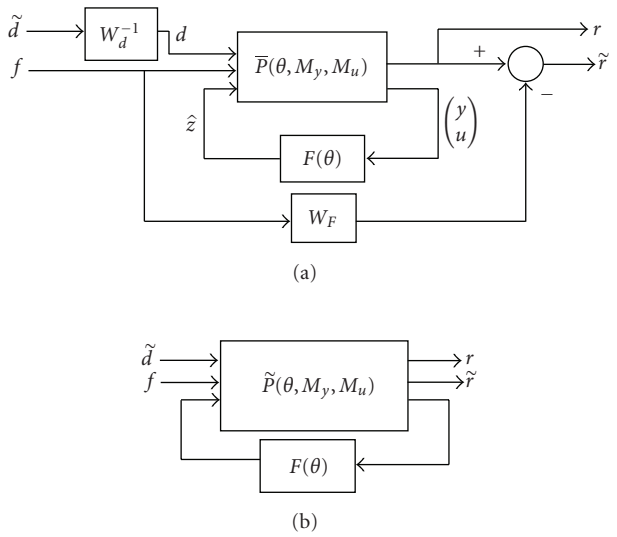

FIGURE 4: Fictitious quadratic H_∞ formulation for the filter design problem.

Remark 2. It is clear that a key feature in the proposed formulation is the a priori choice of the shaping filters W_d and W_f. From a practical point of view, it is required that the residuals r are as "big" and as "fast" as possible, when a fault occurs. Then, if the considered faults manifest themselves in low frequencies, this leads to select W_f as a low pass filter with the static gain and the cutting frequency, the highest possible. With regards to the robustness objectives, it is required that the effects of the disturbances on the residuals are as "small" as possible. This implies to choose the gain of W_d as "small" as possible in the frequency range where the energy content of the disturbances is located. In other words, it is required a high attenuation level of the disturbances on the residuals in the appropriate frequencies (see Section 3 where a practical case is presented). However, both sensitivity to faults and robustness against disturbances might be not achieved in some cases. Faults having similar frequency characteristics as those of disturbances might go undetected. In such cases, the proposed formulation provides a framework to find a good balance between fault sensitivity and robustness via the construction of the shaping filters W_d and W_f. Finally, note that the work reported in [16, 17] could be an interesting method to select W_d and W_f.

2.2.2. Synthesis of the FDI filter

In the following, a solution is derived in terms of a SDP (Semi Definite Programming) problem. To proceed, let $\{A_{wd}, B_{wd}, C_{wd}, D_{wd}\}$ and $\{A_{wF}, B_{wF}, C_{wF}, D_{wF}\}$ be the state-space representations of W_d^{-1} and W_F respectively, and denote n_{wd} and n_{wF} the associated order, that is, $A_{wd} \in R^{n_{wd} \times n_{wd}}$ and $A_{wF} \in R^{n_{wF} \times n_{wF}}$. Using some linear algebra manipulations, it can be verified from (14) that the matrices $\widetilde{A}(\theta)$, $\widetilde{B}(\theta)$, $\widetilde{C}(\theta)$ and $\widetilde{D}(\theta)$ of the state-space representation of $\widetilde{P}(\theta, M_y, M_u)$ are defined according to:

$$\widetilde{A}(\theta) = \begin{pmatrix} A(\theta) & B_d(\theta)C_{wd} & 0 \\ 0 & A_{wd} & 0 \\ 0 & 0 & A_{wF} \end{pmatrix}, \quad \widetilde{A}(\theta) \in R^{(n+n_{wd}+n_{wF}) \times (n+n_{wd}+n_{wF})}, \tag{31}$$

$$\widetilde{B}(\theta) = (\widetilde{B}_1(\theta) \mid \widetilde{B}_2) = \begin{pmatrix} B_d(\theta)D_{wd} & B_f(\theta) & 0 \\ B_{wd} & 0 & 0 \\ 0 & B_{wF} & 0 \end{pmatrix}, \quad \widetilde{B}(\theta) \in R^{(n+n_{wd}+n_{wF}) \times (q_{\tilde{d}}+q_f+q_r)}, \tag{32}$$

$$\widetilde{C}(\theta) = \begin{pmatrix} \widetilde{C}_1(\theta) \\ \widetilde{C}_2(\theta) \end{pmatrix} = \begin{pmatrix} (M_y \quad M_u)C(\theta) & (M_y \quad M_u)D_d(\theta)C_{wd} & 0 \\ (M_y \quad M_u)C(\theta) & (M_y \quad M_u)D_d(\theta)C_{wd} & -C_{wF} \\ C(\theta) & D_d(\theta)C_{wd} & 0 \end{pmatrix}, \quad \widetilde{C}(\theta) \in R^{(2q_r+m+p) \times (n+n_{wd}+n_{wF})}, \tag{33}$$

$$\widetilde{D}(\theta) = \begin{pmatrix} \widetilde{D}_{11}(\theta) & \widetilde{D}_{12} \\ \widetilde{D}_{21}(\theta) & \widetilde{D}_{22} \end{pmatrix} = \begin{pmatrix} (M_y \quad M_u)D_d(\theta)D_{wd} & (M_y \quad M_u)D_f(\theta) & -I_{q_r} \\ (M_y \quad M_u)D_d(\theta)D_{wd} & [(M_y \quad M_u)D_f(\theta) - D_{wF}] & -I_{q_r} \\ D_d(\theta)D_{wd} & D_f(\theta) & 0 \end{pmatrix}, \quad \widetilde{D}(\theta) \in R^{(2q_r+m+p) \times (q_{\tilde{d}}+q_f+q_r)}. \tag{34}$$

Having in mind the definition of $\widetilde{A}(\theta)$, $\widetilde{B}(\theta)$, $\widetilde{C}(\theta)$, and $\widetilde{D}(\theta)$, it can be noted that the H_∞ optimization problem formulated by (30) is non convex since it involves simultaneously the residual structuring matrices M_y and M_u and the filter state-space matrices $A_F(\theta)$, $B_F(\theta)$, $C_F(\theta)$, and $D_F(\theta)$. A solution to this problem may consist in chosen heuristically M_y and M_u. However, as it has been outlined in [10], there is no guarantee to the optimal solution.

The following lemma which is an adaptation of Proposition 1 in [8] for our purpose, gives the solution to this problem. The proof is omitted here as it can be found in [8].

Lemma 2. *Let $\widetilde{A}(\Pi_i)$, $\widetilde{B}(\Pi_i)$, $\widetilde{C}(\Pi_i)$, $\widetilde{D}(\Pi_i)$ $\forall i = 1, \ldots, N$ be the evaluation of $\widetilde{A}(\theta)$, $\widetilde{B}(\theta)$, $\widetilde{C}(\theta)$, $\widetilde{D}(\theta)$ at each vertex Π_i of the polytope Θ. Assume that $\widetilde{C}_2(\theta)$ and $\widetilde{D}_{21}(\theta)$ do not depend of θ (see Remark 3 for a discussion about this assumption) and let $N_s = (\widetilde{C}_2 \quad \widetilde{D}_{21})^\perp$. Then, there exists a solution of (31) if and only if there exists $\gamma < 1$ and $M_y \in R^{q_r \times m}$ and $M_u \in R^{q_r \times p}$ and two symmetric matrices $R \in R^{(n+n_{wd}+n_{wF}) \times (n+n_{wd}+n_{wF})} > 0$ and $S \in R^{(n+n_{wd}+n_{wF}) \times (n+n_{wd}+n_{wF})} > 0$ solving the following SDP*

problem involving $2N+1$ *LMI constraints:*

$$\begin{aligned}&\min \gamma\\ &s.t.\begin{pmatrix}\widetilde{A}(\Pi_i)R+R\widetilde{A}^T(\Pi_i) & \widetilde{B}_1(\Pi_i)\\ \widetilde{B}_1^T(\Pi_i) & -\gamma I\end{pmatrix}<0,\quad i=1,\dots,N\end{aligned} \tag{35}$$

$$\begin{pmatrix}N_S & 0\\ 0 & I\end{pmatrix}^T\begin{pmatrix}\widetilde{A}^T(\Pi_i)S+SA(\Pi_i) & S\widetilde{B}_1(\Pi_i) & \widetilde{C}_1^T(\Pi_i)\\ \widetilde{B}_1^T(\Pi_i)S & -\gamma I & \widetilde{D}_{11}^T(\Pi_i)\\ \widetilde{C}_1(\Pi_i) & \widetilde{D}_{11}(\Pi_i) & -\gamma I\end{pmatrix}\begin{pmatrix}N_S & 0\\ 0 & I\end{pmatrix}<0,\quad i=1,\dots,N \tag{36}$$

$$\begin{pmatrix}R & I\\ I & S\end{pmatrix}\geq 0. \tag{37}$$

Moreover, $F(\theta)$ *is a full order filter if* $n_F=n+n_{wd}+n_{wF}$. *The state space realization of the LPV filter* $F(\theta)$ *is then computed using the barycentric coordinates of* Θ *given by* (7), *so that:*

$$\begin{pmatrix}A_F(\theta) & B_F(\theta)\\ C_F(\theta) & D_F(\theta)\end{pmatrix}=\sum_{i=1}^{N}\beta_i\begin{pmatrix}A_F(\Pi_i) & B_F(\Pi_i)\\ C_F(\Pi_i) & D_F(\Pi_i)\end{pmatrix} \tag{38}$$

$A_F(\Pi_i)$, $B_F(\Pi_i)$, $C_F(\Pi_i)$, *and* $D_F(\Pi_i)$ $\forall i=1,\dots,N$ *are the state space matrices of the* N *LTI filters* $F(\Pi_i)$ $\forall i=1,\dots,N$ *that are deduced from the unique solution* (R,S,M_y,M_u,γ) *following the procedure described in [14].*

Remark 3. As it is outlined in Lemma 2, it is required that $\widetilde{C}_2$ and $\widetilde{D}_{21}$ do not depend on θ. This assumption is also done for N_S to be computed. If, by construction, such an assumption is not verified, the solution consists in post filtering $(y^T\ \ u^T)^T$ by a LTI filter at a high cutting frequency. This solution has already been proposed in [14].

3. APPLICATION: THE SECONDARY CIRCUIT OF A NPP

To illustrate the benefits of the proposed approach, experimental results obtained from the secondary circuit of a Nuclear Power Plant (NPP) are provided in this section.

In a NPP, the secondary circuit erosion can occur in the steam generators, releasing radio nuclides into the secondary coolant. This problem is now well understood and has been the subject of some studies initiated by EDF (Eléctricité De France) for its pressurized water reactors (PWR) to overcome and master the steam generator corrosion problems. The main degradation process is to be controlled by careful optimization of the secondary water chemistry. There is a need to ensure that the optimum secondary chemistry regime is selected and maintained. So, the process of erosion—corrosion of steel piping and other components is of critical importance during operation of a NPP. Feed water pH is adjusted by hydrazine, so that the pH is maintained within the limits specified by the nuclear authority (norm ISO-14253-1).

The NPP under consideration is a 900 MW pressurized water reactors (PWR), located in France. During the winter 2002, and thanks to a mandatory period of maintenance operations, it has been possible to measure and record a set of experimental data on the secondary circuit. The aim was to optimally control hydrazine and pH through an adaptive LQG control scheme. The designed controller has been successfully tested under real operational conditions [18].

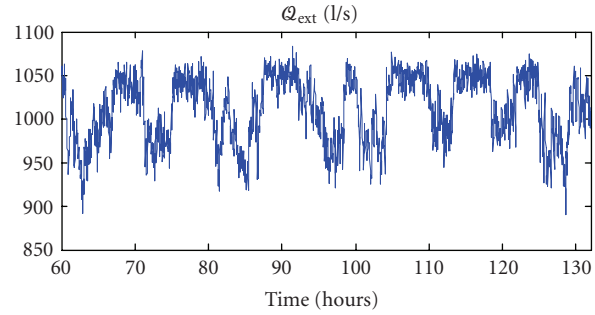

FIGURE 5: The time varying parameter $Q_{ext}(t)$.

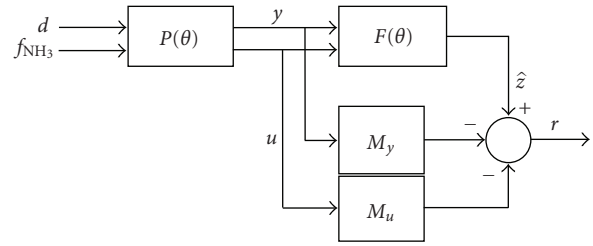

FIGURE 6: Filter $F(\theta(t))$ synthesized scheme.

The dynamics of hydrazine and ammoniac concentrations behavior in the secondary circuit of the NPP can be expressed as follows:

$$\begin{aligned}V\frac{d}{dt}[N_2H_4]&=-Q_{ext}(t)\cdot[N_2H_4]+u(t-\tau)\\ V\frac{d}{dt}[NH_3]&=\frac{4}{3}Q_{ext}(t)([N_2H_4]-[O_2])-\beta\cdot[NH_3]\end{aligned} \tag{39}$$

V is the circuit's water volume, Q_{ext} the water extraction flow rate of the condenser and β is a parameter depending of the NPP operating conditions. $[N_2H_4]$, $[NH_3]$, and $[O_2]$ represent hydrazine, ammoniac and oxygen concentrations respectively. u is the flow rates of the pumps used to inject hydrazine in the circuit. Moreover, the system present a time delay ($\tau=560$ s) corresponding to the chemical reaction after the introduction of hydrazine in the circuit. It is assumed that the pH is measured, that is,

$$\mathrm{pH}=14+\frac{1}{2}\log\left(K_b[NH_3]+K_{Mo}[Mo]\right)+n_{\mathrm{pH}}, \tag{40}$$

where n_{pH} denotes the measurement noise, $[Mo]$ also denotes the morpholine concentration, K_b and K_{Mo} are the basicity constants of the ammoniac and morpholine respectively.

Taken into account the dynamical equations (39), it follows that

$$\begin{aligned}\dot{x}(t) &= \begin{pmatrix} -\frac{\beta}{V} & \frac{4Q_{\text{ext}}(t)}{3V} \\ 0 & -\frac{Q_{\text{ext}}(t)}{V} \end{pmatrix} x(t) + \begin{pmatrix} 0 \\ \frac{1}{V} \end{pmatrix} u(t-\tau) \\ &\quad + \begin{pmatrix} -\frac{4Q_{\text{ext}}(t)}{3V} \\ 0 \end{pmatrix} [\text{O}_2](t) \\ y(t) &= \begin{pmatrix} 1 & 0 \\ 0 & 1 \end{pmatrix} x(t) + \begin{pmatrix} n_{\text{NH}_3}(t) \\ n_{\text{N}_2\text{H}_4}(t) \end{pmatrix}, \end{aligned} \tag{41}$$

where $x = ([\text{NH}_3]\ [\text{N}_2\text{H}_4])^T$ represents the state vector. $n_{\text{N}_2\text{H}_4}$ represents the measurement noise of the hydrazine sensor. n_{NH_3} is the image of the measurement noise of the pH sensor via the relation (40). Then, since (40) is static we will consider that an ammoniac concentration measure is available through the pH sensor. Characteristics of n_{NH_3} are then deduced from the following equation, which is the inverse of (40):

$$[\text{NH}_3] + n_{\text{NH}_3} = \frac{10^{2[\text{pH}-14-n_{\text{pH}}]} - K_{Mo}[Mo]}{K_b}. \tag{42}$$

Figure 5 presents the behavior of the time varying parameter $Q_{\text{ext}}(t)$ during a period of 3 days. We assume here that $Q_{\text{ext}}(t)$ is not affected by the considered faults. As it can be seen on Figure 5, $Q_{\text{ext}}(t)$ varies between $Q_{\min}$ and $Q_{\max}$ with:

$$\begin{aligned} Q_{\min} &= 878\,\text{l/s} \\ Q_{\max} &= 1097\,\text{l/s}. \end{aligned} \tag{43}$$

The considered faults are hydrazine sensor faults and pH sensor faults. Note that monitoring of pH sensors is a key feature for well functioning the overall system.

The relation between the ammoniac measurement and the pH measurement is only algebraic (see (41)), then the pH sensor fault is directly transmitted to the ammoniac measurement. Therefore, we can consider an ammoniac sensor fault in place of a pH sensor fault. Consequently, the following state space representation derived from (42) models the failing behavior of the secondary circuit (the notations are chosen to be consistent with those used in Section 2):

$$G(\theta): \begin{cases} \dot{x} = \begin{pmatrix} -\frac{\beta}{V} & \frac{4\theta(t)}{3V} & 0 \\ 0 & -\frac{\theta(t)}{V} & \frac{2}{\tau V} \\ 0 & 0 & -\frac{2}{V} \end{pmatrix} x + \begin{pmatrix} 0 \\ -\frac{1}{V} \\ 2 \end{pmatrix} u \\ \qquad + \begin{pmatrix} -\frac{4\theta(t)}{3V} \\ 0 \\ 0 \end{pmatrix} [\text{O}_2] \\ y = \begin{pmatrix} 1 & 0 & 0 \\ 0 & 1 & 0 \end{pmatrix} x + \begin{pmatrix} 0 \\ 0 \end{pmatrix} u + \begin{pmatrix} n_{\text{NH}_3}(t) \\ n_{\text{N}_2\text{H}_4}(t) \end{pmatrix} d_1 \\ \qquad + \begin{pmatrix} 1 & 0 \\ 0 & 1 \end{pmatrix} \begin{pmatrix} n_{\text{NH}_3}(t) \\ n_{\text{N}_2\text{H}_4}(t) \end{pmatrix} \end{cases} \tag{44}$$

f_{NH_3} represent ammoniac sensor faults and $f_{\text{N}_2\text{H}_4}$ hydrazine sensor faults. In this model, the time delay due to actuators is approximated using a first order Pade approximation. The model (44) corresponds to the model described in Figure 1, where $878 \le \theta(t) = Q_{\text{ext}}(t) \le 1097$. It follows that the considered polytope $\Theta = \{\theta : 878 \le \theta \le 1097\}$ becomes a simple segment since $\dim(\theta) = 1$.

For the FDI purpose, two filters $F_1(\theta)$ and $F_2(\theta)$ are computed such that the two residuals $r_1(t)$ and $r_2(t)$ satisfy the following requirements:

(i) $r_1(t)$ is sensitive to pH sensor faults through the (fictitious) ammoniac sensor and robust to hydrazine sensor faults.
(ii) $r_2(t)$ is sensitive to hydrazine sensor faults and robust to ammoniac sensor faults.

This method allows to isolate sensor faults uniquely. Therefore, we consider a different model for each filter to be synthesized. For the design of $F_1(\theta)$, the following model is used

$$G_1(\theta): \begin{cases} \dot{x} = \begin{pmatrix} -\frac{\beta}{V} & \frac{4\theta(t)}{3V} & 0 \\ 0 & -\frac{\theta(t)}{V} & \frac{2}{\tau V} \\ 0 & 0 & -\frac{2}{V} \end{pmatrix} x + \begin{pmatrix} 0 \\ -\frac{1}{V} \\ 2 \end{pmatrix} u \\ \qquad + \begin{pmatrix} -\frac{4\theta(t)}{3V} & 0 & 0 & 0 \\ 0 & 0 & 0 & 0 \\ 0 & 0 & 0 & 0 \end{pmatrix} d_1 + \begin{pmatrix} 0 \\ 0 \\ 0 \end{pmatrix} f_{\text{NH}_3} \\ y = \begin{pmatrix} 1 & 0 & 0 \\ 0 & 1 & 0 \end{pmatrix} x + \begin{pmatrix} 0 \\ 0 \end{pmatrix} \\ \qquad u + \begin{pmatrix} 0 & 1 & 0 & 0 \\ 0 & 0 & 1 & 1 \end{pmatrix} d_1 + \begin{pmatrix} 1 \\ 0 \end{pmatrix} f_{\text{NH}_3}, \end{cases} \tag{45}$$

where the disturbances vector d_1 includes the oxygen concentration, the measurement noises and the hydrazine sensor fault, that is, $d_1 = [[\text{O}_2]\ n_{\text{NH}_3}\ n_{\text{N}_2\text{H}_4}\ f_{\text{N}_2\text{H}_4}]^T$. For the design of $F_2(\theta)$, the following model is retained

$$G_2(\theta): \begin{cases} \dot{x} = \begin{pmatrix} -\frac{\beta}{V} & \frac{4\theta(t)}{3V} & 0 \\ 0 & -\frac{\theta(t)}{V} & \frac{2}{\tau V} \\ 0 & 0 & -\frac{2}{V} \end{pmatrix} x + \begin{pmatrix} 0 \\ -\frac{1}{V} \\ 2 \end{pmatrix} u \\ \qquad + \begin{pmatrix} \frac{4\theta(t)}{3V} & 0 & 0 & 0 \\ 0 & 0 & 0 & 0 \\ 0 & 0 & 0 & 0 \end{pmatrix} d_2 + \begin{pmatrix} 0 \\ 0 \\ 0 \end{pmatrix} f_{\text{N}_2\text{H}_4} \\ y = \begin{pmatrix} 1 & 0 & 0 \\ 0 & 1 & 0 \end{pmatrix} x + \begin{pmatrix} 0 \\ 0 \end{pmatrix} \\ \qquad u + \begin{pmatrix} 0 & 1 & 0 & 1 \\ 0 & 0 & 1 & 0 \end{pmatrix} d_2 + \begin{pmatrix} 1 \\ 1 \end{pmatrix} f_{\text{N}_2\text{H}_4}, \end{cases} \tag{46}$$

where the augmented disturbances vector takes into account the ammoniac sensor faults; $d_2 = [[\mathrm{O_2}]\ \ n_{\mathrm{NH_3}}\ \ n_{\mathrm{N_2H_4}}\ \ f_{\mathrm{NH_3}}]^T$.

According to the methodology developed in the Section 2, two polytopic models $P_1(\theta)$ and $P_2(\theta)$ are built as illustrated on Figure 2. To save place and for a better understanding, the different steps are only detailed for $F_1(\theta)$. Here, because the system is placed in an open-loop control law, it follows from $G_1(\theta)$ that (for clarity the index "1" is ignored from now):

$$P(\theta):\begin{cases}\dot{x} = \begin{pmatrix} -\dfrac{\beta}{V} & \dfrac{4\theta(t)}{3V} & 0 \\ 0 & -\dfrac{\theta(t)}{V} & \dfrac{2}{\tau V} \\ 0 & 0 & -\dfrac{2}{V} \end{pmatrix} x \\ \qquad + \begin{pmatrix} 0 & -\dfrac{4\theta(t)}{3V} & 0 & 0 & 0 \\ -\dfrac{1}{V} & 0 & 0 & 0 & 0 \\ 2 & 0 & 0 & 0 & 0 \end{pmatrix} d + \begin{pmatrix} 0 \\ 0 \\ 0 \end{pmatrix} f_{\mathrm{NH_3}} \\ \begin{pmatrix} y \\ u \end{pmatrix} = \begin{pmatrix} 1 & 0 & 0 \\ 0 & 1 & 0 \\ 0 & 0 & 0 \end{pmatrix} x + \begin{pmatrix} 0 & 0 & 1 & 0 & 0 \\ 0 & 0 & 0 & 1 & 1 \\ 1 & 0 & 0 & 0 & 0 \end{pmatrix} d \\ \qquad + \begin{pmatrix} 1 \\ 0 \\ 0 \end{pmatrix} f_{\mathrm{NH_3}}, \end{cases} \tag{47}$$

where $d = [u\ \ [\mathrm{O_2}]\ \ n_{\mathrm{NH_3}}\ \ n_{\mathrm{N_2H_4}}\ \ f_{\mathrm{N_2H_4}}]^T$. Following the developments in Section 2, the fault detector design problem turns out to be the design of $(F(\theta), M_y, M_u)$ satisfying the following objectives:

$$\begin{aligned} \left\| T_{rd}(\theta) \right\|_\infty &< \gamma_1 \\ \left\| T_{rf}(\theta) \right\|_{\mathrm{sens}} &> \gamma_2 \end{aligned} \tag{48}$$

Figure 6 gives an illustration of this problem.

Finally, following the method describes in Section 2, the problem is recasted into the setup depicted in Figure 3 where the model $\overline{P}(\theta, M_y, M_u)$ is defined according to:

$$\overline{P}(\theta, M_y, M_u) = \begin{pmatrix} -\dfrac{\beta}{V} & \dfrac{4\theta(t)}{3V} & 0 & 0 & -\dfrac{4\theta(t)}{3V} & 0 & 0 & 0 & 0 & 0 \\ 0 & -\dfrac{\theta(t)}{V} & \dfrac{2}{\tau V} & \dfrac{1}{V} & 0 & 0 & 0 & 0 & 0 & 0 \\ 0 & 0 & -\dfrac{2}{\tau} & 2 & 0 & 0 & 0 & 0 & 0 & 0 \\ M_{y_1} & M_{y_2} & 0 & M_u & 0 & M_{y_1} & M_{y_2} & M_{y_2} & M_{y_1} & -1 \\ 1 & 0 & 0 & 0 & 0 & 1 & 0 & 0 & 1 & 0 \\ 0 & 1 & 0 & 0 & 0 & 0 & 1 & 1 & 0 & 0 \\ 0 & 0 & 0 & 1 & 0 & 0 & 0 & 0 & 0 & 0 \end{pmatrix} \tag{49}$$

M_{y_1} and M_{y_2} are the two components of the structuring matrix M_y.

As it is outlined in Remark 2 an important step in the proposed method is the choice of the shaping filters W_d and W_f. Similarly to the developments presented in Section 2, W_d is refereed to the robustness objectives against d and W_f to the sensitivity requirements against $f_{\mathrm{NH_3}}$. Here, due to the definition of d, it is natural to choose W_d such as:

$$W_d = \mathrm{diag}(W_u, W_{[\mathrm{O_2}]}, W_{n_{\mathrm{NH_3}}}, W_{n_{\mathrm{N_2H_4}}}, W_{[\mathrm{N_2H_4}]}). \tag{50}$$

The weighting functions W_u, $W_{[\mathrm{O_2}]}$, $W_{n_{\mathrm{NH_3}}}$, $W_{n_{\mathrm{N_2H_4}}}$, $W_{[\mathrm{N_2H_4}]}$ and W_f allow to manage separately the robustness objectives against u, $[\mathrm{O_2}]$, $n_{\mathrm{NH_3}}$, $n_{\mathrm{N_2H_4}}$, $f_{\mathrm{N_2H_4}}$ and $f_{\mathrm{NH_3}}$ respectively. The interested reader can refer to [10] or [19] if necessary. These weighting functions are deduced from an off line spectral analysis procedure of available measurements according to:

$$\begin{aligned} W_u &= \gamma_u \frac{(1 + 1{,}7 \cdot 10^3\ \mathrm{s})^2}{(1 + 10^3\ \mathrm{s})^2} \\ W_{[\mathrm{O_2}]} &= \gamma_{[\mathrm{O_2}]} \frac{1 + 1{,}5 \cdot 10^4\ \mathrm{s}}{1 + 10^2\ \mathrm{s}} \\ W_{n_{\mathrm{NH_3}}} &= \gamma_{n_{\mathrm{NH_3}}} \frac{\mathrm{s} + 2 \cdot 10^{-2}}{\mathrm{s} + 1 \cdot 10^{-5}} \\ W_{n_{\mathrm{N_2H_4}}} &= \gamma_{n_{\mathrm{N_2H_4}}} \frac{\mathrm{s} + 2 \cdot 10^{-2}}{\mathrm{s} + 1 \cdot 10^{-5}} \\ W_{[\mathrm{N_2H_4}]} &= \gamma_{[\mathrm{N_2H_4}]} \frac{1 + 10^3\ \mathrm{s}}{1 + 10^{-3}\ \mathrm{s}} \\ W_f &= \gamma_2 \frac{1}{1 + 10^3\ \mathrm{s}}. \end{aligned} \tag{51}$$

The parameters γ_u, $\gamma_{[\mathrm{O_2}]}$, $\gamma_{n_{\mathrm{NH_3}}}$, $\gamma_{n_{\mathrm{N_2H_4}}}$, $\gamma_{[\mathrm{N_2H_4}]}$ and γ_2 allow to manage the gain of the weighting functions separately. They are optimized by performing an iterative refinement. Remember that the goal is to minimize the effects of disturbances on the residual $r(t)$ and maximize the effects of faults on $r(t)$. The numerical values of them have been fixed to

$$\begin{gathered} \gamma_u = 0.025, \quad \gamma_{[\mathrm{O_2}]} = 10^{-4}, \quad \gamma_{n_{\mathrm{NH_3}}} = \gamma_{n_{\mathrm{N_2H_4}}} = 0.1, \\ \gamma_{[\mathrm{N_2H_4}]} = 2 \cdot 10^{-5}, \quad \gamma_2 = 2. \end{gathered} \tag{52}$$

The method described in Section 2.2.2 is then used to synthesize the filter $F(\theta)$, and the structuring matrices M_y and M_u. For the SDP optimization problem computation, the SDPT3 solver is used.

To analyze the computed solution, the principal gains $\overline{\sigma}(T_{dr}^k(j\omega))$ and $\underline{\sigma}(T_{f_{\mathrm{NH_3}}r}(j\omega))$ of the closed loop transfers $T_{dr}^k(j\omega)$ and $T_{f_{\mathrm{NH_3}}r}(j\omega)$ are plotted versus the objectives W_d^k and W_f for some $\theta \in \Theta$ (see Figure 7). The notation "k" is introduced to outline that the analysis is performed with respect to each component of d. As it can be seen on the figures, for each synthesis, $\overline{\sigma}(T_{dr}^k(j\omega)) < \overline{\sigma}(W_d^k(j\omega))\ \forall \omega$ and $\underline{\sigma}(T_{f_{\mathrm{NH_3}}r}(j\omega)) > \underline{\sigma}(W_f(j\omega))\ \forall \omega \in \Omega \approx [0; 10^{-4}[$rd/s for all considered values of $\theta(t)$. This indicates that the requirements (48) are satisfied for the considered values of θ and by virtue of Lemma 2, we know that it still yields for all values of θ.

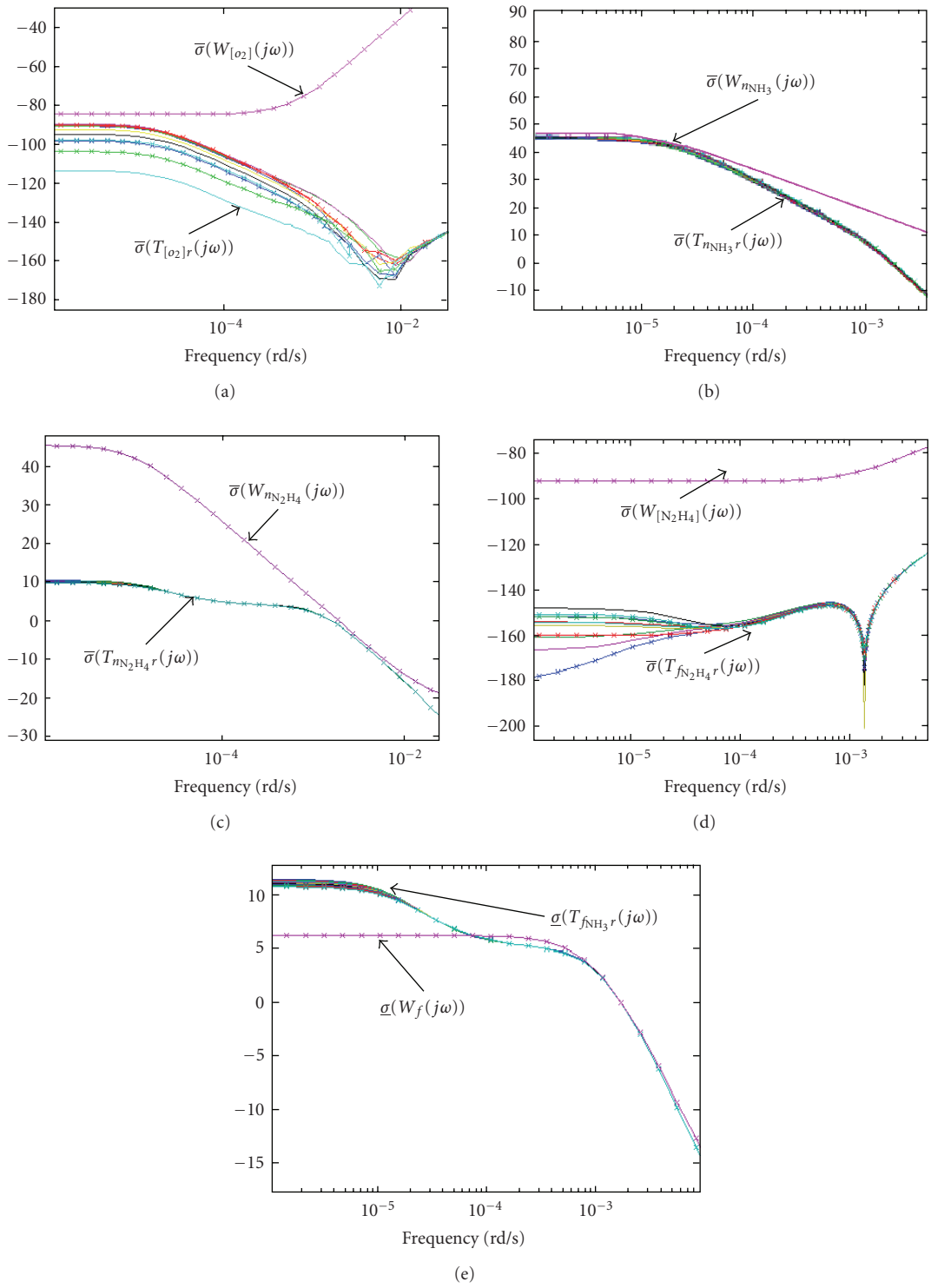

FIGURE 7: Behavior of the principal gains of the closed loop transfers $T_{dr}^{k}(j\omega)$ and $T_{f_{NH_3}r}(j\omega)$ versus the shaping objective filters (in dB).

Simulation results

The FDI unit is implemented within the simulator of the secondary circuit. For simulating faults, a variation of ten percent of sensors measurements between $t = 80$ hours and $t = 85$ hours for the pH sensor and between $t = 120$ hours and $t = 125$ hours for the hydrazine sensor is made. Figures 8, 9 and 10 illustrate the behavior of the residual signals $r_1(t)$ and $r_2(t)$ in both fault free and faulty situations for the aforementioned period of 3 days. As expected, it can be seen from figures that $r_1(t)$ is only sensitive to pH sensor faults and $r_2(t)$ is only sensitive to hydrazine sensor faults.

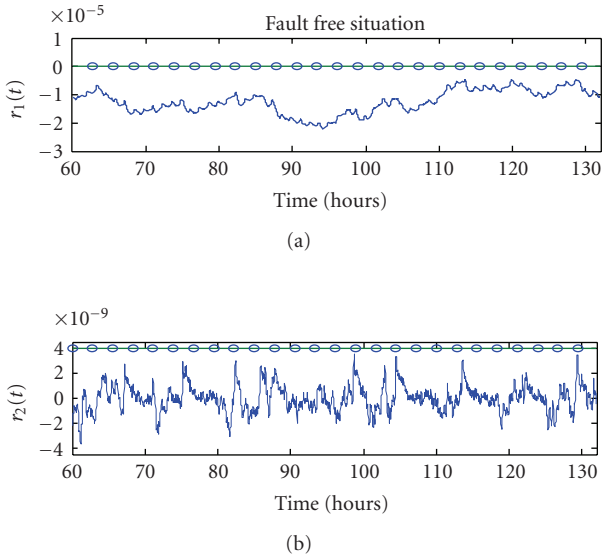

FIGURE 8: Behavior of $r_i(t)$, $i = 1, 2$ and the decision test-fault-free situation.

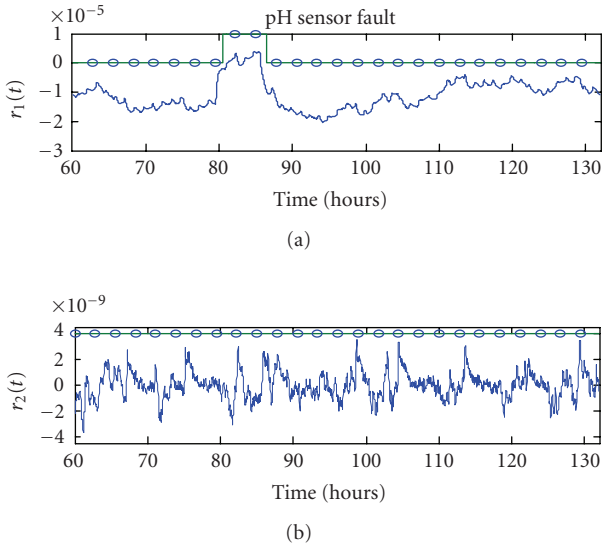

FIGURE 9: Behavior of $r_i(t)$, $i = 1, 2$ and the decision test-pH sensor fault (80 h–85 h).

Finally, a sequential Wald decision test is also implemented within the simulator to make a final decision about the faults. The probabilities of non-detection and false alarms have been fixed to 0.1%. The results are presented in Figures 8, 9 and 10. As it can be seen, all faults are successfully detected and isolated.

4. CONCLUSION

The problem which is addressed in this paper is that of designing FDI filters for dynamic systems that can be described by LPV polytopic models. The method can be seen as a generalization of the well known H_∞/H_- setting for LTI systems. The H_∞ norm for LPV systems is used to formulate the robustness specifications and a new index, that is, the H_{sens} index, which is deduced from the H-norm for LTI systems, is introduced for fault sensitivity specifications. As a result, various design goals and trades-off can be formulated and managed in a systematic way by means of some high level design parameters formulated in terms of dynamic weighting functions. A key feature of the proposed technique is that the remaining control and measurement canals are optimally merged to build the fault indicating signals. The resulting static matrices are also optimized via LMI together with the dynamic FDI filter. The proposed technique is also appropriate for fault diagnosis in nonlinear systems which can be approximated efficiently by LPV models to cover a wider range of operating, and to cope with rapid parameter variations. The method has been successfully applied to experimental data set coming from the secondary circuit of a nuclear power plant in France.

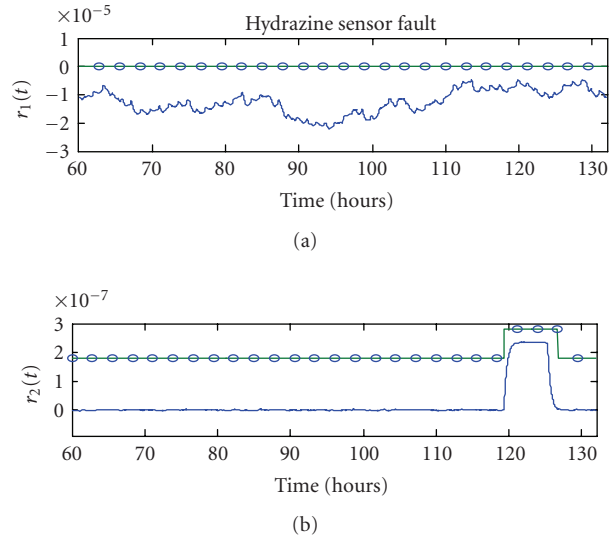

FIGURE 10: Behavior of $r_i(t)$, $i = 1, 2$ and the decision test-hydrazine sensor fault (120 h–125 h).

ACKNOWLEDGMENT

The authors would like to thank Prof. Kemin Zhou for his valuable comments and suggestions that help us to clarify some key features.

REFERENCES

[1] J. Chen and R. J. Patton, *Robust Model-Based Fault Diagnosis for Dynamic Systems*, Kluwer Academic, Norwell, Mass, USA, 1999.

[2] P. Frank, S. Ding, and B. Köppen-Seliger, in *Proceedings of the 4th Symposium on Fault detection, Safety and Supervision of Technical Processes (SAFEPROCESS '00)*, pp. 16–27, Budapest, Hungary, June 2000, IFAC.

[3] V. Venkatasubramanian, R. Rengaswamy, K. Yin, and S. N. Kavuri, "A review of process fault detection and diagnosis—part I: quantitative model-based methods," *Computers & Chemical Engineering*, vol. 27, no. 3, pp. 293–311, 2003.

[4] A. E. Marcos, *A linear parameter varying model of the boeing 747-100/200 longitudinal motion*, Ph.D. thesis, University of Minesota, Minneapolis, Minn, USA, 2001.

[5] F. Bruzelius, S. Pettersson, and C. Breitholtz, "Linear parameter-varying descriptions of nonlinear systems," in *Proceedings of the American Control Conference*, vol. 2, pp. 1374–1379, Boston, Mass, USA, June-July 2004.

[6] J. Bokor and G. Balas, "Detection filter design for LPV systems—a geometric approach," *Automatica*, vol. 40, no. 3, pp. 511–518, 2004.

[7] M. Rodrigues, D. Theilliol, and D. Sauter, "Design of a robust polytopic unknown input observer for FDI: application for systems described by a multi-model representation," in *Proceedings of the 44th IEEE Conference on Decision and Control and European Control Conference (CDC-ECC '05)*, pp. 6268–6273, Seville, Spain, December 2005.

[8] D. Henry and A. Zolghadri, "Robust fault diagnosis in uncertain linear parameter-varying systems," in *Proceedings of the IEEE International Conference on Systems, Man and Cybernetics (SMC '04)*, vol. 6, pp. 5165–5170, The Hague, The Netherlands, October 2004.

[9] S. X. Ding, T. Jeinsch, P. M. Frank, and E. L. Ding, "A unified approach to the optimization of fault detection systems," *International Journal of Adaptive Control and Signal Processing*, vol. 14, no. 7, pp. 725–745, 2000.

[10] D. Henry and A. Zolghadri, "Design and analysis of robust residual generators for systems under feedback control," *Automatica*, vol. 41, no. 2, pp. 251–264, 2005.

[11] D. Henry and A. Zolghadri, "Design of fault diagnosis filters: a multi-objective approach," *Journal of the Franklin Institute*, vol. 342, no. 4, pp. 421–446, 2005.

[12] M. L. Rank and H. Niemann, "Norm based design of fault detectors," *International Journal of Control*, vol. 72, no. 9, pp. 773–783, 1999.

[13] A. Saberi, A. A. Stoorvogel, P. Sannuti, and H. Niemann, "Fundamental problems in fault detection and identification," *International Journal of Robust and Nonlinear Control*, vol. 10, no. 14, pp. 1209–1236, 2000.

[14] P. Apkarian, P. Gahinet, and G. Becker, "Self-scheduled $\mathcal{H}^\infty$ control of linear parameter-varying systems: a design example," *Automatica*, vol. 31, no. 9, pp. 1251–1261, 1995.

[15] J. M. Biannic, *Commande robuste des systèmes à paramètres variables. Application en aéronautique*, Ph.D. thesis, Centre d'études et de Recherche de Toulouse, Department DERA, Toulouse, France, 1996.

[16] E. Frisk and L. Nielsen, "Robust residual generation for diagnosis including a reference model for residual behavior," *Automatica*, vol. 42, no. 3, pp. 437–445, 2006.

[17] A. Varga, "Numerically reliable methods for optimal design of fault detection filters," in *Proceedings of the 44th IEEE Conference on Decision and Control and European Control Conference (CDC-ECC '05)*, pp. 2391–2396, Seville, Spain, December 2005.

[18] F. Marshall, A. Zolghadri, and S. Ygorra, "Mise en œuvre d'une commande optimale en vue de contrôler le pH et les paramètres chimiques qui participent au maintien des conditions de corrosion minimum dans le circuit secondaire d'une centrale nucléaire de type REP," Internal Report, LAPS-EDF, Bordeaux, France, 2002.

[19] D. Henry and A. Zolghadri, "Norm-based design of robust FDI schemes for uncertain systems under feedback control: comparison of two approaches," *Control Engineering Practice*, vol. 14, no. 9, pp. 1081–1097, 2006.

Hindawi Publishing Corporation
Journal of Control Science and Engineering
Volume 2008, Article ID 152030, 10 pages
doi:10.1155/2008/152030

Research Article

Design and Assessment of a Multiple Sensor Fault Tolerant Robust Control System

S. S. Yang[1] and J. Chen[2]

[1] *Department of Electrical Engineering, University of Malaya, 50603 Kuala Lumpur, Malaysia*
[2] *School of Engineering and Design, Brunel University West London, Uxbridge, Middlesex UB8 3PH, UK*

Correspondence should be addressed to J.Chen, jie.chen@brunel.ac.uk

Received 29 December 2006; Revised 21 September 2007; Accepted 12 December 2007

Recommended by Jakob Stoustrup

This paper presents an enhanced robust control design structure to realise fault tolerance towards sensor faults suitable for multi-input-multioutput (MIMO) systems implementation. The proposed design permits fault detection and controller elements to be designed with considerations of stability and robustness towards uncertainties, besides multiple faults environment on a common mathematical platform. This framework can also cater to systems requiring fast responses. A design example is illustrated with a fast, multivariable, and unstable system, that is, the double inverted pendulum system. Results indicate the potential of this design framework to handle fast systems with multiple sensor faults.

1. INTRODUCTION

Growing demands for plant or system availability, reliability, and survivability have prompted active research in fault tolerant control systems (FTCSs) [1, 2]. FTCSs are designed to accommodate component faults automatically by ensuring overall system stability and acceptable performance. A typical FTCS design incorporating separate control and fault detection elements can achieve fault tolerance objectives, but without due considerations given to significant interactions between the elements such as those described in [3, 4]. In addition, addressing issues concerning uncertainties is crucial as practical problems associated with variations in actual plant operating range are undesirable.

Fault detectors are typically based upon the use of process models [5–7]. Data from the monitored plant is input to these algorithms and the outputs are compared with the corresponding plant outputs. If there are discrepancies, then it is an indication that at least one fault has occurred. The model-based approach to designing sensor FTCS employs mathematical manipulation of available signals, that is, analytical redundancy, via suitably designed controllers to accommodate for faults rather than using extra hardware (sensors/actuators).

1.1. Integrating control and fault detection in FTCS

An integrated approach [8–11] where fault detection and controller elements are designed with consideration to the overall system stability or interaction is favourable as the reliability of operation can be determined in a mathematically sound setting offering fast control responses in addition to the availability of the established solution for incorporating robustness towards uncertainties.

In this paper, a robust controller-based MIMO FTCS which integrates the fault detection and controller elements in a single design is presented. A fault indicating residual is utilised as a function of control. The residual signals act as weighting factors, which put corresponding emphasis on nominal controller and fault accommodating controller. The FTCS structure proposed allows the plant to be controlled by a nominal controller that ensures the achievement of best performance objectives, when sensor faults and uncertainties are not present, while preserving the stability at a lower degree of system performance in the presence of major sensor faults [11, 12]. The proposed structure can handle systems with fast responses, multiple sensor faults, and modelling uncertainties.

Note that purely robust control-based FTCS such as described in [13, 14] ensures robustness towards minor faults

only; faults are modelled as very small perturbations on the system. As demonstrated by [13, 14], it is not possible for a purely robust control structure to maintain high performance, when faults are not present as they are designed using worst case criterion.

2. PROBLEM STATEMENT

Assuming that the MIMO plants and controllers are described mathematically in state-space form as follows:

$$\begin{aligned} \dot{x}(t) &= Ax(t) + Bu(t), \\ y(t) &= Cx(t) + Du(t), \end{aligned} \tag{1}$$

where $x \in R^n$ is state vector, $u \in R^l$ is the input vector, while $y \in R^m$ is the measured output vector.

A, B, C, and D are known matrices with appropriate dimensions related to the system dynamics. In addition, $\overline{\sigma}(M)$ denotes the largest singular value of M. H_∞ denotes the Banach space of bounded analytic functions with the ∞ norm defined as $\|F\|_\infty = \sup_\omega \overline{\sigma}(F(j\omega))$ for any $F \in H_\infty$.

Definition 1. All MIMO transfer matrix representations have appropriate dimensions and are proper real-rational matrices, stabilisable, and detectable. A state space rational proper transfer function is denoted by

$$G(s) = \begin{bmatrix} A & B \\ C & D \end{bmatrix} = C(sI - A)^{-1}B + D. \tag{2}$$

Furthermore, let P be a block matrix,

$$P = \begin{bmatrix} P_{11} & P_{12} \\ P_{21} & P_{22} \end{bmatrix}. \tag{3}$$

Therefore, the linear fractional transformation of P over F is defined as

$$F_l(P, F) = P_{11} + P_{12}F(I - P_{22}F)^{-1}P_{21}, \tag{4}$$

where F is assumed to have appropriate dimensions and $(I - P_{22}F)^{-1}$ is well defined.

2.1. Sensor faults defined

Sensor fault symptoms can be observed as measurements that are unavailable, incorrect, or unusually noisy. These faults may occur individually or concurrently or simultaneously, resulting in total system failure or degradation in performance. Significant information about the influence of faults on a process cannot be known without the inclusion of its model in the design. Additive faults provide a suitable framework for sensor faults and are modelled as additional input signals to a system [5],

$$\begin{aligned} \dot{x}(t) &= Ax(t) + Bu(t), \\ y'(t) &= Cx(t) + Du(t) + f_s(t), \end{aligned} \tag{5}$$

where $f_s(t) \in R^m$ denote sensor faults. Hence

$$y(s) = G_p(s)u(s). \tag{6}$$

The variable $y(s)$ denotes all available sensor outputs. When output sensor faults occur in the plant as shown in (5), the measured outputs become

$$y'(s) = y(s) + f_s(s). \tag{7}$$

Due to the existence of fault represented by $f_s(s)$, a conventional controller cannot usually satisfy required performance and the closed-loop control system may even become unstable. A sensor fault-compensating controller can be introduced to augment a nominal controller designed for best performance. However, since the structure of the system as seen in Figure 1 is virtually an internal model controller [15], conditions for physical realizability need to be observed. To ensure that the fault-compensating controller, Q is well defined and proper, the transfer matrix representation from $f_s(s)$ to controller output $u(s)$ must exist and is also proper. Therefore,

$$f_s(s) = W_s(s)f_s'(s). \tag{8}$$

By appropriate use of input weight, $W_s(s)$, the input $f_s'(s)$ can be normalised and transformed into the physical input, $f_s(s)$. Consideration of such sensor fault models has been shown to be suitable for use in formulating the FTCS objectives for the rejection of sensor faults as an optimisation problem. Uncertainties affecting the sensors can also be classified as a subset of $f_s(s)$. Figure 1 shows the block diagram illustrating the interconnections assumed for the formulation H_∞ problem associated with the proposed FTCS design.

2.2. Fault indicating residuals

The presence of sensor faults and uncertainty vectors defined in Section 2.1 can be reflected by a fault indicating residual, since a filtered estimation can be obtained via coprime factorisation of the plant model, $G_p(s)$ [11, 12]. Let

$$G_p(s) = \widetilde{M}^{-1}(s)\widetilde{N}(s). \tag{9}$$

Hence, from (8) and (9), the fault indicating residual denoted by $f_r(s)$ can be defined as

$$\begin{aligned} f_r(s) &= \widetilde{N}(s)u(s) - \widetilde{M}(s)y'(s) \\ &= \widetilde{N}(s)u(s) - \widetilde{M}(s)[y(s) + f_s(s)] \\ &= -\widetilde{M}(s)W_s(s)f'(s). \end{aligned} \tag{10}$$

2.3. Integrating the controller element

Now, since $f_r(s)$ reflects the presence of faults and uncertainty, it can be utilised as an input to the fault compensating controller. The perturbations caused can then be minimised by control actions due to the nominal controller and fault compensating controller. The control signal vector can be expressed as follows:

$$u(s) = u_k(s) + u_q(s), \tag{11}$$

where

$$u_k(s) = K(s)e(s) \tag{12}$$

and $u_k(s)$ denotes nominal controller ($K(s)$) output, and $u_q(s)$ denotes sensor fault compensator ($Q(s)$) output. Error from feedback is denoted by $e(s)$ whereby $r(s)$ denotes input demand. Thus, from (10), $f_r(s)$ is utilised in the following manner:

$$u_q(s) = Q(s)f_r(s) = -Q(s)\widetilde{M}(s)W_s(s)f_s'(s). \tag{13}$$

From (6), (7), and (8), $e(s)$ can be expressed as

$$\begin{aligned} e(s) &= r(s) - y'(s) \\ &= r(s) - y(s) - f_s(s) \\ &= r(s) - G_p(s)u(s) - W_s(s)f_s'(s). \end{aligned} \tag{14}$$

By substituting (12), (13), and (14) into (11), the following is derived:

$$\begin{aligned} u(s) = {} & \left(I + K(s)G_p(s)\right)^{-1} \\ & \times \left\{K(s)r(s) - \left(K(s) + \left[Q(s)\widetilde{M}(s)\right]\right)W_s(s)f'_s(s)\right\}. \end{aligned} \tag{15}$$

Thus,

$$\begin{aligned} y'(s) = {} & G_p(s)(I + K(s)G_p(s))^{-1} \\ & \times \left\{K(s)r(s) - \left(K(s) + \left[Q(s)\widetilde{M}(s)\right]\right)W_s(s)f'_s(s)\right\}. \end{aligned} \tag{16}$$

The plant output expression in (16) shows that in the absence of sensor faults and uncertainties, the output closed-loop system is only reliant on the nominal controller $K(s)$, allowing for high performance during healthy operation. Note that the fault detection scheme generating the above-mentioned fault indicating residual does not need to be made robust, since the fault indicating residual is mainly used as an activating signal for $Q(s)$. It is thus not essential to identify nor to estimate the source of the faults, hence even if the presence of $f_r(s)$ is due to uncertainties and not faults in the sensors, $Q(s)$ will still provide the necessary control signals to compensate for such perturbations thereby introducing robustness to the system.

2.4. Sensor fault compensator realisation

The sensor fault compensator $Q(s)$ is integrated into the framework by utilising $f_r(s)$ as a function of control. The design $Q(s)$ is achieved with the H_∞ technique. A performance weights $W_{\text{ftc}}(s)$ can be defined to establish post-fault performance requirements, which emphasise on stability rather than high performance. The corresponding solution for achieving $Q(s)$ is by minimising the following optimisation criterion:

$$\gamma = \min_{Q(s)} \left\| F_l[P_f(s), Q(s)] \right\|_\infty. \tag{17}$$

Therefore, the standard H_∞ problem is specified in (17) for which the corresponding transfer functions from $f_s'(s)$ to $z(s)$ must satisfy. If the controller $Q(s)$ in (17) is found, then the closed-loop system is said to have robust performance towards uncertainty and sensor faults; it is well known that a system satisfies robust performance if and only if it is robustly stable with respect to norm-bounded matrix perturbation [16]. The equivalent linear fractional transformation (LFT) block diagram for the H_∞ problem stated above is shown in Figure 2.

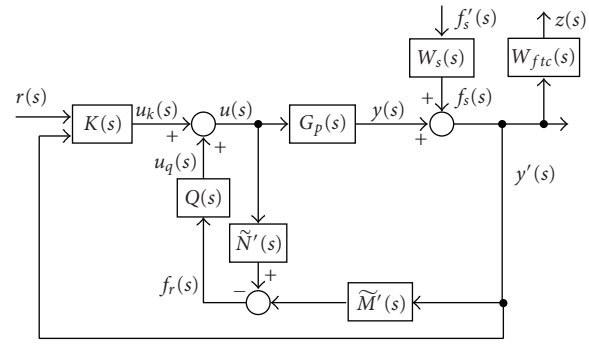

Figure 1: Block diagram representation of H_∞ problem formulation for the proposed FTCS design.

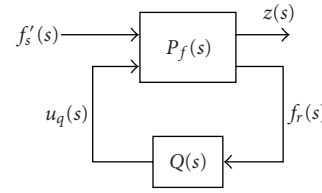

Figure 2: The LFT representation of the proposed FTCS.

Thus,

$$\begin{bmatrix} z(s) \\ f_r(s) \end{bmatrix} = \underbrace{\begin{bmatrix} P_{11}(s) & P_{12}(s) \\ P_{21}(s) & P_{22}(s) \end{bmatrix}}_{P_s(s)} \begin{bmatrix} f_s'(s) \\ u_q(s) \end{bmatrix}. \tag{18}$$

From (10), P_{21} and P_{12} can be derived as

$$\begin{aligned} P_{21}(s) &= -\widetilde{M}(s)W_s(s), \\ P_{12}(s) &= 0. \end{aligned} \tag{19}$$

Now, note that

$$\begin{aligned} u_k(s) &= K(s)\left(r(s) - y'(s)\right) \\ &= K(s)\left(r(s) - G_p(s)u(s) - W_s(s)f_s'(s)\right) \\ &= K(s)r(s) - K(s)G_p(s)\left[u_k(s) + u_q(s)\right] - K(s)W_s(s)f_s'(s), \end{aligned} \tag{20}$$

and thus,

$$\begin{aligned} u_k(s) = {} & \left(I + K(s)G_p(s)\right)^{-1}K(s)r(s) \\ & - \left(I + K(s)G_p(s)\right)^{-1}K(s)W_s(s)f_s'(s) \\ & - \left(I + K(s)G_p(s)\right)^{-1}K(s)G_p(s)u_k(s). \end{aligned} \tag{21}$$

Also

$$\begin{aligned} z(s) &= W_{\text{ftc}}(s)y'(s) \\ &= W_{\text{ftc}}(s)\left[G_p(s)u(s) + W_s(s)f_s'(s)\right] \\ &= W_{\text{ftc}}(s)G_p(s)u_k(s) \\ &\quad + W_{\text{ftc}}(s)G_p(s)u_q(s) \\ &\quad + W_{\text{ftc}}(s)W_s(s)f_s'(s). \end{aligned} \tag{22}$$

Substituting (21) into (22),

$$\begin{aligned} z(s) = {} & W_{\text{ftc}}(s)G_p(s)\left(I+K(s)G_p(s)\right)^{-1}K(s)r(s) \\ & - W_{\text{ftc}}(s)G_p(s)(I+K(s)G_p(s))^{-1}K(s)G_p(s)u_q(s) \\ & + W_{\text{ftc}}(s)G_p(s)uq(s) - W_{\text{ftc}}(s)G_p(s)(I+K(s)G_p(s))^{-1} \\ & \times K(s)W_s(s)f_s'(s) + W_{\text{ftc}}(s)W_s(s)f_s'(s). \end{aligned} \tag{23}$$

Ignoring the reference input $r(s)$, we have

$$\begin{aligned} P_{11}(s) &= -W_{\text{ftc}}(s)G_p(s)\left(I+K(s)G_p(s)\right)^{-1} \\ &\quad \times K(s)W_s(s) + W_{\text{ftc}}(s)W_s(s) \\ &= W_{\text{ftc}}(s)\left\{I - G_p(s)\left(I+K(s)G_p(s)\right)^{-1}K(s)\right\}W_s(s) \\ &= W_{\text{ftc}}(s)\left(1+G_p(s)K(s)\right)^{-1}W_s(s), \\ P_{12}(s) &= -W_{\text{ftc}}(s)G_p(s)\left(I+K(s)G_p(s)\right)^{-1} \\ &\quad \times K(s)G_p(s) + W_{\text{ftc}}(s)G_p(s) \\ &= W_{\text{ftc}}(s)\left\{I - G_p(s)\left(I+K(s)G_p(s)\right)^{-1}K(s)\right\}G_p(s) \\ &= W_{\text{ftc}}(s)\left(1+G_p(s)K(s)\right)^{-1}G_p(s). \end{aligned} \tag{24}$$

Note that the following matrix operation (Zhou, Doyle & Glover, 1996, page 23) has been used in the derivation of (24):

$$\begin{aligned} & A_{11}^{-1} + A_{11}^{-1}A_{12}(A_{22} - A_{21}A_{11}^{-1}A_{12})^{-1}A_{21}A_{11}^{-1} \\ & \quad = (A_{11} - A_{12}A_{22}^{-1}A_{21})^{-1}. \end{aligned} \tag{25}$$

With the conditions laid out, the closed-loop system shown above is guaranteed to be tolerant to sensor faults and modelling uncertainty, stable for any nonlinear, time varying, and stable $K(s)$ and $Q(s)$ due to the minimisation of the transfer matrix between fault-generating signal $f_s'(s)$ to the performance evaluation signal $z(s)$.

3. A NUMERICAL SIMULATION EXAMPLE

An experimental study of the FTCS implementation on a double inverted pendulum system for tolerance towards sensor faults is shown next to illustrate the feasibility of the proposed design method. The implementation is tested for fault tolerance towards sensors in nominal and under plant uncertainty conditions.

3.1. The double inverted pendulum system

The double inverted pendulum system is an example of a chaotic system. The system is a fast, multivariable, nonlinear, and unstable process. The pendulum system is a standard classical control test rig for the verification of different control methods, and is among the most difficult systems to control in the field of control engineering. Similar to the single inverted pendulum problem, the control task for the double inverted pendulum is to stabilise the two pendulums. The position of the carriage on the track is controlled quickly and accurately, so that the pendulums are always erected in their inverted position during such movements.

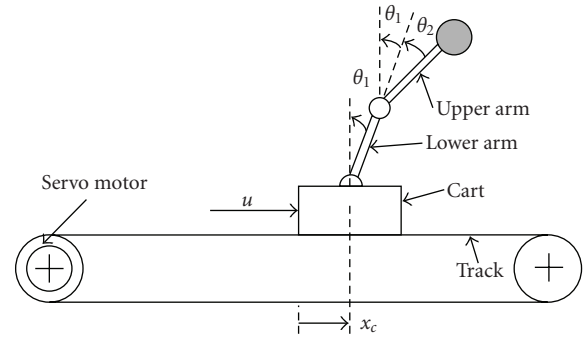

Figure 3: Schematic diagram of the pendulum system.

The double inverted pendulum system is made up of two aluminium arms connected to each other with the lower arm attached to a cart placed on a guiding rail, as illustrated in Figure 3. Data used in this case study has been obtained from [9]. The aluminium arms are constrained to rotate within a single plane and the axis of rotation is perpendicular to the direction of the force acting on the cart motion f. The cart can move along a linear low-friction track and is moved by a belt driven by a servo motor system. Sensors providing measurements of cart position x_c, the pendulums angles θ_1 and θ_2, controller output, u, and motor current i are assumed available for the purpose of control. The control law has to regulate the lower-arm angle and upper-arm angle, θ_1 and θ_2, respectively, from an initial condition, and the control of the position of the cart x_c from an initial position.

3.2. Nominal high-performance controller

An H_∞ loop shaping controller, as high-performance nominal controller K for the MIMO system, is designed using the *MATLAB* command *ncfsyn*.m. The specification function W_p is augmented to K in the manner shown in Figure 4. Sensors for detecting e_x (cart positional error), θ_1 and θ_2, are fault prone sensors. Motor voltage and current are denoted by u and i, respectively. The controller output variable is the corresponding motor voltage demand u. The controller performance was tested on the *SIMULINK* model of the double inverted pendulum. Initial conditions are with $\theta_1 = 0.05$ rad and $\theta_2 = -0.04$ rad. The cart movement command signal r_c is initiated at 0.5 m and at -0.5 m after 50 seconds, is shown in Figure 5, while system responses are shown in Figure 6. It is observed that the output responses are within limits of specifications, and the cart position set points have been achieved in a stable and smooth manner.

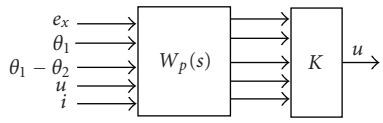

Figure 4: The H_∞ loop-shaping controller K with specification function.

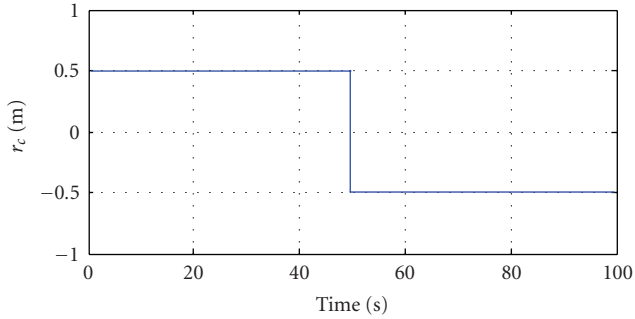

Figure 5: Command signal requiring the cart to move from 0.5 m to −0.5 m.

3.3. FTCS design and implementation

The nominal model of the double inverted pendulum model is described by its left coprime factors to ensure well posedness. The double inverted pendulum model without modelling uncertainty is considered for the representation of the nominal plant in the fault indicating residual generator setup. Fault indicating residuals are denoted by $f_{\theta 1}$, $f_{\theta 2}$ and f_{ex} for faults in the corresponding sensors.

The interconnection of the system is setup and the design of the controller sensor fault compensating controller, Q is automated with the command *hinfsyn.m* provided in *MATLAB's μ-analysis and synthesis toolbox* [17], which iteratively solves the optimisation criterion set out in (17). When γ value of below 1 is obtained, the solution of a satisfactory Q is used. This condition is only met with relaxations to the effects of additive faults, as it is obvious that total failure cannot be handled. Note that the performance weights $W_{\text{ftc}}(s)$ (shown in the appendix) to establish postfault performance requirements reuse the elements in the original specification function W_p, which are related to the fault prone sensors, that is, sensors providing measurements of cart position x_c, the pendulums angles θ_1 and θ_2. The block diagram showing the augmentation of Q to nominal controller K is illustrated in Figure 7.

3.4. Tests and results

The following responses have been recorded from testing the FTCS by simulating the occurrence of faults in the relevant sensors. Sensor effectiveness indicating faults are simulated as deterioration of performance; 0%: no fault, 100%: total failure. Results are shown for conditions with and without modelling uncertainty. Responses of the inverted double pendulum system performances with the proposed FTCS, H_∞, and μ controllers are recorded for comparison purposes.

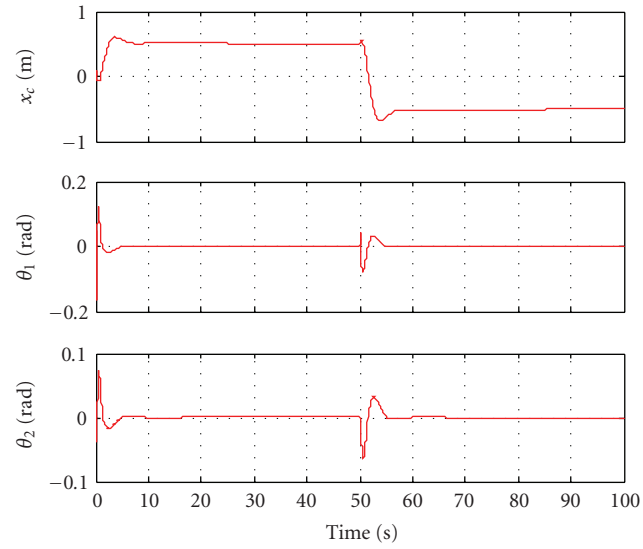

Figure 6: System responses with K implementation (position of cart x_c is shown instead of cart position error e_x).

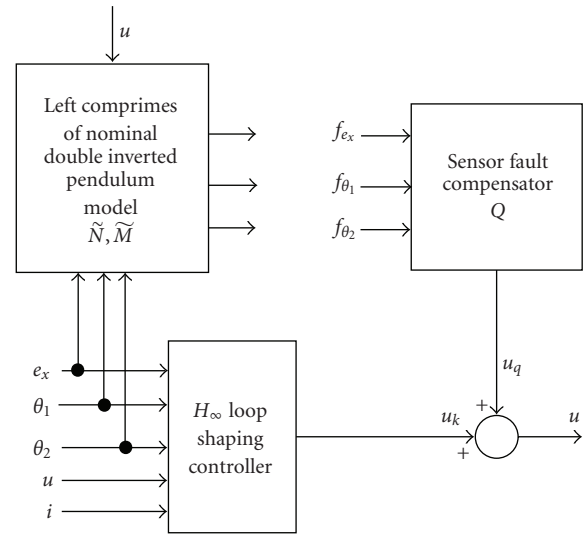

Figure 7: Block diagram of sensor fault compensator Q augmented to nominal controller K in the FTCS structure.

Nominal response, without modelling uncertainties and sensor faults

Nominal performances of all controllers for healthy system are recorded in Figure 8. Apparently the proposed FTCS produces faster cart positioning response compared to all other control system responses, initiating slightly higher overshoots in θ_1 and θ_2.

Multiple sensor faults without plant uncertainty

Multiple sensor faults are assumed to occur at 2, 4, and 6 seconds after the simulation has been initiated (e_x at 90% deterioration, θ_1 at 20% deterioration, and θ_2 at 10% deterioration, resp.). The output responses are shown in Figure 9.

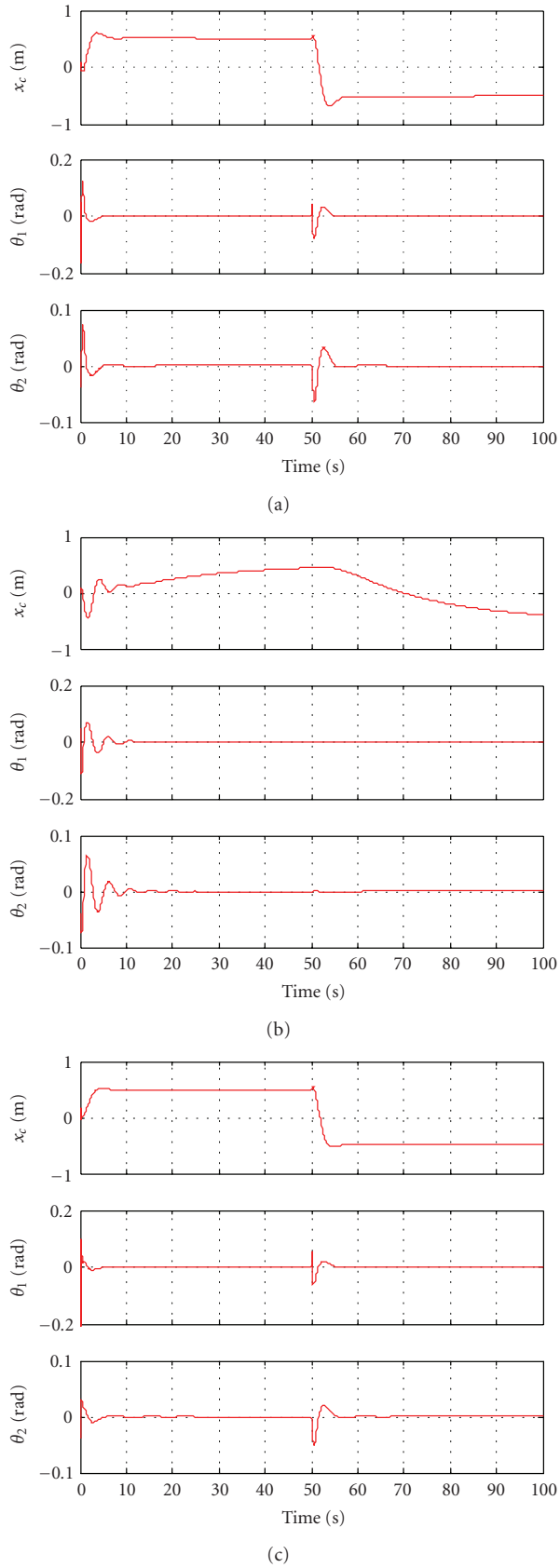

Figure 8: Nominal double inverted pendulum system responses of all controllers under healthy conditions. (a) —- FTCS, (b) ... H_∞ controller, and (c) - - - μ controller.

Observe that the proposed FTCS and the μ controller handled the faults and managed to achieve satisfactory control responses. However, stability could not be maintained by the H_∞ controller.

Multiple sensor faults with plant uncertainty

Tests for control systems to handle system uncertainty and multiple sensor faults were also performed. Conditions were made similar to the tests performed for the nominal system with multiple sensor faults. The supremacy of the proposed FTCS to accommodate for faults even under the influence of system uncertainties is seen in Figure 10.

The H_∞ controller could not handle this mode of fault and oscillates beyond control as shown. Meanwhile, both the proposed FTCS and the μ controller handled the fault satisfactorily.

Further discussion

Overall, the proposed FTCS has managed to handle all pre- and postfault conditions satisfactorily, while maintaining the highest level of stability in all test scenarios. Although it seems that the μ controller could handle faults and modelling uncertainty as well as the proposed FTCS, it could not handle certain cases of single faults such as the cases shown in Figure 11 for the effect of θ_2 sensor fault at 10% deterioration. Responses of μ control system is too oscillatory and unstable.

4. CONCLUSION

The proposed FTCS has been observed to have managed all faults simulated in the nominal performance tests, while the two other control systems could not consistently maintain stability in a majority of fault scenario. Robust performance assessments showing the performance of the control systems when faced with system uncertainty in addition to sensor faults were also simulated. Again, it is observed that fault tolerance capability of the proposed FTCS has been maintained. The proposed improvement to the model-based FTCS structure provides a potential framework for the realisation of an integrated MIMO FTCS. This design framework is suitable as it inherently incorporates fault residuals as feedback and allows the application of established robust MIMO control design concept. The test results show the capability of the proposed FTCS to maintain availability and an acceptable level of performance for multiple deteriorated sensor conditions.

APPENDIX

Transfer matrix of Q:

$$\begin{aligned} \frac{u_q(s)}{f_{ex}(s)} &= \frac{\alpha_1}{\beta_1}, \\ \frac{u_q(s)}{f_{\theta 1-\theta 2}(s)} &= \frac{u_q(s)}{f_{\theta 3}(s)} = \frac{\alpha_2}{\beta_2}, \\ \frac{u_k(s)}{f_{ex}(s)} &= \frac{\alpha_3}{\beta_3}, \end{aligned} \tag{A.1}$$

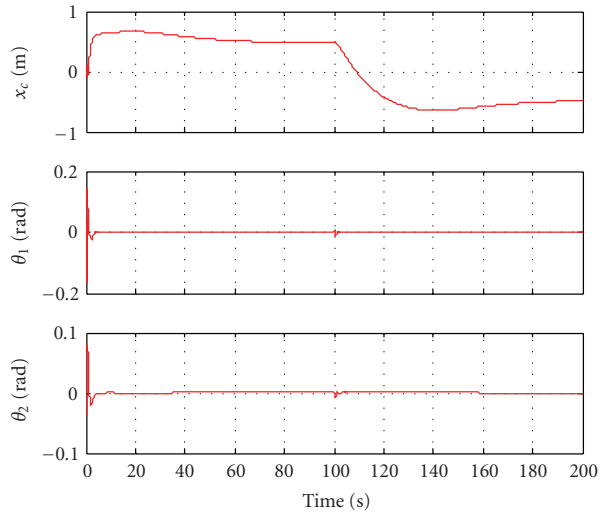

(a)

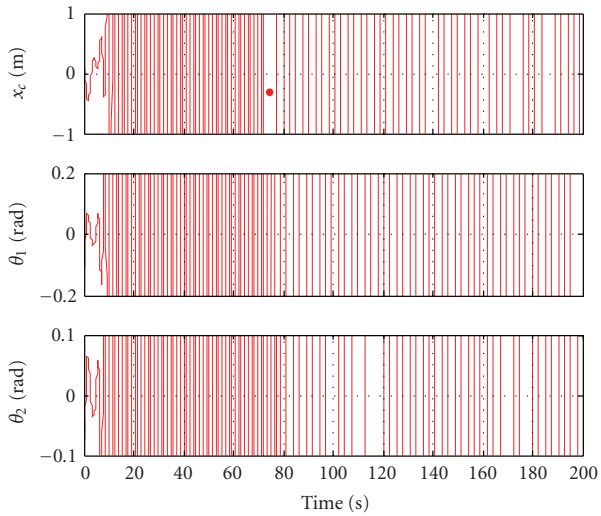

(b)

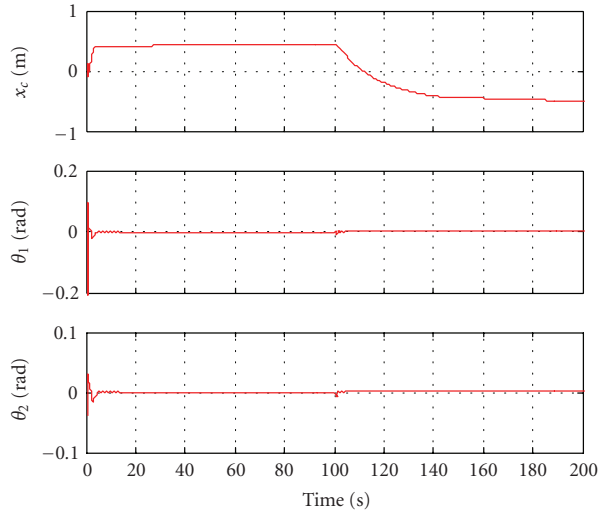

(c)

FIGURE 9: System responses of all controllers under multiple sensor fault condition, without modelling uncertainty. (a) —- FTCS, (b) . . . H_∞ controller, and (c) - - - μ controller.

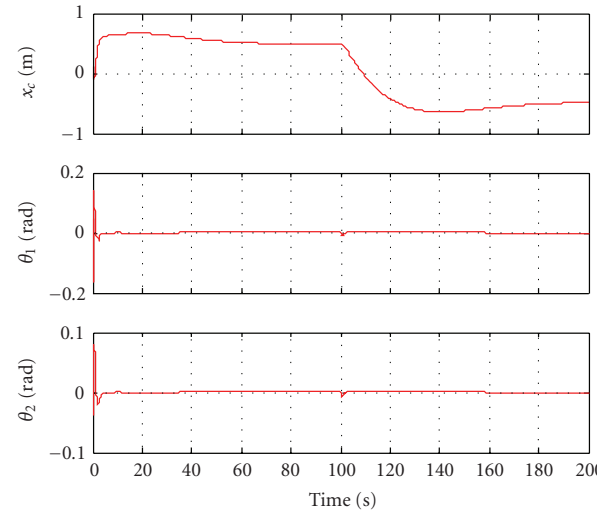

(a)

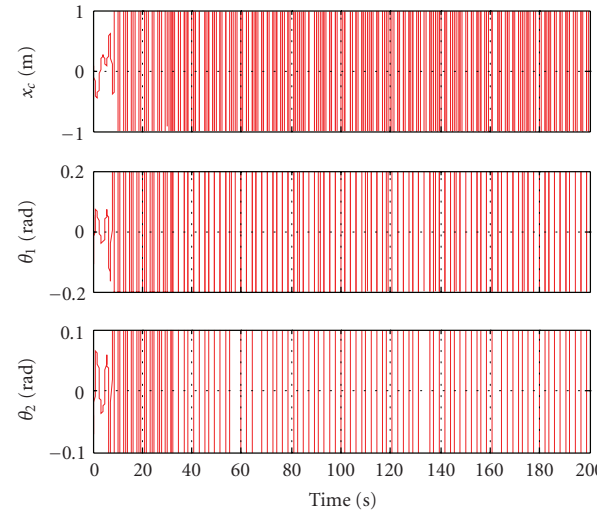

(b)

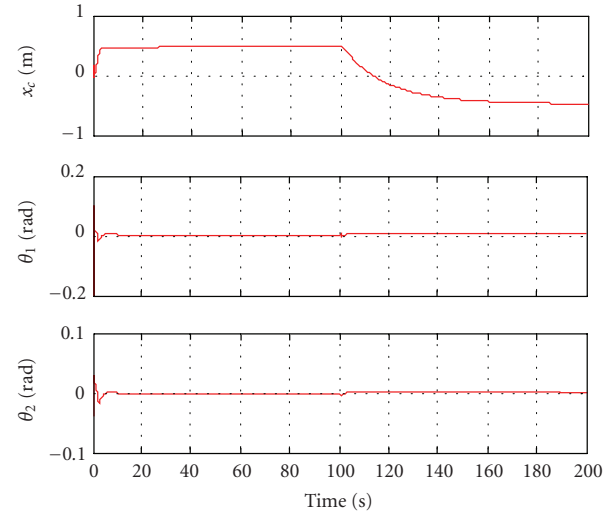

(c)

FIGURE 10: System responses of all controllers under multiple sensor fault condition with modelling uncertainty. (a) —- FTCS, (b) . . . H_∞ controller, and (c) - - - μ controller.

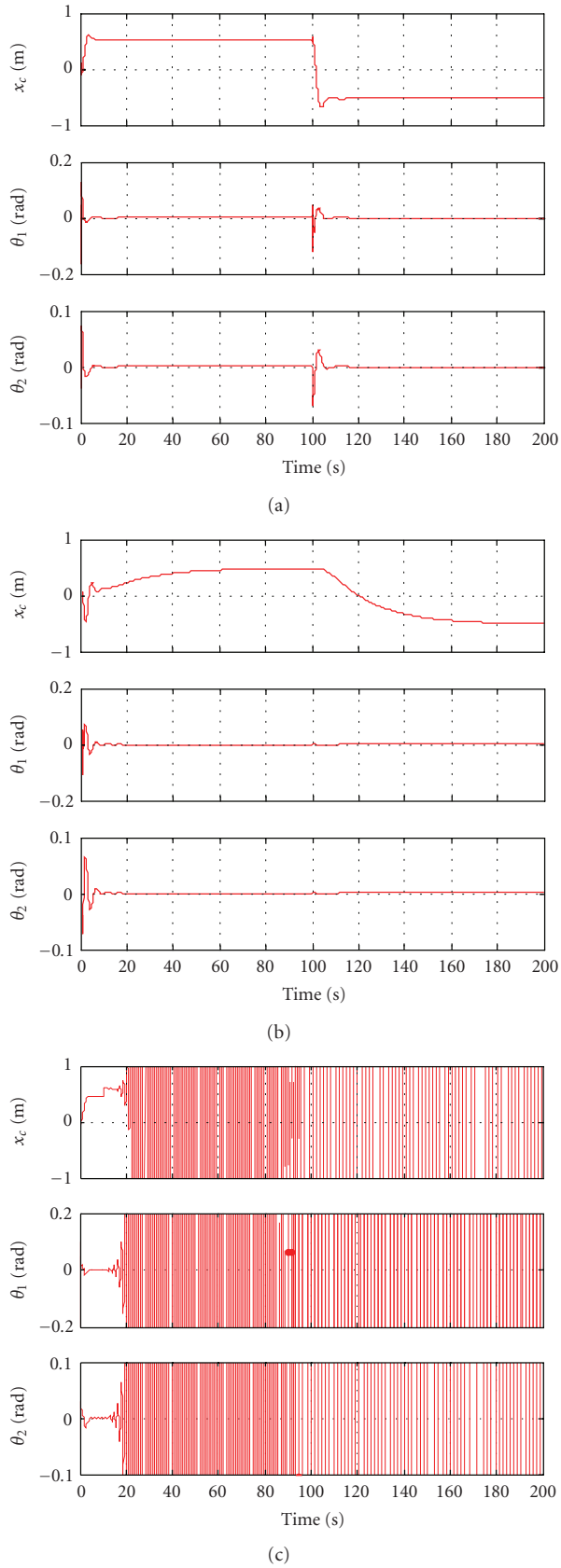

FIGURE 11: System responses of all controllers under θ_2 sensor fault at 10% deterioration, without uncertainties. (a) —- FTCS, (b) ... H_∞ controller, and (c) - - - μ controller.

where $\alpha_1 = (0.0001s^7 + 0.0025s^6 + 0.0465s^5 + 0.3162s^4 + 1.5660s^3 + 2.5422s^2 + 1.0939s - 0.1242)$, $\beta_1 = 0.0004s^7 + 0.0088s^6 + 0.1299s^5 + 0.6940s^4 + 2.8528s^3 + 3.3483s^2 + 2.4253s + 0.1423$, $\alpha_2 = 10^{-3}(-0.0001s^7 - 0.0032s^6 - 0.0603s^5 - 0.3832s^4 - 1.8085s^3 - 2.176s^2 - 0.9779s + 0.0841)$, $\beta_2 = 0.0004s^7 + 0.0088s^6 + 0.1299s^5 + 0.6940s^4 + 2.8528s^3 + 3.3483s^2 + 2.4253s + 0.1423$, $\alpha_3 = (0.0001s^7 + 0.0016s^6 + 0.0223s^5 + 0.1791s^4 + 0.8204s^3 + 1.9258s^2 + 1.7793s + 0.2839)$, $\beta_3 = 0.0006s^7 + 0.0137s^6 + 0.1474s^5 + 0.8104s^4 + 2.8431s^3 + 4.6326s^2 + 3.8566s + 1.5476$.

Transfer matrix of K:

$$\begin{aligned}
\frac{u_k(s)}{e_x(s)} &= \frac{\alpha_4}{\beta_4},\\
\frac{u_k(s)}{\theta_1(s)} &= \frac{\alpha_5}{\beta_5},\\
\frac{u_k(s)}{\theta_3(s)} &= \frac{\alpha_6}{\beta_6},\\
\frac{u_k(s)}{u(s)} &= \frac{\alpha_7}{\beta_7},\\
\frac{u_k(s)}{i(s)} &= \frac{\alpha_8}{\beta_8},
\end{aligned} \tag{A.2}$$

where $\alpha_4 = (0.0001s^7 + 0.0016s^6 + 0.0223s^5 + 0.1791s^4 + 0.8204s^3 + 1.9258s^2 + 1.7793s + 0.2839)$, $\beta_4 = 0.0006s^7 + 0.0137s^6 + 0.1474s^5 + 0.8104s^4 + 2.8431s^3 + 4.6326s^2 + 3.8566s + 1.5476$, $\alpha_5 = (0.003s^7 + 0.061s^6 + 0.740s^5 + 4.942s^4 + 17.436s^3 + 26.050s^2 + 16.23s + 4.898)$, $\beta_5 = 0.0006s^7 + 0.0137s^6 + 0.1474s^5 + 0.8104s^4 + 2.8431s^3 + 4.6326s^2 + 3.8566s + 1.5476$, $\alpha_6 = (-0.005s^7 - 0.115s^6 - 1.333s^5 - 8.249s^4 - 25.938s^3 - 35.97s^2 - 21.914s - 6.633)$, $\beta_6 = 0.0006s^7 + 0.0137s^6 + 0.1474s^5 + 0.8104s^4 + 2.8431s^3 + 4.6326s^2 + 3.8566s + 1.5476$, $\alpha_7 = (-0.00006s^7 - 0.00149s^6 - 0.01616s^5 - 0.08897s^4 - 0.30832s^3 - 0.49612s^2 - 0.40571s - 0.16099)$, $\beta_7 = 0.0006s^7 + 0.0137s^6 + 0.1474s^5 + 0.8104s^4 + 2.8431s^3 + 4.6326s^2 + 3.8566s + 1.5476$, $\alpha_8 = (-0.00006s^7 - 0.00159s^6 - 0.01862s^5 - 0.06867s^4 - 0.10104s^3 - 0.04271s^2 - 0.01119s - 0.01105)$, $\beta_8 = 0.0006s^7 + 0.0137s^6 + 0.1474s^5 + 0.8104s^4 + 2.8431s^3 + 4.6326s^2 + 3.8566s + 1.5476$.

Postfault performance weight matrix:

$$W_p = \begin{bmatrix} W_e & 0 & 0 \\ 0 & W_{\theta 1} & 0 \\ 0 & 0 & W_{\theta 2} \end{bmatrix}, \tag{A.3}$$

where

(i) $W_e = 25/(50s + 1)$ denotes the performance weight related to e_x;

(ii) $W_{\theta 1} = 50/(s + 10)$ denotes the performance weight related to θ_1;

(iii) $W_{\theta 2} = 45/(s + 10)$ denotes the performance weight related to θ_2.

The performance function of the signals provided is weighted to characterise the following limits:

(i) limiting cart position tracking error e_x at 0 m at high frequency and relaxed for low frequency at a maximum error of 0.04 m;

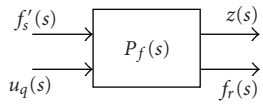

Figure 12

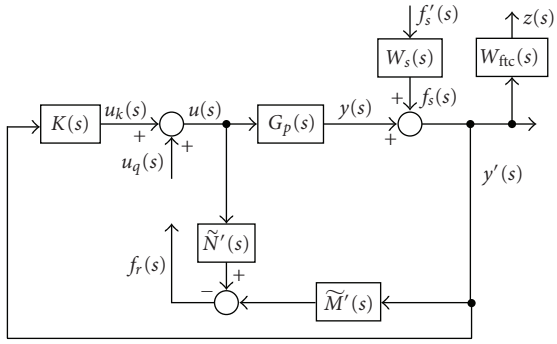

Figure 13

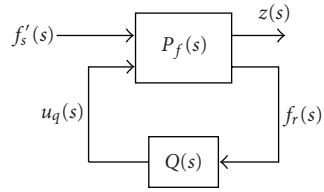

Figure 14

(ii) limiting the vertical to lower arm angle θ_1 at 0 *radians* at high frequency and relaxed for low frequency at a maximum angle of 0.20 *radians;*
(iii) limiting the vertical to upper arm angle θ_2 at 0 *radians* at high frequency and relaxed for low frequency at a maximum angle of 0.22 *radians.*

System interconnection and synthesis of Q(s)

The appropriate system interconnection structure of P(s) which is the outer loop of the FTCS inclusive of the nominal controller, K(s),and fault indicating generation elements needs to be formed using MATLAB μ-toolbox instruction *sysic.m* [17]. Hence, Figure12 is equivalent to Figure13.

Following that, the sensor fault compensating controller, Q(s), which is an H^∞ controller closing the inner loop of the FTCS (i.e., closing the loop for the system interconnection obtained from P(s) shown above), can be solved with the MATLAB instruction, *hinfsyn.m* [17]. Since

$$[k] = \text{hinfsyn}(p, \text{nmeas}, \text{ncon}, \text{gmin}, \text{gmax}, \text{tol}, \text{ricmethd}, \text{epr}, \text{epp}), \tag{A.4}$$

hence, in this case,

(i) k denotes the calculated H^∞ controller, that is, Q(s);
(i) p denotes system interconnection P(s) as shown above;
(iii) nmeas denotes number of fault indicating signals;
(iv) ncont denotes the number of control inputs;
(v) gmin, gmax, tol, and so on are as denoted in [17].

Finally, the closed-loop interconnection with Q(s) is shown as in Figure 14.

ACKNOWLEDGMENTS

The authors gratefully acknowledge funding from Brunel University and the University of Malaya in order to complete this work.

REFERENCES

[1] M. Blanke, M. Staroswiecki, and N. E. Wu, "Concepts and methods in fault-tolerant control," in *Proceedings of the American Control Conference (ACC '01)*, vol. 4, pp. 2606–2620, Arlington, Va, USA, June 2001.
[2] R. J. Patton, "Fault-tolerant control: the 1997 situation," in *Proceedings of the IFAC Symposium on Fault Detection, Supervision and Safety for Technical Processes (SAFEPROCESS '97)*, vol. 2, pp. 1033–1055, Hull, UK, August 1997.
[3] M. Gopinathan, R. K. Mehra, and J. C. Runkle, "Hot isostatic pressing furnaces: their modeling and predictive fault-tolerant control," *IEEE Control Systems Magazine*, vol. 20, no. 6, pp. 67–82, 2000.
[4] M. R. Napolitano, Y. An, and B. A. Seanor, "A fault tolerant flight control system for sensor and actuator failures using neural networks," *Aircraft Design*, vol. 3, no. 2, pp. 103–128, 2000.
[5] J. Chen and R. J. Patton, *Robust Model Based Fault Diagnosis for Dynamic Systems*, Kluwer Academic Publishers, Dordrecht, The Netherlands, 1999.
[6] R. Isermann, "Supervision, fault-detection and fault-diagnosis methods—an introduction," *Control Engineering Practice*, vol. 5, no. 5, pp. 639–652, 1997.
[7] R. J. Patton and J. Chen, "Observer-based fault detection and isolation: robustness and applications," *Control Engineering Practice*, vol. 5, no. 5, pp. 671–682, 1997.
[8] H. Niemann and J. Stoustrup, "Integration of control and fault detection: nominal and robust design," in *Proceedings of the IFAC Symposium on Fault Detection, Supervision and Safety for Technical Processes (SAFEPROCESS '97)*, vol. 1, pp. 341–346, Hull, UK, August 1997.
[9] H. Niemann and J. Stoustrup, "Passive fault tolerant control of a double inverted pendulum—a case study," *Control Engineering Practice*, vol. 13, no. 8, pp. 1047–1059, 2005.
[10] J. Stoustrup, M. J. Grimble, and H. Niemann, "Design of integrated systems for the control and detection of actuator/sensor faults," *Sensor Review*, vol. 17, no. 2, pp. 138–149, 1997.
[11] K. Zhou and Z. Ren, "A new controller architecture for high performance, robust, and fault-tolerant control," *IEEE Transactions on Automatic Control*, vol. 46, no. 10, pp. 1613–1618, 2001.
[12] D. U. Campos-Delgado and K. Zhou, "Fault tolerant control of a gyroscope system," in *Proceedings of the American Control Conference (ACC '01)*, vol. 4, pp. 2688–2693, Arlington, Va, USA, June 2001.
[13] M. Akesson, "Integrated control and fault detection for a mechanical servo process," in *Proceedings of the IFAC Symposium on Fault Detection, Supervision and Safety for Technical Processes (SAFEPROCESS '97)*, vol. 2, pp. 1252–1257, Hull, UK, August 1997.
[14] J. Eich and B. Sattler, "Fault tolerant control system design using robust control techniques," in *Proceedings of the IFAC Symposium on Fault Detection, Supervision and Safety for Technical*

Processes (SAFEPROCESS '97), vol. 2, pp. 1246–1251, Hull, UK, August 1997.

[15] M. Morari and E. Zafiriou, *Robust Process Control*, Prentice-Hall, Englewood Cliffs, NJ, USA, 1989.

[16] K. Zhou, J. C. Doyle, and K. Glover, *Robust and Optimal Control*, Prentice-Hall, Englewood Cliffs, NJ, USA, 1996.

[17] G. J. Balas, J. C. Doyle, K. Glover, A. Packard, and R. Smith, *μ-Analysis and Synthesis Toolbox*, The Mathworks, Natick, Mass, USA, 2001.

Hindawi Publishing Corporation
Journal of Control Science and Engineering
Volume 2008, Article ID 274313, 18 pages
doi:10.1155/2008/274313

Research Article

Design and Analysis of Robust Fault Diagnosis Schemes for a Simulated Aircraft Model

M. Benini,[1] M. Bonfè,[1] P. Castaldi,[2] W. Geri,[2] and S. Simani[1]

[1] *Department of Engineering, University of Ferrara, Via Saragat 1, 44100 Ferrara, Italy*
[2] *Aerospace Engineering Faculty, University of Bologna, Via Fontanelle 40, 40136 Forlì, Italy*

Correspondence should be addressed to S. Simani, ssimani@ing.unife.it

Received 30 March 2007; Revised 27 September 2007; Accepted 20 December 2007

Recommended by Jakob Stoustrup

Several procedures for sensor fault detection and isolation (FDI) applied to a simulated model of a commercial aircraft are presented. The main contributions of the paper are related to the design and the optimisation of two FDI schemes based on a linear polynomial method (PM) and the nonlinear geometric approach (NLGA). The FDI strategies are applied to the aircraft model, characterised by tight-coupled longitudinal and lateral dynamics. The robustness and the reliability properties of the residual generators related to the considered FDI techniques are investigated and verified by simulating a general aircraft reference trajectory. Extensive simulations exploiting the Monte Carlo analysis tool are also used for assessing the overall performance capabilities of the developed FDI schemes, in the presence of turbulence, measurement, and model errors. Comparisons with other disturbance-decoupling methods for FDI based on neural networks (NNs) and unknown input kalman filter (UIKF) are finally reported.

1. INTRODUCTION

Increasing demands on reliability for safety critical systems such as aircraft or spacecraft require robust control and fault diagnosis capabilities as these systems are potentially subjected to unexpected anomalies and faults in actuators, input-output sensors, components, or subsystems. Consequently, fault diagnosis capabilities and requirements for aerospace applications have recently been receiving a great deal of attention in the research community [1, 2]. A fault diagnosis system needs to detect and isolate the presence and location of the faults, on the basis also of the control system architectures. Development of appropriate techniques and solutions for these tasks are known as the fault detection and isolation (FDI) problem. There are, broadly speaking, two main approaches for addressing the FDI problem, namely, hardware-based and model-based techniques [3, 4]. A common and important approach in model-based techniques is known as the residual-based method. A number of researchers have developed residual-based methods for dynamic systems such as the parity space [5], state estimation [6], unknown input observer (UIO), Kalman filters (KFs) [3], and parameter identification [6].Intelligent techniques [7] can be also exploited. Furthermore, the Massoumnia's geometric method [8] was successfully extended to nonlinear systems [9, 10]. A crucial issue with any FDI scheme is its robustness properties and a viable procedure for practical application of FDI techniques is really necessary. Moreover, robust FDI for the case of aircraft systems and applications is still an open problem for further research.

The first part of this work deals with the residual generator design for the FDI of input-output sensors of a general aviation aircraft subject to turbulence, wind gust disturbances, and measurement noises. The developed PM scheme belongs to the parity space approach [5] and it is based on an input-output polynomial description of the system under diagnosis. In particular, the use of input-output forms allows to easily obtain the analytical description for the disturbance-decoupled residual generators. These dynamic filters, organised into bank structures, are able to achieve fault isolation properties. An appropriate choice of their parameters allows to maximise robustness with respect to both measurement noise and modelling errors, while optimising fault sensitivity characteristics. The development of NLGA methodology is based on the works by De Persis and Isidori [10]. It was shown that the problem of the FDI for nonlinear systems is solvable if and only if there is an unobservability distribution that leads to a quotient subsystem which is unaffected

by all faults but one. If such a distribution exists, an appropriate coordinate transformations in the state space can be exploited for designing a residual generator only for the observable subsystem. This technique was applied for the first time to a vertical takeoff and landing (VTOL) aircraft with reference to a reduced-order model [11]. The NLGA residual generators have been designed in order to be analytically decoupled from the vertical and lateral components of the wind (gusts and turbulence). Moreover, a new full analytical developed mixed $\mathcal{H}_-/\mathcal{H}_\infty$ optimisation is proposed in order to design the NLGA residual generators so that a good tradeoff between the fault sensitivity and the robustness with respect to measurements and model errors is achieved. The designed residual generators have been tested on a PIPER PA-30 aircraft flight simulator that was implemented in Matlab-Simulink environments. With respect to the related works by the same authors [12, 13], the main contribution of this paper regards the enhancement in the designs of the proposed FDI schemes. Moreover, the final performances have been evaluated by adopting a typical aircraft reference trajectory embedding several steady-state flight conditions, such as straight flight phases and coordinated turns. Comparisons with different disturbance-decoupling methods for FDI based on neural networks (NNs) and unknown input Kalman filter (UIKF) have been also provided. Finally, extensive experiments exploiting Monte Carlo analysis are used for assessing the overall capabilities of the developed FDI methods, in the presence of uncertainty, measurement, and modelling errors.

2. AIRCRAFT MODEL OVERVIEW

This section recalls briefly the description of the monitored aircraft whose main parameters and variables are reported in Table 1.

The considered aircraft simulation model consists of a PIPER PA-30, based on the classical nonlinear 6 degrees of freedom (DoF) rigid body formulation [14] whose motion occurs as a consequence of applied forces and moments (aerodynamic, propulsive, and gravitational). A set of local approximations for these forces has been computed and scheduled depending on the values assumed by true airspeed (TAS), curvature radius, flight path angle, altitude, and flap deflection. In this way, it is possible to obtain a mathematical model for each flight condition. This model is suitable for a state-space representation, as it can be made explicit. The parameters in the analytic representation of the aerodynamic actions have been obtained from wind tunnel experimental data, and the aerodynamic actions are expressed along the axes of the wind reference system. It should be observed that aerodynamic forces and moments are not implemented by the classical linearised expressions (stability derivatives) but by means of cubic splines approximating the nonlinear experimental curves. The nonlinear 6 DoF model has been completed by means of the PIPER PA-30 propulsion system consisting of two 4-pistons aspirated engines, with the throttle valve aperture δ_{th} as input and the overall thrust intensity as output. The overall simulation model, used to perform all the following tests, consists of the aircraft 6 DoF flight dynamics and the engine model completed with the model of input-output sensors, the servo actuators, the atmosphere turbulence Dryden description, the wind gust disturbances, and a classical autopilot. Moreover, the sensor models embed all the possible sources of disturbance (calibration and alignment errors, scale factor, white and coloured noises, limited bandwidth, g-sensitivity, gyro drift, etc.).

Table 1: Nomenclature.

α	Angle of attack
β	Angle of sideslip
p_ω	Roll rate
q_ω	Pitch rate
r_ω	Yaw rate
ϕ	Bank angle
θ	Elevation angle
ψ	Heading angle
n_e	Engine shaft angular rate
$\begin{bmatrix} I_x & 0 & -I_{xz} \\ 0 & I_y & 0 \\ -I_{xz} & 0 & I_z \end{bmatrix}$	Inertia moment matrix
V	True airspeed (TAS)
δ_e	Elevator deflection angle
δ_a	Aileron deflection angle
δ_r	Rudder deflection angle
δ_{th}	Throttle aperture percentage
H	Altitude
γ	Flight path angle
m	Airplane mass
ω_u, ω_v, ω_w	Wind gust components

The linear model used by the proposed PM FDI approach described in Section 3 embeds the linearisation both of the 6 DoF model and of the propulsion system as follows:

$$\dot{x}(t) = Ax(t) + Bc(t) + Ed(t) \tag{1}$$

with

$$\begin{aligned} x(t) &= [\Delta V(t)\Delta\alpha(t)\Delta\beta(t)\Delta p_\omega(t)\Delta q_\omega(t)\Delta r_\omega(t) \\ &\quad \cdots \Delta\phi(t)\Delta\theta(t)\Delta\psi(t)\Delta n_e(t)]^T, \\ c(t) &= [\Delta\delta_e(t)\Delta\delta_a(t)\Delta\delta_r(t)\Delta\delta_{\text{th}}(t)]^T, \\ d(t) &= [w_u(t)w_v(t)w_w(t)]^T, \end{aligned} \tag{2}$$

where Δ denotes the variations of the considered variables while $c(t)$ and $d(t)$ are the control inputs and the disturbances, respectively. The disturbance contribution of the wind gusts as air velocity components, w_u, w_v, and w_w, along body axes was also considered. The output equation associated with the model (1) is of the type $y(t) = Cx(t)$, where the rows of C correspond to rows of the identity matrix, depending on the measured variables.

On the other hand, regarding the NLGA FDI scheme described in Section 4, it requires a nonlinear input affine

system [10], but the adopted simulation model of the aircraft does not fulfil this requirement. For this reason, the following simplified aircraft model is used:

$$\begin{aligned}
\dot{V} &= -\frac{\left(C_{D0}+C_{D\alpha}\alpha+C_{D\alpha_2}\alpha^2\right)}{m}V^2 \\
&\quad + g(\sin\alpha\cos\theta\cos\phi-\cos\alpha\sin\theta) \\
&\quad + \frac{\cos\alpha}{m}\frac{t_p}{V}(t_0+t_1n_e)\delta_{\text{th}}+w_v\sin\alpha, \\
\dot{\alpha} &= -\frac{(C_{L0}+C_{L\alpha}\alpha)}{m}V+\frac{g}{V}(\cos\alpha\cos\theta\cos\phi+\sin\alpha\sin\theta) \\
&\quad + q_\omega+\frac{\sin\alpha}{m}\frac{t_p}{V^2}(t_0+t_1n_e)\delta_{\text{th}}+\frac{\cos\alpha}{V}w_v, \\
\dot{\beta} &= \frac{\left(C_{D0}+C_{D\alpha}\alpha+C_{D\alpha_2}\alpha^2\right)\sin\beta+C_{Y\beta}\beta\cos\beta}{m}V \\
&\quad + g\frac{\cos\theta\sin\phi}{V}+p_\omega\sin\alpha-r_\omega\cos\alpha \\
&\quad + \frac{\cos\alpha\sin\beta}{m}\frac{t_p}{V^2}(t_0+t_1n_e)\delta_{\text{th}}+\frac{1}{V}w_\ell, \\
\dot{p}_\omega &= \frac{(C_{l\beta}\beta+C_{lp}p_\omega)}{I_x}V^2+\frac{(I_y-I_z)}{I_x}q_\omega r_\omega+\frac{C_{\delta_a}}{I_x}V^2\delta_a, \\
\dot{q}_\omega &= \frac{(C_{m0}+C_{m\alpha}\alpha+C_{mq}q_\omega)}{I_y}V^2+\frac{(I_z-I_x)}{I_y}p_\omega r_\omega \\
&\quad + \frac{C_{\delta_e}}{I_y}V^2\delta_e+\frac{t_d}{I_y}\frac{t_p}{V}(t_0+t_1n_e)\delta_{\text{th}}, \\
\dot{r}_\omega &= \frac{(C_{n\beta}\beta+C_{nr}r_\omega)}{I_z}V^2+\frac{(I_x-I_y)}{I_z}p_\omega q_\omega+\frac{C_{\delta_r}}{I_z}V^2\delta_r, \\
\dot{\phi} &= p_\omega+(q_\omega\sin\phi+r_\omega\cos\phi)\tan\theta, \\
\dot{\theta} &= q_\omega\cos\phi-r_\omega\sin\phi, \\
\dot{\psi} &= \frac{(q_\omega\sin\phi+r_\omega\cos\phi)}{\cos\theta} \\
\dot{n}_e &= t_nn_e^3+\frac{t_f}{n_e}(t_0+t_1n_e)\delta_{\text{th}},
\end{aligned} \tag{3}$$

where $C_{(\cdot)}$ are the aerodynamic coefficients; $t_{(\cdot)}$ are the engine parameters; and w_v, w_l are the vertical and lateral wind disturbance components. In particular, the model of (3) has been obtained on the basis of some assumptions.In particular, the expressions of aerodynamic forces and moments have been represented by means of series expansions in the neighbourhood of the steady-state flight condition, then only the main terms are considered. The engine model has been simplified by linearising the power with respect to the angular rate behaviour in the neighbourhood of the trim point. The second-order coupling between the longitudinal and lateral-directional dynamics have been neglected. The x-body axis component of the wind has been neglected. In fact, the aircraft behaviour is much more sensitive to the y-body and z-body axis wind components. Finally, the rudder effect in the equation describing the β dynamics has been neglected. It is worth noting that Section 5 has shown that the designs and the simulations of the NLGA residual generators are robust with respect to the last approximation. In fact, the model of the β dynamics will never be used.

3. PM RESIDUAL GENERATORS

Let us consider the input-output representation of a continuous-time, time-invariant linear dynamic system affected by faults and disturbances in the form

$$P(s)y(t) = Q_c(s)c(t)+Q_d(s)d(t)+Q_f(s)f(t), \tag{4}$$

where $y(t)\in\Re^m$ is the output vector, $c(t)\in\Re^{l_c}$ is the input vector, $d(t)\in\Re^{l_d}$ is the disturbance vector, and $f(t)\in\Re^{l_f}$ is the fault vector; $P(s)$, $Q_c(s)$, $Q_d(s)$, and $Q_f(s)$ are known polynomial matrices of proper dimensions.

Models of type (4) can be frequently found in practice by applying well-known physical laws to describe the input-output dynamical links of various systems. Algorithms to transform multivariable state-space models to equivalent multiple-input-multiple-output (MIMO) polynomial representations and vice versa are available [15]. Suitable software routines for multivariable system transformations have been implemented by the authors in the Matlab environment. In fact, the Matlab software for state-space and transfer function conversions is not able to manage directly MIMO models, since they are considered as concatenations of single-input-single-output (SISO) systems.

An important aspect of the residual generator design concerns the decoupling properties of the disturbance $d(t)$. The decoupling can be obtained premultiplying all the terms of (4) by the matrix $L(s)\in\mathcal{N}_l(Q_d(s))$, that is, the left null-space of the matrix $Q_d(s)$:

$$L(s)P(s)y(t)-L(s)Q_c(s)c(t) = L(s)Q_f(s)f(t). \tag{5}$$

Hence, the residual generator for the system of (4) is represented by

$$\begin{aligned}
R(s)r(t) &= L(s)P(s)y(t)-L(s)Q_c(s)c(t) \\
&= L(s)Q_f(s)f(t),
\end{aligned} \tag{6}$$

where it is assumed that $r(t)\in\Re$ and $L(s)$ is a polynomial row vector. The polynomial $R(s)$ can be arbitrarily selected among the polynomials with degree greater than or equal to n_r^*, where n_r^* is the maximum row-degree of the pair $\{L(s)P(s), L(s)Q_c(s)\}$. Moreover, if all the roots of $R(s)$ lie in the open left-half s-plane, it assures the stability of the filter of (6). Without loss of generality, it is assumed that $R(0)=1$.

Remark 1. If the matrix $Q_d(s)$ is of full-column rank (i.e., rank $Q_d(s)=l_d$), $\mathcal{N}_l(Q_d(s))$ has dimension $m-l_d$. Therefore, a polynomial matrix $B(s)$, whose rows represents a minimal polynomial basis of $\mathcal{N}_l(Q_d(s))$, has $m-l_d$ rows and m columns.

This work is focused on the problem of detecting and isolating additive faults acting on the input and output sensors of the monitored system. If the input-output measurements

are modelled by the relations of (7):

$$\begin{aligned} c^*(t) &= c(t) + f_c(t), \\ y^*(t) &= y(t) + f_o(t), \end{aligned} \tag{7}$$

the system of (4) becomes

$$P(s)\big(y^*(t) - f_o(t)\big) = Q_c(s)\big(c^*(t) - f_c(t)\big) + Q_d(s)d(t), \tag{8}$$

under the assumptions that $Q_f(s)f(t) = [-Q_c(s), P(s)] \cdot [f_c^T(t), f_o^T(t)]^T$. Thus, the residual generator of (6) is written as

$$\begin{aligned} R(s)r(t) &= L(s)P(s)y^*(t) - L(s)Q_c(s)c^*(t) \\ &= L(s)P(s)f_o(t) - L(s)Q_c(s)f_c(t). \end{aligned} \tag{9}$$

Remark 2. The residual generator described by (7) and (9) can be seen as an errors-in-variables (EIV) model [16] with respect the input and output variables, as the measurements that feed the residual function are affected by additive faults. This description highlights the importance of the residual generator in the form of (9).

Remark 3. The diagnostic capabilities of the residual generator of (6) strongly depend on the choice of the terms $L(s)$ and $R(s)$. This paper proposes a method for the design of these polynomials, under the assumption that $f(t)$ is a scalar and, consequently, $Q_f(s)$ is a vector. The rationale of this assumption is commented in Section 3.2 where the fault isolation method is proposed.

In the following, the freedom design in the selection of the rows of the polynomial matrix $L(s)$ is investigated when $q = m - l_d \geq 2$. These degrees of freedom are used to optimise the sensitivity properties of $r(t)$ with respect to the fault $f(t)$, for example, by maximising the steady-state gain of the transfer function $G_f(s) = L(s)Q_f(s)/R(s)$.

If $b_i(s)$ $(i = 1, \ldots, q)$ are the row vectors of the basis $B(s)$, $L(s)$ can be expressed as linear combination of these vectors:

$$L(s) = \sum_{i=1}^{q} k_i b_i(s), \tag{10}$$

where k_i are real constants maximising:

$$\lim_{s\to 0} \frac{1}{R(s)} \left[\sum_{i=1}^{q} k_i b_i(s)\right] Q_f(s) = \left[\sum_{i=1}^{q} k_i b_i(0)\right] Q_f(0) \tag{11}$$

with the constraint

$$\sum_{i=1}^{q} k_i^2 = 1. \tag{12}$$

Under these assumptions, when the fault $f(t)$ is a step-function of magnitude F,the steady-state residual value is

$$\lim_{t\to\infty} r(t) = \lim_{s\to 0} \frac{L(s)Q_f(s)}{R(s)} \frac{F}{s} = \left[\sum_{i=1}^{q} k_i b_i(0)\right] Q_f(0)F. \tag{13}$$

If the following real vectors are defined as

$$k = \begin{bmatrix} k_1 \\ k_2 \\ \vdots \\ k_q \end{bmatrix}, \qquad a = B(0)Q_f(0) = \begin{bmatrix} a_1 \\ a_2 \\ \vdots \\ a_q \end{bmatrix}, \tag{14}$$

the problem of the maximisation of the residual fault sensitivity can be recast as follows.

Proposition 1. *Given the vector a, the vector k that maximises the steady-state fault sensitivity, that is, the function W given by the expression*

$$W = a^T k = \sum_{i=1}^{q} a_i k_i, \tag{15}$$

under the constraint of (12)*, can be found by solving*

$$\widetilde{k} = \arg\ \max W(k). \tag{16}$$

The solution to the problem described by Proposition 1 can be derived as follows. The constraint of (12) describes a hypersphere, whilst the expression of the function of (15) is a hyperplane. The unknown coefficients k must belong to both the hyperplane and the hypersphere. Therefore, the points of tangency between the hypersphere and the hyperplane represents the solutions that maximise or minimise W. As shown below, the solution of the problem described by Proposition 1 exists and is unique.

Proof. From (12), k_1 is expressed as a function of k_2, $k_3, \ldots, k_q$, and it is substituted into (15):

$$W = a_1\sqrt{1 - k_2^2 - k_3^2 - \cdots - k_q^2} + a_2k_2 + \cdots + a_qk_q. \tag{17}$$

By computing $\nabla W = 0$, that is,

$$\begin{aligned} \frac{\partial W}{\partial k_2} &= \frac{1}{2}a_1 \frac{-2k_2}{\sqrt{1 - k_2^2 - k_3^2 - \cdots - k_q^2}} + a_2 = 0, \\ \frac{\partial W}{\partial k_3} &= \frac{1}{2}a_1 \frac{-2k_3}{\sqrt{1 - k_2^2 - k_3^2 - \cdots - k_q^2}} + a_3 = 0, \\ &\vdots \\ \frac{\partial W}{\partial k_q} &= \frac{1}{2}a_1 \frac{-2k_q}{\sqrt{1 - k_2^2 - k_3^2 - \cdots - k_q^2}} + a_q = 0, \end{aligned} \tag{18}$$

and squaring the expression, after algebraic manipulation:

$$\begin{aligned} a_2^2 &= (a_2^2 + a_1^2)k_2^2 + a_2^2k_3^2 + \cdots + a_2^2k_q^2, \\ a_3^2 &= a_3^2k_2^2 + (a_3^2 + a_1^2)k_3^2 + \cdots + a_3^2k_q^2, \\ &\vdots \\ a_q^2 &= a_q^2k_2^2 + a_q^2k_3^2 + \cdots + (a_q^2 + a_1^2)k_q^2, \end{aligned} \tag{19}$$

an expression in the form of $Ax = b$ is obtained, where

$$A = \begin{bmatrix} (a_2^2 + a_1^2) & a_2^2 & \cdots & a_2^2 \\ a_3^2 & (a_3^2 + a_1^2) & \cdots & a_3^2 \\ \vdots & \vdots & \ddots & \vdots \\ a_q^2 & a_q^2 & \cdots & (a_q^2 + a_1^2) \end{bmatrix},$$
$$x = \begin{bmatrix} k_2^2 \\ k_3^2 \\ \vdots \\ k_q^2 \end{bmatrix}, \qquad b = \begin{bmatrix} a_2^2 \\ a_3^2 \\ \vdots \\ a_q^2 \end{bmatrix}. \tag{20}$$

The unknown vector $\widetilde{x}$, under the constraint of (12), can be expressed as follows:

$$\widetilde{x} = \begin{bmatrix} 1 - \sum_{i=1}^{q-1} (A^{-1}b)_i \\ A^{-1}b \end{bmatrix}, \tag{21}$$

where $(A^{-1}b)_i$ is the ith element of the vector $A^{-1}b$. The vector $\widetilde{x}$ represents the squares of the solution of the problem of Proposition 1.

Let us indicate Ω the set of the vectors k whose elements are the square roots of the elements of $\widetilde{x}$. As every element can be taken both with signs "+" and "−", such vectors are 2^q. Therefore, the solution $\widetilde{k}$ of Proposition 1 can be reformulated as

$$\widetilde{k} = \arg\max_{k \in \Omega} W(k). \tag{22}$$

□

Remark 4. The matrix A can be expressed as $A = E + a_1^2 I_{q-1}$, where E is a matrix with equal columns. If $a_1 \neq 0$, this assumption guarantees the existence of A^{-1}, and consequently the existence and the uniqueness of the solution $A^{-1}b$. Obviously, if $a_1 = 0$ and $a_j \neq 0$, it is sufficient to express k_j as function of the remaining variables and to reapply the same procedure.

Remark 5. The same solution can be found by maximising the function $|W|$. Due to the symmetry properties, the maximisation of $|W|$ admits two solutions corresponding to the maximum and the minimum of the function W. Moreover, the choice of the quadratic constraint of (12) guarantees the unicity of the solution to the problem of Proposition 1.

Remark 6. The problem described by Proposition 1 could have been solved also in a numerical way, that is, by searching k that maximises W on the surface of the q-dimensional hypersphere. However, the computational cost of this numerical solution can be a drawback when q is big.

3.1. PM residual design

Section 3 has shown how to maximise the steady-state gain of the continuous-time transfer function $G_f(s) = L(s)Q_f(s)/R(s)$ trough a suitable choice of the real vector k (i.e., $k = \widetilde{k}$). The design of the filter of (6) has been completed here by introducing a method for assigning both the zeros and the poles of the continuous-time transfer function $G_f(s)$. The zeros and poles location influences the transient characteristics (maximum overshoot, delay time, rise time, settling time, etc.) of the filter of (6). In many applications, these characteristics must be kept within tolerable or prescribed limits in order to guarantee good performances of the filter in terms, for example, of fault detection times and false-alarm probabilities.

Remark 7. When $k = \widetilde{k}$, the polynomial $L(s)Q_f(s) = k^T B(s)Q_f(s)$ is fixed and no freedom degree is left to arbitrarily assign the zeros. In order to solve this problem, a polynomial vector $k(s)$ can be considered. Under this assumption, $L(s)$ still belongs to the subspace $\mathcal{N}_l(Q_d(s))$, where the terms k_i are polynomial coefficients.

The previous consideration leads to introduce the polynomial $E(s) = k^T(s)B(s)Q_f(s)$, where $k(s)$ is a q-dimensional polynomial vector whose ith element has the form

$$k_i(s) = \sum_{j=0}^{n_k} k_i^j s^j. \tag{23}$$

The degree n_k and the $q \times n_k$ coefficients k_i^j are freedom design ($j \neq 0$) that are exploited for obtaining the desired roots of the polynomial $E(s)$. However, in order to maximise the steady-state gain, as shown in Section 3, the following condition must hold:

$$k(0) = \widetilde{k} = \begin{bmatrix} \widetilde{k}_1 \\ \widetilde{k}_2 \\ \vdots \\ \widetilde{k}_q \end{bmatrix} \iff k_i^0 = \widetilde{k}_i, \quad i = 1, \ldots, q. \tag{24}$$

Definition 1. $H(s)$ is the reference polynomial whose roots are the zeros to be assigned:

$$H(s) = \sum_{j=0}^{n_h} h^j s^j. \tag{25}$$

Since the constraint of (24) must hold, $H(0) = \widetilde{k}^T B(0) \cdot Q_f(0)$. Obviously, this assumption does not provide any restriction on the roots assignable. Under the previous considerations, the zero assignment and pole placement problem is formulated as follows.

Proposition 2. *The degree n_k and the coefficients k_i^j have to be determined under the constraint of* (24) *in order to obtain $E(s) = H(s)$.*

Proof. In Section 3, the polynomial vector $a(s) = B(s)Q_f(s)$ was defined. Its ith element is a known polynomial of a

certain degree, n_{a_i}. If n_a is defined as follows:

$$n_a = \max_{i=1,\ldots,q} n_{a_i}, \tag{26}$$

the ith element of $a(s)$ can be always written as a polynomial of degree n_a:

$$a_i(s) = \sum_{j=0}^{n_a} a_i^j s^j \tag{27}$$

by imposing that $a_i^j = 0$ when $j > n_{a_i}$.

As $E(s) = k^T(s)a(s)$, by multiplying (23) and (27), it results

$$E(s) = \sum_{i=1}^{q} \sum_{j=0}^{n_k+n_a} \left(\sum_{\alpha+\beta=j} k_i^\alpha a_i^\beta \right) s^j = \sum_{j=0}^{n_k+n_a} e^j s^j, \tag{28}$$

where

$$e^j = \sum_{i=1}^{q} \sum_{\alpha+\beta=j} k_i^\alpha a_i^\beta. \tag{29}$$

Equations (28) and (29) assume that $k_i^\alpha = 0$ when $\alpha > n_k$ and $a_i^\beta = 0$ when $\beta > n_a$. Note that the coefficients $e^1, \ldots, e^{n_k+n_a}$ depend on the freedom design $k_i^1, \ldots, k_i^{n_k}$. On the other hand, e^0 is fixed as the coefficients k_i^0 are assigned by (24).

Let us suppose that $n_h \leq n_k + n_a$. By imposing $E(s) = H(s)$, from (29) and (25), the following expressions are computed:

$$\sum_{i=1}^{q} \sum_{\alpha+\beta=j\ (\alpha\neq 0)} k_i^\alpha a_i^\beta = h^j - \sum_{i=1}^{q} k_i^0 a_i^j, \quad j = 1, \ldots, n_k + n_a. \tag{30}$$

Equations (24) and (30) represent a linear system with n_k+n_a equations and $q \times n_k$ unknowns, which can be expressed in the classical form $Ax = b$, where

$$A = \begin{bmatrix} a_1^0 & \cdots & a_q^0 & 0 & \cdots & 0 & & 0 & \cdots & 0 \\ \vdots & \ddots & \vdots & a_1^0 & \cdots & a_q^0 & & & & \\ a_1^{n_a} & \cdots & a_q^{n_a} & \vdots & \ddots & \vdots & & & & \\ 0 & \cdots & 0 & a_1^{n_a} & \cdots & a_q^{n_a} & & \vdots & \ddots & \vdots \\ 0 & \cdots & 0 & 0 & \cdots & 0 & & & & \\ & & & & & & \ddots & & & \\ \vdots & \ddots & \vdots & \vdots & \ddots & \vdots & & 0 & \cdots & 0 \\ & & & & & & & a_1^0 & \cdots & a_q^0 \\ & & & & & & & \vdots & \ddots & \vdots \\ 0 & \cdots & 0 & 0 & \cdots & 0 & & a_1^{n_a} & \cdots & a_q^{n_a} \end{bmatrix},$$

$$x = \begin{bmatrix} k_1^1 \\ \vdots \\ k_q^1 \\ k_1^2 \\ \vdots \\ k_q^2 \\ \vdots \\ \vdots \\ k_1^{n_k} \\ \vdots \\ k_q^{n_k} \end{bmatrix}, \qquad b = \begin{bmatrix} h^1 - \sum_{i=1}^{q} k_i^0 a_i^1 \\ \vdots \\ h^{n_a} - \sum_{i=1}^{q} k_i^0 a_i^{n_a} \\ h^{n_a+1} \\ \vdots \\ h^{n_a+n_k} \end{bmatrix}. \tag{31}$$

The degree n_k of the polynomials $k_i(s)$ has to be chosen in order to obtain a solvable system (i.e., rank A = rank $[A\ b]$). □

In order to understand the proposed solution, the following points should be considered.

(i) The choice of n_k must guarantee that the relations $n_h \leq n_k + n_a$ are satisfied.

(ii) When $q \geq 2$, the difference between the number of unknown terms and the number of equations, that is, $(q-1) \times n_k - n_a$, is greater than zero if n_k is selected sufficiently high.

(iii) Even if the system admits solutions, the inverse of the matrix A may not exist; in such case there are infinite solutions and the one associated to the pseudoinverse of A, that is, A^+b can be computed.

Remark 8. The use of a polynomial vector $k(s)$ instead of a real vector k has the drawback of increasing the complexity of the residual generator. Many FDI applications require that

$$\frac{G_f(s)}{G_f(0)} = \frac{F(0)}{F(s)}, \tag{32}$$

where $F(s)$ is an arbitrary polynomial. These cases do not require a $k(s)$ such that $E(s) = G_f(0)$, but it is enough considering $k = \widetilde{k}$ and imposing

$$R(s) = \frac{E_0(s)F(s)}{G_f(0)F(0)}, \tag{33}$$

where $E_0(s) = \widetilde{k}B(s)Q_f(s)$. However, there is a restriction on the choice of $F(s)$. In fact, due to the realisability condition, $\deg\{F(s)\} > n_r^* - \deg\{E_0(s)\}$. Moreover, the method cannot be applied if $E_0(s)$ admits one or more roots with positive real part, as the residual generator would become unstable. These cases require an approximate solution.

Remark 9. This section is focused on the design of residual generators on the basis of a given reference function with

disturbance-decoupling and fault sensitivity maximisation properties. The pole location influences the transient dynamics of the designed residual filters, while the steady-state properties depend on the PM residual design, as it maximises the residual steady-state values with respect to step faults affecting input and output sensors. The poles of the residual functions could be optimised with respect to both fault and disturbance terms, as shown, for example, in a work by the same authors [17].

3.2. PM fault isolation

This section addresses the design problem of residual generator banks for the isolation of faults affecting the input and the output sensors. This design is performed by using the disturbance-decoupling method suggested in Section 3.

To univocally isolate a fault concerning one of the *output sensors*, under the hypotheses that the input sensors and the remaining output sensors are fault-free, a bank of residual generator filters is used. The number of these generators is equal to the number m of the system outputs, and the ith device ($i = 1, \dots, m$) is driven by all but the ith output and all the inputs of the system. In this case, a fault on the ith output sensor affects all but the ith residual generator.

In presence of a fault on the jth output sensor, the measured output $y^*(t)$ can be expressed as follows:

$$y^*(t) = y(t) + f_{o_j}(t), \tag{34}$$

with

$$f_{o_j}(t) = \begin{bmatrix} 0 & \cdots & 0 & h_{o_j}(t) & 0 & \cdots & 0 \end{bmatrix}^T, \tag{35}$$

where $h_{o_j}(t)$ represents the jth output fault function.

In these conditions, the system of (4) becomes

$$P(s)y^*(t) - p_j(s)h_{o_j}(t) = Q_c(s)c(t) + Q_d(s)d(t), \tag{36}$$

where $p_j(s)$ is the jth column of the matrix $P(s)$.

Let us indicate $L_{o_i}(s)$ a polynomial row vector belonging to the basis of the left null space of the matrix $[Q_d(s) \mid p_i(s)]$. The expression of the ith filter when a fault is acting on the jth output sensor is obtained by multiplying (36) by $L_{o_i}(s)$:

$$\begin{aligned} R_{o_i}(s)r_{o_i}(t) &= L_{o_i}(s)P^i(s)y^{*i}(t) - L_{o_i}(s)Q_c(s)c(t) \\ &= \begin{cases} L_{o_i}(s)p_j(s)h_{o_j}(t) & \text{for } j \neq i, \\ 0 & \text{for } j = i, \end{cases} \end{aligned} \tag{37}$$

where $P^i(s)$ is the matrix obtained by deleting from $P(s)$ the ith column, and $y^{*i}(t)$ represents the $(m-1)$-dimensional vector obtained by deleting from $y^*(t)$ its ith component.

From the comparison between (37) and (6) with $f(t) \in \Re$ if $q' = m - l_d - 1 \geq 2$, the methods shown in Sections 3 and 3.1 can be exploited for the design of the ith filter. In particular, the parameters of this filter can be properly chosen in order to optimise its performances when a fault is acting on the jth output sensor.

In more detail, as shown in Section 3, $L_{o_i}(s)$ is chosen to maximise the steady-state gain in the presence of the fault $f_{o_j}(t)$. Moreover, as shown in Section 3.1, $R_{o_i}(s)$ is chosen to obtain a fixed behaviour of the transfer function due to the fault $f_{o_j}(t)$.

It is worth noting that the similar design technique can be used for *input sensor* fault isolation.

The problem requirements determine the selection of the specific fault with respect to which the design depends. Most often in practice, it is important to obtain *good* performance with respect to all possible faults rather than *optimal* behaviour with respect to one specific fault. In this situation, a different design of the filter behaviour for each fault situation is needed.

4. NLGA RESIDUAL GENERATORS

The considered NLGA to the FDI problem is suggested in [18] and formally developed in [10]. It consists in finding, by means of a coordinate change in the state space and in the output space, an observable subsystem which, if possible, is affected by the fault and not affected by disturbance. In this way, necessary and sufficient conditions for the FDI problem to be solvable are given. Finally, a residual generator can be designed on the basis of the model of the observable subsystem.

More precisely, the approach considers a nonlinear system model in the form

$$\begin{aligned} \dot{x} &= n(x) + g(x)c + \ell(x)f + p(x)d, \\ y &= h(x) \end{aligned} \tag{38}$$

in which the state vector $x \in \mathcal{X}$ (an open subset of $\Re^{\ell_n}$), $c(t) \in \Re^{\ell_c}$ is the control input vector, $f(t) \in \Re$ is the fault, $d(t) \in \Re^{\ell_d}$ the disturbance vector (embedding also the faults which have to be decoupled), and $y \in \Re^{\ell_m}$ the output vector; whilst $n(x)$, $\ell(x)$, the columns of $g(x)$ and $p(x)$ are smooth vector fields; and $h(x)$ is a smooth map.

Therefore, if P represents the distribution spanned by the column of $p(x)$, the NLGA method can be devised as it follows: first, determine the largest observability codistribution contained in $P^\perp$, denoted with Ω^* [10].

If $\ell(x) \notin \Omega^*$, the design procedure can continue, otherwise, the fault is not detectable; whenever the previous condition is satisfied, it can be found a surjection Ψ_1 and a function Φ_1 fulfilling $\Omega^* \cap \operatorname{span}\{dh\} = \operatorname{span}\{d(\Psi_1 \circ h)\}$ and $\Omega^* = \operatorname{span}\{d(\Phi_1)\}$, respectively. The functions $\Psi(y)$ and $\Phi(x)$ defined as

$$\Psi(y) = \begin{pmatrix} \overline{y}_1 \\ \overline{y}_2 \end{pmatrix} = \begin{pmatrix} \Psi_1(y) \\ H_2 y \end{pmatrix}, \qquad \Phi(x) = \begin{pmatrix} \overline{x}_1 \\ \overline{x}_2 \\ \overline{x}_3 \end{pmatrix} = \begin{pmatrix} \Phi_1(x) \\ H_2 h(x) \\ \Phi_3(x) \end{pmatrix} \tag{39}$$

are (local) diffeomorphisms, where H_2 is a selection matrix (i.e., a matrix in which any row has all 0 entries but one, which is equal to 1), $\Phi_1(x)$ represents the measured part of the state which is affected by f and not affected by d, and

$\Phi_3(x)$ represents the not measured part of the state which is affected by f and by d.

In the new (local) coordinate defined previously, the system of (38) is described by the relations in the form

$$\begin{aligned}
\dot{\overline{x}}_1 &= n_1(\overline{x}_1,\overline{x}_2) + g_1(\overline{x}_1,\overline{x}_2)c + \ell_1(\overline{x}_1,\overline{x}_2,\overline{x}_3)f,\\
\dot{\overline{x}}_2 &= n_2(\overline{x}_1,\overline{x}_2,\overline{x}_3) + g_2(\overline{x}_1,\overline{x}_2,\overline{x}_3)c\\
&\quad + \ell_2(\overline{x}_1,\overline{x}_2,\overline{x}_3)f + p_2(\overline{x}_1,\overline{x}_2,\overline{x}_3)d,\\
\dot{\overline{x}}_3 &= n_3(\overline{x}_1,\overline{x}_2,\overline{x}_3) + g_3(\overline{x}_1,\overline{x}_2,\overline{x}_3)c\\
&\quad + \ell_3(\overline{x}_1,\overline{x}_2,\overline{x}_3)f + p_3(\overline{x}_1,\overline{x}_2,\overline{x}_3)d,\\
\overline{y}_1 &= h(\overline{x}_1),\\
\overline{y}_2 &= \overline{x}_2
\end{aligned} \tag{40}$$

with $\ell_1(\overline{x}_1,\overline{x}_2,\overline{x}_3)$ not identically zero. Denoting $\overline{x}_2$ with $\overline{y}_2$ and considering it as an independent input, it can be singled out the $\overline{x}_1$-subsystem:

$$\begin{aligned}
\dot{\overline{x}}_1 &= n_1(\overline{x}_1,\overline{y}_2) + g_1(\overline{x}_1,\overline{y}_2)c + \ell_1(\overline{x}_1,\overline{y}_2,\overline{x}_3)f,\\
\overline{y}_1 &= h(\overline{x}_1),
\end{aligned} \tag{41}$$

which is affected by the single fault f and decoupled from the disturbance vector. This subsystem has been exploited for the design of the residual generator for the FDI of the fault f.

As already described in Section 2, the proposed NLGA FDI scheme is designed on the basis of a model structure of the input affine type as described in [10]. For this reason, the aircraft simulation model has been simplified and the nonlinear model of (3) has been considered for the NLGA design.

Under these assumptions, by means of computations detailed in [19], the residual generators for detecting the faults affecting the aircraft input sensors are obtained. In particular, the residual generator for the elevator $r_{\delta_e}(t)$, with $k_{\delta_e} > 0$, is described by the relation

$$\begin{aligned}
\dot{\xi}_1 &= \frac{V^2}{m}\left[-(C_{D0} + C_{D\alpha}\alpha + C_{D\alpha_2}\alpha^2)\cos\alpha\right]\\
&\quad + \frac{V^2}{m}(C_{L0} + C_{L\alpha}\alpha)\sin\alpha - g\sin\ \theta\\
&\quad + Vq_\omega\sin\alpha - \frac{(C_{m0} + C_{m\alpha}\alpha + C_{mq}q_\omega)}{mt_d}V^2\\
&\quad - \frac{(I_z - I_x)}{mt_d}p_\omega r_\omega - \frac{C_{\delta_e}}{mt_d}V^2\delta_e\\
&\quad + k_{\delta_e}\left[\left(V\cos\alpha - \frac{I_y}{mt_d}q_\omega\right) - \xi_1\right],\\
r_{\delta_e} &= \left(V\cos\alpha - \frac{I_y}{mt_d}q_\omega\right) - \xi_1.
\end{aligned} \tag{42}$$

The aileron residual generator $r_{\delta_a}(t)$, with $k_{\delta_a} > 0$, has the form

$$\begin{aligned}
\dot{\xi}_2 &= \frac{(C_{l\beta}\beta + C_{lp}p_\omega)}{I_x}V^2 + \frac{(I_y - I_z)}{I_x}q_\omega r_\omega\\
&\quad + \frac{C_{\delta_a}}{I_x}V^2\delta_a + k_{\delta_a}(p_\omega - \xi_2),\\
r_{\delta_a} &= p_\omega - \xi_2.
\end{aligned} \tag{43}$$

The rudder residual generator $r_{\delta_r}(t)$, with $k_{\delta_r} > 0$, is written in the form

$$\begin{aligned}
\dot{\xi}_3 &= \frac{(C_{n\beta}\beta + C_{nr}r_\omega)}{I_z}V^2 + \frac{(I_x - I_y)}{I_z}p_\omega q_\omega\\
&\quad + \frac{C_{\delta_r}}{I_z}V^2\delta_r + k_{\delta_r}(r_\omega - \xi_3),\\
r_{\delta_r} &= r_\omega - \xi_3.
\end{aligned} \tag{44}$$

The throttle residual generator $r_{\delta_{\text{th}}}(t)$, with $k_{\delta_{\text{th}}} > 0$, has the form

$$\begin{aligned}
\dot{\xi}_4 &= t_n n_e^3 + \frac{t_f}{n_e}(t_0 + t_1 n_e)\delta_{\text{th}} + k_{\delta_{\text{th}}}(n_e - \xi_4),\\
r_{\delta_{\text{th}}} &= n_e - \xi_4.
\end{aligned} \tag{45}$$

Remark 10. It is worth observing that each residual generator is affected by a single input sensor fault and is decoupled from the wind components and the faults affecting the remaining input sensors. This feature can be obtained by defining a different $p(x)$ for each residual generator design [19]. In this way, the tuning of the residual generator gains k_{δ_e}, k_{δ_a}, k_{δ_r}, and $k_{\delta_{th}}$ can be carried out independently. Finally, by a straightforward analysis, the positive sign of each gain is a necessary and sufficient condition for the asymptotic stability of the dynamics (42)–(45).

A procedure optimising the tradeoff between the fault sensitivity and the robustness to the modelling errors and disturbances of the generic residual generator is proposed in the next section.

4.1. NLGA robustness improvement

The proposed NLGA-based scheme consists of two design steps:

(1) the structural decoupling of critical disturbances (wind gust and turbulence) and critical modelling errors can be obtained as described in Section 4;
(2) the nonlinear residual generators robustness is improved by minimising the effects of both noncritical disturbances and modelling errors, whilst maximising the fault effects on the residual signals.

In order to apply the robustness improvement procedure presented in this section, the considered framework is restricted to suitable scalar components of the $\overline{x}_1$-subsystem (41). In particular, the vectors $\overline{x}_1$ and $\overline{y}_1$ are decomposed as follows:

$$\overline{x}_1 = \begin{bmatrix}\overline{x}_{11}\\ \overline{x}_{1c}\end{bmatrix}, \qquad \overline{y}_1 = \begin{bmatrix}\overline{y}_{11}\\ \overline{y}_{1c}\end{bmatrix}, \tag{46}$$

where $\overline{x}_{11} \in \Re$, $\overline{y}_{11} \in \Re$, and, correspondingly, it follows that

$$n_1(\cdot) = \begin{bmatrix} n_{11}(\cdot) \\ n_{1c}(\cdot) \end{bmatrix}, \quad g_1(\cdot) = \begin{bmatrix} g_{11}(\cdot) \\ g_{1c}(\cdot) \end{bmatrix}, \quad \ell_1(\cdot) = \begin{bmatrix} \ell_{11}(\cdot) \\ \ell_{1c}(\cdot) \end{bmatrix} \tag{47}$$

Let us consider the following conditions:

$$\overline{y}_{11} = h_{11}(\overline{x}_{11}) \qquad \overline{y}_{1c} = h_{1c}(\overline{x}_{1c}) \qquad \ell_{11}(\cdot) \neq 0\,, \tag{48}$$

where $h_{11}(\cdot)$ is a smooth map and $h_{1c}(\cdot)$ is an invertible smooth map. It is important to highlight that if the constraints (48) are satisfied, the decomposition (46)-(47) can always be applied to obtain the following $\overline{x}_{11}$-subsystem:

$$\begin{aligned} \dot{\overline{x}}_{11} &= n_{11}(\overline{x}_{11}, \overline{y}_{1c}, \overline{y}_2) + g_{11}(\overline{x}_{11}, \overline{y}_{1c}, \overline{y}_2)c \\ &\quad + \ell_{11}(\overline{x}_{11}, \overline{y}_{1c}, \overline{y}_2, \overline{x}_3) f, \\ \overline{y}_{11} &= h_{11}(\overline{x}_{11}). \end{aligned} \tag{49}$$

As can be seen in [19], the conditions (48) are satisfied for the considered aircraft application, hence, from now on, the scalar $\overline{x}_{11}$-subsystem (49) is referred to in place of the $\overline{x}_1$-subsystem (41).

It can be noted that the tuning of the residual generator gains, in the framework of the $\overline{x}_{11}$-subsystem (49), cannot be properly carried out. In fact, the critical disturbances are structurally decoupled but the noncritical ones are not considered. For this reason, to achieve robustness of the residual generators, the tuning of the gains is performed by embedding the description of the noncritical disturbances in the $\overline{x}_{11}$-subsystem as follows:

$$\begin{aligned} \dot{\overline{x}}_{11} &= n_{11}(\overline{x}_{11}, \overline{y}_{1c}, \overline{y}_2) + g_{11}(\overline{x}_{11}, \overline{y}_{1c}, \overline{y}_2)c \\ &\quad + \ell_{11}(\overline{x}_{11}, \overline{y}_{1c}, \overline{y}_2, \overline{x}_3) f + e(\overline{x}_{11}, \overline{y}_{1c}, \overline{y}_2, \overline{x}_3)\zeta, \\ \overline{y}_{11} &= \overline{x}_{11} + \nu, \end{aligned} \tag{50}$$

where, to simplify the treatment without loss of generality (accordingly to the considered aircraft application), the state variable $\overline{x}_{11}$ is supposed to be directly measured. Moreover, the variable $\nu \in \Re$ is the measurement noise on $\overline{x}_{11}$. Finally, the variable $\zeta \in \Re$ and the related scalar field $e(\cdot)$ represent the noncritical effects which have not been considered in the simplified aircraft model (3) used for the NLGA scheme.

The following system, which is referred to as *filter form*, represents a generic scalar residual generator (based on the subsystem (50)) to which (42)–(45) belong as a particular case

$$\begin{aligned} \dot{\xi}_f &= n_{11}(\overline{y}_{11}, \overline{y}_{1c}, \overline{y}_2) + g_{11}(\overline{y}_{11}, \overline{y}_{1c}, \overline{y}_2)c + k_f(\overline{y}_{11} - \xi_f), \\ r_f &= \overline{y}_{11} - \xi_f, \end{aligned} \tag{51}$$

where the gain k_f has to be tuned in order to minimise the effects of the disturbances ζ and ν whilst maximise the effects of the fault f on the residual r_f. The quantification both of the disturbances and of the fault effects on the residual can be obtained by defining the estimation error

$$\widetilde{x}_f = \overline{x}_{11} - \xi_f, \tag{52}$$

which allows to write the following equivalent residual model:

$$\begin{aligned} \dot{\widetilde{x}}_f &= n_{11}(\overline{x}_{11}, \overline{y}_{1c}, \overline{y}_2) - n_{11}(\overline{y}_{11}, \overline{y}_{1c}, \overline{y}_2) \\ &\quad + g_{11}(\overline{x}_{11}, \overline{y}_{1c}, \overline{y}_2)c - g_{11}(\overline{y}_{11}, \overline{y}_{1c}, \overline{y}_2)c \\ &\quad + \ell_{11}(\overline{x}_{11}, \overline{y}_{1c}, \overline{y}_2, \overline{x}_3) f + e(\overline{x}_{11}, \overline{y}_{1c}, \overline{y}_2, \overline{x}_3)\zeta \\ &\quad - k_f \widetilde{x}_f - k_f \nu, \\ r_f &= \widetilde{x}_f + \nu. \end{aligned} \tag{53}$$

In order to apply the effective mixed $\mathcal{H}_-/\mathcal{H}_\infty$ approach [3, 20] to tune k_f, the system (53) has to be linearised in the neighbourhood of a stationary flight condition, as suggested in [2] with reference to the $\mathcal{H}_\infty$ optimisation of nonlinear unknown input observers. It is worth observing that the considered aircraft application is characterised by small excursions of the state, input, and output variables with respect to their trim values $\overline{x}_{10}$, $\overline{x}_{30}$, c_0, $\overline{y}_{10}$, and $\overline{y}_{20}$, hence the robustness of the nonlinear residual generator is achieved. The linearisation of (53) is the following:

$$\begin{aligned} \dot{\widetilde{x}}_f &= -k_f \widetilde{x}_f - k_f \nu + \mathrm{mf} + \breve{q}\breve{\zeta}, \\ r_f &= \widetilde{x}_f + \nu, \end{aligned} \tag{54}$$

where

$$\begin{aligned} a' &= \left.\frac{\partial n_{11}(\cdot)}{\partial \overline{x}_{11}}\right|_{(\overline{x}_{10}, \overline{y}_{20})}, \qquad b = g_{11}(\cdot)|_{(\overline{x}_{10}, \overline{y}_{20})}, \\ m &= \ell_{11}(\cdot)|_{(\overline{x}_{10}, \overline{y}_{20}, \overline{x}_{30})}, \qquad q = e(\cdot)|_{(\overline{x}_{10}, \overline{y}_{20}, \overline{x}_{30})}, \\ \breve{q}\breve{\zeta} &= q\zeta - a'\nu. \end{aligned} \tag{55}$$

Now, it is important to note that in place of the residual generators in the *filter form* (51), the following *observer form* of the residual generators can be used:

$$\begin{aligned} \dot{\xi}_o &= n_{11}(\xi_o, \overline{y}_{1c}, \overline{y}_2) + g_{11}(\xi_o, \overline{y}_{1c}, \overline{y}_2)c + k_o(\overline{y}_{11} - \xi_o), \\ r_o &= \overline{y}_{11} - \xi_o. \end{aligned} \tag{56}$$

For the same reasons previously described, the estimation error $\widetilde{x}_o$ is introduced:

$$\widetilde{x}_o = \overline{x}_{11} - \xi_o, \tag{57}$$

hence

$$\begin{aligned} \dot{\widetilde{x}}_o &= n_{11}(\overline{x}_{11}, \overline{y}_{1c}, \overline{y}_2) - n_{11}(\xi_o, \overline{y}_{1c}, \overline{y}_2) \\ &\quad + g_{11}(\overline{x}_{11}, \overline{y}_{1c}, \overline{y}_2)c - g_{11}(\xi_o, \overline{y}_{1c}, \overline{y}_2)c \\ &\quad + \ell_{11}(\overline{x}_{11}, \overline{y}_{1c}, \overline{y}_2, \overline{x}_3) f + e(\overline{x}_{11}, \overline{y}_{1c}, \overline{y}_2, \overline{x}_3)\zeta \\ &\quad - k_o \widetilde{x}_o - k_o \nu, \\ r_o &= \widetilde{x}_o + \nu. \end{aligned} \tag{58}$$

The linearisation of (58) is

$$\begin{aligned} \dot{\widetilde{x}}_o &= (a' - k_o)\widetilde{x}_o - k_o \nu + \mathrm{mf} + q\zeta, \\ r_o &= \widetilde{x}_o + \nu. \end{aligned} \tag{59}$$

Both the linearised models (54) and (59) of the residual generators in the *filter form* and *observer form*, respectively, can be represented by the following *general form*:

$$\begin{aligned}\dot{\widetilde{x}} &= (a-k)\widetilde{x} + (E_1 - kE_2)\varepsilon + \mathrm{mf},\\ r &= \widetilde{x} + E_2\varepsilon\end{aligned} \tag{60}$$

with $E_1 = [cce_{11} \quad 0]$ as well as the following positions:

$$\begin{aligned}&\text{general form} \quad \widetilde{x} \quad \varepsilon \quad r \quad a \quad k \quad e_{11} \quad E_2\\ &\text{filter form} \quad \widetilde{x}_f \quad \begin{bmatrix}\check{\zeta}\\ \nu\end{bmatrix} \quad r_f \quad 0 \quad k_f \quad \check{q} \quad \begin{bmatrix}0 & 1\end{bmatrix}\\ &\text{observer form} \quad \widetilde{x}_o \quad \begin{bmatrix}\zeta\\ \nu\end{bmatrix} \quad r_o \quad a \quad k_o \quad q \quad \begin{bmatrix}0 & 1\end{bmatrix}.\end{aligned} \tag{61}$$

On the basis of (60) and (61), the mixed $\mathcal{H}_-/\mathcal{H}_\infty$ [3, 20] procedure is developed for the robustness improvement of the residual generators both in the *filter* and *observer* form. Since the considered NLGA residual generators are scalar, the $\mathcal{H}_-/\mathcal{H}_\infty$ procedure leads to a new analytical solution.

The following definition will be used throughout the section.

Definition 2. The norms $\mathcal{H}_\infty$ and $\mathcal{H}_-$ of a stable transfer function G are defined as

$$\|G\|_\infty = \sup_{\omega\geq 0} \overline{\sigma}[G(j\omega)], \qquad \|G\|_- = \underline{\sigma}[G(j0)], \tag{62}$$

where $\overline{\sigma}$ represents the maximum singular value, whilst $\underline{\sigma}$ the minimum singular value. The problem of the tradeoff between disturbances robustness and fault sensitivity is stated as follows.

Problem 1 (Mixed $\mathcal{H}_-/\mathcal{H}_\infty$ residual robustness improvement). Given two scalars $\beta > 0$ and $\gamma > 0$, find the set $\mathcal{K}$ defined as:

$$\mathcal{K} = \{k \in \Re : (a-k) < 0,\ \|G_{r\varepsilon}\|_\infty < \gamma,\ \|G_{rf}\|_- > \beta\}, \tag{63}$$

where

$$G_{r\varepsilon}(s) = (s-a+k)^{-1}(E_1 - kE_2) + E_2, \tag{64}$$

$$G_{rf}(s) = (s-a+k)^{-1}m. \tag{65}$$

In order to obtain the analytical solution of Problem 1, the following propositions are given.

Proposition 3. *For all $k \in \Re, (a-k) < 0$, then*

$$\left\|G_{r\varepsilon}\right\|_\infty^2 = \max\left\{1, \frac{(e_{11}^2 + a^2)}{(k-a)^2}\right\}, \tag{66}$$

$$\sup_{\{k\in\Re:(a-k)<0\}} \left\|G_{r\varepsilon}\right\|_\infty = +\infty. \tag{67}$$

Proof. From the definition (64)

$$G_{r\varepsilon}(s) = \left[\frac{e_{11}}{s-a+k} \quad \frac{s-a}{s-a+k}\right], \tag{68}$$

hence it is possible to write

$$\begin{aligned}\{\overline{\sigma}[G_{r\varepsilon}(j\omega)]\}^2 &= \frac{e_{11}^2}{(k-a)^2+\omega^2} + \frac{a^2+\omega^2}{(k-a)^2+\omega^2}\\ &= \frac{(e_{11}^2+a^2)+\omega^2}{(k-a)^2+\omega^2}\end{aligned} \tag{69}$$

so that it follows

$$\left\|G_{r\varepsilon}\right\|_\infty^2 = \sup_{\xi\geq 0} \frac{(e_{11}^2+a^2)+\xi}{(k-a)^2+\xi}. \tag{70}$$

From the last expression, it is straightforward to obtain (66) and (67). □

Proposition 4. *The set*

$$\mathcal{K}_\gamma = \{k \in \Re : (a-k) < 0,\ \left\|G_{r\varepsilon}\right\|_\infty < \gamma,\ \gamma > 1\} \tag{71}$$

is given by

$$k > \underline{k} \quad \text{with } \underline{k} = a + \frac{\sqrt{e_{11}^2+a^2}}{\gamma}. \tag{72}$$

Proof. By means of Proposition 3, it is possible to write

$$\frac{(e_{11}^2+a^2)}{(k-a)^2} < \gamma^2, \tag{73}$$

which holds for

$$k > a + \frac{\sqrt{e_{11}^2+a^2}}{\gamma}. \tag{74}$$

□

Proposition 5. *If $\gamma > 1$, then $\{\|G_{rf}\|_- : \|G_{r\varepsilon}\|_\infty < \gamma\}$ is given by*

$$0 < \|G_{rf}\|_- < \beta_{\max}(\gamma) \quad \text{where } \beta_{\max}(\gamma) = \frac{m\gamma}{\sqrt{e_{11}^2+a^2}}. \tag{75}$$

Proof. From the definition (65), it results $G_{rf}(s) = m/(s - a+k)$ and assuming, without loss of generality, that $m > 0$, it follows $\|G_{rf}\|_- = m/(k-a)$. By imposing $\|G_{rf}\|_- > \beta$ with $\beta > 0$, the constraint $k < a + (m/\beta)$ has to hold. Then, by recalling the result of Proposition 4, the maximum feasible value of β fulfilling the constraint $\|G_{r\varepsilon}\|_\infty < \gamma$ is given by

$$\underline{k} = a + \frac{m}{\beta_{\max}(\gamma)}, \tag{76}$$

hence

$$\beta_{\max}(\gamma) = \frac{m}{\underline{k}-a} = \frac{m\gamma}{\sqrt{e_{11}^2+a^2}}. \tag{77}$$

□

Theorem 1. *Given $\gamma > 1$ and $\beta \in]0, \beta_{\max}(\gamma)[$, the set $\mathcal{K}$ fulfilling the constraints of Problem 1 is given by*

$$\mathcal{K} = \left\{ k \in \mathcal{R} : k \in]\underline{k}, \overline{k}[, \underline{k} = a + \frac{m}{\beta_{\max}(\gamma)}, \overline{k} = a + \frac{m}{\beta} \right\}. \tag{78}$$

Proof. The proof of the theorem is not reported, as it is straightforward from Propositions 3, 4, and 5. □

Remark 11. Let us consider the following performance index to maximise

$$J = \frac{\|G_{rf}\|_-}{\|G_{r\varepsilon}\|_\infty}. \tag{79}$$

From (66), it follows

$$\|G_{r\varepsilon}\|_\infty = \begin{cases} 1, & k > \left(a + \sqrt{e_{11}^2 + a^2}\right) \\ \dfrac{\sqrt{e_{11}^2 + a^2}}{k - a}, & a < k \le \left(a + \sqrt{e_{11}^2 + a^2}\right) \end{cases} \tag{80}$$

hence

$$J = \begin{cases} \dfrac{m}{k - a}, & k > \left(a + \sqrt{e_{11}^2 + a^2}\right), \\ \dfrac{m}{\sqrt{e_{11}^2 + a^2}}, & a < k \le \left(a + \sqrt{e_{11}^2 + a^2}\right). \end{cases} \tag{81}$$

From (81), it can be observed that

$$J = \frac{m}{k - a} < \frac{m}{\sqrt{e_{11}^2 + a^2}}, \quad k > \left(a + \sqrt{e_{11}^2 + a^2}\right). \tag{82}$$

In this way, the maximum value of the performance index J is

$$J_{\max} = \frac{m}{\sqrt{e_{11}^2 + a^2}} \quad \forall k \in \mathcal{K}_{\mathcal{J}} = \left\{ k \in \Re : a < k \le \left(a + \sqrt{e_{11}^2 + a^2}\right) \right\}. \tag{83}$$

The method proposed in this paper guarantees the maximum value of the performance index J as well as the constraints $\|G_{r\varepsilon}\|_\infty < \gamma$ and $\|G_{rf}\|_- > \beta$ if $\beta \ge m/\sqrt{e_{11}^2 + a^2}$.

In fact, from $\beta \ge m/\sqrt{e_{11}^2 + a^2}$ it follows

$$\|G_{rf}\|_- = \frac{m}{k - a} > \beta \ge \frac{m}{\sqrt{e_{11}^2 + a^2}}, \tag{84}$$

hence $k < (a + \sqrt{e_{11}^2 + a^2})$.

Finally, from (75) it is always possible to find a β such that

$$\frac{m}{\sqrt{e_{11}^2 + a^2}} \le \beta \le \beta_{\max}(\gamma) \quad \forall \gamma > 1. \tag{85}$$

On the basis of Theorem 1, k can be designed by means of the following procedure.

Procedure 1. (1) Choose $\gamma > 1$ to obtain a desired level of disturbance attenuation.

(2) Compute $\beta_{\max}(\gamma)$ and choose $\beta \in]0, \beta_{\max}(\gamma)[$ to obtain a desired level of fault sensitivity.

(3) Choose $k \in]\underline{k}, \overline{k}[$, with $\underline{k} = a + m/\beta_{\max}(\gamma)$ and $\overline{k} = a + m/\beta$.

(4) Apply the chosen gain k to the k_f of (51) or to the k_o of (56) if the NLGA residual generator is in the *filter form* or in the *observer form*, respectively.

5. FDI PERFORMANCE ESTIMATION

To show the diagnostic characteristics brought by the application of the proposed FDI schemes to general aviation aircrafts, some numerical results obtained in the Matlab and Simulink environments are reported. The final performances that are achieved with the developed FDI schemes are finally reported. These performances are evaluated by means of extensive simulations applied to the aircraft simulation model. This section presents also some comparisons of the developed PM and NLGA FDI strategies with NN and UIKF FDI schemes.

The designed PM residual generator filters are fed by the 4 component input vector $c(t)$ and the 9 component output vector $y(t)$ acquired from the simulation aircraft model previously described. In particular, a bank of 4 residual generator filters has been used to detect input sensor faults regarding the 4 input control variables. Moreover, in order to obtain the fault isolation properties, each residual generator function of the considered bank is fed by all but one of the 4 control input signals and by the 9 output variables. Obviously, the residual generator bank has been designed to be decoupled from the 3 component wind disturbance vector $d(t) = [w_u(t), w_v(t), w_w(t)]^T$. As to the NLGA residual generator filters, the aircraft synthesis model of (3), adopted for the design, is simplified with respect to the simulation model. Analogously to the PM, the approximations of the NLGA synthesis nonlinear model are related to a particular steady-state flight condition. For this reason, the switching for the NLGA FDI scheme is also required when a generic reference trajectory is followed. Hence, it is important to evaluate the robustness characteristic of a single design of NLGA residual generators when a large set of flight conditions is dealt with.

It is worth noting that the aircraft reference trajectories are typically made up of a sequence of steady-state flight conditions, each one described by the associated input state output set point and the linearised model of (1). As a consequence, all the FDI linear techniques are usually implemented by switching among the residual generators related to the different steady-state flight conditions. The target of this work is to reduce the switching by adopting robust PM residual generators. In particular, the robustness is achieved by using the same residual generators for a large set of flight conditions. The chosen single steady-state flight condition for designing both of the PM and of the NLGA residual

generators is a coordinated turn characterised as follows:

(i) the true airspeed is 50 m/s;
(ii) the curvature radius is 1000 m;
(iii) the flight-path angle is 0°;
(iv) the altitude is 330 m;
(v) the flap deflection is 0°.

This represents one of most general flight condition due to the coupling of the longitudinal and lateral dynamics. Moreover, it is used in simulation to highlight the performances of the proposed methods in the nominal flight condition.

Regarding the PM, the detection properties of the filters in terms of fault sensitivity and disturbance rejection can be achieved according to Section 3. The synthesis of the dynamic filters for FDI has been performed by choosing a suitable linear combination of residual generator functions. This choice has to maximise the steady-state gain of the transfer functions between input sensor fault signals. The roots of the $R(s)$ polynomial matrix have been optimised for maximising the fault detection promptness, as well as to minimise the occurrence of false alarms. In order to assess the PM diagnosis technique, different fault sizes have been simulated on each sensor. Single faults in the input sensors have been generated by producing abrupt (step) and ramp (slowly developing) faults in the input signals $c(t)$. The residual signals indicate fault occurrence according to whether their values are lower or higher than the thresholds fixed in fault-free conditions. The residual processing methods can be based on simple residual geometrical analysis or comparison with fixed thresholds [3]. More complex residual evaluation can rely on statistical properties of the residuals and hypothesis testing [6], or based on adaptive thresholds, that is, the so-called threshold selector [21].

In this paper, the threshold test for FDI is performed with the logic described by (86):

$$\begin{aligned} &\overline{r} - \nu\sigma_r \le r(t) \le \overline{r} + \nu\sigma_r \quad \text{for } f(t) = 0, \\ &r(t) < \overline{r} - \nu\sigma_r \quad \text{or} \quad r(t) > \overline{r} + \nu\sigma_r \quad \text{for } f(t) \neq 0, \end{aligned} \tag{86}$$

that is, the comparison of $r(t)$ with respect its statistical normal characteristics. $\overline{r}$ and σ_r^2 are the normal values for the mean and variance of the fault-free residual, respectively. In order to separate normal from faulty behaviour, the tolerance parameter ν (normally $\nu \ge 3$) is selected and properly tuned. Hence, by a proper choice of the parameter ν, a good trade-off can be achieved between the maximisation of fault detection probability and the minimisation of false-alarm probability. In practice, the threshold values depend on the residual error amount due to measurement errors, linearised model approximations, and disturbance signals that are not completely decoupled.

Thus, in this case, a suitable value of $\nu = 4$ for the computation of the positive and negative thresholds in (86) has been considered. To summarise the performances of the PM FDI scheme, the minimal detectable step faults on the various input sensors are collected in Table 2.

On the other hand, the minimal detectable ramp faults are reported in Table 3.

Table 2: PM FDI technique: minimal *step* faults with $\nu = 4$.

$c_i(t)$	Variable	Fault size	Delay time
Elevator	δ_e	2°	18 s
Aileron	δ_a	3°	6 s
Rudder	δ_r	4°	8 s
Throttle aperture %	δ_{th}	2%	15 s

Table 3: PM FDI technique: minimal *ramp* faults with $\nu = 4$.

$c_i(t)$	Variable	Fault size	Delay time
Elevator	δ_e	0.11°/s	26 s
Aileron	δ_a	0.50°/s	11 s
Rudder	δ_r	0.49°/s	12 s
Throttle aperture %	δ_{th}	0.13°/s	19 s

Table 4: NLGA FDI technique: minimal *step* faults with $\nu = 8$.

$c_i(t)$	Variable	Fault size	Delay time
Elevator	δ_e	2°	5 s
Aileron	δ_a	2°	3 s
Rudder	δ_r	2°	6 s
Throttle aperture %	δ_{th}	6%	3 s

Table 5: NLGA FDI technique: minimal *ramp* faults with $\nu = 8$.

$c_i(t)$	Variable	Fault size	Delay time
Elevator	δ_e	0.21°/s	11 s
Aileron	δ_a	0.45°/s	12 s
Rudder	δ_r	0.32°/s	10 s
Throttle aperture %	δ_{th}	0.15°/s	15 s

Concerning the NLGA, the synthesis of the residual generators has been performed by using filter gains that optimise the fault sensitivity and reduce as much as possible the occurrence of false alarms due to model uncertainties and to disturbances not completely decoupled. This robustness requirement has been fulfilled by designing the residual gains according to the Procedure 1. For example, with reference to the fourth residual generator, Procedure 1 has led to $K_{\delta_{\text{th}}} = 1$ which satisfies the norm bounds $\gamma = 1.2$ and $\beta = 400$. This guarantees a good separation of the residual signal with $\|f\|_{\mathcal{L}_2} \ge 0.05$ and $\|d\|_{\mathcal{L}_2} \le 10$, where $\mathcal{L}_2$-norm is considered.

In order to assess the NLGA diagnosis technique, single step and ramp faults have been used. Moreover, also in this case the threshold values have been chosen in simulation according to (86). A suitable value of $\nu = 8$ for the computation of the positive and negative thresholds in (86) has been considered. For what concern NLGA FDI scheme, the minimal detectable step faults on the various input sensors are summarised in Table 4.

On the other hand, the minimal detectable input sensor ramp faults are reported in Table 5.

The minimal detectable step fault values in Tables 2, 3, 4, and 5 are expressed in the unit of measure of the sensor signals. The fault step sizes and ramp slopes are relative to the

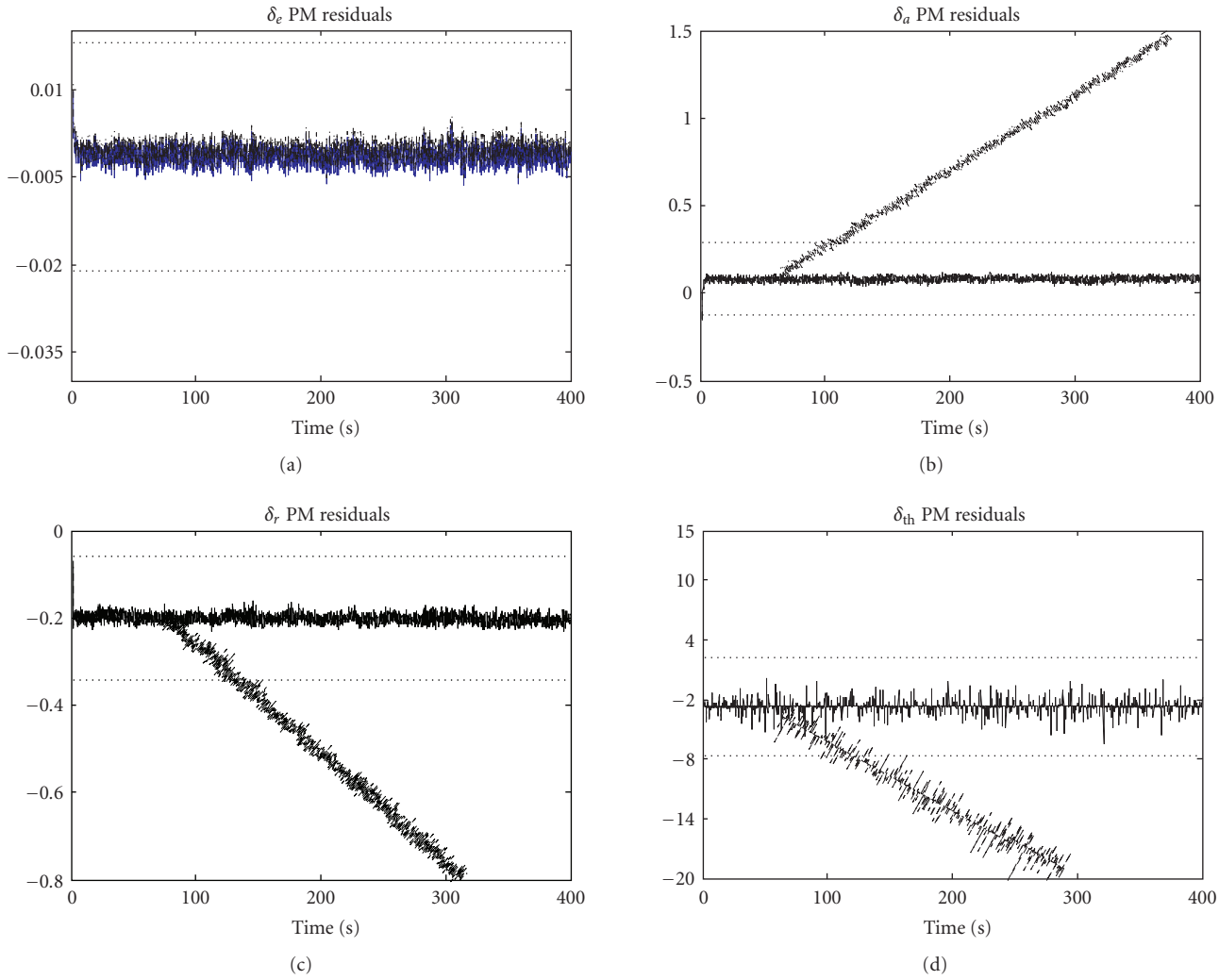

FIGURE 1: PM residuals for the 1st input sensor ramp fault $f_{c_1}(t)$ isolation with $\nu = 4$.

case in which the occurrence of a fault is detected and isolated as soon as possible. The detection delay times represent the worst case results, as they are evaluated on the basis of the time taken by the slowest residual function to cross the settled threshold. These experiments represent a further validation of the residual generator robustness with respect to the fault type, as the the residual function sensitivity was optimised only with respect to step faults.

As an example, Figure 1 shows the 4 PM residual functions generated for the complete trajectory. On the basis of the fault-free and faulty conditions, this bank provides the correct isolation of the considered input sensor *ramp* fault.

The horizontal lines represent the levels of the fault-free thresholds that are settled according to test (86) with $\nu = 4$. The first residual function depicted in Figure 1, provides also the isolation of the fault $f_c(t)$ regarding the 1st input sensor.

The second example of Figure 2 shows the 4 residual functions generated by the NLGA filter bank applied to the complete aircraft trajectory. The horizontal lines represent the thresholds with $\nu = 12$. Note that, due to the NLGA design technique, only the 1st residual related to the δ_e signal of the filter bank is sensitive to a *ramp* fault affecting the 1st input sensor.

5.1. Reliability and robustness evaluation

In this section, the robustness characteristics of the proposed PM and NLGA FDI schemes have been evaluated and compared also with respect to the UIKF scheme [3] and the NN technique [7]. In particular, a bank of UIKF has been exploited for diagnosing faults of the monitored process. This technique seems to be robust with respect to the modelling uncertainties, the system parameter variations, and the measurement noise, which can obscure the performance of an FDI system by acting as a source of false faults. The procedure recalled here requires the design of a UIKF bank and the basic scheme is the standard one: a set of measured variables of the system is compared with the corresponding signals estimated by filters to generate residual functions. The diagnosis has been performed by detecting the changes of UIKF residuals caused by a fault. The FDI input sensor scheme exploits a

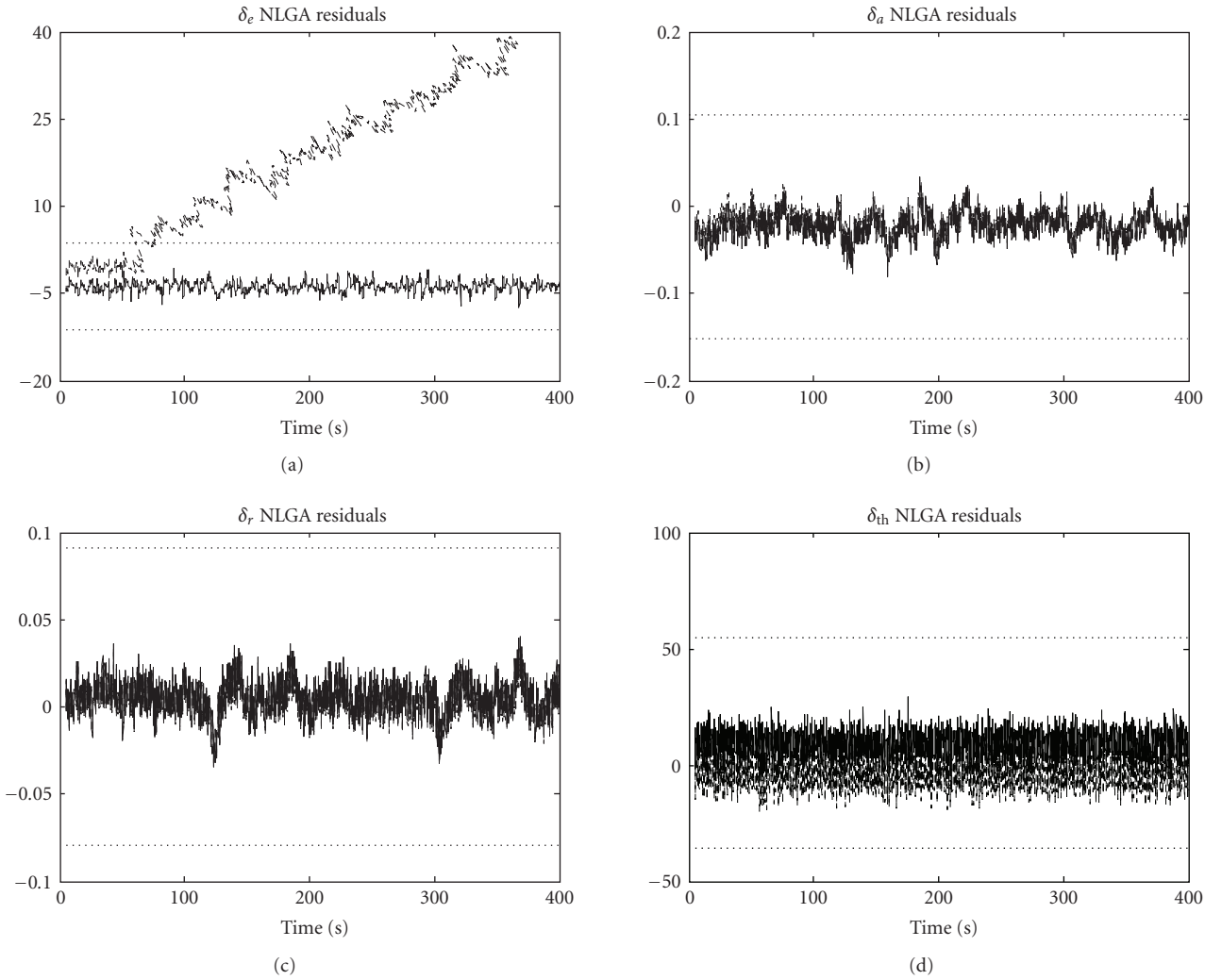

Figure 2: NLGA residuals for the 1st input sensor fault isolation with $\nu = 12$.

number of KF equal to the number of input variables. Each filter is designed to be insensitive to a different input sensor of the process and its disturbances (the so-called unknown inputs). Moreover, the considered UIKF bank was obtained by following the design technique described in [3, Section 3.5, pages 99–105], whilst the noise covariance matrices were estimated as described in [22, Section 3.3, pages 70–74 and Section 4.6, pages 130-131]. Each of the 4 UIKF of the bank was decoupled from both one input sensor fault and the wind gust disturbance component, thus providing the optimal filtering of the input-output measurement noise sequences. On the other hand, a dynamic NN bank has been exploited in order to find the dynamic connection from a particular fault regarding the input sensors to a particular residual. In this case, the learning capability of NN is used for identifying the nonlinear dynamics of the monitored plant. The dynamic NN provides the prediction of the process output with an arbitrary degree of accuracy, depending on the NN structure, its parameters, and a sufficient number of neurons. Once the NN has been properly trained, the residuals have been computed as the difference between predicted and measured process outputs. The FDI is therefore achieved by monitoring residual changes. The NN learning is typically an offline procedure. Normal operation data are acquired from the monitored plant and are exploited for the NN training. Regarding the NN FDI method and according to a generalised observer scheme (GOS) [3], a bank of 4 time-delayed three-layers multilayer perceptron (MLP) NN with 15 neurons in the input layer, 25 neurons in the hidden layer, and 1 neuron in the output layer is implemented. Each NN was designed to be insensitive to each input sensor fault, and the NN were trained in order to provide the optimal output prediction on the basis of the training pattern and target sequences [7].

In the following of this section, the performances of the different FDI schemes have been evaluated by considering a more complex aircraft trajectory. This has been obtained by means of the guidance and control functions of a standard autopilot which stabilises the aircraft motion towards the reference trajectory as depicted in Figure 3. The reference trajectory is made up of 4 branches (2 straight flights and 2 turn flights) so that a closed path is obtained. It is worth observing that only 2 steady-state flight conditions are used to follow

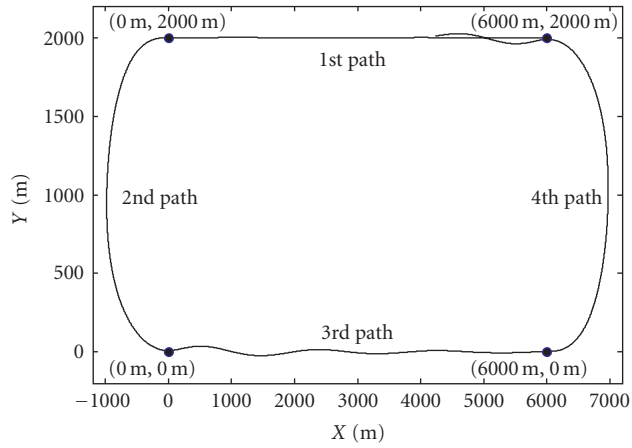

Figure 3: Aircraft complete trajectory example.

Table 6: Performances of the FDI schemes for a complete aircraft trajectory.

Variable	PM	NLGA	UIKF	NN
ν	4	12	9	5
δ_e	4°	3°	4°	3°
δ_a	5°	3°	5°	4°
δ_r	5°	3°	4°	4°
δ_{th}	7%	10%	11%	12%
Mean detection delay	26 s	25 s	31 s	27 s

alternatively the 4 branches of the reference trajectory:

(i) *straight flight condition:* true airspeed = 50 [m/s]; radius of curvature = ∞; flight-path angle = 0°; altitude = 330 [m]; flap deflection = 0°;

(ii) *turn flight condition:* true airspeed = 50 [m/s]; radius of curvature = 1000 [m]; flight-path angle = 0°; altitude = 330 [m]; flap deflection = 0°.

The reference turn flight condition is used to design the PM and the NLGA filters. The achieved results are reported in Tables 2 and 4, respectively. The performed tests represent a also a possible reliability evaluation of the considered FDI techniques. In fact, in this case the diagnosis requires that the residual generators are robust with respect to the flight conditions that do not match the nominal trajectory used for the design.

As an example, the fault-free and faulty residuals generated by the designed NN and UIKF banks are shown in Figures 4 and 5, respectively.

Table 6 summarises the results obtained by considering the observers and filters (corresponding to the PM, NLGA, UIKF,and NN) for the input sensor FDI whose parameters have been designed and optimised for the steady-state coordinated turn represented by the 2nd reference flight condition of the complete trajectory. Table 6 reports the performances of the considered FDI techniques in terms of the minimal detectable step faults on the various input sensors, as well as the corresponding parameters ν for the residual evaluation of (86). The mean detection delay is also reported in Table 6 in order to compare the effectiveness of the different FDI schemes.

The choice of ν has been performed with reference to the particular flight conditions involved in the complete trajectory following. In particular, the selected value of ν for each FDI observer or filter represents a tradeoff between two objectives, that is, for increasing the residual fault sensitivity and promptness, as well as for minimising the occurrence of false alarms due to the switching among the reference flight conditions needed to stabilise the aircraft motion towards the reference trajectory. Table 6 shows how the proper design of the parameter ν allows to obtain good performances with all the considered FDI schemes, hence the robustness with respect to the proposed complete trajectory is always achieved.

It is worth noting that the NLGA has a theoretical advantage by taking into account the nonlinear dynamics of the aircraft. However, the behaviour of the related nonlinear residual generators is quite sensitive to the model uncertainties due to variation of the flight condition. In fact, the NLGA FDI scheme requires high values of ν which have to be increased (from 8 to 12 in this work) when the aircraft motion regarding the complete trajectory is considered in place of the nominal flight condition. In particular, even though the analysis was restricted just to the aircraft turn phase of the complete trajectory, a performance worsening would happen, since the steady-state condition (nominal flight condition) is quite far to be reached. However, the filter design based on the NLGA lead to a satisfactory fault detection, above all in terms of promptness. On the other hand, regarding the PM, it is rather simple to note the good FDI performances, even if optimisation stages can be required. The ν values selected for the PM are lower, but the related residual fault sensitivities are even smaller. Similar comments can be made for the UIKF and NN techniques.

The simulation model applied to the complete trajectory is an effective way to test the performances of the proposed FDI methods with respect to modelling mismatch and measurement errors. The obtained results demonstrate the reliability of the PM-, NLGA-, UIKF-, and NN-based FDI schemes as long as proper design procedures are adopted.

5.2. Monte Carlo analysis

In this section, further experiment results have been reported. They regard the performance evaluation of the developed FDI scheme with respect to uncertainty acting on the system. Hence, the simulation of different fault-free and faulty data sequences was performed by exploiting the aircraft Matlab-Simulink simulator and a *Monte Carlo analysis* implemented in the Matlab environment. The Monte Carlo tool is useful at this stage as the FDI performances depend on the residual error magnitude due to the system uncertainty, as well as the signal $c(t)$ and $y(t)$ measurement errors. It is worth noting how the Monte Carlo simulations have been achieved by perturbing the parameters of the PM filter residuals by additive white Gaussian noises with standard deviation values equal to a fixed percentage p of the element values. The same experiments have been performed by statistically varying the main parameters of the NLGA filters. In

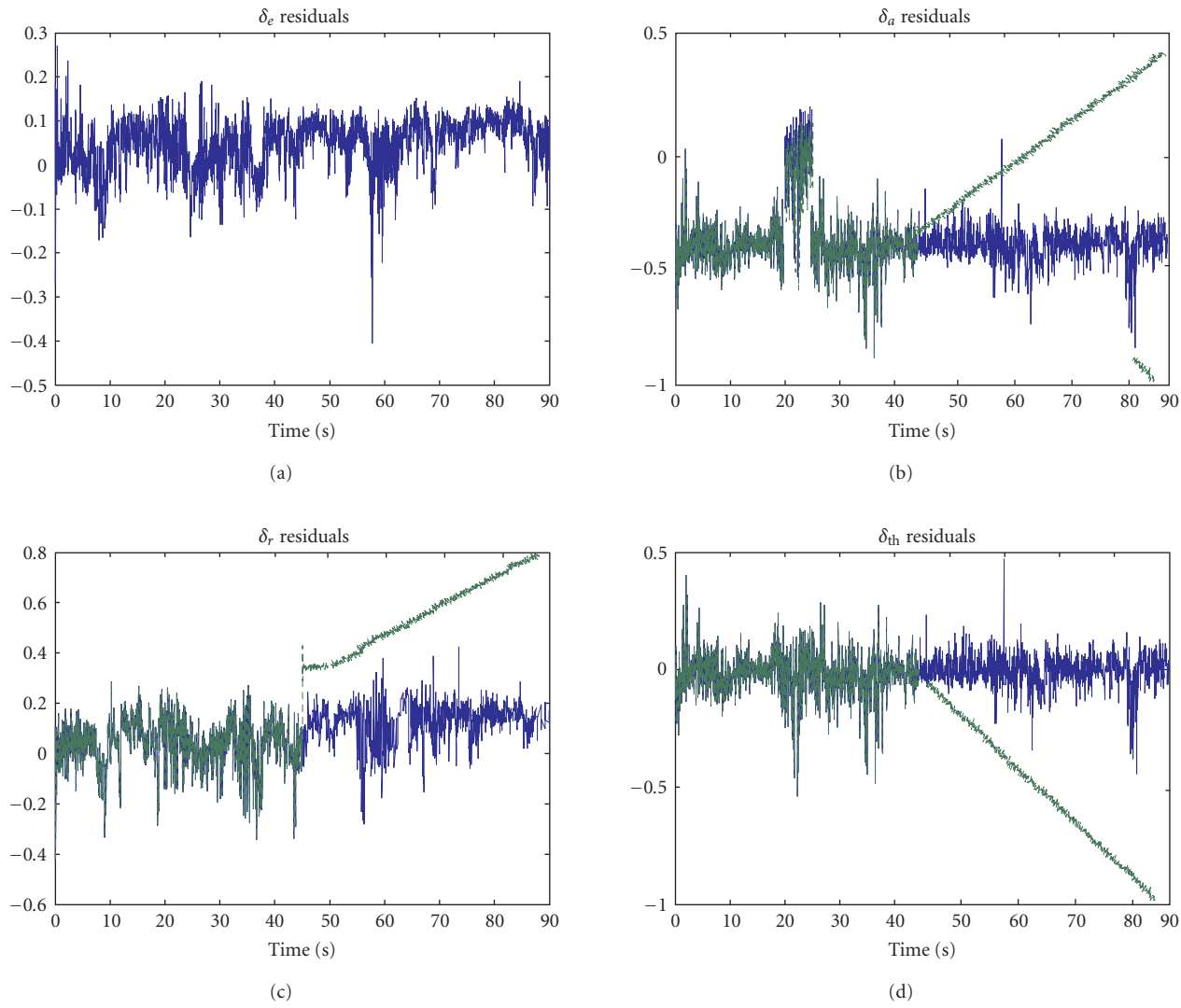

Figure 4: NN residuals with *ramp* fault.

these conditions, the Monte Carlo analysis represents a further method for estimating the reliability and the robustness of the developed FDI schemes, when applied to the considered aircraft.

For robustness and reliability experimental analysis of the FDI schemes, some performance indices have been used. The performances of the FDI method are then evaluated on a number of Monte Carlo runs equal to 1000. This number of simulations is carried out to determine the indices listed below with a given degree of accuracy.

False-Alarm Probability (r_{fa}): the number of wrongly detected faults divided by total fault cases.

Missed-Fault Probability(r_{mf}): for each fault, the total number of undetected faults, divided by the total number of times that the fault case occurs.

True Detection/Isolation Probability (r_{td}, r_{ti}): for a particular fault case, the number of times it is correctly detected/isolated, divided by total number of times that the fault case occurs.

Mean Detection/Isolation Delay (τ_{md}, τ_{mi}): for a particular fault case, the average detection/isolation delay time.

These indices are hence computed for the number of Monte Carlo simulations and for each fault case. Table 7summarises the results obtained by considering the PM dynamic filters for the input sensor FDI for a complete aircraft trajectory and with $p = 10\%$.

The same analysis can be applied again to the residual generated by means of the NLGA, NN, and UIKF FDI schemes. The results are summarised in Tables 8, 9, and 10.

Tables 7, 8, 9, and 10 show how the proper design of the dynamic filters with a proper choice of the FDI thresholds allow to achieve false-alarm and missed-fault probabilities less than 0.6%, detection and isolation probabilities bigger than 99.4%, with minimal detection and isolation delay times. The results demonstrate also that Monte Carlo simulation is an effective tool for testing and comparing the design robustness of the proposed FDI methods with respect to modelling

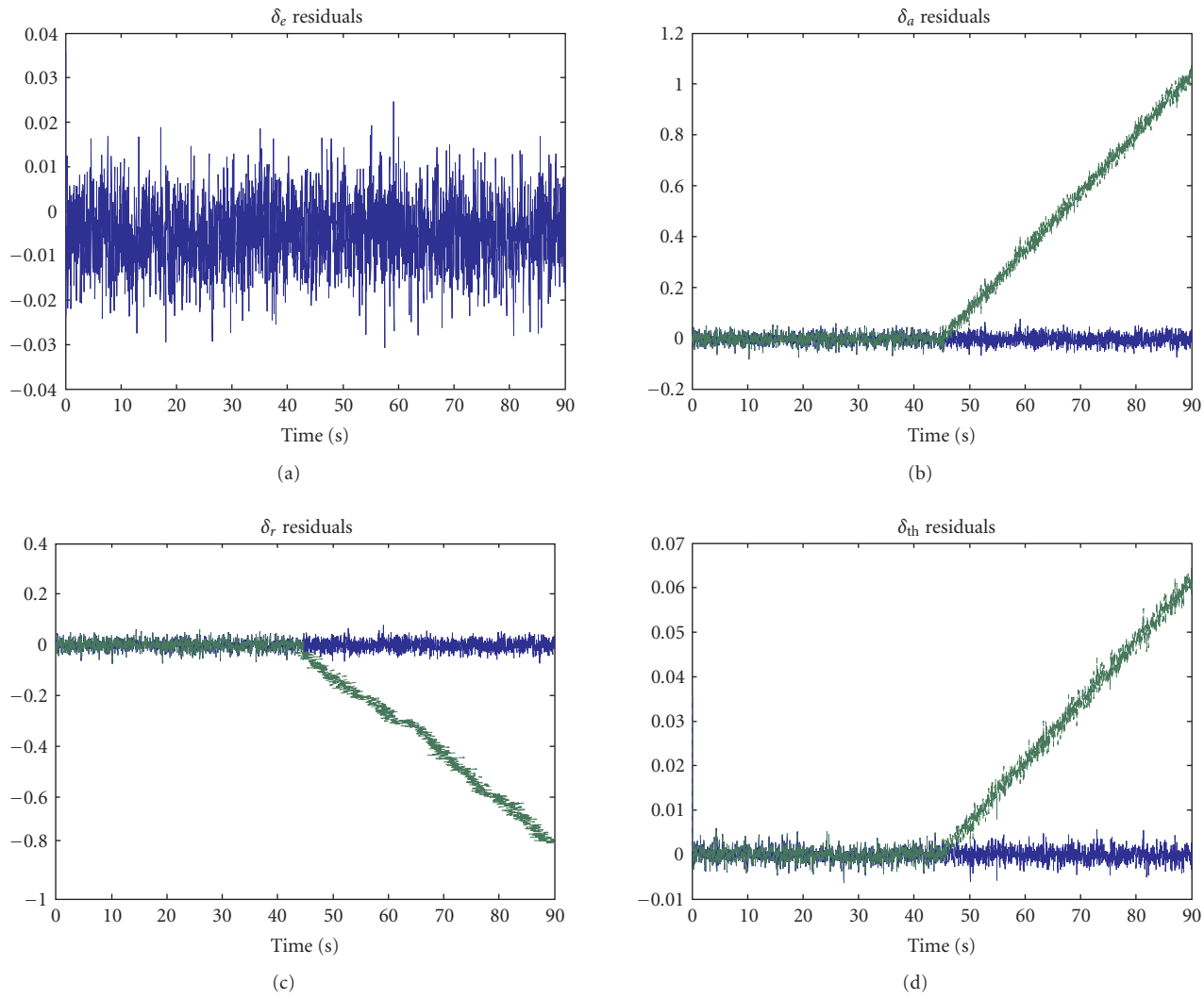

Figure 5: UIKF residuals with *ramp* fault.

Table 7: PM Monte Carlo analysis with $\nu = 4$ and $p = 10\%$.

Faulty sensor	r_{fa}	r_{mf}	r_{td}, r_{ti}	τ_{md}, τ_{mi}
δ_e	0.002	0.003	0.997	27 s
δ_a	0.001	0.001	0.999	18 s
δ_r	0.002	0.003	0.997	25 s
δ_{th}	0.003	0.002	0.998	35 s

Table 8: NLGA Monte Carlo analysis with $\nu = 12$ and $p = 10\%$.

Faulty sensor	r_{fa}	r_{mf}	r_{td}, r_{ti}	τ_{md}, τ_{mi}
δ_e	0.003	0.004	0.996	30 s
δ_a	0.002	0.002	0.998	15 s
δ_r	0.001	0.001	0.999	23 s
δ_{th}	0.004	0.003	0.997	32 s

Table 9: NN Monte Carlo analysis with $\nu = 5$.

Faulty sensor	r_{fa}	r_{mf}	r_{td}, r_{ti}	τ_{md}, τ_{mi}
δ_e	0.004	0.005	0.995	33 s
δ_a	0.003	0.003	0.997	23 s
δ_r	0.004	0.004	0.996	29 s
δ_{th}	0.005	0.003	0.997	38 s

Table 10: UIKF Monte Carlo analysis with $\nu = 9$.

Faulty sensor	r_{fa}	r_{mf}	r_{td}, r_{ti}	τ_{md}, τ_{mi}
δ_e	0.003	0.004	0.996	26 s
δ_a	0.002	0.002	0.998	17 s
δ_r	0.001	0.002	0.998	26 s
δ_{th}	0.004	0.003	0.997	37 s

uncertainty ($p = 10\%$) and fixed measurement errors. This last simulation technique example hence facilitates an assessment of the reliability of the developed, analysed, and applied FDI methods.

6. CONCLUSION

The paper provided the development and application of two FDI techniques based on a PM scheme and on an NLGA method, respectively. The PM procedure led to residual generators optimising the tradeoff between disturbance-decoupling and fault sensitivity. Moreover, the application of the PM FDI scheme resulted robust with respect to model uncertainties. On the other hand, the NLGA relies on a novel design scheme based on the structural decoupling of disturbances and modelling errors, Thus, the mixed $\mathcal{H}_-/\mathcal{H}_\infty$ optimisation of the tradeoff between fault sensitivity, disturbances, and modelling errors has been proposed. The PM and NLGA residual generators were tested by considering a nonlinear aircraft simulator model that takes into account also the wind gusts, the Dryden turbulence, the input-output sensors measurement errors, as well as the engine and the servo actuators. Moreover, in order to verify the robustness characteristics and the achievable performances of the approaches, the simulation results considered a typical aircraft reference trajectory consisting of several steady-state flight conditions. The effectiveness of the developed PM and NLGA FDI schemes was shown by simulations and a comparison with widely used data-driven and model-based disturbance-decoupling FDI schemes, such as NN and UIKF diagnosis methods, was provided. The reliability and the robustness properties of the proposed residual generators to model uncertainty and disturbances and measurement noise for the aircraft nonlinear model were investigated via Monte Carlo simulations. Further works extensive comparative studies for robustness of the FDI algorithms when applied to real data.

REFERENCES

[1] A. Marcos, S. Ganguli, and G. J. Balas, "An application of H_∞ fault detection and isolation to a transport aircraft," *Control Engineering Practice*, vol. 13, no. 1, pp. 105–119, 2005.

[2] F. Amato, C. Cosentino, M. Mattei, and G. Paviglianiti, "A direct/functional redundancy scheme for fault detection and isolation on an aircraft," *Aerospace Science and Technology*, vol. 10, no. 4, pp. 338–345, 2006.

[3] J. Chen and R. J. Patton, *Robust Model-Based Fault Diagnosis for Dynamic Systems*, Kluwer Academic Publishers, Dordrecht, The Netherlands, 1999.

[4] R. Isermann, *Fault-Diagnosis Systems: An Introduction from Fault Detection to Fault Tolerance*, Springer, Berlin, Germany, 1st edition, 2005.

[5] J. Gertler, *Fault Detection and Diagnosis in Engineering Systems*, Marcel Dekker, New York, NY, USA, 1998.

[6] M. Basseville and I. V. Nikiforov, *Detection of Abrupt Changes: Theory and Application*, Prentice Hall, Upper Saddle River, NJ, USA, 1993.

[7] J. Korbicz, J. M. Koscielny, Z. Kowalczuk, and W. Cholewa, Eds., *Fault Diagnosis: Models, Artificial Intelligence, Applications*, Springer, Berlin, Germany, 1st edition, 2004.

[8] M. A. Massoumnia, *A geometric appoach to failure detection and identification in linear systems*, Ph.D. thesis, Massachusetts Institute of Technology, Cambridge, Mass, USA, 1986.

[9] H. Hammouri, M. Kinnaert, and E. H. El Yaagoubi, "Observer-based approach to fault detection and isolation for nonlinear systems," *IEEE Transactions on Automatic Control*, vol. 44, no. 10, pp. 1879–1884, 1999.

[10] C. De Persis and A. Isidori, "A geometric approach to nonlinear fault detection and isolation," *IEEE Transactions on Automatic Control*, vol. 45, no. 6, pp. 853–865, 2001.

[11] C. De Persis, R. De Santis, and A. Isidori, "Nonlinear actuator fault detection and isolation for a VTOL aircraft," in *Proceedings of the American Control Conference (ACC '01)*, vol. 6, pp. 4449–4454, Arlington, Va, USA, June 2001.

[12] M. Bonfè, P. Castaldi, W. Geri, and S. Simani, "Fault detection and isolation for on-board sensors of a general aviation aircraft," *International Journal of Adaptive Control and Signal Processing*, vol. 20, no. 8, pp. 381–408, 2006.

[13] M. Bonfè, P. Castaldi, W. Geri, and S. Simani, "Design and performance evaluation of residual genertors for the FDI of an aircraft," *International Journal of Automation and Computing*, vol. 4, no. 2, pp. 156–163, 2007.

[14] B. L. Stevens and F. L. Lewis, *Aircraft Control and Simulation*, John Wiley & Son, New York, NY, USA, 2nd edition, 2003.

[15] R. P. Guidorzi, "Invariants and canonical forms for systems stuctural and parametric identification," *Automatica*, vol. 17, no. 1, pp. 117–133, 1981.

[16] S. Van Huffel and P. Lemmerling, Eds., *Total Least Squares and Errors-in-Variables Modeling: Analysis, Algorithms and Applications*, Springer, Berlin, Germany, 1st edition, 2002.

[17] M. Bonfè, S. Simani, P. Castaldi, and W. Geri, "Residual generator computation for fault detection of a general aviation aircraft," in *Proceedings of the 16th IFAC Symposium on Automatic Control in Aerospace (ACA '04)*, vol. 2, pp. 318–323, St. Petersburg, Russia, June 2004.

[18] C. De Persis and A. Isidori, "On the observability codistributions of a nonlinear system," *Systems and Control Letters*, vol. 40, no. 5, pp. 297–304, 2000.

[19] P. Castaldi, W. Geri, M. Bonfè, and S. Simani, "Nonlinear actuator fault detection and isolation for a general aviation aircraft," in *Proceedings of the 17th IFAC Symposium on Automatic Control in Aerospace (ACA '07)*, vol. CD-Rom, pp. 1–6, Toulouse, France, June 2007.

[20] M. Hou and R. J. Patton, "LMI approach to H_-/H_∞ fault detection observers," in *Proceedings of the 1996 UKACC International Conference on Control (CONTROL '96)*, pp. 305–310, Exeter, UK, September 1996.

[21] A Emami-Naeini, M. M. Akhter, and S. M. Rock, "Effect of model uncertainty on failure detection: the threshold selector," *IEEE Transactions on Automatic Control*, vol. 33, no. 12, pp. 1106–1116, 1988.

[22] S. Simani, C. Fantuzzi, and R. J. Patton, *Model-Based Fault Diagnosis in Dynamic Systems Using Identification Techniques*, Advances in Industrial Control, Springer, London, UK, 1st edition, 2002.

Hindawi Publishing Corporation
Journal of Control Science and Engineering
Volume 2008, Article ID 523749, 11 pages
doi:10.1155/2008/523749

Research Article

Stability of Discrete Systems Controlled in the Presence of Intermittent Sensor Faults

Rui Vilela Dionísio[1, 2] and João M. Lemos[3, 2]

[1] *Laboratório de Instrumentação e Medida, Escola Superior de Tecnologia de Setúbal, Instituto Politécnico de Setúbal, Campus do IPS, Estefanilha, 2910-761 Setúbal, Portugal*
[2] *Instituto de Engenharia de Sistemas e Computadores-Investigação e Desenvolvimento em Lisboa, Rua Alves Redol 9, 1000-029 Lisboa, Portugal*
[3] *Instituto Superior Técnico, Universidade Técnica de Lisboa, Avenida Rovisco Pais, 1049-001 Lisboa, Portugal*

Correspondence should be addressed to Rui Vilela Dionísio, rvilela@est.ips.pt

Received 10 April 2007; Accepted 7 October 2007

Recommended by Jakob Stoustrup

This paper presents sufficient conditions for stability of unstable discrete time invariant models, stabilized by state feedback, when interrupted observations due to intermittent sensor faults occur. It is shown that the closed-loop system with feedback through a reconstructed signal, when, at least, one of the sensors is unavailable, remains stable, provided that the intervals of unavailability satisfy a certain time bound, even in the presence of state vanishing perturbations. The result is first proved for linear systems and then extended to a class of Hammerstein systems.

1. INTRODUCTION

In recent years, the mass advent of digital communication networks and systems has boosted the integration of teleoperation in feedback control systems. Applications like unmanned vehicles [1] or internet-based real time control [2] provide significant examples raising, in turn, new problems.

This paper deals with one of such problems, if the communication channel through which feedback information passes is not completely reliable, sensors' measurements may not be available to the controller during some intervals of time. In such a situation, one has to couple the controller with a block, hereafter called supervisor, which is able to discriminate between intervals of signal availability (availability time T_{a_i}) and unavailability (unavailability time $T_{u_{i+1}}$), and to generate an estimate of the plant's state during this $T_{u_{i+1}}$ intervals. Methods for detection and estimation for abruptly changing systems [3] can be applied in the problem considered here. For that purpose an algorithm based on Bayesian decision could be implemented, for example.

Somehow related with the problem of temporary sensor unavailability presented in this paper are the problem of data packet dropout, and the problem of network-induced delay, in networked control systems [4, 5].

Moreover, the approach suggested in this paper can be compared with different techniques based, for example, on the idea of the unknown input observer, as suggested in [6]. On the other hand, it is obvious to exploit Kalman filters and fuzzy logic for sensor fusion, applied to autonomous underwater vehicle systems, as described in [7]. It was, also, shown in [8, 9] that the design of fault-tolerant observers can be successfully applied to the control of rail traction drives. Finally, the stability analysis for a real application example in the presence of intermittent faults is described in [10].

Biomedical applications provide, as well, examples in that the sensor used for feedback is intermittently unavailable. In [11] the artifacts in the neuromuscular blockade level measurement in patients subject to general anaesthesia are modeled as sensor faults. The occurrence of these faults is detected with a Bayesian algorithm and, during the periods of unavailability of the signal, the feedback controller is fed with an estimate generated by a model.

It is shown, throughout the paper, that with the above described scheme, the controlled open-loop unstable plant will be stable (in some sense, to be defined later) if the time

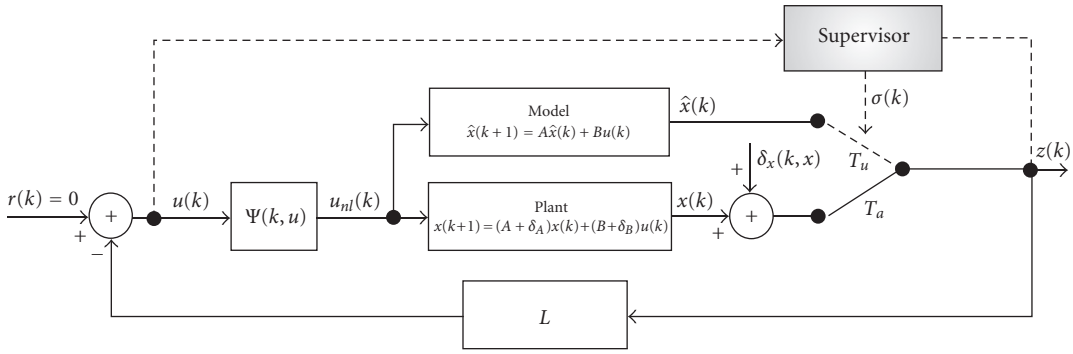

Figure 1: Block diagram of a discrete feedback system with nonlinear actuator and interrupted observations supervisor.

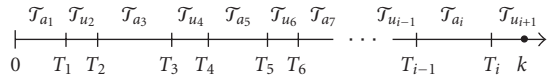

Figure 2: Operation time line with availability intervals alternating with unavailability intervals.

interval, during which at least one of the sensors measure is unavailable, is somehow "small", and that the Euclidean norm of the state $x(k)$, at the end of each $T_{u_{i+1}}$ interval, is a monotonic descent sequence. Moreover, if the plant state is perturbed by a class of vanishing perturbations $\delta_x(k,x)$, similar stability results are derived.

The contributions of the paper consist in providing sufficient conditions for stability of feedback controlled open-loop unstable systems with intermittent sensors faults. Linear as well as nonlinear systems are considered.

This paper is organized in four sections and two appendices. After this introduction, Section 2 makes a detailed system description referring the functionality of the supervisor in terms of detection and estimation of the state, and the way the feedback system with linear as well as with nonlinear actuators behaves when intermittent sensors faults occur. Section 3 presents two theorems with sufficient conditions, one for uniform stability of the system with linear and nonlinear actuators, and respective corollaries, also with sufficient conditions, and the other for uniform exponential stability and descent monotonicity of the Euclidean norm of the state $x(k)$ at the end of each $T_{u_{i+1}}$ interval. Moreover, Section 3 presents two other theorems, again with sufficient conditions, that prove that the system with linear and nonlinear actuators, subject to a vanishing perturbation, is asymptotically stable. In Section 4 conclusions are drawn. Appendix A.1 gives a full proof of Theorem 1 and Corollaries 1 and 2, and Appendix A.2 gives a full proof of Theorem 2 and Corollaries 3 and 4.

2. SYSTEM DESCRIPTION

The system depicted in Figure 1 is composed of two subsystems: (i) the supervisor responsible for detection of sensors' measures interruptions, and for switching state feedback from plant to model and from model to plant; (ii) the plant and the model rendered stable through state feedback.

An example of supervisor based on Bayesian inference is provided in [12, 13]. It is beyond the scope of this paper to detail this block.

The supervisor decides whether the state $x(k)$ is being correctly measured by the sensors or not and commands the switch signal $\sigma(k)$. During the time intervals in which the sensors do not provide a reliable measure of the actual plant state (it is admitted that the state coincides with the output) one possibility is to replace it by an estimate $\hat{x}(k)$ obtained from a plant model. This yields a loss of performance with respect to the ideal situation in which the sensors are always available, and may pose stability problems if the plant is open-loop unstable.

In order to understand the system functioning, consider the time line of operation, depicted in Figure 2, divided in alternate intervals where all sensors operate correctly (T_{a_j}, with $j = 1, 3, 5, 7, \ldots, i$), and where, at least, one of them fails (T_{u_j}, with $j = 2, 4, 6, \ldots, i-1, i+1$) being replaced by the model estimate. Note that the index j does not represent discrete instants of time, but is rather used to enumerate both the availability, T_{a_j}, and the unavailability, T_{u_j}, intervals. These intervals are identified in script font in the upper part of the time line of Figure 2. The time instants corresponding to the beginning of each interval, wether it is an availability or an unavailability interval, are represented in the lower part of the time line of Figure 2. Let k_0 denote the beginning of one such intervals. It is assumed that the first interval always corresponds to an availability interval, and that the intervals are open at their end. Furthermore, the time analysis always finishes in an unavailability interval at time k. Therefore, in a complete time sequence there are $(i+1)$ intervals, where $(i+1)$ is an even number.

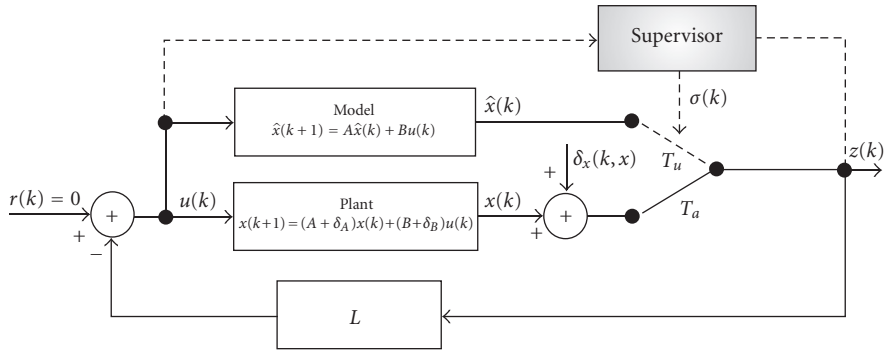

Figure 3: Block diagram of a discrete feedback system with linear actuator, and interrupted observations supervisor.

The model initial sate $\hat{x}$ is made equal to the last available observation of the state x when an interrupted observation occurs ($\hat{x}(k_0) = x(k_0) = x(k_0 - 1)$), since the sate x is no longer available.

3. STABILITY RESULTS

Three distinct situations regarding system's stability are considered. In the first case, the nonlinear function $\psi(u(k))$ does not exist ($\psi(u(k)) = I$; see Figure 3). Moreover, the perturbation function $\delta_x(k,x)$ is also considered not to exist ($\delta_x(k,x) = 0$, see Figure 3). The second case is referred to the feedback system with nonlinear actuator function $\psi(u(k))$ but, also, without the perturbation function $\delta_x(k,x)$; see Figure 1. The third case considers the existence of the perturbation function $\delta_x(k,x)$ in both feedback systems, with linear actuator, and with nonlinear actuator.

In all the situations the reference signal, $r(k)$, is considered to be zero, for all $k \geq 0$ (regulation problem).

Throughout the text, matrices norms are the ones induced by the Euclidean norm of vectors, being given by their largest singular value ($\|A\| = \sigma_{\max}[A] = \sigma_A \geq 0$).

3.1. System with linear input

Consider Figure 3 with $\delta_x(k,x) = 0$, and $r(k) = 0$, for all $k \geq 0$. The plant and the model depicted are described in the state-space form by (1) and (2), respectively

$$x(k+1) = (A+\delta_A)x(k) + (B+\delta_B)u(k), \tag{1}$$
$$\hat{x}(k+1) = A\hat{x}(k) + Bu(k) \tag{2}$$

with x and $\hat{x} \in \mathbb{R}^n$, accessible for direct measurement, $u \in \mathbb{R}^p$, A, B, δ_A, and δ_B are of appropriate dimensions, and (A,B) is controllable. Moreover, δ_A and δ_B represent modeling uncertainties. It is assumed that the plant is time invariant, and open-loop unstable. The state feedback of signal $z(k)$, yielded by the sensor

$$u(k) = -Lz(k), \tag{3}$$

is implemented by L, a matrix of feedback gains assumed to stabilize the model. Furthermore, $z(k) = x(k)$ during availability intervals, when all sensors are working properly, and $z(k) = \hat{x}(k)$ during unavailability intervals, when measuring interruptions take place.

During availability intervals the plant state equation is

$$x(k+1) = [(A+\delta_A) - (B+\delta_B)L]x(k) \tag{4}$$

and during unavailability intervals the plant state equation is

$$x(k+1) = (A+\delta_A)x(k) - (B+\delta_B)L\hat{x}(k). \tag{5}$$

Define the plant closed-loop dynamics matrix as

$$A_{\delta_{\mathrm{CL}}} := (A+\delta_A) - (B+\delta_B)L = A_\delta - B_\delta L, \tag{6}$$

the model closed-loop dynamics matrix as

$$A_{\mathrm{CL}} := A - BL, \tag{7}$$

the plant open and closed-loop transition matrices

$$\begin{aligned} \Phi_\delta(k,k_0) &:= A_\delta^{k-k_0}, \\ \Phi_{\delta_{\mathrm{CL}}}(k,k_0) &:= A_{\delta_{\mathrm{CL}}}^{k-k_0}, \end{aligned} \tag{8}$$

and the model open and closed-loop transition matrices

$$\begin{aligned} \Phi(k,k_0) &:= A^{k-k_0}, \\ \Phi_{\mathrm{CL}}(k,k_0) &:= A_{\mathrm{CL}}^{k-k_0}. \end{aligned} \tag{9}$$

Theorem 1. *Consider the closed-loop system of Figure 3 with the unstable model in open-loop (bounded by $\|\Phi(k,k_0)\| \leq \alpha\beta^{k-k_0}$ with $\alpha \geq 1$ and $\beta > 1$, finite constants) rendered stable in closed-loop ($\|\Phi_{CL}(k,k_0)\| \leq \gamma\lambda^{k-k_0}$ with $\gamma \geq 1$ a finite constant and $0 \leq \lambda < 1$), through proper design of L. Consider, also, that $\sigma_B := \|B\|$, $\sigma_L := \|L\|$, and that model uncertainties are bounded $\|\delta_A\| \leq \sigma_{\delta_A}$, and $\|\delta_B\| \leq \sigma_{\delta_B}$. The system with initial condition $x(0) = x_0$ is globally uniformly stable provided that the total unavailability time T_u, up to discrete time k inside the unavailability interval $T_{u_{i+1}}$, satisfies the bound*

$$\begin{aligned} T_u < {} & \frac{\log M_1}{\log(\beta + \alpha\cdot\sigma_{\delta_A})} - \frac{(i+1)}{2} \\ & \cdot \frac{\log\left[(1 + (\sigma_B + \sigma_{\delta_B})\sigma_L\cdot\gamma/(\beta + \alpha\cdot\sigma_{\delta_A} - \lambda))\alpha\gamma\right]}{\log(\beta + \alpha\cdot\sigma_{\delta_A})} \\ & - T_a \frac{\log(\lambda + \gamma\Sigma)}{\log(\beta + \alpha\cdot\sigma_{\delta_A})} \end{aligned} \tag{10}$$

with $M_1 \geq 1$, a finite constant, and $\Sigma := \sigma_{\delta_A} + \sigma_{\delta_B} \cdot \sigma_L$ is such that verifies

$$0 \leq \Sigma < \frac{1-\lambda}{\gamma}, \tag{11}$$

T_a is the total availability time.

A result derived from the previous theorem is stated on the following corollary.

Corollary 1. *Under the assumptions of Theorem 1, $\|x(T_j)\|$, for $j = 0, 2, 4, \ldots, i-1$, (the state norm at the beginning of each availability interval) is a monotonic descent sequence provided that the unavailability interval $T_{u_{i-1}}$ satisfies*

$$T_{u_{i-1}} < \frac{\log\left[\left(1 + (\sigma_B + \sigma_{\delta_B})\sigma_L \cdot \gamma / (\beta + \alpha \cdot \sigma_{\delta_A} - \lambda)\right)\alpha\gamma\right]}{\log(\beta + \alpha \cdot \sigma_{\delta_A})} - T_{a_{i-2}} \frac{\log(\lambda + \gamma\Sigma)}{\log(\beta + \alpha \cdot \sigma_{\delta_A})} \tag{12}$$

and $\Sigma := \sigma_{\delta_A} + \sigma_{\delta_B} \cdot \sigma_L$ is such that verifies

$$0 \leq \Sigma < \frac{1-\lambda}{\gamma}, \tag{13}$$

$T_{a_{i-2}}$ is the availability time previous to $T_{u_{i-1}}$.

Concerning global uniform exponential stability, consider the next corollary.

Corollary 2. *Under the assumptions of Theorem 1, the system with initial condition $x(0) = x_0$ is globally uniformly exponentially stable provided that the total unavailability time T_u, up to discrete time k inside the unavailability interval $T_{u_{i+1}}$, satisfies*

$$T_u < \frac{\log M_2}{\log\left((\beta + \alpha \cdot \sigma_{\delta_A})/N_2\right)} - \frac{(i+1)}{2} \cdot \frac{\log\left[\left(1 + (\sigma_B + \sigma_{\delta_B})\sigma_L \cdot \gamma / (\beta + \alpha \cdot \sigma_{\delta_A} - \lambda)\right)\alpha\gamma\right]}{\log\left((\beta + \alpha \cdot \sigma_{\delta_A})/N_2\right)} - T_a \frac{\log\left((\lambda + \gamma\Sigma)/N_2\right)}{\log\left((\beta + \alpha \cdot \sigma_{\delta_A})/N_2\right)} \tag{14}$$

with $M_2 \geq 1$, a finite constant, and $\Sigma := \sigma_{\delta_A} + \sigma_{\delta_B} \cdot \sigma_L$ is such that verifies

$$0 \leq \Sigma < \frac{1-\lambda}{\gamma} \tag{15}$$

and $0 \leq N_2 < 1$ is a constant constrained to

$$N_2 > \lambda + \gamma\Sigma, \tag{16}$$

T_a is the total availability time.

A proof of the theorem and of the corollaries is presented in Appendix A.1.

Remark 1. The constraint $\Sigma < (1-\lambda)/\gamma$ is imposed to assure that the plant closed-loop transition matrix is such that $\|\Phi_{\delta_{CL}}(k, k_0)\| \leq \gamma(\lambda + \gamma\Sigma)^{k-k_0}$ with $0 \geq (\lambda + \gamma\Sigma) < 1$ (see the proof in Appendix A.1).

Remark 2. Notice that since $(\beta + \alpha \cdot \sigma_{\delta_A}) > 1$ and $0 \leq (\lambda + \gamma\Sigma) < 1$, then the bound on T_u has a monotonous crescent linear relation with T_a in the result from Theorem 1, and $T_{u_{i-1}}$ also has a monotonous crescent linear relation with $T_{a_{i-2}}$ in the result from Corollary 1.

Remark 3. The constant N_2 (in Corollary 2) represents an upper bound on the rate of exponential decay of the overall system. If $N_2 < \lambda + \gamma\Sigma$, then the result of Corollary 2 would indicate a negative solution for T_u, which, clearly, is not possible, since $T_u \in [0, \infty[$. Being $N_2 > \lambda + \gamma\Sigma$, then the bound on T_u has also a monotonous crescent linear relation with T_a, as mentioned in the previous remark.

Remark 4. Concerning Theorem 1 and Corollary 2, constants M_1 and M_2 represent an offset term for the upper bound function on the evolution of $\|x(k)\|$. The bigger these constants are, the more conservative is the referred upper bound on uniform stability and uniform exponential stability, respectively.

Remark 5. Theorem 1 and Corollaries 1 and 2 present only conservative sufficient stability conditions for the system of Figure 3.

3.2. System with nonlinear input

Consider Figure 1 with $\delta_x(k, x) = 0$, and $r(k) = 0$, for all $k \geq 0$. The plant and the model depicted are described in the state-space form by (17) and (18), respectively,

$$x(k+1) = (A + \delta_A)x(k) + (B + \delta_B)u_{\text{nl}}(k), \tag{17}$$

$$\hat{x}(k+1) = A\hat{x}(k) + Bu_{\text{nl}}(k), \tag{18}$$

with x and $\hat{x} \in \mathbb{R}^n$, accessible for direct measurement, u and $u_{\text{nl}} \in \mathbb{R}^p$, A, B, δ_A, and δ_B are of appropriate dimensions, and (A, B) is controllable. Moreover, δ_A and δ_B represent modeling uncertainties. It is assumed that the plant is time invariant, and open-loop unstable.

The vector u_{nl} represents the nonlinear input to both the plant and the model, $u_{\text{nl}}(k) = \psi(k, u)$. A memoryless nonlinearity, $\psi : [0, \infty[\times \mathbb{R}^p \to \mathbb{R}^p$, is said to satisfy a sector condition globally [14] if

$$\left[\psi(k,u) - K_{\min}u(k)\right]^T \left[\psi(k,u) - K_{\max}u(k)\right] \leq 0 \tag{19}$$

for all $t \geq 0$, for all $u \in \mathbb{R}^p$, for some real matrices $K_{\min}$ and $K_{\max}$, where $K = K_{\max} - K_{\min}$ is a positive definite symmetric matrix. The nonlinearity $\psi(k, u)$ is said to belong to a sector $[K_{\min}, K_{\max}]$.

Proposition 1. *Consider $K_{\min} = -(\gamma_2/2)I$ and $K_{\max} = (\gamma_2/2)I$ with γ_2 a finite positive constant. The nonlinearity $\psi(k, u)$ can be decomposed in a linear component and a nonlinear component, [15]*

$$\psi_s(k,u) = \psi(k,u) - K_{\min}u(k), \tag{20}$$

where $\psi_s(k, u)$ represents the nonlinear component and verifies the sector condition

$$\psi_s^T(k,u)\left[\psi_s(k,u) - Ku(k)\right] \leq 0. \tag{21}$$

Proof. This result is straightforward using (20) in (19), and considering matrix K definition. □

Proposition 2. *For the defined matrices $K_{\min}$ and $K_{\max}$, the memoryless sector nonlinearity $\psi(k,u)$ is bounded by $\|\psi(k,u)\| \le (\gamma_2/2)\|u(k)\|$, for all $t \ge 0$, for all $u \in \mathbb{R}^p$.*

Proof. Replacing $K_{\min}$ and $K_{\max}$ by their respective values in (19), and since $\psi^T(k,u)u(k)$ is a scalar, yields

$$||\psi(k,u)||^2 - \left(\frac{\gamma_2}{2}\right)^2 ||u(k)||^2 \le 0. \tag{22}$$

By definition $\|\psi(k,u)\| \ge 0$, $\|u(k)\| \ge 0$, and $\gamma_2/2 > 0$, which implies

$$||\psi(k,u)|| \le \frac{\gamma_2}{2}||u(k)||. \tag{23}$$

□

In order to find a bound on $\psi_s(k,u)$ starting from (20), using (23), and $K_{\min}$ definition, it follows that

$$||\psi_s(k,u)|| \le \gamma_2||u(k)||. \tag{24}$$

The state feedback of signal $z(k)$, yielded by the sensor

$$u(k) = -Lz(k), \tag{25}$$

is implemented by L, a matrix of feedback gains assumed to stabilize the model. Furthermore, $z(k) = x(k)$ during availability intervals, when all sensors are working properly, and $z(k) = \hat{x}(k)$ during unavailability intervals, when measuring interruptions take place.

During availability intervals, the plant state equation is

$$\begin{aligned} x(k+1) = {} & [(A+\delta_A) - (B+\delta_B)K_{\min}L]x(k) \\ & + (B+\delta_B)\psi_s(-Lx(k)) \end{aligned} \tag{26}$$

and during unavailability intervals, the plant state equation is

$$\begin{aligned} x(k+1) = {} & (A+\delta_A)x(k) + (B+\delta_B) \\ & .(\psi_s(-L\hat{x}(k)) - K_{\min}L\hat{x}(k)). \end{aligned} \tag{27}$$

Define the plant closed-loop dynamics matrix as

$$\overline{A}_{\delta_{\mathrm{CL}}} := (A+\delta_A) - (B+\delta_B)K_{\min}L = A_\delta - B_\delta K_{\min}L, \tag{28}$$

the model closed-loop dynamics matrix as

$$\overline{A}_{\mathrm{CL}} := A - BK_{\min}L, \tag{29}$$

the plant open and closed-loop transition matrices as

$$\begin{aligned} \Phi_\delta(k,k_0) &:= (A+\delta_A)^{k-k_0} = A_\delta^{k-k_0}, \\ \overline{\Phi}_{\delta_{\mathrm{CL}}}(k,k_0) &:= \overline{A}_{\delta_{\mathrm{CL}}}^{k-k_0}, \end{aligned} \tag{30}$$

the model open and closed-loop transition matrices as

$$\begin{aligned} \Phi(k,k_0) &:= A^{k-k_0}, \\ \overline{\Phi}_{\mathrm{CL}}(k,k_0) &:= \overline{A}_{\mathrm{CL}}^{k-k_0}, \end{aligned} \tag{31}$$

and matrix $P = K_{\min}L$, considered to stabilize the model in closed loop.

Theorem 2. *Consider the closed-loop system of Figure 1 where the model is unstable in open-loop (bounded by $\|\Phi(k,k_0)\| \le \alpha\beta^{k-k_0}$, with $\alpha \ge 1$, and $\beta > 1$, finite constants), rendered stable in closed-loop ($\|\overline{\Phi}_{\mathrm{CL}}(k,k_0)\| \le \gamma\lambda^{k-k_0}$, with $\gamma \ge 1$ a finite constant, and $0 \le \lambda < 1$), through proper design of P. The nonlinearity $\psi_s(k,u)$ satisfies $\|\psi_s(k,u)\| \le \gamma_2\|u(k)\|$ for all $t \ge 0$, for all $u \in \mathbb{R}^p$. Consider, also, that $\sigma_B := \|B\|$, $\sigma_L := \|L\|$, $\sigma_P := \|P\|$ and that model uncertainties are bounded $\|\delta_A\| \le \sigma_{\delta_A}$ and $\|\delta_B\| \le \sigma_{\delta_B}$. The system with initial condition $x(0) = x_0$ is globally uniformly stable provided that the total unavailability time T_u, up to discrete time k inside the unavailability interval $T_{u_{i+1}}$, satisfies the bound*

$$\begin{aligned} T_u < {} & \frac{\log M_1}{\log(\beta + \alpha\cdot\sigma_{\delta_A})} - \frac{(i+1)}{2} \\ & \cdot \frac{\log\left[\left(1 + \dfrac{(\sigma_B+\sigma_{\delta_B})(\sigma_P+\gamma_2\cdot\sigma_L)\gamma}{(\beta+\alpha\cdot\sigma_{\delta_A}) - (\lambda+\gamma\sigma_{\delta_B}\cdot\gamma_2\cdot\sigma_L)}\right)\alpha\gamma\right]}{\log(\beta+\alpha\cdot\sigma_{\delta_A})} \\ & - T_a\frac{\log[(\lambda+\gamma\Sigma) + \gamma(\sigma_B+\sigma_{\delta_B})\gamma_2\cdot\sigma_L]}{\log(\beta+\alpha\cdot\sigma_{\delta_A})} \end{aligned} \tag{32}$$

with $M_1 \ge 1$, a finite constant, and $\Sigma := \sigma_{\delta_A} + \sigma_{\delta_B}\cdot\sigma_P$ is such that verifies

$$0 \le \Sigma < \frac{1-\lambda}{\gamma} \tag{33}$$

and γ_2 is the less of the following two inequalities:

$$\begin{aligned} \gamma_2 &< \frac{1-(\lambda+\gamma\Sigma)}{\gamma(\sigma_B+\sigma_{\delta_B})\sigma_L}, \\ \gamma_2 &< \frac{\beta+\alpha\cdot\sigma_{\delta_A}-\lambda}{\gamma\cdot\sigma_{\delta_B}\cdot\sigma_L}, \end{aligned} \tag{34}$$

T_a is the total availability time.

As in the previous subsection the following two corollaries are derived.

Corollary 3. *Under the assumptions of Theorem 1, $\|x(T_j)\|$, for $j = 0, 2, 4, \ldots, i-1$, (the state norm at the beginning of each availability interval) is a monotonic descent sequence provided that the unavailability interval $T_{u_{i-1}}$ satisfies*

$$\begin{aligned} T_{u_{i-1}} < {} & -\frac{\log\left[\left(1 + \dfrac{(\sigma_B+\sigma_{\delta_B})(\sigma_P+\gamma_2\cdot\sigma_L)\gamma}{(\beta+\alpha\cdot\sigma_{\delta_A}) - (\lambda+\gamma\sigma_{\delta_B}\cdot\gamma_2\cdot\sigma_L)}\right)\alpha\gamma\right]}{\log(\beta+\alpha\cdot\sigma_{\delta_A})} \\ & - T_{a_{i-2}}\frac{\log[(\lambda+\gamma\Sigma) + \gamma(\sigma_B+\sigma_{\delta_B})\gamma_2\cdot\sigma_L]}{\log(\beta+\alpha\cdot\sigma_{\delta_A})} \end{aligned} \tag{35}$$

and $\Sigma := \sigma_{\delta_A} + \sigma_{\delta_B}\cdot\sigma_L$ is such that verifies

$$0 \le \Sigma < \frac{1-\lambda}{\gamma} \tag{36}$$

and γ_2 is the less of the following two inequalities:

$$\gamma_2 < \frac{1-(\lambda+\gamma\Sigma)}{\gamma(\sigma_B+\sigma_{\delta_B})\sigma_L},$$
$$\gamma_2 < \frac{\beta+\alpha\cdot\sigma_{\delta_A}-\lambda}{\gamma\cdot\sigma_{\delta_B}\cdot\sigma_L}, \tag{37}$$

$T_{a_{i-2}}$ is the availability time previous to $T_{u_{i-1}}$.

Corollary 4. *Under the assumptions of Theorem 2, the system with initial condition $x(0)=x_0$ is globally uniformly exponentially stable provided that the total unavailability time T_u, up to discrete time k inside the unavailability interval $T_{u_{i+1}}$, satisfies*

$$T_u < \frac{\log M_2}{\log\left((\beta+\alpha\cdot\sigma_{\delta_A})/N_2\right)} - \frac{(i+1)}{2} \cdot \frac{\log\left[\left(1+\frac{(\sigma_B+\sigma_{\delta_B})(\sigma_P+\gamma_2\cdot\sigma_L)\gamma}{(\beta+\alpha\cdot\sigma_{\delta_A})-(\lambda+\gamma\sigma_{\delta_B}\cdot\gamma_2\cdot\sigma_L)}\right)\alpha\gamma\right]}{\log\left((\beta+\alpha\cdot\sigma_{\delta_A})/N_2\right)} - T_a\frac{\log\left(((\lambda+\gamma\Sigma)+\gamma(\sigma_B+\sigma_{\delta_B})\gamma_2\cdot\sigma_L)/N_2\right)}{\log\left((\beta+\alpha\cdot\sigma_{\delta_A})/N_2\right)} \tag{38}$$

with $M_1 \geq 1$, a finite constant, and $\Sigma := \sigma_{\delta_A}+\sigma_{\delta_B}\cdot\sigma_P$ is such that verifies

$$0 \leq \Sigma < \frac{1-\lambda}{\gamma} \tag{39}$$

and γ_2 is the less of the following two inequalities:

$$\gamma_2 < \frac{1-(\lambda+\gamma\Sigma)}{\gamma(\sigma_B+\sigma_{\delta_B})\sigma_L},$$
$$\gamma_2 < \frac{\beta+\alpha\cdot\sigma_{\delta_A}-\lambda}{\gamma\cdot\sigma_{\delta_B}\cdot\sigma_L}, \tag{40}$$

and $0 \leq N_2 < 1$ is a constant constrained to

$$N_2 > (\lambda+\gamma\Sigma)+\gamma(\sigma_B+\sigma_{\delta_B})\gamma_2\cdot\sigma_L, \tag{41}$$

T_a is the total availability time.

A proof of the theorem and of the corollaries is presented in Appendix A.2.

Remark 6. Notice that since $(\beta+\alpha\cdot\sigma_{\delta_A}) > 1$ then it must be $(\lambda+\gamma\Sigma)+\gamma(\sigma_B+\sigma_{\delta_B})\gamma_2\cdot\sigma_L < 1$, which leads to (34), (37), and (40), so that the bound on T_u has a monotonous crescent linear relation with T_a in the result from Theorem 2, and $T_{u_{i-1}}$ also has a monotonous crescent linear relation with $T_{a_{i-2}}$ in the result from Corollary 3.

Remark 7. The constant N_2 (in Corollary 4) represents an upper bound on the rate of exponential decay of the overall system. If $N_2 < (\lambda+\gamma\Sigma)+\gamma(\sigma_B+\sigma_{\delta_B})\gamma_2\cdot\sigma_L$, then the result of Corollary 4 would indicate a negative solution for T_u, which, clearly, is not possible, since $T_u \in [0,\infty[$. Being $N_2 > (\lambda+\gamma\Sigma)+\gamma(\sigma_B+\sigma_{\delta_B})\gamma_2\cdot\sigma_L$, then the bound on T_u has also a monotonous crescent linear relation with T_a, as mentioned in the previous remark.

Remark 8. Concerning Theorem 2 and Corollary 4, constants M_1 and M_2 represent, once again, an offset term for the upper bound function on the evolution of $\|x(k)\|$. The bigger these constants are, the more conservative is the referred upper bound on uniform stability and uniform exponential stability, respectively.

Remark 9. Theorem 2 and Corollaries 3 and 4 present only conservative sufficient stability conditions for the system of Figure 1.

3.3. Perturbed system with linear and nonlinear inputs

Consider that both systems depicted in Figures 1 and 3, suffer the influence of perturbation $\delta_x(k,x)$, where $\delta_x : [0,\infty[\times D \to \mathbb{R}^n$ is piecewise continuous in k and locally Lipschitz in x on $[0,\infty[\times D$, and $D \subset \mathbb{R}^n$ is a domain that contains the origin $x=0$. Also, $\|\delta_x(k,x)\| \leq \epsilon\|x(k)\|$ for all $k \geq 0$, for all $x \in D$, and ϵ is a nonnegative constant, meaning that the perturbation satisfies a linear growth bound, therefore, considering a vanishing perturbation, [14].

During availability intervals T_{a_j}, for $j = 1,3,5,\ldots,i$, both systems can be represented by the autonomous equation

$$x(k+1) = F(k,x), \tag{42}$$

where $F(k,x)$, for the system depicted in Figure 3, is

$$F(k,x) = A_{\delta_{\mathrm{CL}}}x(k), \quad k \in T_{a_j}, \tag{43}$$

and for the system depicted in Figure 1, $F(k,x)$ is

$$F(k,x) = \overline{A}_{\delta_{\mathrm{CL}}}x(k) + (B+\delta_B).\psi_s(-Lx(k)), \quad k \in T_{a_j}. \tag{44}$$

Clearly, $F(0)=0$ in both situations (from (19) and matrices' $K_{\min}$ and $K_{\max}$ definition in Proposition 1, the sector memoryless nonlinearity verifies $\psi_s(0)=0$). Recalling the state equations (5) and (27) during unavailability intervals T_{u_j}, for $j = 2,4,6,\ldots,i+1$, and the fact that the initial model state $\hat{x}$ is made equal to the last available observation of the state x when an interrupted observation occurs, $(\hat{x}(k_0)=x(k_0)=x(k_0-1))$, it is clearly understood that if the state becomes zero during an availability interval, then it will remain zero for all time instants belonging to any unavailability interval that may occur. The function's $F(k,x)$ branch related with the unavailability interval is not of obvious writing in terms only of $x(k)$. It has an easier writing in terms of $x(k)$ and of $\hat{x}(k)$. Nevertheless, since these two states are related at the switching time between availability and unavailability intervals (as recalled above), it can be understood that during an unavailability interval, $F(k,x)$ exists.

It is important to stress out that an unavailability interval cannot occur without having previously existed an availability interval. Bearing this in mind, it is possible to state that $F(0)=0$, for all $k \geq 0$, (including availability and unavailability intervals).

Also, linear and nonlinear systems were proved to be globally uniformly exponentially stable, under the conditions

of Corollaries 2 and 4, respectively, therefore, both $F(k,x)$ are Lipschitz not only near the origin, but in $\mathbb{R}^n$, and verify $\|F(x_1) - F(x_2)\| \leq L_v\|x_1 - x_2\|$.

Combining the results from Corollaries 2 and 4 with the above comments, and with the result presented in [16], is reproduced in the next theorem.

Theorem 3. *Let $F : \mathbb{R}^n \to \mathbb{R}^n$ satisfy a Lipschitz condition in a neighborhood of the origin, with $F(0) = 0$. If the origin is an exponentially stable fixed point of $x(k+1) = F(x(k))$, it is an asymptotically stable fixed point of the perturbed system $\overline{x}(k+1) = F(\overline{x}(k)) + \delta_x(k,\overline{x})$.*

This leads to the next two theorems.

Theorem 4. *The nonperturbed system from Figure 3, $x(k+1) = F(k,x)$, verifying Corollary 2 and Theorem 3 sufficient conditions, has a globally asymptotically stable fixed point of the perturbed system $\overline{x}(k+1) = F(\overline{x}(k)) + \delta_x(k,\overline{x})$ in the origin, and $\delta_x : [0,\infty[\times D \to \mathbb{R}^n$ is piecewise continuous in k and locally Lipschitz in x on $[0,\infty[\times D$, and $D \subset \mathbb{R}^n$ is a domain that contains the origin $x = 0$. Also, $\|\delta_x(k,x)\| \leq \epsilon\|x(k)\|$ for all $k \geq 0$, for all $x \in D$ with ϵ a nonnegative constant satisfies a linear growth bound.*

Theorem 5. *It is the same redaction of Theorem 4, but considering the system from Figure 1.*

Remark 10. These results are global since both $F(k,x)$ are Lipschitz continuous in $\mathbb{R}^n$, and the original systems are uniformly exponentially stable, [16].

4. CONCLUSIONS

The paper presents and proves sufficient conditions that allow a discrete time analysis of sensor unavailability (interrupted observations) intervals, bounding these intervals in order to state that the unstable open-loop plant represented in Figure 1, when controlled in closed-loop, is globally uniformly exponentially stable. These results are proved under the existence of modeling uncertainties and if plant state vanishing perturbations occur, then global asymptotical stability is achieved for the perturbed system. The results were proved for either systems with linear actuators, or with memoryless sector nonlinear actuators.

It is interesting to note that in a related work [4], a similar conservative theoretical result regarding uniform exponential stability is reported, showing that longer intervals of unavailability can be reached in practice and that these theoretical results might be too conservative for practical purposes.

APPENDIX

Throughout the appendix, the matrices norms are the ones induced by the Euclidean norm of vectors, being given by their largest singular values.

Consider the discrete time line represented in Figure 2. The intervals where the sensors yield correct measures are designated as T_{a_j}, with $j = 1,3,5,7,\ldots,i$, and the intervals where the observations are interrupted are designated as T_{u_j}, with $j = 2,4,6,\ldots,i-1,i+1$. Let the discrete time instant k_0 denote the beginning of a generic interval.

Since it will be often used in the following proofs, a Gronwall-Bellman type of inequality for sequences is presented [17].

Lemma 1. *Suppose the scalar sequences $v(k)$ and $\phi(k)$ are such that $v(k) \geq 0$ for $k \geq k_0$, and*

$$\phi(k) \leq \begin{cases} \Psi, & k = k_0, \\ \Psi + \eta \sum_{j=k_0}^{k-1} v(j)\phi(j), & k \geq k_0 + 1, \end{cases} \tag{A.1}$$

where Ψ and η are constants with $\eta \geq 0$. Then

$$\phi(k) \leq \Psi \prod_{j=k_0}^{k-1} [1 + \eta v(j)]. \tag{A.2}$$

Consider, also, the sum of the $(k-k_0)$ terms of a geometric progression with ratio r,

$$\sum_{j=k_0}^{k-1} r^j = \frac{r^{k_0} - r^k}{1-r}. \tag{A.3}$$

If $|r| < 1$, then, as $k \to \infty$, (A.3) becomes

$$\sum_{j=k_0}^{k-1} r^j = \frac{r^{k_0}}{1-r}. \tag{A.4}$$

A.1. Stability proofs for system with linear input

Proof of Theorem 1. Consider the system depicted in Figure 3. During availability time intervals T_{a_j}, with $j = 1,3,5,7,\ldots,i$, it is $z(k) = x(k)$, and the plant state $x(k)$ evolves according to

$$x(k) = \Phi_{\delta_{\mathrm{CL}}}(k,k_0)x(k_0), \quad k \geq k_0 + 1. \tag{A.5}$$

On the other hand, during unavailability time intervals T_{u_j}, with $j = 2,4,6,\ldots,i-1,i+1$, it is $z(k) = \hat{x}(k)$, the model state $\hat{x}(k)$ evolves according to

$$\hat{x}(k) = \Phi_{\mathrm{CL}}(k,k_0)\hat{x}(k_0), \quad k \geq k_0 + 1, \tag{A.6}$$

and the plant state $x(k)$ evolves according to

$$x(k) = \Phi_\delta(k,k_0)x(k_0) - \sum_{j=k_0}^{k-1} \Phi_\delta(k,j+1)(B+\delta_B)L\hat{x}(j), \quad k \geq k_0 + 1. \tag{A.7}$$

Replacing (A.6) in (A.7), and knowing that the model initial sate $\hat{x}$ is made equal to the last available observation of

the state x when an interrupted observation occurs ($\hat{x}(k_0) = x(k_0) = x(k_0 - 1)$), the plant state $x(k)$ evolution is

$$x(k) = \Phi_\delta(k, k_0)x(k_0) - \sum_{j=k_0}^{k-1} \Phi_\delta(k, j+1)(B + \delta_B)L\Phi_{\mathrm{CL}}(j, k_0)x(k_0), \quad k \geq k_0 + 1. \tag{A.8}$$

It is assumed that the model in closed-loop is stable and bounded by $\|\Phi_{\mathrm{CL}}(k, k_0)\| \leq \gamma\lambda^{k-k_0}$, $k \geq k_0$, with $0 \leq \lambda < 1$ and $\gamma \geq 1$, and that the model is unstable in open-loop, but bounded by $\|\Phi(k, k_0)\| \leq \alpha\beta^{k-k_0}$, $k \geq k_0$, with $\beta > 1$ and $\alpha \geq 1$.

For bounded model uncertainties $\|\delta_A\| \leq \sigma_{\delta_A}$, and considering the bound on $\|\Phi(k, k_0)\|$, with $\beta > 1$ (this corresponds to assume an unfavorable situation), it can be proved through the use of Lemma 1, if δ_A is seen as a perturbation in the system $x(k+1) = (A + \delta_A)x(k)$, [17], that $\|\Phi_\delta(k, k_0)\| \leq \alpha(\beta + \alpha\cdot\sigma_{\delta_A})^{k-k_0}$, with $(\beta + \alpha\cdot\sigma_{\delta_A}) > 1$. This means, as expected, that if the model dynamics are open-loop unstable, then there will be a δ_A such that the plant dynamics will be open-loop unstable (the use of a continuity argumentation could also explain such assertion). A similar proof can be given for the stability of the plant in closed-loop since the model is stable in closed-loop ($\|\Phi_{\mathrm{CL}}(k, k_0)\| \leq \gamma\lambda^{k-k_0}$, with $0 \leq \lambda < 1$). Again, recurring to Lemma 1, and considering that $(\delta_A - \delta_B L)$ is seen as a perturbation in the system $x(k+1) = [(A + \delta_A) - (B + \delta_B)L]x(k)$, it can be proved that $\|\Phi_{\delta_{\mathrm{CL}}}(k, k_0)\| \leq \gamma(\lambda + \gamma\Sigma)^{k-k_0}$, $k \geq k_0$, with $0 \leq \Sigma < (1 - \lambda)/\gamma$, and $\Sigma := \sigma_{\delta_A} + \sigma_{\delta_B}\cdot\sigma_L$.

Upper bounds for (A.5) during availability time intervals, and for (A.8) during unavailability time intervals, are obtained, respectively

$$||x(k)|| = ||\Phi_{\delta_{\mathrm{CL}}}(k, k_0)x(k_0)||, \tag{A.9}$$

$$||x(k)|| = \left|\left|\Phi_\delta(k, k_0)x(k_0) - \sum_{j=k_0}^{k-1} \Phi_\delta(k, j+1)(B + \delta_B)L\Phi_{\mathrm{CL}}(j, k_0)x(k_0)\right|\right|. \tag{A.10}$$

Starting from (A.9), yields

$$||x(k)|| \leq \gamma(\lambda + \gamma\Sigma)^{k-k_0}||x(k_0)|| \tag{A.11}$$

and for (A.10), recalling that $\|B\| := \sigma_B$, $\|\delta_B\| \leq \sigma_{\delta_B}$, and $\|L\| := \sigma_L$,

$$||x(k)|| \leq \left(\alpha(\beta + \alpha\cdot\sigma_{\delta_A})^{k-k_0} + \sum_{j=k_0}^{k-1} \alpha(\beta + \alpha\cdot\sigma_{\delta_A})^{k-j-1}(\sigma_B + \sigma_{\delta_B})\sigma_L\gamma\lambda^{j-k_0}\right) \cdot||x(k_0)||. \tag{A.12}$$

Since $0 \leq \lambda/(\beta + \alpha\cdot\sigma_{\delta_A}) < 1$, and considering (A.4), after some calculations

$$||x(k)|| \leq \left[1 + (\sigma_B + \sigma_{\delta_B})\frac{\sigma_L\cdot\gamma}{\beta + \alpha\cdot\sigma_{\delta_A} - \lambda}\right] . \alpha(\beta + \alpha\cdot\sigma_{\delta_A})^{k-k_0}\cdot||x(k_0)||. \tag{A.13}$$

The complete state evolution from time instant $k = 0$, up to the final time instant at $k \in T_{u_{i+1}}$, is given by the alternate product of (A.5) by (A.8), where $\hat{x}(k_0) = x(k_0) = x(k_0 - 1)$ is considered. Applying results (A.11) and (A.13) to this product originates

$$\begin{aligned} ||x(k)|| \leq{}& \left[1 + (\sigma_B + \sigma_{\delta_B})\frac{\sigma_L\cdot\gamma}{\beta + \alpha\cdot\sigma_{\delta_A} - \lambda}\right]\alpha(\beta + \alpha\cdot\sigma_{\delta_A})^{k-T_i} \\ &\cdot\gamma(\lambda + \gamma\Sigma)^{(T_i-1)-T_{i-1}} \\ &\cdots\left[1+(\sigma_B+\sigma_{\delta_B})\frac{\sigma_L\cdot\gamma}{\beta + \alpha\cdot\sigma_{\delta_A} - \lambda}\right]\alpha(\beta+\alpha\cdot\sigma_{\delta_A})^{T_2-T_1} \\ &\cdot\gamma(\lambda + \gamma\Sigma)^{T_1-1}\cdot||x_0|| \\ ={}& c_1^{(i+1)/2}\cdot(\beta + \alpha\cdot\sigma_{\delta_A})^{T_u}\cdot(\lambda + \gamma\Sigma)^{T_a}\cdot||x_0||, \end{aligned} \tag{A.14}$$

where T_u and T_a represent the entire duration of all unavailability and availability time intervals, respectively, and

$$c_1 := \left[1 + (\sigma_B + \sigma_{\delta_B})\frac{\sigma_L\cdot\gamma}{\beta + \alpha\cdot\sigma_{\delta_A} - \lambda}\right]\alpha\gamma. \tag{A.15}$$

In order for the system to be uniformly stable, it must verify $\|x(k)\| \leq M_1\|x(k_0)\|$, $k \geq k_0$, with $M_1 \geq 1$. Therefore, from (A.14)

$$\begin{aligned} &c_1^{(i+1)/2}\cdot(\beta + \alpha\cdot\sigma_{\delta_A})^{T_u}\cdot(\lambda + \gamma\Sigma)^{T_a} \leq M_1 \\ &\quad\Longrightarrow T_u \leq \frac{\log M_1 - ((i+1)/2)\log c_1 - T_a\log(\lambda + \gamma\Sigma)}{\log(\beta + \alpha\cdot\sigma_{\delta_A})}. \end{aligned} \tag{A.16}$$

Replacing (A.15) in (A.16) gives the desired result from Theorem 1 subject to the constraint $\Sigma < (1 - \lambda)/\gamma$, and the result holds globally since it is valid for any $\|x(k_0)\|$. □

Proof of Corollary 1. Consider the Euclidean norm of $x(k)$ at discrete times $k = T_{i-1}$, and $k = T_{i-3}$, at the end of the unavailability intervals $T_{u_{i-1}}$, and $T_{u_{i-3}}$, respectively. In order for $\|x(T_j)\|$, for $j = 0, 2, 4, 6, \ldots, i-1$, to be a monotonic descent sequence, it should verify

$$\frac{||x(T_{i-1})||}{||x(T_{i-3})||} < 1 \tag{A.17}$$

equivalently, from the first two lines of (A.14), and considering (A.15)

$$c_1(\beta + \alpha\cdot\sigma_{\delta_A})^{T_{i-1}-T_{i-2}}\cdot(\lambda + \gamma\Sigma)^{(T_{i-2}-1)-T_{i-3}} < 1 \tag{A.18}$$

or, since $T_{i-1} - T_{i-2} = T_{u_{i-1}}$, and $(T_{i-2} - 1) - T_{i-3} = T_{a_{i-2}}$

$$T_{u_{i-1}} < \frac{-\log c_1 - T_{a_{i-2}}\log(\lambda + \gamma\Sigma)}{\log(\beta + \alpha\cdot\sigma_{\delta_A})}. \tag{A.19}$$

Replacing (A.15) in (A.19) gives the desired result from Corollary 1 subject to the constraint $\Sigma < (1-\lambda)/\gamma$, and the result holds globally since it is valid for any $\|x(k_0)\|$. □

Proof of Corollary 2. In order for the system to be uniformly exponentially stable, it must verify $\|x(k)\| \leq M_2 N_2^{k-k_0}\|x(k_0)\|$, $k \geq k_0$, with $M_2 \geq 1$, and $0 \leq N_2 < 1$. Therefore, from (A.14) and considering $k_0 = 0$, and $(k - k_0) = T_u + T_a$,

$$c_1^{(i+1)/2}\cdot\left(\beta+\alpha\cdot\sigma_{\delta_A}\right)^{T_u}\cdot\left(\lambda+\gamma\Sigma\right)^{T_a} \leq M_2 N_2^{T_u+T_a}$$
$$\Longrightarrow T_u \leq \frac{\log M_2 - ((i+1)/2)\log c_1 - T_a \log\left((\lambda+\gamma\Sigma)/N_2\right)}{\log\left((\beta+\alpha\cdot\sigma_{\delta_A})/N_2\right)}. \tag{A.20}$$

Replacing (A.15) in (A.20) gives the desired result from Corollary 2 subject to the constraint $\Sigma < (1-\lambda)/\gamma$, and the result holds globally since it is valid for any $\|x(k_0)\|$. □

A.2. Stability proofs for system with nonlinear input

Proof of Theorem 2. Consider the system depicted in Figure 1. During availability time intervals T_{a_j}, with $j = 1, 3, 5, 7, \ldots, i$, it is $z(k) = x(k)$, and the plant state $x(k)$ evolves according to

$$x(k) = \overline{\Phi}_{\delta_{\mathrm{CL}}}(k,k_0)x(k_0) + \sum_{j=k_0}^{k-1}\overline{\Phi}_{\delta_{\mathrm{CL}}}(k,j+1)\left(B+\delta_B\right) \cdot \psi_s(-Lx(j)), \quad k \geq k_0+1. \tag{A.21}$$

On the other hand, during unavailability time intervals T_{u_j}, with $j = 2, 4, 6, \ldots, i-1, i+1$, it is $z(k) = \hat{x}(k)$, the model initial sate $\hat{x}$ is made equal to the last available observation of the state x when an interrupted observation occurs ($\hat{x}(k_0) = x(k_0) = x(k_0-1)$), the model state $\hat{x}(k)$ evolves according to

$$\hat{x}(k) = \overline{\Phi}_{\mathrm{CL}}(k,k_0)x(k_0) + \sum_{j=k_0}^{k-1}\overline{\Phi}_{\mathrm{CL}}(k,j+1)B\psi_s(-L\hat{x}(j)), \quad k \geq k_0+1 \tag{A.22}$$

and the plant state $x(k)$ evolves according to

$$x(k) = \Phi_\delta(k,k_0)x(k_0) + \sum_{j=k_0}^{k-1}\Phi_\delta(k,j+1)\left(B+\delta_B\right) \cdot\left[\psi_s(-L\hat{x}(j)) - P\hat{x}(j)\right], \quad k \geq k_0+1. \tag{A.23}$$

It is assumed that the model in closed-loop is stable and bounded by $\|\overline{\Phi}_{\mathrm{CL}}(k,k_0)\| \leq \gamma\lambda^{k-k_0}$, $k \geq k_0$, with $0 \leq \lambda < 1$ and $\gamma \geq 1$, and that the model is unstable in open-loop, but bounded by $\|\Phi(k,k_0)\| \leq \alpha\beta^{k-k_0}$, $k \geq k_0$, with $\beta > 1$ and $\alpha \geq 1$.

For bounded model uncertainties $\|\delta_A\| \leq \sigma_{\delta_A}$, and considering the bound on $\|\Phi(k,k_0)\|$ with $\beta > 1$ (this corresponds to assume an unfavorable situation), it was proved in Appendix A.1 that $\|\Phi_\delta(k,k_0)\| \leq \alpha(\beta+\alpha\cdot\sigma_{\delta_A})^{k-k_0}$ with $(\beta+\alpha\cdot\sigma_{\delta_A}) > 1$. A similar proof can be given for the stability of the plant in closed-loop since the model is stable in closed-loop ($\|\overline{\Phi}_{\mathrm{CL}}(k,k_0)\| \leq \gamma\lambda^{k-k_0}$ with $0 \leq \lambda < 1$). Recurring to Lemma 1, and considering that $(\delta_A - \delta_B P)$ is seen as a perturbation in the system $x(k+1) = [(A+\delta_A) - (B+\delta_B)P]x(k)$, it can be proved that $\|\overline{\Phi}_{\delta_{\mathrm{CL}}}(k,k_0)\| \leq \gamma(\lambda+\gamma\Sigma)^{k-k_0}$, $k \geq k_0$ with $0 \leq \Sigma < (1-\lambda)/\gamma$, and $\Sigma := \sigma_{\delta_A} + \sigma_{\delta_B}\cdot\sigma_P$, [17].

Upper bounds for (A.21) during availability time intervals, and for (A.23) during unavailability time intervals, are obtained, respectively

$$\|x(k)\| = \left\|\overline{\Phi}_{\delta_{\mathrm{CL}}}(k,k_0)x(k_0) + \sum_{j=k_0}^{k-1}\overline{\Phi}_{\delta_{\mathrm{CL}}}(k,j+1)\left(B+\delta_B\right)\psi_s(-Lx(j))\right\|,$$
$$\|x(k)\| = \left\|\Phi_\delta(k,k_0)x(k_0) + \sum_{j=k_0}^{k-1}\Phi_\delta(k,j+1)\left(B+\delta_B\right) \cdot\left[\psi_s(-L\hat{x}(j)) - P\hat{x}(j)\right]\right\|. \tag{A.24}$$

From (A.24), recalling that $\|B\| := \sigma_B$, $\|\delta_B\| \leq \sigma_{\delta_B}$, $\|L\| := \sigma_L$ and considering (24) yield, respectively

$$\|x(k)\| \leq \gamma(\lambda+\gamma\Sigma)^{k-k_0}\cdot\|x(k_0)\| + \sum_{j=k_0}^{k-1}\gamma(\lambda+\gamma\Sigma)^{k-j-1}\cdot\left(\sigma_B+\sigma_{\delta_B}\right)\gamma_2\cdot\sigma_L\cdot\|x(j)\|, \tag{A.25}$$

$$\|x(k)\| \leq \alpha(\beta+\alpha\cdot\sigma_{\delta_A})^{k-k_0}\cdot\|x(k_0)\| + \sum_{j=k_0}^{k-1}\alpha(\beta+\alpha\cdot\sigma_{\delta_A})^{k-j-1} \cdot\left(\sigma_B+\sigma_{\delta_B}\right)\left(\sigma_P+\gamma_2\cdot\sigma_L\right)\cdot\|\hat{x}(j)\|. \tag{A.26}$$

Applying Lemma 1 to (A.25) gives

$$\|x(k)\| \leq \gamma\left[(\lambda+\gamma\Sigma) + \gamma\left(\sigma_B+\sigma_{\delta_B}\right)\gamma_2\cdot\sigma_L\right]^{k-k_0}\cdot\|x(k_0)\|. \tag{A.27}$$

An upper bound for (A.22) is obtained from

$$\|\hat{x}(k)\| \leq \gamma\lambda^{k-k_0}\cdot\|x(k_0)\| + \sum_{j=k_0}^{k-1}\gamma\lambda^{k-j-1}\sigma_B\cdot\gamma_2\cdot\sigma_L\cdot\|\hat{x}(j)\|. \tag{A.28}$$

Applying Lemma 1 and recalling that $\hat{x}(k_0) = x(k_0) = x(k_0-1)$ yield

$$\|\hat{x}(k)\| \leq \gamma\left(\lambda+\gamma\cdot\sigma_B\cdot\gamma_2\cdot\sigma_L\right)^{k-k_0}\cdot\|x(k_0)\|. \tag{A.29}$$

Using (A.29) in (A.26),

$$||x(k)|| \leq \left[\alpha(\beta+\alpha\cdot\sigma_{\delta_A})^{k-k_0} + \alpha(\sigma_B+\sigma_{\delta_B})(\sigma_P+\gamma_2\cdot\sigma_L)\gamma \cdot (\beta+\alpha\cdot\sigma_{\delta_A})^{k-1}\cdot(\lambda+\gamma\cdot\sigma_B\cdot\gamma_2\cdot\sigma_L)^{-k_0} \cdot \sum_{j=k_0}^{k-1}\left(\frac{\lambda+\gamma\cdot\sigma_B\cdot\gamma_2\cdot\sigma_L}{\beta+\alpha\cdot\sigma_{\delta_A}}\right)^j\right]\cdot||x(k_0)||. \tag{A.30}$$

Making use of (A.3) in (A.30) gives

$$||x(k)|| \leq \left[\alpha(\beta+\alpha\cdot\sigma_{\delta_A})^{k-k_0} + \alpha(\sigma_B+\sigma_{\delta_B})(\sigma_P+\gamma_2\cdot\sigma_L)\gamma \cdot \frac{(\beta+\alpha\cdot\sigma_{\delta_A})^{k-k_0} - (\lambda+\gamma\cdot\sigma_B\cdot\gamma_2\cdot\sigma_L)^{k-k_0}}{(\beta+\alpha\cdot\sigma_{\delta_A}) - (\lambda+\gamma\cdot\sigma_B\cdot\gamma_2\cdot\sigma_L)}\right] \cdot||x(k_0)||. \tag{A.31}$$

Providing $\gamma_2 < (\beta+\alpha\cdot\sigma_{\delta_A}-\lambda)/(\gamma\cdot\sigma_B\cdot\sigma_L)$, and considering (A.4), after some calculations, (A.31) yields

$$||x(k)|| \leq \left[1+\frac{(\sigma_B+\sigma_{\delta_B})\cdot(\sigma_P+\gamma_2\cdot\sigma_L)\gamma}{(\beta+\alpha\cdot\sigma_{\delta_A})-(\lambda+\gamma\cdot\sigma_B\cdot\gamma_2\cdot\sigma_L)}\right] \cdot\alpha(\beta+\alpha\cdot\sigma_{\delta_A})^{k-k_0}\cdot||x(k_0)||. \tag{A.32}$$

From this point on, the demonstration follows closely the one of Theorem 1 (see Appendix A.1), and applying results (A.27) and (A.32) originates

$$||x(k)|| \leq c_2^{(i+1)/2}\cdot(\beta+\alpha\cdot\sigma_{\delta_A})^{T_u} \cdot\left[(\lambda+\gamma\Sigma)+\gamma(\sigma_B+\sigma_{\delta_B})\gamma_2\cdot\sigma_L\right]^{T_a}\cdot||x_0||, \tag{A.33}$$

where T_u and T_a represent the entire duration of all unavailability and availability time intervals, respectively, and

$$c_2 := \left[1+\frac{(\sigma_B+\sigma_{\delta_B})\cdot(\sigma_P+\gamma_2\cdot\sigma_L)\gamma}{(\beta+\alpha\cdot\sigma_{\delta_A})-(\lambda+\gamma\cdot\sigma_B\cdot\gamma_2\cdot\sigma_L)}\right]\alpha\gamma. \tag{A.34}$$

In order for the system to be uniformly stable, it must verify $\|x(k)\| \leq M_1\|x(k_0)\|$, $k \geq k_0$ with $M_1 \geq 1$. Therefore, from (A.33)

$$c_2^{(i+1)/2}\cdot(\beta+\alpha\cdot\sigma_{\delta_A})^{T_u}\cdot\left[(\lambda+\gamma\Sigma)+\gamma(\sigma_B+\sigma_{\delta_B})\gamma_2\cdot\sigma_L\right]^{T_a} \leq M_1 \Longrightarrow T_u \leq \frac{\log M_1 - ((i+1)/2)\log c_2}{\log(\beta+\alpha\cdot\sigma_{\delta_A})} - \frac{T_a\log\left[(\lambda+\gamma\Sigma)+\gamma(\sigma_B+\sigma_{\delta_B})\gamma_2\cdot\sigma_L\right]}{\log(\beta+\alpha\cdot\sigma_{\delta_A})}. \tag{A.35}$$

Replacing (A.34) in (A.35) gives the desired result from Theorem 2 subject to the constraints $\Sigma < (1-\lambda)/\gamma$, and $\gamma_2 < (\beta+\alpha\cdot\sigma_{\delta_A}-\lambda)/(\gamma\cdot\sigma_B\cdot\sigma_L)$. The result holds globally since it is valid for any $\|x(k_0)\|$. □

Proof of Corollary 3. Consider the Euclidean norm of $x(k)$ at discrete times $k = T_{i-1}$, and $k = T_{i-3}$, at the end of the unavailability intervals $T_{u_{i-1}}$, and $T_{u_{i-3}}$, respectively. In order for $\|x(T_j)\|$, for $j = 0, 2, 4, 6, \ldots, i-1$, to be a monotonic descent sequence, it should verify

$$\frac{||x(T_{i-1})||}{||x(T_{i-3})||} < 1. \tag{A.36}$$

This proof is outlined in the very same way as Corollary 1 proof, therefore, the following equation yields naturally after Theorem 2 proof calculations:

$$T_{u_{i-1}} < \frac{-\log c_2 - T_{a_{i-2}}\log\left[(\lambda+\gamma\Sigma)+\gamma(\sigma_B+\sigma_{\delta_B})\gamma_2\cdot\sigma_L\right]}{\log(\beta+\alpha\cdot\sigma_{\delta_A})}. \tag{A.37}$$

Replacing (A.34) in (A.37) gives the desired result from Corollary 3 subject to the constraints $\Sigma < (1-\lambda)/\gamma$, and $\gamma_2 < (\beta+\alpha\cdot\sigma_{\delta_A}-\lambda)/(\gamma\cdot\sigma_B\cdot\sigma_L)$. The result holds globally since it is valid for any $\|x(k_0)\|$. □

Proof of Corollary 4. In order for the system to be uniformly exponentially stable, it must verify $\|x(k)\| \leq M_2N_2^{k-k_0}\|x(k_0)\|$, $k \geq k_0$, with $M_2 \geq 1$, and $0 \leq N_2 < 1$. Therefore, from (A.33), and considering $k_0 = 0$, and $(k-k_0) = T_u + T_a$,

$$c_2^{(i+1)/2}\cdot(\beta+\alpha\cdot\sigma_{\delta_A})^{T_u}\cdot\left[(\lambda+\gamma\Sigma)+\gamma(\sigma_B+\sigma_{\delta_B})\gamma_2\cdot\sigma_L\right]^{T_a} \leq M_2N_2^{T_u+T_a} \Longrightarrow T_u \leq \frac{\log M_2 - ((i+1)/2)\log c_2}{\log((\beta+\alpha\cdot\sigma_{\delta_A})/N_2)} - \frac{T_a\log\left(\dfrac{\left[(\lambda+\gamma\Sigma)+\gamma(\sigma_B+\sigma_{\delta_B})\gamma_2\cdot\sigma_L\right]}{N_2}\right)}{\log((\beta+\alpha\cdot\sigma_{\delta_A})/N_2)}. \tag{A.38}$$

Replacing (A.34) in (A.38) gives the desired result from Corollary 4 subject to the constraints $\Sigma < (1-\lambda)/\gamma$ and $\gamma_2 < (\beta+\alpha\cdot\sigma_{\delta_A}-\lambda)/(\gamma\cdot\sigma_B\cdot\sigma_L)$. The result holds globally since it is valid for any $\|x(k_0)\|$. □

ACKNOWLEDGMENT

This work was produced in the framework of the project IDEA—Integrated Design for Automated Anaesthesia, PTDC/EEA-ACR/69288/2006.

REFERENCES

[1] E. Halberg, I. Kaminer, and A. Pascoal, "Development of a flight test system for unmanned air vehicle," *IEEE Control Systems*, vol. 19, no. 1, pp. 55–65, 1999.

[2] J. W. Overstreet and A. Tzes, "An Internet-based real-time control engineering laboratory," *IEEE Control Systems*, vol. 19, no. 5, pp. 19–34, 1999.

[3] J. Tugnait, "Detection and estimation for abruptly changing systems," *Automatica*, vol. 18, pp. 607–615, 1982.

[4] W. Zhang, M. S. Branicky, and S. M. Phillips, "Stability of networked control systems," *IEEE Control Systems*, vol. 21, no. 1, pp. 84–99, 2001.
[5] T. Estrada, H. Lin, and P. J. Antsaklis, "Model-based control with intermittent feedback," in *Proceedings of the 14th Mediterranean Conference on Control and Automation (MED '06)*, pp. 1–6, Ancona, Italy, June 2006.
[6] H. Yang and M. Saif, "Observer design and fault diagnosis for state-retarded dynamical systems," *Automatica*, vol. 34, no. 2, pp. 217–227, 1998.
[7] D. Loebis, R. Sutton, J. Chudley, and W. Naeem, "Adaptive tuning of a Kalman filter via fuzzy logic for an intelligent AUV navigation system," *Control Engineering Practice*, vol. 12, no. 12, pp. 1531–1539, 2004.
[8] S. M. Bennett, R. J. Patton, and S. Daley, "Sensor fault-tolerant control of a rail traction drive," *Control Engineering Practice*, vol. 7, no. 2, pp. 217–225, 1999.
[9] C. J. Lopez-Toribio and R. J. Patton, "Takagi-Sugeno fuzzy fault-tolerant control for a non-linear system," in *Proceedings of the 38th IEEE Conference on Decision and Control (CDC '99)*, vol. 5, pp. 4368–4373, Phoenix, Ariz, USA, December 1999.
[10] O. R. Gonzalez, W. S. Gray, A. Tejada, and S. Patilkulkarni, "Stability analysis of upset recovery methods for electromagnetic interference," in *Proceedings of the 40th IEEE Conference on Decision and Control*, vol. 5, pp. 4134–4139, Orlando, Fla, USA, December 2001.
[11] J. M. Lemos, H. Magalhães, T. Mendonça, and R. V. Dionísio, "Control of neuromuscular blockade in the presence of sensor faults," *IEEE Transactions on Biomedical Engineering*, vol. 52, no. 11, pp. 1902–1911, 2005.
[12] J. M. Lemos, H. Magalhães, R. V. Dionísio, and T. Mendonça, "Control of physiological variables in the presence of interrupted feedback measurements," in *Proceedings of the 16th International Conference on Systems Engineering (ICSE '03)*, vol. 2, pp. 433–438, Coventry, UK, September 2003.
[13] R. V. Dionísio and J. Lemos, "Stability results for discrete systems controlled in the presence of interrupted observations," in *Proceedings of the 11th IEEE Mediterranean Conference on Control and Automation (MED '03)*, Rhodes, Greece, June 2003.
[14] H. K. Khalil, *Nonlinear Systems*, Prentice Hall, Upper Saddle River, NJ, USA, 2nd edition, 1996.
[15] W. M. Haddad and V. Kapila, "Static output feedback controllers for continuous-time and discrete-time systems with input non-linearities," *European Journal of Control*, vol. 4, pp. 22–31, 1998.
[16] P. O. M. Scokaert, J. B. Rawlings, and E. S. Meadows, "Discrete-time stability with perturbations: application to model predictive control," *Automatica*, vol. 33, no. 3, pp. 463–470, 1997.
[17] W. J. Rugh, *Linear System Theory*, Prentice-Hall, Upper Saddle River, NJ, USA, 2nd edition, 1996.

Hindawi Publishing Corporation
Journal of Control Science and Engineering
Volume 2008, Article ID 723292, 7 pages
doi:10.1155/2008/723292

Research Article

Actuator Fault Diagnosis with Robustness to Sensor Distortion

Qinghua Zhang

INRIA-IRISA, Campus de Beaulieu, 35042 Rennes Cedex, France

Correspondence should be addressed to Qinghua Zhang, zhang@irisa.fr

Received 1 April 2007; Revised 15 August 2007; Accepted 11 November 2007

Recommended by Jakob Stoustrup

Actuator fault diagnosis is often studied under strong assumptions on available sensors. Typically, it is assumed that the sensors are either fault free or sufficiently redundant. The purpose of this paper is to present a new method for *actuator* fault diagnosis which is robust to *sensor* distortion. It does not require sensor redundancy to compensate sensor distortion. The essential assumption is that sensor distortions are strictly monotonous. Despite the nonlinear and unknown nature of distortions, such sensors still provide useful information for fault diagnosis. The robustness of the presented diagnosis method is analyzed, as well as its ability to detect actuator faults. A numerical example is provided to illustrate its efficiency.

1. INTRODUCTION

In the design of modern control systems, fault diagnosis is often considered for component faults, sensor faults, and actuator faults. Various methods for fault diagnosis are generally based on the processing of sensor signals [1–3]. Many methods for *actuator* fault diagnosis assume reliable fault-free *sensors*, see, for instance, [4, 5]. For methods simultaneously dealing with actuator and sensor faults, it is typically assumed that there is sufficient redundancy among the sensors such that at any moment, the valid sensors can provide the information required for faults diagnosis. For mass production, it is important to use as less sensors as possible to reduce production cost. In such situations, fault diagnosis cannot uniquely rely on redundant sensors. Moreover, still for the purpose of cost reduction, sensors used in mass production may be highly nonlinear. If the sensor nonlinearity is well known, it can often be electronically compensated. Unfortunately, sometimes sensor nonlinearity varies within the production, and for each piece in use, the nonlinearity varies during its normal life duration. For example, most oxygen sensors used in cars equipped with catalytic converters are highly nonlinear. They roughly indicate if the oxygen concentration is over or below a reference value. Nevertheless, such sensors are sufficient for the purpose of engine control. It is then important to develop fault diagnosis methods relying on the same sensors. In this paper, unknown nonlinear behaviors of sensors are generally called *sensor distortion*.

The purpose of this paper is to present a method for actuator fault diagnosis which is robust to sensor distortion. It is assumed that each sensor can be affected by an *unknown* and *arbitrary*, but *strictly monotonous*, nonlinearity. The monotonousness is a weak assumption since any non monotonous distortion would make the sensor information useless. Remark that saturation is not a strictly monotonous nonlinearity, and thus is excluded in the proposed method. Nevertheless, a correctly working sensor should not be saturated when it is in its normal working range.

Robust methods for fault diagnosis has been studied in different contexts by many authors. In [6], a method based on adaptive wavelet analysis is proposed. The method studied in [7] uses generalized frequency response functions. Kullback discrimination information is used as a fault detection index in [8]. In [9], some faults of induction motors are detected by Fourier analysis of frequency signatures. (See the references cited in these publications for more information.) Compared to these existing results, the novelty of the method presented in this paper is its ability to deal with unknown nonlinear sensor distortions without requiring sensor redundancy.

The preliminary results presented in [10] are further developed in this paper, in particular, the analysis of the proposed robust detection method is completed with the characterization of the faults which can be detected.

The paper is organized as follows. The problem considered in this paper is formulated in Section 2. Fault detection

and isolation are, respectively, studied in Sections 3 and 4. A numerical example is presented in Section 5. Some concluding remarks are given in Section 6.

2. PROBLEM STATEMENT

The considered linear state-space system with sensor distortion is formulated as

$$\dot{x}(t) = Ax(t) + B\,\mathrm{diag}(u(t))\theta + w(t), \tag{1a}$$
$$z(t) = Cx(t) + v(t), \tag{1b}$$
$$y(t) = h(z(t)), \tag{1c}$$

where $x(t) \in \mathbb{R}^n$ is the state, $u(t) \in \mathbb{R}^l$ the input, $z(t) \in \mathbb{R}^m$ the output before sensor distortion, $y(t) \in \mathbb{R}^m$ the output after sensor distortion, and $w(t) \in \mathbb{R}^n$ and $v(t) \in \mathbb{R}^m$ represent bounded modeling uncertainties. The notation $\mathrm{diag}(u(t))$ denotes the diagonal matrix formed by the components of the input vector $u(t)$, and the vector $\theta \in \mathbb{R}^l$ is a coefficient vector introduced to describe the efficiency loss of actuators (multiplicative actuator faults). For fault-free actuators, θ takes the nominal value θ_0.

For notation simplicity, the parenthesis (t) of the time-dependent variables will not be written unless necessary.

Sensor distortion is modeled by the component-wisely defined nonlinear function h: let z_i and y_i be, respectively, the ith component of z and y, $i = 1, \ldots, m$, then

$$y_i = h_i(z_i). \tag{2}$$

Assumption 1. Each sensor distortion $h_i : \mathbb{R} \to \mathbb{R}$ is an unknown, but a strictly monotonously increasing, function. In other words, for any $\xi_1, \xi_2 \in \mathbb{R}$,

$$\xi_1 < \xi_2 \Longrightarrow h_i(\xi_1) < h_i(\xi_2). \tag{3}$$

Assumption 2. The system dynamics matrix A is asymptotically stable, that is, the eigenvalues of A have negative real parts.

Remark 1. No additive uncertainty is assumed in the sensor distortion equation (1c) since the arbitrary unknown monotonous nonlinear function can take into account some sensor distortion uncertainty. On the other hand, if it is assumed that

$$y = h(z) + \varepsilon, \tag{4}$$

where ε is some additive uncertainty, define

$$\begin{aligned} \widetilde{v} &= h^{-1}\big[h(Cx + v) + \varepsilon\big] - Cx, \\ \widetilde{z} &= Cx + \widetilde{v}, \end{aligned} \tag{5}$$

then (4) can be replaced by

$$y = h(\widetilde{z}) \tag{6}$$

which is in the form of (1c). Of course, in order to limit $\widetilde{v}$, some regularity of h should be assumed.

With the above formulation, the problem considered in this paper is the detection and isolation of multiplicative actuator faults, modeled as changes in the coefficient vector θ, despite the unknown sensor distortions.

3. FAULT DETECTION

The main difficulty of the problem formulated in the previous section is caused by the *unknown* sensor distortions. The key question is how to use the information provided by such sensors. Because of the unknown nature of h_i, for each measured value of $y_i = h_i(z_i)$, the corresponding value of z_i is completely unknown, and even the sign of z_i is unknown. The strict monotonousness of h_i assumed in Assumption 1 is not helpful in this aspect. However, it is important to make the following observation. For any two time instants t and τ, Assumption 1 implies that

$$\mathrm{sign}\big[z_i(t) - z_i(\tau)\big] = \mathrm{sign}\big[y_i(t) - y_i(\tau)\big]. \tag{7}$$

In other words, the relative sign of z_i at different time instants is known from the sensor output y_i measured at these time instants. Remark that t and τ are two arbitrary and independent time instants, and either one can be earlier than the other one. Since the absolute value $|z_i(t) - z_i(\tau)|$ is completely unknown, the relative sign is thus the only information about $z_i(t) - z_i(\tau)$ provided by the sensor output. This information will be the basis for the design of fault detection and isolation algorithms in this paper. Such information can also be used for the identification of Wiener systems [11].

Let $Z(s)$, $U(s)$, $W(s)$, and $V(s)$ be, respectively, the Laplace transforms of $z(t)$, $u(t)$, $w(t)$, and $v(t)$. It is then derived from (1a), (1b), and (1c) (by assuming zero initial state) that

$$Z(s) = C(sI - A)^{-1}B\,\mathrm{diag}\big(U(s)\big)\theta + C(sI - A)^{-1}W(s) + V(s). \tag{8}$$

Define

$$\Phi(t) = \mathfrak{L}^{-1}\Big[C(sI - A)^{-1}B\,\mathrm{diag}\big(U(s)\big)\Big], \tag{9}$$
$$\zeta(t) = \mathfrak{L}^{-1}\Big[C(sI - A)^{-1}W(s) + V(s)\Big], \tag{10}$$

where $\mathfrak{L}^{-1}$ is the inverse Laplace transform operator. Then

$$z(t) = \Phi(t)\theta + \zeta(t), \tag{11a}$$
$$y(t) = h(z(t)). \tag{11b}$$

Notice that $\Phi(t) \in \mathbb{R}^{m \times l}$ depends on $u(t)$ and can be computed through (9), whereas $\zeta(t) \in \mathbb{R}^m$ depends on modeling uncertainties $w(t)$, $v(t)$ and is unknown.

Remark 2. Zero initial condition of the state x has been assumed when (8) was derived. The asymptotic stability condition (Assumption 2) is not explicitly used in the above reasoning, but it ensures well-behaved computation of Φ through (9). To some extent, this stability condition allows also to tolerate nonzero initial states which are asymptotically forgotten. If the system was not asymptotically stable, then, in principle, an observer should be used in the computation of Φ. However, it is difficult to design observers with sensors distorted by unknown nonlinear functions.

Let ϕ_i be the ith row of Φ and ζ_i be the ith component of ζ, then the ith row of (11a) writes

$$z_i(t) = \phi_i(t)\theta + \zeta_i(t). \tag{12}$$

For any two time instants t and τ, it is obvious that

$$\operatorname{sign}[z_i(t) - z_i(\tau)][z_i(t) - z_i(\tau)] \geq 0. \tag{13}$$

Substitute $z_i(t)$ and $z_i(\tau)$ with the last equality, then, for constant θ,

$$\operatorname{sign}[z_i(t) - z_i(\tau)][(\phi_i(t) - \phi_i(\tau))\theta + \zeta_i(t) - \zeta_i(\tau)] \geq 0. \tag{14}$$

Remind the relative sign equality (7), then

$$\operatorname{sign}[y_i(t) - y_i(\tau)][(\phi_i(t) - \phi_i(\tau))\theta + \zeta_i(t) - \zeta_i(\tau)] \geq 0, \tag{15}$$

or equivalently

$$\begin{aligned} -\operatorname{sign}[y_i(t) - y_i(\tau)][\phi_i(t) - \phi_i(\tau)]\theta \\ \leq \operatorname{sign}[y_i(t) - y_i(\tau)][\zeta_i(t) - \zeta_i(\tau)]. \end{aligned} \tag{16}$$

Let θ_0 be the nominal value of θ (corresponding to fault-free actuators), a residual $r_i(t,\tau)$ for actuator fault detection can be generated as

$$r_i(t,\tau) = -\operatorname{sign}[y_i(t) - y_i(\tau)][\phi_i(t) - \phi_i(\tau)]\theta_0. \tag{17}$$

It then follows from (16) that, in the fault-free case,

$$r_i(t,\tau) \leq \operatorname{sign}[y_i(t) - y_i(\tau)][\zeta_i(t) - \zeta_i(\tau)]. \tag{18}$$

This result leads to the following proposition.

Proposition 1. *If $|\zeta_i(t)| \leq \lambda$ for some constant λ and any t, then the residual $r_i(t,\tau)$ defined in (17) satisfies, in the fault-free case, that is, $\theta = \theta_0$, the inequality*

$$r_i(t,\tau) \leq 2\lambda. \tag{19}$$

Proof. Let us first consider the case $y_i(t) \neq y_i(\tau)$, then it follows from the inequality (18) that

$$\begin{aligned} r_i(t,\tau) &\leq |r_i(t,\tau)| \\ &\leq |\zeta_i(t) - \zeta_i(\tau)| \\ &\leq |\zeta_i(t)| + |\zeta_i(\tau)| \leq 2\lambda. \end{aligned} \tag{20}$$

Now for the case $y_i(t) = y_i(\tau)$, it follows trivially from the inequality (18) that

$$r_i(t,\tau) \leq 0 \leq 2\lambda. \tag{21}$$

□

Remind that $\zeta_i(t)$ is a component of the variable $\zeta(t)$ depending on the bounded modeling uncertainties $w(t)$ and $v(t)$, as defined in (10). The boundedness of $w(t)$ and $v(t)$, together with Assumption 2, implies the boundedness of $\zeta(t)$. For practical convenience, the residual threshold should be directly derived from the assumed bounds of $w(t)$ and $v(t)$. It would require nontrivial error bound propagation through (10). Techniques of interval analysis or set-membership computation [12] can be applied for this purpose. This topic is not further discussed in this paper.

Proposition 1 guarantees the absence of false detection if fault detection is made by comparing the residual $r_i(t,\tau)$ with the threshold 2λ. However, it does not tell what are the faults which can be detected with such a decision rule. In general, robust fault detection methods are based on conservative decision rules, preventing the detection of some faults. In publications about robust fault detection, typically robustness results are provided, but the analysis about the set of faults which can be detected is usually absent, because it is often difficult to characterize the detectable faults in a robust detection framework. In contrast, for the method proposed in this paper, the faults which can be detected are clearly characterized as follows.

Proposition 2. *Assume that the system matrix pair (A, B) is controllable, $\theta \neq 0$, and $\theta_0 \neq 0$. For the faulty actuator parameter vector $\theta \neq \theta_0$, if there does not exist any positive real number α such that $\theta = \alpha\theta_0$, then there exist an input signal $u(t)$ and time instants t and τ such that*

$$r_i(t,\tau) > 2\lambda \tag{22}$$

for each $i = 1, \ldots, m$, where λ is a positive constant such that $|\zeta_i(t)| \leq \lambda$.

Proof. This proof applies to the residual $r_i(t,\tau)$ for each $i = 1, \ldots, m$.

Define the vector

$$\nu = \beta\left(\|\theta\|^{-1}\theta - ||\theta_0||^{-1}\theta_0\right), \tag{23}$$

where the norm $\|\theta\| = \sqrt{\theta^T\theta}$ and β is a *positive* number to be specified later. Then

$$\begin{aligned} \nu^T\theta &= \beta\left(\|\theta\| - ||\theta_0||^{-1}\theta_0^T\theta\right) \\ &= \beta\|\theta\|\left(1 - ||\theta_0||^{-1}\|\theta\|^{-1}\theta_0^T\theta\right) \geq 0, \end{aligned} \tag{24}$$

where the last inequality follows from the fact that $|\theta_0^T\theta| \leq \|\theta_0\|\|\theta\|$.

Notice that the equality

$$\left|\theta_0^T\theta\right| = ||\theta_0||\|\theta\| \tag{25}$$

would imply $\theta = \alpha\theta_0$ for some $\alpha > 0$, that is, the case excluded in Proposition 2. Therefore,

$$\nu^T\theta = \beta\left(\|\theta\| - ||\theta_0||^{-1}\theta_0^T\theta\right) > 0. \tag{26}$$

Similarly, it is also shown that

$$\nu^T\theta_0 = \beta\left(\|\theta\| - ||\theta_0||^{-1}\theta_0^T\theta\right) < 0. \tag{27}$$

It then follows that

$$\operatorname{sign}\left[\nu^T\theta\right]\nu^T\theta_0 < 0. \tag{28}$$

For given values of θ and θ_0, the value of β in (23) is chosen large enough such that

$$\begin{aligned} \left|\nu^T\theta\right| &> 2\lambda, \\ \left|\nu^T\theta_0\right| &> 2\lambda. \end{aligned} \tag{29}$$

Now, let us consider ϕ_i, the ith *row* of the matrix Φ defined in (9). If there is an input signal $u(t)$ such that $\phi_i(t) - \phi_i(\tau) = \nu^T$ for two time instants t and τ, then the inequality (28) leads to

$$\operatorname{sign}\big[(\phi_i(t) - \phi_i(\tau))\theta\big](\phi_i(t) - \phi_i(\tau))\theta_0 < 0. \tag{30}$$

Notice that the existence of such input signals is ensured by the controllability of the matrix pair (A, B).

Because $|(\phi_i(t) - \phi_i(\tau))\theta| = |\nu^T\theta| > 2\lambda \geq |\zeta_i(t) - \zeta_i(\tau)|$, the sign of $(\phi_i(t) - \phi_i(\tau))\theta + (\zeta_i(t) - \zeta_i(\tau))$ is determined by the sign of $(\phi_i(t) - \phi_i(\tau))\theta$, thus

$$\begin{aligned}&\operatorname{sign}\big[(\phi_i(t) - \phi_i(\tau))\theta + (\zeta_i(t) - \zeta_i(\tau))\big]\\ &\quad = \operatorname{sign}\big[(\phi_i(t) - \phi_i(\tau))\theta\big].\end{aligned} \tag{31}$$

This last equality, together with the inequality (30), leads to

$$\operatorname{sign}\big[(\phi_i(t) - \phi_i(\tau))\theta + (\zeta_i(t) - \zeta_i(\tau))\big](\phi_i(t) - \phi_i(\tau))\theta_0 < 0, \tag{32}$$

or equivalently

$$\begin{aligned}&\operatorname{sign}\big[z_i(t) - z_i(\tau)\big](\phi_i(t) - \phi_i(\tau))\theta_0 < 0,\\ &\operatorname{sign}\big[y_i(t) - y_i(\tau)\big](\phi_i(t) - \phi_i(\tau))\theta_0 < 0.\end{aligned} \tag{33}$$

Remind that $|[\phi_i(t) - \phi_i(\tau)]\theta_0| = |\nu^T\theta_0| > 2\lambda$, then

$$\operatorname{sign}\big[y_i(t) - y_i(\tau)\big][\phi_i(t) - \phi_i(\tau)]\theta_0 < -2\lambda. \tag{34}$$

Therefore, the residual as defined in (17) satisfies

$$r_i(t, \tau) > 2\lambda. \tag{35}$$

□

If t is the current time instant, then $r_i(t, \tau)$ can be computed for different past time instant τ. In order to reduce the effect of modeling uncertainties, $r_i(t, \tau)$ can be averaged over different values of τ in a sliding window. The computation of the residul from *sampled signals* is summarized as follows.

Residual generation algorithm summary

Assume that $\Phi(t)$ and $y(t)$ are sampled[1] at discrete time instants $1, 2, \ldots, N$. Choose the sliding window length $0 < L < N$ for residual averaging. For each sensor number $i = 1, 2, \ldots, m$, a residual is computed, for $k \geq L + 1$, through the formulas

$$\begin{aligned}r_i(k, s) &= -\operatorname{sign}\big[y_i(k) - y_i(s)\big][\phi_i(k) - \phi_i(s)]\theta_0,\\ \overline{r}_i(k) &= \frac{1}{L}\sum_{s=k-L}^{k-1} \max\big(r_i(k, s), 0\big).\end{aligned} \tag{36}$$

Notice that the max function is used to exclude negative values of $r_i(k, s)$ in the computation of the average value.

[1] For notation simplicity, the sampling period is assumed to be 1 here.

4. FAULT ISOLATION

After the detection of an actuator fault, the purpose of fault isolation is to figure out which actuators are faulty. In terms of (11a) and (11b), it amounts to deciding which components of θ have deviated from the nominal value θ_0.

It should be first remarked that, because of the arbitrary unknown function h, it is not possible to detect or isolate any proportional changes in all the components of θ. In other words, for any value $\alpha \in \mathbb{R}$, the parameter vector $\theta_1 = \alpha\theta_0$ cannot be distinguished from θ_0 based on the known signals $\Phi(t)$ and $y(t)$. For the same reason, if all the components of θ, except one, have changed, it is not possible to determine which one has not changed.

After having clarified the limitation related to unknown sensor distortion, let us look for an algorithm for fault isolation. The basic idea is to design residuals similar to (17), but capable of rejecting some actuator faults. Each designed residual should be insensitive to some of the possible actuator faults, whereas sensitive to the others. The actually occurred fault can then be isolated by comparing such residuals.

Let P be a permutation matrix, that is, a matrix obtained by permuting the rows of the $l \times l$ identity matrix I_l (remind that l is the number of actuators). Divide P into two submatrices P_f and P_s, respectively, composed of l_f and $l_s = l - l_f$ rows of P. Then it can be easily verified that

$$P_f^T P_f + P_s^T P_s = I_l. \tag{37}$$

The notations $P_f\theta$ and $P_s\theta$ will be used to select, respectively, the assumed *faulty* components and *sound* (or fault-free) components of θ. It is derived from (11a) that

$$z(t) = \Phi(t)P_f^T P_f\theta + \Phi(t)P_s^T P_s\theta + \zeta(t). \tag{38}$$

If P_s is assumed to select the components of θ corresponding to sound actuators, then, even after the occurrence of actuator faults, the equality

$$P_s\theta = P_s\theta_0 \tag{39}$$

still holds. Define

$$\theta_f \triangleq P_f\theta, \tag{40}$$

then

$$z(t) = \Phi(t)P_f^T\theta_f + \Phi(t)P_s^T P_s\theta_0 + \zeta(t). \tag{41}$$

For the purpose of fault isolation, different partitions of P into (P_f, P_s) should be considered. For each particular partition, a residual will be designed to be insensitive to changes in the corresponding subvector $\theta_f = P_f\theta$. Such a residual is said to be rejecting changes in θ_f. The rejection method used in the following is the estimation of θ_f from measure signals.

For two time instants t, τ, Assumption 1 implies (by rewriting inequality (15)) that

$$\begin{aligned}\operatorname{sign}\big[y_i(t) - y_i(\tau)\big]\big[(\phi_i(t) - \phi_i(\tau))P_f^T\theta_f + (\phi_i(t) - \phi_i(\tau))\\ \times P_s^T P_s\theta_0 + \zeta_i(t) - \zeta_i(\tau)\big] \geq 0.\end{aligned} \tag{42}$$

For a given set of signals $\Phi(t)$, $y(t)$ sampled at discrete time instants $1, 2, \ldots, N$, the value of θ_f can be estimated by minimizing the error term $\zeta_i(t) - \zeta_i(\tau)$ in the inequality (42) where the time instants t, τ are replaced by all pairs among the sampling instants $1, 2, \ldots, N$.

Because $y_i(t) < y_i(s)$ and $y_i(s) < y_i(\tau)$ imply $y_i(t) < y_i(\tau)$, there would be too much redundancy if all the possible pairs among $1, 2, \ldots, N$ were considered in (42). In order to reduce redundancy, for each sensor y_i, the data samples are sorted according to the values of $y_i(t)$, and only the neighboring pairs are considered. The algorithm is summarized as follows.

Residual generation algorithm summary

For each chosen partition of P into (P_f, P_s), the residuals rejecting changes in $\theta_f = P_f\theta$ are computed as follows. For each sensor number $i = 1, 2, \ldots, m$, sort the data such that

$$y_i\left(k_1^i\right) \le y_i\left(k_2^i\right) \le \cdots \le y_i\left(k_N^i\right). \tag{43}$$

Solve the constrained optimization problem

$$\min_{\theta_f} \max_{1\le i\le m,\, 1\le j\le N-1} \tilde{\zeta}_i(j), \tag{44}$$

subject to the constraints, for $i = 1, 2, \ldots, m$ and $j = 1, 2, \ldots, N-1$,

$$\begin{aligned}&\left[\phi_i\left(k_j^i\right) - \phi_i\left(k_{j+1}^i\right)\right]P_f^T\theta_f \\ &\quad+\left[\phi_i\left(k_j^i\right) - \phi_i\left(k_{j+1}^i\right)\right]P_s^TP_s\theta_0 + \tilde{\zeta}_i(j) \le 0.\end{aligned} \tag{45}$$

The corresponding sequences

$$\tilde{\zeta}_i(1), \tilde{\zeta}_i(2), \ldots, \tilde{\zeta}_i(N-1), \quad i = 1, 2, \ldots, m, \tag{46}$$

are the residuals rejecting changes in θ_f.

Remark that the inequality (45) corresponds to the inequality (42) where the omitted $\operatorname{sign}[y_i(k_j^i) - y_i(k_{j+1}^i)]$ is always negative due to the sorted sequence, and accordingly, the inequality changes from "$\ge$" to "$\le$".

The constrained minimization (44)-(45) can be easily reformulated in the form of a standard linear programing problem. There are efficient numerical algorithms for its solution [13].

Proposition 3. *If the true parameter vector θ governing* (11a) *satisfies $P_s\theta = P_s\theta_0$, and if $|\zeta_i(t)| \le \lambda$ for some constant λ and any t, then the residual $\tilde{\zeta}_i(j)$, solution of the constrained optimization problem* (44)-(45), *satisfies*

$$\tilde{\zeta}_i(j) \le 2\lambda. \tag{47}$$

Proof. The proof of this result is quite straightforward. Let us first derive from (11a), (11b), and (37) that

$$\begin{aligned}&\left[\phi_i\left(k_j^i\right) - \phi_i\left(k_{j+1}^i\right)\right]P_f^TP_f\theta + \left[\phi_i\left(k_j^i\right) - \phi_i\left(k_{j+1}^i\right)\right]P_s^TP_s\theta \\ &\quad+\zeta_i\left(k_j^i\right) - \zeta_i\left(k_{j+1}^i\right) = z_i\left(k_j^i\right) - z_i\left(k_{j+1}^i\right) \le 0,\end{aligned} \tag{48}$$

where the indices k_j^i, k_{j+1}^i come from the sequence sorting $y_i(k)$ as in (43).

It is assumed that $P_s\theta = P_s\theta_0$. Then the above inequality shows that there exist a value of θ_f (equal to $P_f\theta$) and a value of $\tilde{\zeta}_i(j)$ (equal to $\zeta_i(k_j^i) - \zeta_i(k_{j+1}^i)$) such that the inequality (45) is satisfied. These values of θ_f and $\tilde{\zeta}_i(j)$ do not necessarily correspond to the solution of the constrained optimization problem (44)-(45), however, the optimal solution certainly has a value of $\tilde{\zeta}_i(j)$ not larger than $\zeta_i(k_j^i) - \zeta_i(k_{j+1}^i)$. Therefore,

$$\tilde{\zeta}_i(j) \le \zeta_i\left(k_j^i\right) - \zeta_i\left(k_{j+1}^i\right) \le 2\lambda. \tag{49}$$

□

Property (47) has been proved under the assumption $P_s\theta = P_s\theta_0$. It can be shown that (47) holds also if $P_s\theta = \alpha P_s\theta_0$ for any $\alpha \in \mathbb{R}$ because of the unknown sensor distortion function.

For fault isolation, various matrices P_s are assumed and the corresponding residuals are computed. Then property (47) can be used to decide if each assumed P_s is correct or not. Alternatively, for different matrices P_s of the same size, the values of the residuals can also be compared for fault isolation.

Keep in mind that fault isolation cannot distinguish the cases such that $P_s\theta = \alpha P_s\theta_0$. For reliable fault isolation, the following assumption is required.

Assumption 3. There exists a permutation matrix P such that, for P_s composed of some rows of P,

$$P_s\theta = P_s\theta_0, \tag{50}$$

and there does not exist any $\widetilde{P}_s \ne P_s$ (except for $\widetilde{P}_s$ composed of a subset of permutated rows of P_s) such that

$$\widetilde{P}_s\theta = \alpha\widetilde{P}_s\theta_0, \tag{51}$$

for some scalar real value α.

5. NUMERICAL EXAMPLE

In this section, the presented fault diagnosis method will be illustrated with a simulated distillation column.

In [14, page 223], a distillation column is modeled with a transfer function matrix with three control inputs: top draw flow rate, side draw flow rate, and bottom temperature control, and three outputs: top draw composition, side draw composition, and bottom reflux temperature. In order to illustrate the possibility of fault diagnosis with only one output sensor, let us consider the model relating the three inputs and one of the outputs, the bottom reflux temperature. The transfer function model is

$$Z(s) = \frac{4.38e^{-20s}}{33s+1}U_1(s) + \frac{4.42e^{-22s}}{44s+1}U_2(s) + \frac{7.20}{19s+1}U_3(s). \tag{52}$$

Note that the known time delays at the inputs do not cause any serious difficulty for fault diagnosis, though the on-line computation has to be delayed accordingly.

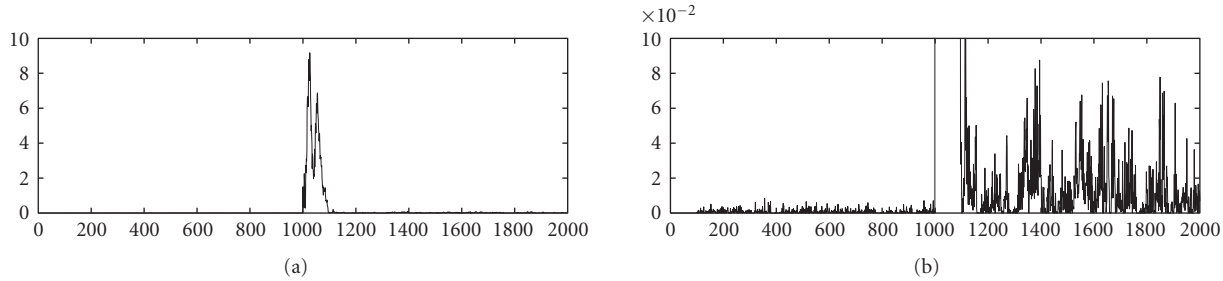

Figure 1: Fault detection residual. The same residual is plotted twice at different scales. The time unit is the minute.

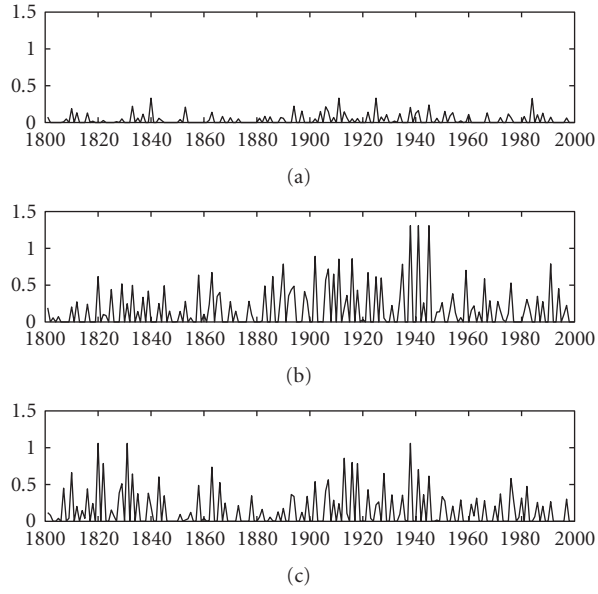

Figure 2: Fault isolation residuals. The time unit is the minute. Top: residual rejecting the fault of actuator 1. Middle: residual rejecting the fault of actuator 2. Bottom: residual rejecting the fault of actuator 3.

Numerical simulation is first made in continuous time. The three input variables are randomly drawn with uniform distributions ranged within the intervals [20, 40] (mol/min), [10, 30] (mol/min) and [10, 20] (°C). The simulated noise-free output is disturbed by an additive bandlimited noise with noise power 0.01 and unitary sample time. Then the sensor distortion function

$$h(z) = \frac{100}{1 + e^{-0.2(z-320)}} + 10 \tag{53}$$

is applied. In this monotonously increasing function, the additive constant 10 has been added to illustrate the robustness of the proposed method to sensor bias (shifting error). Finally, the distorted sensor output $y(t)$ sampled at the period of one minute is corrupted by a random noise uniformly distributed within the interval $[-0.05, 0.05]$ (°C). The simulated data is recorded during 2000 minutes after an initial simulation of 1000 minutes to avoid the initial transient period. At the beginning, all the actuators are fault free. At the 1000th minute (of the recorded duration), a factor of 0.8 is applied to the first actuator, simulating an actuator fault.

The residual for fault detection, computed with the averaging window length $L = 100$, is illustrated in Figure 1. In Figure 1(a) showing the residual in full scale, there is a strong transient behavior of the residual after occurrence of the actuator fault (at the 1000th minute). This transient behavior is in favor of a fast detection of the actuator fault. In order to view better the residual outside the transient period, it is plotted in Figure 1(b) in a finer scale. The detected fault is clearly confirmed by the residual after the transient period.

For fault isolation, three residuals are computed with the signals from the 1801th minute to the 2000th minute. Each of the three residuals is designed to reject a fault affecting one of the three actuators. The residuals rejecting the faults of actuator 1, 2, and 3 are, respectively, plotted in the top, middle, and bottom pictures of Figure 2. The first residual is clearly smaller than the two others, indicating that the hypothesis of a fault affecting the first actuator is the most likely one, which corresponds to the actually simulated fault.

6. CONCLUSION

Despite unknown nonlinear distortions of sensors, the information provided by such sensors is still useful for fault diagnosis, even when there is no redundant sensors, if the distortions are strictly monotonous. The monotonousness is a weak assumption since nonmonotonous distortion would make the sensor information useless. The main idea of the method presented in this paper is about how to use the information provided by such sensors. Because of the unknown nature of nonlinear distortion, neither the absolute value of the measured physical variable nor its sign can be determined from the sensor signal. The strict monotonousness of the nonlinear distortion is not helpful in this aspect. However, for any two different time instants, the relative sign of the measured variable is preserved by the monotonous nonlinear distortion. By using the information residing in the relative sign of sensor signals, the method for actuator fault diagnosis presented in this paper is conceptually robust to sensor distortions, as illustrated by the numerical example presented in this paper.

REFERENCES

[1] M. Basseville and I. Nikiforov, *Detection of Abrupt Changes: Theory and Applications*, Information and System Sciences Series, Prentice-Hall, Englewood Cliffs, NJ, USA, 1993.

[2] J. J. Gertler, *Fault Detection and Diagnosis in Engineering Systems*, Marcel Dekker, New York, NY, USA, 1998.

[3] J. Chen and R. J. Patton, *Robust Model-Bsed Fault Diagnosis for Dynamic Systems*, Kluwer Academic Publishers, Dordrecht, The Netherlands, 1999.

[4] M.-A. Massoumnia, G. C. Verghese, and A. S. Willsky, "Failure detection and identification," *IEEE Transactions on Automatic Control*, vol. 34, no. 3, pp. 316–321, 1989.

[5] C. De Persis and A. Isidori, "A geometric approach to nonlinear fault detection and isolation," *IEEE Transactions on Automatic Control*, vol. 46, no. 6, pp. 853–865, 2001.

[6] P. W. Tse, W.-X. Yang, and H. Y. Tam, "Machine fault diagnosis through an effective exact wavelet analysis," *Journal of Sound and Vibration*, vol. 277, no. 4-5, pp. 1005–1024, 2004.

[7] H. Ma, C. Han, X. Kong, G. Wang, J. Xu, and X. Zhu, "A chaos-GFRF based fault diagnosis method," in *Proceedings of IEEE Conference on Cybernetics and Intelligent Systems (ICCIs '04)*, vol. 2, pp. 1314–1317, Singapore, December 2004.

[8] K. Kumamaru, K. Inoue, and T. Iwamura, "Improved approach to KDI-based fault detection for non-linear black-box systems," in *Proceedings of the SICE Annual Conference*, vol. 1, pp. 927–932, Sapporo, Japan, August 2004.

[9] M. E. H. Benbouzid, H. Nejjari, R. Beguenane, and M. Vieira, "Induction motor asymmetrical faults detection using advanced signal processing techniques," *IEEE Transactions on Energy Conversion*, vol. 14, no. 2, pp. 147–152, 1999.

[10] Q. Zhang, "A method for actuator fault diagnosis with robustness to sensor distortion," in *Proceedings of the 6th IFAC Symposium on Fault Detection, Supervision and Safety of Technical Processes (SAFEPROCESS '06)*, Beijing, China, August-September 2006.

[11] Q. Zhang, A. Iouditski, and L. Ljung, "Identification of Wiener system with monotonous nonlinearity," in *Proceedings of IFAC Symposium on System Identification*, Newcastle, Australia, March 2006.

[12] R. B. Kearfott and V. Kreinovich, Eds., *Applications of Interval Computations*, Kluwer Academic Publishers, Boston, Mass, USA, 1996.

[13] D. Den Hertog, *Interior point approach to linear, quadratic, and convex programming: algorithms and complexity*, Kluwer Academic Publishers, Dordrecht, The Netherlands, 1994.

[14] T. Glad and L. Ljung, *Control Theory: Multivariable and Nonlinear Methods*, Taylor & Francis, New York, NY, USA, 2000.

Hindawi Publishing Corporation
Journal of Control Science and Engineering
Volume 2008, Article ID 189064, 9 pages
doi:10.1155/2008/189064

Research Article

Stability Guaranteed Active Fault-Tolerant Control of Networked Control Systems

Shanbin Li, Dominique Sauter, Christophe Aubrun, and Joseph Yamé

Centre de Recherche en Automatique de Nancy (CRAN-UMR 7039), Nancy Université, CNRS, BP 239, 54506 Vandoeuvre-lès-Nancy Cedex, France

Correspondence should be addressed to Joseph Yamé, joseph.yame@cran.uhp-nancy.fr

Received 4 May 2007; Revised 15 October 2007; Accepted 9 December 2007

Recommended by Jakob Stoustrup

The stability guaranteed active fault-tolerant control against actuators failures and plant uncertainties in networked control systems (NCSs) is addressed. A detailed design procedure is formulated as a convex optimization problem which can be efficiently solved by existing software. An illustrative example is given to show the efficiency of the proposed method for network-based control for uncertain systems.

1. INTRODUCTION

Fault-tolerant control (FTC) techniques against actuator faults can be classified into two groups [1]: passive and active approaches. In passive FTC systems, a single controller with fixed structure/parameters is used to deal with all possible failure scenarios which are assumed to be known a priori. Consequently, the passive controller is usually conservative. Furthermore, if a failure out of those considered in the design occurs, the stability and performance of the closed-loop system might not be guaranteed. Such potential limitations of passive approaches provide a strong motivation for the development of methods and strategies for active FTC (AFTC) systems.

In contrast to passive FTC systems, AFTC techniques rely on a real-time fault detection and isolation (FDI) scheme and a controller reconfiguration mechanism. Such techniques allow a flexibility to select different controllers according to different component failures, and therefore better performance of the closed-loop system can be expected. However, this holds true when the FDI process does not make an incorrect or delayed decision [2]. Some preliminary results have been obtained on AFTC which is immune to *imperfect* FDI process [3, 4]. In [5], the latter issue is further discussed in a classical setting (i.e., point-to-point control) by using the guaranteed cost control approach and online controller switching in order to ensure stability of the closed-loop system at all times. The aim of this paper is to extend the results in [5] to uncertain plants controlled over digital communication networks. In such networks, the information transfer from sensors to controllers and from controllers to actuators is not instantaneous but suffers communication delays. Such communication delays can be highly variable due to their strong dependence on variable network conditions such as congestion and channel quality. These network-induced delays may impact adversely on the stability and performance of the control system [6, 8]. Networked control systems (NCSs) are now pervasive (see, e.g., the recent special issue of the proceedings of the IEEE [7]), and such systems are long-running real-time systems which should function in a correct manner even in the presence of failures. This makes the issue of fault tolerant control in NCS an important one and entails designing strategies to cope with some of the fundamental problems introduced by the network such as bandwidth limitations, quantization and sampling effects, message scheduling and communication delays. Motivated by the above considerations, we address the problem of fault tolerant control in NCSs with time-varying delays. Specifically, we extend the results of [5] for the stabilization of a plant, subject to model *uncertainties* and *actuator faults*, which is controlled over a communication network that induces time-varying but bounded delays.

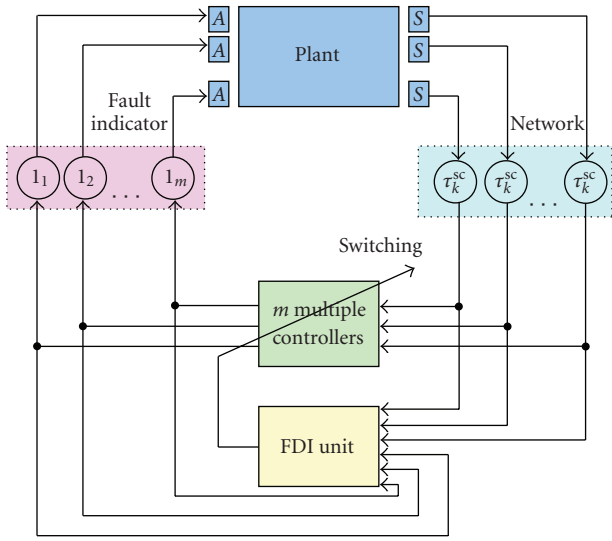

Figure 1: Networked control system with actuator failures.

The outline of the paper is as follows. In Section 2, a network-based control model for an uncertain plant subject to actuator failures is proposed and the guaranteed cost control problem is formulated. In Section 3, the detailed procedure for designing the NCSs-based fault-tolerant controller is given. Section 4 presents a design example to illustrate the benefit of the proposed FTC design procedure. Finally, conclusions are given in Section 5. The proof of the main theorem of the paper is reported in the appendix.

2. PROBLEM STATEMENT

Figure 1 shows the basic networked control architecture which is considered in this paper and which consists of a single uncertain plant, with few sensors and actuators, controlled by a digital controller in a centralized structure.

The delays induced by the network in the closed-loop control system are modeled as time-varying quantities $\tau(k) = \tau_k^{sc}$ arising from the communication delays between sensors and controllers at time k. Without loss of generality, we assume that there are no transmission time-delays between the controllers and the actuators. The actuators might be subject to faults during the system operation. Thus, taking into account the potential failures of actuators, the interconnection of the uncertain discrete-time plant and a discrete-time controller through the digital communication link as depicted in Figure 1 can be described by the following dynamical and state-delayed feedback equations:

$$x(k+1) = (A + D\Delta(k)E)x(k) + B\mathcal{L}u(k), \quad (1)$$

$$x(0) = x_0, \quad (2)$$

$$u(k) = Kx(k - \tau(k)), \quad (3)$$

where $x(k) \in \mathcal{R}^n$ is the state of the uncertain plant, $u(k) \in \mathcal{R}^m$ is the control input, A, B, D, E are all real constant matrices, and matrix K is the controller gain matrix to be designed. The time-varying matrix $\Delta(k)$ represents norm-bounded *parameter* uncertainties and satisfies the bound $\Delta(k)^T\Delta(k) \leq I$ where I denotes the identity matrix with appropriate dimension. The constant matrices D and E characterize the structure of these parameter uncertainties. The fault indicator matrix $\mathcal{L}$ is given by

$$\mathcal{L} = \text{diag}\{l_1, \ldots, l_m\} \quad (4)$$

with $l_j \in \{0, 1\}$ for $j = 1, 2, \ldots, m$, where $l_j = 1$ means that the jth actuator is in healthy state, whereas the jth actuator is meant to experience a total failure when $l_j = 0$. Having a finite number of actuators, the set of possible related failure modes is also finite and, by abuse of notation, we denote this set by

$$\mathcal{L} = \{\mathcal{L}^1, \mathcal{L}^2, \ldots \mathcal{L}^N\} \quad (5)$$

with $N = 2^m - 1$. Each failure mode $\mathcal{L}^i$, $(i = 1, 2 \ldots, N)$ is therefore an element of the set $\mathcal{L}$. We also view $\mathcal{L}^i$ as a matrix, that is, as a particular pattern of matrix $\mathcal{L}$ in (4) depending on the values of l_j $(j = 1, 2, \ldots m)$. Throughout, when $\mathcal{L}$ is invoked as a matrix, it will mean that matrix $\mathcal{L}$ varies over the set of matrices in (5). Note that the faulty mode $\mathcal{L}^i$ in the NCS architecture of Figure 1 is estimated by the FDI unit. In order to ensure that system (1) should remain controllable, we assume that the set $\mathcal{L}$ excludes the element $\text{diag}\{0, 0, \ldots, 0\}$, that is, at least one actuator should be healthy.

We further assume that the time-varying delays $\tau(k)$ lie between the following positive integer bounds τ_m and τ_M, that is,

$$\tau_m \leq \tau(k) \leq \tau_M. \quad (6)$$

Given positive definite symmetric matrices Q_1 and Q_2, we consider the quadratic cost function

$$J = \sum_{k=0}^{\infty} [x^T(k)Q_1x(k) + u^T(k)Q_2u(k)], \quad (7)$$

and with respect to this cost function, we define the guaranteed cost controller in the event of actuator failures as follows.

Definition 1. If there exists a control law $u(k)$ and a positive scalar J^* such that for all admissible uncertainties $\Delta(k)$ and all failure modes $\mathcal{L}^i \in \mathcal{L}$ the closed-loop system (1)–(3) is stable with cost function (7) satisfying $J \leq J^*$, then J^* is said to be a guaranteed cost and $u(k)$ a guaranteed cost controller for the uncertain system (1).

In Section 3, we will proceed through two main steps to design a cost guaranteed active fault tolerant control in the NCS framework. These steps are

(i) construct a fault-tolerant controller (i.e., a robust controller), with structure as given by (3), which achieves the smallest possible value for J^* under all admissible plant uncertainties and all actuator failure modes;
(ii) redesign that part of the above controller associated to only one fault-free actuator in order to improve the robust performance without loss of the stability property of the design in step (i); step (ii) repeats for all m actuators and results in a bank of m controllers.

It follows from inequality $m \le N = 2^m - 1$, that the cardinality of the bank of controllers (which is equal to the number of actuators) is less than the cardinality of the set $\mathcal{L}$ of faulty modes. For each faulty mode $\mathcal{L}^i$, the controller to be switched on should be the best as ranked with respect to a closed-loop performance index. In this paper, we will not address the switching and reconfiguration mechanisms; we focus on the design of the bank of m controllers.

3. AFTC DESIGN FOR NCS

3.1. Robust stability

In this subsection, we establish a sufficient condition for the existence of a guaranteed cost network-based controller for the uncertain plant (1). Note that the control law (3) applied to plant (1) results in the following system:

$$x(k+1) = A_1 x(k) + B\mathcal{L}Kx(k-\tau(k)), \tag{8}$$

where $A_1 = A + D\Delta(k)E$. The cost function associated to system (8) is therefore

$$J = \sum_{k=0}^{\infty} x_e^T(k) Q x_e(k), \tag{9}$$

where $x_e^T(k) = [x^T(k), x^T(k-\tau(k))]$ and $Q = \operatorname{diag}\{Q_1, K^T Q_2 K\}$. Under the assumptions made in Section 2, we can state the following result.

Theorem 1. *If there exist a gain matrix K, a scalar $\epsilon > 0$, symmetric positive-definite matrices $P_1 \in \mathcal{R}^{n\times n}$, $R \in \mathcal{R}^{n\times n}$, $S \in \mathcal{R}^{n\times n}$, and matrices $P_2 \in \mathcal{R}^{n\times n}$, $P_3 \in \mathcal{R}^{n\times n}$, $W \in \mathcal{R}^{2n\times 2n}$, $M \in \mathcal{R}^{2n\times n}$ such that the following matrix inequalities are satisfied:*

$$\begin{bmatrix} \Gamma & P^T \begin{bmatrix} 0 \\ B\mathcal{L}K \end{bmatrix} - M & \begin{bmatrix} E^T \\ 0 \end{bmatrix} \\ * & -R + K^T Q_2 K & 0 \\ * & * & -\epsilon I \end{bmatrix} < 0, \tag{10}$$

$$\begin{bmatrix} W & M \\ * & S \end{bmatrix} \ge 0 \tag{11}$$

with

$$\begin{aligned} \Gamma &= P^T \begin{bmatrix} 0 & I \\ A - I & -I \end{bmatrix} + \begin{bmatrix} 0 & I \\ A - I & -I \end{bmatrix}^T P \\ &\quad + \epsilon P^T \begin{bmatrix} 0 & 0 \\ 0 & DD^T \end{bmatrix} P + \begin{bmatrix} \mu R + Q_1 & 0 \\ 0 & P_1 + \tau_M S \end{bmatrix} \\ &\quad + \tau_M W + [\, M \;\; 0\,] + [\, M \;\; 0\,]^T, \\ \mu &= 1 + (\tau_M - \tau_m), \qquad P = \begin{bmatrix} P_1 & 0 \\ P_2 & P_3 \end{bmatrix}, \end{aligned} \tag{12}$$

then system (8) is asymptotically stable and the cost function (9) satisfies the inequality

$$\begin{aligned} J &\le x^T(0) P_1 x(0) + \sum_{l=-\tau_M}^{-1} x^T(l) R x(l) \\ &\quad + \sum_{\theta=-\tau_M+1}^{0} \sum_{l=-1+\theta}^{-1} y^T(l) S y(l) \\ &\quad + \sum_{\theta=-\tau_M+2}^{-\tau_M+1} \sum_{l=\theta-1}^{-1} x^T(l) R x(l), \end{aligned} \tag{13}$$

where $y(l) = x(l+1) - x(l)$.

Proof. See the appendix. □

Remark 2. The "$*$" sign represents blocks that are readily inferred by symmetry.

Remark 3. Note that the upper bound in (13) depends on the initial condition of system (8). To remove the dependence on the initial condition, we suppose that the initial state of system (8) might be arbitrary but belongs to the set $\mathcal{S} = \{x(l) \in \mathcal{R}^n : \; x(l) = U\nu, \nu^T\nu \le 1, l = -\tau_M, -\tau_M + 1, \ldots, -\tau_m\}$, where U is a given matrix. Inequality (13) leads to

$$J \le \lambda_{\max}(U^T P_1 U) + \rho_1 \lambda_{\max}(U^T R U) + \rho_2 \lambda_{\max}(U^T S U), \tag{14}$$

where $\lambda_{\max}(\cdot)$ denotes the maximum eigenvalue of matrix $(\cdot)$, $\rho_1 = \mu(\tau_M + \tau_m)/2$, and $\rho_2 = 2\tau_M(\tau_M + 1)$.

3.2. Step (i): Controller Design

Now, we derive the guaranteed cost controller in terms of the feasible solutions to a set of linear matrix inequalities.

Using Sherman-Morrison matrix inversion formula, we have

$$P^{-1} = \begin{bmatrix} P_1^{-1} & 0 \\ -P_3^{-1} P_2 P_1^{-1} & P_3^{-1} \end{bmatrix}. \tag{15}$$

In the sequel, we will denote $X = P_1^{-1}$, $Y = P_3^{-1}$, and $Z = -P_3^{-1} P_2 P_1^{-1}$. We further restrict M to the following case in order to obtain a linear matrix inequality (LMI) (see, e.g., [9]):

$$M = \delta P^T \begin{bmatrix} 0 \\ B\mathcal{L}K \end{bmatrix}, \tag{16}$$

where δ is a scalar parameter. Pre- and postmultiply (10) by $\operatorname{diag}\{(P^{-1})^T, P_1^{-1}, I\}$ and $\operatorname{diag}\{P^{-1}, P_1^{-1}, I\}$, respectively; also pre- and postmultiply (11) by $\operatorname{diag}\{(P^{-1})^T, P_1^{-1}\}$ and $\operatorname{diag}\{P^{-1}, P_1^{-1}\}$ and denote

$$\begin{aligned} L &= P_1^{-1} R P_1^{-1}, \qquad F = K P_1^{-1}, \qquad \overline{S} = S^{-1}, \\ (P^{-1})^T W P^{-1} &= \begin{bmatrix} \overline{W}_1 & \overline{W}_2 \\ * & \overline{W}_3 \end{bmatrix}. \end{aligned} \tag{17}$$

Applying the Schur complement and expanding the block matrices, we obtain the following result under the assumptions made in Section 2.

Theorem 2. *Suppose that for a prescribed scalar δ, there exist a scalar $\epsilon > 0$, matrices $X > 0$, Y, Z, F, $L > 0$, $\overline{S} > 0$, $\overline{W}_1$, $\overline{W}_2$, $\overline{W}_3$, such that the following matrix inequalities are satisfied:*

$$\begin{bmatrix} \Psi_1 & \Psi_2 & 0 & \Psi_{41} \\ * & \Psi_3 & (1-\delta)B\mathcal{L}F & \Psi_{42} \\ * & * & -L & \Psi_{43} \\ * & * & * & \Psi_5 \end{bmatrix} < 0, \tag{18}$$

$$\begin{bmatrix} \overline{W}_1 & \overline{W}_2 & 0 \\ * & \overline{W}_3 & \delta B\mathcal{L}F \\ * & * & X\overline{S}^{-1}X \end{bmatrix} \geq 0, \tag{19}$$

where

$$\begin{aligned} \Psi_1 &= Z + Z^T + \mu L + \tau_M \overline{W}_1, \\ \Psi_2 &= Y + X(A-I)^T - Z^T + \tau_M \overline{W}_2 + \delta(B\mathcal{L}F)^T, \\ \Psi_3 &= -Y - Y^T + \tau_M \overline{W}_3 + \epsilon DD^T, \\ \begin{bmatrix} \Psi_{41} \\ \Psi_{42} \\ \Psi_{43} \end{bmatrix} &= \begin{bmatrix} XE^T & \tau_M Z^T & 0 & X & Z^T \\ 0 & \tau_M Y^T & 0 & 0 & Y^T \\ 0 & 0 & F^T & 0 & 0 \end{bmatrix}, \\ \Psi_5 &= \operatorname{diag}\{-\epsilon I, -\tau_M \overline{S}, -Q_2^{-1}, -Q_1^{-1}, -X\}. \end{aligned} \tag{20}$$

Then, the control law

$$u(k) = FX^{-1}x(k-\tau(k)) \tag{21}$$

is a guaranteed cost networked control law for system (1) *and the corresponding cost function satisfies*

$$\begin{aligned} J \leq{}& \lambda_{\max}(U^T X^{-1} U) + \rho_1 \lambda_{\max}(U^T X^{-1} L X^{-1} U) \\ &+ \rho_2 \lambda_{\max}(U^T \overline{S}^{-1} U), \end{aligned} \tag{22}$$

where $\rho_1 = \mu(\tau_M + \tau_m)/2$ and $\rho_2 = 2\tau_M(\tau_M + 1)$.

Remark 4. From (22), we establish the following inequalities:

$$\begin{bmatrix} -\alpha I & U^T \\ * & -X \end{bmatrix} < 0, \qquad \begin{bmatrix} -\beta I & U^T \\ * & -XL^{-1}X \end{bmatrix} < 0,$$
$$\begin{bmatrix} -\gamma I & U^T \\ * & -\overline{S} \end{bmatrix} < 0, \tag{23}$$

where α, β, and γ are scalars to be determined. It is worth noting that condition (23) is not an LMI because of the term $-XL^{-1}X$. This is also the case for condition (19) which is not an LMI because of the term $X\overline{S}^{-1}X$. Note that for any matrix $X > 0$ we have

$$X\overline{S}^{-1}X \geq 2X - \overline{S}, \qquad XL^{-1}X \geq 2X - L. \tag{24}$$

Given a prescribed scalar δ, the design problem of the optimal guaranteed cost controller can be formulated therefore as the following optimization problem:

$$\text{OP1:} \min_{\epsilon, X, Y, Z, F, L, \overline{S}, \overline{W}_1, \overline{W}_2, \overline{W}_3} (\alpha + \rho_1\beta + \rho_2\gamma)$$
$$\text{s.t.} \begin{cases} \text{(i)} & \text{inequality (18)}, \\ \text{(ii)} & \begin{bmatrix} \overline{W}_1 & \overline{W}_2 & 0 \\ * & \overline{W}_3 & \delta B\mathcal{L}F \\ * & * & 2X - \overline{S} \end{bmatrix} \geq 0, \\ \text{(iii)} & \begin{bmatrix} -\alpha I & U^T \\ * & -X \end{bmatrix} < 0, \begin{bmatrix} -\beta I & U^T \\ * & -2X + L \end{bmatrix} < 0, \\ & \begin{bmatrix} -\gamma I & U^T \\ * & -\overline{S} \end{bmatrix} < 0. \end{cases} \tag{25}$$

Clearly, the above optimization problem (25) is a convex optimization problem which can be effectively solved by existing LMI software [10]. Thus, the minimization of $\alpha+\rho_1\beta+\rho_2\gamma$ implies the minimization of the cost in (9). By applying a simple one-dimensional search over δ for a certain τ_M, a global optimum cost can be found.

3.3. Robust Stability with at least a fault-free actuator

Based on the controller designed in Theorem 2, let us assume that actuator i is fault-free, then we can redesign the i th row of controller gain matrix K to improve the robust performance for the system against actuator failures. We can rewrite the overall control system as

$$x(k+1) = A_1 x(k) + (B_{\bar{i}}\mathcal{L}_{\bar{i}}K_{\bar{i}} + b_i k_i)x(k-\tau(k)), \tag{26}$$

where $A_1 = A + D\Delta(k)E$, matrix $K_{\bar{i}}$ is obtained by deleting the ith row from K, $B_{\bar{i}}$ is obtained by deleting the ith column from B, and $\mathcal{L}_{\bar{i}}$ is obtained by deleting ith row and ith column from $\mathcal{L}$. The cost function associated to system (26) reads as

$$J = \sum_{k=0}^{\infty} x_e^T(k) Q x_e(k) \tag{27}$$

with $x_e^T(k) = [x^T(k), x^T(k-\tau(k))]$, $Q = \operatorname{diag}\{Q_1, k_i^T Q_{2i} k_i + K_{\bar{i}}^T Q_{2\bar{i}} K_{\bar{i}}\}$, where $Q_{2\bar{i}}$ is obtained by deleting the ith row and ith column from Q_2. With regard to system (26) where $K_{\bar{i}}$ is assumed to be known, we have the following result.

Theorem 3. *If there exist a gain matrix k_i, a scalar $\epsilon > 0$, symmetric positive-definite matrices $P_1 \in \mathcal{R}^{n\times n}$, $R \in \mathcal{R}^{n\times n}$, $S \in \mathcal{R}^{n\times n}$, and matrices $P_2 \in \mathcal{R}^{n\times n}$, $P_3 \in \mathcal{R}^{n\times n}$, $W \in \mathcal{R}^{2n\times 2n}$,*

$M \in \mathcal{R}^{2n\times n}$ such that the following matrix inequalities are satisfied:

$$\begin{bmatrix} \Gamma & P^T\begin{bmatrix} 0 \\ B_{\bar{i}}\mathcal{L}_{\bar{i}}K_{\bar{i}} + b_i k_i \end{bmatrix} - M & \begin{bmatrix} E^T \\ 0 \end{bmatrix} \\ * & -R + k_i^T Q_{2i} k_i + K_{\bar{i}}^T Q_{2\bar{i}} K_{\bar{i}} & 0 \\ * & * & -\epsilon I \end{bmatrix} < 0, \tag{28}$$

$$\begin{bmatrix} W & M \\ * & S \end{bmatrix} \geq 0, \tag{29}$$

then, system (26) *is asymptotically stable and the cost function* (27) *satisfies inequality* (13).

Proof. The proof is similar to the proof of Theorem 1. □

3.4. Step (ii): Controller Redesign

Proceeding as in step (i), we restrict M to the following case in order to obtain an LMI:

$$M = \delta P^T \begin{bmatrix} 0 \\ b_i k_i \end{bmatrix}, \tag{30}$$

where δ is a scalar parameter. Pre- and postmultiply (28) with $\mathrm{diag}\{(P^{-1})^T, P_1^{-1}, I\}$ and $\mathrm{diag}\{P^{-1}, P_1^{-1}, I\}$, respectively; also pre- and postmultiply (29) with $\mathrm{diag}\{(P^{-1})^T, P_1^{-1}\}$ and $\mathrm{diag}\{P^{-1}, P_1^{-1}\}$, respectively, and denote

$$L = P_1^{-1} R P_1^{-1}, \qquad F^* = k_i P_1^{-1}, \qquad \overline{S} = S^{-1},$$
$$(P^{-1})^T W P^{-1} = \begin{bmatrix} \overline{W}_1 & \overline{W}_2 \\ * & \overline{W}_3 \end{bmatrix}. \tag{31}$$

The Schur complement trick leads to the following controller redesign result.

Theorem 4. *Suppose that for a prescribed scalar δ, there exist a scalar $\epsilon > 0$, matrices $X > 0$, Y, Z, F^*, $L > 0$, $\overline{S} > 0$, $\overline{W}_1$, $\overline{W}_2$, $\overline{W}_3$, such that the following matrix inequalities are satisfied:*

$$\begin{bmatrix} \widetilde{\Psi}_1 & \widetilde{\Psi}_2 & 0 & \widetilde{\Psi}_{41} \\ * & \widetilde{\Psi}_3 & B_{\bar{i}}\mathcal{L}_{\bar{i}}K_{\bar{i}}X + (1-\delta)b_i F^* & \widetilde{\Psi}_{42} \\ * & * & -L & \widetilde{\Psi}_{43} \\ * & * & * & \widetilde{\Psi}_5 \end{bmatrix} < 0, \tag{32}$$

$$\begin{bmatrix} \overline{W}_1 & \overline{W}_2 & 0 \\ * & \overline{W}_3 & \delta b_i F^* \\ * & * & X\overline{S}^{-1}X \end{bmatrix} \geq 0, \tag{33}$$

where

$$\widetilde{\Psi}_1 = Z + Z^T + \mu L + \tau_M \overline{W}_1,$$
$$\widetilde{\Psi}_2 = Y + X(A-I)^T - Z^T + \tau_M \overline{W}_2 + \delta(b_i F^*)^T,$$
$$\widetilde{\Psi}_3 = -Y - Y^T + \tau_M \overline{W}_3 + \epsilon D D^T,$$
$$\begin{bmatrix} \widetilde{\Psi}_{41} \\ \widetilde{\Psi}_{42} \\ \widetilde{\Psi}_{43} \end{bmatrix} = \begin{bmatrix} XE^T & \tau_M Z^T & 0 & 0 & X & Z^T \\ 0 & \tau_M Y^T & 0 & 0 & 0 & Y^T \\ 0 & 0 & (F^*)^T & XK_{\bar{i}}^T & 0 & 0 \end{bmatrix}, \tag{34}$$
$$\widetilde{\Psi}_5 = \mathrm{diag}\{-\epsilon I, -\tau_M \overline{S}, -Q_{2i}^{-1}, -Q_{2\bar{i}}^{-1}, -Q_1^{-1}, -X\}.$$

Then, the ith control law

$$u_i(k) = F^* X^{-1} x(k - \tau(k)) \tag{35}$$

is a guaranteed cost networked control law of system (26) *and the corresponding cost function satisfies*

$$J \leq \lambda_{\max}(U^T X^{-1} U) + \rho_1 \lambda_{\max}(U^T X^{-1} L X^{-1} U) + \rho_2 \lambda_{\max}(U^T \overline{S}^{-1} U), \tag{36}$$

where $\rho_1 = \mu(\tau_M + \tau_m)/2$ and $\rho_2 = 2\tau_M(\tau_M + 1)$.

Given a prescribed scalar δ, the redesign problem of the optimal guaranteed cost controller can be formulated as the following convex optimization problem:

$$\text{OP2:} \min_{\epsilon, X, Y, Z, F^*, L, \overline{S}, \overline{W}_1, \overline{W}_2, \overline{W}_3} (\alpha + \rho_1\beta + \rho_2\gamma)$$
$$\text{s.t.} \begin{cases} \text{(i)} & \text{inequality (32)}, \\ \text{(ii)} & \begin{bmatrix} \overline{W}_1 & \overline{W}_2 & 0 \\ * & \overline{W}_3 & \delta b_i F^* \\ * & * & 2X - \overline{S} \end{bmatrix} \geq 0, \\ \text{(iii)} & \begin{bmatrix} -\alpha I & U^T \\ * & -X \end{bmatrix} < 0, \begin{bmatrix} -\beta I & U^T \\ * & -2X + L \end{bmatrix} < 0, \\ & \begin{bmatrix} -\gamma I & U^T \\ * & -\overline{S} \end{bmatrix} < 0. \end{cases} \tag{37}$$

4. ILLUSTRATIVE EXAMPLE

The dynamics are described by the following matrices:

$$A = \begin{bmatrix} 0.9 & 0 \\ 0.2 & 0.5 \end{bmatrix}, \qquad B = \begin{bmatrix} 0.2 & 0.1 \\ 0 & -0.1 \end{bmatrix},$$
$$D = \begin{bmatrix} 0 & 0.1 \\ 0.1 & 0 \end{bmatrix}, \qquad E = \begin{bmatrix} 0.1 & 0 \\ 0.1 & -0.1 \end{bmatrix}, \tag{38}$$

and the design parameters are chosen as

$$Q_1 = \begin{bmatrix} 1 & 0 \\ 0 & 1 \end{bmatrix}, \qquad Q_2 = \begin{bmatrix} 0.1 & 0 \\ 0 & 0.1 \end{bmatrix}, \qquad U = \begin{bmatrix} 1 & 0 \\ 0 & 1 \end{bmatrix}. \tag{39}$$

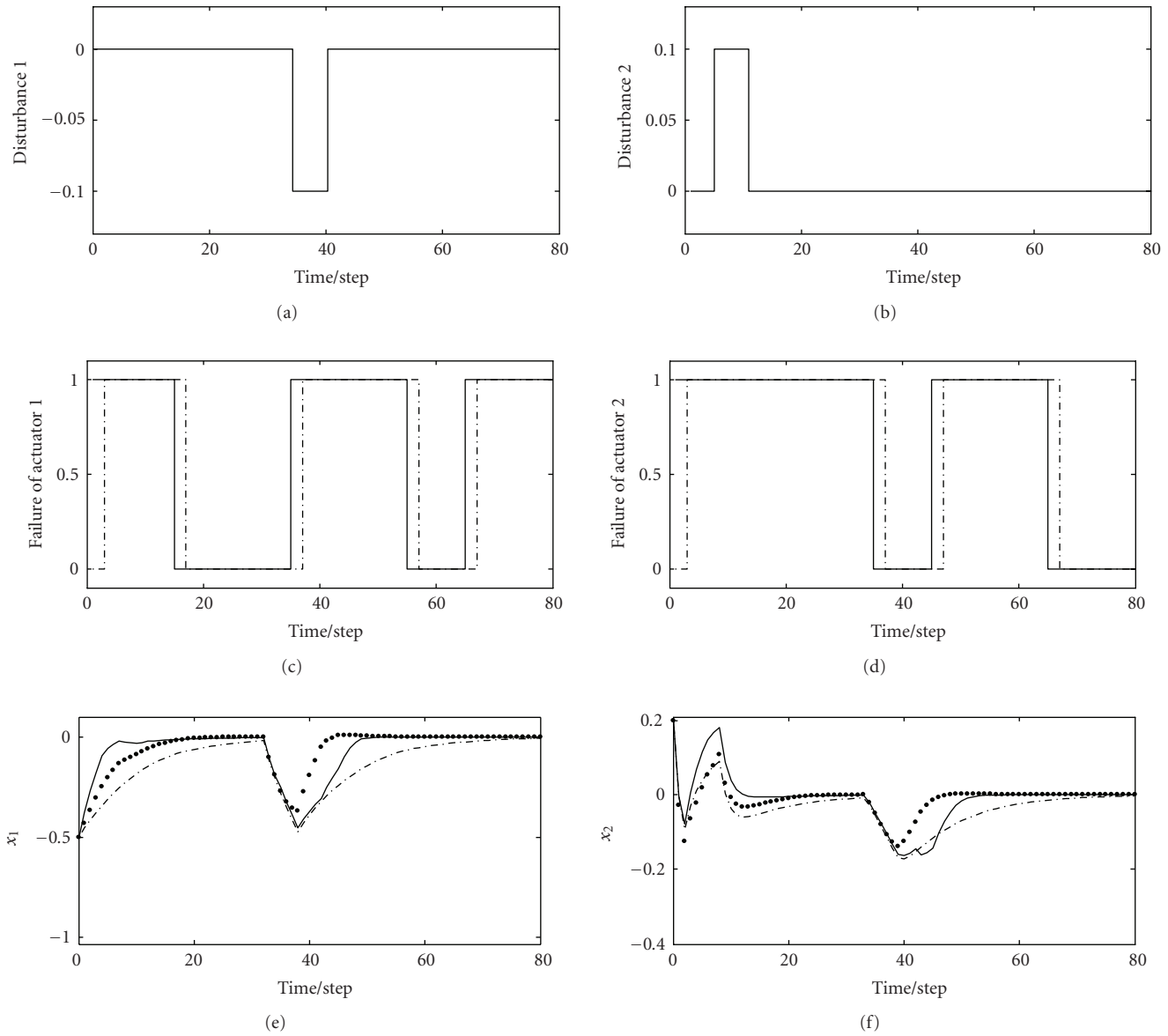

Figure 2: Disturbance, actuator failures, and state response.

When $\tau_m = 1, \tau_M = 2$, and $\delta = 1$, by OP1 (25), the cost is obtained as $J_1 = 61.6653$ and the fault-tolerant controller can be designed for step (i):

$$\begin{bmatrix} k_1 \\ k_2 \end{bmatrix} = \begin{bmatrix} -0.0812 \times 10^{-5} & -0.1333 \times 10^{-5} \\ -0.1865 \times 10^{-5} & -0.3060 \times 10^{-5} \end{bmatrix}. \tag{40}$$

In step (ii), by OP2 (37), the cost and the feedback gains are redesigned as

$$\begin{aligned} J_2 &= 39.0026, \qquad k_1^* = \begin{bmatrix} -0.8776 & -0.2857 \end{bmatrix}, \\ J_3 &= 49.9616, \qquad k_2^* = \begin{bmatrix} -0.6494 & -0.4161 \end{bmatrix}. \end{aligned} \tag{41}$$

As a result, the two controllers are determined as follows:

$$\begin{aligned} \#1 : \begin{bmatrix} k_1^* \\ k_2 \end{bmatrix} &= \begin{bmatrix} -0.8776 & -0.2857 \\ -0.1865 \times 10^{-5} & -0.3060 \times 10^{-5} \end{bmatrix}, \\ \#2 : \begin{bmatrix} k_1 \\ k_2^* \end{bmatrix} &= \begin{bmatrix} -0.0812 \times 10^{-5} & -0.1333 \times 10^{-5} \\ -0.6494 & -0.4161 \end{bmatrix}. \end{aligned} \tag{42}$$

Figure 2 reports the simulation for two failures scenarios of the actuators. For this simulation, the time-varying norm-bounded uncertain matrix $\Delta(k)$ is taken as

$$\Delta(k) = \begin{pmatrix} \sin(\pi k) & 0 \\ 0 & \cos(\pi k) \end{pmatrix}, \tag{43}$$

which clearly satisfies the bound $\Delta(k)^T\Delta(k) \le I$. The left column of Figure 2 is related to failures of actuator 1 and the right column is related to failures of actuator 2. Note also that for these two failures scenarios the system has been disturbed by step disturbances entering *additively* in the state equations. This is illustrated in the simulation where the step disturbance 1 shown in Figure 2(a) disturbs the state variables at time instant 35 and disappears at time instant 40. The step disturbance 2 shown in Figure 2(b) disturbs the system at time instant 5 and disappears at time instant 10. In Figure 2(c), the solid line represents the failure of actuator 1 which occurs at time instant 15 and disappears at time instant 35, occurs again at time instant 55 and disappears at time instant 65. In Figure 2(d), the solid line represents the failure of actuator 2 which occurs at time instant 35 and disappears at time instant 45, occurs again at time instant 65 and disappears at time instant 80. The delay of fault detection is assumed to be 3 time steps, which is represented by dot-dashed lines as shown in Figures 2(c) and 2(d). Under the above simulation setting, the state responses are shown in Figures 2(e) and 2(f):

(i) the dotted line represents the state response for controller-switching sequence N°1 : #2 is the initial controller, and #1 is switched-on at time instant 38, then #2 at time instant 48, #1 at time instant 68;
(ii) the solid line represents the state response for controller-switching sequence N°2 : #1 is the initial controller, and #2 is switched-on at time instant 38, then #1 at time instant 48, #2 at time instant 68;
(iii) the dot-dashed line represents the state response under the fault tolerant control (i.e., robust control) of step (i).

The trace of matrices $(x^*)(x^*)^T$/(simulation time) is used as a performance measure for comparison, where x^* represents the state trajectory in the different schemes and the simulation time is 80 seconds. After computation, we obtain for the above three control schemes the traces $Tr_1 = 0.0279, Tr_2 = 0.0338, Tr_3 = 0.0499$, which means that $Tr_1 < Tr_2 < Tr_3$. We conclude that the proposed method for sequence N°1 is the best control scheme. We also observe that for all possible switching sequences with controllers in the designed controllers bank, the proposed active FTC is able to guarantee at least the closed-loop stability of the overall system.

5. CONCLUSION

In this paper, the stability guaranteed active fault tolerant control against actuators failure in networked control system with time-varying but bounded delays has been addressed. Plants with norm-bounded parameter uncertainty have been considered, where the uncertainty may appear in the state matrix. Modelling network-induced delays as communication delays between sensors and actuators, linear memoryless state feedback fault-tolerant controllers have been developed through LMI-based methods. A simulation example has been presented to show the potentials of the proposed method for fault-tolerant control in networked control systems.

APPENDIX

PROOF OF THEOREM 1

The following matrix inequalities are essential for the proof of Theorem 1.

Lemma 5 (see [11]). *Assume that $a(\cdot) \in \mathcal{R}^{n_a}$, $b(\cdot) \in \mathcal{R}^{n_b}$, and $N(\cdot) \in \mathcal{R}^{n_a\times n_b}$. Then, for any matrices $X \in \mathcal{R}^{n_a\times n_a}$, $Y \in \mathcal{R}^{n_a\times n_b}$, and $Z \in \mathcal{R}^{n_b\times n_b}$, the following holds:*

$$-2a^TNb \le \begin{bmatrix} a \\ b \end{bmatrix}^T \begin{bmatrix} X & Y-N \\ Y^T-N^T & Z \end{bmatrix} \begin{bmatrix} a \\ b \end{bmatrix}, \tag{A.1}$$

where $\left[\begin{smallmatrix} X & Y \\ Y^T & Z \end{smallmatrix}\right] \ge 0$.

Lemma 6 (see [12]). *Let Y be a symmetric matrix and let H, E be given matrices with appropriate dimensions, then*

$$Y + HFE + E^TF^TH^T < 0 \tag{A.2}$$

holds for all F satisfying $F^TF \le I$, if and only if there exists a scalar $\epsilon > 0$ such that

$$Y + \epsilon HH^T + \epsilon^{-1}E^TE < 0. \tag{A.3}$$

Proof. Note that $x(k-\tau(k)) = x(k) - \sum_{l=k-\tau(k)}^{k-1} y(l)$, where $y(l) = x(l+1) - x(l)$. Then from system (8) we have

$$0 = (A_1 + B\mathcal{L}K - I)x(k) - y(k) - B\mathcal{L}K \sum_{l=k-\tau(k)}^{k-1} y(l). \tag{A.4}$$

Choose the Lyapunov-Krasovskii function candidates as follows:

$$V(k) = V_1(k) + V_2(k) + V_3(k), \tag{A.5}$$

where

$$\begin{aligned} V_1(k) &= x^T(k)P_1x(k), \\ V_2(k) &= \sum_{l=k-\tau(k)}^{k-1} x^T(l)Rx(l), \\ V_3(k) &= \sum_{\theta=-\tau_M}^{-1} \sum_{l=k+\theta}^{k-1} y^T(l)Sy(l) \\ &\quad + \sum_{\theta=-\tau_M+2}^{-\tau_m+1} \sum_{l=k+\theta-1}^{k-1} x^T(l)Rx(l) \end{aligned} \tag{A.6}$$

Taking the forward difference for the Lyapunov functional $V_1(k)$, we have

$$\Delta V_1(k) = 2x^T(k)P_1y(k) + y^T(k)P_1y(k). \tag{A.7}$$

From (A.4), we have

$$2x^T(k)P_1y(k) = 2\eta^T(k)P^T \begin{bmatrix} y(k) \\ N - B\mathcal{L}K \sum_{l=k-\tau(k)}^{k-1} y(l) \end{bmatrix}, \tag{A.8}$$

where $N = (A_1 + B\mathcal{L}K - I)x(k) - y(k), \eta^T(k) = [x^T(k)\ y^T(k)]$. Choose constant matrices W, M, and S satisfying (11); by Lemma 5, we have

$$\begin{aligned} -2\sum_{l=k-\tau(k)}^{k-1} \eta^T(k)P^T\begin{bmatrix}0\\ B\mathcal{L}K\end{bmatrix} y(l) &\le \tau_M \eta^T(k)W\eta(k) + \sum_{l=k-\tau_M}^{k-1} y^T(l)Sy(l) \\ &\quad + 2\eta^T(k)\left\{M - P^T\begin{bmatrix}0\\ B\mathcal{L}K\end{bmatrix}\right\}(x(k) - x(k-\tau(k))). \end{aligned} \tag{A.9}$$

Similarly,

$$\begin{aligned} \Delta V_2(k) &= x^T(k)Rx(k) - x^T(k-\tau(k))Rx(k-\tau(k)) \\ &\quad + \sum_{l=k+1-\tau(k+1)}^{k-1} x^T(l)Rx(l) - \sum_{k-\tau(k)+1}^{k-1} x^T(l)Rx(l). \end{aligned} \tag{A.10}$$

Note that

$$\begin{aligned} &\sum_{l=k+1-\tau(k+1)}^{k-\tau_m} x^T(l)Rx(l) \\ &\quad = \sum_{l=k+1-\tau_m}^{k-1} x^T(l)Rx(l) + \sum_{l=k+1-\tau(k+1)}^{k-\tau_m} x^T(l)Rx(l) \\ &\quad \le \sum_{l=k+1-\tau(k)}^{k-1} x^T(l)Rx(l) + \sum_{l=k+1-\tau_M}^{k-\tau_m} x^T(l)Rx(l). \end{aligned} \tag{A.11}$$

So, we have

$$\begin{aligned} \Delta V_2(k) &\le x^T(k)Rx(k) - x^T(k-\tau(k))Rx(k-\tau(k)) \\ &\quad + \sum_{l=k+1-\tau_m}^{k-\tau_m} x^T(l)Rx(l). \end{aligned} \tag{A.12}$$

Furthermore, we have

$$\begin{aligned} \Delta V_3(k) &= \tau_M y^T(k)Sy(k) - \sum_{l=k+1-\tau_m}^{k-1} y^T(l)Sy(l) \\ &\quad + (\tau_M - \tau_m)x^T(k)Rx(k) - \sum_{l=k+1-\tau_m}^{k-\tau_m} x^T(l)Rx(l). \end{aligned} \tag{A.13}$$

Combining (9) and (A.7)–(A.13), we have

$$\begin{aligned} \Delta V(k) &\le \xi^T(k)[\Theta_0(\tau_m,\tau_M) + \hat{D}\Delta(k)\hat{E} + \hat{E}^T\Delta^T(k)\hat{D}^T]\xi(k) \\ &\quad - x_e^T(k)Qx_e(k), \end{aligned} \tag{A.14}$$

where

$$\begin{aligned} \xi^T(k) &= [\ \eta^T(k)\ \ x^T(k-\tau(k))\ ], \\ \hat{D}^T &= \left[[0D^T]P\ \ 0\right], \hat{E} = \left[[E0]0\right], \\ \Theta_0(\tau_m,\tau_M) &= \begin{bmatrix}\Gamma_0 & P^T\begin{bmatrix}0\\ B\mathcal{L}K\end{bmatrix} - M\\ * & -R + K^TQ_2K\end{bmatrix}, \\ \Gamma_0 &= \Gamma - \epsilon P^T\begin{bmatrix}0 & 0\\ 0 & DD^T\end{bmatrix}P. \end{aligned} \tag{A.15}$$

By Lemma 6, we have

$$\begin{aligned} \Delta V(k) &\le \xi^T(k)[\Theta_0(\tau_m,\tau_M) + \epsilon\hat{D}\hat{D}^T + \epsilon^{-1}\hat{E}^T\hat{E}]\xi(k) \\ &\quad - x_e^T(k)Qx_e(k). \end{aligned} \tag{A.16}$$

It is worth observing that matrix $[\Theta_0(\tau_m,\tau_M) + \epsilon\hat{D}\hat{D}^T + \epsilon^{-1}\hat{E}^T\hat{E}]$ is the Schur complement of $-\epsilon I$ in the matrix of the left-hand side of inequality (10). Therefore, the negative definiteness of matrix $[\Theta_0(\tau_m,\tau_M) + \epsilon\hat{D}\hat{D}^T + \epsilon^{-1}\hat{E}^T\hat{E}]$ resulting from inequality (10) implies that

$$\Delta V(k) \le -x_e^T(k)Qx_e(k). \tag{A.17}$$

Summing both sides of the above inequality from 0 to ∞ leads to

$$\begin{aligned} \sum_{k=0}^{\infty}\Delta V(k) &= V(\infty) - V(0) \\ &\le -\sum_{k=0}^{\infty} x_e^T(k)Qx_e(k) = -J \end{aligned} \tag{A.18}$$

which, from system stability, yields

$$J \le V(0), \tag{A.19}$$

that is, inequality (13). □

ACKNOWLEDGMENTS

The authors would like to thank the anonymous reviewers for their constructive comments and suggestions that have improved the quality of the manuscript. This work is supported by the French National Research Agency (Agence Nationale de la Recherche, ANR) project SafeNECS (Safe-Networked Control Systems) under Grant no. ANR-ARA SSIA-NV-15.

REFERENCES

[1] M. Blanke, M. Kinnaert, J. Lunze, and M. Staroswiecki, *Diagnosis and Fault-Tolerant Control*, Springer, Berlin, Germany, 2003.

[2] M. Mariton, "Detection delays, false alarm rates and the reconfiguration of control systems," *International Journal of Control*, vol. 49, no. 3, pp. 981–992, 1989.

[3] M. Mahmoud, J. Jiang, and Y. Zhang, "Stabilization of active fault tolerant control systems with imperfect fault detection and diagnosis," *Stochastic Analysis and Applications*, vol. 21, no. 3, pp. 673–701, 2003.

[4] N. E. Wu, "Robust feedback design with optimized diagnostic performance," *IEEE Transactions on Automatic Control*, vol. 42, no. 9, pp. 1264–1268, 1997.

[5] M. Maki, J. Jiang, and K. Hagino, "A stability guaranteed active fault-tolerant control system against actuator failures," *International Journal of Robust and Nonlinear Control*, vol. 14, no. 12, pp. 1061–1077, 2004.

[6] W. Zhang, M. S. Branicky, and S. M. Phillips, "Stability of networked control systems," *IEEE Control Systems Magazine*, vol. 21, no. 1, pp. 84–99, 2001.

[7] P. Antsaklis and J. Baillieul, "Special issue on technology of networked control systems," *Proceedings of the IEEE*, vol. 95, no. 1, pp. 5–8, 2007.

[8] Y. Tipsuwan and M.-Y. Chow, "Control methodologies in networked control systems," *Control Engineering Practice*, vol. 11, no. 10, pp. 1099–1111, 2003.

[9] W.-H. Chen, Z.-H. Guan, and X. Lu, "Delay-dependent guaranteed cost control for uncertain discrete-time systems with delay," *IEE Proceedings: Control Theory and Applications*, vol. 150, no. 4, pp. 412–416, 2003.

[10] P. Gahinet, A. Nemirovsky, A. J. Laub, and M. Chilali, *LMI Control Toolbox—for Use with Matlab*, The Math Works, Natick, Mass, USA, 1995.

[11] Y. S. Moon, P. Park, W. H. Kwon, and Y. S. Lee, "Delay-dependent robust stabilization of uncertain state-delayed systems," *International Journal of Control*, vol. 74, no. 14, pp. 1447–1455, 2001.

[12] Y. Wang, L. Xie, and C. E. de Souza, "Robust control of class uncertain nonlinear systems," *Systems and Control Letters*, vol. 19, no. 2, pp. 139–149, 1992.

Hindawi Publishing Corporation
Journal of Control Science and Engineering
Volume 2008, Article ID 265189, 10 pages
doi:10.1155/2008/265189

Research Article

Reliability Monitoring of Fault Tolerant Control Systems with Demonstration on an Aircraft Model

Hongbin Li,[1] Qing Zhao,[1] and Zhenyu Yang[2]

[1] *Department of Electrical and Computer Engineering, University of Alberta, Edmonton, AB, Canada T6G 2V4*
[2] *Department of Computer Science and Engineering, Aalborg University Esbjerg, Niels Bohrs Vej 8, 6700 Esbjerg, Denmark*

Correspondence should be addressed to Qing Zhao, qingzhao@ece.ualberta.ca

Received 4 April 2007; Revised 6 September 2007; Accepted 13 November 2007

Recommended by Kemin Zhou

This paper proposes a reliability monitoring scheme for active fault tolerant control systems using a stochastic modeling method. The reliability index is defined based on system dynamical responses and a safety region; the plant and controller are assumed to have a multiple regime model structure, and a semi-Markov model is built for reliability evaluation based on the safety behavior of each regime model estimated by using Monte Carlo simulation. Moreover, the history data of fault detection and isolation decisions is used to update its transition characteristics and reliability model. This method provides an up-to-date reliability index as demonstrated on an aircraft model.

1. INTRODUCTION

In order to meet high reliability requirement of safety-critical processes, major progress has been made in fault tolerant control systems (FTCSs). FTCSs usually employ fault detection and isolation (FDI) schemes and reconfigurable controllers to accommodate fault effects, also known as active FTCSs. Most work on reconfigurable controller design is performed under the assumption of perfect FDI detections. However, imperfect FDI results are inevitable owing to disturbances or modeling uncertainties and may corrupt designated reliability requirement. Therefore, it is necessary to validate the design of FTCSs from a reliability perspective.

The reliability of FTCSs has been investigated using various methods. The key problem is to set up appropriate reliability models with control objectives and safety requirements incorporated. As fault occurrences and system failures are rare events, dynamic models are usually not suitable for reliability analysis. For example, Wu used serial-parallel block diagrams and Markov models for evaluation purpose, and defined a coverage concept to relate reliability and control actions [1]. Walker proposed Markov and semi-Markov models to describe the transitions of fault and FDI modes, but control actions are not considered [2]. In previous work, we considered static model-based control objectives and built a semi-Makov model from imperfect FDI and hard-deadline concepts [3, 4]. However, in many practical systems, the safety and reliability of operation are often assessed based on dynamic system responses. For instance, reliability in structural control is defined as the probability of system outputs outcrossing safety boundaries and evaluated by using Gaussian approximation [5]. Also, an online available reliability monitoring scheme using updated information may aid maintenance scheduling, provide prealarming, and avoid emergent overhauls. How to evaluate reliability when it is defined based on system trajectory and how to implement an online-monitoring scheme are the main motivations of this paper.

The objectives of this paper are threefold. First of all, a steady-state test (SST) is proposed to reduce false alarms of FDI decisions. The stochastic modeling of such an FDI scheme is studied based on which the transition characteristics of FDI modes can be described. The second objective is to develop a reliability evaluation scheme for FTCSs based on system dynamic responses and safety boundary. At last, online monitoring features are considered, such as estimation of FDI transition parameters based on history data and timely update of reliability index to reflect up-to-date system behavior.

The remainder of this paper is organized as follows: the assumptions and system structure are given in Section 2; FDI scheme, modeling, and parameter estimation are discussed in Section 3; the determination of outcrossing failure rates and hard-deadlines are discussed in Section 4; the reliability model construction is discussed in Section 5 followed by a demonstration example of an F-14 aircraft model in Section 6.

2. ASSUMPTIONS AND SYSTEM STRUCTURE

Assumption 1. The considered plant is assumed to have finite fault modes, and dynamics under each fault mode can be effectively represented by a linear system model.

Fault modes are represented by a set S with N integers; $\{\mathcal{M}_i : i \in S\}$ represents the set of dynamical plant models under various fault modes; $\{\mathcal{K}_j : j \in S\}$ denotes a set of reconfigurable controllers in a switching structure. $\mathcal{K}_j$ is designed for fault mode j based on $\mathcal{M}_j$, $j \in S$. However, true fault modes are usually not directly known, so an FDI scheme is used to generate estimates of fault modes, which may deviate from true fault modes with error probabilities.

Assumption 2. FDI scheme is assumed to generate a fault estimate based on a batch of measurements and calculations for every fixed period T_c.

This assumption states a cyclic feature of FDI, such as statistical tests and interactive multiple model (IMM) Kalman filters [6]. FDI modes are represented by a discrete-time stochastic process $\eta_n \in S$, where $n \in \mathbb{N}$, the set of nonnegative integers. The time duration between consecutive discrete indices is equal to FDI detection period T_c. $\mathcal{K}_j$ is put in use when $\eta_n = j$, $j \in S$. Corresponding to η_n, a discrete-time stochastic process ζ_n denotes true fault mode. In reliability engineering, constant failure rates are usually assumed for the main part of component life cycle. In such a case, ζ_n can be described as a Markov chain [7], and its transition probabilities are denoted as $G_{ij} = \Pr\{\zeta_{n+1} = j \mid \zeta_n = i\}$, $i, j \in S$.

Remark 1. The semi-Markov process can be used as a general FDI model. It can describe any type of sojourn time distribution; in contrast, the Markov process model accepts exponential sojourn time distributions only. More discussions can be found in [4].

Assumption 3. System performance is assumed to be represented by a vector signal $z(t)$. Safety region, denoted as Ω, is assumed to be a fixed region in the space of $z(t)$ bounded by its safety threshold. Failure is assumed to occur when $z(t)$ exceeds a safety region for the first time.

This assumption intends to define an appropriate reliability index based on system dynamical response. It is common in control systems to use a signal $z(t)$ to represent performance, and $z(t)$ is usually to be kept at small values against influences from exogenous disturbances, modeling uncertainties, and dynamical characteristic changes caused by faults. Safety region Ω is assumed to be fixed and known a priori. The scenario that $z(t)$ exceeds Ω represents lost of control and system failures. More discussions on this assumption can be found in [8].

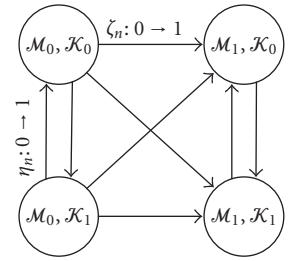

Figure 1: Transitions among regime models.

Definition 1. For a time interval from 0 to t, the reliability function $R(t)$ is defined as the following probability:

$$R(t) = \Pr\{\forall 0 \le \tau \le t, z(\tau) \in \Omega\}. \tag{1}$$

Mean time to failure (MTTF) is defined as the expected time of satisfactory operation:

$$\text{MTTF} = \int_0^\infty R(t)dt. \tag{2}$$

Remark 2. Different from repairs relying on human intervention when system operation is stopped, control actions are executed automatically and can be deemed as an internal actions of FTCSs. Therefore, MTTF represents the mean operational time without human intervention before failure.

Compared with ζ_n and η_n, $z(t)$ is typically a fast changing function determined by both continuous and discrete dynamics. As shown in Figure 1, ζ_n and η_n are two regime modes and determine the transitions among regime models. When $\zeta_n = i$ and $\eta_n = j$ are fixed, $z(t)$ evolves according to plant model $\mathcal{M}_i$ and controller $\mathcal{K}_j$. As a result of this hybrid dynamics, directly evaluating $R(t)$ and MTTF is a difficult problem. Therefore, a discrete-time semi-Markov chain X_n is constructed for reliability evaluation purpose. The main idea is that the hybrid system is decomposed into various regime models; each regime model is then evaluated for related safety characteristics, and X_n is constructed to integrate these characteristics with transition parameters of regime modes and to solve its transition probabilities for reliability evaluation. The structure and main components of reliability monitoring scheme are illustrated in Figure 2.

Semi-Markov reliability model X_n is the kernel component for calculating MTTF. It is constructed based on the following parameters: (1) the transition rates of ζ_n, called plant failure rates, (2) the estimates of ζ_n from FDI and confirmation test, called confirmed fault modes, (3) the parameters of η_n estimated from history data, called FDI transition characteristics, (4) the probability of $z(t)$ crossing safety boundary during an FDI cycle T_c when $\zeta_n = \eta_n$, called failure outcrossing rates, (5) the average number of periods before crossing safety boundary when $\zeta_n \neq \eta_n$, called hard deadlines. Among

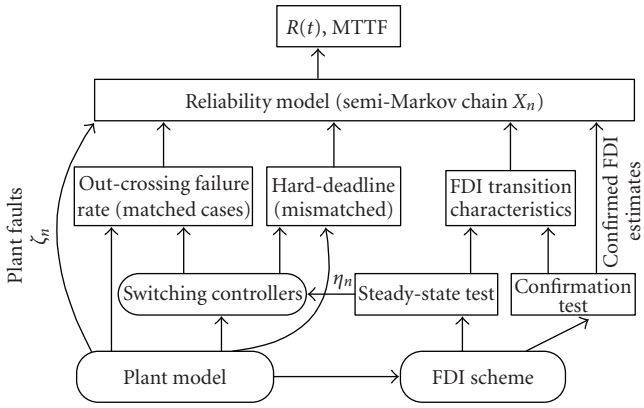

Figure 2: System structure.

these parameters, the second and third ones can be updated online.

3. FDI SCHEME AND ITS CHARACTERIZATION

3.1. Steady-state tests

It is well known that false alarm and missing detection rates are two conflicting quality criteria of FDI. One is usually improved at the cost of degrading the other. What is worse, the general rules of adjusting FDI to improve these two criteria simultaneously are often not known. For example, in a scheme based on IMM Kalman filters, it is not clear how to determine Markov interaction parameters. Considering that most false alarms last for short time only, an SST strategy is adopted for postprocessing FDI decisions.

SST requires that, when FDI decision changes, new decision is accepted only when it stays the same for a minimum number of detection cycles. Let $T_{\mathrm{SST}j}$ denote the required number of consistent cycles for FDI mode j, $j \in S$. The effectiveness of this SST strategy relies on the distribution of false alarm durations. For example, if a nonnegative discrete random variable λ_0 denotes the false alarm duration when system fault mode $\zeta_n = 0$, $T_{\mathrm{SST}0}$ can be taken as $(1-\alpha)$-quantile of λ_0, $0 < \alpha < 1$, meaning

$$\Pr\{\lambda_0 > T_{\mathrm{SST}0}\} \le \alpha, \tag{3}$$

which implies that false alarm probability can be reduced by ratio α when accepting FDI decisions after $T_{\mathrm{SST}0}$. The weakness of this method is additional detection time delay of $T_{\mathrm{SST}j}$ when fault occurs. However, this happens only under rare occurrences of faults. Compared with the improvement on relatively more frequently transitions of FDI modes, this weakness is acceptable.

Detection decisions from SST are represented by η_n and used for controller reconfigurations. In Figure 2, the confirmation test is an SST with large test period to further reduce false alarm probability to a negligible level. It generates confirmed fault modes, which are used with FDI trajectories for updating transition parameters of η_n and reliability index.

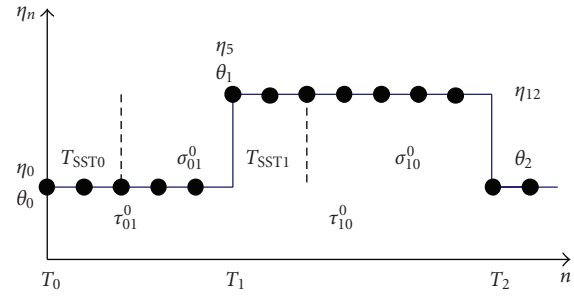

Figure 3: A sample path of η_n.

3.2. Stochastic models

A sample path of η_n is given in Figure 3. Let $\theta_m \in S$ and $T_m \in \mathbb{N}$ denote the FDI mode and cycle index, respectively, after the mth transition of η_n, $m \in \mathbb{N}$. For example, in Figure 3, $\theta_1 = \eta_5$ and $T_2 = 5$. θ_m and T_m together determine FDI trajectory, and $\eta_n = \theta_{S_n}$, where $S_n = \sup\{m \in \mathbb{N} : T_m \le n\}$ is the discrete-time counting process of the number of jumps in $[1, n]$. $(\theta, T) \triangleq \{\theta_m, T_m : m \in \mathbb{N}\}$ is called a discrete-time Markov renewal process if

$$\begin{aligned}&\Pr\{\theta_{m+1} = j, T_{m+1} - T_m = l \mid \theta_0, \ldots, \theta_m; T_0, \ldots, T_m\}\\ &\quad = \Pr\{\theta_{m+1} = j, T_{m+1} - T_m = l \mid \theta_m\}\end{aligned} \tag{4}$$

holds for fixed $\zeta_{T_m} = \zeta_{T_m+1} = \cdots = \zeta_{T_{m+1}} = k$, $k, j \in S$, $l, m \in \mathbb{N}$. $\eta_n = \theta_m$ is then called the associated discrete-time semi-Markov chain of (θ, T). It can be shown that θ_m is a Markov chain, and its transition probability matrix is denoted by P^k.

Given $\zeta_{T_m} = \zeta_{T_m+1} = \cdots = \zeta_{T_{m+1}} = k$, let $\tau^k_{ij} = T_{m+1} - T_m$ if $\theta_m = i$ and $\theta_{m+1} = j$, $i, j, k \in S$. τ^k_{ij} is the sojourn time of η_n between its transition to state i at T_m and the consecutive transition to j at T_{m+1}. If the transition destination state is not specified, let τ^k_i denote the sojourn time at state i.

As shown in Figure 3, τ^k_{ij} is the sum of two variables: a constant $T_{\mathrm{SST}i}$ for SST period and a random sojourn time σ^k_{ij}. Let $h^k_{ij}(l)$ and $g^k_{ij}(l)$ denote the discrete distribution functions of τ^k_{ij} and σ^k_{ij} respectively, which have the following relations:

$$h^k_{ij}(l) = \Pr\{\tau^k_{ij} = l\} = \begin{cases} 0, & l \le T_{\mathrm{SST}i}, \\ g^k_{ij}(l - T_{\mathrm{SST}i}), & l > T_{\mathrm{SST}i}. \end{cases} \tag{5}$$

This semi-Markov description provides a general model on FDI mode transitions, but it involves a large number of parameters. The transition characteristics of η_n are jointly determined by P^k and h^k_{ij} (or g^k_{ij}). If S contains N fault modes, there are N transition probability matrices P^k and N^3 distribution functions h^k_{ij}. If each h^k_i follows geometric distribution, the description of η_n may degenerate to a hypothetical Markov model η'_n.

All Markov chains can be considered as a special type of semi-Markov chains. If η_n can be modeled as a Markov chain

with transition probability matrix denoted by H^k for $\zeta_n = k$, the following relations hold:

$$P_{ij}^k = \frac{H_{ij}^k}{1 - H_{ii}^k}, \tag{6}$$

$$h_{ij}^k(l) = \left(H_{ii}^k\right)^{l-1} H_{ij}^k, \tag{7}$$

$$h_i^k(l) = \left(H_{ii}^k\right)^{l-1} \left(1 - H_{ii}^k\right). \tag{8}$$

It is obvious that h_i^k is a geometric distribution. In fact, this is an essential property of Markov chain, as shown in the following lemma.

Lemma 1. *A discrete-time semi-Markov chain degenerates to a Markov chain if and only if the sojourn time at each state (when subsequent state is not specified) follows geometric distribution.*

The proof is given in the appendix. When T_{SST} is nonzero, the sojourn time of η_n does not follow geometric distribution owing to this deterministic constant, and Lemma 1 cannot be directly applied. However, as T_{SST} is known, a hypothetical process η_n' can be constructed by setting T_{SST} to zeros; if the sojourn time of η_n' is geometrically distributed, it can be described as a Markov chain; the original sojourn time of η_n can be recovered by adding T_{SST} to that of η_n'. This method may greatly reduce the number of parameters for characterizing FDI results.

3.3. Transition parameter estimation

FDI transition parameters can be estimated as an offline test on FDI when both fault mode and FDI detection results are known. This estimation can also be carried out online using FDI history data and confirmed fault modes.

When η_n is modeled as a semi-Markov chain, P^k and h_{ij}^k (or g_{ij}^k) are parameters to be estimated. P^k can be estimated from the transition history of η_n. For example, when ζ_n is kept as a constant k, if there are M_{ij} transitions from i to j among all M transitions leaving i, the ijth element of P^k can be estimated as $\hat{P}_{ij}^k = M_{ij}/M$.

The estimation of sojourn time distribution g_{ij}^k can be completed in two steps: the histogram of sojourn time is firstly examined to select a standard distribution such that nonparametric estimation is converted to a parametric one; $\hat{g}_{ij}^k$ is then obtained by estimating unknown parameters in distribution functions.

If $\hat{g}_{ij}^k$ follows geometric distribution for all $i, j, k \in S$, η_n can be described as a hypothetical Markov chain η_n' under the hypothesis that $T_{\mathrm{SST}i} = 0$. As a result, transition probability H_{ij}^k from i to j and sojourn time τ_i^k at i have the following relation:

$$\Pr\{\tau_i^k = n\} = \left(H_{ii}^k\right)^{n-1} \left(1 - H_{ii}^k\right). \tag{9}$$

Therefore, $E(\tau_i^k) = 1/(1 - H_{ii}^k)$, and H_{ii}^k can be estimated by

$$\hat{H}_{ii}^k = \begin{cases} 1 - \dfrac{1}{\sum_{l=1}^{M} \tau_i^k(l)/M}, & \dfrac{\sum_{l=1}^{M} \tau_i^k(l)}{M} \neq 0, \\ 1, & \text{otherwise}, \end{cases} \tag{10}$$

where $\tau_i^k(l)$ denote M sojourn time samples at state i, $l = 1, \ldots, M$. H_{ij}^k can be estimated based on the transition frequency from state i to j:

$$\hat{H}_{ij}^k = \frac{\left(1 - \hat{H}_{ii}^k\right) w_{ij}^k}{M}, \tag{11}$$

where $1 - \hat{H}_{ii}^k$ is a normalization coefficient and w_{ij}^k represents the number of FDI transitions from i to j.

4. OUTCROSSING FAILURE RATES AND HARD-DEADLINES

Owing to FDI delays or incorrect decisions, controller $\mathcal{K}_i$ may be used for its designated regime model $\mathcal{M}_i$ (namely, matched cases) and other model $\mathcal{M}_j$, $i \neq j$ (namely, mismatched cases). Matched cases usually account for major operation time, while mismatched cases often appear as temporary operation.

Definition 2. The outcrossing failure rate in matched cases is defined as

$$\nu_{ii} \triangleq \Pr\{\exists \tau,\ nT_{\mathrm{c}} < \tau \leq (n+1)T_{\mathrm{c}}, \\ z(\tau) \notin \Omega \mid z(nT_{\mathrm{c}}) \in \Omega,\ \zeta_n = \eta_n = i\}, \quad i \in S. \tag{12}$$

Monte Carlo simulation can be used for estimating ν_{ii}: sample simulations are performed by using generated sample uncertain plant model and sample disturbance input; the simulation time when system fails is called a sample time-to-failure. With a large number of time-to-failure samples obtained, ν_{ii} can be estimated as the ratio between T_{c} and sample mean of time-to-failure.

Mismatched cases are usually temporary operation caused by FDI false alarms or delays, and system may return to matched cases if $z(t)$ does not diverge to unsafe region. So, it is important to find out the average tolerable time before system failure. This time limit is called hard-deadline, denoted by $T_{\mathrm{hd}ij}$ for $\zeta_n = i$ and $\eta_n = j$. It can also be estimated by sample mean of time-to-failure using Monte Carlo simulations.

5. RELIABILITY MODEL CONSTRUCTION

The states of semi-Markov chain X_n for reliability evaluation are classified into two groups: one unique failure state, denoted by s_{F}, and multiple functional states, defined as state combinations of $\zeta_n = i$ and $\eta_n = j$, denoted as s_{ij}, $i, j \in S$. For example, if two types of faults are considered in the plant, ζ_n includes states of fault-free, fault type 1, fault type 2, and both fault 1 and fault 2, represented by $S = \{0, 1, 2, 3\}$, and X_n contains 17 states.

The semi-Markov kernel of X_n is denoted as $Q(\cdot, \cdot, m)$, representing the one-time transition probability in m cycles. It is determined by the following parameters: (1) transition characteristics of fault and FDI modes, (2) outcrossing failure rate in state s_{ii} denoted by ν_{ii}, (3) hard-deadline in state s_{ij} denoted by $T_{\mathrm{hd}ij}$, (4) FDI SST period denoted by $T_{\mathrm{SST}j}$ for FDI mode j.

Let us begin with the case that FDI mode can be described as a hypothetical Markov chain η_n' with transition probability denoted by H_{ij}^k. The calculation of Q is classified into the following cases.

Case 1. The transitions from functional states to themselves are not defined and the corresponding elements are assigned as zeros:

$$Q(s_{ii}, s_{ii}, m) = 0, \quad Q(s_{ij}, s_{ij}, m) = 0, \quad i, j \in S. \tag{13}$$

Case 2. Failure state s_F is absorbing:

$$Q(s_F, s_F, m) = \begin{cases} 1, & m = 1, \\ 0, & m > 1. \end{cases} \tag{14}$$

Case 3. Initial states are matched states s_{ii}:

$$\begin{aligned}
&Q(s_{ii}, s_F, m) \\
&= \begin{cases} (1 - v_{ii})^{m-1} G_{ii}^{m-1} v_{ii}, & m \le T_{\mathrm{SST}i}, \\ p_{ii}\left[(1 - v_{ii}) G_{ii} H_{ii}^i\right]^{(m - T_{\mathrm{SST}i} - 1)} v_{ii}, & m > T_{\mathrm{SST}i}, \end{cases} \\
&Q(s_{ii}, s_{ji}, m) \\
&= \begin{cases} (1 - v_{ii})^{m-1} G_{ii}^{m-1} (1 - v_{ii}) G_{ij}, & m \le T_{\mathrm{SST}i}, \\ p_{ii}\left[(1 - v_{ii}) G_{ii} H_{ii}^i\right]^{(m - T_{\mathrm{SST}i} - 1)} (1 - v_{ii}) G_{ij} H_{ii}^i, & m > T_{\mathrm{SST}i}, \end{cases} \\
&Q(s_{ii}, s_{ij}, m) \\
&= \begin{cases} 0, & m \le T_{\mathrm{SST}i}, \\ p_{ii}\left[(1 - v_{ii}) G_{ii} H_{ii}^i\right]^{(m - T_{\mathrm{SST}i} - 1)} (1 - v_{ii}) G_{ii} H_{ij}^i, & m > T_{\mathrm{SST}i}, \end{cases} \\
&Q(s_{ii}, s_{kj}, m) \\
&= \begin{cases} 0, & m \le T_{\mathrm{SST}i}, \\ p_{ii}\left[(1 - v_{ii}) G_{ii} H_{jj}^k\right]^{(m - T_{\mathrm{SST}i} - 1)} (1 - v_{ii}) G_{ik} H_{ij}^i, & m > T_{\mathrm{SST}i}, \end{cases}
\end{aligned} \tag{15}$$

where $p_{ii} = \Pr\{X_1 = X_2 = \cdots = X_{T_{\mathrm{SST}i}} = s_{ii} \mid X_0 = s_{ii}\} = (1 - v_{ii})^{T_{\mathrm{SST}i}} G_{ii}^{T_{\mathrm{SST}i}}$, $i \neq j, k \neq i, i, j, k \in S$.

The derivation of these equations are based on Markov transition probabilities and the decomposition of each event. For example,

$$\begin{aligned}
&Q(s_{ii}, s_F, m) \\
&\quad = \Pr\{X_1 = X_2 = \cdots = X_{m-1} = s_{ii},\ X_m = s_F \mid X_0 = s_{ii}\} \\
&\quad = \Pr\{X_1 = X_2 = \cdots = X_{m-1} = s_{ii} \mid X_0 = s_{ii}\} \\
&\qquad \times \Pr\{X_1 = s_F \mid X_0 = s_{ii}\}.
\end{aligned} \tag{16}$$

Considering the SST of FDI, if $m \le T_{\mathrm{SST}i}$,

$$\begin{aligned}
&\Pr\{X_1 = X_2 = \cdots = X_{m-1} = s_{ii} \mid X_0 = s_{ii}\} \\
&\quad = (1 - v_{ii})^{m-1} G_{ii}^{m-1}.
\end{aligned} \tag{17}$$

If $m > T_{\mathrm{SST}i}$,

$$\begin{aligned}
&\Pr\{X_1 = X_2 = \cdots = X_{m-1} = s_{ii} \mid X_0 = s_{ii}\} \\
&\quad = \Pr\{X_1 = X_2 = \cdots = X_{T_{\mathrm{SST}i}} = s_{ii} \mid X_0 = s_{ii}\} \\
&\qquad \times \left[(1 - v_{ii}) G_{ii} H_{ii}^i\right]^{(m - T_{\mathrm{SST}i} - 1)}.
\end{aligned} \tag{18}$$

$Q(s_{ii}, s_F, m)$ can be obtained by combining these two probabilities with $\Pr\{X_1 = s_F \mid X_0 = s_{ii}\} = v_{ii}$.

Case 4. Mismatched states, s_{ij}, $i \neq j$. When $m \le T_{\mathrm{SST}j}$, the transition probability of $X(t)$ to any other state is zero because of SST period. When $T_{\mathrm{SST}j} < m \le T_{\mathrm{hd}ij}$, the probability of $X(t)$ transiting to any other state is zero except to s_{ii}. The above reasoning is based on the facts that FDI rarely jumps to other false modes when current mode is incorrect, and mean fault occurrence time is in a much higher order compared with a short false FDI detection period. Therefore, when $T_{\mathrm{SST}j} < m \le T_{\mathrm{hd}ij}$,

$$\begin{aligned}
Q(s_{ij}, s_F, m) &= 0, \\
Q(s_{ij}, s_{ii}, m) &= (H_{jj}^i)^{m - T_{\mathrm{SST}j} - 1} H_{ji}^i, \quad j \neq l,\ j, l \in S.
\end{aligned} \tag{19}$$

When $m > T_{\mathrm{hd}ij} + 1$, X_n jumps to s_F at the earliest time $m = T_{\mathrm{hd}ij} + 1$ only:

$$\begin{aligned}
Q(s_{ij}, s_F, T_{\mathrm{SST}i} + 1) &= 1 - \sum_{k = T_{\mathrm{SST}i} + 1}^{T_{\mathrm{hd}ij}} Q(s_{ij}, s_{ii}, m) \\
&= 1 - \frac{1 - (H_{jj}^i)^{T_{ij} - T_{\mathrm{SST}j} + 1}}{1 - H_{jj}^i} H_{ji}^i.
\end{aligned} \tag{20}$$

In the general cases, η_n is modeled as a semi-Markov chain, and the competition probabilities methods discussed in [4] can be utilized.

Definition 3. Given $\zeta_n = i$ and $\eta_n = j$, the combinational mode is denoted as (i, j), $i, j \in S$. Suppose $(\zeta_{n+1}, \eta_{n+1}) = \cdots = (\zeta_{n+m-1}, \eta_{n+m-1}) = (i, j)$ and the next combinational mode after the consequent transition of ζ_n or/and η_n at $n+m$ is $(\zeta_{n+m}, \eta_{n+m}) = (k, l)$, where $k \neq i$ or/and $l \neq j$, $k, j \in S$. The probability of this event is called the competition probability, denoted by $\rho_{(i,j) \rightarrowtail (k,l)}(m)$.

The calculation formulas of $\rho_{(i,j) \rightarrowtail (k,l)}(m)$ were derived in [4, Section 3] and are omitted here for brevity. As the states of X_n are mainly defined as the state combinations of ζ_n and η_n, the calculation of the semi-Markov kernel of X_n is simplified when $\rho_{(i,j) \rightarrowtail (k,l)}(m)$ is available, as shown in the following listed formulas:

$$\begin{aligned}
Q(s_{ii}, s_{kl}, m) &= (1 - v_{ii})^m \rho_{(i,i) \rightarrowtail (k,l)}(m), \\
Q(s_{ii}, s_F, m) &= (1 - v_{ii})^{m-1} v_{ii}, \\
Q(s_{ii}, s_{ii}, m) &= 0, \\
Q(s_{ij}, s_{kl}, m) &= \begin{cases} \rho_{(i,j) \rightarrowtail (k,l)}(m), & m \le T_{\mathrm{hd}ij},\ k = l = i, \\ 0, & \text{otherwise}, \end{cases} \\
Q(s_{ij}, s_F, m) &= \begin{cases} 0, & m \le T_{\mathrm{hd}ij}, \\ 1 - \sum_{m=1}^{T_{\mathrm{hd}ij}} Q(s_{ij}, s_{ii}, m), & m > T_{\mathrm{hd}ij}, \end{cases} \\
Q(s_F, s_F, m) &= \begin{cases} 1, & m = 1, \\ 0, & m > 1. \end{cases}
\end{aligned} \tag{21}$$

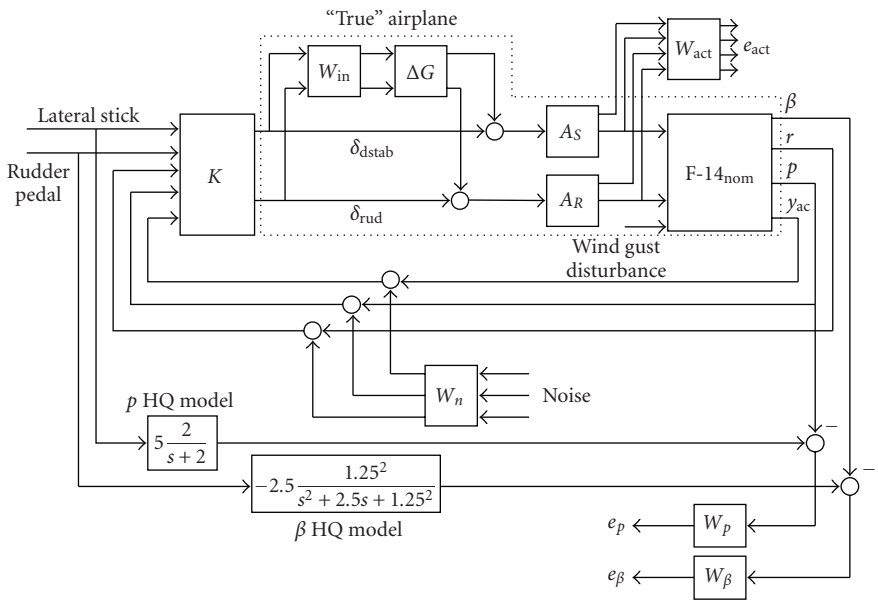

Figure 4: Control design diagram for F-14 lateral axis (Courtesy of The MathWorks, Inc.).

Although these formulas appear to be simpler, both the parameter estimation and competition probability calculations need much more calculation burden than the first case when FDI decision is modeled as a hypothetical Markov chain. Once X_n is constructed, calculation of reliability function and MTTF are straightforward using available formulas [9].

6. DEMONSTRATION ON AN F-14 AIRCRAFT MODEL

6.1. Model description

A control problem of F-14 aircraft was presented in [10], and also used as a demonstration example in MATLAB Robust Control Toolbox.[1] This problem considers the design of a lateral-directional axis controller during powered approach to a carrier landing with two command inputs from the pilot: lateral stick and rudder pedal. At an angle-of-attack of 10.5 degrees and airspeed of 140 knots, the nominal linearized F-14 model has four states: lateral velocity, yaw rate, roll rate, and roll angle, denoted by v, r, p, and ϕ, respectively, two control inputs: differential stabilizer deflection and rudder deflection, denoted by δ_{dstab} and δ_{rud}, respectively, and four outputs: roll rate, yaw rate, lateral acceleration, and side-slip angle, denoted by p, r, y_{ac}, and β, respectively. The system dynamics equations are ignored here, and can be loaded in MATLAB 7.1 using command "load F14nominal." An additional disturbance input is added to represent the wind gust effects.

The control objective is to have desired handling quality (HQ) responses from lateral stick to roll rate p and from rudder pedal to side-slip angle β. Under fault-free modes, the HQ models are $5(2/(s+2))$ and $-2.5(1.25^2/(s+2.5s+1.25^2))$; when fault occurs, HQ models degrade to $5(1/(s+1))$ and $-2.5(0.75^2/(s+1.5s+0.75^2))$, respectively.

The system block diagram is shown in Figure 4, where F-14$_{\text{nom}}$ represents the nominal linearized F-14 model, and A_S and A_R the actuator models. e_p and e_β represent the weighted model matching errors. Actuator energy is described by e_{act}, and noise is added to the measured output after antialiasing filters.

The considered fault occurs in two actuators. Under fault-free mode, their transfer functions are

$$A_S = A_R = \frac{25}{s+25}. \tag{22}$$

Two types of actuator faults are considered here, each has mean occurrence time 10^5 of FDI periods or its failure rate is 10^{-5}. Under fault type 1, the transfer function of A_S becomes

$$A_S' = 0.5\frac{15}{s+15}. \tag{23}$$

Under fault type 2, the transfer function of A_R becomes

$$A_R' = 0.5\frac{10}{s+10}. \tag{24}$$

These fault modes are described as the change of actuator gains and time constants. The set of fault modes is denoted by $S = \{0, 1, 2, 3\}$, representing fault-free, fault type 1, type 2, and simultaneous occurrence of both.

6.2. Performance characterization of controller and FDI

Four H_∞ controllers are designed for each fault mode to achieve nominal HQ control objectives under fault-free

[1] MATLAB and Robust Control Toolbox are the trademarks of The MathWorks, Inc.

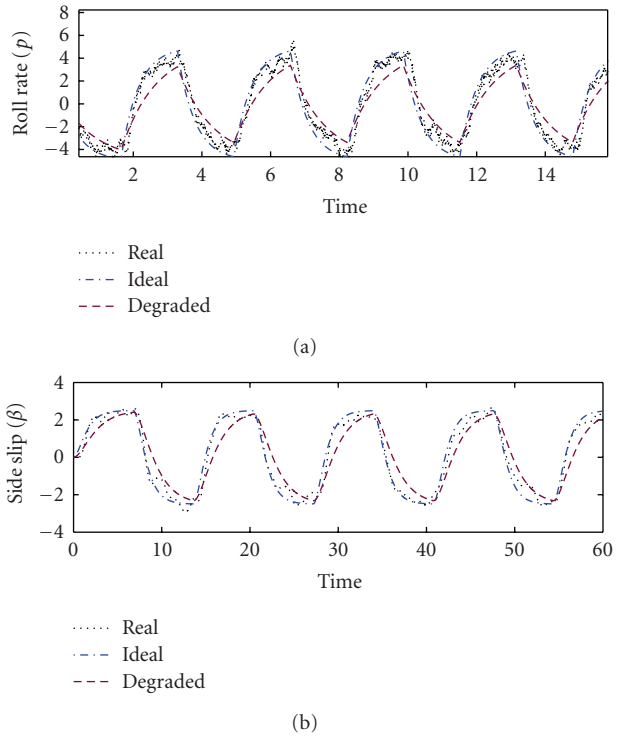

FIGURE 5: Output trajectories.

mode and degraded HQ performance under fault modes. Typical output trajectories under fault-free mode are shown in Figure 5, where the curves labeled with "Real" represent the measured outputs, "Ideal" the outputs under nominal HQ performance, and "Degraded" the outputs under degraded HQ performance. The absolute minimal matching errors between the real responses and the expected outputs under ideal HQ performance are shown in Figure 6, which are assumed to represent system safety behaviors. When these matching errors go over the safety limits, 30% of expected output, aircraft is considered as failed.

An IMM FDI is constructed to detect fault occurrences. To reduce false alarms, a steady-state test strategy is applied on FDI decisions with $T_{\mathrm{SST}j} = 6$ for any FDI mode j. A typical FDI trajectory is shown in Figure 7. It is clear that the steady FDI mode is free of false alarms in the shown time period. But detection time delays are introduced when fault occurs at 20 and 50 seconds, respectively.

To represent FDI detection characteristics, a batch of fault and FDI history data is collected for statistical estimation. First, histograms of FDI delays are generated to check its distribution type. When there is no fault, the histogram of FDI sojourn time at fault-free mode is shown in Figure 8. It clearly resembles a geometric distribution. Equations (10)-(11) are then used to estimate Markov transition probabilities, and those under fault-free mode are obtained as

$$H^0 = \begin{bmatrix} 0.9990 & 0 & 0.0010 & 0.0000 \\ 1.0000 & 0 & 0 & 0 \\ 0.1330 & 0 & 0.8670 & 0 \\ 0.5000 & 0 & 0 & 0.5000 \end{bmatrix}. \quad (25)$$

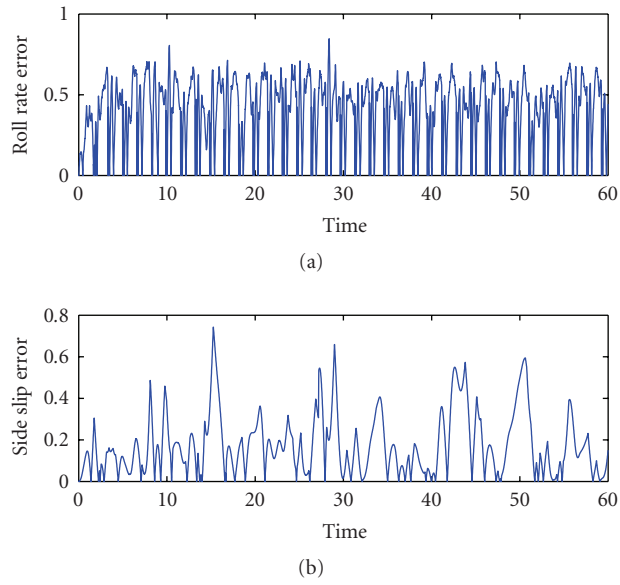

FIGURE 6: The trajectories of matching errors.

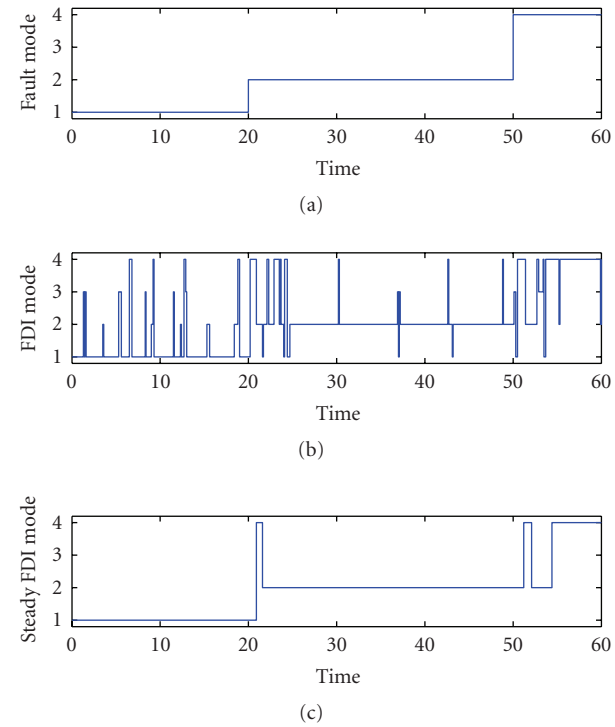

FIGURE 7: FDI trajectory.

Note that $H^0(2,1) = 1$ and $H^0(2,2) = 0$ represent the transition probabilities of FDI from a false alarm state. Estimated based on the given history data, these values imply that the FDI leaves false alarm state in one transition cycle. But there may exist estimation error, and the true value of $H^0(2,2)$ may be close to but not exact zero.

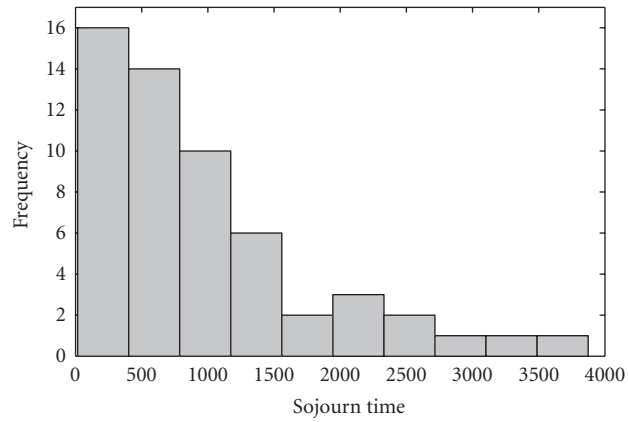

Figure 8: Histogram of FDI sojourn time.

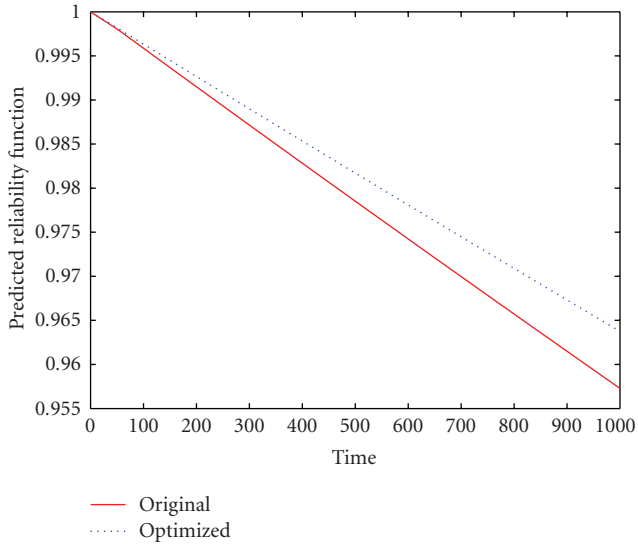

Figure 9: Reliability functions comparison.

As a result of FDI false alarms, missing detections, and detection delays, controllers may be engaged for various fault modes for which they are not designed. So, it is necessary to evaluate system behavior under all possible combinations of FDI and fault modes. Here, Monte Carlo simulations are adopted with the following settings: (1) command stick inputs are square waves with frequency as a random variable ranging from 0.2 to 2 Hertz, (2) wind gust disturbances and sensor measurement noises are assumed to be Gaussian processes, (3) actuator saturation effects limit control inputs to 20 and 30, respectively, (4) system failure is assumed to occur when model matching errors go over 30% of stick commands. For example, with fault mode 2 occurred and $\mathcal{K}_2$ engaged, mean time to system failure is 57 403 seconds when controller $\mathcal{K}_2$ is used, and 6 seconds when $\mathcal{K}_1$ is used. Considering the sampling period to be 0.1 second for IMM FDI, the outcrossing failure rate and hard-deadline are $\nu_{22} = 1/574030$, $T_{\text{hd}21} = 60$.

6.3. Reliability evaluation

Reliability semi-Markov model can be constructed based on fault transition rates, FDI transition parameters, outcrossing failure rate, and hard-deadlines. Predicted reliability function and MTTF can be thereby calculated. By using MTTF as an objective, an optimization is performed on T_{SST}. It is found that MTTF will be improved from 27 727 to 32 605 seconds if $T_{\text{SST}j}$ is reduced from 6 to 1. A comparison of reliability functions before and after this optimization is shown in Figure 9. It is clearly shown that reliability index is improved.

Comparisons on the transition probabilities between these two SST periods are shown in Figure 10, in which each subfigure gives the transition probability curves from s_{00} to other states. For example, the subfigure at the first row and second column shows that the transition probabilities to s_{01} are increased from 0 to about 0.008. This is a natural result of increased false alarms when reducing $T_{\text{SST}j}$. In fact, when $T_{\text{SST}j} = 1$, new Markov transition parameters H'^0 become

$$H'^0 = \begin{bmatrix} 0.9822 & 0.0017 & 0.0122 & 0.0038 \\ 0.2634 & 0.7366 & 0 & 0 \\ 0.1989 & 0 & 0.8011 & 0 \\ 0.3530 & 0 & 0 & 0.6470 \end{bmatrix}. \quad (26)$$

Compared with H^0, the element on the first row and second column is increased from 0 to 0.0017, a confirmation of increased false alarms. On the other hand, detection delays are reduced approximately from 6 to 1, and system stays less time under mismatched fault and FDI cases. Overall, MTTF is improved.

This evaluation procedure can be completed in an online manner. Estimated FDI transition parameters H and current mode of ζ_n provided by confirmed test on FDI can be used to provide updated MTTF based on this most recent information.

7. CONCLUSIONS

A reliability monitoring scheme for FTCSs is reported in this paper. The scheme contains two postprocessing strategies on FDI results to provide estimated fault mode for control reconfiguration and confirmed mode for updating reliability. The stochastic transitions of FDI mode is represented by a semi-Markov chain with parameters estimated from history data. Under geometric sojourn time distributions, FDI mode can be described by an equivalent hypothetical Markov chain that simplifies its model and reliability analysis. Safety and satisfactory operation of system is defined by system trajectories and safety boundaries; the probability of violating this safety criterion under fixed fault and FDI modes is estimated using Monte Carlo simulations. Overall reliability evaluation is obtained through a semi-Markov model constructed by integrating FDI transition characteristics and failure probabilities under each regime model. This scheme provides timely monitoring on the reliability index of FTCSs, and was demonstrated on an F-14 aircraft model.

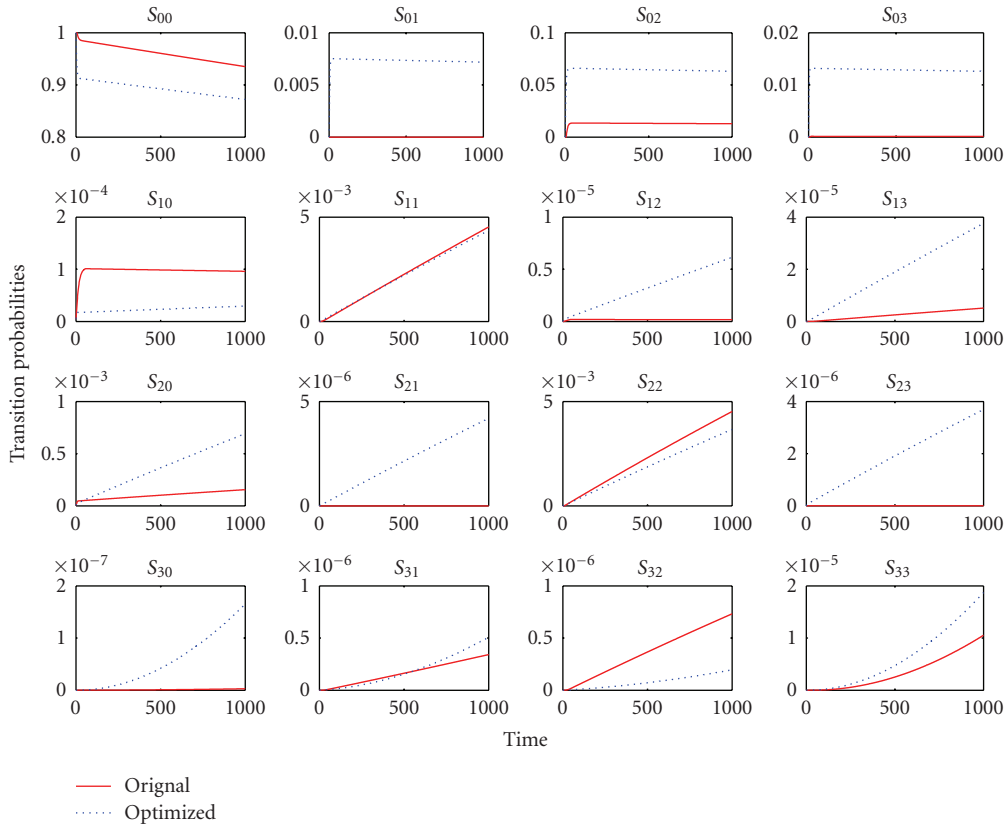

Figure 10: Comparison of transition probabilities.

APPENDIX

Proof of Lemma 1. The "only if" part is trivial as shown in (8). Let η_n denote a semi-Markov chain; the associated Markov renewal processes are denoted as θ_m and T_m, and the sojourn time distribution h_i^k when subsequent state is not specified is in geometric distribution:

$$\begin{aligned}&\Pr\{\eta_{n+1}=j \mid \eta_1,\ldots,\eta_n\}\\&\quad=\Pr\{\eta_{n+1}=j \mid \theta_1,\ldots,\theta_{S_n},T_1,\ldots,T_{S_n}\}.\end{aligned}\tag{A.1}$$

If $\theta_{S_n}=j$,

$$\begin{aligned}&\Pr\{\eta_{n+1}=j \mid \eta_1,\ldots,\eta_n\}\\&\quad=\Pr\{T_{S_n+1}>n+1 \mid \theta_1,\ldots,\theta_{S_n},T_1,\ldots,T_{S_n},T_{S_n+1}>n\}\\&\quad=\Pr\{T_{S_n+1}>n+1 \mid \theta_{S_n},T_{S_n},T_{S_n+1}>n\}\\&\quad=\Pr\{T_{S_n+1}-T_{S_n}>n+1-T_{S_n} \mid \theta_{S_n},T_{S_n+1}-T_{S_n}>n-T_{S_n}\}\\&\quad=\Pr\{T_{S_n+1}-T_{S_n}>1 \mid \theta_{S_n}\}\\&\quad=\Pr\{\eta_{n+1}=j \mid \eta_n\};\end{aligned}\tag{A.2}$$

otherwise, $\theta_{S_n}\neq j$, and we have

$$\begin{aligned}&\Pr\{\eta_{n+1}=j \mid \eta_1,\ldots,\eta_n\}\\&\quad=\Pr\{\theta_{S_n+1}=j,T_{S_n+1}=n+1 \mid \theta_1,\ldots,\theta_{S_n},\\&\qquad T_1,\ldots,T_{S_n},T_{S_n+1}>n\}\\&\quad=\Pr\{\theta_{S_n+1}=j,T_{S_n+1}=n+1 \mid \theta_{S_n},T_{S_n},T_{S_n+1}>n\}\\&\quad=\Pr\{\theta_{S_n+1}=j,T_{S_n+1}-T_{S_n}=n+1-T_{S_n} \mid \theta_{S_n},\\&\qquad T_{S_n+1}-T_{S_n}>n-T_{S_n}\}\\&\quad=\Pr\{\theta_{S_n+1}=j,T_{S_n+1}-T_{S_n}=1 \mid \theta_{S_n}\}\\&\quad=\Pr\{\eta_{n+1}=j \mid \eta_n\}.\end{aligned}\tag{A.3}$$

In the above derivations, the memoryless property of geometric distributions has been used:

$$\begin{aligned}&\Pr\{T_{S_n+1}-T_{S_n}>n+1-T_{S_n} \mid T_{S_n+1}-T_{S_n}>n-T_{S_n}\}\\&\qquad=\Pr\{T_{S_n+1}-T_{S_n}>1\},\\&\Pr\{T_{S_n+1}-T_{S_n}=n+1-T_{S_n} \mid T_{S_n+1}-T_{S_n}>n-T_{S_n}\}\\&\qquad=\Pr\{T_{S_n+1}-T_{S_n}=1\}.\end{aligned}\tag{A.4}$$

The Markov property of η_n is proved, so η_n is a Markov chain. □

REFERENCES

[1] N. E. Wu, "Coverage in fault-tolerant control," *Automatica*, vol. 40, no. 4, pp. 537–548, 2004.

[2] B. Walker, "Fault tolerant control system reliability and performance prediction using semi-Markov models," in *Proceedings of Safeprocess*, pp. 1053–1064, Kingston Upon Hull, UK, 1997.

[3] H. Li, Q. Zhao, and Z. Yang, "Reliability modeling of fault tolerant control systems," to appear in *International Journal of Applied Mathematics and Computer Science*.

[4] H. Li and Q. Zhao, "Reliability evaluation of fault tolerant control with a semi-Markov fault detection and isolation model," *Proceedings of the Institution of Mechanical Engineers Part I*, vol. 220, no. 5, pp. 329–338, 2006.

[5] J. Song and A. Der Kiureghian, "Joint first-passage probability and reliability of systems under stochastic excitation," *Journal of Engineering Mechanics*, vol. 132, no. 1, pp. 65–77, 2006.

[6] Y. Zhang and X. R. Li, "Detection and diagnosis of sensor and actuator failures using IMM estimator," *IEEE Transactions on Aerospace and Electronic Systems*, vol. 34, no. 4, pp. 1293–1313, 1998.

[7] W. Kuo and M. Zuo, *Optimal Reliability Modeling*, John Wiley & Sons, Hoboken, NJ, USA, 2002.

[8] R. V. Field Jr. and L. A. Bergman, "Reliability-based approach to linear covariance control design," *Journal of Engineering Mechanics*, vol. 124, no. 2, pp. 193–199, 1998.

[9] V. Barbu, M. Boussemart, and N. Limnios, "Discrete-time semi-Markov model for reliability and survival analysis," *Communications in Statistics: Theory and Methods*, vol. 33, no. 11, pp. 2833–2868, 2004.

[10] G. J. Balas, A. K. Packard, J. Renfrow, C. Mullaney, and R. T. M'Closkey, "Control of the F-14 aircraft lateral-directional axis during powered approach," *Journal of Guidance, Control, and Dynamics*, vol. 21, no. 6, pp. 899–908, 1998.

Hindawi Publishing Corporation
Journal of Control Science and Engineering
Volume 2008, Article ID 310652, 13 pages
doi:10.1155/2008/310652

Research Article

Fault-Tolerant Control of a Distributed Database System

N. Eva Wu,[1] Matthew C. Ruschmann,[1] and Mark H. Linderman[2]

[1] *Department of Electrical and Computer Engineering, Binghamton University, Binghamton, NY 13902-6000, USA*
[2] *US Air Force Research Laboratories at Rome Research Site, Rome, NY 13441-4505, USA*

Correspondence should be addressed to N. Eva Wu, evawu@binghamton.edu

Received 31 December 2006; Accepted 11 September 2007

Recommended by Kemin Zhou

Optimal state information-based control policy for a distributed database system subject to server failures is considered. Fault-tolerance is made possible by the partitioned architecture of the system and data redundancy therein. Control actions include restoration of lost data sets in a single server using redundant data sets in the remaining servers, routing of queries to intact servers, or overhaul of the entire system for renewal. Control policies are determined by solving Markov decision problems with cost criteria that penalize system unavailability and slow query response. Steady-state system availability and expected query response time of the controlled database are evaluated with the Markov model of the database. Robustness is addressed by introducing additional states into the database model to account for control action delays and decision errors. A robust control policy is solved for the Markov decision problem described by the augmented state model.

1. INTRODUCTION

A database, as described in [1], is a shared collection of related data and the description of this data, designed to meet the information needs of a client. A recent study by Wu et al. [2] on a distributed database system, as shown in Figure 1, revealed the benefits of a conscientious design of redundant architecture and the application of state information-based control. Such benefits were quantified in terms of mean time to system failure, steady-state availability, expected response time, and service overhead. The database system was viewed as a queuing network [3, 4] and mathematically modeled as a Markov chain [5]. The control authorities considered included the ability to restore the lost data sets in a single server and the ability to route service requests. In order to obtain an analytic model of manageable size for scrutinizing the effects of control, the queuing network was restricted to the closed type with a query population of three. In addition, all the event lifetime distributions were assumed to be exponential. A simulation study conducted by Metzler [6] using Arena [7, 8] with the above restrictions removed supported the conclusions in [2].

The first objective of this paper is to provide justification that the control policy applied in the aforementioned study [2] is optimal in a well defined sense. To that end, a Markov decision problem [9, 10] is formulated and the solution that minimizes a total expected discounted cost is sought. For the purpose of illustration, a simple problem that disregards the query states is set up, for which the policy developed in [2] is confirmed to be optimal.

In reality, however, it is not practical to monitor every state variable in a network. As a result, knowledge on a certain set of states is inferred based on the observables. On the other hand, a control action, in response to a state transition such as an occurrence of a server failure, must wait until a process of diagnosing the failure state [11] is complete. The time required for diagnosis is assumed to be a random variable and the outcome of the diagnosis usually has some degree of uncertainty as well. If servers must communicate through wireless channels, the likelihood of an erroneous decision and a delayed action is drastically increased. Recognizing that the assumption of instantaneous accessibility of the state information in the database system could lead to overly optimistic conclusions on system performance, Wu et al. [12] took a further step to analyze the effects of control action delays and decision errors for the same database system. Their analysis concluded that delays and errors can significantly degrade the performance of the database system.

Therefore, the second objective of the paper is to seek a robust control policy that mitigates the effects of such control action delays and decision errors. A robust solution obviously has a strong dependence on how uncertainties are

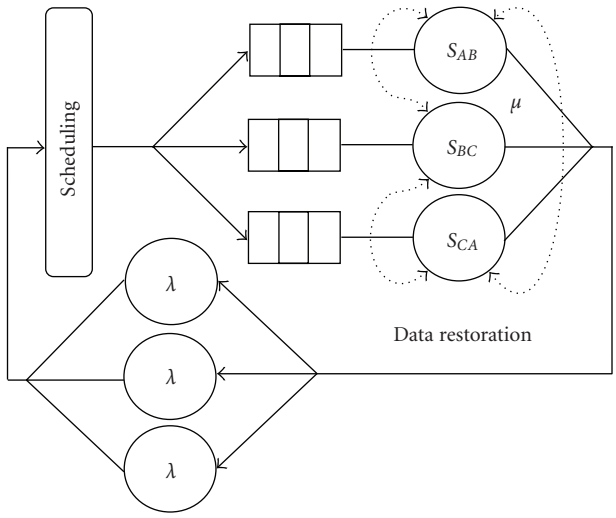

Figure 1: A queuing network representation of a partitioned database system with three servers.

modeled. This paper establishes an uncertain database model following the basic principles presented in [12]. The new model also captures the effect of routing delays of queries from a failed server to remote intact servers. A new Markov decision problem is then formulated and solved. Due to the increased dimension of the problem, approximate solutions are sought via numerical means.

This paper presents a novel model of a replicated data store wherein a set of information is partitioned and each partition is stored on multiple servers. This work is motivated by the recognition of the need for greatly enhanced availability of information management systems in air operations [13]. It addresses the desirability of hardware replication and state-information-controlled restoration, whereas published works in the field of distributed database and replication have discussed specific protocols and software failures [14].

The paper is organized as follows: Section 2 describes the baseline model of the controlled database system shown in Figure 1; Section 3 formulates and solves a Markov decision problem that justifies the control policy applied to the baseline model; Section 4 presents an approach to modeling control action delays and decision errors; Section 5 formulates and solves, using dynamic programming, a Markov decision problem with an uncertain model containing delays and errors, and analyzes the robustly controlled system in terms of system availability and query response time in the presence of control action delays and decision errors.

2. BASELINE MODEL AND NOTATION FOR A CONTROLLED DATABASE SYSTEM

The description of a baseline model for a replicated data store follows to a large extent that of Wu et al. [2]. In particular, a system of three servers is studied, each storing two partitions out of a total of three. Each partition has one "primary" server and one "secondary" server.

The distributed database system in Figure 1 contains three servers in parallel to answer three classes, A, B, and C, of queries for which relevant information can be found in the partitioned data sets, A, B, and C, of the database, respectively. Server S_{MN} would contain the data set corresponding to class M as the primary set and a reproduction of data set N as the secondary set. Alternate secondary data sets are reproduced in order to automate restoration of failed servers within the database. The failure of a server implies the loss of two sets of data within the server. A system level failure is declared when two servers fail, in which case one set of data is completely lost. The queues preceding servers S_{AB}, S_{BC}, and S_{CA} are named Q_{AC}, Q_{BC}, and Q_{CA}, respectively. All queues are of sufficient capacity in the baseline model. Service is provided on a first-come-first-served (FCFS) basis at each server.

The three delay elements of average delay $1/\lambda$ imply that there are always three queries present in the system at any given time. A new query is generated at a delay element with rate λ upon the completion of the service to a query at one of the servers. The delay elements are also intended to be reflective of the response time to the querying customers by other service nodes in the system that are not explicitly modeled. Any new query is assumed to have a likelihood of ρ_{IJ} to visit server S_{IJ}, where IJ can be AB, BC, or CA.

The use of a queuing network model for the database is based on its suitability to involve control actions and to capture their effects on the system performance. The model is built in this study with the premise that event life distributions have been established for the process of query generation ($\exp(\lambda) \equiv 1 - e^{-\gamma t}$), the process of service completion ($\exp(\mu)$), the process of server failure ($\exp(\nu)$), the process of data restoration ($\exp(\gamma)$), and the process of system overhaul ($\exp(\omega)$) when the failed database system is repaired. All such processes are independent. Standard statistical methods that involve data collection, parameter estimation, and goodness of fit tests exist [15] for identifying event life distributions. Alternative distributions and goodness of these assumptions were investigated in [6]. Since all event lives are assumed to be exponentially distributed, the database system can be conveniently modeled as a Markov chain specified by a state space $\mathcal{X}$, an initial state probability mass function (pmf) $\pi_x(0)$, and a set of state transition rates Λ.

2.1. Model specification

State space $\mathcal{X}$

A state name is coded with a 6-digit number indicative of all queue lengths and server states in the system. With some abuse of notations, a valid state representation is given by $Q_{AB}Q_{BC}Q_{CA}S_{AB}S_{BC}S_{CA}$, where queue length Q_{AB}, Q_{BC}, $Q_{CA} \in \{0, 1, 2, 3\}$ with total length $L \equiv Q_{AB} + Q_{BC} + Q_{CA} \leq 3$ limited by the three entities available in the closed-queue system. The server states S_{AB}, S_{BC}, $S_{CA} \in \{0, 1, 2\}$ are further defined as "2" $\equiv$ data are lost in both the primary and the secondary sets in a server, "1" $\equiv$ the data in the primary set have been restored and data in the secondary set have not been restored, and "0" $\equiv$ data in both primary set and secondary set in a server are intact. A server is said to be in the

down state if it is either at states "1" or "2." For example, state 110020 indicates that server S_{AB} is up with one customer in its queue, server S_{BC} is down with both sets of data lost and one customer in its queue, and server S_{CA} is up and idle. Note that the queue length includes the customer being served. There are 540 valid states in the baseline system. The total number of states is reduced to 147 when all the states representing system level failures are aggregated into seven states memorizing the possible queue length distributions and exploiting the symmetry of the three servers. A set of alternative state names are assigned from $\mathcal{X} = \{1, 2, \ldots, 147\}$ with 000000 mapped to $x = 1$ and the aggregated system failure state mapped to $x = 141, \ldots, 147$. Although the symmetry of the system allows further reduction on the number of states to 56, the 147-state model is retained for clarity of presentation.

Initial state pmf $\{\pi_x(0),\ x = 1, 2, \ldots, 147\}$

It is assumed that the database system starts operation from state $x = 1(000000)$, that is, the initial state probability is given by vector $\pi(0) = [1\ 0 \ldots 0]$.

Set of state transition functions $p_{i,j}(t)$

Events that trigger the transitions and the corresponding transition rates are given as follows. A newly generated query enters one of the servers with rate $(3-L)\times\lambda/3$. A query is answered at a server with rate μ. A complete data loss occurs at a server with rate ν. Data in the primary data set of a server are restored with rate γ or repaired with overhaul rate ω. Data in the secondary data set of the server are restored with rate γ, following the restoration of the primary data set. The failed database system is always renewed with overhaul rate ω.

Let $X \in \mathcal{X}$ denote the random state variable at time t. The set of state transition functions is given by

$$p_{i,j}(t) \equiv P[X(t) = j \mid X(0) = i], \quad i, j = 1, 2, \ldots, 147. \tag{1}$$

The continuous-time Markov chain can be solved from the forward Chapman-Kolmogorov equation [5, 10]

$$\dot{P}(t) = P(t)Q(u(x)), \quad P(0) = I, \quad P(t) = [p_{i,j}(t)] \tag{2}$$

and $Q(u(x))$ is called an infinitesimal generator or a rate transition matrix whose (i, j)th entry is given by the rate associated with the transition from current state i to next state j. (See [2] for the complete rate transition.) Control variable $u(x)$ will be defined shortly. State probability mass function at time t,

$$\pi(t) = [\pi_1(t) \quad \pi_2(t) \quad \ldots \quad \pi_{147}(t)], \quad t \geq 0, \tag{3}$$

is computed by

$$\pi(t) = \pi(0)P(t). \tag{4}$$

At this point, a baseline Markov model for the database system of Figure 1 has been established. Since transition rate matrix Q is dependent on control actions, the state transition functions $p_{i,j}(t)$ are being controlled, as are the state probabilities.

2.2. Control Policy

Our intention is to eliminate all single point failures. Our approach is to base the control actions on the state information, which effectively alter the transition rates when loss of data occurs in a single server. The possible set of control actions includes restoration, overhaul, and no decision needed. There is one admissible set of control actions at each state. A state of no decision needed has an empty admissible set.

Taking into consideration the symmetry of the model, the control policy considered for this study is summarized as follows:

$$u(x) = \begin{cases} 0, & \text{upon entering the state of one server failure, system overhauls;} \\ 1, & \text{upon entering the state of one server failure, system restores.} \end{cases} \tag{5}$$

The presence of control in the transition rate matrix is seen via $u(x)$ and $\overline{u}(x) = 1 - u(x)$. The values of $u(x)$ represent specific control actions associated with data restoration $(u(x) = 1)$ or system overhaul $(\overline{u}(x) = 1)$, respectively. Previously in [2], system overhaul is considered only at state $x = 141$ through $x = 147$.

2.3. Performance measures

Two of the four performance measures defined in [2] are reintroduced: steady-state availability A_{sys} and expected response time $E[R]$. These will be used later to validate the control policies that are derived under cost criteria intended to improve both A_{sys} and $E[R]$.

Steady-state availability

Suppose as soon as the database system reaches a system level failure, an overhaul process starts. Suppose, with a rate ω, the system is repaired, and at the completion of the repair, the system immediately starts to operate again. In this case, the Markov chain becomes irreducible, and a unique steady-state distribution exists [5, 10]. The steady-state availability, which can be roughly thought of as the fraction of time the database system is upto, is computed in [2] by

$$A_{\text{sys}} = 1 - \pi_F(\infty), \tag{6}$$

where $\pi_F(\infty)$ is the sum of the system level failure state probabilities determined by solving

$$\pi(\infty)Q = 0, \quad \sum_{x=1}^{147} \pi_x(\infty) = 1. \tag{7}$$

Expected query response time

Query response time is the amount of time elapsing from the instant a query enters a queue until it completes service [10]. With server failures, the average response time $E[R]$ is calculated as the expectation of the ratio of total amount of time that all queries spend waiting for service in queue, plus

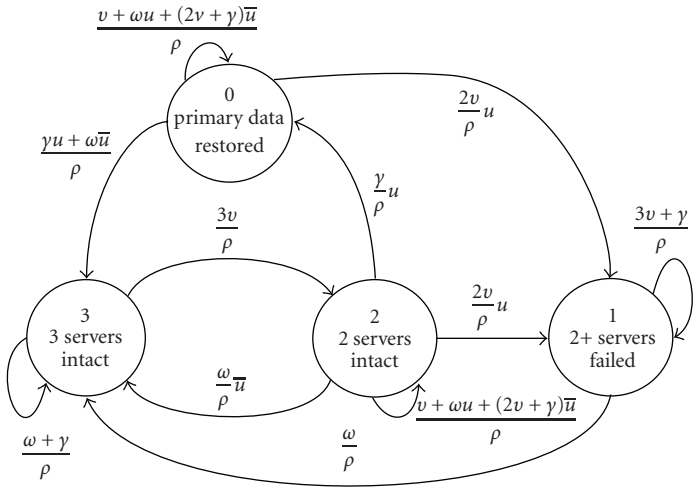

Figure 2: Markov chain model of the database reflecting only the server states.

their service times to the number of queries that are serviced. Consider, again, the irreducible chain modeling of the system in Figure 1. Let $I_{i,j}$ be the indicator function associated with transition from state i to state j that indicates a query arrival. Let N_i be the total number of queries in queue at state i. Then the total expected number of queries in queue at the steady state is given by

$$E[X] = \sum_{i=1}^{147} \pi_i(\infty) N_i, \tag{8}$$

and the arrival rate at steady-state is

$$\lambda_s = \sum_{i=1}^{147} \pi_i(\infty) \sum_{i=1}^{147} I_{ij} q_{ij}. \tag{9}$$

The calculation of the response time at steady-state then follows Little's Law [4, 10] $E[X] = \lambda_s E[R]$.

3. RESTORATION AS SOLUTION TO MARKOV DECISION PROBLEM

Intuition suggests that by restoring the lost data sets in a single failed server, overhaul can be avoided, and therefore, the stationary control policy $u(x)$ given in (5) ought to render service more available. However, the restoration process occupies one of the remaining servers, and therefore, may prolong the average response time of the system to queries. This section formulates and solves a Markv decision problem (MDP) for the database system to justify the optimality of the restoration policy used in [2].

The Markov decision problem considered in this paper assumes that a cost $C(i, u)$ is incurred at every state transition, where i is the state entered and u is a control action selected from a set of admissible actions [9, 10]. The solution amounts to determining a stationary policy $\pi = \{u_0(x_0), u_1(x_1), \dots\}$ that minimizes the following expected total discounted cost:

$$V_\pi(x_0) = E_\pi \sum_{k=0}^{\infty} \alpha^k C(X_k, u_k), \tag{10}$$

where $0 < \alpha < 1$ is a discount factor.

To simplify the presentation, state information on representing service demand is ignored for the moment. In this case, the inherent symmetry of the database system leads to a very simple 4-state Markov model as shown in Figure 2. As a result, the finite population assumption can be relaxed, that is, the closed queuing network of Figure 1 can either remain closed or can be revised to an open queuing network. In addition, query handling in the event of a server failure becomes completely unrestricted. Two different methods of query handling are to be examined in this section.

(1) Each arrival query has equal likelihood to seek information in data sets A, B, or C, but only the primary data set is available for query service in each server, and the secondary server is there to restore data in a failed server.
(2) Upon a server failure, queries are rerouted to the two remaining servers where the secondary data sets also participate in query service though only one of the two intact servers can provide service to only two of the three classes of queries during restoration.

The distinction in these two cases is captured in transition probabilities and in transition cost $C(i, u)$. Fault-tolerant control policies are now developed for the two cases.

3.1. Secondary data set reserved for lost data restoration

This subsection derives the optimal control policy with the first method for handling queries; each arrival query has equal likelihood to seek information in data sets A, B, or C, but only the primary data set is available for query service in

Table 1: One step cost $C(x_k, u_k)$.

State	$u = 1$	$u = 0$
3	0	0
2	$1/\gamma$	$1/\omega$
1	$1/\omega$	$1/\omega$
0	$1/\gamma$	$1/\omega$

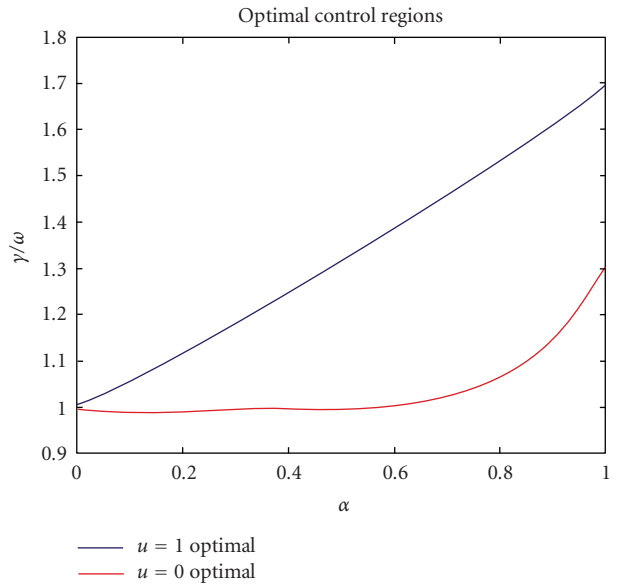

Figure 3: Optimal policy on the $(\alpha, \gamma/\omega)$ graph.

each server, and the secondary server is there to restore data in a failed server.

Figure 2 shows a discrete time Markov chain model for this case. This model is obtained by the application of a uniformization procedure [10] with a uniform rate $\rho = 3\nu+\omega+\gamma$ that is greater than any total outgoing transition rates at any state of the original continuous time Markov process. All parameters in Figure 2 have been defined earlier.

A fault-tolerant control policy essentially determines whether to occupy one of the two working servers to restore the data in the failed server or to overhaul the entire system at the state of one server failure. It is determined by how the designer penalizes a control action at any given state. Table 1 specifies the one step cost at each state.

Let $X_k \in \{1, 2, 3, 4\}$ denote the random state variable at $t = k/\rho$ in the discrete time Markov chain. Control action $u(x_k) = 1$(or 0, or φ) indicates the system's decision to (or not to overhaul, or not to act) restore a failed server. $C(x_k, u_k)$ in Table 1 is the cost incurred when control action u_k is taken based on x_k. It has been shown that under the condition $0 \le C(j, u) < \infty$ for all j and all u that belongs to some finite admissible sets U_j, the minimal cost $V^*(i)$ satisfies the following optimality equation [9, 10]:

$$V(i) = \min_{u \in U_i} \left\{ C(i,u) + \alpha \sum_j p_{i,j} V(j) \right\}, \tag{11}$$

where $p_{i,j}$ have been marked in Figure 2. In addition, policy π^* is optimal if and only if it yields $V^*(i)$ for all i. The four optimality equations can be expressed explicitly based on (11):

$$\begin{aligned}
V(0) = \min_u \Bigg\{ & \underbrace{\frac{1}{\omega} + \alpha\frac{3\nu+\gamma}{\rho} V(0) + \alpha\frac{\omega}{\rho} V(3)}_{u=0}, \\
& \underbrace{\frac{1}{\gamma} + \alpha\frac{\nu+\omega}{\rho} V(0) + \alpha\frac{2\nu}{\rho} V(1) + \alpha\frac{\gamma}{\rho} V(3)}_{u=1} \Bigg\}; \\
V(1) = \min_u \Bigg\{ & \frac{1}{\omega} + \alpha\frac{3\nu+\gamma}{\rho} V(1) + \alpha\frac{\omega}{\rho} V(3), \\
& \frac{1}{\omega} + \alpha\frac{3\nu+\gamma}{\rho} V(1) + \alpha\frac{\omega}{\rho} V(3) \Bigg\}; \\
V(2) = \min_u \Bigg\{ & \frac{1}{\omega} + \alpha\frac{2\nu+\gamma}{\rho} V(2) + \alpha\frac{\omega}{\rho} V(3), \\
& \frac{1}{\gamma} + \alpha\frac{\gamma}{\rho} V(0) + \alpha\frac{2\nu}{\rho} V(1) + \alpha\frac{\nu+\omega}{\rho} V(2) \Bigg\}; \\
V(3) = \min_u \Bigg\{ & \alpha\frac{3\nu}{\rho} V(2) + \alpha\frac{\omega+\gamma}{\rho} V(3), \\
& \alpha\frac{3\nu}{\rho} V(2) + \alpha\frac{\omega+\gamma}{\rho} V(3) \Bigg\}.
\end{aligned} \tag{12}$$

The above equations are solved for $V^*(i)$, for $i = 0, 1, 2, 3$, using *Mathematica* [16]. Figure 3 is created with $\omega = 10\nu$ and $\alpha \in [0, 1)$. It can be seen that, when the ratio of γ to ω is above the blue curve, $u = 1$ (restoration) is optimal at all states, whereas $u = 0$ (overhaul) is optimal when γ/ω is below the red curve. Between the two curves, $\{u(2) = \varphi, u(0) = \varphi\}$ is optimal, for transition from state "2" to state "0" implies restoration of primary data set, which cannot occur with control action $u(2) = 0$. Therefore, the mid-region optimal policy does not take place in the operation of the database system.

Note that $\gamma/\omega = 5$ in [2], which lies above the blue curve in Figure 3 for any $\alpha \in [0, 1)$. Therefore, the always-restore policy implemented in [2] is optimal under the cost structure defined in Table 1.

3.2. Secondary data set available for both query service and data restoration

This subsection considers the second method of query handling upon a server failure: overhaul can only occur at state "1," which implies that queries of the failed server are rerouted to the two remaining servers where the secondary data sets also participate in query service though only one of the two intact servers can provide service to only two of the three classes of queries during restoration.

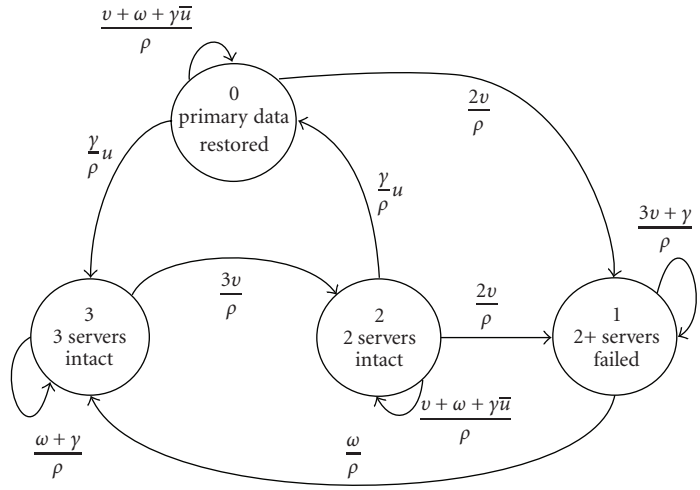

FIGURE 4: Markov chain model of the database where overhaul does not occur until a second server failure.

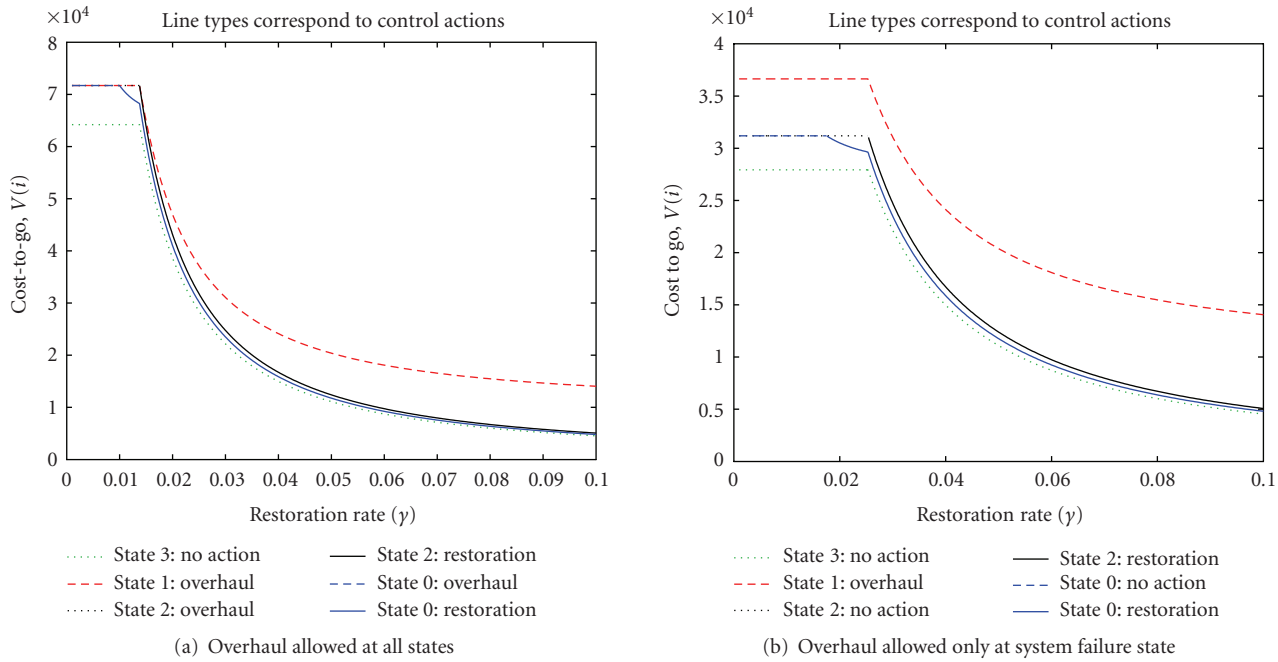

(a) Overhaul allowed at all states

(b) Overhaul allowed only at system failure state

FIGURE 5: Minimum cost-to-go versus restoration rate for the 4-state model with cost criteria of Table 1.

The uniformized Markov chain model is shown in Figure 4. In this case,

$$u(x) = \begin{cases} 0, & \text{upon entering the state of one server} \\ & \text{failure, system awaits,} \\ 1, & \text{upon entering the state of one server} \\ & \text{failure, system restores,} \end{cases} \tag{13}$$

overhaul is held until a second server fails, and all classes of queries rely on the service of the two operating servers in the meantime.

Figures 5(a) and 5(b) compare the optimal cost-to-go's of the two methods of query handling as functions of restoration rate γ at fixed $\omega = 10\nu$ and $\nu = 0.001$. Different line types specify different control actions. In Figure 5(b), for example, no control action is taken at state "0" unless $\gamma \geq 1.8\omega$ where restoration takes place; the system is always overhauled at state "1;" no control action is taken at state "2" unless $\gamma \geq 2.6\omega$ where restoration takes place; and no control action is ever taken at state "3." It is seen that control policy change occurs at a higher ratio of γ/ω with the second method (policy change at $\gamma = .026$ in Figure 5(b)) than that with the first method (policy change at $\gamma = .014$ in

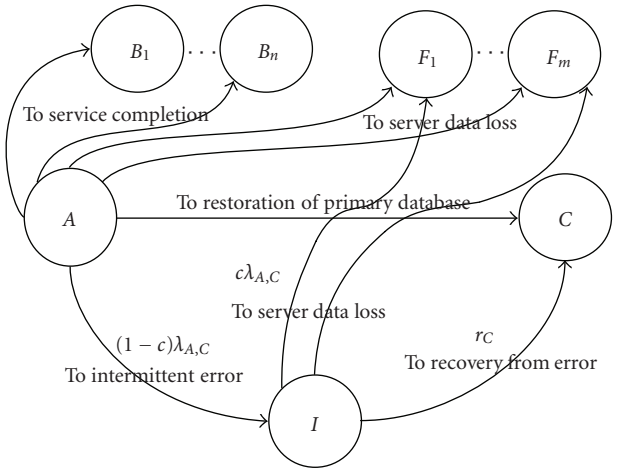

FIGURE 6: Decision error modeling with an intermittent error state.

Figure 5(a)). Despite the slight favor toward overhaul, the optimality of the "always-restore" policy applied in [2] still holds with the second method at the nominal parameter values $\mu = 12$, $\gamma = 0.05$, and $\omega = 0.01$, where $\gamma/\omega = 5 > 2.6$.

4. AUGMENTED MODEL INCLUDING CONTROL DELAYS AND DECISION ERRORS

This section establishes a full-state model to include the effects of decision errors and control action delays upon entering a state of a single server failure. The first two subsections follow [12] that treated these separately as the effect of decision errors when a control action is taken incorrectly but immediately upon entering a state, and the effect of delayed control actions when a correct control action is taken but after some time delay. There are deterministically diagnosable systems for which the only cost of diagnosis is time [11]. The third subsection presents a new model to be used in robust control policy design that combines the two augmented models and introduces also delays due to rerouting queries from failed sever to intact servers.

4.1. Modeling the effect of erroneous decisions

The control action considered in this study is state information based. Upon entering a state, for instance, A, any information deficiency can result in uncertainty in decision making as to whether to take a control action or what control actions to take. In this case, every decision carries a risk [17].

A decision error in the database system could include the possibility that upon a server failure, the wrong server is identified as being failed. More specifically, S_{AB}, for instance, has failed. However, S_{CA} is mistakenly observed as the failed server. Based on the false information, the control action would be for S_{BC} to restore data set C in S_{CA}, whereas S_{AB} would be expected to continue to work. As a consequence, none of the servers can process queries for a period of time, and the database system is said to have entered an intermittent error state. It is assumed that from this state, only transitions representing service completion can occur. Figure 6 depicts a generic representation of such a case.

Without loss of generality, let A be a state that is entered upon the loss of both data sets in a server. Let C be the state entered upon the completion of primary data set restoration associated with the data loss. Let B_1 through B_n be the states representing completion of services at other n servers. Let $G_1, \ldots, G_l$ be the state entered upon the arrival of a new query in one of the queues. (G_i are not shown explicitly in Figure 6.) Let F_1 through F_m be the states entered upon data loss at other m servers. An intermittent state I is introduced, as shown in Figure 6, to allow the representation of imperfect decision making upon entering A. Therefore, there is an intermittent error state for each state that involves outgoing transitions with weakened control authorities due to some decision errors. In the database system of Figure 1, 60 states are added to the original 147 states of baseline model. It is assumed that once the primary data set restoration takes place for a particular server, the secondary data set restoration proceeds without a decision error.

Let $\lambda_{A,C}$ denote the transition rate from state A to state C in the absence of decision error in the restoration of the primary database associated with the most recent data loss. Let c be the probability of successful restoration, given that the event of restoration occurs. $(1 - c)$ then is referred to as the thinning [5] of the Poisson arrival process associated with the restoration. The split of rate $\lambda_{A,C}$ into rate $c\lambda_{A,C}$ and rate $(1 - c)\lambda_{A,C}$ is sometimes also called a decomposition of a Poisson arrival process into type 1 with probability w and type 2 with probability $(1 - c)$.

An imperfect decision corresponds to the value of c being less than unity. As a consequence, the authority of control that is supposed to reinforce the restoration process is weakened. The smaller the value of c, the weaker the control authority is.

The rate of recovery from decision error is denoted by r_C. To state the fact that recovery from an intermittent error state to restoration cannot be faster than the error-free ($c = 1$) restoration process, $r_C \leq \lambda_{A,C}$ is enforced. On the other hand, the outgoing transition rates from the intermittent error state to the states of data loss in other servers, that is, from I to $F_i, i = 1, 2, \ldots, m$, are bounded below by the corresponding rates going from A to F_i. These transitions further reduce the likelihood of reaching state C.

It is now shown that decision errors always degrade the performance in terms of the state transition probability P_{AC} which is the probability that restoration to state C occurs given current state A. It turns out that this probability is readily obtained for a Markov chain

$$P_{AC} = \frac{c\lambda_{AC}}{\Lambda(A)}, \tag{14}$$

where

$$\Lambda(A) = \lambda_{AB_1} + \cdots + \lambda_{AB_n} + \cdots + \lambda_{AF_1} + \cdots + \lambda_{AF_m} + \lambda_{AC} \tag{15}$$

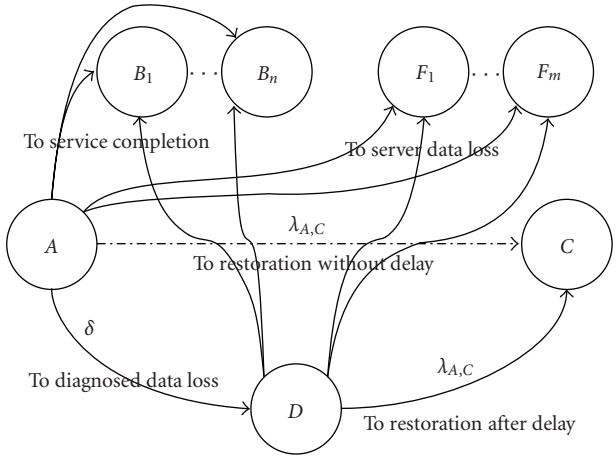

Figure 7: Control action delay modeling with a single-stage delay state.

without decision error, in which case $w = 1$ in (14), and

$$\Lambda(A) = \lambda_{AB_1} + \cdots + \lambda_{AB_n} + \lambda_{AF_1} + \cdots + \lambda_{AF_m} + c\lambda_{AC} + (1-c)\lambda_{AC} \tag{16}$$

with decision error, in which case $c < 1$. Note that (15) and (16) are the same, and both enter (14). Therefore, (14) is proportional to c, and is largest at $c = 1$ when there is no decision error.

4.2. Modeling the effect of delayed control actions

Time required for diagnosis [11] can be regarded as the universal cause of a control action delay. An example of the control action delay in the database system shown in Figure 1 would be that a total loss of data in a server is not immediately observed. As a result, the action of data restoration is delayed.

As in the previous subsection, let A be a state that is entered upon a total loss of data in a server. Let C be the state entered upon the completion of primary database restoration associated with the data loss. States B_1 through B_n and states F_1 through F_m also follow the earlier definitions. Figure 7 depicts a proposed model capable of describing a delayed restoration action by an exponentially distributed random amount with average δ^{-1} units of time upon entering state A. With a single-stage delay for each state entered upon a total loss of data in a server, another 60 states are added to the baseline model.

In a more general case, there can be an N-phased delay implemented in the augmented model by inserting N states D_1 through D_N in series between states A and C. Each state D_i retains outgoing transitions to all B_1 through B_n, and F_1 through F_m, in addition to transition to D_{i+1}. The total amount of delay before restoration action is bounded below by random variable $D = D_1 + \cdots + D_N$, with a generalized Erlang distribution [5];

$$\mathcal{L}^{-1}\left\{\prod_{i=1}^{N}\frac{\delta_i}{s+\delta_i}\right\}. \tag{17}$$

One may use an N-stage Erlang to approach a constant delay, an N-state hyperexponential to approach a highly uncertain delay, or a mixture of the two to acquire more general properties [10] in its distribution.

Note that there are two significant differences between the decision error model of Figure 6 and the control delay model of Figure 7. First, the link to *restoration of primary database* is present in Figure 7 with a smaller likelihood of transition, whereas the link to *restoration without delay* is absent in Figure 7. In addition, all links to *service completion* are absent in Figure 6, but are present in Figure 7. Therefore, each case has its distinct nature.

4.3. Full-state model of the controlled database system

Referring again to the closed queuing network view of the distributed database system in Figure 1, this section presents its augmented model that incorporates all three sources of uncertainties: decision errors (Section 4.1), control action delays (Section 4.2), and routing delays. Routing delays are incurred when queries at a failed server are rerouted to the remaining intact servers.

Rerouting of queries becomes desirable when the queries observe a server failure after they have entered the queue preceding the server. An exponentially distributed random routing time is introduced with rate τ/sec for this purpose. A routing delay is assumed independent of a control action delay. The former captures the random time of diagnosis, whereas the latter captures random time of transmission of queries among servers. Model augmentation amounts to adding new transitions among existing states without the need for new states.

In order to establish a full state model with all uncertainty types, the representation of the composite state variable is modified to $x = Q_{AB}Q_{BC}Q_{CA}S_{AB}S_{BC}S_{CA}U$, where $Q_{IJ} \in \{0,1,2,3\}$ and $S_{IJ} \in \{0,1,2\}$ as in the baseline model described in Section 2; newly introduced uncertainty variable $U \in \{0,1,2\}$ with "1" = control delayed and "2" = wrong decision made. This results in a 267 state-model. By exploiting symmetry, the 256 $(147+60+60)$ state model can be reduced to a 96-state model. The binary control variables are defined as follows: $u_1 = 1$ to restore, $u_2 = 1$ to overhaul, and $u_3 = 1$ to reroute queries.

The states, the transitions, and the transition rates of the uncertain model are summarized in Figure 8, based on which transition matrix Q of a Markov chain can be built and used in the next section for robust control policy design. τ in Figure 8 is the newly introduced query transmission rate when the action for rerouting is called for. Error probability $\bar{c}$ relates to c in Figure 6 through $\bar{c} = 1 - c$. Subscript "p" denotes "primary" and "s" denotes "secondary." Use of symmetry is reflected in server state S_f and arrival rates λ_1, λ_2, and λ_3.

	State #	States					Arrivals						Completions			Failures			Delay	Restorations				Overhaul	Reroute
		$\mathcal{Q}_{AB}$	$\mathcal{Q}_{BC}$	$\mathcal{Q}_{CA}$	S_f	U	λ_1	λ_2	λ_3	Overhaul			μ_p			ν			δ	$c\gamma_p$	$c\gamma_s$	$\bar{c}\gamma_p$	$\bar{c}\gamma_s$	ω	τ
Available	**1**	0	0	0	0	0	2	2	2	0	0	0	0	0	0	29	29	29	0	0	0	0	0	0	0
	2	1	0	0	0	0	4	3	3	0	0	0	1	0	0	32	30	31	0	0	0	0	0	0	0
	3	1	1	0	0	0	7	6	5	0	0	0	2	2	0	38	37	36	0	0	0	0	0	0	0
	4	2	0	0	0	0	8	7	6	0	0	0	2	0	0	35	33	34	0	0	0	0	0	0	0
	5	1	1	1	0	0	0	0	0	0	0	0	3	3	3	39	39	39	0	0	0	0	0	0	0
	6	1	2	0	0	0	0	0	0	0	0	0	4	3	0	44	43	40	0	0	0	0	0	0	0
	7	2	1	0	0	0	0	0	0	0	0	0	3	4	0	45	41	42	0	0	0	0	0	0	0
	8	3	0	0	0	0	0	0	0	0	0	0	4	0	0	48	46	47	0	0	0	0	0	0	0
Secondary restore	**9**	0	0	0	1	0	12	11	10	50	50	50	0	0	0	0	49	49	0	0	1	0	0	1	0
	10	0	0	1	1	0	17	16	13	51	51	52	0	0	9	0	50	50	0	0	2	0	0	2	0
	11	0	**1**	0	1	0	18	14	16	51	52	51	0	9	0	0	50	50	0	0	2	0	0	2	0
	12	1	0	0	1	0	15	18	17	52	51	51	0	0	0	0	50	50	0	0	2	0	0	2	10
	13	0	0	2	1	0	21	20	26	55	54	56	0	0	10	0	52	52	0	0	4	0	0	4	0
	14	0	**2**	0	1	0	24	27	22	54	56	55	0	11	0	0	52	52	0	0	4	0	0	4	0
	15	2	0	0	1	0	28	25	23	56	55	54	0	0	0	0	52	52	0	0	4	0	0	4	17
	16	0	**1**	1	1	0	19	22	20	53	55	54	0	10	11	0	51	51	0	0	3	0	0	3	0
	17	1	0	1	1	0	23	19	21	54	53	55	0	0	12	0	51	51	0	0	3	0	0	3	13
	18	1	**1**	0	1	0	25	24	19	55	54	53	0	12	0	0	51	51	0	0	3	0	0	3	16
	19	1	**1**	1	1	0	0	0	0	0	0	0	0	17	18	0	53	53	0	0	5	0	0	5	20
	20	0	**1**	2	1	0	0	0	0	0	0	0	0	13	16	0	54	54	0	0	6	0	0	6	0
	21	1	0	2	1	0	0	0	0	0	0	0	0	0	17	0	55	55	0	0	7	0	0	7	26
	22	0	**2**	1	1	0	0	0	0	0	0	0	0	16	14	0	55	55	0	0	7	0	0	7	0
	23	2	0	1	1	0	0	0	0	0	0	0	0	0	15	0	54	54	0	0	6	0	0	6	21
	24	1	**2**	0	1	0	0	0	0	0	0	0	0	18	0	0	54	54	0	0	6	0	0	6	22
	25	2	**1**	0	1	0	0	0	0	0	0	0	0	15	0	0	55	55	0	0	7	0	0	7	19
	26	0	0	3	1	0	0	0	0	0	0	0	0	0	13	0	56	56	0	0	8	0	0	8	0
	27	0	**3**	0	1	0	0	0	0	0	0	0	0	14	0	0	56	56	0	0	8	0	0	8	0
	28	3	0	0	1	0	0	0	0	0	0	0	0	0	0	0	56	56	0	0	8	0	0	8	23
Observation delay	**29**	0	0	0	2	0	32	31	30	50	50	50	0	0	0	0	49	49	57	0	0	0	0	1	0
	30	0	0	1	2	0	37	36	33	51	51	52	0	0	29	0	50	50	58	0	0	0	0	2	0
	31	0	1	0	2	0	38	34	36	51	52	51	0	29	0	0	50	50	59	0	0	0	0	2	0
	32	1	0	0	2	0	35	38	37	52	51	51	0	0	0	0	50	50	60	0	0	0	0	2	0
	33	0	0	2	2	0	41	40	46	55	54	56	0	0	30	0	52	52	61	0	0	0	0	4	0
	34	0	2	0	2	0	44	47	42	54	56	55	0	31	0	0	52	52	62	0	0	0	0	4	0
	35	**2**	0	0	2	0	48	45	43	56	55	54	0	0	0	0	52	52	63	0	0	0	0	4	0
	36	0	1	1	2	0	39	42	40	53	55	54	0	30	31	0	51	51	64	0	0	0	0	3	0
	37	1	0	1	2	0	43	39	41	54	53	55	0	0	32	0	51	51	65	0	0	0	0	3	0
	38	1	1	0	2	0	45	44	39	55	54	53	0	32	0	0	51	51	66	0	0	0	0	3	0
	39	1	1	1	2	0	0	0	0	0	0	0	0	37	38	0	53	53	67	0	0	0	0	5	0
	40	0	1	2	2	0	0	0	0	0	0	0	0	33	36	0	54	54	68	0	0	0	0	6	0
	41	1	0	2	2	0	0	0	0	0	0	0	0	0	37	0	55	55	69	0	0	0	0	7	0
	42	0	2	1	2	0	0	0	0	0	0	0	0	36	34	0	55	55	70	0	0	0	0	7	0
	43	**2**	0	1	2	0	0	0	0	0	0	0	0	0	35	0	54	54	71	0	0	0	0	6	0
	44	1	2	0	2	0	0	0	0	0	0	0	0	38	0	0	54	54	72	0	0	0	0	6	0
	45	**2**	1	0	2	0	0	0	0	0	0	0	0	35	0	0	55	55	73	0	0	0	0	7	0
	46	0	0	3	2	0	0	0	0	0	0	0	0	0	33	0	56	56	74	0	0	0	0	8	0
	47	0	3	0	2	0	0	0	0	0	0	0	0	34	0	0	56	56	75	0	0	0	0	8	0
	48	**3**	0	0	2	0	0	0	0	0	0	0	0	0	0	0	56	56	76	0	0	0	0	8	0
Failure	**49**	0	0	0	3	0	50	50	50	50	50	50	0	0	0	0	49	49	0	0	0	0	0	1	0
	50	1	0	0	3	0	52	51	51	52	51	51	0	0	0	0	50	50	0	0	0	0	0	2	0
	51	1	1	0	3	0	55	54	53	55	54	53	0	0	0	0	51	51	0	0	0	0	0	3	0
	52	**2**	0	0	3	0	56	55	54	56	55	54	0	0	0	0	52	52	0	0	0	0	0	4	0
	53	1	1	1	3	0	0	0	0	0	0	0	0	0	0	0	53	53	0	0	0	0	0	5	0
	54	1	**2**	0	3	0	0	0	0	0	0	0	0	0	0	0	54	54	0	0	0	0	0	6	0
	55	**2**	1	0	3	0	0	0	0	0	0	0	0	0	0	0	55	55	0	0	0	0	0	7	0
	56	**3**	0	0	3	0	0	0	0	0	0	0	0	0	0	0	56	56	0	0	0	0	0	8	0
Primary restoration	**57**	0	0	0	2	1	60	59	58	50	50	50	0	0	0	0	49	49	0	9	0	77	0	1	0
	58	0	0	**1**	2	1	65	64	61	51	51	52	0	0	57	0	50	50	0	10	0	78	0	2	0
	59	0	1	0	2	1	66	62	64	51	52	51	0	57	0	0	50	50	0	11	0	79	0	2	0
	60	1	0	0	2	1	63	66	65	52	51	51	0	0	0	0	50	50	0	12	0	80	0	2	58
	61	0	0	**2**	2	1	69	68	74	55	54	56	0	0	58	0	52	52	0	13	0	81	0	4	0
	62	0	2	0	2	1	72	75	70	54	56	55	0	59	0	0	52	52	0	14	0	82	0	4	0
	63	**2**	0	0	2	1	76	73	71	56	55	54	0	0	0	0	52	52	0	15	0	83	0	4	65
	64	0	1	**1**	2	1	67	70	68	53	55	54	0	58	59	0	51	51	0	16	0	84	0	3	0
	65	1	0	**1**	2	1	71	67	69	54	53	55	0	0	60	0	51	51	0	17	0	85	0	3	61
	66	1	1	0	2	1	73	72	67	55	54	53	0	60	0	0	51	51	0	18	0	86	0	3	64
	67	1	1	**1**	2	1	0	0	0	0	0	0	0	65	66	0	53	53	0	19	0	87	0	5	68
	68	0	1	**2**	2	1	0	0	0	0	0	0	0	61	64	0	54	54	0	20	0	88	0	6	0
	69	1	0	**2**	2	1	0	0	0	0	0	0	0	0	65	0	55	55	0	21	0	89	0	7	74
	70	0	2	**1**	2	1	0	0	0	0	0	0	0	64	62	0	55	55	0	22	0	90	0	7	0
	71	**2**	0	**1**	2	1	0	0	0	0	0	0	0	0	63	0	54	54	0	23	0	91	0	6	69
	72	1	2	0	2	1	0	0	0	0	0	0	0	66	0	0	54	54	0	24	0	92	0	6	70
	73	**2**	1	0	2	1	0	0	0	0	0	0	0	63	0	0	55	55	0	25	0	93	0	7	67
	74	0	0	**3**	2	1	0	0	0	0	0	0	0	0	61	0	56	56	0	26	0	94	0	8	0
	75	0	3	0	2	1	0	0	0	0	0	0	0	62	0	0	56	56	0	27	0	95	0	8	0
	76	**3**	0	0	2	1	0	0	0	0	0	0	0	0	0	0	56	56	0	28	0	96	0	8	71
Rework primary restoration	**77**	0	0	0	2	2	80	79	78	50	50	50	0	0	0	0	49	49	0	9	0	57	0	1	0
	78	0	0	**1**	2	2	85	84	81	51	51	52	0	0	77	0	50	50	0	10	0	58	0	2	0
	79	0	1	0	2	2	86	82	84	51	52	51	0	77	0	0	50	50	0	11	0	59	0	2	0
	80	1	0	0	2	2	83	86	85	52	51	51	0	0	0	0	50	50	0	12	0	60	0	2	78
	81	0	0	**2**	2	2	89	88	94	55	54	56	0	0	78	0	52	52	0	13	0	61	0	4	0
	82	0	2	0	2	2	92	95	90	54	56	55	0	79	0	0	52	52	0	14	0	62	0	4	0
	83	**2**	0	0	2	2	96	93	91	56	55	54	0	0	0	0	52	52	0	15	0	63	0	4	85
	84	0	1	**1**	2	2	87	90	88	53	55	54	0	78	79	0	51	51	0	16	0	64	0	3	0
	85	1	0	**1**	2	2	91	87	89	54	53	55	0	0	80	0	51	51	0	17	0	65	0	3	81
	86	1	1	0	2	2	93	92	87	55	54	53	0	80	0	0	51	51	0	18	0	66	0	3	84
	87	1	1	**1**	2	2	0	0	0	0	0	0	0	85	86	0	53	53	0	19	0	67	0	5	88
	88	0	1	2	2	2	0	0	0	0	0	0	0	81	84	0	54	54	0	20	0	68	0	6	0
	89	1	0	**2**	2	2	0	0	0	0	0	0	0	0	85	0	55	55	0	21	0	69	0	7	94
	90	0	2	**1**	2	2	0	0	0	0	0	0	0	84	82	0	55	55	0	22	0	70	0	7	0
	91	**2**	0	**1**	2	2	0	0	0	0	0	0	0	0	83	0	54	54	0	23	0	71	0	6	89
	92	1	2	0	2	2	0	0	0	0	0	0	0	86	0	0	54	54	0	24	0	72	0	6	90
	93	**2**	1	0	2	2	0	0	0	0	0	0	0	83	0	0	55	55	0	25	0	73	0	7	87
	94	0	0	**3**	2	2	0	0	0	0	0	0	0	0	81	0	56	56	0	26	0	74	0	8	0
	95	0	3	0	2	2	0	0	0	0	0	0	0	82	0	0	56	56	0	27	0	75	0	8	0
	96	3	0	0	2	2	0	0	0	0	0	0	0	0	0	0	56	56	0	28	0	76	0	8	91

FIGURE 8: Transitions and transition rates of the uncertain database state model.

5. ROBUST CONTROL POLICY DESIGN

This section seeks robust control policies as solutions to the Markov decision problem:

$$V_{\pi^*}(x_0) = \min_{\pi} E_{\pi} \sum_{k=0}^{\infty} \alpha^k C(X_k, \mathbf{u}_k), \quad x_0 \in \mathcal{X} = \{1, 2, \ldots, 95, 96\}, \tag{18}$$

where $0 < \alpha < 1$, $\pi = \{\mathbf{u}_0, \mathbf{u}_1, \ldots\}$ is the control policy sought, $\mathbf{u} = (u_1, u_2, u_3)$, and $u_i \in \{0, 1\}$. $u_1 = 1$ to restore, $u_2 = 1$ to overhaul, and $u_3 = 1$ to reroute queries, as defined in Section 4.3. Note that the full-state model enables the designer to consider service demand and to weigh availability against response time. Thus two cost criteria are established. The first criterion,

$$C(x_k, \mathbf{u}_k) = \frac{Q_1(x_k) + Q_2(x_k) + Q_3(x_k)}{\mu}, \tag{19}$$

penalizes long queues that cannot effectively reduce in time due to server failure, and thus favors response time. The second criterion, shown in the following table, penalizes prolonged service time, again, due to server failure, and thus favors availability.

The size of the state space suggests numerical means for solutions. Mathematical programs will be applied to obtain the solutions. The steady-state availability and the expected query response time of the controlled database system with the optimal policy will then be examined under various conditions.

5.1. Optimal policy design via mathematical programming

The rate transition matrix $Q(\mathbf{u}(x))$ of the 96-state model can be obtained based on Figure 8 established in Section 4.3. This $Q(\mathbf{u}(x))$ depends on $\mathbf{u}(x) = (u_1(x), u_2(x), u_3(x))$, $u_i \in \{0, 1\}$. State probability equation

$$\dot{\pi}(t) = \pi(t) Q(\mathbf{u}(x)) \tag{20}$$

originated from the forward Chapman-Kolmogorov (2) can now be uniformized to yield a discrete time Markov chain

$$\pi(k+1) = \pi(k)\left[I + \frac{1}{\rho} Q(\mathbf{u}(x))\right], \tag{21}$$

where uniform rate ρ can be chosen to be

$$\rho = 3\lambda + 3\nu + \tau + \delta + \gamma + \mu + \omega. \tag{22}$$

Recall optimality (11)

$$V(i) = \min_{\mathbf{u} \in \mathbf{U}_i} \left\{ C(i, \mathbf{u}) + \alpha \sum_j p_{i,j} V(j) \right\}, \quad i \in \mathcal{X}, \tag{23}$$

as an alternative characterization of the solution to Markov decision problem (18), which produces a system of 96 equations.

Dynamic programming is the most natural numerical approach to policy design (18) because (11) is derived through taking limit of a finite horizon dynamic program [9, 10]

$$V_{k+1}(j) = \min_{\mathbf{u} \in \mathbf{U}_j} \left\{ C(j, \mathbf{u}) + \alpha \sum_{r \in \mathcal{X}} p_{j,r} V_k(r) \right\}, \quad k = 1, 2, \ldots, N-1, \tag{24}$$

where $\alpha < 1$, and terminal cost $V_0(j) = 0$, forall $j \in \mathcal{X}$. In this case the optimal cost is given by $V_N(x_0)$, $x_0 \in \mathcal{X}$. More specifically, with $\mathbf{u}$ taking values in a finite set, the minimal cost-to-go from x_0 of the 96-state Markov decision process satisfies

$$\lim_{N \to \infty} V_N(x_0) = V^*(x_0), \quad x_0 \in \mathcal{X} = \{1, 2, \ldots, 95, 96\}, \tag{25}$$

where $V_N(x_0)$ is the minimal cost-to-go from x_0 of an N-step finite horizon process.

The solution to a dynamic program results from an iterative calculation backwards along the horizon from $V_0(j)$ to the first step $V_N(j)$. For the dynamic programming calculation to converge to the true cost-to-go, N must be significantly large, and must be less than 1.

Linear programming [18] can be considered as an alternative numerical approach to the solution of the Markov decision problem. In this case, the set of optimality equations is turned into a set of affine constraints on the set of optimization variables $\{V(i)\}$, and the problem can be formally stated as follows:

$$\text{Maximize} \quad V(1) + V(2) + \cdots + V(95) + V(96) \tag{26}$$

$$\text{subject to} \quad V(i) \geq 0, \quad i \in \mathcal{X} = \{1, \ldots, 96\}, \tag{27}$$

$$V(i) \leq \left[C(i, \mathbf{u}) + \alpha \sum_i p_{i,j} V(j) \right] \Bigg|_{\mathbf{u}} \quad \forall \mathbf{u} \in \mathbf{U_i}, i \in \mathcal{X}. \tag{28}$$

The equivalence of the linear program formulation (26)–(28) and the optimality equation formulation can be easily established. First, (27) is trivially satisfied for all i in both formulations because one-step cost $C(i, \mathbf{u})$ is always nonnegative.

Suppose $(V(1), \ldots, V(96))$ is the linear program solution. Then there must be one active (equality achieved) constraint for each of the affine inequality constraints of the form $V(i) \leq \cdots$ for each i. Suppose for some j, the constraint(s) $V(j)$ is not active. Then $V(j)$ can be increased until one of the inequality constraints becomes active without violating the rest of the inequality constraints because $\alpha p_{i,j} < 1$ as coefficient of $V(j)$ on the right side of the inequality constraints (28). This, however, contradicts the assumption that $\sum_i V(i)$ is maximum. Therefore, $(V(1), \ldots, V(96))$ is also the solution to the optimality equations (28).

Assume now that $(V(1), \ldots, V(96))$ satisfies the optimality equations. It then automatically satisfies the inequality

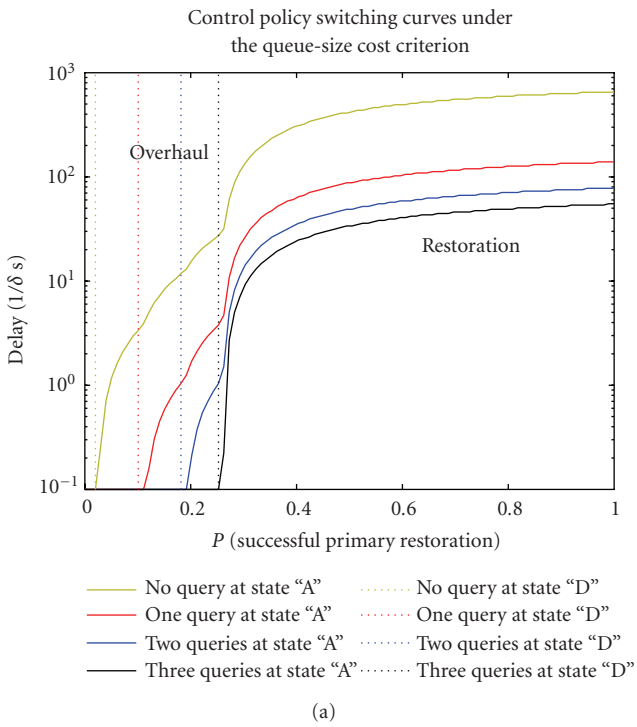

FIGURE 9: (a) Switching curves of the optimal policy under discounted queue size. (b) Partial database model containing both control action delay and decision error.

constraints (28), of which 96 are active, one for each $V(i)$ appearing on the left side. Suppose $\sum_i V(i)$ is not maximum. There is at least a $V(j)$ for some j that is smaller than the corresponding cost in max $\sum_i V(i)$, which implies that the corresponding constraint(s) for $V(j) < \cdots$ is (are) slack or inactive. This contradicts that $V(j)$ satisfies the optimality equation. Therefore, $(V(1), \ldots, V(96))$ must also be the solution of the linear program formulation (28). The equivalence is thus established.

The function linprog in MATLAB's Optimization Toolbox [19] solves the maximization problem above. The active constraints are checked with a MATLAB script to determine the optimal control policy.

The computational complexity of the dynamic program and that of the linear program are now compared. Finding the solution to a linear program generally requires a computation time proportional to n^2m [18] when $m \geq n$, where n is the number of optimization variables, and m is the number of constraints. The computational complexity of an iterative dynamic programming solution can be approximated by assuming that each iteration is a series of linear programs. The linear programming solution to the set of optimality equations is of course a single linear program.

The number of control variables, u, the number of states, s, and the horizon length, N, are critical to the computation time of these methods. First, consider the iterative method as a series of linear programs. Each individual iteration along the N-step horizon consists of s individual linear programs. Each individual linear program has u variables and $2u$ constraints. Therefore, the computation time is proportional to $Ns(u^2 2u) = Ns(2u^3)$. Now, consider the method of solving the optimality equations through linear programming. The single linear program has s variables and $2^u s$ constraints. Hence, its computation time is proportional to $s^2 2^u s = s^3 2^u$.

Although the computation time grows faster for the linear program as the number of states increases, the horizon N is typically much larger than s^2 for small discount factorin β in $\alpha = \rho/(\beta + \rho)$. Therefore, the linear program is more efficient for moderate numbers of states and small discount factors.

5.2. Availability and response time under robust control policy

A selected set of results on the robust control policies solved via mathematical programming are presented in this subsection, and the system availability and query response time under some of the optimal policies are examined.

5.2.1. Restoration-overhaul switching

Under the cost criterion (19) (minimum total discounted queue size), the optimal policy depends on the number of queries in the queue behind the failed server. No action is taken to overhaul the system until the two active queues are empty and the buildup of queries behind the failed server is significant. Figure 9(a) depicts a switching curve of of the control policy between overhaul and restoration before (solid) and after (dotted) state D in Figure 9(b) is reached. Policy switching is determined by the amount of control action delay, the decision error probability, and the number of queries in the failed server. It can be seen that, while the two active queues are occupied or after the primary data is successfully restored, restoration is performed on the failed server as long as the server performing the restoration does not have any customers waiting in its queue.

Under the cost criterion stated in Table 2 (minimally reduced service time), the optimal policy always attempts to

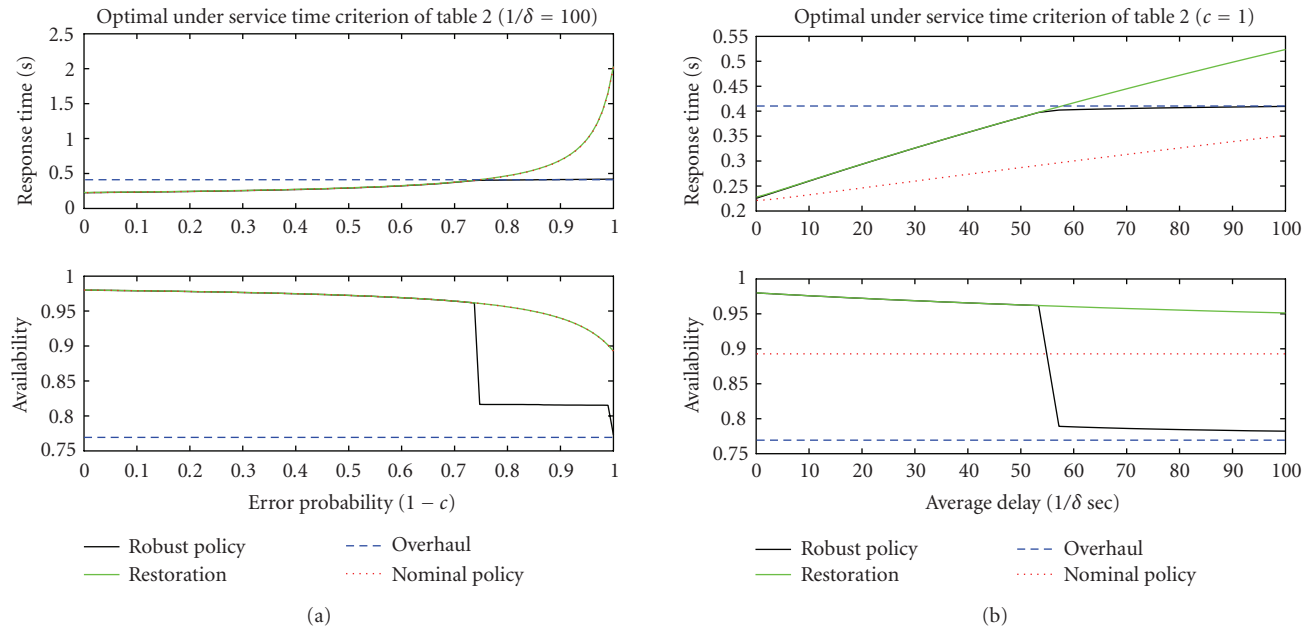

Figure 10: Response time (upper panel) and availability (lower panel) resulting from robust control policy (solid black) and nominal control policy (dotted red) versus (a) decision error $(1 - c)$ and (b) control delay $(1/\delta)$.

Table 2: Discounted service rate with service demand consideration.

Current state x_k	One-step cost $C(x_k, \mathbf{u}_k)$
The database is fully functional	0
One unavailable server has a queue	$1/\mu$
Two unavailable servers have a queue	$2/\mu$
All servers are unavailable and have a queue	$3/\mu$

restore the failed server as long as the server performing the restoration does not have any queries waiting in its queue. The only exception is when three queries are piled into any single queue. In this case, overhaul occurs when the uncertainties are significant.

5.2.2. *Performance under nominal and robust policies, and effect of routing delay*

This subsection examines the system steady-state availability and the expected query response under the robust policy, where random control delay and decision error are explicitly modeled, and under nominal policy where uncertainties are ignored. The results are similar for policies derived with either the queue size criterion (19) or the service time criterion (Table 2). The robust policy shows two distinct features in Figures 10(a) and 10(b); it switches control action when uncertainties (delay and error) becomes significant, and it balances between availability and response time in this situation.

The routing only policy does not attempt to restore the single failed server. Instead, queries are routed to an empty queue whenever the subsequent server contains the data for the query. The system is overhauled upon a second server failure. It offers some advantage in response time over the always-restore policy when there is no routing delay, as shown in Figure 11(a). It is also seen that the robust optimal policy experience improved performance with rerouting authority. However, a routing delay of about one second is significant enough to discourage the use of the routing-only policy, as shown in Figure 11(b).

6. CONCLUSIONS

Uncertainties due to control delays, transmission delays, and decision errors in the distributed database system degrade the performance of the database system performance in terms of availability and response time. Restoration remains to be the optimal policy over a significant range of uncertainties. Beyond boundaries of the range, however, the optimal control policy switches to overhaul. By formulating and solving a Markov decision problem, the robustness of the control policies is investigated. Boundaries for which optimal actions alter are shown to exist and are quantified. The robust policies are shown to provide the best compromise among competing interests.

The authors have also investigated the optimal control policy for the database under the open queuing network setting in the face of delays and errors. Simulations with SimEvents [20] show that response time further depends on the arrival rate of queries. Simulation results will be reported

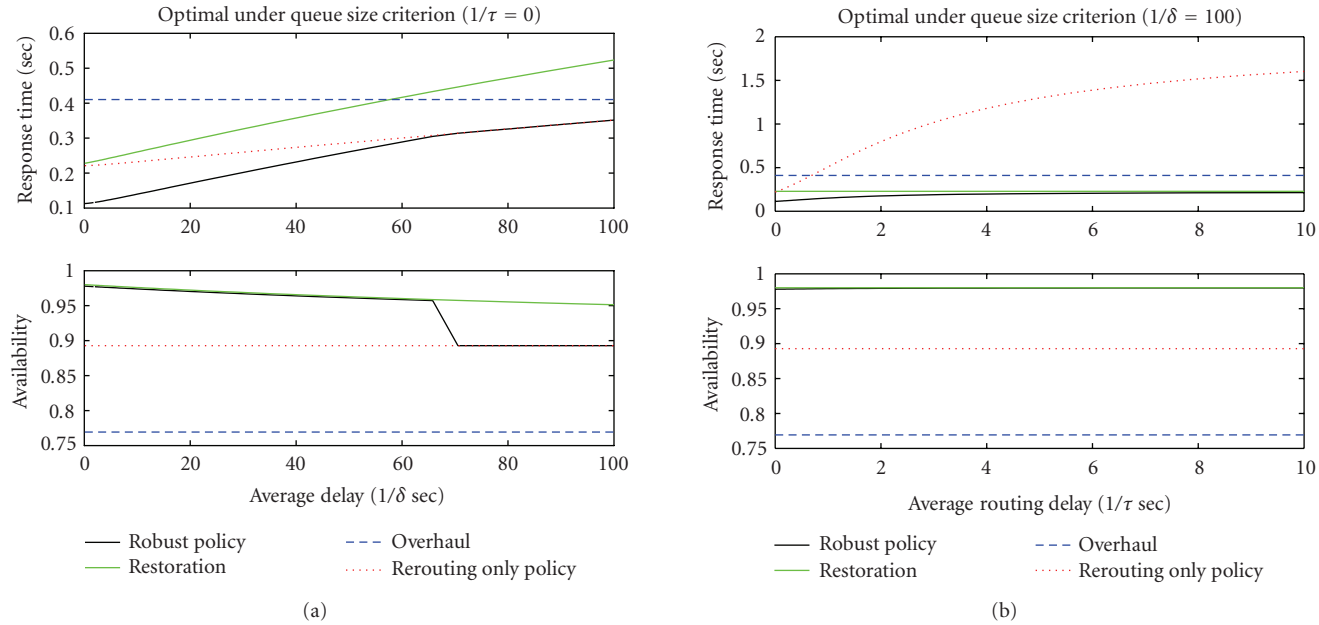

FIGURE 11: Response time (upper panel) and availability (lower panel) resulting from robust control policy (solid black) and routing only policy (dotted red) versus (a) control delay ($1/\delta$) and (b) routing delay ($1/\tau$).

separately. Simulation study of larger networks has also been planned.

ACKNOWLEDGMENT

This work was supported in part by AFOSR under Grants FA9550-06-0456 and FA9550-06-10249.

REFERENCES

[1] T. Connolly and C. Begg, *Database Solutions: A Step by Step Guide to Building Databases*, Pearson/Addison Wesley, New York, NY, USA, 2nd edition, 2004.

[2] N. E. Wu, J. M. Metzler, and M. H. Linderman, "Supervisory control of a database unit," in *Proceedings of the 44th IEEE Conference on Decision and Control and European Control Conference (CDC-ECC '05)*, pp. 7615–7620, Seville, Spain, December 2005.

[3] L. Kleinrock, *Queueing Systems: Volume 2: Computer Applications*, John Wiley & Sons, New York, NY, USA, 1976.

[4] G. Bolch, S. Greiner, H. de Meer, and K. S. Trivedi, *Queueing Networks and Markov Chains: Modeling and Performance Evaluation with Computer Science Applications*, John Wiley & Sons, New York, NY, USA, 1998.

[5] E. P. C. Kao, *An Introduction to Stochastic Processes*, Duxbury Press, New York, NY, USA, 1997.

[6] J. M. Metzler, "The effect of supervisory control on a redundant database unit," M.S. thesis, Binghamton University, Vestal, NY, USA, 2005.

[7] Arena, Academic Version 7.01.00, Rockwell Software, 2004.

[8] W. D. Kelton, R. P. Sadowski, and D. T. Sturrock, *Simulation with Arena*, McGraw-Hill, New York, NY, USA, 3rd edition, 2004.

[9] D. P. Bertsekas, *Dynamic Programming and Optimal Control*, vol. 1, 2, Athena Scientific, Belmont, Mass, USA, 1995.

[10] C. G. Cassandras and S. Lafortune, *Introduction to Discrete Event Systems*, Kluwer Academic Publishers, Dordrecht, The Netherlands, 1999.

[11] D. Thorsley and D. Teneketzis, "Diagnosability of stochastic discrete-event systems," *IEEE Transactions on Automatic Control*, vol. 50, no. 4, pp. 476–492, 2005.

[12] N. E. Wu, J. M. Metzler, and M. H. Linderman, "Controlled database unit subject to control delays and decision errors," in *Proceedings of the 8th International Workshop on of Discrete Event Systems (WODES '06)*, pp. 131–136, Michigan, Mich, USA, July 2006.

[13] N. E. Wu and T. Busch, "Reconfiguration of C2 architecture for improved availability to support air operations," *IEEE Transactions on Aerospace and Electronics*, vol. 43, no. 2, pp. 795–805, 2007.

[14] A. A. Helal, A. A. Heddaya, and B. K. Bhargava, *Replication Techniques in Distributed Systems*, Kluwer Academic Publishers, Norwell, Mass, USA, 1996.

[15] S. Zacks, *Introduction to Reliability Analysis: Probability Models and Statistics Methods*, Springer, New York, NY, USA, 1992.

[16] S. Wolfram, *Mathematica 5.2*, Wolfram Media, Champaign, Ill, USA, 3rd edition, 2005.

[17] N. E. Wu, "Coverage in fault-tolerant control," *Automatica*, vol. 40, no. 4, pp. 537–548, 2004.

[18] S. Boyd and L. Vandenberghe, *Convex Optimization*, Cambridge University Press, New York, NY, USA, 2004.

[19] MathWorks, "Optimization Toolbox User's Guide, for Use with MATLAB, Version 3," The MathWorks, 2006.

[20] MathWorks, "SimEvents User's Guide, for Use with Simulink," The MathWorks, 2006.